

12-1-2011

Part I, Unified Pharmacophore Protein Models of the Benzodiazepine Receptor Subtypes ; Part II, Subtype

Terrill S. Clayton
University of Wisconsin-Milwaukee

Follow this and additional works at: <https://dc.uwm.edu/etd>



Part of the [Biochemistry Commons](#), and the [Pharmacology Commons](#)

Recommended Citation

Clayton, Terrill S., "Part I, Unified Pharmacophore Protein Models of the Benzodiazepine Receptor Subtypes ; Part II, Subtype" (2011). *Theses and Dissertations*. 2442.
<https://dc.uwm.edu/etd/2442>

This Dissertation is brought to you for free and open access by UWM Digital Commons. It has been accepted for inclusion in Theses and Dissertations by an authorized administrator of UWM Digital Commons. For more information, please contact open-access@uwm.edu.

PART I. UNIFIED PHARMACOPHORE PROTEIN MODELS OF THE
BENZODIAZEPINE RECEPTOR SUBTYPES

PART II. SUBTYPE SELECTIVE LIGANDS FOR $\alpha 5$ GABA(A) /BZ RECEPTORS

VOLUME I

by

Terrill S. Clayton

A Dissertation Submitted in
Partial Fulfillment of the
Requirements for the Degree of

Doctor of Philosophy
in Chemistry

at

The University of Wisconsin-Milwaukee

December 2011

UMI Number: 3520610

All rights reserved

INFORMATION TO ALL USERS

The quality of this reproduction is dependent upon the quality of the copy submitted.

In the unlikely event that the author did not send a complete manuscript and there are missing pages, these will be noted. Also, if material had to be removed, a note will indicate the deletion.



UMI 3520610

Published by ProQuest LLC 2012. Copyright in the Dissertation held by the Author.

Microform Edition © ProQuest LLC.

All rights reserved. This work is protected against unauthorized copying under Title 17, United States Code.



ProQuest LLC
789 East Eisenhower Parkway
P.O. Box 1346
Ann Arbor, MI 48106-1346

PART I. UNIFIED PHARMACOPHORE PROTEIN MODELS OF THE
BENZODIAZEPINE RECEPTOR SUBTYPES

PART II. SUBTYPE SELECTIVE LIGANDS FOR $\alpha 5$ GABA(A) /BZ RECEPTORS

by

Terrill S. Clayton

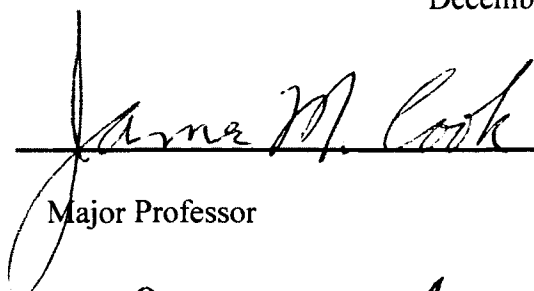
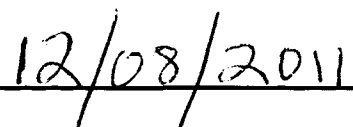
A Dissertation Submitted in
Partial Fulfillment of the
Requirements for the Degree of


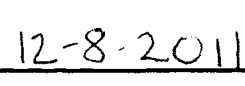
Doctor of Philosophy
in Chemistry

at

The University of Wisconsin-Milwaukee

December 2011

 
Major Professor Date

 
Graduate School Approval Date

ABSTRACT

PART I. UNIFIED PHARMACOPHORE PROTEIN MODELS OF THE
BENZODIAZEPINE RECEPTOR SUBTYPES
PART II. SUBTYPE SELECTIVE LIGANDS FOR $\alpha 5$ GABA(A) /BZ RECEPTORS

by

Terrill S. Clayton

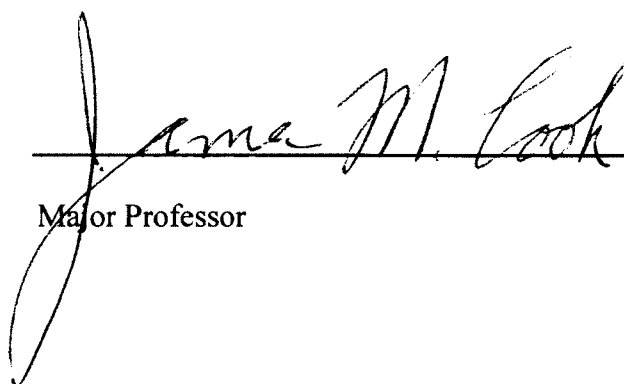
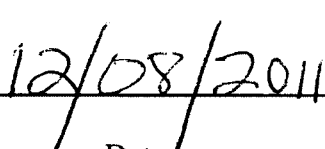
University of Wisconsin-Milwaukee, 2011
Under the Supervision of Professor James M. Cook

Part I. New models of unified pharmacophore/receptors have been constructed guided by the synthesis of subtype selective compounds in light of recent developments both in ligand synthesis and structural studies of the binding site itself. The evaluation of experimental data in combination with comparative models of the $\alpha 1\beta 2\gamma 2$, $\alpha 2\beta 2\gamma 2$, $\alpha 3\beta 2\gamma 2$ and $\alpha 5\beta 2\gamma 2$ GABA(A) receptors has led to an orientation of the pharmacophore model within the benzodiazepine binding site (Bz BS). These results not only are important for the rational design of new selective ligands, but also for the identification and evaluation of possible roles which specific residues may have within the benzodiazepine binding pocket. More importantly, the process summarized here may be used as a general template to help scientists develop novel ligands for receptors for which the three dimensional structure has not yet been confirmed by X-ray crystallography or cryo-electron microscopy. Presented here are new models of the $\alpha 1\beta 2\gamma 2$, $\alpha 2\beta 2\gamma 2$, $\alpha 3\beta 2\gamma 2$ and $\alpha 5\beta 2\gamma 2$ GABA(A) receptors which have incorporated

homology models built based on the acetylcholine binding protein. These new models will further our ability to understand structural characteristics of ligands which act as agonists, antagonists, or inverse agonists to the Bz BS of the GABA(A) receptor. This approach will also serve as a powerful model for structure based approaches carried out using ligand-protein docking methods.

Part II. An effective strategy to alleviate memory deficits would be to enhance memory and cognitive processes by augmenting the impact of acetylcholine released from cholinergic neurons of the hippocampus. Using the included volume pharmacophore presented in Part I, a number of $\alpha 5$ selective compounds were synthesized, notably PWZ-029. PWZ-029 was examined in rats in the passive and active avoidance, spontaneous locomotor activity, elevated plus maze and grip strength tests which are indicative of the effects on memory acquisition, locomotor activity, anxiety, and muscle tone. Improvement of task learning was shown at a dose of 5mg/kg in passive avoidance test without effect on anxiety or muscle tone. Moderate negative modulation at GABA(A) receptors containing the $\alpha 5$ subunit using a moderate inverse agonist such as PWZ-029, is a sufficient condition for eliciting enhanced encoding/consolidation of declarative memory. Using low temperature NMR and X-ray analysis, it was shown that enhanced selectivity and potent *in vitro* affinity of $\alpha 5$ selective benzodiazepine dimers was possible with aliphatic linkers of 3 to 5 carbons in length. Although originally proposed to enhance solubility, oxygen-containing linkers caused the dimer to fold back on itself leading to the inability of dimers to enter the binding pocket. In addition, studies of a series of PWZ-029 analogs found that the electrostatic potential near the ligands' terminal substituent correlated with its binding selectivity toward the $\alpha 5\beta 2\gamma 2$ versus $\alpha 1\beta 2\gamma 2$ BzR/

GABA(A) ergic isoform. Investigations further found that compound PWZ-029, which exhibits reasonable binding selectivity toward GABA(A) receptors containing the $\alpha 5$ subunit and possesses a favorable electrophysiological profile, was able to attenuate scopolamine induced contextual memory impairment in mice. This compound appears to be useful (Harris, Delorey et al.) for the treatment of cognitive deficits in rodents as well as primates (Rowlett et al.) and may well be a compound for the treatment of patients with Alzheimers disease.

 
Major Professor Date

To
My parents William and Elizabeth Clayton
and
My wife Tracey
and
My daughters Makenna, Madison, and Leah

TABLE OF CONTENTS

Introduction.....	1
Recent Alignment of Non-Classical Bz Binding Site Ligands Support the Unified Pharmacophore/Receptor Model	9
Zopiclone and its Active Enantiomer (Lunesta®)	10
SH-053 Benzodiazepine Enantiomers	12
Flavonoids.....	16
Analogues of 8-Chloropyrazolo[5,1-c][1,2,4]-benzotriazine 5-oxide (3)	19
Dimer Affinity for the Binding Site.....	21
Beta-Carbolines	29
Application of β -Carbolines to Treat Alcohol Addiction.....	33
Structure Activity Relationships of β -Carbolines.....	38
The β CCt Bivalent Ligands	43
WYS8	45
3-Substituted β -Carbolines	49
Chiral 3-Substituted β -Carbolines.	52
Efficacy of α 1 Preferring Ligands in Oocytes at GABA(A) Receptor Channels	55
Ligands that Occupy the L ₂ Region and are Selective for α 5 Containing Receptors;	58
RY-24 and Related Analogs	58
QH-II-066	65
The Interactive Compound Table	67
Evidence from Covalently Reactive Ligands Allows One to Position the L ₂ Lipophilic Pocket	68

The A ₂ Descriptor and the L _{DI} Region.....	70
Included Volume Analysis of Ligands Binding to Receptors Containing Different Alpha Subunits	71
The Previous Benzodiazepine Subtype Selective Receptor Pharmacophore Models	73
Recent Discovery of Alpha 5 Volume Differences	76
Computer Modeling Methods.....	83
The Updated Included Volume Analysis Models.....	85
The $\alpha 1\beta 3\gamma 2$ Receptor Subtype	85
The $\alpha 2\beta 3\gamma 2$ Receptor Subtype	95
The $\alpha 3\beta 3\gamma 2$ Receptor Subtype	103
The $\alpha 4\beta 3\gamma 2$ Receptor Subtype	109
The $\alpha 5\beta 3\gamma 2$ Receptor Subtype	112
The $\alpha 6\beta 3\gamma 2$ Receptor Subtype	124
QSAR.....	127
The $\alpha 1\beta 3\gamma 2$ Receptor Subtype	128
The $\alpha 2\beta 3\gamma 2$ Receptor Subtype	130
The $\alpha 3\beta 3\gamma 2$ Receptor Subtype	132
The $\alpha 5\beta 3\gamma 2$ Receptor Subtype	134
Comparative Model of the Benzodiazepine Binding Site	138
Combining Homology Model and Experimental Evidence.....	143
Construction of the Unified Pharmacophore/Receptor Model	150
Homology Models of the Benzodiazepine Receptor	155
Protein Models of the $\alpha 1\beta 3\gamma 2$, $\alpha 2\beta 3\gamma 2$, $\alpha 3\beta 3\gamma 2$ and $\alpha 5\beta 3\gamma 2$ Subtypes.....	163

Docking Studies Using AutoDock 4.2.....	175
Docking WYS8.....	177
Future Work.....	180
Part II. Subtype Selective Ligands for $\alpha 5$ GABA(A) /Bz Receptors.....	181
Introduction.....	181
$\alpha 5$ Selective Ligands	185
Pharmacology	193
History of GABA(A) / Benzodiazepine Receptors	198
Synthesis of 8-Substituted imidazobenzodiazepines	201
Included Volume Analysis of Ligands Binding to Receptors Containing $\alpha 5$ Subunits ..	206
SH-053 Analogs.....	207
Dimeric Benzodiazepines	211
QH-II-066	221
Affect on Passive Avoidance Learning in Rats of a Modest Inverse Agonist (PWZ-029) with Functional Selectivity at GABA(A) Receptors Containing $\alpha 5$ Subunits	225
Electrophysiological Experiments	229
Passive Avoidance	230
Active Avoidance	231
Locomotor Activity Assay	232
Whole Chamber-Activity.....	233
Central/Peripheral Distance	235
Antagonism of the Effect of PWZ-029 (Figure 116).....	235
Elevated Plus Maze.....	238

Activity-Related Parameters	238
Anxiety-Related Parameters (Figure 117)	238
Grip Strength Test.....	240
Experimental Procedure.....	246
Electrophysiological Experiments (with Sieghart et al.)	246
Behavioral Experiments (with Savic et al.)	248
Passive Avoidance (PA) Paradigm	249
Two-Way Active Avoidance (AA) Paradigm (with Savic et al.)	249
Measurement of Locomotor Activity (with Savic et al.).....	250
Behavior on the Elevated Plus Maze (EPM) (with Savic et al.).....	250
Grip Strength Test (with Savic et al.)	251
Statistical Analysis.....	251
Sedative Influence of $\alpha 5$ Benzodiazepine Site Agonists or Stereotypical Behavior?.....	252
Rotarod Performance	256
Statistical Analysis.....	257
Results.....	258
Elevated Plus Maze.....	259
Anxiety-Related Parameters (Figure 121)	262
SH-053-S-CH3-2'F	264
Anxiety-related parameters (Figure 123).....	266
SH-053-R-CH3	268
Motor Activity Assay	268
Central/Peripheral Distance	271
Rotarod Test.....	272

Discussion.....	272
Behavioral Effects Due to Differences in Activity at $\alpha 1$ Plus $\alpha 5$ Versus $\alpha 2$ Plus $\alpha 3$ Subunits	277
Drugs.....	280
Competition Binding Assays	280
Electrophysiological Experiments (with Sieghart et al.)	281
Behavioral Experiments (with Savic et al.)	283
Measurement of Locomotor Activity	284
Behavior in the Elevated Plus Maze.....	284
Behavior in the Morris Water Maze	285
Statistical Analysis.....	287
Competition Binding Assays	288
Electrophysiological Experiments	289
Results.....	291
Motor Activity Assay	291
Elevated Plus Maze.....	293
Morris Water Maze.....	299
Discussion.....	309
Search for Subtype Selective Ligands for $\alpha 5\beta 3\gamma 2$ Subtypes	318
Results.....	321
Discussion.....	325
Chemistry.....	335
Computational Assessment of Benzodiazepine Influence on Contextual Memory	337
Organization of the Study	344

Binding and Activational Selectivity in the Development of a Palliative Memory Agent.	347
Validation of 3D Pharmacophore for Sedation and Contextual Memory Endpoints by 3D- Database Search and Testing (Harris, Delorey, Clayton et al.)	356
3D-QSAR (COMSIA) Models of $\alpha 5\beta 2\gamma 2$ and $\alpha 1\beta 2\gamma 2$ Receptor Isoforms.	359
Fragment QSAR: Facets Effecting Differential Binding Between $\alpha 1\beta 2\gamma 2$ and $\alpha 5\beta 2\gamma 2$ GABA(A) Receptor Isoforms.....	364
Computational Assessment of Molecular Properties Correlated with Electrophysiological Response	370
COMSIA analyses	372
$5\beta 2\gamma 2$ BzR/GABA(A)ergic Subtype Selective Bivalent Antagonists Reverse Scopolomine Induced Cognitive Impairment.....	382
Xli356 and PWZ-029 PDSP data	388
Preparation of Cloned mRNA	393
Functional Expression of GABA(A) Receptors	393
Electrophysiological Experiments with Sieghart et al. ⁵⁰⁸	394
In vivo Assessments	395
Pavlovian Fear Conditioning	395
Conformational Libraries for Pharmacophore/Overlap Rule Development.....	396
Initial Pharmacophore Development	397
Validation of Overlap Rules/Pharmacophores Via Database Searches.....	398
Quantum Chemical Evaluation of Properties in Conformations Complying with Pharmacophores for Use in QSAR.....	398

Fragment and 3D-QSAR Analyses.....	399
Molecular Modeling, Synthesis, and Pharmacological Studies of Some Tetracyclic 1,3-Diazepinium Chlorides (with Grant et al.)	400
Pharmacology	402
Animals.....	403
Preparation of Drug Samples.....	403
Hippocratic Screen 1.....	403
Hippocratic Screen 2.....	404
Statistical Analysis.....	404
Hippocratic Screen 1.....	404
Hippocratic Screen 2.....	405
Decreased Motor Activity.....	405
Ataxia.....	406
Loss of Righting Reflex.....	406
Pinnal Reflex	408
Molecular Modeling	409
The Role of $\alpha 1$ and $\alpha 5$ containing GABA(A) Receptors in Mediating Diazepam Effects on Spontaneous Locomotor Activity and Water Maze Learning and Memory in Rats ..	414
Drugs.....	415
Behavioral Experiments by Savic et al. ^{429, 528}	416
Measurement of Locomotor Activity	416
Behavior in the Morris Water Maze	417
Statistical Analysis.....	420
Results.....	421

Motor Activity Assay	422
Morris Water Maze.....	426
Where To Go From Here- Next Generation Ligands	444
Biology	466
$\alpha 5\beta 2\gamma 2$ Selective Ligands Attenuate Scopolamine Induced Contextual Memory Impairment.....	471
Experimental.....	475
Competition Binding Assays	475
Preparation of Cloned mRNA (with Dr. R. Furtmüller, Dr. Ramerstorfer and Dr. W. Sieghart). ^{545, 546}	475
Functional Expression of GABA(A) Receptors (with Dr. R. Furtmüller, Dr. Ramerstorfer and Dr. W. Sieghart). ^{36, 37}	476
Electrophysiological Experiments (with Dr. R. Furtmüller, Dr Ramerstorfer and Dr. W. Sieghart). ^{64, 310}	477
Synthesis of Bivalents.....	478
Materials and General Instrumentation.....	480
Competition Binding Assays	481
Radioligand Binding Assays (Drs. McKernan and Atack) ⁵⁵¹	481
1,3-Bis(8-acetyleno-5,6-dihydro-5-methyl-6-oxo-4H-imidazo[1,5a][1,4]benzodiazepine- 3-carboxy) propyl diester 1	482
1,5-Bis(8-acetyleno-5,6-dihydro-5-methyl-6-oxo-4H-imidazo[1,5a][1,4] benzodiazepine - 3carboxy) pentyl diester 18 (XLi210)	483
1,3-Bis(8-ethyl-5,6-dihydro-5-methyl-6-oxo-4H-imidazo[1,5a][1,4]benzodiazepine-3- carboxy) propyl diester 3 (XLi356).....	483

Bis(8-acetyleno-5,6-dihydro-5-methyl-6-oxo-4H-imidazo[1,5-a][1,4]benzodiazepine-3-carboxy) dimethyl glycol diester 23 (XLi374)	484
8-Bromo-6-phenyl-4H-benzo[f]imidazo[1,5-a][1,4]diazepine-3-carboxylic acid	484
1, 3-Bis(8-bromo-6-phenyl-4H-benzo[f]imidazo[1,5-a][1,4]diazepine-3-carboxy) propyl diester.....	485
1,3-Bis(8-trimethylsilylacetylenyl-6-phenyl-4H-benzo[f]imidazo[1,5-a][1,4]-diazepine-3-carboxy) propyl diester	485
1,3-Bis(8-acetylenyl-6-phenyl-4H-benzo[f]imidazo[1,5-a][1,4]diazepine-3-carboxy)propyl diester	486
Bis(8-bromo-6-phenyl-4H-benzo[f]imidazo[1,5-a][1,4]diazepine-3-carboxy) diethylene glycol diester.....	487
Bis(8-trimethylsilylacetylenyl-6-phenyl-4H-benzo[f]imidazo[1,5-a][1,4]diazepine-3-carboxy) diethylene glycol diester.....	488
Bis(8-acetylenyl-6-phenyl-4H-benzo[f]imidazo[1,5-a][1,4]diazepine-3-carboxy) diethylene glycol diester	488
X-ray Crystallographic Data.....	489
Audio Cued Data for Xli356.....	489
References.....	490
Appendix I. Key Amino Acid Sequences.....	539
Data Table 1. Amino acid sequence of the alpha subunit of the acetylcholine receptor in the <i>lymnaea stagnalis</i> (Great Pond Snail)	539
Data Table 2. Amino acid sequence of the alpha subunit of the acetylcholine receptor in the <i>Torpedo californica</i> (Pacific Electric Ray).....	539

Data Table 3. Amino acid sequence of the alpha 1 subunit of the rat GABA(A) receptor	539
Data Table 4. Amino acid sequence of the gamma 2 subunit of the rat GABA(A) receptor	540
Data Table 5. Amino acid sequence of the alpha 1 subunit of the human GABA(A) receptor	540
Data Table 6. Amino acid sequence of the gamma 2 subunit of the human GABA(A) receptor	541
Data Table 7. Amino acid sequence of the Beta 2 Subunit of the Human GABA(A) Receptor	541
Appendix II.	542
Data Table 8. Coordinates of the Pharmacophore	542
Appendix III. Pharmacology	543
Extraction of Diazepam from Valium® Tablets (5 mg).....	543
Hippocratic Screen Activities	543
Appendix IV. Tetracyclic 1,3-Diazepinium Chemistry (with Grant et al.)	545
Experimental Data for the Tetracyclic 1,3-Diazepinium Chlorides	550
Chemistry	550
General Preparation of 6-Methoxy-3-Methylbenzofuran-2-Carboxamides (5a-h)	550
6-Methoxy-3-methyl- <i>N</i> -(pyridin-2-yl)benzofuran-2-carboxamide (5a).....	551
Di-(6-methoxy-3-methylbenzofuran-2-carbonyl)(3-methylpyridin-2-yl)amine (9).....	551
6-Methoxy-3-methyl- <i>N</i> -(4-methylpyridin-2-yl)benzofuran-2-carboxamide (5c)	552
6-Methoxy-3-methyl- <i>N</i> -(5-methylpyridin-2-yl)benzofuran-2-carboxamide (5d)	552
Di-(6-methoxy-3-methylbenzofuran-2-carbonyl)(5-methylpyridin-2-yl)amine (10).....	553

6-Methoxy-3-methyl- <i>N</i> -(6-methylpyridin-2-yl)benzofuran-2-carboxamide (5e)	553
<i>N</i> -(5-Chloropyridin-2-yl)-6-methoxy-3-methylbenzofuran-2-carboxamide (5f)	554
6-Methoxy-3-methyl- <i>N</i> -(pyrimidin-2-yl)benzofuran-2-carboxamide (5g)	554
6-Methoxy-3-methyl- <i>N</i> -(3-methylpyridin-2-yl)benzofuran-2-carboxamide (5b)	554
5,6-Dimethoxy-3-methyl- <i>N</i> -(pyridin-2-yl)benzofuran-2-carboxamide (5h)	555
General Preparation of Bromomethyl Amides (6a–h)	556
3-(Bromomethyl)-6-methoxy- <i>N</i> -(pyridin-2-yl)benzofuran-2-carboxamide (6a)	556
3-(Bromomethyl)-6-methoxy- <i>N</i> -(4-methylpyridin-2-yl)benzofuran-2-carboxamide (6c)	556
3-(Bromomethyl)-6-methoxy- <i>N</i> -(5-methylpyridin-2-yl)benzofuran-2-carboxamide (6d)	557
3-(Bromomethyl)-6-methoxy- <i>N</i> -(6-methylpyridin-2-yl)benzofuran-2-carboxamide (6e)	557
3-(Bromomethyl)- <i>N</i> -(5-chloropyridyl)-6-methoxybenzofuran-2-carboxamide (6f)	558
3-Methoxy-6-oxo-7,13-dihydro-6 <i>H</i> -benzofuro[2,3- <i>e</i>]pyrimido[1,2- <i>a</i>][1,3]diazepin-12- ium bromide (11)	558
3-(Bromomethyl)-5,6-dimethoxy- <i>N</i> -(pyridin-2-yl)benzofuran-2-carboxamide (6h)	559
Preparation of Chloromethyl Amides (7a–f and 7h)	559
3-(Chloromethyl)-6-methoxy- <i>N</i> -(pyridin-2-yl)benzofuran-2-carboxamide (7a)	560
3-(Chloromethyl)-6-methoxy- <i>N</i> -(4-methylpyridin-2-yl)benzofuran-2-carboxamide (7c)	560
3-(Chloromethyl)-6-methoxy- <i>N</i> -(6-methylpyridin-2-yl)benzofuran-2-carboxamide (7e)	560
3-Chloromethyl- <i>N</i> -(5-chloropyridin-2-yl)-6-methoxybenzofuran-2-carboxamide (7f) ..	561

3-(Chloromomethyl)-5,6-dimethoxy- <i>N</i> -(pyridin-2-yl)benzofuran-2-carboxamide (7h)	561
Preparation of Tetracyclic Salts (8a–f, 8h)	561
3-Methoxy-6-oxo-7,13-dihydro-6 <i>H</i> -benzofuro[2,3- <i>e</i>]pyrido[1,2- <i>a</i>][1,3]diazepin-12-ium chloride (8a)	562
3-Methoxy-8-methyl-6-oxo-7,13-dihydro-6 <i>H</i> -benzofuro[2,3- <i>e</i>]pyrido[1,2- <i>a</i>][1,3]diazepin-12-ium chloride (8b)	562
3-Methoxy-9-methyl-6-oxo-7,13-dihydro-6 <i>H</i> -benzofuro[2,3- <i>e</i>]pyrido[1,2- <i>a</i>][1,3]diazepin-12-ium chloride (8c)	563
3-Methoxy-10-methyl-6-oxo-7,13-dihydro-6 <i>H</i> -benzofuro[2,3- <i>e</i>]pyrido[1,2- <i>a</i>][1,3]diazepin-12-ium chloride (8d)	563
3-Methoxy-11-methyl-6-oxo-7,13-dihydro-6 <i>H</i> -benzofuro[2,3- <i>e</i>]pyrido[1,2- <i>a</i>][1,3]diazepin-12-ium chloride (8e)	564
10-Chloro-3-methoxy-6-oxo-7,13-dihydro-6 <i>H</i> -benzofuro[2,3- <i>e</i>]pyrido[1,2- <i>a</i>][1,3]diazepin-12-ium chloride (8f)	564
2,3-Dimethoxy-6-oxo-7,13-dihydro-6 <i>H</i> -benzofuro[2,3- <i>e</i>]pyrido[1,2- <i>a</i>][1,3]diazepin-12-ium chloride (8h)	565
Appendix V. UWM Compound Table	566
Appendix VI. PDSP Activity Data	717
Appendix VII. In Vitro Metabolic Stability of Selected Compounds Using Human Liver Microsomes	759
Curriculum Vitae	771

LIST OF FIGURES

Figure 1. Proposed topology of a GABA(A) receptor subunit. The extracellular domain begins with the N-terminus and M1-M4 represents the four transmembrane domains. ¹⁰ ...2	2
Figure 2. Longitudinal (A) and cross-sectional (B) schematic representations of the ligand-gated ion channel. The numbers 1-4 refer to the M1-M4 segments. The M2 segment contributes to the majority of the pore lining within the membrane lipid bilayer. ¹⁰3	3
Figure 3. Longitudinal homology model of the human $\alpha 1\beta 2\gamma 2$ ligand gated ion channel ¹⁰4	4
Figure 4. Cross-sectional homology model of the human $\alpha 1\beta 2\gamma 2$ ligand gated ion channel ¹¹5	5
Figure 5. Membrane potential over time during the transmission of a nerve signal. A hyperpolarized state represents a potential further away from the threshold potential.8	8
Figure 6. Structure of the sedative-hypnotic zopiclone 1, its alignment within the pharmacophore/receptor model and the model rotated 90°.11	11
Figure 7. Alignment of zopiclone 1 (left) and its active enantiomer (right) in the included volume of the pharmacophore/receptor model for the $\alpha 1\beta 3\gamma 2$ subtype.12	12
Figure 8. Structures and conformations of SH-053-S-CH3 (A1-A3) and SH-053-R-CH3 (B1-B3) in the $\alpha 2\beta_{2/3}\gamma 2$ subtype included volume. A3 and B3 are the pharmacophore model rotated 90° in a clockwise direction.15	15

Figure 9. Concentration-effect curves for SH-053-S-CH3 and SH-053-R-CH3 on $\alpha 1\beta 3\gamma 2$, $\alpha 2\beta 3\gamma 2$, $\alpha 3\beta 3\gamma 2$, and $\alpha 5\beta 3\gamma 2$ GABA(A) receptors. Data points represent means \pm SEM from at least 4 oocytes from ≥ 2 batches. ⁵⁸	16
Figure 10. Alignment of 2 within the included volume of the $\alpha 2\beta 3\gamma 2$ subtype.....	18
Figure 11. A series of flavone-related analogs that were inactive at the Bz BS.....	19
Figure 12. Alignment of N-oxide ligand 3 (black) overlaid with diazepam (cyan) within the unified pharmacophore/receptor model and rotated 90° (right side).	21
Figure 13. Alignments of XLi-093 27 (white) and Ro15-1788 21 (cyan) within the included volume of the $\alpha 5\beta 3\gamma 2$ subtype. ⁵⁵	24
Figure 14. Crystal structures of the linear XLi-093 (27, above) and the folded DMH-III-96 (30, below). ^{33, 68, 69}	25
Figure 15. Alignment of DMH-III-96 (30) within the included volume of the $\alpha 5\beta 3\gamma 2$ subtype. It was apparent that the folded conformation prevented it from binding to this GABA(A) subtype.	27
Figure 16. Alignment of WY-S-2 (25, left) and WY-S-6 (26, right) within the included volume of the $\alpha 1\beta 3\gamma 2$ subtype.	28
Figure 17. Flexidocking of β CCT to the unified pharmacophore receptor model of the $\alpha 1\gamma 2$ model of the protein subunits	29
Figure 18. In vitro binding affinities of a series of $\alpha 1$ selective BzR ligands (K_i in nM)..	39
Figure 19. Efficacy of β CCT in modulating GABA at recombinant GABA $\alpha 1-\alpha 5$ receptors ¹⁶⁴ in <i>Xenopus</i> oocytes: comparison with other BzR antagonists.....	41
Figure 20. Orthogonal views of CoMFA contour maps for the affinity of 6-benzyl-substituted β -carboline at the $\alpha 1\beta 3\gamma 2$ BzR. Orthogonal view of CoMFA contour maps	

for the $\alpha 1\beta 3\gamma 2$ receptor subtype with 6-benzyl-substituted β -carbolines modeled by Huang. ^{71, 158} Green contours represent areas of positive steric interaction at a contribution level of 85%, which would result in reduced binding affinity. Blue contours represent areas of positive charge interaction at a level of 85%, which would increase the affinity of a ligand.....	44
Figure 21. Overlap of diazepam and β CCt in the previous two dimensional pharmacophore/receptor model.	46
Figure 22. Efficacy of β CCt in modulating GABA at recombinant GABA $\alpha 1-\alpha 5$ receptors ^{135, 183, 184} in <i>Xenopus</i> oocytes: comparison with other BzR antagonists.	56
Figure 23. Subtype efficacy of RY-24 (83), Dose response curves for RY-24 in oocytes expressing different subunit combinations of GABA(A) receptors. Subtype combinations are indicated in legends. cRNA-injected <i>Xenopus</i> oocytes were held at -60 mV under two-electrode voltage clamp. Increasing concentrations of RY-24 were superfused together with a GABA concentration eliciting ~ 20% of the maximal current amplitude. RY-24 was pre-applied for 30 sec before the addition of GABA, which was co-applied with the drugs until a peak response was observed. Data were normalized for each curve assuming 100% for the response in the absence of RY-24. RY-24 was made up and diluted as stock solution in DMSO. Final DMSO concentrations perfusing the oocyte were 0.1%. Values are presented as mean \pm SD of at least 4 oocytes from at least 2 batches.	61
Figure 24. Suppression of alcohol-motivated responding by RY-24 (83) and RY-23 (84) 18	64

Figure 25. Comparison of non-selective diazepam (black) with the $\alpha 5$ -selective QH-ii-066 (cyan) when aligned within the unified pharmacophore/ receptor model.	66
Figure 26. Diazepam in the pharmacophore receptor model and the key residues $\gamma 2A79$ and $\gamma 2T81$	71
Figure 27. Overlap between pairs of previous included volumes derived from receptor subtype selective ligands:	1
Figure 28. Included volume and ligand occupation of the SH-053-2'F-S-CH3 and SH-053-2'F-R-CH3 enantiomers in the $\alpha 5$ and $\alpha 2$ BzR subtypes.....	78
Figure 29. The Milwaukee-based unified pharmacophore	81
Figure 30. The schematic representation of the descriptors for the inclusive BzR pharmacophore. ²⁵¹	83
Figure 31. Overlay of selected compounds for $\alpha 1\beta 3\gamma 2$ subtype from Table 8	94
Figure 32. Updated $\alpha 1\beta 3\gamma 2$ subtype (solid) overlayed with the previous model (line). ...	95
Figure 33. Overlay of compounds selective for $\alpha 2\beta 3\gamma 2$ subtype.....	102
Figure 34. Updated $\alpha 2\beta 3\gamma 2$ subtype (solid) overlayed with the previous model (line). .	102
Figure 35. Overlay of compounds selective for $\alpha 3\beta 3\gamma 2$ subtype.....	108
Figure 36. Updated $\alpha 3\beta 3\gamma 2$ subtype (solid) overlayed with the previous model (line). .	109
Figure 37. Overlay of selected compounds selective for $\alpha 4\beta 3\gamma 2$ subtype	111
Figure 38. Updated $\alpha 4\beta 3\gamma 2$ subtype (solid) overlayed with the previous model (line). .	111
Figure 39. Overlay of selected compounds selective for $\alpha 5\beta 3\gamma 2$ subtype	121
Figure 40. Updated $\alpha 5\beta 3\gamma 2$ subtype (solid) overlayed with the previous model (line). .	121

Figure 41. Overlay of the $\alpha 5\beta 3\gamma 2$ receptor (yellow) subtype with the $\alpha 1\beta 3\gamma 2$ receptor (magenta) subtype. Orange surfaces indicate overlapping regions.	122
Figure 42. Overlay of the $\alpha 5\beta 3\gamma 2$ receptor (yellow) subtype with the $\alpha 1\beta 3\gamma 2$ receptor (magenta) subtype (Figure 42 rotated 90°). Orange surfaces indicate overlapping regions.	123
Figure 43. Overlay of selected compounds selective for $\alpha 6\beta 3\gamma 2$ subtype	126
Figure 44. Updated $\alpha 6\beta 3\gamma 2$ subtype (solid) overlayed with the previous model (line)..	126
Figure 45. Steric (left) and electrostatic maps of $\alpha 1\beta 3\gamma 2$ receptor subtype shown in transparent mode as seen from the classic perspective.....	128
Figure 46. Steric (left) and electrostatic maps of $\alpha 1\beta 3\gamma 2$ receptor subtype shown in transparent mode as seen from the classic perspective rotated 90°.....	129
Figure 47. Steric (left) and electrostatic maps of $\alpha 1\beta 3\gamma 2$ receptor subtype shown in line mode as seen from the classic perspective.	129
Figure 48. Steric (left) and electrostatic maps of $\alpha 1\beta 3\gamma 2$ receptor subtype shown in line mode as seen from the classic perspective rotated 90°.....	130
Figure 49. Steric (left) and electrostatic maps of $\alpha 2\beta 3\gamma 2$ receptor subtype shown in transparent mode as seen from the classic perspective.....	130
Figure 50. Steric (left) and electrostatic maps of $\alpha 2\beta 3\gamma 2$ receptor subtype shown in transparent mode as seen from the classic perspective rotated 90°.....	131
Figure 51. Steric (left) and electrostatic maps of $\alpha 2\beta 3\gamma 2$ receptor subtype shown in line mode as seen from the classic perspective.	131

Figure 52. Steric (left) and electrostatic maps of $\alpha 2\beta 3\gamma 2$ receptor subtype shown in line mode as seen from the classic perspective rotated 90°	132
Figure 53. Steric (left) and electrostatic maps of $\alpha 3\beta 3\gamma 2$, receptor subtype shown in transparent mode as seen from the classic perspective.....	132
Figure 54. Steric (left) and electrostatic maps of $\alpha 3\beta 3\gamma 2$, receptor subtype shown in transparent mode as seen from the classic perspective rotated 90°	133
Figure 55. Steric (left) and electrostatic maps of $\alpha 3\beta 3\gamma 2$, receptor subtype shown in line mode as seen from the classic perspective.	133
Figure 56. Steric (left) and electrostatic maps of $\alpha 3\beta 3\gamma 2$ receptor subtype shown in line mode as seen from the classic perspective rotated 90°	134
Figure 57. Steric (left) and electrostatic maps of $\alpha 5\beta 3\gamma 2$ receptor subtype shown in transparent mode as seen from the classic perspective.....	134
Figure 58. Steric (left) and electrostatic maps of $\alpha 5\beta 3\gamma 2$ receptor subtype shown in transparent mode as seen from the classic perspective rotated 90°	135
Figure 59. Steric (left) and electrostatic maps of $\alpha 5\beta 3\gamma 2$ receptor subtype shown in line mode as seen from the classic perspective.	135
Figure 60. Steric (left) and electrostatic maps of $\alpha 5\beta 3\gamma 2$ receptor subtype shown in line mode as seen from the classic perspective rotated 90°	136
Figure 61. Clockwise from the top left, line maps of the $\alpha 1\beta 3\gamma 2$, $\alpha 2\beta 3\gamma 3$, $\alpha 3\beta 3\gamma 2$, and $\alpha 5\beta 3\gamma 2$ CoMFA.....	137
Figure 62. Absolute subunit arrangement of the $\alpha 1\beta 2\gamma 2$ GABA(A) receptor when viewed from the synaptic cleft.....	139

Figure 63. Alignment and homology model depiction of the so called “loops A-F” and flanking regions of the human sequences of the Bz recognition site in different subunits.	140
Figure 64. Ribbon illustration of the GABA(A) BzR binding pocket conceived by Clayton et al. ^{198, 276, 277}	143
Figure 65. Flumazenil	144
Figure 66. Diazepam docking pose in $\alpha 1\gamma 2$. The beta subunit is not in the binding pocket.	145
Figure 67. High resolution image of diazepam docking pose in $\alpha 1\gamma 2$ binding pocket.	146
Figure 68. Orthogonal views of the location of residues with respect to pharmacophore in the $\alpha 1\beta 3\gamma 2$ BzR binding pocket	149
Figure 69. Unified model of the $\alpha 1\gamma 2$ subtype benzodiazepine receptor with diazepam docked in the binding site.	150
Figure 70. Alignments of several Bz BS ligands within the pharmacophore model.	154
Figure 71. Orthogonal views of the homopentameric acetylcholine binding protein crystallized from <i>Lymnaea stagnalis</i> . The subunits have been assigned different colors for clarity	157
Figure 72. Single subunit of acetylcholine binding protein crystallized from <i>Lymnaea stagnalis</i> (side view)	159
Figure 73. Single subunit of acetylcholine binding protein crystallized from <i>Lymnaea stagnalis</i> (top view)	160
Figure 74. The $\alpha 1\beta 3\gamma 2$ subtype receptor with key residues shown	164
Figure 75. The benzodiazepine binding site of the $\alpha 1\beta 3\gamma 2$ receptor	164

Figure 76. The benzodiazepine binding site of the $\alpha 1\beta 3\gamma 2$ receptor rotated 90°	165
Figure 77. The $\alpha 2\beta 3\gamma 2$ subtype receptor with key residues shown	166
Figure 78. The benzodiazepine binding site of the $\alpha 2\beta 3\gamma 2$ receptor	166
Figure 79. The benzodiazepine binding site of the $\alpha 2\beta 3\gamma 2$ receptor rotated 90°	167
Figure 80. The $\alpha 3\beta 3\gamma 2$ subtype receptor with key residues shown	167
Figure 81. The benzodiazepine binding site of the $\alpha 3\beta 3\gamma 2$ receptor within the active site	168
Figure 82. The benzodiazepine binding site of the $\alpha 3\beta 3\gamma 2$ receptor rotated 90°	168
Figure 83. The benzodiazepine binding site of the $\alpha 1\beta 3\gamma 2$ receptor with diazepam in the binding pocket.	169
Figure 84. The benzodiazepine binding site of the $\alpha 1\beta 3\gamma 2$ receptor rotated 90° with diazepam in the binding site	170
Figure 85. The benzodiazepine binding site of the $\alpha 1\beta 3\gamma 2$ receptor rotated 90° (reverse direction) with diazepam in the binding site.....	171
Figure 86. The $\alpha 5\beta 3\gamma 2$ subtype receptor with key residues shown with diazepam in the binding site.....	172
Figure 87. The benzodiazepine binding site of the $\alpha 5\beta 3\gamma 2$ receptor with diazepam in the binding site.....	172
Figure 88. The benzodiazepine binding site of the $\alpha 5\beta 3\gamma 2$ receptor rotated 90° with diazepam in the binding site	173
Figure 89. Flexidock fit of WYS8	174
Figure 90. Setting the autogrid in Autodock for the Bz BS protein	176

Figure 91. WYS8	177
Figure 92. Rotatable bonds are identified along with root atom in ligand WYS8	178
Figure 93. AutoDock result rendering was performed using Tripos Benchware.	178
Figure 94. Alpha 5 selective compounds.....	186
Figure 95. Xli093 aligned in the included volume of the pharmacophore receptor model for the $\alpha 5\beta 3\gamma 2$ subtype	188
Figure 96. Xli093 in cognition enhancement (Wenger unpublished).....	188
Figure 97. The $\alpha 5$ selective agonist DM-I-81	190
Figure 98. Xli356 and RY10 were screened in stably expressed HEK cells.....	195
Figure 99. GABA function in <i>C. elegans</i>	199
Figure 100. Synthesis of 8-substituted imidazobenzodiazepine bivalent ligands	202
Figure 101. Visual and audio qured data for Xli356.....	1
Figure 102. Updates of the $\alpha 5\beta 2\gamma 2$ subtype (solid) overlayed with the previous model (line).....	207
Figure 103. SH053 compounds in the $\alpha 2$ pharmacophore/receptor model.....	209
Figure 104. Concentration-effect curves for SH-053-S-CH3 and SH-053-R-CH3 on $\alpha 1\beta 3\gamma 2$, $\alpha 2\beta 3\gamma 2$, $\alpha 3\beta 3\gamma 2$, and $\alpha 5\beta 3\gamma 2$ GABA(A) receptors. Data points represent means \pm SEM from at least 4 oocytes from ≥ 2 batches.....	210
Figure 105. Alignment of XLi-093 1 (white) and Ro15-1788 20 (cyan) within the included volume of the $\alpha 5\beta 3\gamma 2$ subtype.....	213
Figure 106. Crystal structures of the linear XLi-093 1 (left) and the folded DMH-III-96 19 (right).	1

Figure 107. Alignment of DMH-III-96 within the included volume of the $\alpha 5\beta 3\gamma 2$ subtype. It is apparent that the folded conformation prevented it from binding to this GABA(A) subtype.	215
Figure 108. Subtype efficacy of RY-24.....	218
Figure 109. Suppression of alcohol-motivated responding by RY-24 and RY-23. ¹⁸⁵ ...	220
Figure 110. Comparison of non-selective diazepam (black) with the $\alpha 5$ -selective QH-ii-066 (cyan) when aligned within the unified pharmacophore/ receptor model.	222
Figure 111. <i>In vitro</i> efficacy of PWZ-029 in <i>Xenopus</i> oocytes.....	228
Figure 112. The effects of DMCM (0.2 mg/kg) and PWZ-029 (2, 5 and 10 mg/kg) on retention performance in a passive-avoidance task (*P<0.05 compared to solvent (SOL) group). Number of animals per treatment group: 10.	230
Figure 113. The effects of DMCM (0.2 mg/kg) and PWZ-029 (2, 5 and 10 mg/kg) on acquisition (a) and retention (b) performance in an active-avoidance task (*P<0.05 compared to solvent (SOL) group). Number of animals per treatment group: 8.	232
Figure 114. DMCM (2 mg/kg) and PWZ-029 (5,10 and 20 mg/kg)	234
Figure 115. The effects of DMCM (2 mg/kg) and PWZ-020 (5,10 and 20 mg/kg) on the distance travelled in 5-min intervals in the activity assay. *P<0.05 compared to solvent (SOL) group.....	235
Figure 116. Antagonism of selected ligands (SH = SH-053-).....	237
Figure 117. DMCM and PWZ-029 in open arm experiments	239
Figure 118. Structures and conformations of SH-053-S-CH3 (A1-A3) and SH-053-R-CH3 (B1-B3) in the included volume of the pharmacophore receptor model for the $\alpha 2$ subtype.....	256

Figure 119. Illustrated here are the concentration-effects curves for SH-053-S-CH3 (A) and SH-053-R-CH3 (B) on $\alpha 1\beta 3\gamma 2$, $\alpha 2\beta 3\gamma 2$, $\alpha 3\beta 3\gamma 2$, and $\alpha 5\beta 3\gamma 2$ GABA(A) receptors, using an EC3 GABA concentration. Data points represent means \pm SEM from at least 4 oocytes from ≥ 2 batches.	259
Figure 120. Diazepam (DZP) and SH-053-S-CH3 on closed arm entries and EPM.....	261
Figure 121. Illustrated here are the effects of diazepam (1.25 mg/kg) and SH-053-S-CH3 (10, 20 and 30 mg/kg) on the a) distance travelled on open arms, b) percentage of entries in open arms and c) percentage of time spent on open arms of the EPM. *P<0.05 compared to solvent (SOL) group.	263
Figure 122. Illustrated here are the effects of diazepam (1.25 mg/kg) and SH-053-S-CH3-2'F (10, 20 and 30 mg/kg, designated as S-CH3-2'F) on the a) closed arm entries, b) total arm entries and c) total distance travelled in the EPM. Number of animals per treatment (Figure 120-121, for SOL through SH-053-S-CH3-2'F 30 mg/kg) was 10	265
Figure 123. Illustrated here are the effects of diazepam (1.25 mg/kg) and SH-053-S-CH3-2'F (10, 20 and 30 mg/kg, designated as S-CH3-2'F) on the a) distance travelled on open arms, b) percentage of entries in open arms and c) percentage of time spent on open arms of the EPM.....	267
Figure 124. Whole chamber activity	269
Figure 125. Distance travelled in activity	271
Figure 126. Illustrated here are the concentration-effect curves for diazepam, zolpidem, SH-053-2'N, SH-053-S-CH3-2'F SH-053-R-CH3-2'F and JY-XHe-053 on $\alpha 1\beta 3\gamma 2$ (■), $\alpha 2\beta 3\gamma 2$ (▲), $\alpha 3\beta 3\gamma 2$ (◆), and $\alpha 5\beta 3\gamma 2$ (▼) GABA(A) receptors, using an EC3 GABA	

concentration. Data points represent means \pm SEM from at least four oocytes from ≥ 2 batches.290

Figure 127. Illustrated here are the effects of diazepam (DZP 1.25 and 2.5 mg/kg) and SH-053-2'N 30 mg/kg (left graphs, a1 and b1), JY-XHe-053 (2.5, 5, 10, 20 and 40 mg/kg) (middle graphs, a2 and b2) and DZP 2 mg/kg and SH-053-R-CH3-2'F (10, 20 and 30 mg/kg) (right graphs, a3 and b3) on distance travelled in the central (hatched bars) and peripheral (open bars) zone of the activity chamber during 45 or 30 minute of recording (total activity corresponds to the height of the whole bar) (upper graphs, a1, a2 and a3) as well as on distance travelled in 5-minute intervals (lower graphs, b1, b2 and b3). *,** and ***, $P < 0.05$; 0.01 and 0.001, respectively, compared to solvent (SOL) group in each of three experiments. Numbers of animals per treatment group for consecutive groups on each of panels were 8, 8, 7, 8 (left); 8, 6, 6, 8, 8, 6 (middle) and 7, 5, 7, 8, 8 (right).....292

Figure 128. Illustrated here are the effects of diazepam (DZP 1.25 mg/kg) and SH-053-2'N (10, 20 and 30 mg/kg) on the a) closed arm entries, b) total arm entries and c) total distance travelled in the EPM. * $P < 0.05$ compared to solvent (SOL) group. Number of animals per treatment group (Figure 131- 132, for SOL through SH-053-2'N 30 mg/kg, respectively): 6, 6, 5, 6, 6.....295

Figure 129. Illustrated here are the effects of diazepam (1.25 mg/kg) and SH-053-2'N (10, 20 and 30 mg/kg) on the a) distance travelled on open arms, b) percentage of entries in open arms and c) percentage of time spent on open arms of the EPM. * $P < 0.05$ compared to solvent (SOL) group.297

Figure 130. Illustrated here are the influences of JY-XHe-053 (0; 2.5; 5; 10; 20 and 40 mg/kg) on the a) distance traveled on open arms, b) percentage of entries in open arms

and c) percentage of time spent on open arms of the EPM. Number of animals per treatment group (for SOL through JY-XHe-053 40 mg/kg) was 7.	299
Figure 131. Illustrated here are the effects of a) zolpidem (ZOL 0.5, 1 and 2 mg/kg), b) SH-053-2'N, SH-053-S-CH3-2'F and SH-053-R-CH3-2'F (all dosed at 30 mg/kg) and c) JY-XHe-053 (5; 20 and 40 mg/kg), on latency to platform. *,** and ***, P<0.05; 0.01 and 0.001, respectively, compared to solvent (SOL) group in each of three experiments. In graph a): +, ++, and +++, P<0.05; 0.01 and 0.001, respectively, compared to ZOL 0.5 group; #, P<0.05 compared to ZOL 1.0 group; ^ and ^^, P<0.05 and 0.01, ZOL 1 group compared to ZOL 0.5 group. In graph b): ++, P<0.01 compared to SH-053-S-CH3-2'F (30mg) group. Number of animals per each treatment group was 8 in a) and b), and 7 in c).	301
Figure 132. Scheme representing the virtual division of the water maze used in the analysis of rats' performance	304
Figure 133. Illustrated here are the effects of SH-053-2'N, SH-053-S-CH3-2'F and SH-053-R-CH3-2'F, all dosed at 30 mg/kg, on a) path efficiency during 5-day acquisition sessions and b) number of entries to the zone of previous days' position of platform in the probe trial.....	306
Figure 134. Illustrated here are the effects of b) zolpidem (ZOL 2), c) JY-XHe-053 (30mg), d) SH-053-2'N (30mg), e) SH-053-R-CH3-2'F and f) SH-053-S-CH3-2'F (30mg) (all doses in mg/kg) on the distance rats travelled in the NE quadrant and target region during 5-day acquisition trials in the water maze. The numbers inside the columns are the percent of the distance swam inside the target (NE) quadrant which was travelled in the target region. Control values (SOL) given in a) are taken from the experiment with ZOL. Numbers of animals are as in Figure 128.	308

Figure 135. Crystal structures of Xli-093, DMH-D-053, and DM-III-96.	321
Figure 136. Aromatic region of ¹ H NMR spectra of 19 in CD ₂ Cl ₂ at variable temperatures.....	323
Figure 137. Aromatic region of ¹ H NMR spectra of 6 in CD ₂ Cl ₂ at different temperatures.	324
Figure 138. Aromatic region of ¹ H NMR spectra of 1 in MeOH- <i>d</i> ₄ at different temperatures.....	326
Figure 139. Aromatic region of proton spectra of 19 in MeOH- <i>d</i> ₄ at different temperatures.....	327
Figure 140. Partial HSQC spectrum of 19 in MeOH- <i>d</i> ₄ at 298 K.	328
Figure 141. Bivalent ligand 1 (Xli093) aligned in the included volume of the pharmacophore/receptor model for the α5β3γ2 subtype.	329
Figure 142. The linkers of the bivalent ligands.	330
Figure 143. The conformations for dimethoxymethane.	331
Figure 144. Newman projection for linkers B, C and D.....	333
Figure 145. Diverse training set used to develop pharmacophores (overlap rules), COMSIA for binding to α1βxy2 and α5βxy2 GABA(A) receptor subtypes. S and R refer to the molecular conformation.....	346
Figure 146. Examples illustrating subtle variations in scaffold substitutions that modulate behavioral profiles of each of the selected benzodiazepine ligands	1
Figure 147. Structures of RY23/RY24/ and RY80 along with the electrophysiological characterization of RY24	351
Figure 148. PWZ-029 within the pharmacophore/receptor model for the α5β3γ2 GABA(A) BzR subtype	353

Figure 149. Harris pharmacophore. The inset table displays the distances between the pharmacophore points (1,2 = hydrogen bond acceptor, 3 = hydrophobic terminus, 4 = aliphatic/aromatic centroid with LUMO, 5 = ring system containing hydrogen bond acceptor) identified in benzodiazepines binding to and activating GABA(A) receptor subtypes associated with sedation and memory. In the upper right panel is a graphical depiction of 3D pharmacophore points for compounds having at the sedation and memory endpoints corresponding to the table in the upper left. Lower left and right panels show the overlap of several compounds complying with the sedation and memory pharmacophores, respectively, illustrating some of the commonalities: green spheres represent hydrogen bond acceptors, red spheres represent the polar core ring system, purple ring centroid represents the aromatic ring, LUMO center, blue sphere represents the hydrophobic group at one end of the ligands.....357

Figure 150. Selected structures retrieved from pharmacophore directed searches of the Maybridge Chemical Database with indicated binding affinities (IC_{50} , $[H^3]Ro15-4513$ competition in a cell based binding assay, see Methods Section) to GABA(A) receptors with either the $\alpha1\beta2\gamma2$ or $\alpha5\beta2\gamma2$ stoichiometry.359

Figure 151. COMSIA based on overlap rules and observed binding affinities for BZD training set ligands at $\alpha1\beta2\gamma2$ subunits.362

Figure 152. COMSIA model predictive of compounds binding to the $\alpha5\beta2\gamma2$ GABA(A) receptor isoform.....363

Figure 153. Selected benzodiazepines employed in the fragment QSAR analyses for $\alpha1\beta3\gamma2$ and $\alpha5\beta3\gamma2$ binding.....367

Figure 154. Computed electrostatic potentials (computed using density function theory (B3LYP/6-3G**) evaluated on the van der Waals surfaces of compounds showing selectivity of binding to $\alpha 5\beta 3\gamma 2$ versus $\alpha 1\beta 3\gamma 2$	368
Figure 155. Fragment QSAR for the binding of compounds in figure 145 to $\alpha 5\beta 3\gamma 2$ (left) and $\alpha 1\beta 3\gamma 2$ (right) receptor isoforms, illustrating, via the derived QSAR relations at the bottom of the figures, that the electrostatic contributions (EL min) are more important for ligand binding to the $\alpha 5\beta 3\gamma 2$ receptor isoform than to the $\alpha 1\beta 3\gamma 2$ isoform, as indicated by the larger magnitude of the coefficient of the electrostatic term for the $\alpha 5\beta 3\gamma 2$ isoform compared to that for the $\alpha 1\beta 3\gamma 2$ isoform. SE = standard error.	368
Figure 156. COMSIA analyses (bottom) for the electrophysiological responses ($\ln[E(\alpha 5) + 100]$) of the imidazobenzodiazepines from Figure 153 relative to the $\alpha 5\beta 3\gamma 2$ GABA(A) receptor isoform. The molecular superposition used to perform the COMSIA is shown (above). This COMSIA analyses highlights the importance of steric and hydrophobic features in explaining variations in the electrophysiological response: ($\ln[E(\alpha 5) + 100]$) at $\alpha 5\beta 3\gamma 2$ in that these coefficients (0.3 steric/0.06 hydrophobic) are significantly larger than the electrostatic components (0.1 electrostatic).	373
Figure 157. Fragment QSAR analyses of selected properties of the substituents on the common imidazobenzodiazepine template in Table 39. The coefficients of the terms in the QSAR equations indicate the correlations of the magnitude of the fragment Sterimol L (L1 and L2), HOMO-LUMO (HL1 and HL2), and hydrophobicities (HYD1 and HYD2) of the terminal substituents with the resulting electrophysiological response. The finding of significant QSAR coefficients for the fragment Sterimol L values of the second	

substituents (Table 39) is consistent with the initial notion derived from COMSIA analyses (see A) that ligand length is correlated with electrophysiological response.	374
Figure 158. Overlap of ligands studied by Chambers and coworkers with RY10 (above) and Ro15-4513 (below). Note the spatial correspondence of polar (red O/blue N/yellow S atoms) and hydrophobic (grey C/white H) regions.	379
Figure 159. Fragment QSAR for binding at $\alpha 5\beta 3\gamma 2$ with electrophysiological response ($\ln[E(\alpha 5)+100]=0.73 L1+0.22 L2$ (upper panel) and $\ln[E(\alpha 5)+100]= 0.66 L1 +0.21 HL1 +0.09 L2 + 0.04 HL2$) (lower panel) where HL1 and HL2 are the HOMO-LUMO energy differences for the substituents identified in Table 40.....	1
Figure 160. HOMO-LUMO energy differences between inverse agonists and antagonists.	1
Figure 161. Van der Waal representations of compounds RY80, RY10 and their respective bivalent compounds BiRY80 and BiRY10	383
Figure 162. Pavlovian fear conditioned contextual memory. Each mouse was injected ip with either vehicle (0.9% saline containing 2.5% encapsin), 1.5 mg/kg scopolamine, or 1.5 mg/kg scopolamine + drug (top) 10 mg/kg BiRY80 or (center) 10 mg/kg BiRY10 or (bottom) 10 mg/kg PWZ-029. Twenty minutes after injection mice were fear conditioned to the context and tested 24 hours later, well after the drugs and scopolamine have cleared. A reduction in freezing, as observed in mice that received scopolamine alone, is reflective of a low level of contextual memory. Each drug, tested in the absence of scopolamine, was found not to differ significantly from vehicle administered alone; * $p < 0.05$, data not shown; *** $p < 0.001$. N = 12 male C57BL/6J mice per vehicle or drug. This is an important set of results.	385
Figure 163. 30 mg/kg SH-053-R-CH3 in the absence of scopolamine.	387

Figure 164. BzR ligands binding to other receptors. Data represent mean % inhibition (N = 4 determinations) for compounds tested at receptor subtypes.....	389
Figure 165. Comparison of the structure of 1,3-diazinium bromide to 1,4-benzodiazepines.....	1
Figure 166. Effects of 8a, 8c and 8e on diazepam-induced decreased motor activity in mice.....	1
Figure 167. Effects of 8a, 8c and 8e on diazepam-induced ataxia in mice.	1
Figure 168. Effects on 8a, 8c, and 8e on diazepam-induced loss of righting reflex in mice.	1
Figure 169. Effects of 8a, 8c and 8e on pinna reflex in mice when treated with diazepam.	1
Figure 170. a) Alignment of 1,3-diazepinium chloride 8a within the pharmacophore/receptor model for the $\alpha 1\beta 3\gamma 2$ GABA(A) /BzR subtype; b) Alignment of 8a in the model rotated 90°.	1
Figure 171. a) Alignment of 1,3-diazepinium chloride 8c within the pharmacophore/receptor model for the $\alpha 1\beta 3\gamma 2$ GABA(A) /BzR subtype; b) Alignment of 8c in the model rotated to 90° showing methyl group on ring A sticking out into the extracellular region.	1
Figure 172. 1,3-Diazepinium chloride 8a overlaid with diazepam (yellow) in the pharmacophore/receptor model.	1
Figure 173. The scheme representing the virtual division of the water maze used in the analysis of rats' performance.....	418

Figure 174. The effects of diazepam (Sol+DZP 0.5, 1.5 and 5.0 mg/kg) on total distance (a) and distance travelled in 5-min intervals (b). * p<0.05 compared to solvent (Sol+Sol) group;** p<0.01 compared to solvent. Animals per treatment (n=8).....	421
Figure 175. The effect of combinations of drugs.....	422
Figure 176. Mean distance travelled in successive 5-min blocks for groups	423
Figure 177. Latency to platform data	425
Figure 178. Acquisition trials in the water maze.....	431
Figure 179. Acquisition trials in the Morris water maze	433
Figure 180. Distance data during 5 day acquisition trials in the water maze.	436
Figure 181. Overlay of cyclopropyl analogs of PWZ-029	449
Figure 182. Fluoro analogs of the XHe-II-053	454
Figure 183. Alkyl ether fluoro analogs of XHe-II-053.....	454
Figure 184. Binding data for PWZ-029 and Roche Compound 7.	456
Figure 185. Roche Compound 7 docked in the pharmacophore of the $\alpha 5\beta 3\gamma 2$ receptor subtype.....	457
Figure 186. Proposed analog of PWZ-029	458
Figure 187. Proposed analog of PWZ-029.	459
Figure 188. Proposed amine analog of PWZ-029	460
Figure 189. Control compound SH-I-75.....	465
Figure 190. Reversal of Diazepam-induced memory deficit.....	1
Figure 191. In vivo binding assay of Xli-093	1
Figure 192. $\alpha 5$ GABA(A) occupancy in the brain ⁴¹⁶	469
Figure 193. Oocyte and binding data for PWZ-029 by Sieghart et al. ⁴¹⁶	470
Figure 194. Fear conditioned contextual memory	472

Figure 195. Passive avoidance task ^{64, 542-544}	474
---	-----

LIST OF TABLES

Table 1. Action of benzodiazepines at GABA(A) $\alpha 1-6 \beta 3\gamma 2$ receptor subtypes. ^{33, 34}	7
Table 2. Binding affinity at $\alpha x\beta 2\gamma 2$ GABA(A) receptor subtypes (values are reported in nM)	13
Table 3. Affinities of a Series of Flavonoid Ligands for Benzodiazepine Receptors. ⁶¹	17
Table 4. Affinities of a series of 8-chloropyrazolo[5,1-c][1,2,4]benzotriazine 5-oxide ligands at the Bz BS of GABA(A) receptors. ⁶⁶	20
Table 5. Structures and Affinities at the $\alpha x\beta 3\gamma 2$ Subtype.....	22
Table 6. The Molecular Composition and Stable Conformation of Various Bz BS Bivalent Ligands. ND = not determined yet.....	26
Table 7. Affinities (K_i =nM) of 3,6-disubstituted β -carboline at $\alpha x\beta 3\gamma 2$ (x=1-3,5,6) receptor subtypes. ^a	30
Table 8. Affinities (K_i =nM) of 3,6-disubstituted β -carboline at $\alpha x\beta 3\gamma 2$ (x=1-3,5,6) receptor subtypes. ^a	47
Table 9. Affinities (K_i =nM) of 3-substituted β -carboline at $\alpha x\beta 3\gamma 2$ (x=1-3,5,6) receptor subtypes	50
Table 10. Affinities (K_i =nM) of Ether-substituted β -carboline at $\alpha x\beta 3\gamma 2$ (x=1-3,5,6) Receptor Subtypes	52
Table 11. Affinities (K_i =nM) of chiral 3-substituted β -carboline at $\alpha x\beta 3\gamma 2$ (x=1-3,5,6) receptor subtypes	54
Table 12. Affinities (K_i =nM) of Boc-protected 3-substituted β -carboline at $\alpha x\beta 3\gamma 2$ (x=1-3,5,6) receptor subtypes	55

Table 13. Structures and affinities at $\alpha\beta\gamma_2$ recombinant receptors and modulation by β -carbolines. pAg = weak partial agonist; Ag = agonist ^{19, 186}	58
Table 14. Structures and affinities of some $\alpha_5\beta_3\gamma_2$ subtype selective ligands.	60
Table 15. Structures and affinities of 1,4-benzodiazepines.	67
Table 16. Ligands used for affinity labeling studies. ²⁰²	68
Table 17. Binding affinity at $\alpha\beta\gamma_2$ GABA(A) receptor subtypes (values are reported in nM)	78
Table 18. Ligands with potent affinity for α_1 ; ligands bound with K_i values <20 nm at this subtype	85
Table 19. Ligands with potent affinity for α_2 ; ligands bound with K_i values <20 nm at this subtype	95
Table 20. Ligands with potent affinity for α_3 ; ligands bound with K_i values <20 nm at this subtype	103
Table 21. Ligands with potent affinity for α_4 ; ligands bound with K_i values <20 nm at this subtype	109
Table 22. Ligands with potent affinity for α_5 ; ligands bound with K_i values <20 nm at this subtype	112
Table 23. Ligands with potent affinity for α_6 ; ligands bound with K_i values <20 nm at this subtype	124
Table 24. Structures of ligands and their modulation at the α_1 subtype	151
Table 25. Binding data of selected imidazobenzodiazepines	191
Table 26. Binding data of selected imidazobenzodiazepines	192
Table 27. Full panel receptor binding reported for Xli093 and Xli356.....	204

Table 28. Structures and affinities at the $\alpha\beta\gamma 2$ subtype. ^{19, 213} NR = not reported; ANT = antagonist; IA = inverse agonist; ND = not determined yet. Activity is defined for receptor subtype listed in bold.	211
Table 29. The molecular composition and stable conformation of various Bz BS bivalent ligands. ND = not determined yet.	214
Table 30. Structures and affinities of some $\alpha 5\beta\gamma 2$ -subtype selective ligands.	216
Table 31. Structures and affinities of 1,4-benzodiazepines.	223
Table 32. Table 1. PWZ-029 binding affinity (K_i , nM) at human recombinant GABA(A) receptors containing $\beta 3, \gamma 2$ and named α subunit, stably expressed in mouse fibroblast L(tk-) cells ^a	230
Table 33. Binding affinity at $\alpha\beta\gamma 2$ GABA(A) /BZ site subtypes. Measurements were made in duplicate. K_i values are reported in nM.	288
Table 34. Illustrated here is the significant differences among overall influence (averaged for five days of acquisition) on the Morris water maze learning parameters: latency to find the platform (L), distance swam before finding the platform (D), mean swim speed (S) and path efficiency (E) in the dose-response study of zolpidem (ZOL, mg/kg).	300
Table 35. Parameters of water maze performance with zolpidem.	303
Table 36. Stable conformations of selected compounds.	319
Table 37. Concentration-response data for modulation of control GABA EC_{20} by RY024 in different GABA(A) receptor subtypes	352
Table 38. Normalization coefficients and fractions of the components in the COMSIA analyses for A, a diverse training set of benzodiazepines and B, a homogenous set consisting of imidazobenzodiazepines ^a	363

Table 39. Fragment properties for the imidazobenzodiazepines shown in Figure 153...	372
Table 40. (Above) Structures with binding affinities (top number) and efficacies (bottom number) of compounds studied by Chambers et. al. ⁴⁹⁸⁻⁵⁰¹ (Below) Fragments and selected fragment properties for a series of 6,7-dihydro-2-benzothiophen-4(5H)-ones L, B1, Sterimol and electronic HOMO-LUMO (HLn) parameters used in a fragment QSAR for direct comparison with results for the imidazobenzodiazepines shown in Table 39.	377
Table 41. Affinity of 3-methoxy-6-oxo-7,13-dihydro-6 <i>H</i> -benzofuro[2,3- <i>e</i>]pyrido[1,2- <i>a</i>][1,3]diazepin-12-ium chloride, 8a, for $\alpha\chi\beta\gamma_2$ ($x = 1-6$) BzR isoforms.	1
Table 42. Differences among influence of diazepam on water maze learning	426
Table 43. Performance in water maze	427
Table 44. Differences on influences on water maze learning	439
Table 45. Parameters of water maze performance in the probe trial	440
Table 46. Alpha 5 GABA(A) ergic Subtype Selective Ligands	464
Table 47. In vitro metabolic stability of XHE-II-053(1), XHE-II-043 acid(2), HZ-166(3), SR-II-54(4), HZ-166-TMS(5) using human liver microsomes	844
Table 48. In vitro metabolic stability of HJ-I-40(6), EMJ-I-026(7), JY-XHE-053(8), SH-053-2'F-SCH3(9), SH-053-2'F-RCH3(10) using human microsomes	846
Table 49. In vitro metabolic stability of Midazolam using human liver microsomes	850

ACKNOWLEDGEMENTS

I owe a debt of gratitude to Professor James M. Cook for his guidance, encouragement and patience during the course of my studies. From him, I received an education in much more than organic chemistry. I would like to thank the members of my doctoral committee, Professors Feinberg, Arnold, Peng, Chen, Silvaggi, Schwabacher, Pacheco and Moran, for their assistance, suggestions and instructive discussions during my graduate studies at UW-Milwaukee. I am also very grateful to Dr. Föersterling for his instruction, guidance and the donation of his time for the NMR studies. I greatly appreciate Mr. Bob Ponton for his expertise in glassblowing. I would also like to acknowledge Mr. Frank Laib for mass spectral analysis and CHN analysis. I greatly appreciate Dr. Jeffery R. Deschamps for his assistance in X-ray analysis of benzodiazepine ligands and dimers. I am indebted to my colleagues for providing a stimulating and fun environment in which to learn and grow. I would especially like to thank Dr. Xiaoyan Li, Dr. Jun Ma, Dr. Wenyuan Yin and Dr. Srirama Sarma V. V. Pullela for their help and many inspiring discussions during the initial years of my Ph.D program. I would also like to thank my colleagues Dr. Ojas Namjoshi, Dr. Zhijian Wang, Dr. Ranjit Verma, Dr. Michael Lorenz, Ms. Sundari Rallapalli, Dr. M. Shahjahan Kabir, Dr. Edward Merle Johnson, Dr. Yun Teng, and the rest of Professor Cook's current group for providing a great work environment and for their help and advice. A special thanks must go to Dr. Danni Harris, Dr. Timothy Delorey, Dr. Miroslav Savic, Dr. Galen Wenger, Dr. James Rowlett, and Dr. Werner Sieghart for their collaborative work. I would like to acknowledge the financial, academic and technical support of the Department of Chemistry at UW-Milwaukee, the Graduate School at UW-Milwaukee,

and the NIMH. Finally, I would like to thank my wife Tracey, who has always been fully supportive during my studies.

Introduction

The GABA(A) receptor is the major inhibitory neurotransmitter receptor of the central nervous system (CNS) and the site of action of a variety of pharmacologically and clinically important drugs, such as benzodiazepines, barbiturates, neuroactive steroids, anesthetics and convulsants.¹ It is now clear that these receptors regulate the excitability of the brain, anxiety, muscle tone, circadian rhythms, sleep, vigilance, memory, and learning.¹ There are several disease states associated with the improper functioning of this ion channel, including anxiety, epilepsy,² insomnia,³ depression, bipolar disorder,^{4, 5} and schizophrenia,⁶ as well as mild cognitive impairment and Alzheimer's disease.⁷ The role of GABA(A) receptors in drug and alcohol abuse has also been reported.^{8, 9}

GABA(A) receptors are composed of 5 subunits that form a central chloride channel and can belong to different subunit classes. A total of 19 subunits (6 α , 3 β , 3 γ , 1 δ , 1 ϵ , 1 π , 1 θ , 3 ρ) of the GABA(A) receptor have been cloned and sequenced from the mammalian nervous system.⁸ All these polypeptides possess an approximate molecular mass of ~ 50 kD and are structurally related. Each subunit consists of a large extracellular region, which contains several potential glycosylation sites and a characteristic “cys-loop” formed by a covalent bond between two conserved cysteines. This extracellular region is important in contributing to the agonist GABA(A) and modulatory benzodiazepine binding sites. The protein then traverses the lipid bilayer four times and has a large intracellular loop located between transmembrane regions 3 and 4 (M3 and M4). This intracellular region contains possible phosphorylation sites necessary for regulation of the receptor. The homology within each subunit class is about 60 – 80 %, while the homology between subunit classes is about 30 – 40 %. In Figure 1,

the proposed topology of a single GABA(A) receptor subunit is shown. The pentameric structure of a ligand-gated ion channel is shown in Figure 2.⁹

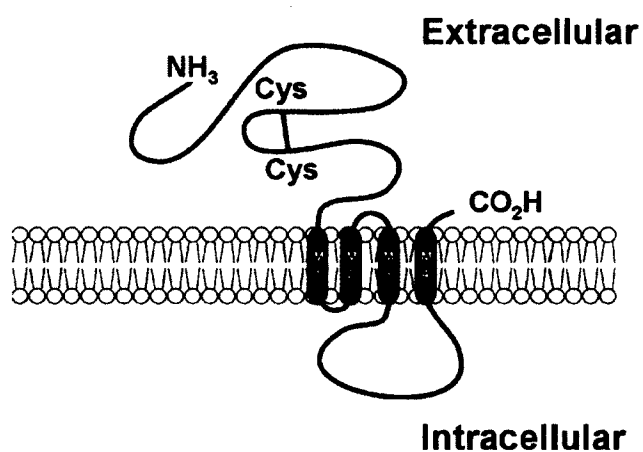


Figure 1. Proposed topology of a GABA(A) receptor subunit. The extracellular domain begins with the N-terminus and M1-M4 represents the four transmembrane domains.¹⁰

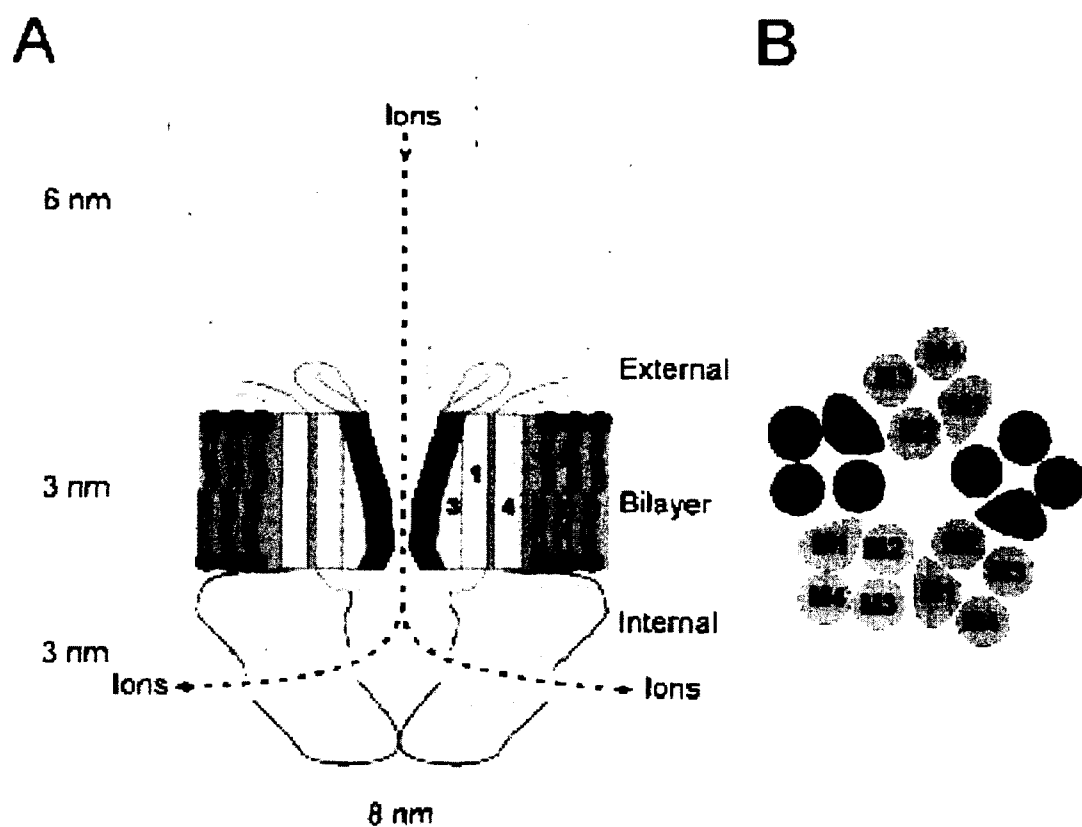


Figure 2. Longitudinal (A) and cross-sectional (B) schematic representations of the ligand-gated ion channel. The numbers 1-4 refer to the M1-M4 segments. The M2 segment contributes to the majority of the pore lining within the membrane lipid bilayer.¹⁰

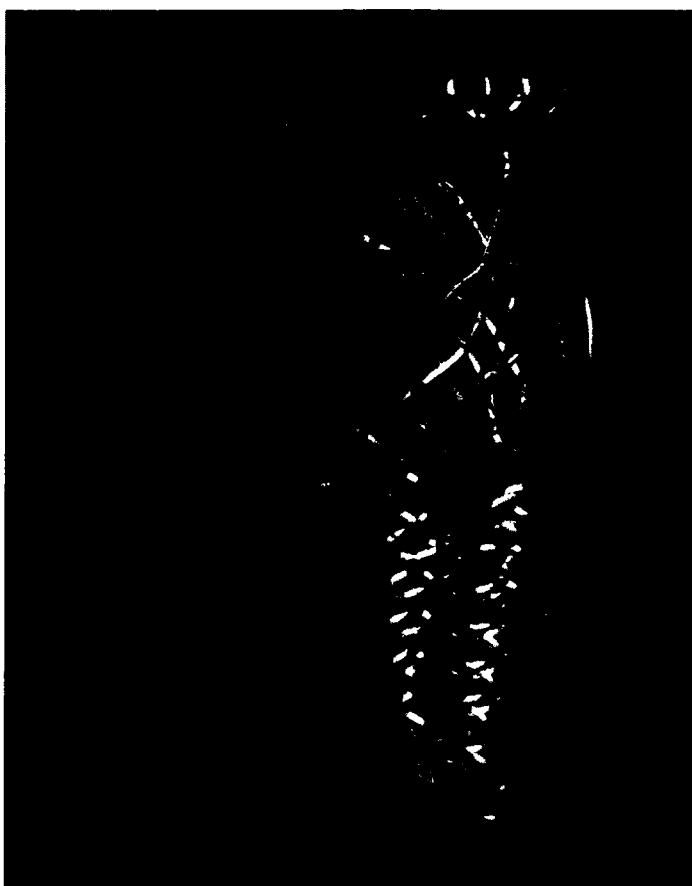


Figure 3. Longitudinal homology model of the human $\alpha 1\beta 2\gamma 2$ ligand gated ion channel¹⁰



Figure 4. Cross-sectional homology model of the human $\alpha 1\beta 2\gamma 2$ ligand gated ion channel¹¹

The GABA(A) ligand gated ion channel (Figures 3 and 4) was constructed in Deep View and rendered here using Tripos Benchware 3D Explorer. The $\alpha 1$ subunits are yellow and magenta, the $\beta 2$ subunits are green and red, while the $\gamma 2$ subunit is blue.¹

The existence of multiple GABA(A) receptor subunits can give rise to a large number of different GABA(A) receptor subtypes.¹²⁻¹⁴ The majority of GABA(A) receptors, however, are composed of 1γ , 2α and 2β subunits. The presence of a γ subunit within a GABA(A) receptor is necessary for the formation of a benzodiazepine binding

site that is located at the interface of an α and γ subunit. Whereas the classical benzodiazepines, such as diazepam or flunitrazepam, exhibit a high affinity for receptors composed of $\alpha 1\beta 2\gamma 2$, $\alpha 2\beta 2\gamma 2$, $\alpha 3\beta 2\gamma 2$ or $\alpha 5\beta 2\gamma 2$ subunits (the diazepam sensitive (DS) receptors), as well as for their less intensively investigated analogues containing the $\gamma 3$ subunit, other benzodiazepine binding site ligands are also able to interact with $\alpha 4\beta 2\gamma 2$ or $\alpha 6\beta 2\gamma 2$ receptors (diazepam insensitive (DI) receptors), or with receptors containing $\gamma 1$ subunits.^{11, 15-17} Receptors containing $\gamma 1$ or $\gamma 3$ subunits exhibit quite a low abundance in the brain^{11, 18-25} and their contribution to the “in vivo” effects of Bz BS ligands currently is unclear.

The concept of receptor multiplicity has been extremely valuable in that different receptor subtypes reside within anatomically distinct regions of the brain and are responsible for different physiological and pathological processes.²⁶ For example, the $\alpha 1\beta 2\gamma 2$ receptor subtype has a prominent role in seizure susceptibility and sedation,²⁷ the $\alpha 2\beta 2\gamma 2$ and possibly the $\alpha 3\beta 2\gamma 2$ subtypes are involved in anxiety, whereas the $\alpha 5\beta 2\gamma 2$ subtype has a prominent role in memory and learning (Table 1).^{28, 29} These distinctions have thus become a motivation for the design of subtype selective ligands in order to elicit a single specific response.³⁰ Differences observed in the action of such drugs may be due to subtype-selective affinity and absolute and/or relative subtype-selective efficacy.^{31, 32} Herein lies the motivation for developing a unified pharmacophoric GABA(A) protein model for each of the GABA(A) benzodiazepine receptor subtypes.

Table 1. Action of benzodiazepines at GABA(A) $\alpha 1$ –6 $\beta 3\gamma 2$ receptor subtypes.^{33, 34}

Subtype	Associated Effect
$\alpha 1$	Sedation, anterograde amnesia, Some anticonvulsant action, ataxia, addiction presumably
$\alpha 2$	Anxiolytic, hypnotic (EEG), some muscle relaxation
$\alpha 3$	Some anxiolytic action, anticonvulsant action at higher dose Maybe some muscle relaxation
$\alpha 4$	Diazepam-insensitive site
$\alpha 5$	Cognition, temporal and spatial memory (Maybe memory component of anxiety)
$\alpha 6$	Diazepam-insensitive site

Agonist binding to the receptor opens an intrinsic chloride ion channel, typically hyperpolarizing the cell membrane or at least opposing depolarization, thereby inhibiting neuronal transmission (Figure 5).

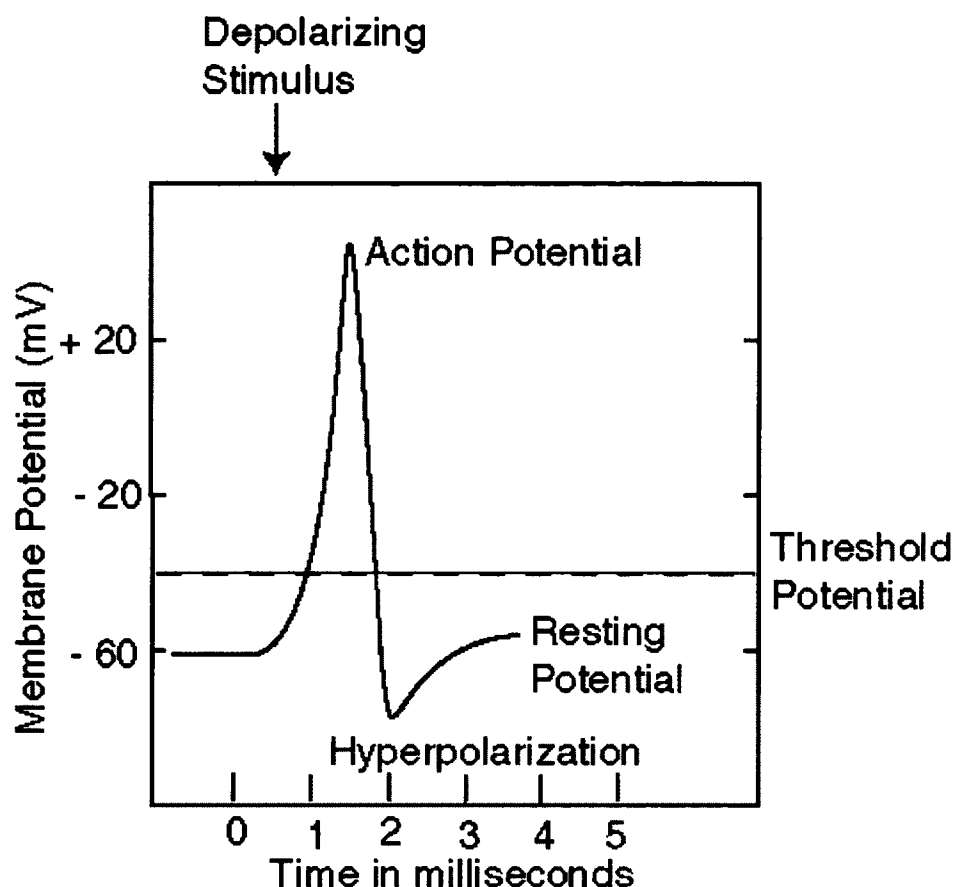


Figure 5. Membrane potential over time during the transmission of a nerve signal. A hyperpolarized state represents a potential further away from the threshold potential.

Benzodiazepine binding site ligands are allosteric modulators. They are unable to induce channel openings themselves, but instead function to vary the frequency, but not the channel opening, times.³⁵⁻³⁷ Positive allosteric modulators at the benzodiazepine binding site (agonists) increase this frequency, while negative allosteric modulators (inverse agonists) decrease the frequency. Currently, it is not clear whether Bz BS ligands allosterically modulate GABA(A) affinity or channel gating. Recent studies^{38, 39} support the view that high-affinity classical benzodiazepines modulate $\alpha 1\beta 2\gamma 2$ GABA(A)

receptors *via* allosteric coupling to channel gating.⁴⁰ Further studies are needed to determine whether the mechanism of modulation varies in different receptor subtypes.

In recent years an initial unified pharmacophore/receptor model for agonists, antagonists and inverse agonists at the Bz BS was developed, using the techniques of chemical synthesis, radioligand binding and receptor mapping.⁴¹ This model did not include a perspective in regard to GABA(A) protein subunits. The overlap of these different modulators within the Bz BS has been supported by experimental data.⁴² Using this ligand-based pharmacophore/receptor model and our new $\alpha 1\beta 2\gamma 2$, $\alpha 2\beta 2\gamma 2$, $\alpha 3\beta 2\gamma 2$, and $\alpha 5\beta 2\gamma 2$ GABA(A) receptor models,⁴³ the experimental data of recent and past years have been evaluated and definite trends with regard to the orientation of the regions of the protein relative to the descriptors of the pharmacophore/receptor model have been identified and are presented here. The need to define such an orientation has already been established,⁴⁴ since it permits inspection of ligand docking studies and the identification of possible roles specific residues may have within the Bz binding site. These roles may then be explored in future studies which involves covalent labeling, site-directed mutagenesis and structure-activity relationships, all of which contribute to the rational design of subtype-specific modulators of the Bz BS of GABA(A) receptors.

Recent Alignment of Non-Classical Bz Binding Site Ligands Support the Unified Pharmacophore/Receptor Model

Besides the major classes of Bz ligands used to define the model, several non-Bz ligands also fit within the pharmacophore/receptor model very well. Examples include zopiclone,**1**, and its active enantiomer, the flavonoid **2** and the 8-chloropyrazolo[5,1-

c][1,2,4]-benzotriazine 5-oxide analog **38**, as illustrated in Figures 6 and 7, as well as Figures 10 and 12.

Zopiclone and its Active Enantiomer (Lunesta®)

Since the sedative-hypnotic zopiclone **1** was first reviewed in *Drugs* in 1986,⁴⁵ a much larger body of clinical data has become available to permit a more detailed comparison of the activity of non-benzodiazepine, zopiclone, with classical benzodiazepines.⁴⁶ Results have shown that, regardless of the duration of action, zopiclone was generally at least as effective as benzodiazepines in the treatment of insomnia, although comparisons between zopiclone and flurazepam have produced inconsistent results. It was observed that zopiclone had a relatively low propensity to elicit residual clinical effects, such as difficulty in waking or reduced morning concentration. While tolerance to the effects of zopiclone was not noticed in short term clinical trials (≥ 4 weeks), the results from longer term studies were conflicting and, therefore, the potential for tolerance during long term administration of zopiclone was unclear. Rebound insomnia to a level above that at baseline can occur after withdrawal of zopiclone. However, on the basis of data from short term studies, this does not appear to be common. Evaluation of prescriptions filled has indicated that zopiclone does not have a high dependence potential, at least in those who are not regular drug abusers/addicts. Zopiclone was well-tolerated in both the elderly and younger patients with insomnia. A bitter after-taste was usually the most common adverse event, but was relatively infrequent at 3.6 % in the largest available post-marketing study. Thus, zopiclone has now been firmly established as an effective and well-tolerated sleep agent.⁴⁶

The structure and alignment of zopiclone within the unified pharmacophore/receptor model is shown in Figure 6. The centroid of the pyridine moiety of zopiclone overlapped with region L_1 of the receptor, while the lone pair of electrons of the carbonyl oxygen (O) atom interacted with H_1 of the receptor to form a hydrogen bond between the ligand and the receptor. A second hydrogen bond was formed between the amide carbonyl oxygen atom lone pair (LP) and H_2 of the receptor protein (Figure 6).

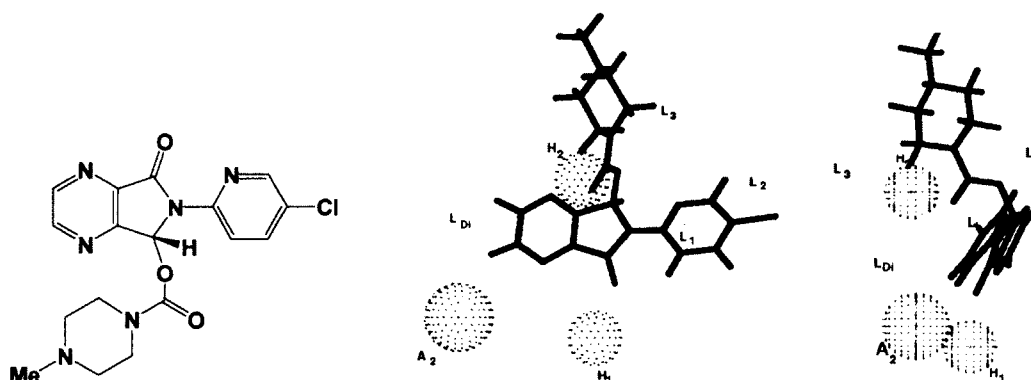


Figure 6. Structure of the sedative-hypnotic zopiclone 1, its alignment within the pharmacophore/receptor model and the model rotated 90°.

However, a recent study by Sepracor⁴⁷ indicated that one of the enantiomers of zopiclone was much more active than zopiclone itself. This may be the result of receptor subtype-selective efficacy or simply a pharmacokinetic effect, but the pharmacophore/receptor model developed here revealed that the active enantiomer fits better into the included volume of the $\alpha 1\beta_{2/3}\gamma 2$ subtype than zopiclone 1 itself (Figure 7). The $\alpha 2$ and $\alpha 3$ subunits are frequently co-expressed with the $\beta 3$ and $\gamma 2$ subunits, which

are particularly evident in hippocampal pyramidal neurons.⁴⁸ This enantiomer (Lunesta) has just been approved by the FDA for treatment of insomnia.

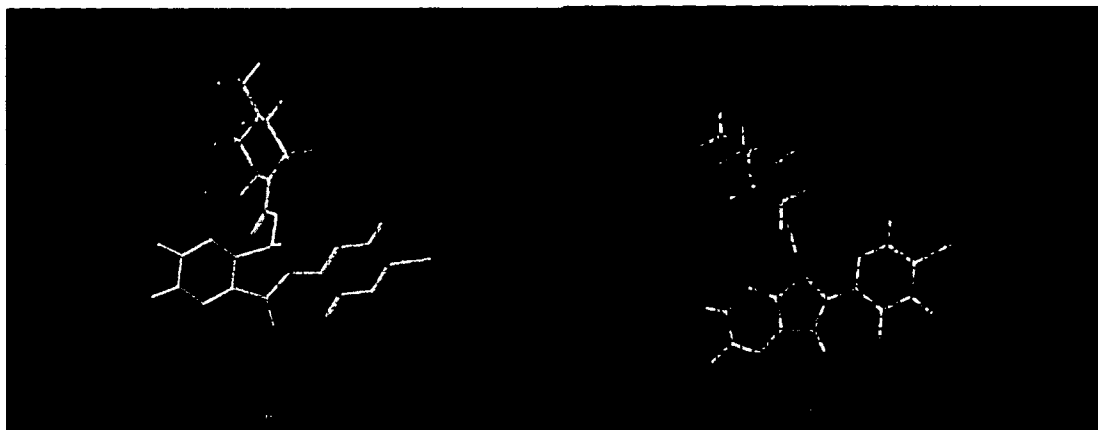


Figure 7. Alignment of zopiclone 1 (left) and its active enantiomer (right) in the included volume of the pharmacophore/receptor model for the $\alpha_1\beta_3\gamma_2$ subtype.

SH-053 Benzodiazepine Enantiomers

Taking into consideration how enantiomers fit into pharmacophores within included volumes, the behavioral activity of three newly-synthesized active Bz enantiomers,^{49, 50} functionally selective for α_2 , α_3 and α_5 -containing subtypes of GABA(A) receptors (SH-053-S-CH3 and SH-053-S-CH3-2'F), or one essentially selective for α_5 subtypes (SH-053-R-CH3) were examined. Motor influence was tested in the elevated plus maze, spontaneous locomotor activity and rotarod test, which are considered primarily predictive of the anxiolytic, sedative and ataxic influence of BZs, respectively. There was substantially diminished ataxic potential of BZ site agonists devoid of α_1 subunit-mediated effects, with preserved anti-anxiety effects at 30 mg/kg of SH-053-S-CH3 and SH-053-S-CH3-2'F. However, all three ligands, dosed at 30 mg/kg, decreased spontaneous locomotor activity, suggesting that sedation may be partly dependent on activity mediated by α_5 -containing GABA(A) receptors.⁵¹ Such an effect

could not have been observed previously, because to date, all apparently non-sedating BZ receptor ligands, which are devoid of activity at $\alpha 1$ -containing GABA(A) receptors, engendered essentially antagonist⁵² or only partial agonist efficacy at $\alpha 5$ -containing GABA(A) receptors.^{49, 50} Therefore, it cannot be ruled out that substantial efficacy at $\alpha 5$ -containing GABA(A) receptors may contribute to sedative effects besides the effects on learning and memory processes.⁴⁶

Table 2. Binding affinity at $\alpha x\beta 2\gamma 2$ GABA(A) receptor subtypes (values are reported in nM)

Compound	$\alpha 1$	$\alpha 2$	$\alpha 3$	$\alpha 4$	$\alpha 5$	$\alpha 6$
SH-053-R-CH3	2026	2377	1183	>5000	949.1	>5000
SH-053-S-CH3	1666	1263	1249	>5000	206.4	>5000
SH-053-2'F-R-CH3	759.1	948.2	768.8	>5000	95.17	>5000
SH-053-2'F-S-CH3	350	141	1237	>5000	19.2	>5000

This effect on locomotor activity is supported by two sets of data which indicate the possibility of substantial motor influence via $\alpha 5$ -GABA(A) receptor modulation: In the spinal cord, somatic and preganglionic motoneurons (lamina IX and lateral cell column) exhibited a moderate to strong staining for the $\alpha 5$ subunit, suggesting a possible influence of receptors containing these subunits in motor behavior.⁵³ In addition, the knock-in mice harboring the $\alpha 5$ subunit insensitive to diazepam are refractory to development of tolerance to the sedative effect of diazepam dosed subchronically. Such a

tolerance development might have been caused by a down regulation of receptors containing $\alpha 5$ subunits in the appropriate brain regions of wild-type mice.⁴² These two sets of evidence indicate that the motor influence of $\alpha 5$ -GABA(A) receptor modulation is not necessarily an indirect consequence of the established effects on learning and memory processes.⁵⁴ Hence, it has been hypothesized^{55, 56} that locomotor activity changes induced by ligands possessing a substantial $\alpha 5$ -efficacy may be, at least in part, caused by modulation at GABA(A) receptors containing the $\alpha 5$ subunit. It therefore could be of importance to avoid substantial agonist potentiation of $\alpha 5$ -subunits by candidate anxiolytic anxiolytics, if clinical sedation is to be avoided. *As a caveat to all studies examining sedation, it should be remembered that a decrease in automatically measured locomotor activity can be due to a variety of causes other than sedation, including the occurrence of stereotypical behavior, motor impairments, or pain.*⁵⁷ To dissect these overlaps in activity and uncertainties, much is expected from required screening of even more subtype selective BZ site ligands in the future.

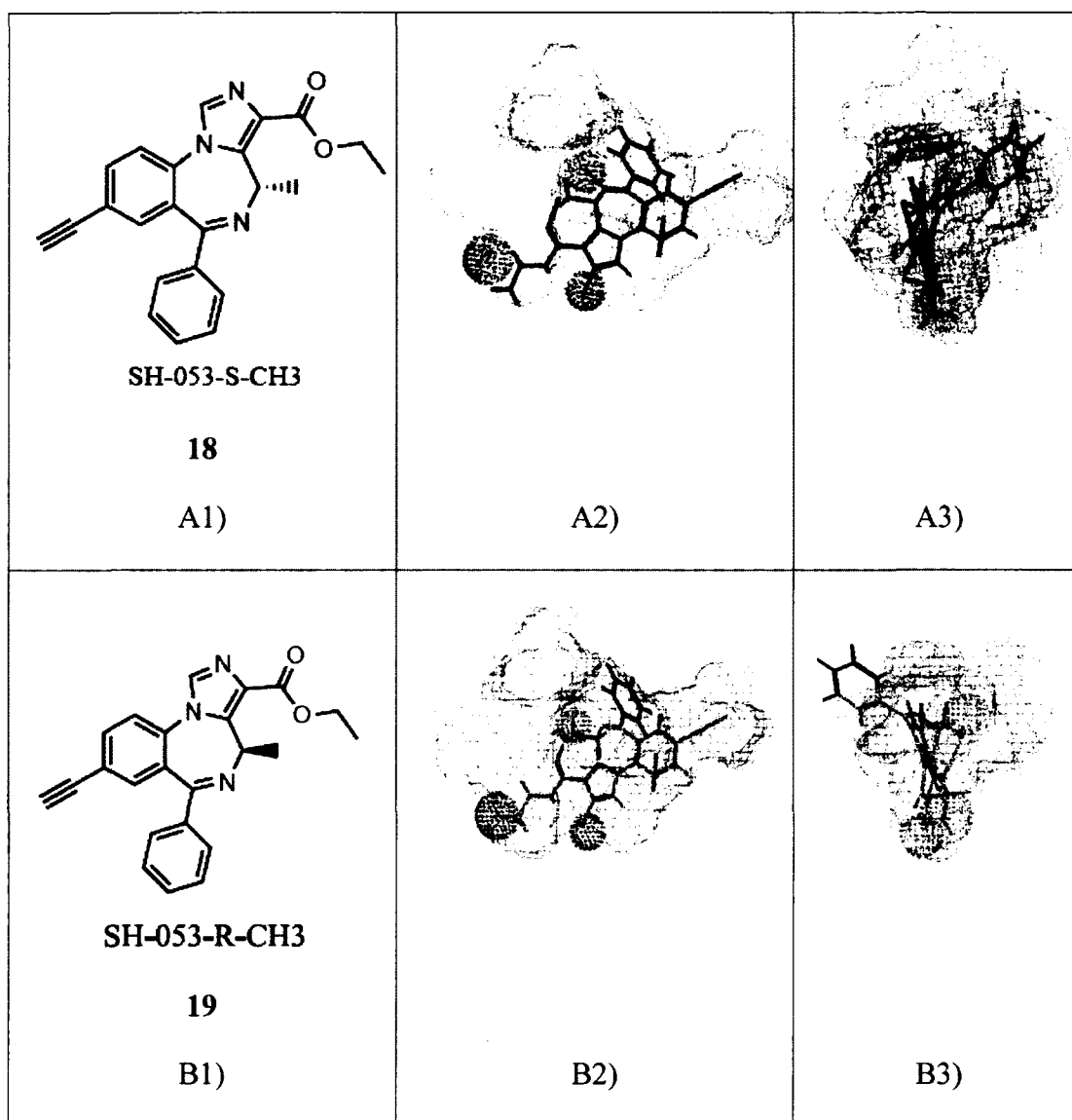


Figure 8. Structures and conformations of SH-053-S-CH₃ (A1-A3) and SH-053-R-CH₃ (B1-B3) in the $\alpha_2\beta_{2\gamma_2}$ subtype included volume. A3 and B3 are the pharmacophore model rotated 90° in a clockwise direction.

The molecular modeling of ligands in the Milwaukee-based pharmacophore was carried out as described by Clayton et al.⁵⁸ SH-053-S-CH₃ fits to the pharmacophore within the included volume of the α_2 subtype (A2). A3 is the A2 image rotated 90° (Figure 8). It can be clearly seen that this conformer fits within the included volume. Below, SH-053-R-CH₃ (see Figure 8B2) is fitted to the pharmacophore in the included

volume of the $\alpha 2$ subtype (B2). B3 is the B2 image rotated 90° . The R-CH₃-function at the prochiral center C(4) changes the conformation of the molecule causing the pendant 6-phenyl group to protrude outside the included volume, consequently this ligand is not efficacious at the $\alpha 2$ subtype (Figure 9). It simply does not interact strongly enough with $\alpha 1\beta 3\gamma 2$, $\alpha 2\beta 3\gamma 2$ or $\alpha 3\beta 3\gamma 2$ receptor subtypes.

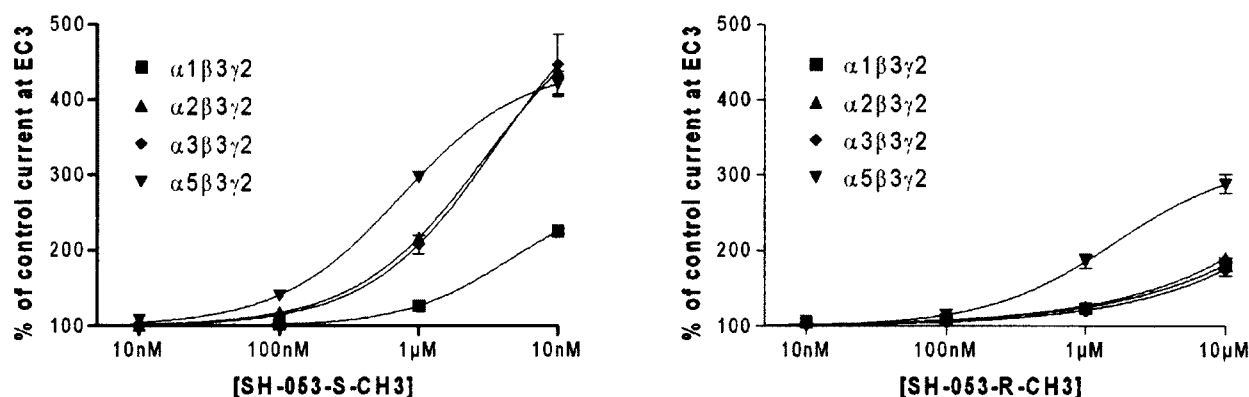


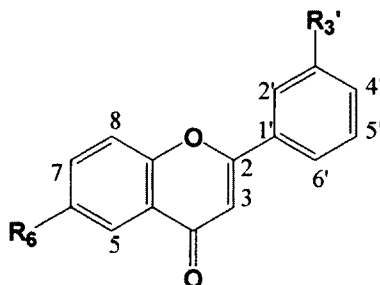
Figure 9. Concentration-effect curves for SH-053-S-CH3 and SH-053-R-CH3 on $\alpha 1\beta 3\gamma 2$, $\alpha 2\beta 3\gamma 2$, $\alpha 3\beta 3\gamma 2$, and $\alpha 5\beta 3\gamma 2$ GABA(A) receptors. Data points represent means \pm SEM from at least 4 oocytes from ≥ 2 batches.⁵⁸

Flavonoids

Flavonoids represent a class of non-Bz ligands that fit extremely well within the unified pharmacophore/receptor model. These compounds are a class of natural products isolated from a variety of herbal plants and have been employed as tranquilizers in folk medicine. They exhibit a wide range of biological activity, such as antiviral, anti-inflammatory, antithrombotic, antioxidant and estrogenic effects.⁵⁹ Flavonoids also display potent anxiolytic effects and appear devoid of myorelaxant, amnesic or sedative actions. Haberlein *et al.* has shown that the steric orientation of the substituents which lie coplanar to the aromatic ring are crucial for ligand affinity to the Bz BS.⁶⁰ This was

especially true for the C(5) and C(6) positions. Furthermore, the recent work of Huang *et al.* indicated that 6,3'-dinitroflavone **2** exhibited a K_i value of 12 nM at the Bz BS (Table 3) and was an extremely potent anxiolytic devoid of muscle relaxant effects. The 6-Br-3'-nitroflavone **4** also demonstrated increased binding affinity, however, the anxiolytic effect was lower than the dinitroanalogue **2**.⁶¹

Table 3. Affinities of a Series of Flavonoid Ligands for Benzodiazepine Receptors.⁶¹



Compound	R ₆	R _{3'}	K _i (nM)
5	F	NO ₂	182
6	Cl	NO ₂	8.0
7	Br	Cl	17.0
8	Cl	Br	23.0
9	Br	Br	19.1
2	NO ₂	NO ₂	12.0
4	Br	NO ₂	1.0

The flavonoids **2**, **4** and **6** fit very well within the unified pharmacophore/receptor model. The alignment of 6,3'-dinitroflavone **2** within the $\alpha 2\beta 3\gamma 2$ subtype is shown in Figure 10. The centroid of the phenyl moiety overlapped with the L₁ region and the 3'-nitro group occupied region L₂, while the lone pair of electrons of the carbonyl oxygen

(O) atom interacted with H₁ to form a hydrogen bond between the ligand and the receptor. A second hydrogen bond was formed between the oxygen lone pair and H₂ of the receptor protein. This alignment essentially agrees with what has been reported by Marder.⁶²



Figure 10. Alignment of 2 within the included volume of the $\alpha 2\beta 3\gamma 2$ subtype.

Recently, some flavone-related analogs were prepared (Figure 11)^{63, 64} by Yu et al. in Milwaukee, however, these flexible ligands with additional lipophilic groups did not bind to any GABA(A) receptor subtype. It is believed that more planar ligands are required for affinity to these subtypes, as the twist chair of the dihydropyran unit prevented the fit required for high affinity binding at the Bz binding site. Together these data, combined with the work of others, indicate the phenyl ring, the carbonyl group and the double bond between C(2) and C(3) of the flavone are the key structural features that contribute to the binding affinity of flavonoids to the Bz binding site. This is in

agreement with the planar or near planar BzR binding site proposed by Hagen in Milwaukee in the 1980's.

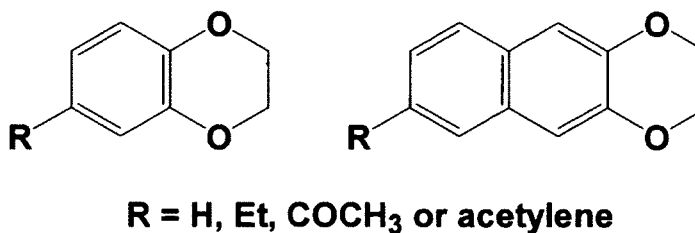


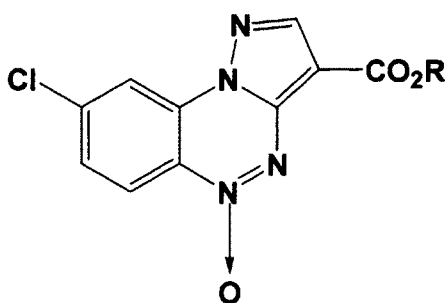
Figure 11. A series of flavone-related analogs that were inactive at the Bz BS.

Analogues of 8-Chloropyrazolo[5,1-c][1,2,4]-benzotriazine 5-oxide (3)

It has been recognized that small structural modifications in the same chemical family can lead to ligands which display different intrinsic activity. Costanzo *et al.* reported that small structural modifications in analogues of 8-chloropyrazolo[5,1-c][1,2,4]-benzotriazine 5-oxide (3) produced ligands that displayed different intrinsic activity (Table 4).⁶⁵ When an aryl ester function occupied position-3, this class of ligands exhibited high affinity at the Bz BS (Table 4, $K_i = 11 - 35$ nM). It was proposed the methoxy group of ligand 3, which bound with an affinity of 1.0 nM, acted as an electron donor group to enhance the π - π stacking interactions between the phenyl ring of this ligand and the imidazole ring of the histidine side chain (H102) in the receptor protein. However, it may also be that the methoxy group enhanced lipophilic interactions within the L₁ region. Costanzo *et al.* proposed that net inductive and resonance effects as well as the electron donating properties ($\sigma = -0.27$) and suitable lipophilic features of the

ligand facilitated this interaction. This has been supported by the current electrostatic maps created by the Milwaukee-based group (see QSAR section).

Table 4. Affinities of a series of 8-chloropyrazolo[5,1-c][1,2,4]benzotriazine 5-oxide ligands at the Bz BS of GABA(A) receptors.⁶⁶



Ligand	R	K _i (nM)
10	Ph	47.5
11	4-F-Ph	146.0
12	2-F-Ph	14.0
13	4-Cl-Ph	49.2
14	2-Cl-Ph	14.4
15	4-Me-Ph	51.9
16	2-Me-Ph	38.3
17	4-NO ₂ -Ph	41.8
18	2-NO ₂ -Ph	106.0
19	4-MeO-Ph	11.6
20	3-MeO-Ph	41.1
3	2-MeO-Ph	1.0

Alignment of N-oxide **3** overlaid with diazepam is shown in Figure 12, wherein the N(1) and N(4) functions hydrogen bond to the H₂ and H₁ donor receptor sites, respectively. It was felt that the 3-ester function fits into a limited dimension lipophilic pocket in the L₁/ L₂ region. Moreover, the orientation of the lone pair of electrons of the

carbonyl oxygen atom of the ester function reinforced the receptor binding by means of a 3-centered hydrogen bond (N(4)/ CO/ H₁). This hydrogen bond, which is similar to that described for the C(3) ester substituent in β -carboline, is also strengthened by the interaction between the 5-oxide group and the nitrogen atom with H₁.

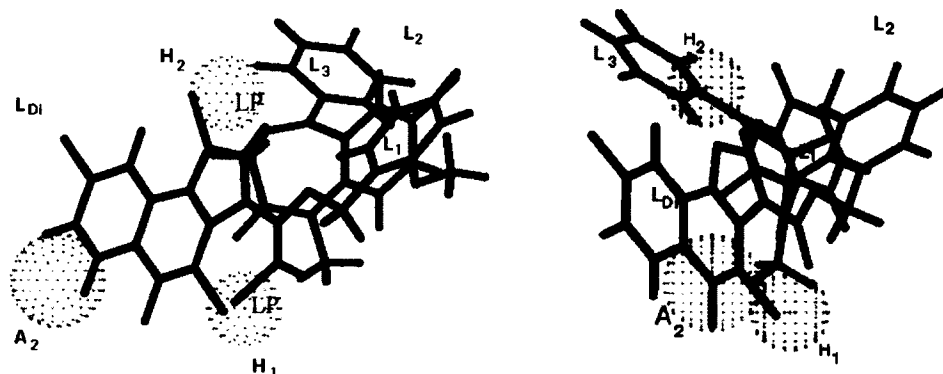
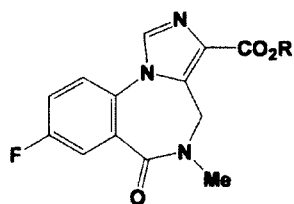
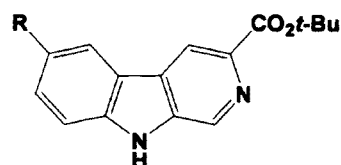
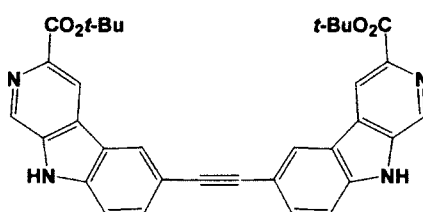
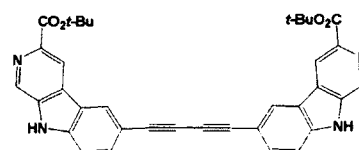
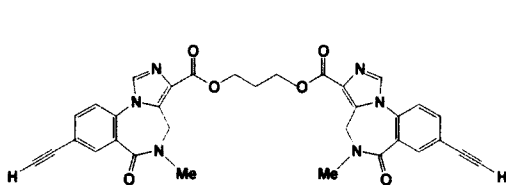
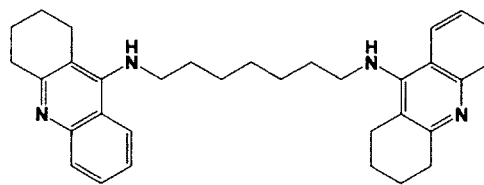
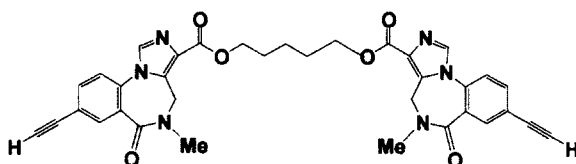
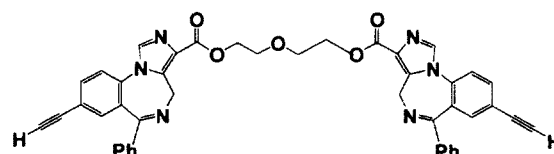


Figure 12. Alignment of N-oxide ligand 3 (black) overlaid with diazepam (cyan) within the unified pharmacophore/receptor model and rotated 90° (right side).

Dimer Affinity for the Binding Site

Some studies which involved monomeric imidazobenzodiazepines (*i*-BZDs) indicated that there may be a limit on the size of the 3'-imidazo substituents the receptor may accommodate.^{64, 66} However, studies that involved bivalent ligands suggested otherwise (Table 5).⁴² It is possible that the spacer for *i*-BZDs dimers threaded the second portion of the bivalent ligand through and/or around the L_{DI}/A₂ region that presented steric hindrance for the monomers. A proposed orientation is illustrated in Figure 13.

Table 5. Structures and Affinities at the $\alpha\beta\gamma 2$ Subtype.Ro15-1788, **21** (R = Et) β -CCT, **22** (R = H)WY-S-8, **23** (R = $\text{---}\equiv\text{---H}$)WY-B-14, **24** (R = $\text{---}\equiv\text{---TMS}$)WY-S-2, **25**WY-S-6, **26**XLi-093, **27**bis(7)-THA, **28**XLi-210, **29**DMH-III-96, **30**

Ligand	K _i (nM) ^a						Activity
	$\alpha 1$	$\alpha 2$	$\alpha 3$	$\alpha 4$	$\alpha 5$	$\alpha 6$	
21 , Ro15-1788	0.8	0.9	1.05	NR	0.6	148	ANT
22 , β -CCT	0.72	15	18.9	NR	110.8	5000	IA
23 , WY-S-8	0.97	111	102	NR	208	1980	ND
24 , WY-B-14	6.8	30	36	2000	108	1000	ND
25 , WY-S-2	30	124	100	300	300	4000	ND
26 , WY-S-6	120	1059	3942	NR	5000	5000	ND
27 , XLi-093	1000	1000	858	1550	15	2000	ANT
28 , bis(7)-THA	NR	NR	NR	NR	NR	NR	ANT
29 , XLi-210	231	661	2666	NR	5.4	54.2	ND
30 , DMH-III-96	460	5000	NR	NR	5000	5000	ND

^aAffinity of compounds at GABA(A) /BzR recombinant subtypes was measured by competition for [³H]flunitrazepam or [³H] Ro15-4513 binding to HEK cell membranes expressing human receptors of composition $\alpha 1\beta 3\gamma 2$, $\alpha 2\beta 3\gamma 2$, $\alpha 3\beta 3\gamma 2$, $\alpha 4\beta 3\gamma 2$, and $\alpha 5\beta 3\gamma 2$ and $\alpha 6\beta 3\gamma 2$.⁶⁴ Data represent the average of at least three determinations with a SEM of $\pm 5\%$.

Design of the bivalent ligand XLi-093 **27** was based on the modeling of the $\alpha 5$ -selective monomer RY-80 **31** in the $\alpha 5$ pharmacophore model. The ability of XLi-093 to bind (Table 5) and fit well within the pharmacophore (Figure 13) required the 3-carbon linker to be in a linear (*versus* folded) conformation. This linear conformation of XLi-093 has been confirmed both in the solid phase (by X-ray) and in solution by NMR spectroscopy (Figure 14).^{64, 66} The *J* values calculated from the dihedral angles (*J* = 5.38) were in excellent agreement with those determined from the solution NMR spectrum (*J* =

6.39). Because this bivalent ligand was the first dimeric $\alpha 5$ -selective ligand reported, the enriched selectivity of this dimer and those similar to it might be entropic in nature since the loss of affinity at the other subtypes was profound.⁶³

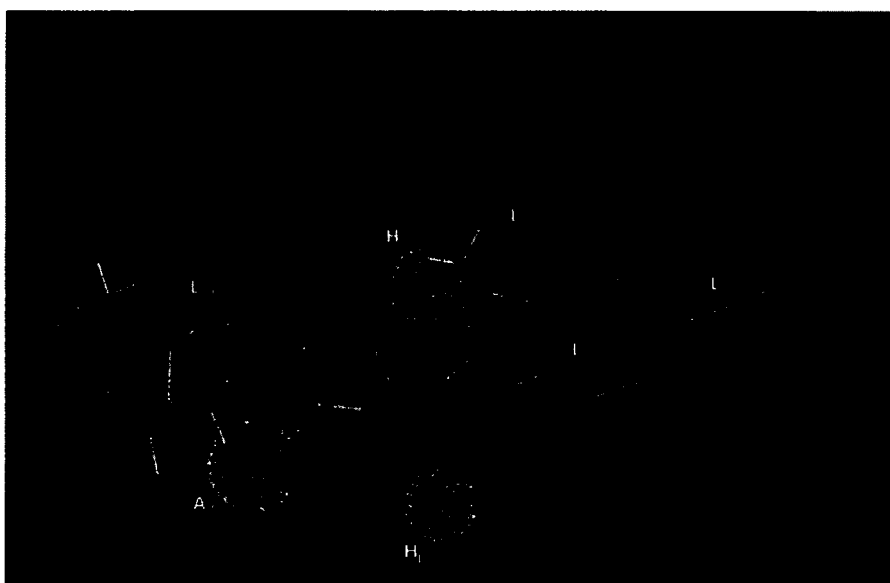


Figure 13. Alignments of XLI-093 27 (white) and Ro15-1788 21 (cyan) within the included volume of the $\alpha 5 \beta 3 \gamma 2$ subtype.⁵⁵

It has been shown *via* crystallographic and solution NMR studies that modification of the aliphatic spacer to a $-\text{CH}_2\text{OCH}_2-$ or a $-(\text{CH}_2)_2\text{O}(\text{CH}_2)_2-$ group, provided the bivalent ligand with a folded conformation (Figure 14).⁶⁷ Modeling of this type of ligand (*e.g.* DMH-III-96 **30**, Figure 15) within the $\alpha 5$ pharmacophore model illustrated the inability of bivalent ligands in the folded conformation to bind, presumably, because they are either too hindered to access the Bz BS or its inability to fit in the included volume binding site space. Current data displaying these trends is shown

in Table 6, while further studies are underway to evaluate the length the lipophilic spacers may contribute toward the selectivity of both the benzodiazepine and β -carboline bivalent ligands (*e.g.* XLi-210, **29** and WY-S-6, **26**). It is clear that the second imidazole unit is protruding into the extracellular domain of the BzR/GABA(A) $\alpha 5$ binding site. This has a profound effect on the ligand design. For it means other homodimers or even heterodimers may bind o BzR/GABA(A)ergic sites.

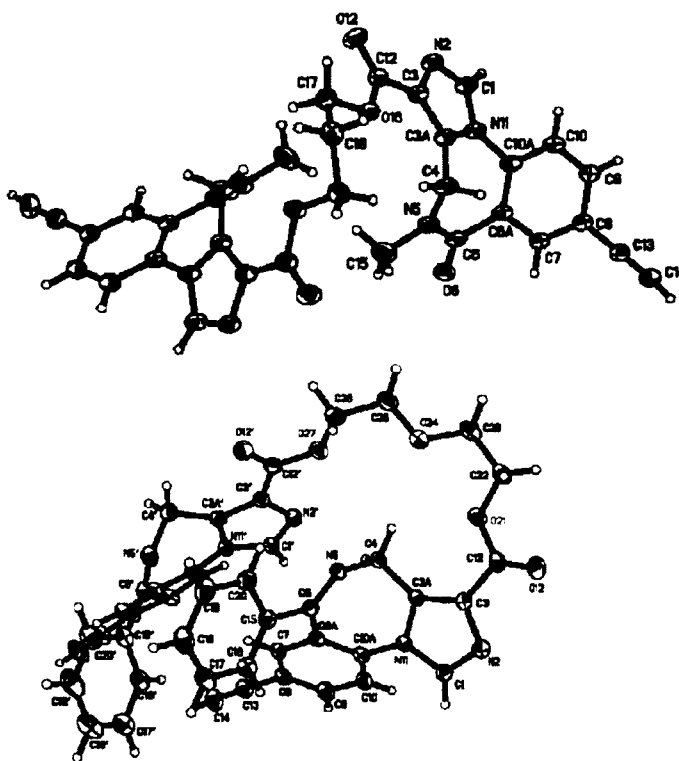
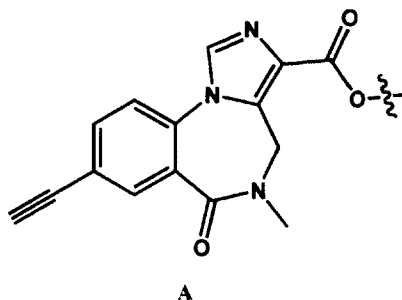


Figure 14. Crystal structures of the linear XLi-093 (**27**, above) and the folded DMH-III-96 (**30**, below).^{33, 68, 69}

Table 6. The Molecular Composition and Stable Conformation of Various Bz BS Bivalent Ligands.
 ND = not determined yet.



Ligand	Monounit 1	Monounit 2	Spacer	Conformation in solution	Crystal structure
27 , XLi-093	A	A	(CH ₂) ₃	linear	linear
29 , XLi -210	A	A	(CH ₂) ₅	linear	ND
46 , XLi -347	A	A	(CH ₂) ₂ O(CH ₂) ₂	folded	ND
47 , XLi-374	A	A	CH ₂ OCH ₂	folded	ND
30 , DMH-III-96	-	-	(CH ₂) ₂ O(CH ₂) ₂	folded	folded

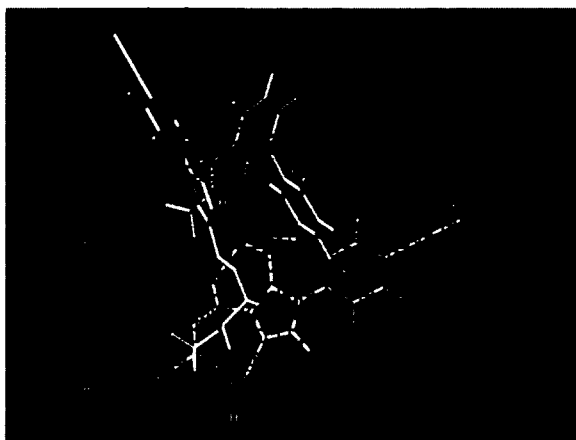


Figure 15. Alignment of DMH-III-96 (30) within the included volume of the $\alpha 5\beta 3\gamma 2$ subtype. It was apparent that the folded conformation prevented it from binding to this GABA(A) subtype.

It is apparent that a folded conformation prevents these types of dimers from binding to this GABA(A) subtype and others as well. This will be discussed further in Part II.

Success of XLi-093 and earlier *in vitro* data on WY-S-8 **23** and WY-B-14 **24** (Table 5) indicated the C(6)-substituent of β -carboline lies in the L_{Di} region of the pharmacophore model or in the extracellular domain of Bz BS. For this reason, the β -CCT dimer, WY-S-2 **25** was designed and synthesized. Although the $\alpha 1$ subtype selectivity was not amplified with this particular β -carboline dimer, the ligand does bind. It was proposed that the two-carbon linker was not long enough and that crowding between the second β -CCT unit and the receptor protein decreased the binding affinity at the $\alpha 1$ subtype, thereby negating potential selectivity.⁷⁰⁻⁷² Further evaluation of the β -CCT bivalent ligand with a bis-acetylene linker (WY-S-6 **26**) was done. Binding data revealed the bis-acetylene linker led to enhanced selectivity but was not as potent as WY-

S-2. It was believed that by increasing the length of the linker, the ligand would have been able to thread itself into the binding site more efficiently (Figure 16).

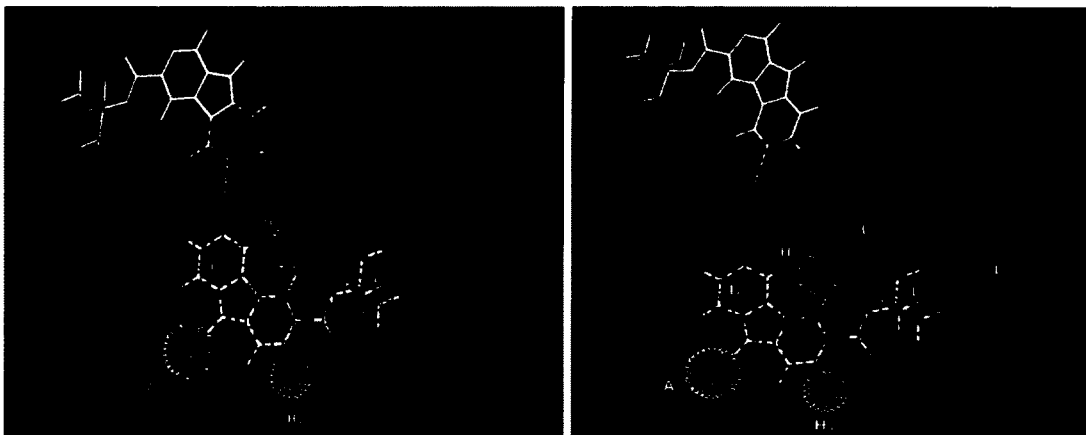


Figure 16. Alignment of WY-S-2 (25, left) and WY-S-6 (26, right) within the included volume of the $\alpha_1\beta_3\gamma_2$ subtype.

Similar to XLi-093, the dimer bis-(7)-THA **28** of Wang *et al.* was found to be a competitive antagonist at the Bz BS in both electrophysiological experiments and receptor binding assays (Table 4).⁶⁰ Although additional experimental data is needed, inspection of the alignment of XLi-093 (Figure 13) and our receptor model (Figure 17) indicated the aliphatic linker of these bivalent ligands would thread the second half of the dimer through the L_{Di}/A_2 regions and toward the solvent accessible space outside of the pocket.

Beta-Carbolines

The crystal structures and molecular mechanics simulations of several β -carbolines has recently been reported.^{33, 73} In general, substitution at C(3) and C(6) had the greatest effect on affinity. Consistent with the interaction with the H₁ descriptor, high affinity ligands were always associated with groups able to interact as hydrogen bond acceptors at C(3). Furthermore, affinity was much lower for constrained β -carbolines which contained the carbonyl group in the *anti* conformation, in agreement with the proposed 3-centered hydrogen bond^{74, 75} afforded by many β -carbolines in the stable *syn* conformation with the H₁ descriptor proposed in Milwaukee years ago.⁶⁵

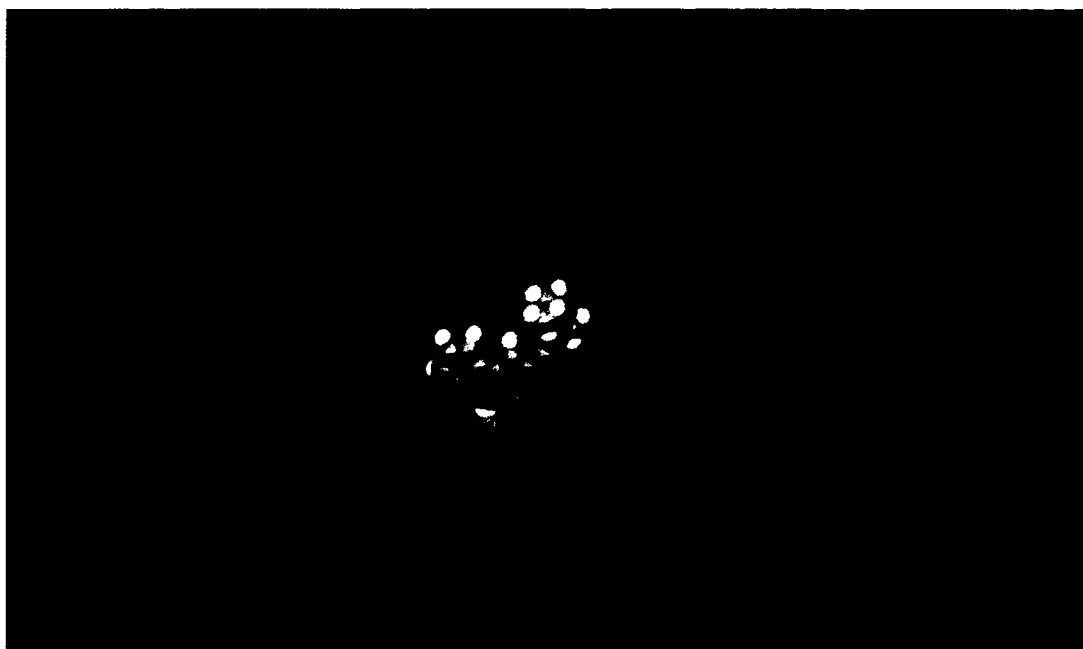
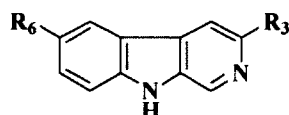
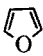
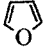
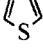
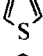
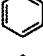



Figure 17. Flexidocking of β CCT to the unified pharmacophore receptor model of the $\alpha_1\gamma_2$ model of the protein subunits

As previously stated, the C(6)-substituent of β -carboline lies in the L_{D1} region of the unified pharmacophore/ receptor model for inverse agonists and antagonists. However, based on the CoMFA studies of Huang *et al.*,⁷⁶ β -carboline agonists have been proposed to take on a vertical alignment with respect to the horizontal alignment of inverse agonists and antagonists. While only four β -carboline have been reported to display agonistic activity, each of these compounds had a 4-methylmethoxy group that permitted interaction with the H_2 descriptor and partial interaction with the region near the entrance to the L_3 pocket (Table 6). It was postulated that 6-PBC **32** should display agonistic activity, and indeed, since partial occupation of a lipophilic region near the C(6)-substituent is probable (relative to ZK-93423 **33**), 6-PBC was a partial agonist.⁴² However, it is likely that the type of activity displayed by 6-PBC may be receptor subtype-dependent, because when evaluated *in vivo*, it inhibited PTZ-induced seizures in a dose-dependent fashion and exhibited anxiolytic activity when evaluated in the elevated plus-maze paradigm. Yet, unlike typical 1,4-benzodiazepines, 6-PBC **32** was devoid of muscle relaxant activity and even antagonized the muscle relaxant/ataxic activity of diazepam.⁷⁷⁻⁷⁹ This is an interesting and unique molecule.

Table 7. Affinities (K_i =nM) of 3,6-disubstituted β -carboline at $\alpha\chi\beta 3\gamma 2$ ($\chi=1-3,5,6$) receptor subtypes.^a



Ligands	R ₆	R ₃	α ₁	α ₂	α ₃	α ₄	α ₅	α ₆
22(βCct)	H	CO ₂ tBu	0.72	15	18.9	1000	111	>5,000
48(βCCE)	H	CO ₂ Et	1.2	4.9	5.7	ND	26.8	2,700
37(3-PBC)	H	OnPr	5.3	52.3	68.8	1000	591	>1,000
49(WYB14)	TMS—≡	CO ₂ tBu	6.8	30	36	2000	108	1000
50(WY-B-25)	TMS—≡	CO ₂ CH ₂ CF ₃	17	59	88	200	1444	>3000
51(WY-B-99-1)	TMS—≡	CO ₂ Et	4.4	4.5	5.58	2000	47	2000
23(WYS8)	H—≡	CO ₂ tBu	0.972	111	102	2000	1473	1980
52(WY-B-26-2)	H—≡	CO ₂ CH ₂ CF ₃	4.5	44.6	42.7	2000	124	2000
53(iodo-βCct)	I	CO ₂ tBu	14.4	44.9	123	>4000	65.3	>4000
54(WY-B-20)	I	CO ₂ CH ₂ CF ₃	12	39	47	2000	122	3000
55(iodo-βCCE)	I	CO ₂ Et	4.8	31	34	1000	286	1000
56(WY-B-08)	I	CO ₂ CH(CF ₃) ₂	78	301	131	3000	681	3000
57(WYS13)		CO ₂ tBu	2.4	13	27.5	NA	163	5000
58(WYB27-1)		CO ₂ CH ₂ CF ₃	26	143	117	3000	127	2000
59(WYS12)		CO ₂ tBu	37	166	314	NA	2861	5000
60(WYB27-2)		CO ₂ CH ₂ CF ₃	9.2	13	72	2000	449	2000
61(WYS15)		CO ₂ tBu	3.63	2.02	44.3	NA	76.5	5000
62(WYB29-2)		CO ₂ CH ₂ CF ₃	25	137	125	2000	299	2000
CMA57	F	COC ₃ H ₇	3.7	27	40	NA	254	>2500
CM-A-82a	C(CH ₃) ₃	CO ₂ tBu	2.78	8.93	24.5	1000	7.49	1000
CM-A-87	F	CO ₂ tBu	1.62	4.54	14.7	1000	4.61	1000
25(WYS2)	Bcct—≡—Bcct		30	124	100	>300	>300	>4000
26(WYS6)	Bcct—≡—≡—Bcct		120	1059	3942	5000	5000	5000

^aAffinity of compounds at GABA(A) /BzR recombinant subtypes was measured by competition for [³H]flunitrazepam or [³H] Ro-15-4513 binding to HEK cell membranes expressing human receptors of composition α1β3γ3, α2β3γ2, α3β3γ2, α4β3γ2, α5β3γ2 and α6β3γ2.⁸⁰ Data represent the average of at least three determinations with a SEM of ±5%.

A series of 3,6-disubstituted β -carbolines was synthesized and evaluated for their *in vitro* affinities at $\alpha_x\beta_3\gamma_2$ GABA(A) /benzodiazepine receptor subtypes by radioligand binding assays in search of α_1 subtype selective ligands. A potential therapeutic application of such analogs is to treat alcohol abuse. Analogues of β -carboline-3-carboxylate-*t*-butyl ester (β CCt, **22**) were synthesized *via* a CDI-mediated process by Yin et al.⁸¹ and the related 6-substituted β -carboline-3-carboxylates **36** including WYS8 (**23**) were synthesized *via* a Sonogashira or Stille coupling process from 6-iodo β CCt (**35**). The bivalent ligands of β CCt (**25** and **26**) were also designed and prepared *via* a palladium-catalyzed homocoupling process to expand the structure-activity relationships (SAR) to larger ligands. Based on the pharmacophore/receptor model, a preliminary SAR study on 34 analogues illustrated that large substituents at position -6 of the β -carbolines were well tolerated.⁸²⁻⁸⁵ As expected, these groups are proposed to project into the extracellular domain (L_{Di} region) of GABA(A) /Bz receptors (see **25** and **26**). Moreover, substituents located at position -3 of the β -carboline nucleus exhibited a conserved stereo interaction in lipophilic pocket L_1 , while N(2) presumably underwent a hydrogen bonding interaction with H_1 . Three novel β -carboline ligands (β CCt, 3PBC and WYS8), which preferentially bound to α_1 BzR subtypes, permitted a comparison of the pharmacological efficacies with a range of classical BzR antagonists (flumazenil, ZK93426) from several different structural groups and indicated these β -carbolines were “near GABA neutral antagonists”. Based on the SAR, the most potent (*in vitro*) α_1 selective ligand was the 6-substituted acetylenyl β CCt (WYS8, **23**). Earlier both β CCt and 3PBC had been shown to reduce alcohol self-administration in alcohol

preferring (P) and high alcohol drinking (HAD) rats but had little or no effect on sucrose self-administration.⁸⁶⁻⁸⁸ 3PBC was also active in baboons (Weerts et al. unpublished results in a poster at a CPDD meeting, manuscript in preparation).^{84, 89}

Application of β -Carbolines to Treat Alcohol Addiction

Alcohol addiction and dependence remain significant public health concerns, impacting physical and mental well-being, family structure and occupational stability.⁹⁰⁻⁹⁵ While advances have been made in the development of novel therapies to treat alcoholism,^{96, 97} alcohol-dependent individuals represent a heterogeneous group,^{79, 98-101} and it is unlikely that a single pharmacological treatment will be effective for all alcoholics. Hence, a better understanding of the neuromechanisms which regulate alcohol seeking behaviors and the design of clinically safe and effective drugs that reduce alcohol addiction and dependence remain a high priority.¹⁰²⁻¹⁰⁴ While the precise neuromechanisms regulating alcohol-seeking behaviors remain unknown, there is now compelling evidence that the GABA(A) receptors within the striatopallidal and extended amygdala system are involved in the "acute" reinforcing actions of alcohol.¹⁰⁵⁻¹⁰⁷ Among the potential GABA(A) receptor isoforms within the VP regulating alcohol-seeking behaviors, GABA receptors containing the α_1 receptor subtype (GABA α_1) appear preeminent. Thus, Criswell and colleagues observed that acute alcohol administration selectively enhanced the effects of iontophoretically applied GABA in the ventral pallidum (VP).⁹⁰ However, no effects were seen in the septum, ventral tegmental area (VTA), and CA1 hippocampus. These data suggest the α_1 Bz/Gaba(A)ergic receptor plays an important role in alcohol-motivated behaviors. Research on the neuroanatomical basis of alcohol reward has shown that the NACC, VTA, VP, central amygdala (CeA),

and hippocampus are all involved in GABAergic regulation of ethanol (EtOH) reinforcement.^{108, 109} Other investigators have identified a dense reciprocal projection from the VP to the NACC,¹¹⁰⁻¹¹² and many of these have been found to be GABAergic neurons.^{105, 113-116} The NACC is now well established as a substrate that regulates the reinforcing properties of abused drugs.^{86, 92, 117, 118} Finally, immunohistochemical¹⁰⁸⁻¹¹² and in situ hybridization studies⁷⁹ have demonstrated that the VP contains one of the highest concentrations of mRNA encoding the $\alpha 1$ subunit in the CNS. These findings, together with pharmacological studies suggest the VP plays a major role in reward-mediated behaviors of psychostimulants and opiates.^{99, 100, 119, 120} This suggests a possible role of the VP- $\alpha 1$ receptors in the euphoric properties of alcohol. Findings of previous studies concluded that inhibition of VP- $\alpha 1$ receptors by the $\alpha 1$ preferring antagonist 3-PBC produced marked reductions on alcohol-maintained responding.^{108, 111} The $\alpha 1$ -mediated suppression at the VP level by 3-PBC showed a high degree of neuroanatomical specificity. Specifically, the $\alpha 1$ -mediated suppression was not observed with the more dorsal placements in the NACC or caudate putamen. The failure of 3-PBC to alter alcohol self-administration in the NACC/striatum is in agreement with previous research which has consistently reported a lack of expression of the $\alpha 1$ transcript in the NACC and caudate.¹⁰⁹⁻¹¹²

An understanding of the neuromechanisms that regulate alcohol drinking is key in the development of drugs to treat alcohol addiction and dependence in humans.^{96, 97} In recent years, much evidence has accumulated in favor of the GABA system;⁷⁹ however, much remains unknown about the role of specific GABA(A) receptor subtypes in regulating ethanol reinforcement. This is due to both a lack of high-affinity and selective

ligands capable of discriminating among the GABA(A) receptor subunits and the heterogeneity of various subunits within the known alcohol reward circuitry.^{73, 121} Of the potential GABA(A) receptors involved in the reinforcing properties of alcohol, evidence suggests the $\alpha 1$ subtype within the VP may play an important role in regulating alcohol-seeking behaviors, as mentioned above. The VP contains one of the highest distributions of $\alpha 1$ subunits in the mesolimbic system.^{73, 122, 123} Acute ethanol administration has been reported to selectively enhance the effects of iontophoretically applied GABA in the VP. These effects correlate highly with [³H] zolpidem binding (an $\alpha 1$ -subtype selective agonist).¹²³⁻¹²⁶

To evaluate the role of the $\alpha 1$ receptor in regulating alcohol reinforcement, 3-propoxy- β -carboline hydrochloride (3-PBC), a mixed benzodiazepine (BDZ) agonist-antagonist with binding selectivity at the $\alpha 1$ receptor was developed.^{108, 109, 111, 127} Compared with the prototypical BDZ agonist zolpidem, 3-PBC exhibited a slightly higher binding selectivity for the $\alpha 1$ receptor.^{79, 124, 128} Preliminary behavioral studies in several species (e.g., rats, mice, and primates) show that 3-PBC is a BDZ antagonist, exhibiting competitive binding-site interactions with BDZ agonists at low to moderate doses (2.5-15 mg/kg).^{73, 124, 129-133} At higher doses (15-60 mg/kg), 3-PBC produces anxiolytic effects in the plus maze that are comparable with those of chlordiazepoxide in alcohol preferring (P) rats.¹²⁴ Thus given the proposed subunit composition of the GABA(A) receptors within the CeA,¹³¹ pharmacological compounds capable of exploiting the $\alpha 1$, $\alpha 2$, and $\alpha 3$ subunit-containing GABA(A) receptors represent optimal tools to evaluate the role of

GABA(A) receptors in alcohol reinforcement and better understand neurobehavior and ethanol responding.

The β -carboline-3-carboxylate-t-butyl ester (β CCt) is a mixed benzodiazepine agonist- antagonist ligand with binding selectivity at α 1 receptors;^{79, 134} β CCt also exhibits some affinity (albeit weaker) for both α 2 and α 3 receptors. Behavioural studies in several species (eg, rats, mice, primates) has shown that β CCt is a BDZ antagonist exhibiting competitive binding site interactions with BDZ agonists over a broad range of doses.^{79, 134} Other studies show that β CCt produced anxiolytic effects in P rodents^{19, 64, 128, 135} and potentiates the anticonflict response induced by α 1 subtype agonists in primates.^{68, 136-142} Thus, β CCt displays a weak agonist-antagonist profile depending on the behavioral task, species, and dose employed.

In studies involving the α 1 subtype, β CCt and 3-PBC were observed to selectively reduce alcohol-motivated behaviors in a variety of experiments.^{68, 73, 133, 137, 138, 143-147} However, unlike the α 5 selective inverse agonist RY-23, both the β -carboline antagonists β CCt and 3-PBC displayed mixed weak agonist-antagonist profiles *in vivo* in alcohol P and HAD rats. Therefore, in addition to being able to study the molecular basis of alcohol reinforcement, α 1 Bz β -carboline ligands which display mixed agonist-antagonist pharmacology in alcohol P and HAD rats may be capable of reducing alcohol intake while eliminating or greatly reducing the anxiety associated with habitual alcohol, abstinence or detoxification. Thus, these types of ligands may be ideal clinical agents for the treatment of alcohol dependent individuals.¹⁴⁸⁻¹⁵³

Consequently, several series of structurally different compounds have been synthesized which possess some α_1 subtype selectivity.¹²⁸ The discovery of high affinity, saturable, and stereospecific ligands for the BzR has been coupled with the demonstration that β -carbolines exhibited an affinity for the BzR.^{148, 154} Some of these agents act on the BzR to induce effects that are functionally opposite (inverse agonists/antagonists) to those of classical BDZs. Consequently, the affinities of a wide variety of β -carbolines have been reported on synaptosomal membranes from this laboratory,^{78, 79} as well as the laboratories of others,^{78, 79} and this prompted a study of the binding affinities of a series of β -carbolines^{48, 73, 155} at 5 recombinant GABA(A) /BzR subtypes ($\alpha_1\beta_3\gamma_2$, $\alpha_2\beta_3\gamma_2$, $\alpha_3\beta_3\gamma_2$, $\alpha_5\beta_3\gamma_2$ and $\alpha_6\beta_3\gamma_2$) expressed from recombinant human cell lines.¹²⁹ In general, this series of β -carboline ligands exhibited some selectivity at α_1 receptor subtypes including β CCt (**22**) and 3-PBC (**70**).⁷⁸ These two ligands displayed a 20-fold and 10-fold selectivity, respectively, for the α_1 subtype over the α_2 and α_3 receptors, as well as over 150-fold selectivity for the α_1 site over the α_5 subtype.^{78, 79, 96, 97, 112} β CCt (**22**) was more selective at the α_1 subtype *in vitro* than the classical α_1 selective agonists zolpidem (**77**) and CL 218872 (**78**).^{156, 157} A number of *in vitro* and *in vivo* studies employing α_1 (e.g., zolpidem, CL 218872,¹²¹ β CCt, and 3-PBC⁷¹) selective ligands suggest the α_1 -containing GABA(A) /Bz receptors of the ventral pallidum (VP) play an important role in regulating alcohol's neurobehavioral effects; particularly alcohol's reinforcing properties as mentioned above.¹²¹

Structure Activity Relationships of β -Carbolines

A predictive 3-D QSAR pharmacophore/receptor model for inverse agonist/antagonist β -carbolines was initially developed *via* Comparative Molecular Field Analysis (CoMFA) and later refined.¹⁵⁸⁻¹⁶¹ Affinities of ligands from 15 different structural classes have been evaluated.¹⁵⁸ Based on this CoMFA study of a series of β -carbolines, Huang *et al.* reported that β -carbolines bind to all diazepam sensitive (DS) sites of the BzR with some selectivity at the $\alpha 1$ containing receptor isoform and this was confirmed by *in vitro* binding affinity of these ligands.¹⁵⁸ A lipophilic region (L_{Di}) of the pharmacophore receptor model appears to be larger in the $\alpha 1$, $\alpha 2$ and $\alpha 3$ -containing receptor isoforms and important for $\alpha 1$ subtype selectivity.¹⁶² More recently, during the design and synthesis of β CCt-related bivalent ligands,¹³⁵ it was found that a series of 3,6-disubstituted β -carbolines (see Figure 18), including 6-iodo- β CCt (**53**) and 6-trimethylsilanyl-ethynyl- β CCt (**49**) possessed $\alpha 1$ subtype selectivity.^{78, 79}

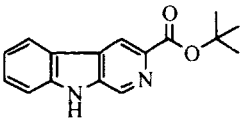
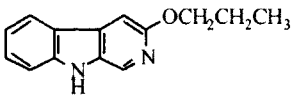
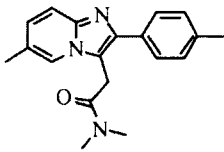
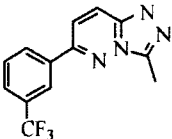
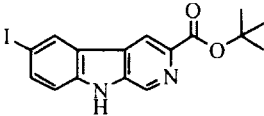
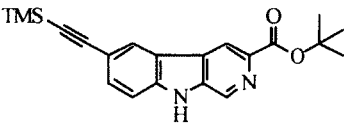
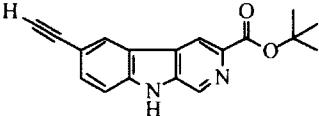
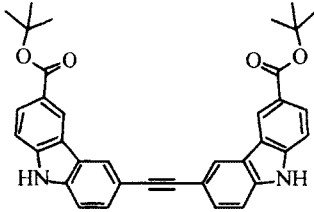
																	
22 β CCt						37 3PBC						7 zolpidem					
α_1	α_2	α_3	α_5	α_6		α_1	α_2	α_3	α_5	α_6		α_1	α_2	α_3	α_5	α_6	
0.72	15	18.9	110.8	>5,000		5.3	52.3	68.8	591	>1000		26.7	156	383	>10,000	>10,000	
																	
78 CL 218872						53 6- iodo- β CCt						49 6-trimethylsilanylethynyl- β CCt					
α_1	α_2	α_3	α_5	α_6		α_1	α_2	α_3	α_5	α_6		α_1	α_2	α_3	α_5	α_6	
57	1964	1161	561	>10,000		14.4	44.9	123	65.3	>4000		6.8	30	36	108	1000	
																	
23 WYS8 (6-ethynyl- β CCt)						25 β CCt bivalent ligand											
α_1	α_2	α_3	α_5	α_6		α_1	α_2	α_3	α_5	α_6							
0.972	111	102	1473	1980		30	124	100	>300	>4000							

Figure 18. In vitro binding affinities of a series of α_1 selective BzR ligands (K_i in nM).

The rigidly linked linear bivalent ligands of β CCt at position “6” did bind to BzR receptors with some α_1 subtype selectivity and may provide the desired α_1 selectivity through specific occupation of the L_{Di} region of the pharmacophore/receptor model.^{79, 126} Although the two 3,6-disubstituted- β -carboline **35** and **36** are less potent than β CCt (**22**), the potent binding affinities observed for **35** and **36** at the α_1 subtype has stimulated the synthesis of the β CCt analogs: 3-substituted- β -carboline as well as 3,6-disubstituted- β -carboline.

On the other hand, these studies also indicated that the selectivity of GABA(A)/BzR site ligands could be described in relation to binding and pharmacological efficacy *in vitro*. This efficacy was based on the capacity of a ligand to modulate GABAergic function.¹⁶³ BzR ligands act to modulate chloride flux over a continuum ranging from positive to negative modulation, with neutral antagonists acting theoretically, at a point on the continuum, with zero intrinsic efficacy (e.g. they bind to the receptor but exhibit no activity).¹⁶³ Consequently, the pharmacological profiles of β CCt and 3-PBC at recombinant $\alpha 1\beta 3\gamma 2$, $\alpha 2\beta 3\gamma 2$, $\alpha 3\beta 3\gamma 2$, $\alpha 4\beta 3\gamma 2$, $\alpha 5\beta 3\gamma 2$ and $\alpha 6\beta 3\gamma 2$ receptor subtypes expressed in *Xenopus oocytes* were investigated.^{78, 128, 163}

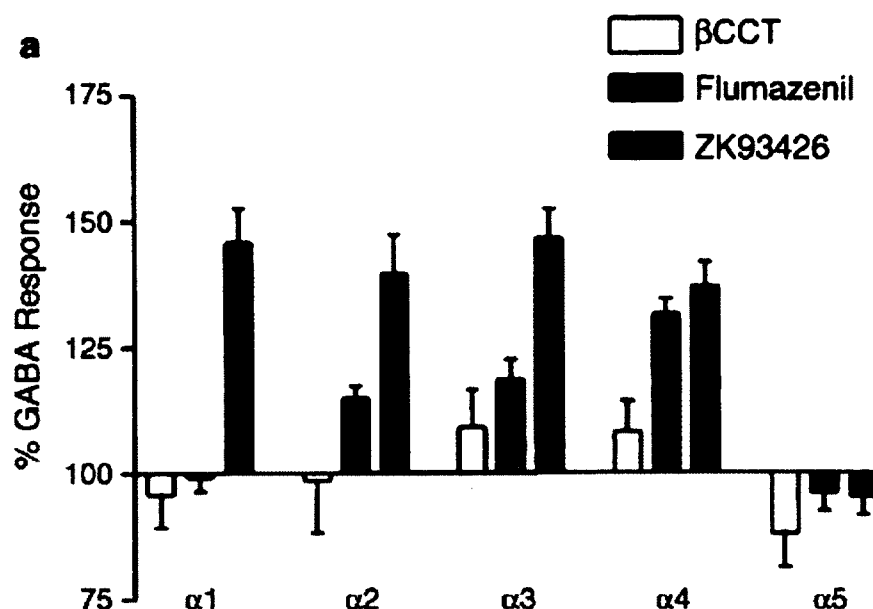


Figure 19. Efficacy of β CCt in modulating GABA at recombinant GABA $\alpha 1$ – $\alpha 5$ receptors¹⁶⁴ in *Xenopus* oocytes: comparison with other BzR antagonists.

Illustrated in Figure 19 is the modulation of GABA(A) $\alpha 1\beta 3\gamma 2$, $\alpha 2\beta 3\gamma 2$, $\alpha 3\beta 3\gamma 2$, $\alpha 4\beta 3\gamma 2$ and $\alpha 5\beta 3\gamma 2$ receptor subunit combinations expressed in *Xenopus* oocytes by β CCt (open bars), flumazenil (shaded bars), and ZK 93426 (black bars). A saturating concentration (1-10 μ M) was coapplied over voltage-clamped oocytes along with an EC_{50} of GABA.

The results of this study illustrated that β CCt was a near “neutral” antagonist (i.e., little or no efficacy) at all receptor subtypes. In fact, the level of intrinsic efficacy of β CCt in oocytes was less at some receptor subtypes than the classical nonselective antagonist flumazenil (Ro15-1788, for which intrinsic efficacy at all BZ-sensitive GABA(A) subtypes was relatively low, but not zero). To date, no compound has been characterized that exhibits zero efficacy at all BzR subtypes, raising the possibility that a compound labeled as an “antagonist” may indeed exhibit functional activity given the right

circumstances. For example, more recently, the efficacies of both β CCt and 3-PBC in the selective reduction of alcohol responding and production of anxiolytic effects were demonstrated in P and HAD rats following oral administration.¹⁶⁵ When compared with naltrexone treatment, these reductions in alcohol responding were more selective and longer in duration.^{42, 121} The antagonist β CCt exhibited either a neutral or low-efficacy agonist response at GABA receptors in oocytes. Although there has been some debate in the literature at present as to whether a ligand's binding or efficacy selectivity was "the more salient factor" in determining a ligand's capacity to function as an alcohol antagonist,^{38, 42, 166, 167} the knowledge of the efficacy of an individual putative anti-alcohol reward ligand across all GABA(A) receptors was indeed critical to the knowledge of their mode of action in the CNS.

Based on the limited availability of data on the series of α 1 "binding" and "efficacy" selective β -carboline (β CCt, 3PBC) as anti-alcohol agents,^{65, 168} a study was designed to expand the SAR and search for better α 1 subtype selective ligands. These compounds may be promising modulators of alcohol-related co-morbid behaviors in alcohol dependence *via* the GABA(A) /BzR system. Although recent evidence suggests a salient role for GABAergic mechanisms in the regulation of excessive alcohol drinking and the negative affective states associated with abstinence, decreased GABAergic tone stemming from chronic alcohol use and withdrawal may serve to generate anxiety.^{121, 169} Thus, compounds that enhance GABAergic tone may be effective and safe treatments for both excessive alcohol drinking and the negative affective states associated with abstinence and may represent novel pharmacotherapies to treat alcoholism.

In this regard, the established pharmacophore/receptor models^{42, 170} of BDZ binding sites was employed to design ligands with respect to the L_{Di} region at position-6, as well as characterize the binding pocket L₁ at position-3. Protein-ligand docking of the α 1 subtype GABA(A) receptor protein and WYS8 illustrated the agreement between the pharmacophore/receptor model and BzR site prediction based on homology modeling.⁷³ The chemistry and pharmacological evaluation of a series of structurally modified analogues of β CCt (**22**) as selective and potent α ₁ subtype-preferring ligands is described. The synthesis of the α 1 selective compound **23** (WYS8) and the structure-activity relationships (SAR) of 3,6-disubstituted β -carboline were also studied.

The β CCt Bivalent Ligands

The *in vitro* biological protocols employed follow the published procedure.⁷⁶ Although the α 1 β 3 γ 2 BzR/GABAergic subtype is very similar in structure to the α 2 and α 3 subtypes, there are slight differences.⁴² One major difference is in region L_{Di}, which appears larger in the α 1 subtype than in either the α 2, or α 3 or α 5 subtypes. This is located near position -6 of β CCt and can be seen in the model of the Comparative Molecular Field Analysis (CoMFA) study for the α 1 subtype (Figure 20).^{71, 158}

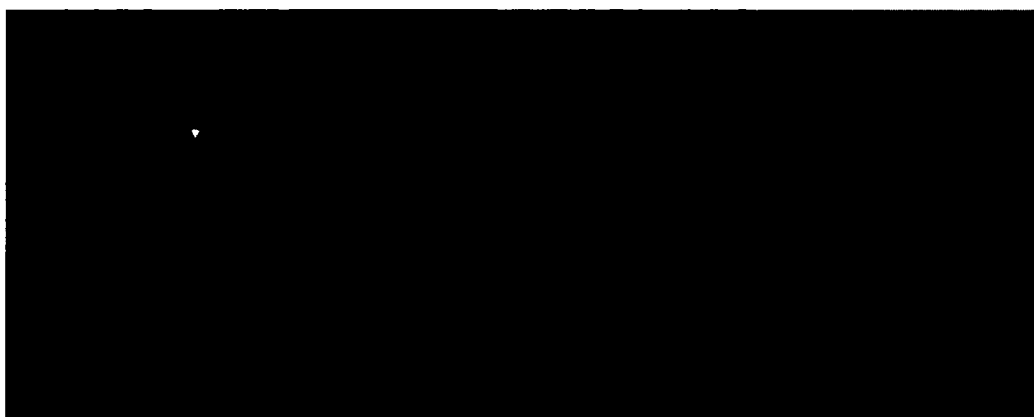


Figure 20. Orthogonal views of CoMFA contour maps for the affinity of 6-benzyl-substituted β -carbolines at the $\alpha 1\beta 3\gamma 2$ BzR. Orthogonal view of CoMFA contour maps for the $\alpha 1\beta 3\gamma 2$ receptor subtype with 6-benzyl-substituted β -carbolines modeled by Huang.^{71, 158} Green contours represent areas of positive steric interaction at a contribution level of 85%, which would result in reduced binding affinity. Blue contours represent areas of positive charge interaction at a level of 85%, which would increase the affinity of a ligand.

Blue contours in the western region of the pharmacophore/receptor model imply positive lipophilic interactions in this area that corresponds to region L_{Di} (a region in the pharmacophore adjacent to the extracellular domain of the receptor) of the unified pharmacophore/receptor model. In this region bulky substituents are tolerated and occupation of this area with substituents appears to enhance affinity or selectivity at $\alpha 1$ subtypes. This knowledge provided an opportunity to introduce a linker between two pharmacophoric β -carboline-3-carboxylate residues in order to design selective and rigid bivalent ligands. Initial efforts to find a novel series of $\alpha 1$ -preferring ligands focused on design and synthesis of β CCt bivalent ligands by Yin^{71, 121} based on molecular modeling. Although the $\alpha 1$ subtype selectivity was not amplified with the particular acetylenyl linked bivalent ligand **25**, the ligand does bind preferentially at $\alpha 1$ subtypes (Table 7). It was proposed the two-carbon linker was not long enough and that crowding between the second β CCt unit and the receptor protein decreased the binding affinity at the $\alpha 1$

subtype, thereby negating some of the potential selectivity. However, these rigidly linked linear bivalent ligands **25** and **26** fit the GABA(A) /BzR pharmacophore/receptor model very well (Figure 16).¹⁷¹ The unit at C-6, presumably, protrudes into the extracellular domain of the BzR, as previously expected,¹⁷² and bound to BzR with some α_1 subtype selectivity.¹⁷³⁻¹⁷⁷ To our knowledge these are the first two rigid bivalent ligands in the β -carboline series, which bind to BzR. Further pharmacological evaluation *in vivo* of the β CCt bivalent ligand with the longer rigid linker should shed light on the above hypothesis and this would also provide some tools to determine the size and exact location of the L_{Di} region.

WYS8

A series of 6-substituted- β -carboline-3-carboxylates have been synthesized and bound *in vitro* to the $\alpha_1\beta_3\gamma_2$ BzR subtype preferentially as compared to other subtypes (see Tables 1-3) by Yin et al.⁶⁵ These ligands have also been modeled in the GABA(A) /BzR pharmacophore model, and the 6-substitutents align well in the L_{Di} region.^{141, 152, 178, 179} Occupation of this region should lead to enhanced selectivity of a ligand at the α_1 containing isoform. Among the new 3,6-disubstituted- β -carbolines, 6-trimethylsilanylethynyl- β CCt **22** has been recently synthesized and found *in vitro* to prefer the α_1 subtype. However, the most selective ligand for the α_1 subtype was WYS8 (**23**). This α_1 subtype selective ligand was 100 fold more selective over the other subtypes. This is the most α_1 subtype selective ligand reported, to date, to these authors' knowledge. This 6-substituted acetylenyl β CCt **23** was 214 fold more selective for α_1 isoforms over α_5 isoforms. Studies of SAR in Table 7 confirmed the occupation of region L_{Di} of the receptor pharmacophore model did enhance α_1 selectivity in

comparison to the affinity of the non-selective ligand diazepam or the $\alpha 5$ selective ligand, RY080. As illustrated in the two dimensional Figure 21, full occupation of the L_{Di} lipophilic region by β -carboline may account for the potency/selectivity of this class of ligands at the $\alpha 1$ subunit. Analysis of the *in vitro* binding data for this series of bulky 6-substituted β -carboline (Table 7) has shown some selectivity for the $\alpha 1$ receptor subtype. In addition, it is important to note that binding affinity in this series of ligands of greater than 400nM usually results in zero efficacy at the subtype at pharmacologically relevant concentrations.

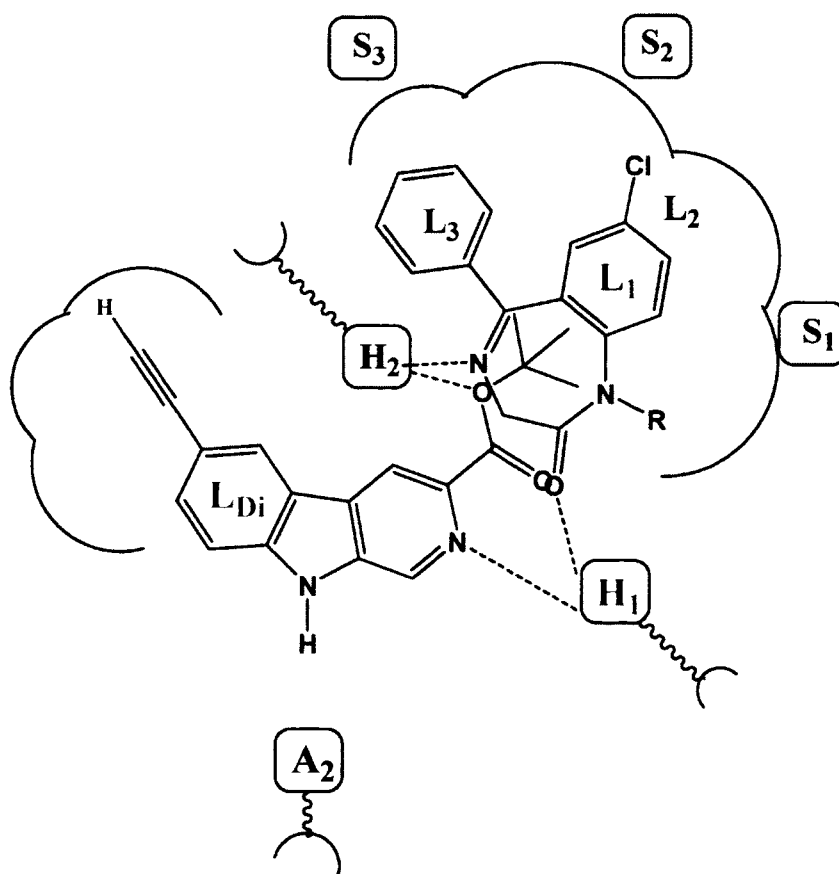
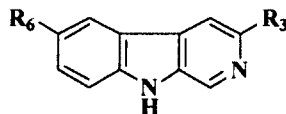


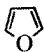
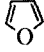
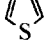
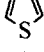

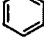
Figure 21. Overlap of diazepam and β CCt in the previous two dimensional pharmacophore/receptor model.

The structure of WYS8 and diazepam is illustrated in a simple representation of the pharmacophore model (Figure 21). WYS8 (blue line) and diazepam (black line) fitted to the inclusive pharmacophore model for the BzR. Sites H_1 and H_2 represent hydrogen bond donor sites on the receptor protein complex, while A_2 represents a hydrogen bond acceptor site necessary for potent inverse activity in vivo. L_1 , L_2 , L_3 and L_{Di} are four lipophilic regions in the binding pharmacophore. Descriptors S_1 , S_2 , and S_3 are regions of negative steric repulsion.

The homology model employed here of the GABA(A) receptor included a number of alternative models for loop C, which was two residues shorter than the template and hence built from a loop database. The final model (Figure 17) was selected based on assessment of model quality^{138, 145, 146} and consistency with published mutational data,^{68, 145, 146} particularly with the T206 side-chain appropriately positioned facing the benzodiazepine-binding pocket. In this illustration, positioning of WYS8 in the BzR was executed using a genetic algorithm in FlexiDock®.

Table 8. Affinities (K_i =nM) of 3,6-disubstituted β -carboline at $\alpha x\beta 3\gamma 2$ ($x=1-3,5,6$) receptor subtypes.^a



Ligands	R ₆	R ₃	α ₁	α ₂	α ₃	α ₄	α ₅	α ₆
22 (βCct)	H	CO₂tBu	0.72	15	18.9	1000	111	>5,000
48 (βCCE)	H	CO₂Et	1.2	4.9	5.7	ND	26.8	2,700
37 (3-PBC)	H	OnPr	5.3	52.3	68.8	1000	591	>1,000
49 (WYB14)	TMS—≡	CO ₂ tBu	6.8	30	36	2000	108	1000
50 (WY-B-25)	TMS—≡	CO ₂ CH ₂ CF ₃	17	59	88	200	1444	>3000
51 (WY-B-99-1)	TMS—≡	CO ₂ Et	4.4	4.5	5.58	2000	47	2000
23 (WYS8)	H—≡	CO ₂ tBu	0.972	111	102	2000	1473	1980
52 (WY-B-26-2)	H—≡	CO ₂ CH ₂ CF ₃	4.5	44.6	42.7	2000	124	2000
53 (iodo-βCct)	I	CO ₂ tBu	14.4	44.9	123	>4000	65.3	>4000
54 (WY-B-20)	I	CO ₂ CH ₂ CF ₃	12	39	47	2000	122	3000
55 (iodo-βCCE)	I	CO ₂ Et	4.8	31	34	1000	286	1000
56 (WY-B-08)	I	CO ₂ CH(CF ₃) ₂	78	301	131	3000	681	3000
57 (WYS13)		CO ₂ tBu	2.4	13	27.5	NA	163	5000
58 (WYB27-1)		CO ₂ CH ₂ CF ₃	26	143	117	3000	127	2000
59 (WYS12)		CO ₂ tBu	37	166	314	NA	2861	5000
60 (WYB27-2)		CO ₂ CH ₂ CF ₃	9.2	13	72	2000	449	2000
61 (WYS15)		CO ₂ tBu	3.63	2.02	44.3	NA	76.5	5000
62 (WYB29-2)		CO ₂ CH ₂ CF ₃	25	137	125	2000	299	2000
CMA57	F	COC ₃ H ₇	3.7	27	40	NA	254	>2500
CM-A-82a	C(CH ₃) ₃	CO ₂ tBu	2.78	8.93	24.5	1000	7.49	1000
CM-A-87	F	CO ₂ tBu	1.62	4.54	14.7	1000	4.61	1000
25 (WYS2)	Bcct—≡—Bcct		30	124	100	>300	>300	>4000
26 (WYS6)	Bcct—≡—≡—Bcct		120	1059	3942	5000	5000	5000

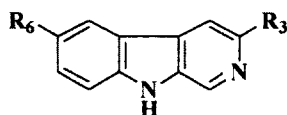
^aThe affinity of compounds at GABA(A) /BzR recombinant subtypes was measured by competition for [³H] or [³H] Ro-15-4513 binding to HEK cell membranes expressing human receptors of composition α1β3γ2, α2β3γ2, α3β3γ2, α4β3γ2, α5β3γ2 and α6β3γ2.^{71, 73, 136, 171} Data represent the average of at least three determinations with a SEM of ±5%.

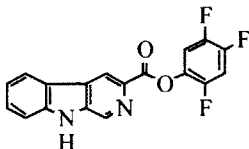
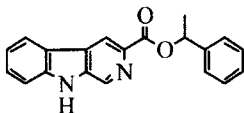
3-Substituted β -Carbolines

It was initially believed by Braestrup, Loew, and others that an ester moiety at position-3 of β -carbolines was required for a ligand to exhibit high affinity binding at Bz binding sites.^{180, 181} However, high affinity binding of β -carbolines including the antagonist 3-propoxy β -carboline (3-P β C, Table 8) demonstrated this was not the case.⁶⁵ Examination of data from additional studies⁶⁵ have suggested that at least two factors affected high affinity binding at BzR with respect to 3-alkoxy substituted β -carbolines,¹⁸² one of which was the lipophilicity of the substituent which interacted at L₁. The L₁ pocket tolerates linear groups up to 4 carbons in length via molecular modeling and receptor binding. Comparison of the *in vitro* receptor binding affinity of the ligands depicted in Table 8 indicated the alkyl ethers **37** and **38** bind potently to α_1 subtypes while the larger branched analog **41** does not; binding affinity is lost, illustrating that the substituent at the 3-position is too large to allow the ligand to bind. Likewise, the 3-benzyloxy β -carboline **42** is also too bulky to fit the L₁ pocket despite its lipophilic nature. The second factor was the ability of the substituent at position-3 to release electron density to the pyridine ring. This enhanced the basicity of the nitrogen atom at N(2) which resulted in a greater ligand-receptor interaction at H₁. Analysis of the binding affinities of the novel trifluoroalkyl esters of β -carboline-3-carboxylic acid further supported this hypothesis (Table 7). The trifluoroalkyl esters exhibited reduced binding affinity at all receptor subtypes when compared to their corresponding alkyl esters (**43** vs. **44**, **45** vs. β CCE). Since the trifluoromethyl group was a strong electron-withdrawing group, when compared to the corresponding alkoxycarbonyl moiety, the 3-trifluoroalkoxycarbonyl substituent would decrease electron density to the pyridine (N2) ring reducing the

basicity of the nitrogen atom. This would result in a weaker ligand-receptor interaction at H_1 . In addition, the trifluoroalkyl group was less lipophilic than the corresponding alkyl moiety, which may result in a weaker interaction at L_1 . Ramachandran and Hanzawa have reported that trifluoromethyl groups are nearly as large as isopropyl or t-butyl functions.^{68, 136} It was possible, the trifluoromethyl substituted ligands are simply too large to exert high affinity binding; however, β CCT (**22**), WY-B-24 (**68**) and CM-A-77 (**69**) all bound with good potency to $\alpha 1$ BzR subtypes, and these ester functions occupy a large molecular volume.

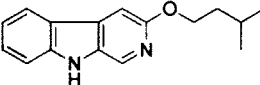
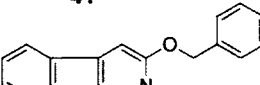
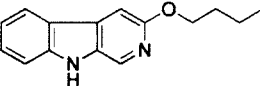
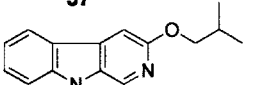
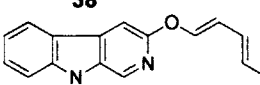
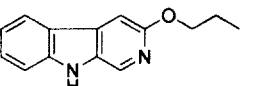
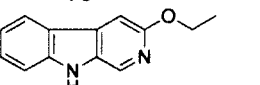
Table 9. Affinities (K_i =nM) of 3-substituted β -carbolines at $\alpha x\beta 3\gamma 2$ ($x=1-3,5,6$) receptor subtypes



Ligands	R ₆	R ₃	α ₁	α ₂	α ₃	α ₄	α ₅	α ₆
48 BCCE	H	CO₂Et	1.2	4.9	5.7	1000	26.8	2700
45	H	CO ₂ CH ₂ CF ₃	3.0	24.5	41.7	>500	125.7	>2000
63(WYB09-1)	H	CO ₂ CH(CF ₃) ₂	3.99	8	32	1000	461	2000
64(WYB23-1)	H	CO ₂ CH ₂ CCl ₃	10	33	43	1000	189	2000
65(WYB17)	H	CO ₂ CH(CH ₃)CCl ₃	2000	2000	2000	3000	2000	5000
66(CMA64)	H	CO ₂ CH(CH ₃)C ₂ H ₅	18	60	116	NA	216	>2000
67(CMA69)	H	CO ₂ CH(CF ₃)C ₂ H ₅	1000	1000	1000	NA	1000	>2000
68(WY-B-24)			22.0	177	44.8	3000	422	3000
69(CM-A-77)			33.5	1000	1000	1000	1000	3000

The affinity of compounds at GABA(A) /BzR recombinant subtypes was measured by competition for [³H]flunitrazepam or [³H] Ro-15-4513 binding to HEK cell membranes expressing human receptors of composition α1β3γ2, α2β3γ2, α3β3γ2, α4β3γ2, α5β3γ2 and α6β3γ2.¹⁷¹ Data represent the average of at least three determinations with a SEM of ±5%.

Table 10. Affinities (K_i =nM) of Ether-substituted β -carbolines at $\alpha x\beta 3\gamma 2$ (x=1-3,5,6) Receptor Subtypes

Ligands	α_1	α_2	α_3	α_5	α_6
 41	350.2	3000	3000	3000	10000
 42	830	3000	3000	10000	10000
 37	36.9	194	245	1000	1000
 38	24.9	123.6	139.2	1000	10000
 39	245	818	859	10000	10000
 70	5.3	52.3	68.8	591	1000
 40	6.43	25.1	28.2	826	1000

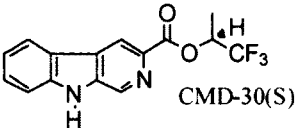
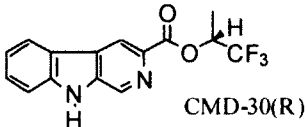
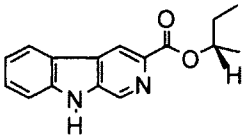
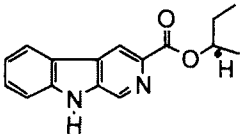
The affinity of compounds at GABA(A) /BzR recombinant subtypes was measured by competition for [3 H]flunitrazepam or [3 H] Ro-15-4513 binding to HEK cell membranes expressing human receptors of composition $\alpha 1\beta 3\gamma 2$, $\alpha 2\beta 3\gamma 2$, $\alpha 3\beta 3\gamma 2$, $\alpha 4\beta 3\gamma 2$, $\alpha 5\beta 3\gamma 2$ and $\alpha 6\beta 3\gamma 2$.^{71, 170} Data represent the average of at least three determinations with a SEM of $\pm 5\%$.

Chiral 3-Substituted β -Carbolines.

Examination of the binding data for the enantiomeric pair of β -carboline sec-butyl esters **73** and **74** (Table 11) indicated that the (R)-enantiomer **74** bound tighter to the

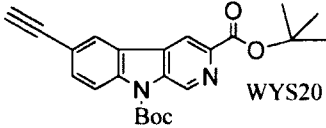
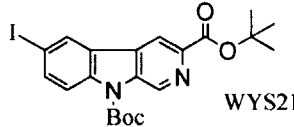
receptor subtypes than the (S) isomer **73**. Although both enantiomers exhibited approximately a 4-fold selectivity for the $\alpha_1\beta_3\gamma_2$ subtype, the (R) isomer remained more potent *in vitro* at all 5 BzR subtypes. Because the receptor subtype selectivity remained about the same for the (R) and (S) isomers, this indicated the stereoenvironment in lipophilic pocket L₁ was highly conserved across the entire series of BzR subtypes in agreement with earlier work on the binding affinities of the enantiomers of the framework-constrained 4,5-substituted pyrroloimidazobenzodiazepines.⁶⁵ It is possible that lipophilic pocket L₁ is simply a large area in the pharmacophore/receptor model with only small steric differences between receptor subtypes. More work will be required to determine if this is the case. A similar result was observed in the case of (R) and (S) isomers of CMD-30. The (R)-enantiomer CMD-30 R (**72**) bound slightly tighter to the receptor subtype than the (S) isomer (**71**) with almost 70 fold more selectivity for the α_1 subtype over the α_5 isoform. In addition, previously it was reported that a hydrogen bond between the N (9) H atom of a β -carboline and the secondary site A₂ in the receptor pharmacophore was required for potent inverse agonist activity *in vivo*.⁷⁹ Therefore, a series of ligands with the Boc group at position-9 such as **75** and **76** were evaluated and were not α_1 subtype selective ligands. In fact, they did not bind to BzR at all in agreement with previous work (Table 12).^{79, 126 73, 126, 133}

Table 11. Affinities (K_i =nM) of chiral 3-substituted β -carbolines at $\alpha x\beta 3\gamma 2$ ($x=1-3,5,6$) receptor subtypes

Ligands		α_1	α_2	α_3	α_4	α_5	α_6
71	 CMD-30(S)	90	931	172	>3000	1847	>2000
72	 CMD-30(R)	27.0	343.3	453	>3000	1847	>2000
73		17	59	88	NA	1444	>3000
74		7.7	32.5	43	NA	69	>2000

The affinity of compounds at GABA(A) /BzR recombinant subtypes was measured by competition for [3 H]flunitrazepam or [3 H] Ro-15-4513 binding to HEK cell membranes expressing human receptors of composition $\alpha 1\beta 3\gamma 2$, $\alpha 2\beta 3\gamma 2$, $\alpha 3\beta 3\gamma 2$, $\alpha 4\beta 3\gamma 2$, $\alpha 5\beta 3\gamma 2$ and $\alpha 6\beta 3\gamma 2$.¹³⁵ Data represent the average of at least three determinations with a SEM of $\pm 5\%$.

Table 12. Affinities (K_i =nM) of Boc-protected 3-substituted β -carboline at $\alpha\beta\gamma 2$ ($x=1-3,5,6$) receptor subtypes

Ligands	α_1	α_2	α_3	α_4	α_5	α_6
<p>75</p>  <p>WYS20</p>	450	5000	ND	ND	5000	5000
<p>76</p>  <p>WYS21</p>	ND	ND	ND	ND	1847	ND

ND = not determined yet (see previous tables for details of receptor binding). Data represent the average of at least three determinations with a SEM of $\pm 5\%$.

Efficacy of α_1 Preferring Ligands in Oocytes at GABA(A) Receptor Channels

The physiological efficacy of β CCt, as compared to other Bz antagonists was investigated across all diazepam sensitive (DS) receptor subunits at recombinant α_1 , α_2 , α_3 , and α_5 receptor subunits in the *Xenopus* oocytes assay and is depicted in Figure 22 by Harvey *et al.*¹⁶³

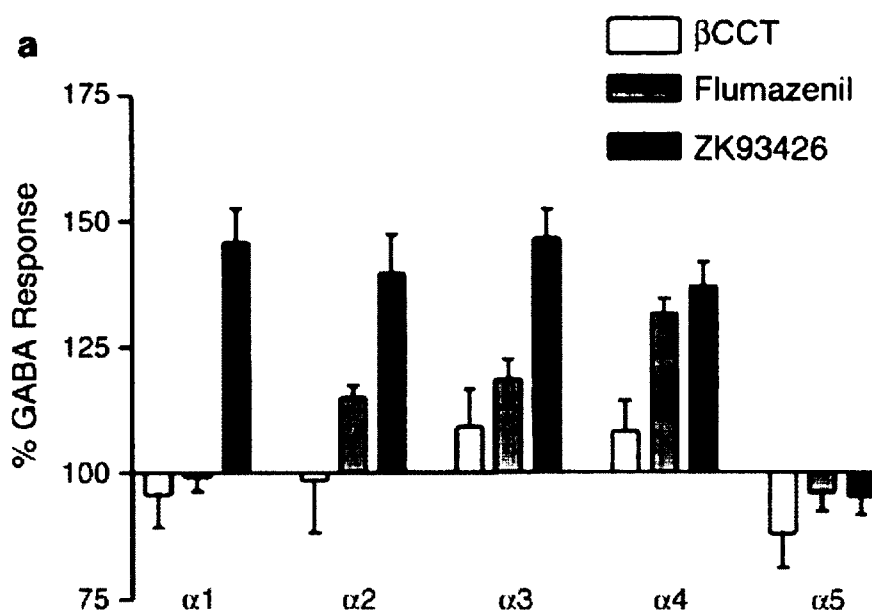


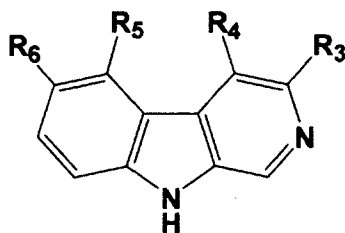
Figure 22. Efficacy of β CCt in modulating GABA at recombinant GABA α 1– α 5 receptors^{135, 183, 184} in *Xenopus* oocytes: comparison with other BzR antagonists.

In comparison to other BzR antagonists such as flumazenil and ZK 93426, as mentioned, β CCt exhibited either a neutral or low-efficacy agonist response at GABA α 1 (96±7%), α 2 (99±10%), α 3 (108±6%), and α 4 (107±5%) receptors. However, a low-efficacy partial inverse agonist response was observed at the α 5 receptor (88±7% of the GABA response) compared to the control diazepam. Flumazenil exhibited an efficacy profile that was qualitatively similar to β CCt at the α 1 (99±5%), α 3 (118±7%), and α 5 (96±6%) subtypes. At the α 2 receptor, flumazenil produced a low-efficacy agonist response (115±4%), while β CCt was GABA neutral (99±10%). Flumazenil also produced a qualitatively similar response to β CCt at the α 4 receptor, albeit the magnitude of GABA potentiation by flumazenil far exceeded that of β CCt (132±6 vs. 108±6%, respectively). However, it is important to note, with regard to α 4/ α 6 β 3 γ 2 subtypes, the

agonist effect was observed at 10 μ M, far above that required for agonist efficacy at the DS subtypes. In contrast, ZK 93426 produced a clear weak agonist profile, potentiating GABAergic activity by $137 \pm 8\%$ and $148 \pm 11\%$ across the $\alpha 1$ – $\alpha 4$ subtypes, but was GABA neutral at the $\alpha 5$ receptor ($96 \pm 6\%$). These findings suggested that β CCt had no appreciable intrinsic efficacy. The rationale for referring to this agent as a “mixed agonist-antagonist” was based on the fact that, despite the ability to potentiate GABA at certain receptor subtypes, it was “GABA neutral” at select doses. In addition, at select doses, β CCt and 3-P β C were capable of competitive antagonism of classical benzodiazepine agonists,⁷³ therefore, the development of subtype-selective antagonists for GABA(A) receptors, such as β CCt, which targeted the GABA(A) $\alpha 1$ receptor as a weak agonist-like antagonist,¹⁸⁵ should facilitate efforts to understand the antialcohol actions of β -carboline in nonhuman primates and humans as well. In the NIMH supported PDSP screen neither β CCt, 3PBC, nor WYS8 exhibited significant interactions at other receptors (See Appendix for PDSP screen or <http://pdsp.med.unc.edu> for details).

Innate elevations of the α_1 and α_2 subunits of the HAD rat may contribute to the capacity of novel β -carboline ligands to function as both anxiolytic agents and alcohol antagonists in this genetic rat line.¹¹¹ These differences may explain the capacity of novel β -carboline ligands to block alcohol drinking and still exhibit anxiolytic actions in the P and HAD alcoholic rats. WYS8 may be a suitable ligand to evaluate as a preclinical agent to reduce alcohol dependence. Its reduced efficacy at the $\alpha 1$ – $\alpha 2$ subunits in potentiating GABA may render it a safe BDZ receptor ligand devoid of synergistic interactions with alcohol and with much less abuse potential.¹⁶

Table 13. Structures and affinities at $\alpha\beta 2\gamma 2$ recombinant receptors and modulation by β -carbolines. pAg = weak partial agonist; Ag = agonist^{19, 186}

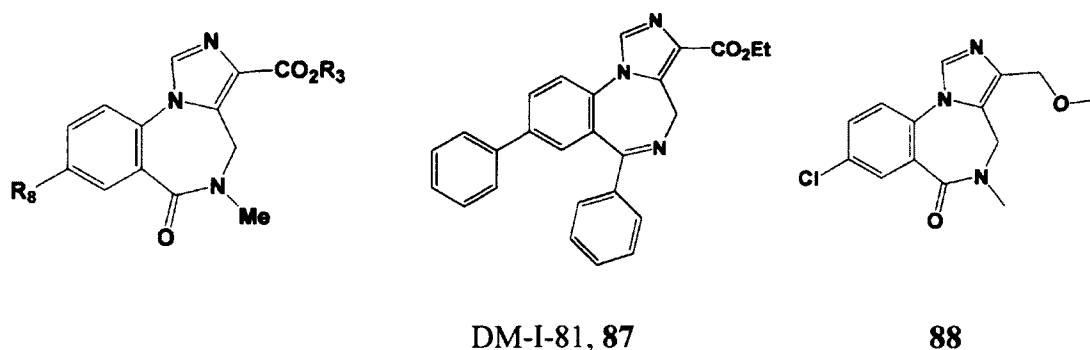


Ligand	K _i (nM)										Activity
	R ₆	R ₅	R ₄	R ₃	$\alpha 1$	$\alpha 2$	$\alpha 3$	$\alpha 4$	$\alpha 5$	$\alpha 6$	
32, 6-PBC	On-Pr	H	MOM	CO ₂ Et	0.49	1.21	2.2	NR	2.39	1343	pAg
33, ZK-93423	OCH ₂ Ph	H	MOM	CO ₂ Et	4.1	4.2	6	NR	4.5	1000	Ag
81, ZK-91296	H	OCH ₂ Ph	MOM	CO ₂ Et	NR	NR	NR	NR	NR	NR	pAg
82, Abecarnil	OCH ₂ Ph	H	MOM	CO ₂ - <i>i</i> -Pr	12.4	15.3	7.5	NR	6	1000	pAg

Ligands that Occupy the L₂ Region and are Selective for $\alpha 5$ Containing Receptors; RY-24 and Related Analogs

Continued interest in the development of $\alpha 5$ selective ligands goes forward in the CNS area for many reasons. One of these involves the localization of these receptors and their presumed importance in developmental biology. Over 30 % of GABA(A) receptors in neonatal rat pups are comprised of $\alpha 5\beta 3\gamma 2$ subtypes, whereas they only comprise about 5 % in adult rats.^{19, 21} In addition, these $\alpha 5$ subtypes are primarily found in the hippocampus,^{16, 187} which prompted interest in memory and learning.¹⁸⁸ From the evaluation of K_i values, it was found that many 8-substituted *i*-BZDs, such as RY-80 31

and RY-24 **83** and their trimethylsilyl precursors **5** and **84** (Table 14) exhibited a significant degree of binding selectivity at the $\alpha 5$ subtype *in vitro*. This observation was in agreement with the previous hypothesis that correct occupation of the L₂ region can promote $\alpha 5$ selectivity of a ligand.²¹ Therefore, the efficacy of the $\alpha 5$ -subtype selective ligand RY-24 **83** was evaluated *in vitro*. Recently, it was determined that this ligand was a potent inverse agonist at the $\alpha 5$ subtype with a much weaker efficacy at the other subtypes (Figure 24). These results confirmed previous binding data, which indicated that this ligand was $\alpha 5$ -selective due to the lipophilic C(8)-substituent which fully occupied the L₂ pocket.¹⁸⁹ The data were also in agreement with previous studies *in vivo*, which indicated that some of these ligands enhanced cognition while other Bz BS ligands were not as effective.^{111, 190} Furthermore, ligands devoid of a lipophilic substituent at the C(8) position showed no selectivity for the $\alpha 5$ subtype (Table 14).

Table 14. Structures and affinities of some $\alpha 5\beta 3\gamma 2$ subtype selective ligands.

Ligand	R_8	R_3	K_i (nM)				
			$\alpha 1$	$\alpha 2$	$\alpha 3$	$\alpha 5$	$\alpha 6$
83 , RY-24		<i>t</i> -Bu	26.9	26.3	18.7	0.4	5.1
84 , RY-23		<i>t</i> -Bu	197	143	255	2.61	58.6
31 , RY-80		Et	28.4	21.4	25.8	0.49	28.8
85 , RY-79		Et	121	142	198	5.0	114
86	H	Et	1.2	2.0	1.1	0.4	> 300
87 , DM-I-81	Ph	NA	> 2000	> 2000	> 2000	176	> 2000
88 , PWZ-029 ^{21, 191}	Cl	NA	>300	>300	>300	38.8	>300

Inspection of the data in Table 14 revealed some observations worth noting. While the lipophilic substituent at R_8 of RY-24 **83** and RY-80 **31** decreased the affinity for $\alpha 1$, $\alpha 2$ and $\alpha 3$ subtypes, it retained affinity for $\alpha 5$ and actually increased affinity for the $\alpha 6$ subtype. Furthermore, selective affinity of *i*-BZDs at the $\alpha 5$ subtype was independent of the occupation of the L_3 pocket, as illustrated by the *in vitro* data of DM-I-81 **87** (Table 14). This data again supports the importance of the occupation of the lipophilic pocket L_2 for potent selectivity at the $\alpha 5$ subtype.

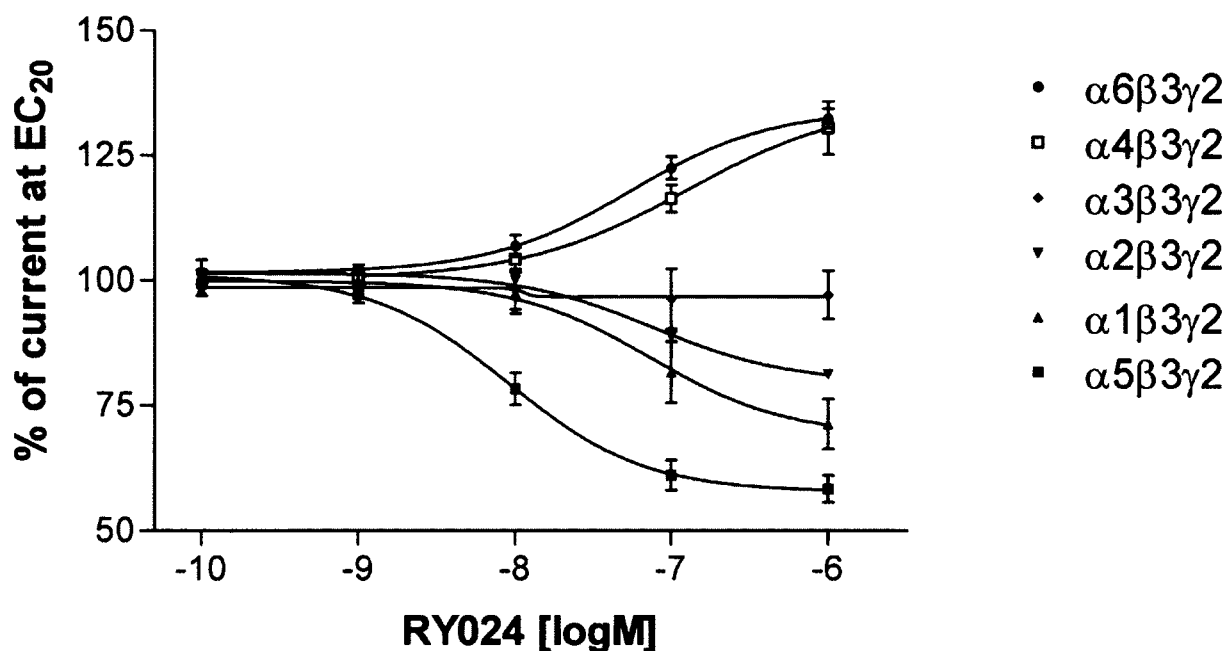


Figure 23. Subtype efficacy of RY-24 (83), Dose response curves for RY-24 in oocytes expressing different subunit combinations of GABA(A) receptors. Subtype combinations are indicated in legends. cRNA-injected *Xenopus* oocytes were held at -60 mV under two-electrode voltage clamp. Increasing concentrations of RY-24 were superfused together with a GABA concentration eliciting $\sim 20\%$ of the maximal current amplitude. RY-24 was pre-applied for 30 sec before the addition of GABA, which was co-applied with the drugs until a peak response was observed. Data were normalized for each curve assuming 100% for the response in the absence of RY-24. RY-24 was made up and diluted as stock solution in DMSO. Final DMSO concentrations perfusing the oocyte were 0.1%. Values are presented as mean \pm SD of at least 4 oocytes from at least 2 batches.

June *et al.* recently reported the neurobehavioral results of RY-23 and RY-24 in rats. In agreement with previous studies,^{79, 183} these $\alpha 5$ selective ligands were highly selective in suppressing ethanol-maintained responding (Figure 25).^{79, 183} As previously stated, the hippocampus contains the greatest concentration of $\alpha 5$ -containing receptors in the CNS,¹⁶ and it is possible that these hippocampal $\alpha 5$ receptors may regulate alcohol-motivated responding following systemic administration of an $\alpha 5$ -selective agent.

Furthermore, RY-24 also antagonized the motor-impairing and sedative effects of ethanol in Long-Evans rats. Combined with additional studies within the ventral pallidum (VP), it has been proposed that the GABAergic systems within the VP and hippocampal pathways may represent new extensions of the mesolimbic ethanol reward circuitry. Although these data do not strongly support a direct role for the modulatory influences of intrinsic efficacy in the behaviors examined, the synthesis of $\alpha 5$ subtype selective ligands provides researchers a unique opportunity to explore the role of this subtype in the neurobehavioral effects of alcohol.^{19, 192} However, the efficacy (inverse agonist, negative modulation) of RY-23 and RY-24 at $\alpha 1$ and $\alpha 2$ subtypes precludes potential clinical uses of such agents for both agents are proconvulsant and RY-24 is also convulsant. The efficacy of PWZ-029 (see below) is more promising in this respect.

In studies involving the $\alpha 1$ subtype, β -CCT and 3-PBC were observed to selectively reduce alcohol-motivated behaviors in a variety of experiments, as mentioned previously.¹⁹³ However, unlike the $\alpha 5$ selective inverse agonist RY-23, both the β -carboline antagonists β -CCT and 3-PBC displayed mixed weak agonist-antagonist profiles *in vivo* in alcohol P and HAD rats. Therefore, in addition to being able to study the molecular basis of alcohol reinforcement, $\alpha 1$ Bz BS ligands which display mixed agonist-antagonist pharmacology in alcohol P and HAD rats may be capable of reducing alcohol intake while eliminating or greatly reducing the anxiety associated with habitual alcohol, abstinence or detoxification. Thus, these types of ligands may be ideal clinical agents for the treatment of alcohol-dependent individuals, as mentioned before.¹⁹⁴

Additional behavioral studies of RY-24 were performed by Helmstetter *et al.* and provided further support for the role of the hippocampus in anxiety and learning.^{191, 192}

Moreover, the data suggested that Bz BSs within the hippocampus are important for the acquisition of fear conditioning. Although this subtype selective ligand has been shown to be an inverse agonist at the $\alpha 5$ subtype,^{191, 192} this study suggested that RY-24 may act as an agonist at other alpha subtypes because larger doses of RY-24 were not as anxiogenic as the smaller doses and resulted in decreased learning. Consistent with the studies of Stephens *et al.* using $\alpha 5$ knock-out mice¹⁸ and the efficacy studies of Lüddens, June and Cook *et al.*,^{195, 196} these findings support the concept that the pharmacology observed depends upon the dose, behavioral paradigm employed and subunit composition activated. Ligands such as RY-24 have proven to be valuable in the study of the biochemical and pharmacological properties of GABA(A) receptors and have permitted insight into the role this protein plays in anxiety and learning.

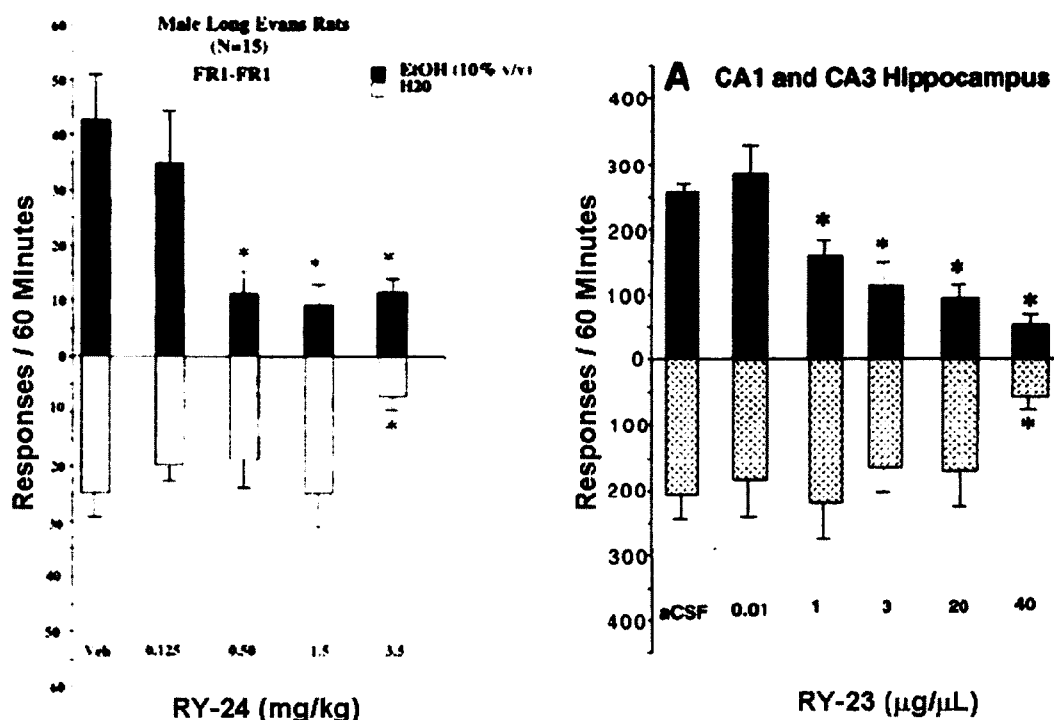


Figure 24. Suppression of alcohol-motivated responding by RY-24 (83) and RY-23 (84)¹⁸

On the left is a dose-response of ip administration of RY-24 (0.0–3.5 mg/kg) and vehicle on responding maintained by ethanol (10 % v/v) (*top panel*) and water (*white bottom panel*) in male Long-Evans rats. On the right is the dose-response of unilateral infusions of RY-23 (0.0–40 µg) in the hippocampus on a concurrent fixed-ratio (FR4) schedule for ethanol (10 % v/v) (*top panel*) and saccharin-maintained (0.025 % v/v) (*grey bottom panel*) responding. For both studies, $*p \leq 0.05$ versus control condition values was determined using ANOVA and *post hoc* Newman-Keuls test. Each bar represents the mean (\pm SEM) ($n = 15$ for RY-24 and $n = 7$ for RY-23).¹⁸

QH-II-066

Due to the pharmacological profile that the negative modulator RY-24 exhibited *in vivo* (enhanced cognition via $\alpha 5$ subtypes), the development of additional $\alpha 5$ subtype selective ligands was pursued. Thus, the 7-acetyleno analog of diazepam, QH-ii-066 **89**, was synthesized and was determined to also exhibit a binding and functional selectivity at the $\alpha 5$ subtype over the $\alpha 1$ subtype (Table 15).¹⁹⁷ This was due to full occupation of the L₂ pocket, relative to diazepam (Figure 25). To our knowledge, this was the first agonist ligand to display some $\alpha 5$ selectivity from the 1,4-benzodiazepine family. Importantly, the 7-cyano congener **90** (Table 15) did not potently bind to recombinant receptors of the $\alpha 5$ subtype, which is in agreement with earlier work of Haefely and Fryer *et al.* on the SAR of 1,4-benzodiazepines.¹⁹⁸⁻²⁰⁴ This cyano ligand also did not exhibit any subtype selectivity, re-emphasizing that occupation of the L₂ region with lipophilic groups is important for $\alpha 5$ selectivity as well as for high affinity.

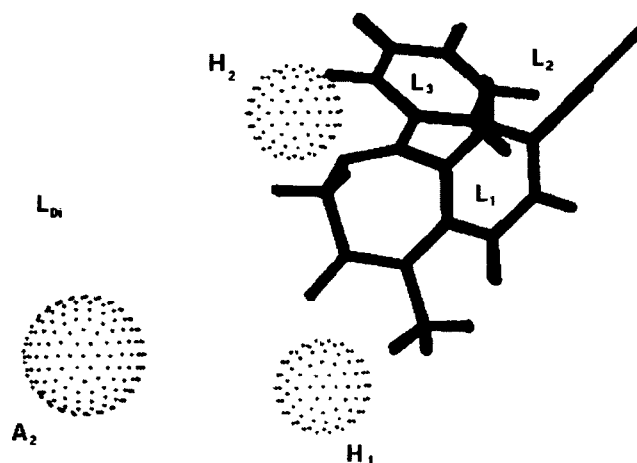
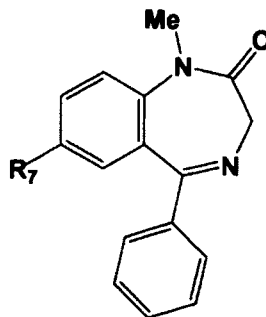
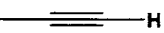


Figure 25. Comparison of non-selective diazepam (black) with the $\alpha 5$ -selective QH-ii-066 (cyan) when aligned within the unified pharmacophore/ receptor model.

The acetylenic moiety of QH-ii-066 increased the occupation of the L_2 region relative to that of diazepam. Furthermore, Lelas and Cook *et al.* have determined that although QH-ii-066 had similar affinity for the DS subtypes in rats, it displayed functional selectivity *in vivo*, with diazepam-like efficacy at the $\alpha 5$ subtype and partial efficacy at the $\alpha 1$ subtype.¹⁹⁸⁻²⁰⁴ The study also indicated that this 7-acetyleno substituted diazepam analog exhibited less potency in protection against MES-induced seizures (maximal electroshock) relative to diazepam than against PTZ-induced (pentylenetetrazol) seizures. Hence, the $\alpha 1$ subtype may play a more prominent role in MES-induced seizures than in PTZ-induced seizures.²⁰³

Table 15. Structures and affinities of 1,4-benzodiazepines.



Ligand	R ₇	K _i (nM)				
		α1	α2	α3	α5	α6
34, diazepam	Cl	14	20	15	11	> 3000
89, QH-ii-066		76.3	42.1	47.4	6.8	> 3000
90	C≡N	320	310	350	265	> 3000

The Interactive Compound Table

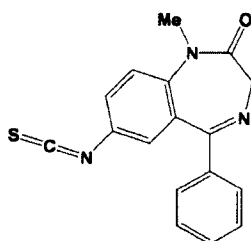
The Milwaukee-based database of compounds has grown to 600-700 compounds. The database designed by Clayton has been entered into a Microsoft Excel with ChemDraw Ultra 12.0 creating an interactive database. The database allows a user to search by K_i value or create mathematical expressions to identify most subtype specific ligands. Additional features of the table are the presence of chemical properties and physical properties (log P), and volume. The program also allows one to search the complete database by substructure, perform similarity searches and R-group analysis. Data can be both imported or exported into other software programs for QSAR and modeling (See complete compound table in Appendix).²⁰¹

Evidence from Covalently Reactive Ligands Allows One to Position the L₂ Lipophilic Pocket

Covalent labeling studies contributed significantly to the determination of residues that are located within the Bz BS.¹⁹⁸

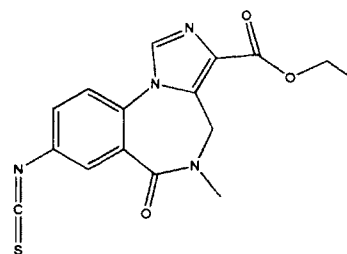
Table 16. Ligands used for affinity labeling studies.²⁰²

Ligand	Activity	Site of Interaction
[³ H]flunitrazepam	agonist	α_1 H102
91 , [³ H]Ro15-4513	inverse agonist	α_1 Y210
92	agonist	α_1 H101C (rat)
93	partial agonist	α_1 H101C, α_1 G157C α_1 V202, α_1 V211C (rat)



92

7-isothiocyano-1,4-benzodiazepine



93

8-isothiocyano imidazolebenzodiazepine

Photoincorporation studies with the agonist [^3H]flunitrazepam identified $\alpha 1\text{H}102$ of the human sequence as the primary site of incorporation.²⁰⁵ McKernan et al. has proposed that flunitrazepam is coupling via the nitro group at the 7-position.^{204, 206} Studies with the inverse agonist [^3H]Ro15-4513 indicated $\alpha 1\text{Y}210$ as the primary site of incorporation.^{35, 173, 204, 207} Thus, the azido group at the 7-position of Ro15-4513 should be in close apposition to $\alpha 1\text{Y}210$, assuming no rearrangement of the photo-activated intermediate. Further information comes from recent studies reporting the covalent coupling of the 7-isothiocyano- derivatives (Rice et al.) of a 1,4-benzodiazepine, (isothiocyanate **92**)²⁰⁴ and of Ro15-1788 (isothiocyanate **93**)^{204, 206} to GABA(A) receptors in which individual amino acid residues had been mutated to cysteines. The primary site of reaction of both substances was the rat $\alpha 1\text{H}101\text{C}$ mutant that is homologous to $\alpha 1\text{H}102$ of the human subunit. Thus, the 7-substituent both of 1,4-benzodiazepines and of imidazodiazepines appears to be in apposition to $\alpha 1\text{H}102$. The imidazobenzodiazepine **93** reacted with additional cysteines in positions corresponding in the human sequence to positions $\alpha 1\text{V}203\text{C}$ and $\alpha 1\text{V}212\text{C}$ in the loop C stem, and with $\alpha 1\text{G}158\text{C}$ in loop B (see alignment in Figure 64). Thus, the 7-substituent of this compound, in agreement with the data from photolabeling H102 with flunitrazepam and Y210 with Ro15-4513, is in apposition to loop A, the loop C base, and additionally loop B.

Thus, all the findings from covalently incorporated ligands given above can be reconciled by placing the 7-substituent, and thus the L2 descriptor of the unified pharmacophore model, between the loop C base near $\alpha 1\text{V}203/\alpha 1\text{V}212/\alpha 1\text{Y}210$ and loop A $\alpha 1\text{H}102$. The homology models reveal that this is not only topologically possible, but

also provides the additional apposition to loop B that is suggested by the reaction of isothiocyanate **93** with rat $\alpha 1G157C$. Thus, the L2 lipophilic pocket is most likely formed by the base of loop C, together with parts of loop A.

The A₂ Descriptor and the L_{DI} Region

Experimental data yields some very convincing evidence for assignment of the A₂ descriptor and the L_{DI} region of lipophilic interaction next to A₂ to protein segments close to residues $\gamma 2A79$ and $\gamma 2T81$ at loop D. Certain imidazobenzodiazepines, which occupy the pharmacophore volume close to A₂ (see Figure 71), are more sensitive to $\gamma 2A79$ mutations than classical benzodiazepines or benzodiazepines that lack a 3'-imidazo substituent. This was shown in a study where mutations of $\gamma 2A79$ and $\gamma 2T81$ had little effect on the binding of the agonists diazepam and flunitrazepam, but in a roughly size dependent fashion decreased the affinities of antagonist Ro15-1788 and inverse agonists Ro15-4513.⁴² In agreement with other studies, midazolam, which lacks a 3' substituent, behaved more closely to classical benzodiazepines than *i*-BZDs.^{1, 208, 209} This trend is enhanced by rigid and bulky 3'-imidazo substituents, altogether suggesting that $\gamma 2A79$ and $\gamma 2T81$ are located close to the region of the Bz BS surrounding the 3' substituent of *i*-BZDs.¹²¹ The localization of the 3'-imidazo substituents in the unified pharmacophore model, thus positions the A₂ and L_{DI} descriptors near residues $\gamma 2A79$ and $\gamma 2T81$ (Figure 71). Further support for this localization comes from the observation that DMCM also loses affinity upon mutagenesis in positions $\gamma 2A79$ and $\gamma 2T81$,^{121, 210} consistent with the alignment of this substance in the pharmacophore. Figure 67 shows that changes to the protein near the A₂ descriptor would in all likelihood not be tolerated by DMCM but

should not impact the efficacy of diazepam (Figure 26). The affect of mutations on positions $\gamma 2A79$ and $\gamma 2T81$ is in agreement with the proposed unified pharmacophore protein model of Milwaukee.^{170, 211, 212}

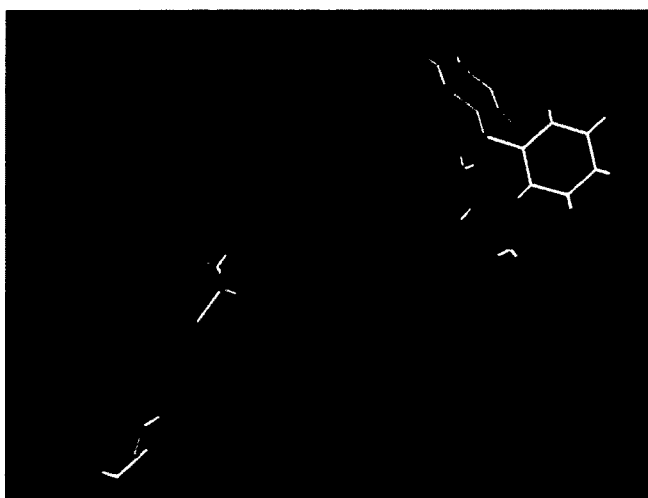


Figure 26. Diazepam in the pharmacophore receptor model and the key residues $\gamma 2A79$ and $\gamma 2T81$

Included Volume Analysis of Ligands Binding to Receptors Containing Different Alpha Subunits

The benzodiazepine binding site of $\alpha\beta\gamma 2$ GABA(A) receptors is strongly influenced by the type of α subunit present in these receptors as indicated by the existence of ligands exhibiting certain selectivity for receptors containing the respective α subunits.¹⁷⁰ If subtype selective ligands are then aligned within the pharmacophore model according to the resulting alignment rules^{33, 213} their included volumes can be

constructed and used to compare the topologies of benzodiazepine binding pockets of different receptor subtypes.²¹⁴ Ligands employed in the included volume for each receptor subtype exhibited potent affinity ($K_i \leq 20$ nM) at the respective receptor subtype. CL-218,872 ($K_i = 57$ nM at α_1) and zolpidem ($K_i = 26.7$ nM at α_1) were added to the included volume of the $\alpha_1\beta_3\gamma_2$ subtype since they are both α_1 -subtype selective ligands. The major differences with regard to volume and affinity are shown below and are important for interpreting experimental data.

The Previous Benzodiazepine Subtype Selective Receptor Pharmacophore Models

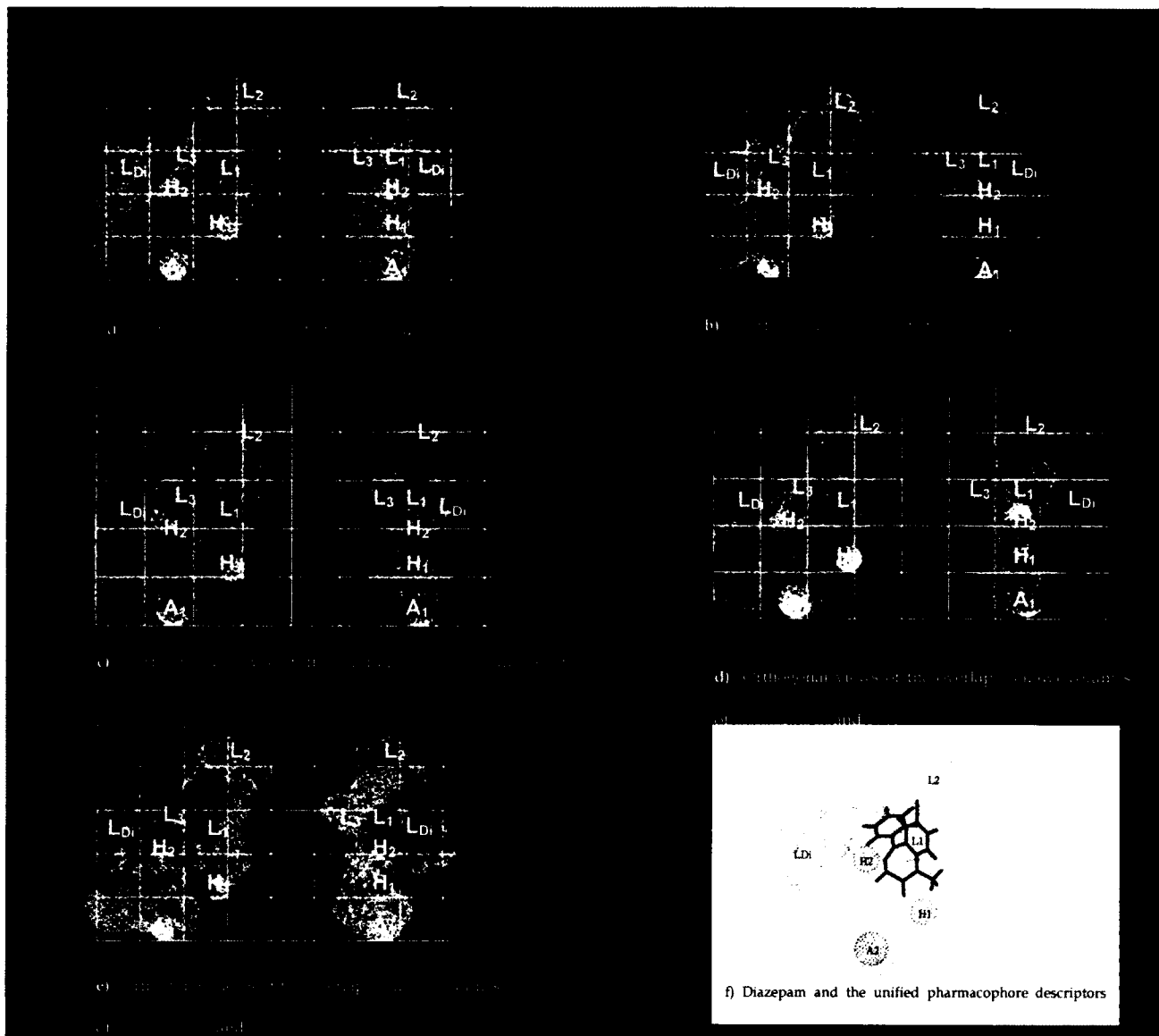


Figure 27. Overlap between pairs of previous included volumes derived from receptor subtype selective ligands:

a) $\alpha 1$ and $\alpha 2$, b) $\alpha 2$ and $\alpha 3$, c) $\alpha 4$ and $\alpha 6$, d) $\alpha 1$ and $\alpha 6$, e) $\alpha 1$ and $\alpha 5$. Yellow color indicates overlapping regions and each grid measures 4 Å in width and height. In order to provide the connection between this figure and other figures, f) shows diazepam and the descriptors of the unified pharmacophore model depicted in the included volume requirement of the $\alpha 1$ subtype ($\alpha 1\beta 3\gamma 2$).

The included volume requirements show some trends that are useful to explain subtype preferences of ligands and that have already guided substance development:

1. *The included volumes of the $\alpha 1$, $\alpha 2$ and $\alpha 3$ subtypes are similar both in size and topology.* This is consistent with the similar affinity profiles these subtypes displayed for classical benzodiazepine agonists, pyrazoloquinolinones and imidazobenzodiazepines (*i*-BZDs).^{33, 34, 213} The included volume of the $\alpha 1$ subtype is slightly different from that of $\alpha 2$ and $\alpha 3$ subtype as indicated by the selective affinities of zolpidem, CL-218,872, 6-substituted β -carboline (e.g. 6-methylbenzyl amino betacarboline) and pyridodiindoles for this subtype and the space needed for accommodating these structures (Figure 27 a,b).^{54, 71} Results from both the SAR studies and the included volume analysis imply that the $\alpha 2$ and $\alpha 3$ subtypes are very similar in shape, polarity and lipophilicity.

2. *The included volumes of the $\alpha 1$ and $\alpha 4$ or $\alpha 6$ subtypes are very different.* From examination of Figure 27d, it is evident that the included volume of the $\alpha 6$ subtype is significantly smaller than that of the $\alpha 1$ subtype. Especially the L_{Di} region is much larger in $\alpha 1$ receptors. Contributions to the L_{Di} region are derived in a large measure from 6-substituted β -carboline and ring-A substituted pyrazoloquinolines, thus implying that occupation of the L_{Di} region may be critical for ligand selectivity at the $\alpha 1$ subtype. This is supported by the finding that the L_{Di} region was also larger for the $\alpha 1\beta 3\gamma 2$ subtype when compared with the $\alpha 5\beta 3\gamma 2$ subtype (Figure 27e).

3. *L_3 region is very small or non-existent for the $\alpha 4$ and $\alpha 6$ DI subtypes.* Based on the inability to bind 1,4-benzodiazepines, the lack of region L_3 was believed to be responsible for the diazepam-insensitivity of these receptor subtypes (Figure 27c, d).⁴² With a few exceptions, β -carboline also do not bind to the $\alpha 6\beta 3\gamma 2$ receptor subtype,

while the smaller *i*-BZDs and pyrazoloquinolinones (CGS series) represent the primary ligands that bind to this subtype.

4. *The L_2 and L_{Di} regions are slightly smaller for the $\alpha 6$ versus the $\alpha 4$ subtype.* The sequence of the $\alpha 4$ subunit is most homologous to the $\alpha 6$ subunit and it was determined that the pharmacological profiles of these DI sites toward classical benzodiazepines are very similar.¹⁹⁵ Differences in the included volume of these DI sites are shown in Figure 27c. *The L_2 region contributes to $\alpha 2$ and $\alpha 5$ selectivity.* It has been observed that ligands with $\alpha 2$ and/or $\alpha 5$ selectivity are generally *i*-BZDs and have a lipophilic C(8)-substituent that occupies the L_2 pocket. Based on ligands from various studies, examination of data in Figure 27 illustrates that the L_2 region is deeper and larger for the $\alpha 2$ and $\alpha 5$ subtypes, respectively, than for the corresponding $\alpha 1$ or $\alpha 6$ subtypes.^{196, 215, 216}

5. This L_2 region seems to account for the selective affinity of ligands at the $\alpha 5$ subtype, as clearly illustrated in Figure 27e, whereas the same region may account for the selective efficacy observed at the $\alpha 2$ subtype. The L_2 region in the $\alpha 5$ subtype is larger than the $\alpha 1$ subtypes. This is a key result. It is the principle difference between $\alpha 5$ subtypes compared to $\alpha 2$ and $\alpha 3$ subtypes, but especially in regard to $\alpha 1$ subtypes (L_2 smaller in $\alpha 1$).

6. The L_3 region is larger in the $\alpha 5$ subtype as compared to the $\alpha 1$, $\alpha 2$, $\alpha 3$, $\alpha 4$ and $\alpha 6$ BzR sites. R analogs of benzodiazepines with pendant phenyls had increased affinity to $\alpha 5$ supporting the larger L_3 pocket in this receptor subtype, while S isomers bound to $\alpha 2$, $\alpha 3$, and $\alpha 5$ subtypes because of different conformational constraints.

Recent Discovery of Alpha 5 Volume Differences

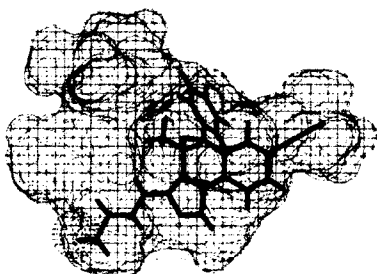
In regard to molecular modeling, depicted in Figure 29 is the included volume and ligand occupation of the SH-053-2'F-S-CH₃ and SH-053-2'F-R-CH₃ enantiomers in the α 5 subtype as well as the α 2 subtype. It is clear a new pocket (L₄), has been located in the α 5 subtype permitting the 2'F(R)-isomer (**94R**) as well as the 2'F(S)-isomer (**94S**) to bind to the α 5 subtype. Examination of both ligands in the α 2 subtype clearly illustrates the analogous region in the α 2 subtype is not present and thus does not accommodate the 2'F(**R**)-isomer(**94R**) for the pendant phenyl lies outside of the included volume in the space allocated for the receptor protein itself.



SH-053-2'F-S-CH3 fits to the pharmacophore in the included volume of the alpha 2 subtype



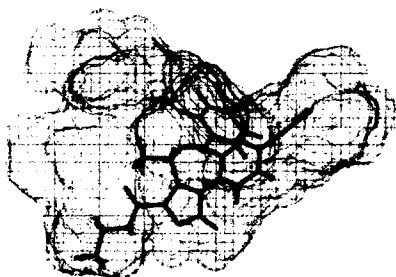
The same image of figure rotated 90°. It can be clearly seen that the molecule fits within the included volume



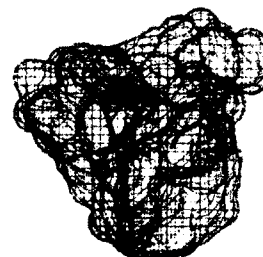
SH-053-2'F-R-CH3 does not fit the pharmacophore in the included volume of the alpha 2 subtype



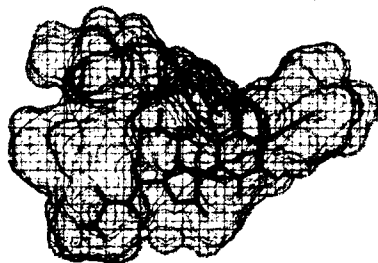
The same image of figure rotated 90°. It can be clearly seen that the conformation of the molecule is such that the pendant 6-phenyl sticks outside the included volume



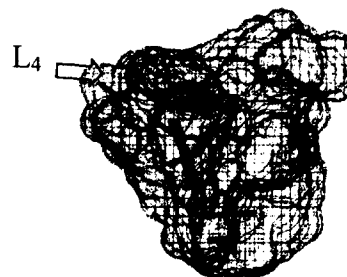
SH-053-2'F-S-CH3 fits the pharmacophore in the included volume of the alpha 5 subtype



The same image of figure rotated 90°. It can be clearly seen that the molecule fits within the included volume



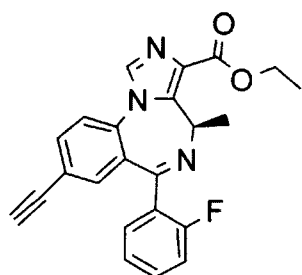
SH-053-2'F-R-CH3 fits the pharmacophore in the included volume of the alpha 5 subtype



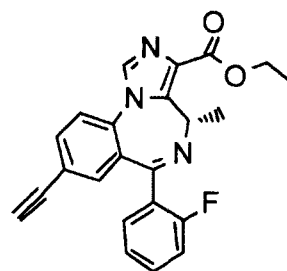
The same image of figure rotated 90°. It can be clearly seen that the molecule fits within the included volume.

Figure 28. Included volume and ligand occupation of the SH-053-2'F-S-CH3 and SH-053-2'F-R-CH3 enantiomers in the $\alpha 5$ and $\alpha 2$ BzR subtypes

Table 17. Binding affinity at $\alpha\beta\gamma 2$ GABA(A) receptor subtypes (values are reported in nM)



SH-053-2'F-R-CH3



SH-053-2'F-S-CH3

Compound	$\alpha 1$	$\alpha 2$	$\alpha 3$	$\alpha 4$	$\alpha 5$	$\alpha 6$
SH-053-R-CH3	2026	2377	1183	>5000	949.1	>5000
SH-053-S-CH3	1666	1263	1249	>5000	206.4	>5000
SH-053-2'F-R-CH3	759.1	948.2	768.8	>5000	95.17	>5000
SH-053-2'F-S-CH3	350	141	1237	>5000	19.2	>5000

Based on this analysis a series of (S) and (R) isomers have been synthesized. The functional selectivity of these ligands was determined by Sieghart et al.⁴⁶ and will be

discussed in Part II. From examination of Figure 28 and Table 17, it is clear the (R)-isomers bound to the $\alpha 5$ subtype while the (S)-isomers were selective for $\alpha 2/\alpha 3/\alpha 5$ subtypes. Work is in progress to determine the *in vitro* potency and *in vivo* pharmacology of the functionally selective (S) and (R) enantiomeric ligands. It is clear, as postulated earlier,²¹⁷ that the major difference in GABA(A) /Bz receptors subtypes stems from differences in asymmetry in the lipophilic pockets L_1 , L_2 , L_3 , L_4 , and L_{Di} in the pharmacophore/receptor model and indicates even better functional selectivity is possible with asymmetric BzR ligands.

The synthetic switching of chirality at the C-4 position of imidazo benzodiazepines to induce subtype selectivity was successful. Moreover, increase of the potency of imidazobenzodiazepines can be achieved by substitution of the 2'-position hydrogen atom with an electron rich atom (fluorine) on the pendant phenyl ring in agreement with Haefly,²¹⁸⁻²²⁰ Fryer,²²¹ and our own work.²²² The biological data on the two enantiomer pairs of benzodiazepine ligands confirm the ataxic activity of BZ site agonists is mediated by $\alpha 1\beta 2/3\gamma 2$ subtypes, as reported.^{222, 223} The anti-anxiety activity of the S isomers was preserved, whereas the confounding sedation was observed in both S isomers (functionally selective for $\alpha 2$, $\alpha 3$ and $\alpha 5$ receptor subtypes) and R isomers (essentially selective for $\alpha 5$ subtype), and appears to involve at least in part agonist activity at $\alpha 5$ BzR subtypes. There are some $\alpha 5$ BzR located in the spinal cord which might be the source of the decrease in locomotion with SH-053-2'F-R-CH₃ and SH-053-2'F-S-CH₃. Hence, in agreement, with many laboratories including our own^{224, 225} that the best potential nonsedative, nonamnesic, antianxiety agents stem from ligands with

agonist efficacy at $\alpha 2$ and $\alpha 3$ subtypes essentially silent at $\alpha 1$ and $\alpha 5$ subtypes (to avoid sedation).^{72, 226}

Structure-activity relationship (SAR) studies have been carried out by a number of research groups on structurally diverse classes of ligands, and have resulted in the formulation of several different pharmacophore/receptor models for the benzodiazepine receptor.¹⁹⁶ Models which attempt to explain ligand efficacy as a function of ligand-receptor interaction at the molecular level have been put forth by Loew,²²⁷ Crippen,²²⁸ Coddington,²²⁹ Fryer,^{33, 34, 68-70, 74, 75, 146, 230-235} Gilli and Borea,^{33, 34} Wermuth,^{33, 34, 68-70, 74, 75, 146, 230-235} and Gardner,^{33, 34} as well as from our own laboratory.^{73, 236}

A comprehensive pharmacophore/receptor model for the BzR was developed using the techniques of chemical synthesis, radioligand binding and receptor mapping.^{19, 71, 73, 169, 170, 237, 238} The model unified the previous models for inverse agonist/antagonist and agonist activity as well as included the recent model for the “diazepam-insensitive” (DI) sites.²³⁹ This unified pharmacophore/receptor model was employed to include agonist, antagonist, and inverse agonist ligands, which encompassed 12 families of structurally diverse ligands (Figure 70).⁷⁵ Four basic anchor points, H₁, H₂, A₂, and L₁, were assigned, and 3 additional lipophilic regions were defined as L₂, L₃, and L_{Di} (see captions in Figure 70 for details); regions S₁, S₂ and S₃ represent negative areas of steric repulsion. As previously reported, the synthesis of both partial agonists and partial inverse agonists has been achieved by using parts of this model.^{62, 72, 170, 226, 240-244}

The cloning, expression and anatomical localization of multiple GABA(A) subunits has facilitated both the identification and design of subtype selective compounds. With the availability of binding data from different recombinant receptor

subtypes, affinities of ligands from a number of different structural classes of ligands have been evaluated.

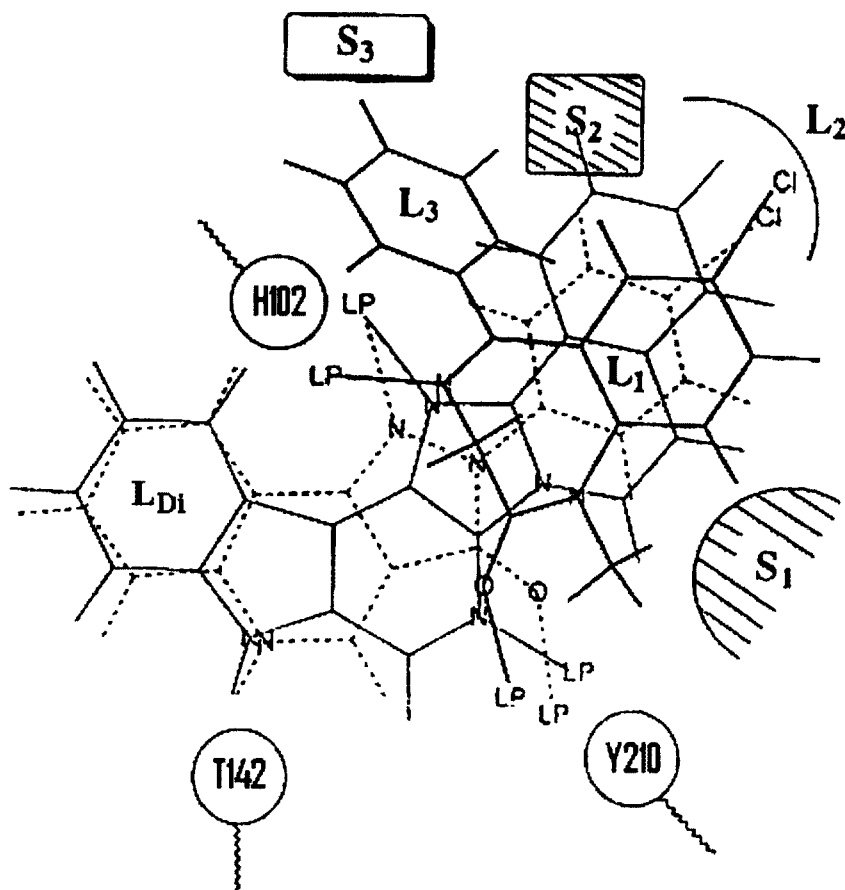


Figure 29. The Milwaukee-based unified pharmacophore

Illustrated in Figure 29 is the pyrazolo[3,4-*c*]quinolin-3-one CGS-9896 (**96**) (dotted line), a diazadiindole (**95**) (thin line), and diazepam (thick line) fitted to the inclusive pharmacophore model for the BzR. Sites H₁ (Y210) and H₂ (H102) represent hydrogen bond donor sites on the receptor protein complex while A₂ (T142) represents a hydrogen bond acceptor site necessary for potent inverse activity *in vivo*. L₁, L₂, L₃ and

L_{Di} are four lipophilic regions in the binding pharmacophore. Descriptors S₁, S₂, and S₃ are regions of negative steric repulsion.

Based on SAR data obtained for these ligands at 6 recombinant BzR subtypes,²⁴⁵⁻²⁴⁹ an effort has been made to establish different pharmacophore/receptor models for BzR subtypes. The alignment of the twelve different structural classes of benzodiazepine receptor ligands was based on the least squares fitting of at least three points. The coordinates of the four anchor points (A₂, H₁, H₂ and L₁) employed in the alignment are outlined in Figure 30. Herein are described the results from ligand-mapping experiments at recombinant BzR subtypes of 1,4-benzodiazepines, imidazobenzodiazepines, β -carbolines, diindoles, pyrazoloquinolinones, and others.²⁵⁰ Some of the differences and similarities among these subtypes can be gleaned from this study and serve as a guide for future drug design.

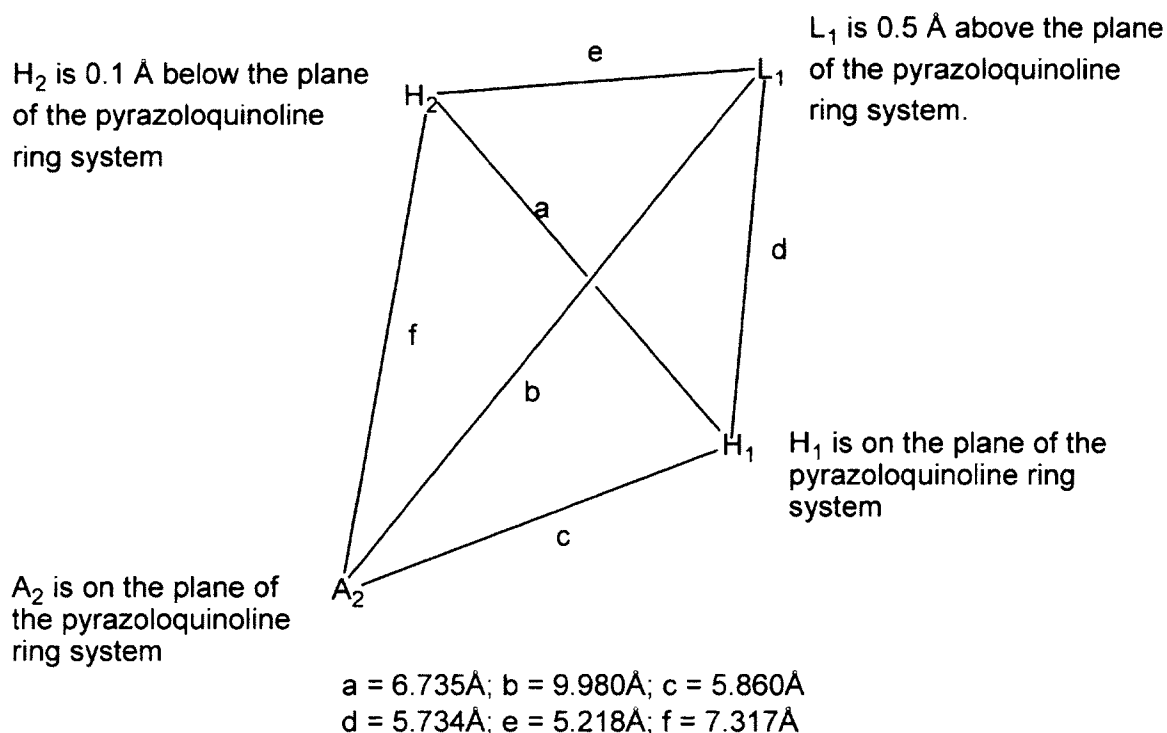


Figure 30. The schematic representation of the descriptors for the inclusive BzR pharmacophore.²⁵¹

Computer Modeling Methods

The core structures of the ligands used to build the pharmacophore and included volume were taken from available x-ray crystallographic coordinates or generated using the SYBYL fragment library.²⁵² The structures which resulted were energy minimized using MM2 (molecular mechanics program 2) or MMFF (Merck molecular force field) force fields.²⁵³⁻²⁵⁶ The subsequent Monte Carlo conformational searches were carried out on MacroModel 4.5 or MacroModel 6.0^{25, 257} on a Silicon Graphics Personal Iris 4D/35 workstation or a Silicon Graphics Octane SI 2P 175 R10000 workstation, respectively. MM2 is a force field developed for hydrocarbons and is the force field of choice for determination of the energies and structures of hydrocarbons.

Recently, the laboratory upgraded to the Linux version of Sybyl 8.1 and ran on RedHat 4.0 Enterprise. On the newer platform, structures were minimized using Tripos force fields. The low energy conformations were then fully optimized *via* molecular orbital calculations at the 3-21G basis set with torsional angles fixed. The structures which resulted were further calibrated with 6-31G* single point calculations at an "SCF=TIGHT" convergence criteria *via* Gaussian 92²⁵⁸ on a Silicon Graphics Indigo² R4400 workstation, or Gaussian 94⁶⁵ on a Silicon Graphics Octane SI2P175R10000 workstation. With ligands containing heavy atoms (bromine or iodine), the necessary 6-31G* basis sets were not included in the commercially available Gaussian 92 and Gaussian 94 programs. These basis sets were taken from splitting the MP4 basis set reported by Andzelm *et al.* and then addition of d functions.⁴⁶

The available *ab initio* 6-31G* geometries of the ligands were used for the included volume analysis. Ligands which possessed BzR affinities of ≤ 20 nM at one recombinant receptor subtype were considered as "active" and used for the included volume analysis for that subtype. Zolpidem, CL 218872 and ligands reported to be more selective for one subtype⁶⁵ were included even though the binding affinities were somewhat higher than 20 nM. Currently the molecular graphics, root-mean-squares (RMS) fit, calculations of centroids of substructures and included volume analyses were carried out by means of SYBYL 6.5⁶⁵ on a Silicon Graphics Octane SI 2P 175 R10000 workstation or Sybyl 8.1 operating on a Dell Vostro 1720. The lengths of hydrogen bond extension vectors (HBV) were set to 1.84 Å, while the C-N-HBV and C=O-HBV valence angles used were chosen to mimic the geometry of an ideal hydrogen bond.

The Updated Included Volume Analysis Models

Illustrated in Figure 32 is the included volume of the updated pharmacophore receptor model of the $\alpha 1\beta 3\gamma 2$ subtype of Clayton et al. The current model for the $\alpha 1\beta 3\gamma 2$ subtype has new features. The cyclopropyl group of CD-214 extended 2 Å past the A₂ descriptor slightly increasing its volume. The trimethylsilyl group of QH-II-82 and WYS7 illustrate how bulky groups are tolerated near the entrance of the binding pocket. Although not as potent, dimers of beta carbolines, WYS2 and WYS6 bound at 30 nm and 120 nm respectively. Their ability to bind, albeit weakly, supports the location of the binding site entrance. The included volume of the $\alpha 1\beta 3\gamma 2$ was previously 1085.7 cubic Angstroms. The volume has now been measured as 1219.2 cubic angstroms. Volume measurements should be used carefully as the binding site is not enclosed and the theoretical opening near L_{DI} is not clearly demarcated. Dimers were excluded from the included volume exercise because although they bound to the receptor, they represented compounds which were felt to extend outside the receptor binding pocket when docked to the protein. Where appropriate, their monomers were included in the included volume analysis. Ligands considered for the included volume in Table 18 exhibited potent binding at $\alpha 1$ subtypes ($K_i \leq 20$ nM) but were not necessarily subtype selective.

The $\alpha 1\beta 3\gamma 2$ Receptor Subtype

Table 18. Ligands with potent affinity for $\alpha 1$; ligands bound with K_i values <20 nm at this subtype

<i>COOK CODE^a</i>	<i>$\alpha 1$</i>	<i>$\alpha 2$</i>	<i>$\alpha 3$</i>	<i>$\alpha 4$</i>	<i>$\alpha 5$</i>	<i>$\alpha 6$</i>
WY-TSC-4(WYS8)	0.007	0.99	1.63		51.04	

<i>COOK CODE^a</i>	$\alpha 1$	$\alpha 2$	$\alpha 3$	$\alpha 4$	$\alpha 5$	$\alpha 6$
SH-TSC-2(BCCT)	0.03	0.0419	0.035		69.32	
QH-II-090(CGS-8216)	0.05	0.08	0.12		0.25	17
XLI-286	0.051	0.064	0.118		0.684	
QH-II-077	0.06	0.08	0.05		0.12	4
QH-II-092	0.07	0.03	0.04	ND	0.17	ND
JYI-57	0.076	0.076	0.131	ND	0.036	ND
QH-II-085	0.08	0.06	0.02	ND	0.08	ND
XHE-II-024	0.09	0.18	0.32	14	0.24	11
PWZ-007A	0.11	0.1	0.09	ND	0.2	10
CGS8216	0.13	ND	ND	ND	ND	46
SPH-121	0.14	1.19	1.72	ND	4	479
QH-II-075	0.18	0.21	0.25	ND	1.3	40
PZII-028	0.2	ND	0.2	ND	0.32	1.9
CGS9895	0.21	ND	ND	ND	ND	9.3
PWZ-0071	0.23	0.17	0.12	ND	0.44	17.31
XHE-III-24	0.25	ND	8	222	10	328
JYI-42	0.257	0.146	0.278	ND	0.256	ND
CGS9896	0.28	ND	ND	ND	ND	181
JYI-64 (C17H12N4FBr)	0.305	1.111	0.62	ND	0.87	5000
PZII-029	0.34	ND	0.79	ND	0.52	10
BRETAZENIL	0.35	0.64	0.2	ND	0.5	12.7
FG8205	0.4	2.08	1.16	ND	1.54	227
YT-5	0.421	0.6034	36.06	ND	1.695	ND
6-PBC	0.49	1.21	2.2	ND	2.39	1343

<i>COOK CODE^a</i>	<i>$\alpha 1$</i>	<i>$\alpha 2$</i>	<i>$\alpha 3$</i>	<i>$\alpha 4$</i>	<i>$\alpha 5$</i>	<i>$\alpha 6$</i>
QH-146	0.49	ND	0.76	ND	7.7	10000
DM-II-90 (C17H12N4BrCl)	0.505	1	0.63	ND	0.37	5000
SPH-165	0.63	2.79	4.85	ND	10.4	1150
BCCt	0.72	15	18.9	ND	110.8	5000
SH-I-048A	0.774	0.1723	0.383	ND	0.11	ND
alprazolam	0.8	0.59	1.43	ND	1.54	10000
Ro15-1788	0.8	0.9	1.05	ND	0.6	148
WYS10 C14H9F3N2O2	0.88	36	25.6	ND	548.7	15.3
WY-B-15	0.92	0.83	0.58	2080	4.42	646
WY-A-99-2(WYS8)	0.972	111	102	2000	208	1980
XHE-III-06a	1	2	1	5	1.8	37
Xli366 C22H21N3O2	1	ND	ND	ND	ND	ND
JYI-59 (C22H13N3O2F4)	1.08	2.6	11.82	ND	11.5	5000
WYSC1 C16H16N2O2	1.094	5.44	12.3	ND	69.8	21.2
MLT-I-70	1.1	1.2	1.1	ND	40.3	1000
SVO-8-30	1.1	5.3	5.3	2.8	0.6	15
BCCE	1.2	4.9	5.7	ND	26.8	2700
XHE-III-04	1.2	2	1.1	219	0.4	500
XLi350 C17H11ClN2O	1.224	1.188	ND	ND	2.9	ND
XHE-III-49	1.3	5.5	4.2	38.7	11.3	85.1
PWZ-009A1	1.34	1.31	1.26	ND	0.84	2.03
DM-239	1.5	ND	0.53	ND	0.14	6.89

<i>COOK CODE^a</i>	<i>$\alpha 1$</i>	<i>$\alpha 2$</i>	<i>$\alpha 3$</i>	<i>$\alpha 4$</i>	<i>$\alpha 5$</i>	<i>$\alpha 6$</i>
XLi351 C21H21ClN2OSi	1.507	0.967	ND	ND	1.985	ND
XLi352 C18H13ClN2O	1.56	0.991	ND	ND	1.957	ND
TG-4-39	1.6	34	24	5.6	1.4	23
TG-II-82	1.6	2.9	2.8	ND	1	1000
CM-A87	1.62	4.54	14.73	1000	4.61	1000
QH-II-082	1.7	1.8	1.6	ND	6.1	100
JYI-49 (C20H12N3O2F4Br)	1.87	2.38	ND	ND	6.7	3390
LJD-III-15E	1.93	14	19	ND	70.8	1000
SPH-38	2	5.4	10.8	ND	18.5	3000
XHE-I-093	2	7.1	8.9	1107	20	1162
MSA-IV-35	2.1	16	21	ND	995	3000
JYI-19 (C23H23N3O3S)	2.176	205	ND	ND	34	12.7
FLUNITRAZEPAM	2.2	2.5	4.5	ND	2.1	2000
YCT-5	2.2	11.46	16.3	ND	200	10000
TJH-IV-51	2.39	17.4	14.5	ND	316	10000
WYS13 C20H18N2O3	2.442	13	27.5	ND	163	5000
YT-III-25	2.531	5.786	5.691	ND	0.095	ND
XHE-III-14	2.6		10	13	2	7
WYS9 C16H15IN2O2	2.72	22.2	23.1	ND	562	122
JYI-47	2.759	2.282	0.511	ND	0.427	ND
CM-A82a	2.78	8.93	24.51	1000	7.49	1000
TG-4-29	2.8	3.9	2.7	2.1	0.18	3.9

<i>COOK CODE^a</i>	$\alpha 1$	$\alpha 2$	$\alpha 3$	$\alpha 4$	$\alpha 5$	$\alpha 6$
XLi268 C17H13BrN4	2.8145	0.6862	ND	ND	0.6243	ND
JYI-54 (C24H15N3O3F4)	2.89	172	6.7	ND	57	1890
MMB-II-74	3	24.5	41.7	500	125.7	1000
MMB-III-016	3	1.97	2	1074	0.26	211
MMB-III-16	3	1.97	2	1074	0.26	211
QH-II-080b	3	3.7	4.7	ND	24	1000
YCT-7A	3	23.8	30.5	ND	240	10000
JYI-32 (C20H15N3O2BrF)	3.07	4.96	ND	ND	2.92	52.24
Ro15-4513	3.3	2.6	2.5	ND	0.26	3.8
XHE-II-017	3.3	10	7	258	17	294
XLi-JY-DMH ANX3	3.3	0.58	1.9	ND	4.4	5000
MLT-II-18	3.4	11.7	11	ND	225	10000
TJH-V-88	3.41		30	ND	140.9	10000
XLI-2TC	3.442	1.673	44.08	ND	1.121	
WYS15 C22H20N2O2	3.63	2.02	44.3	ND	76.5	5000
CM-A57	3.7	27	40	ND	254	1000
XHE-II-006b	3.7	15	12	1897	144	1000
JYI-60 (C17H11N2OF)	3.73	1.635	4.3	ND	1.7	5000
RY-008	3.75	7.2	4.14	ND	1.11	44.3
MLT-II-18	3.9	12.2	24.4	ND	210	10000
OMB-18	3.9	1.2	3.4	1733	0.8	5
WY-B-09-1	3.99	8	32	1000	461	2000

<i>COOK CODE^a</i>	$\alpha 1$	$\alpha 2$	$\alpha 3$	$\alpha 4$	$\alpha 5$	$\alpha 6$
SHU-1-19	4	12	7	48	14	84
ZK 93423	4.1	4.2	6	ND	4.5	1000
WY-B-23-2(WYS11)	4.2	37.7	39	2000	176	69.4
WY-B-23-2(WYS11)	4.2	37.7	73	ND	176	69.4
WY-B-99-1	4.4	4.5	5.58	2000	47	2000
WY-B-26-2	4.45	44.57	42.66	2000	124	2000
XHE-II-006a	4.7	4.4	20	1876	89	3531
CM-B01	4.8	31	34	1000	286	1000
PWZ-085	4.86	13	8.5	ND	0.55	40
MLT-II-16	5.05	10.41	18.4	ND	260	10000
3 PBC	5.3	52.3	68.8	ND	591	1000
MA-3-PROPOXYL	5.3	52.3	68.8	ND	591	1000
TJH-IV-43	5.42	30.19	48.9	ND	475	10000
DMCM	5.69	8.29	4	ND	1.04	134
DM-139	5.8	ND	169	ND	9.25	325
XHE-II-073A (R ENRICHED)	5.9	11	10	15	1.18	140
MSR-I-032	6.2	18.7	4	ND	3.3	74.9
JYI-70 (C19H13N4F)	6.3	2.1	ND	ND	0.56	5000
XLi343 C20H19CIN2OSi	6.375	17.71	ND	ND	150.5	ND
3 EBC	6.43	25.1	28.2	ND	826	1000
DM-146	6.44	ND	148	ND	4.23	247
DM-215	6.74	ND	7.42	ND	0.293	8.28
ZG69A	6.8	16.3	9.2	ND	0.85	54.6

<i>COOK CODE^a</i>	$\alpha 1$	$\alpha 2$	$\alpha 3$	$\alpha 4$	$\alpha 5$	$\alpha 6$
ZG-69a(Ro15-1310)	6.8	16.3	9.2	ND	0.85	54.6
WY-B-14(WYS7)	6.84	30	36	2000	108	1000
YT-II	6.932	0.8712	3.518	ND	5.119	ND
SVO-8-67	7	41	26	15	2.3	191
MLT-II-34	7.04	15.95	22.3	ND	158	1000
SPH-195	7.2	168.5	283.5	ND	271	10000
XHE-I-065	7.2	17	18	500	57	500
ZG-234	7.25	22.14	9.84	ND	0.3	5.25
SH-I-04	7.3	6.136	5.1	ND	7.664	ND
XHE-I-038	7.3	5	34	ND	132	1000
XHE-III-13	7.3	ND	7.1	880	1.6	311
WY-B-25	7.6	40	66	2000	263	2000
CM-A49(R)	7.7	32.5	43	ND	69	1000
SVO-8-14	8	25	8	6.9	0.9	14
TG-4-29	8.3	10.2	6.9	ND	0.4	7.61
XHE-II-002	8.3	18	13	3.9	1.5	11
WY-B-14(WYS7)	8.5	165	245	ND	1786	5000
XHE-II-011	9	60	39	3233	90	1000
WY-B-27-2	9.19	111	72	2000	449	2000
QH-II-063	9.4	9.3	31	ND	7.7	3000
JC184 C13H9BrN2OS	9.606	10.5	ND	ND	6.709	ND
ZG-208	9.7	11.2	10.9	ND	0.38	4.6
RY-I-31	10	45	19	ND	6	1000
WY-B-23-1	10	33	43	1000	189	2000
RY-098	10.1	22.2	16.5	ND	1.68	100

<i>COOK CODE^a</i>	$\alpha 1$	$\alpha 2$	$\alpha 3$	$\alpha 4$	$\alpha 5$	$\alpha 6$
H _z 148 C ₁₈ H ₁₅ N ₃	10.98	5000	ND	ND	256	5000
SVO-8-20	11	40	28	19	8.6	138
XHE-II-073B (S-ENRICHED)	11	17	12	33	2.1	269
SH-I-085	11.08	4.866	13.75	ND	0.24	ND
PWZ-096	11.1	36	16.9	ND	1.07	51.5
ZG-168	11.2	10.7	9.2	ND	0.47	9.4
CM-A77	11.51	51.9	105.16	1000	42.62	1000
WY-B-20	12	39	47	2000	122	3000
ABECARNIL	12.4	15.3	7.5	ND	6	1000
SH-I-89S	12.78	8.562	8.145	ND	3.23	ND
ZG-213	12.8	49.8	30.2	ND	3.5	22.5
EDC-I-071	12.9	83.1	ND	ND	314	5000
MMB-III-14	13	13	6.9	333	1.1	333
DM-173	13.1	ND	38.1	ND	0.78	118
XLI-348	13.56	11.17	1.578	ND	82.05	ND
EDC-I-093	13.6	423	ND	ND	2912	5000
diazepam	14	20	15	ND	11	ND
XLi223 C ₂₂ H ₂₀ BrN ₃ O ₂	14	8.7	18	1000	10	2000
WYSC2 C ₁₅ H ₁₁ F ₃ N ₂ O ₂	14.14	113	170	ND	518	61.2
SH-I-030	14.42	11.04	19.09	ND	1.89	ND
CM-A100	14.49	44.91	123.8	1000	65.31	1000
RY-033	14.8	56	25.3	ND	1.72	22.9
HJ-I-037	15.07	8.127	28.29	ND	0.818	ND
YT-6	15.31	87.8	60.49	ND	1.039	ND

<i>COOK CODE^a</i>	<i>$\alpha 1$</i>	<i>$\alpha 2$</i>	<i>$\alpha 3$</i>	<i>$\alpha 4$</i>	<i>$\alpha 5$</i>	<i>$\alpha 6$</i>
EDC-II-044	15.4	ND	293	ND	323	1000
CM-A58	16	120	184	ND	1000	1012
QH-II-067a	16	31	52	ND	199	3000
CD-214	16.4	48.2	42.5	ND	9.8	168
JYI-06 (C23H23N3O4)	16.5	5.48	5000	ND	12.6	5000
CM-A50(S)	17	59	88	ND	144	1000
RY-061	17	13	6.7	ND	0.3	31
ZG-224	17.1	33.7	50	ND	2.5	30.7
ZG-63A	17.3	21.6	29.1	ND	0.65	4
DM-II-30 (C20H13N3O2BrF3)	17.6	13.4	28.51	ND	7.8	5000
CM-A64	18	60	116	ND	216	1000
RY-071	19	56	91	ND	7.2	266
WZ-113	19.2	13.2	13.4	ND	11.5	300
YT-III-23	19.83	23.65	19.87	ND	1.105	ND
CM-E09b	20	22	19	55	0.45	69
MMB-II-90	20	24	5.7	9	0.25	36

^aAffinity of compounds at GABA(A) /BzR recombinant subtypes was measured by competition for [³H]flunitrazepam or [³H] Ro15-4513 binding to HEK cell membranes expressing human receptors of composition $\alpha 1\beta 3\gamma 2$, $\alpha 2\beta 3\gamma 2$, $\alpha 3\beta 3\gamma 2$, $\alpha 4\beta 3\gamma 2$, $\alpha 5\beta 3\gamma 2$ and $\alpha 6\beta 3\gamma 2$.⁶⁵ Data represent the average of at least three determinations with a SEM of $\pm 5\%$.

As the focus of our research was aimed at diazepam sensitive receptors, additional features to the $\alpha 4\beta 3\gamma 2$ and $\alpha 6\beta 3\gamma 2$ receptors were not identified. The major new feature

identified for the $\alpha 5\beta 3\gamma 2$ receptor was a new L_4 pocket. This new lipophilic pocket was identified with R and S chiral analogs of SH-053.⁶⁵

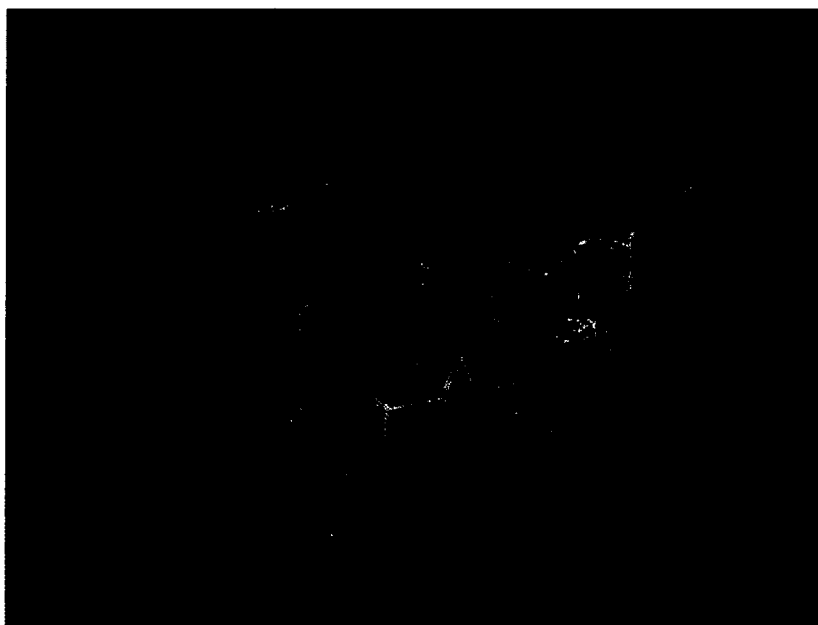


Figure 31. Overlay of selected compounds for $\alpha 1\beta 3\gamma 2$ subtype from Table 8



Figure 32. Updated $\alpha1\beta3\gamma2$ subtype (solid) overlayed with the previous model (line).

The $\alpha2\beta3\gamma2$ Receptor Subtype

Table 19. Ligands with potent affinity for $\alpha2$; ligands bound with K_i values <20 nM at this subtype

<i>COOK CODE^a</i>	$\alpha1$	$\alpha2$	$\alpha3$	$\alpha4$	$\alpha5$	$\alpha6$
QH-II-092	0.07	0.03	0.04	ND	0.17	ND
SH-TSC-2(BCCT)	0.03	0.0419	0.035	ND	69.32	ND
QH-II-085	0.08	0.06	0.02	ND	0.08	ND
XLI-286	0.051	0.064	0.118	ND	0.684	ND
JYI-57	0.076	0.076	0.131	ND	0.036	ND
QH-II-090(CGS-8216)	0.05	0.08	0.12	ND	0.25	17
QH-II-077	0.06	0.08	0.05	ND	0.12	4
PWZ-007A	0.11	0.1	0.09	ND	0.2	10
JYI-42	0.257	0.146	0.278	ND	0.256	ND

<i>COOK CODE^a</i>	$\alpha 1$	$\alpha 2$	$\alpha 3$	$\alpha 4$	$\alpha 5$	$\alpha 6$
PWZ-0071	0.23	0.17	0.12	ND	0.44	17.31
SH-I-048A	0.774	0.1723	0.383	ND	0.11	ND
XHE-II-024	0.09	0.18	0.32	14	0.24	11
QH-II-075	0.18	0.21	0.25	ND	1.3	40
XLi-JY-DMH ANX3	3.3	0.58	1.9	ND	4.4	5000
alprazolam	0.8	0.59	1.43	ND	1.54	10000
YT-5	0.421	0.6034	36.06	ND	1.695	ND
BRETAZENIL	0.35	0.64	0.2	ND	0.5	12.7
XLi268 C17H13BrN4	2.8145	0.6862	ND	ND	0.6243	ND
WY-B-15	0.92	0.83	0.58	2080	4.42	646
YT-II	6.932	0.8712	3.518	ND	5.119	
Ro15-1788	0.8	0.9	1.05	ND	0.6	148
XLi351 C21H21ClN2OSi	1.507	0.967	ND	ND	1.985	ND
WY-TSC-4(WYS8)	0.007	0.99	1.63	ND	51.04	ND
XLi352 C18H13ClN2O	1.56	0.991	ND	ND	1.957	ND
DM-II-90 (C17H12N4BrCl)	0.505	1	0.63	ND	0.37	5000
JYI-64 (C17H12N4FBr)	0.305	1.111	0.62	ND	0.87	5000
XLi350 C17H11ClN2O	1.224	1.188	ND	ND	2.9	ND
SPH-121	0.14	1.19	1.72	ND	4	479
MLT-I-70	1.1	1.2	1.1	ND	40.3	1000
OMB-18	3.9	1.2	3.4	1733	0.8	5

<i>COOK CODE^a</i>	<i>$\alpha 1$</i>	<i>$\alpha 2$</i>	<i>$\alpha 3$</i>	<i>$\alpha 4$</i>	<i>$\alpha 5$</i>	<i>$\alpha 6$</i>
6-PBC	0.49	1.21	2.2	ND	2.39	1343
YT-III-271	32.54	1.26	2.35	ND	103	ND
PWZ-009A1	1.34	1.31	1.26	ND	0.84	2.03
DM-II-72 (C15H10N20BrCl)	5000	1.37	ND	ND	2.02	5000
JYI-60 (C17H11N2OF)	3.73	1.635	4.3	ND	1.7	5000
XLI-2TC	3.442	1.673	44.08	ND	1.121	ND
QH-II-082	1.7	1.8	1.6	ND	6.1	100
TC-YT-II-76	101.1	1.897	5.816	ND	11.99	ND
MMB-III-016	3	1.97	2	1074	0.26	211
MMB-III-16	3	1.97	2	1074	0.26	211
XHE-III-06a	1	2	1	5	1.8	37
XHE-III-04	1.2	2	1.1	219	0.4	500
WYS15 C22H20N2O2	3.63	2.02	44.3	ND	76.5	5000
FG8205	0.4	2.08	1.16	ND	1.54	227
JYI-70 (C19H13N4F)	6.3	2.1	ND	ND	0.56	5000
JYI-47	2.759	2.282	0.511	ND	0.427	ND
JYI-49 (C20H12N3O2F4Br)	1.87	2.38	ND	ND	6.7	3390
FLUNITRAZEPAM	2.2	2.5	4.5	ND	2.1	2000
JYI-59 (C22H13N3O2F4)	1.08	2.6	11.82	ND	11.5	5000
Ro15-4513	3.3	2.6	2.5	ND	0.26	3.8
SPH-165	0.63	2.79	4.85	ND	10.4	1150
YT-II-76	95.34	2.797	0.056	ND	0.04	ND

<i>COOK CODE^a</i>	<i>$\alpha 1$</i>	<i>$\alpha 2$</i>	<i>$\alpha 3$</i>	<i>$\alpha 4$</i>	<i>$\alpha 5$</i>	<i>$\alpha 6$</i>
TG-II-82	1.6	2.9	2.8	ND	1	1000
QH-II-080b	3	3.7	4.7	ND	24	1000
TG-4-29	2.8	3.9	2.7	2.1	0.18	3.9
PS-1-34B C20H17N4BrO	ND	4.198	3.928	ND	ND	ND
ZK 93423	4.1	4.2	6	ND	4.5	1000
XHE-II-006a	4.7	4.4	20	1876	89	3531
WY-B-99-1	4.4	4.5	5.58	2000	47	2000
CM-A87	1.62	4.54	14.73	1000	4.61	1000
OMB-19	22	4.6	20	3333	3.5	40
SH-I-085	11.08	4.866	13.75	ND	0.24	ND
BCCE	1.2	4.9	5.7	ND	26.8	2700
JYI-32 (C20H15N3O2BrF)	3.07	4.96	ND	ND	2.92	52.24
XHE-I-038	7.3	5	34	ND	132	1000
SVO-8-30	1.1	5.3	5.3	2.8	0.6	15
SPH-38	2	5.4	10.8	ND	18.5	3000
WYSC1 C16H16N2O2	1.094	5.44	12.3	ND	69.8	21.2
JYI-06 (C23H23N3O4)	16.5	5.48	5000	ND	12.6	5000
XHE-III-49	1.3	5.5	4.2	38.7	11.3	85.1
YT-III-25	2.531	5.786	5.691	ND	0.095	ND
SH-I-04	7.3	6.136	5.1	ND	7.664	ND
XHE-I-093	2	7.1	8.9	1107	20	1162
RY-008	3.75	7.2	4.14	ND	1.11	44.3
DMH-D-053 (C43H30N6O4)	236	7.4	272	5000	194.2	5000

<i>COOK CODE^a</i>	<i>$\alpha 1$</i>	<i>$\alpha 2$</i>	<i>$\alpha 3$</i>	<i>$\alpha 4$</i>	<i>$\alpha 5$</i>	<i>$\alpha 6$</i>
WY-B-09-1	3.99	8	32	1000	461	2000
HJ-I-037	15.07	8.127	28.29	ND	0.818	ND
DMCM	5.69	8.29	4	ND	1.04	134
SH-I-89S	12.78	8.562	8.145	ND	3.23	ND
XLi223 C22H20BrN3O2	14	8.7	18	1000	10	2000
CM-A82a	2.78	8.93	24.51	1000	7.49	1000
QH-II-063	9.4	9.3	31	ND	7.7	3000
	9.4	9.3	31	ND	7.7	3000
XHE-II-017	3.3	10	7	258	17	294
TG-4-29	8.3	10.2	6.9	ND	0.4	7.61
MLT-II-16	5.05	10.41	18.4	ND	260	10000
JC184 C13H9BrN2OS	9.606	10.5	ND	ND	6.709	ND
ZG-168	11.2	10.7	9.2	ND	0.47	9.4
XHE-II-073A (R ENRICHED)	5.9	11	10	15	1.18	140
XLI-8TC	21.52	11.01	2.155	ND	4.059	ND
SH-I-030	14.42	11.04	19.09	ND	1.89	ND
XLI-348	13.56	11.17	1.578	ND	82.05	ND
ZG-208	9.7	11.2	10.9	ND	0.38	4.6
YT-TC-3	141.4	11.43	118.1	ND	29.22	ND
YCT-5	2.2	11.46	16.3	ND	200	10000
MLT-II-18	3.4	11.7	11	ND	225	10000
XHE-II-O53-ACID	50.35	11.8	44	ND	5.9	5000
SHU-1-19	4	12	7	48	14	84
RY-067	21	12	10	ND	0.37	42

<i>COOK CODE^a</i>	$\alpha 1$	$\alpha 2$	$\alpha 3$	$\alpha 4$	$\alpha 5$	$\alpha 6$
DM-III-01 (C18H12N3O2Br)	5000	12	ND	ND	4.73	5000
MLT-II-18	3.9	12.2	24.4	ND	210	10000
SH-053-2'F	21.99	12.34	34.9	ND	0.671	ND
WYS13 C20H18N2O3	2.442	13	27.5	ND	163	5000
PWZ-085	4.86	13	8.5	ND	0.55	40
MMB-III-14	13	13	6.9	333	1.1	333
RY-061	17	13	6.7	ND	0.3	31
WZ-113	19.2	13.2	13.4	ND	11.5	300
YT-II-83	32.74	13.22	24.1	ND	3.548	ND
DM-II-30 C20H13N3O2BrF3)	17.6	13.4	28.51	ND	7.8	5000
LJD-III-15E	1.93	14	19	ND	70.8	1000
YT-III-272	295.9	14.98	10.77	ND	103.3	ND
BCCt	0.72	15	18.9	ND	110.8	5000
XHE-II-006b	3.7	15	12	1897	144	1000
ABECARNIL	12.4	15.3	7.5	ND	6	1000
MLT-II-34	7.04	15.95	22.3	ND	158	1000
MSA-IV-35	2.1	16	21	ND	995	3000
JYI-04 (C21H23N3O3)	28.3	16	ND	ND	0.51	1.57
PS-1-35 C23H22N5OBr	ND	16.03	24.41	ND	ND	ND
ZG69A	6.8	16.3	9.2	ND	0.85	54.6
ZG-69a(Ro15-1310)	6.8	16.3	9.2	ND	0.85	54.6
YT-III-42	382.9	16.83	44.04	ND	9.77	ND
XHE-I-065	7.2	17	18	500	57	500

<i>COOK CODE^a</i>	<i>$\alpha 1$</i>	<i>$\alpha 2$</i>	<i>$\alpha 3$</i>	<i>$\alpha 4$</i>	<i>$\alpha 5$</i>	<i>$\alpha 6$</i>
XHE-II-073B (S-ENRICHED)	11	17	12	33	2.1	269
TJH-IV-51	2.39	17.4	14.5	ND	316	10000
SH-I-047	1710	17.52	1222	ND	1519	ND
XLi343 C20H19ClN2OSi	6.375	17.71	ND	ND	150.5	ND
XHE-II-002	8.3	18	13	3.9	1.5	11
YT-III-38	1461	18.21	14.63	ND	3999	
JYI-72 (C22H21N4SiF)	48.5	18.5	ND	ND	11.5	5000
MSR-I-032	6.2	18.7	4	ND	3.3	74.9
JC208 C15H10N2OS	22.42	18.89	ND	ND	5.039	ND
diazepam	14	20	15	ND	11	ND

^aAffinity of compounds at GABA(A) /BzR recombinant subtypes was measured by competition for [³H]flunitrazepam or [³H] Ro15-4513 binding to HEK cell membranes expressing human receptors of composition $\alpha 1\beta 3\gamma 2$, $\alpha 2\beta 3\gamma 2$, $\alpha 3\beta 3\gamma 2$, $\alpha 4\beta 3\gamma 2$, $\alpha 5\beta 3\gamma 2$ and $\alpha 6\beta 3\gamma 2$.⁴⁶ Data represent the average of at least three determinations with a SEM of $\pm 5\%$.

Ligands in this table have been selected because they have K_i values < 20 nm at a subtypes.



Figure 33. Overlay of compounds selective for $\alpha 2\beta 3\gamma 2$ subtype

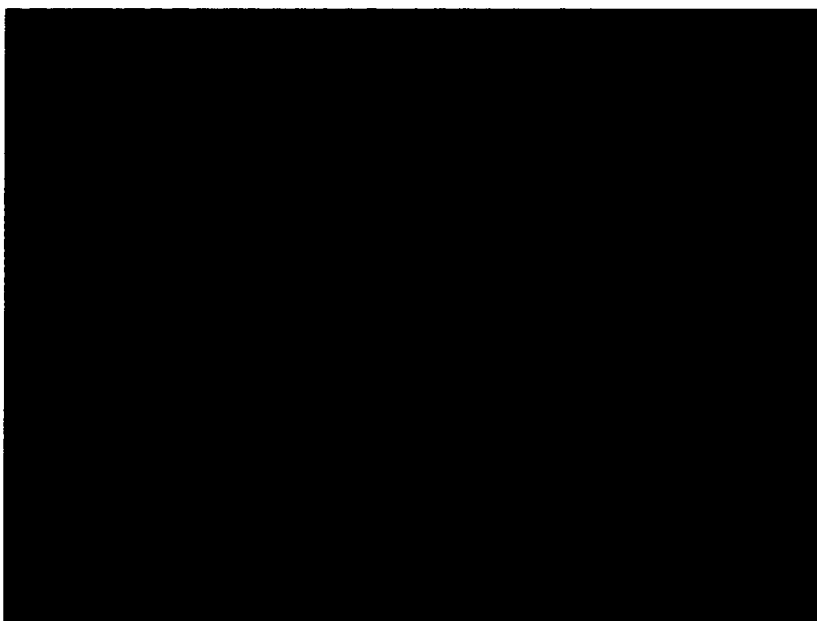


Figure 34. Updated $\alpha 2\beta 3\gamma 2$ subtype (solid) overlaid with the previous model (line).

The $\alpha 3\beta 3\gamma 2$ Receptor Subtype

Table 20. Ligands with potent affinity for $\alpha 3$; ligands bound with K_i values <20 nM at this subtype

<i>COOK CODE^a</i>	$\alpha 1$	$\alpha 2$	$\alpha 3$	$\alpha 4$	$\alpha 5$	$\alpha 6$
QH-II-085	0.08	0.06	0.02	ND	0.08	ND
SH-TSC-2(BCCT)	0.03	0.0419	0.035	ND	69.32	ND
QH-II-092	0.07	0.03	0.04	ND	0.17	ND
QH-II-077	0.06	0.08	0.05	ND	0.12	4
YT-II-76	95.34	2.797	0.056	ND	0.04	ND
PWZ-007A	0.11	0.1	0.09	ND	0.2	10
XLI-286	0.051	0.064	0.118	ND	0.684	ND
QH-II-090(CGS-8216)	0.05	0.08	0.12	ND	0.25	17
PWZ-0071	0.23	0.17	0.12	ND	0.44	17.31
JYI-57	0.076	0.076	0.131	ND	0.036	ND
BRETAZENIL	0.35	0.64	0.2	ND	0.5	12.7
PZII-028	0.2	ND	0.2	ND	0.32	1.9
QH-II-075	0.18	0.21	0.25	ND	1.3	40
JYI-42	0.257	0.146	0.278	ND	0.256	ND
XHE-II-024	0.09	0.18	0.32	14	0.24	11
SH-I-048A	0.774	0.1723	0.383	ND	0.11	ND
JYI-55	41.39	ND	0.504	ND	24.75	ND
JYI-47	2.759	2.282	0.511	ND	0.427	ND
DM-239	1.5	ND	0.53	ND	0.14	6.89
WY-B-15	0.92	0.83	0.58	2080	4.42	646
JYI-64 (C17H12N4FBr)	0.305	1.111	0.62	ND	0.87	5000
DM-II-90 (C17H12N4BrCl)	0.505	1	0.63	ND	0.37	5000

<i>COOK CODE^a</i>	$\alpha 1$	$\alpha 2$	$\alpha 3$	$\alpha 4$	$\alpha 5$	$\alpha 6$
QH-146	0.49	ND	0.76	ND	7.7	10000
PZII-029	0.34	ND	0.79	ND	0.52	10
WYS19 C26H32N2O4Si	ND	ND	0.89	ND	ND	ND
XHE-III-06a	1	2	1	5	1.8	37
Ro15-1788	0.8	0.9	1.05	ND	0.6	148
MLT-I-70	1.1	1.2	1.1	ND	40.3	1000
XHE-III-04	1.2	2	1.1	219	0.4	500
FG8205	0.4	2.08	1.16	ND	1.54	227
PWZ-009A1	1.34	1.31	1.26	ND	0.84	2.03
alprazolam	0.8	0.59	1.43	ND	1.54	10000
XLI-348	13.56	11.17	1.578	ND	82.05	ND
QH-II-082	1.7	1.8	1.6	ND	6.1	100
WY-TSC-4(WYS8)	0.007	0.99	1.63	ND	51.04	ND
SPH-121	0.14	1.19	1.72	ND	4	479
XLi-JY-DMH ANX3	3.3	0.58	1.9	ND	4.4	5000
MMB-III-016	3	1.97	2	1074	0.26	211
MMB-III-16	3	1.97	2	1074	0.26	211
XLI-8TC	21.52	11.01	2.155	ND	4.059	ND
6-PBC	0.49	1.21	2.2	ND	2.39	1343
YT-III-271	32.54	1.26	2.35	ND	103	ND
Ro15-4513	3.3	2.6	2.5	ND	0.26	3.8
TG-4-29	2.8	3.9	2.7	2.1	0.18	3.9
TG-II-82	1.6	2.9	2.8	ND	1	1000
OMB-18	3.9	1.2	3.4	1733	0.8	5
YT-II	6.932	0.8712	3.518	ND	5.119	ND

<i>COOK CODE^a</i>	$\alpha 1$	$\alpha 2$	$\alpha 3$	$\alpha 4$	$\alpha 5$	$\alpha 6$
PS-1-34B C20H17N4BrO	ND	4.198	3.928	ND	ND	ND
DMCM	5.69	8.29	4	ND	1.04	134
MSR-I-032	6.2	18.7	4	ND	3.3	74.9
RY-008	3.75	7.2	4.14	ND	1.11	44.3
XHE-III-49	1.3	5.5	4.2	38.7	11.3	85.1
JYI-60 (C17H11N2OF)	3.73	1.635	4.3	ND	1.7	5000
FLUNITRAZEPAM	2.2	2.5	4.5	ND	2.1	2000
XLI-317	60.24	24.05	4.562	ND	0.295	ND
QH-II-080b	3	3.7	4.7	ND	24	1000
SPH-165	0.63	2.79	4.85	ND	10.4	1150
SH-I-04	7.3	6.136	5.1	ND	7.664	ND
SVO-8-30	1.1	5.3	5.3	2.8	0.6	15
WY-B-99-1	4.4	4.5	5.58	2000	47	2000
YT-III-25	2.531	5.786	5.691	ND	0.095	ND
BCCE	1.2	4.9	5.7	ND	26.8	2700
MMB-II-90	20	24	5.7	9	0.25	36
TC-YT-II-76	101.1	1.897	5.816	ND	11.99	ND
ZK 93423	4.1	4.2	6	ND	4.5	1000
RY-061	17	13	6.7	ND	0.3	31
JYI-54 (C24H15N3O3F4)	2.89	172	6.7	ND	57	1890
TG-4-29	8.3	10.2	6.9	ND	0.4	7.61
MMB-III-14	13	13	6.9	333	1.1	333
XHE-II-017	3.3	10	7	258	17	294
SHU-1-19	4	12	7	48	14	84

<i>COOK CODE^a</i>	$\alpha 1$	$\alpha 2$	$\alpha 3$	$\alpha 4$	$\alpha 5$	$\alpha 6$
XHE-III-13	7.3	ND	7.1	880	1.6	311
DM-215	6.74	ND	7.42	ND	0.293	8.28
ABECARNIL	12.4	15.3	7.5	ND	6	1000
SVO-8-14	8	25	8	6.9	0.9	14
XHE-III-24	0.25	ND	8	222	10	328
SH-I-89S	12.78	8.562	8.145	ND	3.23	ND
PWZ-085	4.86	13	8.5	ND	0.55	40
XHE-I-093	2	7.1	8.9	1107	20	1162
ZG-168	11.2	10.7	9.2	ND	0.47	9.4
ZG69A	6.8	16.3	9.2	ND	0.85	54.6
ZG-69a(Ro15-1310)	6.8	16.3	9.2	ND	0.85	54.6
ZG-234	7.25	22.14	9.84	ND	0.3	5.25
XHE-II-073A (R ENRICHED)	5.9	11	10	15	1.18	140
RY-067	21	12	10	ND	0.37	42
XHE-III-14	2.6	ND	10	13	2	7
YT-III-272	295.9	14.98	10.77	ND	103.3	ND
SPH-38	2	5.4	10.8	ND	18.5	3000
ZG-208	9.7	11.2	10.9	ND	0.38	4.6
MLT-II-18	3.4	11.7	11	ND	225	10000
DM-II-33 (C20H13N3O2BrCl3)	88.6	85	11.6	ND	26.2	5000
JYI-59 (C22H13N3O2F4)	1.08	2.6	11.82	ND	11.5	5000
XHE-II-006b	3.7	15	12	1897	144	1000
XHE-II-073B (S- ENRICHED)	11	17	12	33	2.1	269

<i>COOK CODE^a</i>	<i>$\alpha 1$</i>	<i>$\alpha 2$</i>	<i>$\alpha 3$</i>	<i>$\alpha 4$</i>	<i>$\alpha 5$</i>	<i>$\alpha 6$</i>
CM-B44(ss)	32	43	12	379	4.3	485
WYSC1 C16H16N2O2	1.094	5.44	12.3	ND	69.8	21.2
JYI-48	75.59	90.68	12.78	ND	31.28	ND
XHE-II-002	8.3	18	13	3.9	1.5	11
RY-076	26	27	13	ND	0.7	22
WZ-113	19.2	13.2	13.4	ND	11.5	300
SH-I-085	11.08	4.866	13.75	ND	0.24	ND
CM-E10	23	26	14	215	0.51	96
TJH-IV-51	2.39	17.4	14.5	ND	316	10000
YT-III-38	1461	18.21	14.63	ND	3999	ND
CM-A87	1.62	4.54	14.73	1000	4.61	1000
diazepam	14	20	15	ND	11	ND
RY-053	49	29	15	ND	1	46
YCT-5	2.2	11.46	16.3	ND	200	10000
RY-098	10.1	22.2	16.5	ND	1.68	100
PWZ-096	11.1	36	16.9	ND	1.07	51.5
XLi223 C22H20BrN3O2	14	8.7	18	1000	10	2000
XHE-I-065	7.2	17	18	500	57	500
SH-I-02B	29.82	1315	18	ND	74.05	ND
MLT-II-16	5.05	10.41	18.4	ND	260	10000
RY-024 C19H19N3O3	26.9	26.3	18.7	ND	0.4	5.1
BCCt	0.72	15	18.9	ND	110.8	5000
LJD-III-15E	1.93	14	19	ND	70.8	1000
CM-E09b	20	22	19	55	0.45	69

<i>COOK CODE^a</i>	$\alpha 1$	$\alpha 2$	$\alpha 3$	$\alpha 4$	$\alpha 5$	$\alpha 6$
RY-I-31	10	45	19	ND	6	1000
SH-I-030	14.42	11.04	19.09	ND	1.89	ND
YT-III-23	19.83	23.65	19.87	ND	1.105	ND
XHE-II-006a	4.7	4.4	20	1876	89	3531
OMB-19	22	4.6	20	3333	3.5	40
XHE-III-06b	32	33	20	299	28.6	740

^aAffinity of compounds at GABA(A) /BzR recombinant subtypes was measured by competition for [³H]flunitrazepam or [³H] Ro15-4513 binding to HEK cell membranes expressing human receptors of composition $\alpha 1\beta 3\gamma 2$, $\alpha 2\beta 3\gamma 2$, $\alpha 3\beta 3\gamma 2$, $\alpha 4\beta 3\gamma 2$, $\alpha 5\beta 3\gamma 2$ and $\alpha 6\beta 3\gamma 2$.⁶⁵ Data represent the average of at least three determinations with a SEM of $\pm 5\%$.

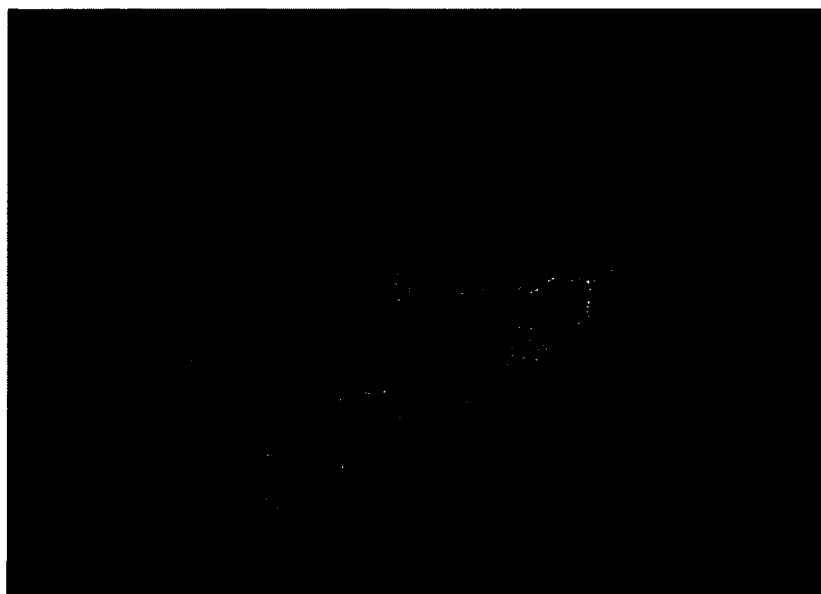


Figure 35. Overlay of compounds selective for $\alpha 3\beta 3\gamma 2$ subtype



Figure 36. Updated $\alpha 3\beta 3\gamma 2$ subtype (solid) overlaid with the previous model (line).

The $\alpha 4\beta 3\gamma 2$ Receptor Subtype

Table 21. Ligands with potent affinity for $\alpha 4$; ligands bound with K_i values <20 nm at this subtype

<i>COOK CODE^a</i>	$\alpha 1$	$\alpha 2$	$\alpha 3$	$\alpha 4$	$\alpha 5$	$\alpha 6$
CM-D45 C19H21N3O4	90.5	65.5	30.3	0.15	1.65	0.23
CM-D44	34.3	56.3	20.7	0.33	0.57	0.92
XHE-III-74	77	105	38	0.42	2.2	5.8
TG-4-29	2.8	3.9	2.7	2.1	0.18	3.9
SVO-8-30	1.1	5.3	5.3	2.8	0.6	15
XHE-II-002	8.3	18	13	3.9	1.5	11
XHE-III-06a	1	2	1	5	1.8	37
RY-080 C17H15N3O3	28.4	21.4	25.8	5.3	0.49	28.8
TG-4-39	1.6	34	24	5.6	1.4	23
SVO-8-14	8	25	8	6.9	0.9	14

<i>COOK CODE^a</i>	<i>$\alpha 1$</i>	<i>$\alpha 2$</i>	<i>$\alpha 3$</i>	<i>$\alpha 4$</i>	<i>$\alpha 5$</i>	<i>$\alpha 6$</i>
RY-023 C22H27N3O3Si	197	142.6	255	7.8	2.61	58.6
MMB-II-90	20	24	5.7	9	0.25	36
XHE-III-14	2.6		10	13	2	7
XHE-II-024	0.09	0.18	0.32	14	0.24	11
XHE-II-073A (R ENRICHED)	5.9	11	10	15	1.18	140
SVO-8-67	7	41	26	15	2.3	191
CM-B31i(ss)	90	184	78	18	4.9	121
SVO-8-20	11	40	28	19	8.6	138

^aAffinity of compounds at GABA(A) /BzR recombinant subtypes was measured by competition for [³H]flunitrazepam or [³H] Ro15-4513 binding to HEK cell membranes expressing human receptors of composition $\alpha 1\beta 3\gamma 2$, $\alpha 2\beta 3\gamma 2$, $\alpha 3\beta 3\gamma 2$, $\alpha 4\beta 3\gamma 2$, $\alpha 5\beta 3\gamma 2$ and $\alpha 6\beta 3\gamma 2$.¹⁷⁰ Data represent the average of at least three determinations with a SEM of $\pm 5\%$.



Figure 37. Overlay of selected compounds selective for $\alpha 4\beta 3\gamma 2$ subtype

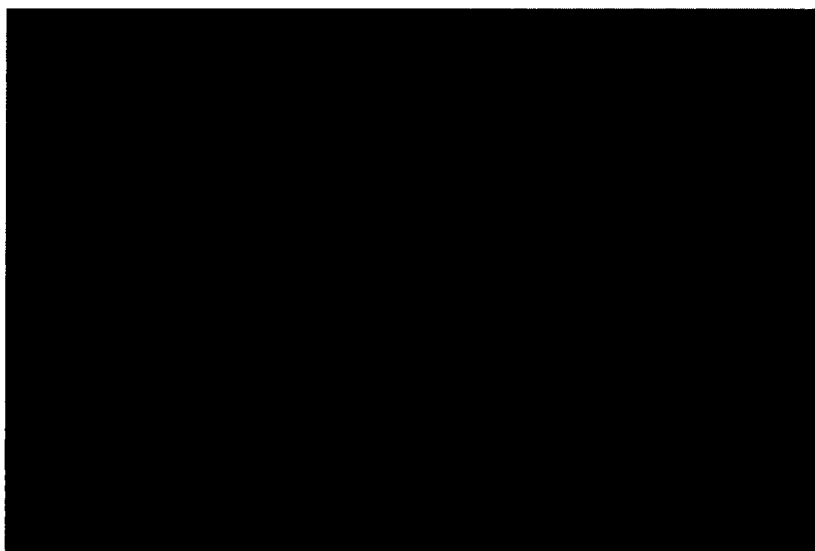


Figure 38. Updated $\alpha 4\beta 3\gamma 2$ subtype (solid) overlaid with the previous model (line).

The $\alpha 5\beta 3\gamma 2$ Receptor Subtype

Table 22. Ligands with potent affinity for $\alpha 5$; ligands bound with K_i values <20 nM at this subtype

<i>COOK CODE^a</i>	$\alpha 1$	$\alpha 2$	$\alpha 3$	$\alpha 4$	$\alpha 5$
JYI-57	0.076	0.076	0.131	ND	0.036
YT-II-76	95.34	2.797	0.056	ND	0.04
QH-II-085	0.08	0.06	0.02	ND	0.08
YT-III-25	2.531	5.786	5.691	ND	0.095
SH-I-048A	0.774	0.1723	0.383	ND	0.11
QH-II-077	0.06	0.08	0.05	ND	0.12
DM-239	1.5	ND	0.53	ND	0.14
QH-II-092	0.07	0.03	0.04	ND	0.17
TG-4-29	2.8	3.9	2.7	2.1	0.18
SH-I-75	1487	989.9	773	ND	0.1825
PWZ-007A	0.11	0.1	0.09	ND	0.2
XHE-II-024	0.09	0.18	0.32	14	0.24
SH-I-085	11.08	4.866	13.75	ND	0.24
MMB-II-90	20	24	5.7	9	0.25
QH-II-090(CGS-8216)	0.05	0.08	0.12	ND	0.25
JYI-42	0.257	0.146	0.278	ND	0.256
MMB-III-016	3	1.97	2	1074	0.26
MMB-III-16	3	1.97	2	1074	0.26
Ro15-4513	3.3	2.6	2.5	ND	0.26
DM-215	6.74	ND	7.42	ND	0.293
XLI-317	60.24	24.05	4.562	ND	0.295
RY-061	17	13	6.7	ND	0.3
ZG-234	7.25	22.14	9.84	ND	0.3

<i>COOK CODE^a</i>	<i>$\alpha 1$</i>	<i>$\alpha 2$</i>	<i>$\alpha 3$</i>	<i>$\alpha 4$</i>	<i>$\alpha 5$</i>
PZII-028	0.2	ND	0.2	ND	0.32
RY-067	21	12	10	ND	0.37
DM-II-90 (C17H12N4BrCl)	0.505	1	0.63	ND	0.37
ZG-208	9.7	11.2	10.9	ND	0.38
XHE-III-04	1.2	2	1.1	219	0.4
TG-4-29	8.3	10.2	6.9	ND	0.4
RY-024 C19H19N3O3	26.9	26.3	18.7	ND	0.4
JYI-47	2.759	2.282	0.511	ND	0.427
PWZ-0071	0.23	0.17	0.12	ND	0.44
CM-E09b	20	22	19	55	0.45
ZG-168	11.2	10.7	9.2	ND	0.47
RY-080 C17H15N3O3	28.4	21.4	25.8	5.3	0.49
BRETAZENIL	0.35	0.64	0.2	ND	0.5
CM-E10	23	26	14	215	0.51
JYI-04 (C21H23N3O3)	28.3	16	ND	ND	0.51
PZII-029	0.34	ND	0.79	ND	0.52
PWZ-085	4.86	13	8.5	ND	0.55
JYI-70 (C19H13N4F)	6.3	2.1	ND	ND	0.56
CM-D44	34.3	56.3	20.7	0.33	0.57
SVO-8-30	1.1	5.3	5.3	2.8	0.6
Ro15-1788	0.8	0.9	1.05	ND	0.6
XLi268 C17H13BrN4	2.8145	0.6862	ND	ND	0.6243

<i>COOK CODE^a</i>	<i>$\alpha 1$</i>	<i>$\alpha 2$</i>	<i>$\alpha 3$</i>	<i>$\alpha 4$</i>	<i>$\alpha 5$</i>
ZG-63A	17.3	21.6	29.1	ND	0.65
SH-053-2'F	21.99	12.34	34.9	ND	0.671
XLI-286	0.051	0.064	0.118	ND	0.684
SH-I-S66	22.93	30.36	55.26	ND	0.69
RY-076	26	27	13	ND	0.7
DM-173	13.1	ND	38.1	ND	0.78
OMB-18	3.9	1.2	3.4	1733	0.8
HJ-I-037	15.07	8.127	28.29	ND	0.818
PWZ-009A1	1.34	1.31	1.26	ND	0.84
ZG69A	6.8	16.3	9.2	ND	0.85
ZG-69a(Ro15-1310)	6.8	16.3	9.2	ND	0.85
JYI-64 (C17H12N4FBr)	0.305	1.111	0.62	ND	0.87
SVO-8-14	8	25	8	6.9	0.9
JYI-03 (C21H21N3O3)	185.4	107	ND	ND	0.954
TG-II-82	1.6	2.9	2.8	ND	1
RY-053	49	29	15	ND	1
YT-6	15.31	87.8	60.49	ND	1.039
DMCM	5.69	8.29	4	ND	1.04
PWZ-096	11.1	36	16.9	ND	1.07
MMB-III-14	13	13	6.9	333	1.1
YT-III-23	19.83	23.65	19.87	ND	1.105
RY-008	3.75	7.2	4.14	ND	1.11
XLI-2TC	3.442	1.673	44.08	ND	1.121
XHE-II-073A (R ENRICHED)	5.9	11	10	15	1.18

<i>COOK CODE^a</i>	$\alpha 1$	$\alpha 2$	$\alpha 3$	$\alpha 4$	$\alpha 5$
QH-II-075	0.18	0.21	0.25	ND	1.3
RY-054	59	44	27	ND	1.3
TG-4-39	1.6	34	24	5.6	1.4
XHE-II-002	8.3	18	13	3.9	1.5
RY-031 (RY-10)	20.4	27	26.1	ND	1.5
FG8205	0.4	2.08	1.16	ND	1.54
alprazolam	0.8	0.59	1.43	ND	1.54
XHE-III-13	7.3	ND	7.1	880	1.6
CM-D45 C19H21N3O4	90.5	65.5	30.3	0.15	1.65
RY-098	10.1	22.2	16.5	ND	1.68
YT-5	0.421	0.6034	36.06	ND	1.695
JYI-60 (C17H11N2OF)	3.73	1.635	4.3	ND	1.7
RY-033	14.8	56	25.3	ND	1.72
XHE-III-06a	1	2	1	5	1.8
SH-I-030	14.42	11.04	19.09	ND	1.89
XLi352 C18H13ClN2O	1.56	0.991	ND	ND	1.957
XLi351 C21H21ClN2OSi	1.507	0.967	ND	ND	1.985
XHE-III-14	2.6	ND	10	13	2
DM-II-72 (C15H10N20BrCl)	5000	1.37	ND	ND	2.02
XHE-II-073B (S- ENRICHED)	11	17	12	33	2.1
FLUNITRAZEPAM	2.2	2.5	4.5	ND	2.1
XHE-III-74	77	105	38	0.42	2.2

<i>COOK CODE^a</i>	<i>$\alpha 1$</i>	<i>$\alpha 2$</i>	<i>$\alpha 3$</i>	<i>$\alpha 4$</i>	<i>$\alpha 5$</i>
SVO-8-67	7	41	26	15	2.3
6-PBC	0.49	1.21	2.2	ND	2.39
RY-058	86	40	85	ND	2.4
ZG-224	17.1	33.7	50	ND	2.5
RY-066	83	60	48	ND	2.6
RY-023 C ₂₂ H ₂₇ N ₃ O ₃ Si	197	142.6	255	7.8	2.61
XLi350 C ₁₇ H ₁₁ ClN ₂ O	1.224	1.188	ND	ND	2.9
JYI-32 (C ₂₀ H ₁₅ N ₃ O ₂ BrF)	3.07	4.96	ND	ND	2.92
SH-I-89S	12.78	8.562	8.145	ND	3.23
MSR-I-032	6.2	18.7	4	ND	3.3
OMB-19	22	4.6	20	3333	3.5
ZG-213	12.8	49.8	30.2	ND	3.5
YT-II-83	32.74	13.22	24.1	ND	3.548
RY-059	89	70	91	ND	3.7
SPH-121	0.14	1.19	1.72	ND	4
RY-047	200	124	79	ND	4
XLI-8TC	21.52	11.01	2.155	ND	4.059
YT-I-38	945.9	326.8	245.9	ND	4.07
DM-146	6.44	ND	148	ND	4.23
CM-B44(ss)	32	43	12	379	4.3
CM-B47	32	63	34	2007	4.4
XLi-JY-DMH ANX3	3.3	0.58	1.9	ND	4.4
WY-B-15	0.92	0.83	0.58	2080	4.42

<i>COOK CODE^a</i>	$\alpha 1$	$\alpha 2$	$\alpha 3$	$\alpha 4$	$\alpha 5$
ZK 93423	4.1	4.2	6	ND	4.5
JYI-12 (C19H16N3O3F3)	91	39	ND	ND	4.5
CM-A87	1.62	4.54	14.73	1000	4.61
DM-III-01 (C18H12N3O2Br)	5000	12	ND	ND	4.73
RY-057	73	85	97	ND	4.8
JYI-15 (C19H14N3O3F3)	205	812	ND	ND	4.8
CM-B31i(ss)	90	184	78	18	4.9
RY-079	121.1	141.9	198.4	159	5
JC208 C15H10N2OS	22.42	18.89	ND	ND	5.039
YT-II	6.932	0.8712	3.518	ND	5.119
XLi270 C19H14N4	36.39	25.81	ND	ND	5.291
XHE-I-051	35	39	42	ND	5.3
MMB-II-87	200	333	107	109	5.4
XLI-210	231	661	2666	ND	5.4
XHE-II-O53-ACID	50.35	11.8	44	ND	5.9
ABECARNIL	12.4	15.3	7.5	ND	6
RY-I-31	10	45	19	ND	6
QH-II-082	1.7	1.8	1.6	ND	6.1
SH-TSC-1(PWZ-029)	362.4	180.3	328.2	ND	6.185
XHE-II-065	1000	409	216	37	6.4
JYI-49 (C20H12N3O2F4Br)	1.87	2.38	ND	ND	6.7

<i>COOK CODE^a</i>	$\alpha 1$	$\alpha 2$	$\alpha 3$	$\alpha 4$	$\alpha 5$
JC184 C13H9BrN2OS	9.606	10.5	ND	ND	6.709
QH-II-066	76.3	42.1	47.4	2000	6.8
	76.3	42.1	47.4	ND	6.8
XLI-381	619.9	285.6	3639	ND	7.051
RY-071	19	56	91	ND	7.2
RY-I-28	283	318	102	ND	7.2
CM-A82a	2.78	8.93	24.51	1000	7.49
YT-III-31	36.39	67.85	129.7	ND	7.59
SH-I-04	7.3	6.136	5.1	ND	7.664
QH-146	0.49	ND	0.76	ND	7.7
QH-II-063	9.4	9.3	31	ND	7.7
	9.4	9.3	31	ND	7.7
JC221 ANX1	106.175	49.405	182	ND	7.7495
DM-II-30 C20H13N3O2BrF3)	17.6	13.4	28.51	ND	7.8
SH-TS-CH3	107.2	50.09	20.95	ND	8.068
RY-073	156	88	122	ND	8.5
SVO-8-20	11	40	28	19	8.6
SHU-221-1	66	41	43	3000	9
YT-III-231	51.09	61.46	26.34	ND	9.124
CM-E09a	176	192	122	490	9.2
DM-139	5.8	ND	169	ND	9.25
YT-III-42	382.9	16.83	44.04	ND	9.77
CD-214	16.4	48.2	42.5	ND	9.8
XHE-III-24	0.25	ND	8	222	10

<i>COOK CODE^a</i>	<i>$\alpha 1$</i>	<i>$\alpha 2$</i>	<i>$\alpha 3$</i>	<i>$\alpha 4$</i>	<i>$\alpha 5$</i>
XLi223 C22H20BrN3O2	14	8.7	18	1000	10
SPH-165	0.63	2.79	4.85	ND	10.4
JYI- 01(C19H20N3O3Br)	59.2	159	96	ND	10.6
diazepam	14	20	15	ND	11
XHE-III-49	1.3	5.5	4.2	38.7	11.3
WZ-113	19.2	13.2	13.4	ND	11.5
JYI-59 (C22H13N3O2F4)	1.08	2.6	11.82	ND	11.5
JYI-72 (C22H21N4SiF)	48.5	18.5	ND	ND	11.5
TC-YT-II-76	101.1	1.897	5.816	ND	11.99
JYI-10 (C17H13N3O3F3Br)	5000	368	ND	ND	12.3
WZ-069	40	30.5	38.5	ND	12.6
JYI-06 (C23H23N3O4)	16.5	5.48	5000	ND	12.6
RY-072	220	150	184	ND	12.7
JYI-14 (C17H14N3O3F3)	32	25	ND	ND	13
XHE-II-053	287	45	96	1504	13.8
Xli-347 C34H28N6O7	828.05	690.2	ND	ND	13.87
SHU-1-19	4	12	7	48	14
CM-C28(SR)	176	752	244	290	14
CM-E11	333	308	161	394	14
XHE-II-012	49	24	31	1042	14
MMB-III-018	117	140	78	3500	14

<i>COOK CODE^a</i>	<i>$\alpha 1$</i>	<i>$\alpha 2$</i>	<i>$\alpha 3$</i>	<i>$\alpha 4$</i>	<i>$\alpha 5$</i>
MMB-III-18	117	140	78	3500	14
CM-B31c(ss)	118	319	173	37	15
CM-B45	230	557	336	265	15
XLI-093	1000	1000	858	1550	15
DM-II-20 (C22H14N3O2F3)	54.3	27.14	35.68	ND	15.35
XLi269 C22H22N4Si	221.8	154.2	ND	ND	15.51
SH-O53-S-CH3-2'F	350	141	1237	ND	16
JYI-13 (C21H16N3O4F3)	5000	63.7	ND	ND	16
CM-B34	472	451	223	114	17
XHE-II-017	3.3	10	7	258	17
JC222 C16H12N2OS	86.7	45.11	ND	ND	17.63
SPH-38	2	5.4	10.8	ND	18.5
WZ-070	72.7	30.7	53.2	ND	18.6
	73	31	53	ND	19
RY-069	692	622	506	ND	19
SH-053-2'F-S-CH3	468.2	33.27	291.5	ND	19.2
XHE-I-093	2	7.1	8.9	1107	20

^aAffinity of compounds at GABA(A) /BzR recombinant subtypes was measured by competition for [³H]flunitrazepam or [³H] Ro15-4513 binding to HEK cell membranes expressing human receptors of composition $\alpha 1\beta 3\gamma 2$, $\alpha 2\beta 3\gamma 2$, $\alpha 3\beta 3\gamma 2$, $\alpha 4\beta 3\gamma 2$, $\alpha 5\beta 3\gamma 2$ and $\alpha 6\beta 3\gamma 2$.²⁵⁹ Data represent the average of at least three determinations with a SEM of $\pm 5\%$.

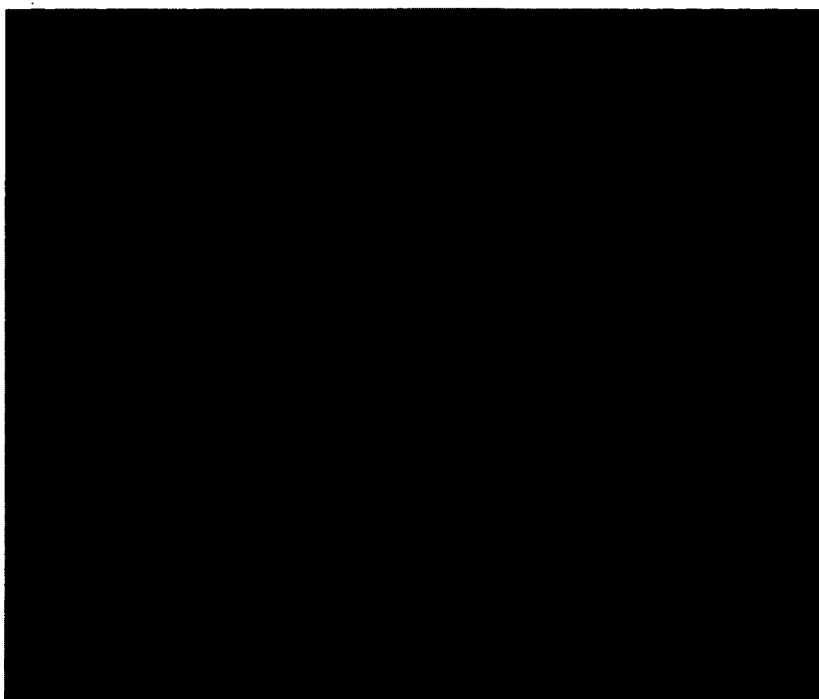


Figure 39. Overlay of selected compounds selective for $\alpha 5\beta 3\gamma 2$ subtype

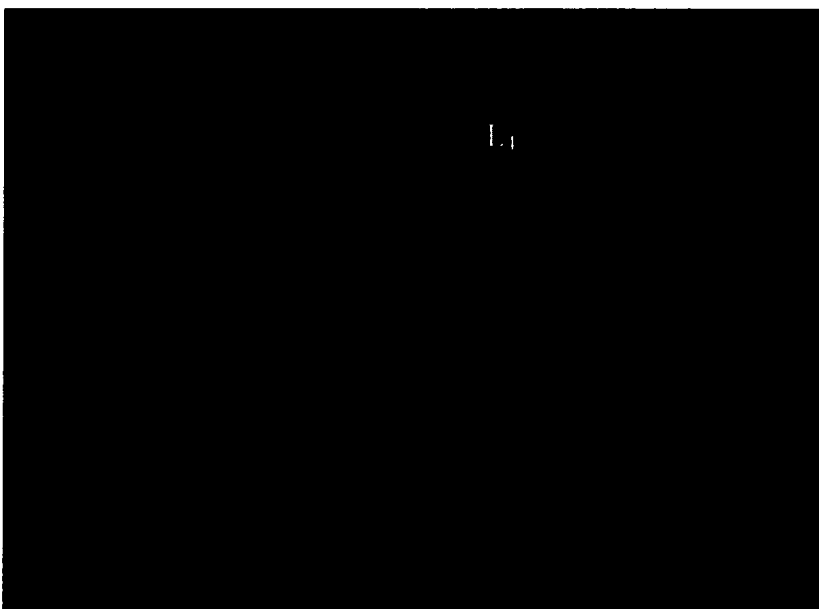


Figure 40. Updated $\alpha 5\beta 3\gamma 2$ subtype (solid) overlaid with the previous model (line).

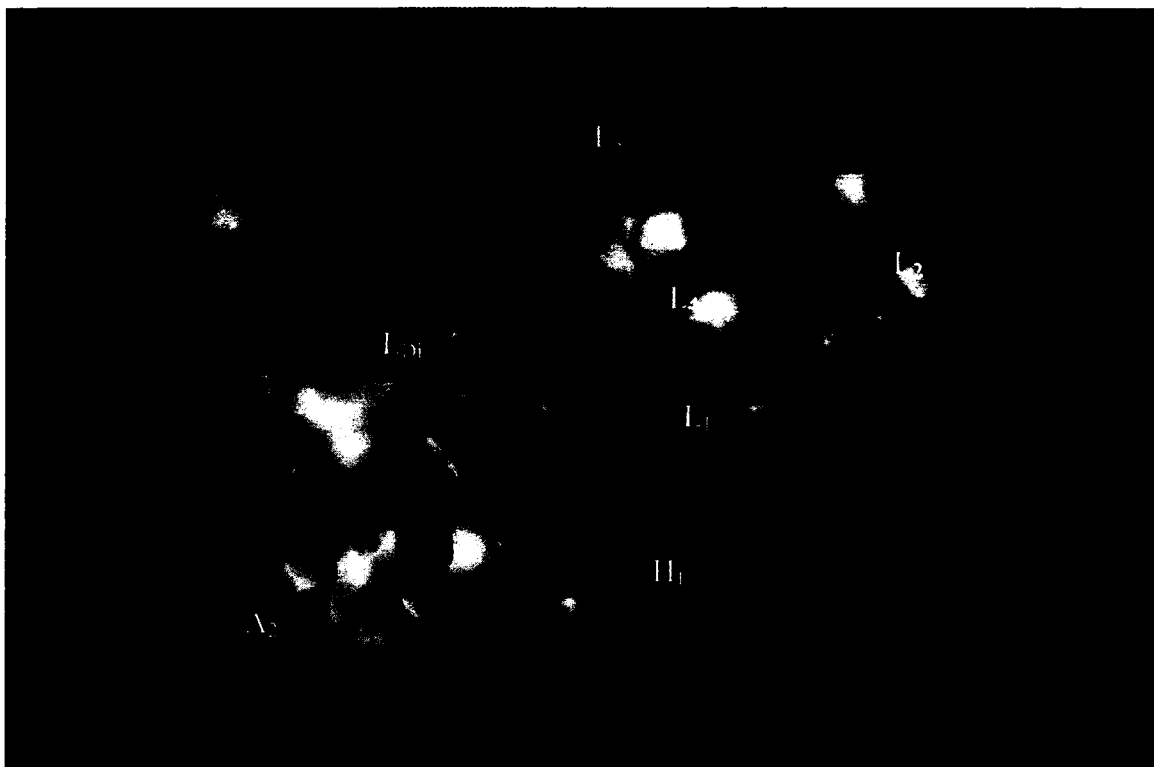


Figure 41. Overlay of the $\alpha 5 \beta 3 \gamma 2$ receptor (yellow) subtype with the $\alpha 1 \beta 3 \gamma 2$ receptor (magenta) subtype. Orange surfaces indicate overlapping regions.



Figure 42. Overlay of the $\alpha 5 \beta 3 \gamma 2$ receptor (yellow) subtype with the $\alpha 1 \beta 3 \gamma 2$ receptor (magenta) subtype (Figure 42 rotated 90°). Orange surfaces indicate overlapping regions.

The multiple volume contours displayed in Figure 33-42 were created using the mvolume function (multiple volume contour function in Sybyl and compounds with binding affinity at the receptor less than or equal to 20 nm. To create the overlays, first, the display (dsp) and contour (cnt) files were created for the $\alpha 5 \beta 3 \gamma 2$ receptor subtype and the $\alpha 1 \beta 3 \gamma 2$ receptor subtype by overlaying the compounds for each of these receptors (given above). Using the mvolume function, a logical expression was entered to create the surfaces making up the union as well as the included volume for each receptor subtype itself. It is clear from the included volume overlay that the L_2 pocket is deeper for the $\alpha 5$ subtype as determined previously. The new L_4 pocket can be distinguished as

the new yellow region of the $\alpha 5\beta 3\gamma 2$ subtype which is due to recently designed R-isomers by Huang.²⁶⁰

The $\alpha 6\beta 3\gamma 2$ Receptor Subtype

Table 23. Ligands with potent affinity for $\alpha 6$; ligands bound with K_i values <20 nm at this subtype

<i>COOK CODE^a</i>	<i>$\alpha 1$</i>	<i>$\alpha 2$</i>	<i>$\alpha 3$</i>	<i>$\alpha 4$</i>	<i>$\alpha 5$</i>	<i>$\alpha 6$</i>
CM-D45 C19H21N3O4	90.5	65.5	30.3	0.15	1.65	0.23
CM-D44	34.3	56.3	20.7	0.33	0.57	0.92
JYI-04 (C21H23N3O3)	28.3	16	ND	ND	0.51	1.57
PZII-028	0.2	ND	0.2	ND	0.32	1.9
PWZ-009A1	1.34	1.31	1.26	ND	0.84	2.03
JYI-01 (C19H20N3O3Br)	59.2	159	96	ND	10.6	2.88
JYI-03 (C21H21N3O3)	185.4	107	ND	ND	0.954	3.34
Ro15-4513	3.3	2.6	2.5	ND	0.26	3.8
TG-4-29	2.8	3.9	2.7	2.1	0.18	3.9
JYI-11 (C22H22N3O3F3Si)	5000	5000	ND	ND	648	3.97
QH-II-077	0.06	0.08	0.05	ND	0.12	4
ZG-63A	17.3	21.6	29.1	ND	0.65	4
ZG-208	9.7	11.2	10.9	ND	0.38	4.6
OMB-18	3.9	1.2	3.4	1733	0.8	5
RY-024 C19H19N3O3	26.9	26.3	18.7	ND	0.4	5.1
ZG-234	7.25	22.14	9.84	ND	0.3	5.25
XHE-III-74	77	105	38	0.42	2.2	5.8

<i>COOK CODE^a</i>	$\alpha 1$	$\alpha 2$	$\alpha 3$	$\alpha 4$	$\alpha 5$	$\alpha 6$
JYI-12 (C19H16N3O3F3)	91	39	ND	ND	4.5	6.8
DM-239	1.5	ND	0.53	ND	0.14	6.89
XHE-III-14	2.6	ND	10	13	2	7
TG-4-29	8.3	10.2	6.9	ND	0.4	7.61
DM-215	6.74	ND	7.42	ND	0.293	8.28
JYI-13 (C21H16N3O4F3)	5000	63.7	ND	ND	16	8.38
CGS9895	0.21	ND	ND	ND	ND	9.3
ZG-168	11.2	10.7	9.2	ND	0.47	9.4
PWZ-007A	0.11	0.1	0.09	ND	0.2	10
PZII-029	0.34	ND	0.79	ND	0.52	10
XHE-II-024	0.09	0.18	0.32	14	0.24	11
XHE-II-002	8.3	18	13	3.9	1.5	11
BRETAZENIL	0.35	0.64	0.2	ND	0.5	12.7
JYI-19 (C23H23N3O3S)	2.176	205	ND	ND	34	12.7
SVO-8-14	8	25	8	6.9	0.9	14
SVO-8-30	1.1	5.3	5.3	2.8	0.6	15
WYS10 C14H9F3N2O2	0.88	36	25.6	ND	548.7	15.3
QH-II-090(CGS- 8216)	0.05	0.08	0.12	ND	0.25	17
PWZ-0071	0.23	0.17	0.12		0.44	17.31

^aThe affinity of compounds at GABA(A) /BzR recombinant subtypes was measured by competition for [³H]flunitrazepam binding to HEK cell membranes expressing human receptors of composition $\alpha 1\beta 3\gamma 2$, $\alpha 2\beta 3\gamma 2$, $\alpha 3\beta 3\gamma 2$, $\alpha 4\beta 3\gamma 2$, $\alpha 5\beta 3\gamma 2$ and $\alpha 6\beta 3\gamma 2$.²⁶⁰ Data represent the average of at least three determinations with a SEM of $\pm 5\%$.

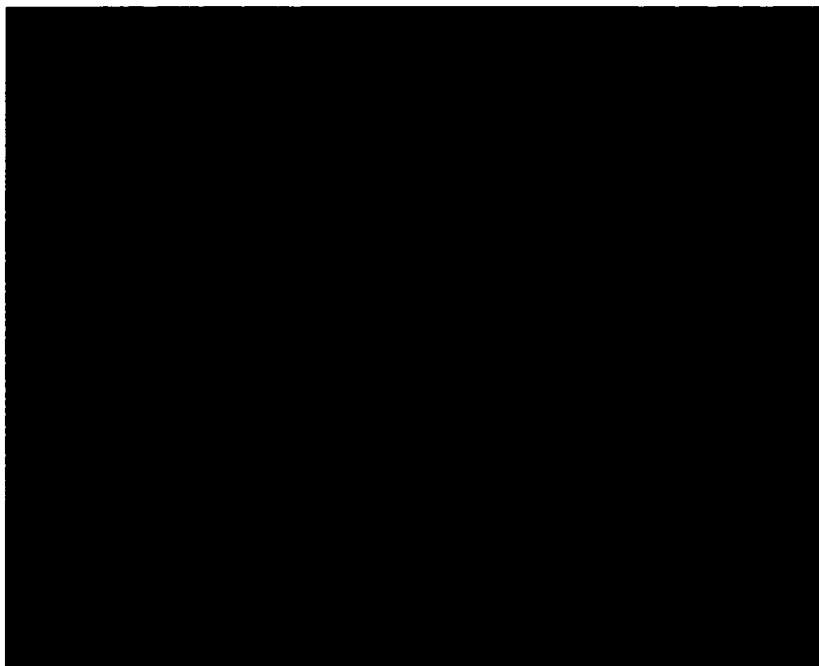


Figure 43. Overlay of selected compounds selective for $\alpha 6\beta 3\gamma 2$ subtype

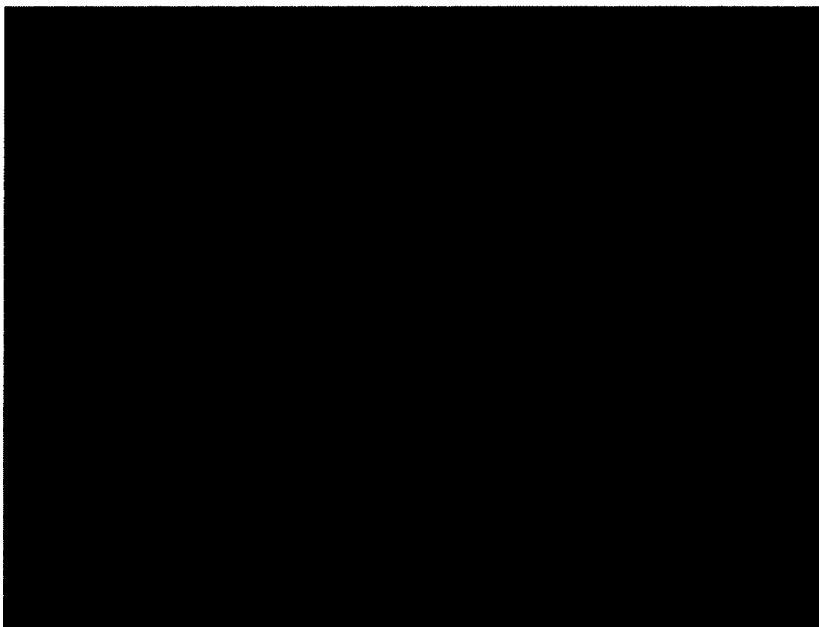


Figure 44. Updated $\alpha 6\beta 3\gamma 2$ subtype (solid) overlaid with the previous model (line).

QSAR

A non-traditional quantitative structure activity relationship (QSAR) project was executed to observe steric and electrostatic preferences for each receptor subtype. A subset of the compounds used in each subtype pharmacophore model were chosen with a good cross-section of scaffold variety. The compounds used in the COMFA maps are the imidazobenzodiazines published previously³⁹ and additionally, alternative scaffolds which bound with <20nm at the respective subtype (see compound table in Appendix V).

The interest here was in creation of steric and electrostatic maps of the comparative molecular field analyses (COMFA) created from molecular spreadsheets. A variety of compounds selective for each subtype were selected and placed into a dataset used to build the CoMFA models. Activities (K_i values) were converted to logarithmic units for this study. A CoMFA descriptor set was created based on the $-\log(K_i)$ of over 70 structures. The goal was to derive an alternative three dimensional shape of the receptor using biological activity of the most selective compounds. Structures were determined by crystal structure where available or by calculation. Charges were provided based on the Gasteiger-Huckel model. Conformations were kept consistent based on previous studies of low energy conformations.^{38, 40} It should be noted that this was not a traditional QSAR study as nonselective compounds were excluded. Therefore, K_i values did not cross 3 log units. This was acceptable since the goal was not to create a predictive QSAR predictive algorithm, rather a map of the receptor based on sterics and electrostatics. Hydrogen acceptor radii were set to 3.0 and the hydrogen donor radii

were set to 2.6 based on recommendations from Certara (Tripos). Analyses were executed using PLS (partial least squares).

For each of the following QSAR models, green areas represent desirable steric bulk and yellow represents undesirable steric bulk. Positive electrostatic contributions are represented by blue and negative electrostatic contributions are represented by red.

The $\alpha 1\beta 3\gamma 2$ Receptor Subtype



Figure 45. Steric (left) and electrostatic maps of $\alpha 1\beta 3\gamma 2$ receptor subtype shown in transparent mode as seen from the classic perspective.

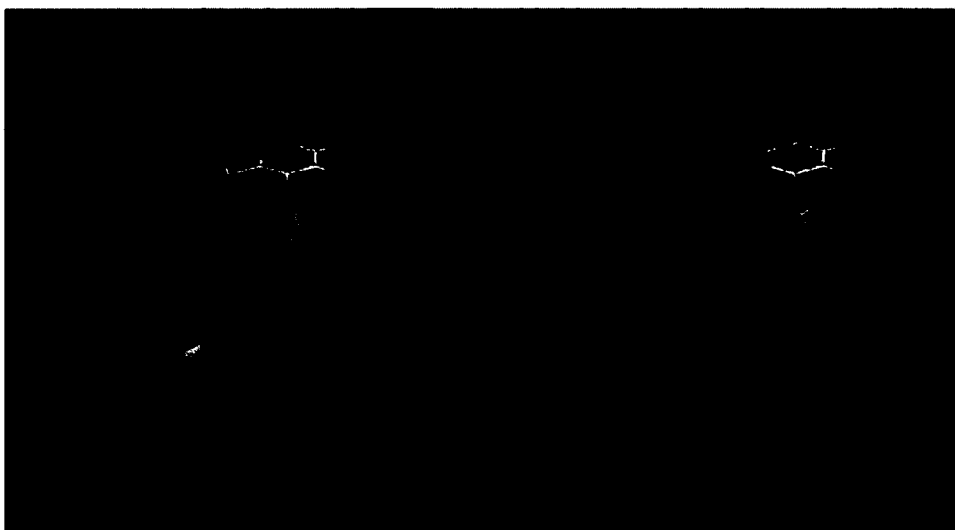


Figure 46. Steric (left) and electrostatic maps of $\alpha 1\beta 3\gamma 2$ receptor subtype shown in transparent mode as seen from the classic perspective rotated 90° .

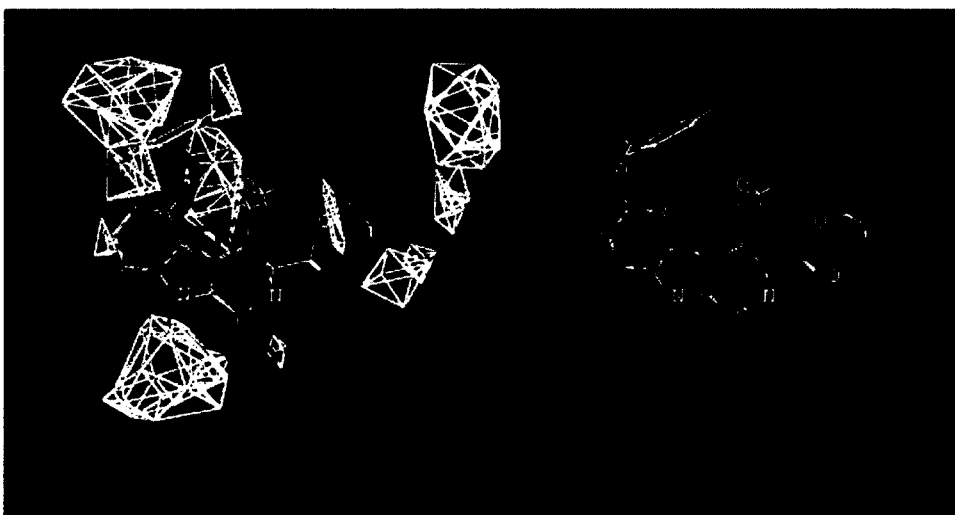


Figure 47. Steric (left) and electrostatic maps of $\alpha 1\beta 3\gamma 2$ receptor subtype shown in line mode as seen from the classic perspective.

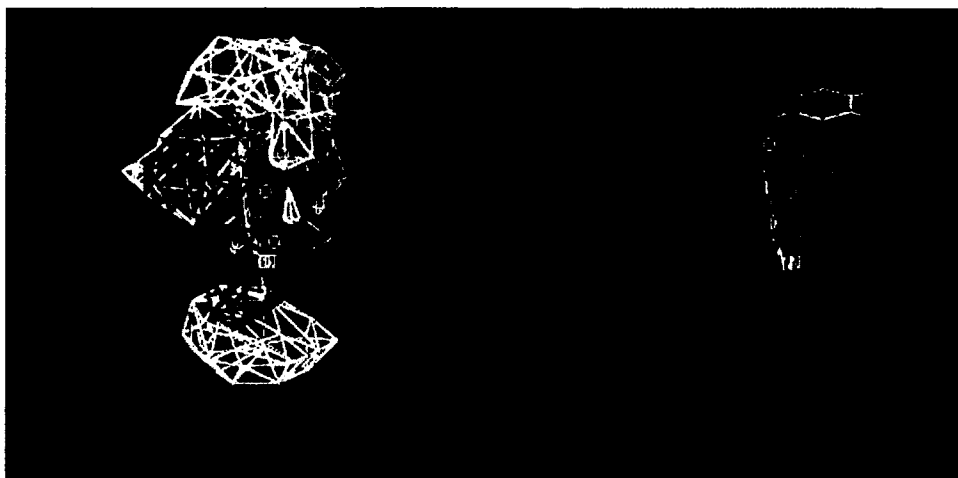


Figure 48. Steric (left) and electrostatic maps of $\alpha1\beta3\gamma2$ receptor subtype shown in line mode as seen from the classic perspective rotated 90°.

The $\alpha2\beta3\gamma2$ Receptor Subtype



Figure 49. Steric (left) and electrostatic maps of $\alpha2\beta3\gamma2$ receptor subtype shown in transparent mode as seen from the classic perspective.

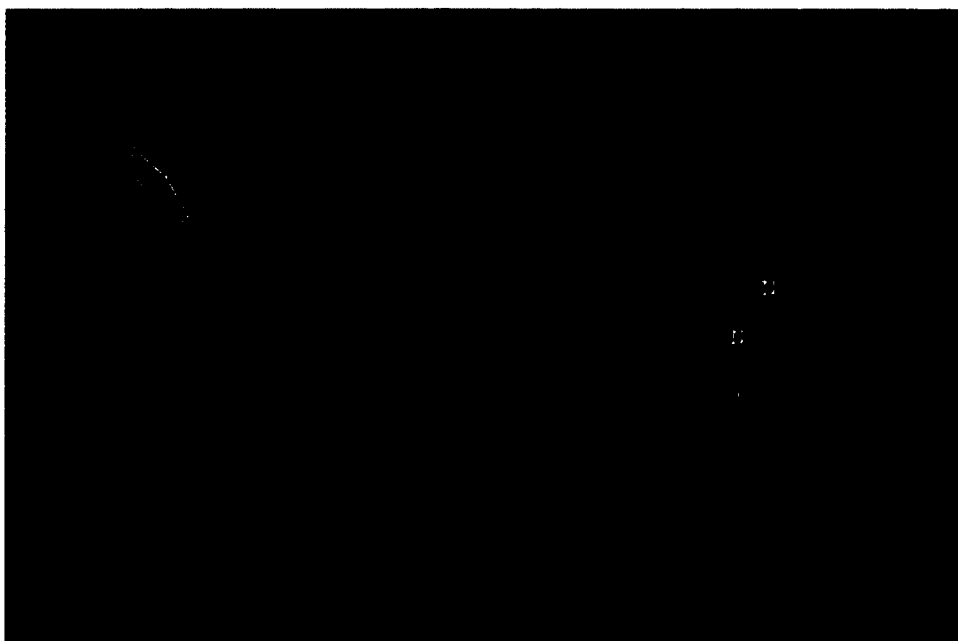


Figure 50. Steric (left) and electrostatic maps of $\alpha 2 \beta 3 \gamma 2$ receptor subtype shown in transparent mode as seen from the classic perspective rotated 90°.

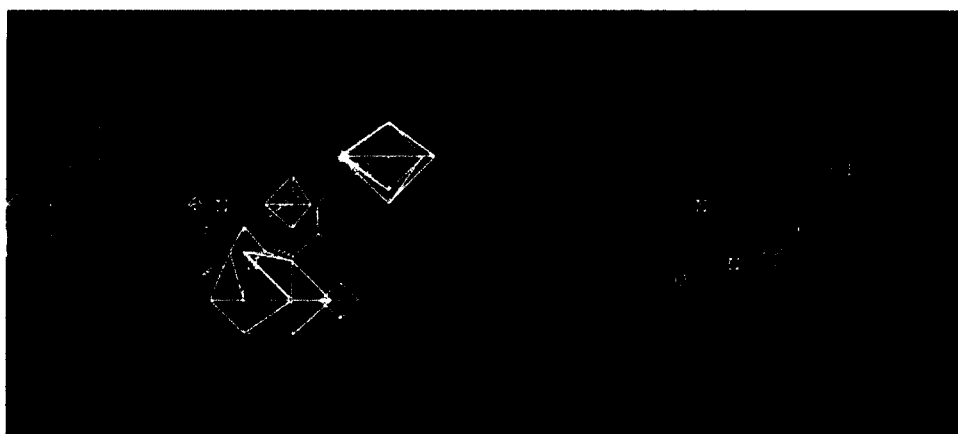


Figure 51. Steric (left) and electrostatic maps of $\alpha 2 \beta 3 \gamma 2$ receptor subtype shown in line mode as seen from the classic perspective.

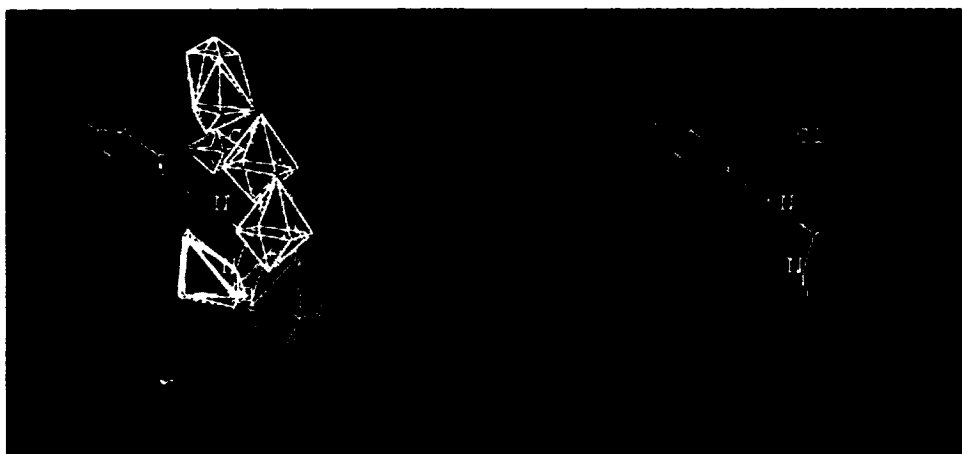


Figure 52. Steric (left) and electrostatic maps of $\alpha 2 \beta 3 \gamma 2$ receptor subtype shown in line mode as seen from the classic perspective rotated 90° .

The $\alpha 3 \beta 3 \gamma 2$ Receptor Subtype

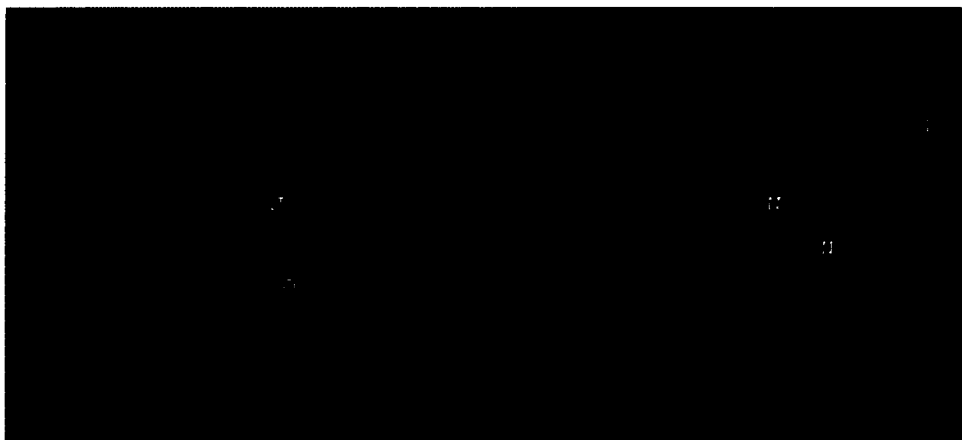


Figure 53. Steric (left) and electrostatic maps of $\alpha 3 \beta 3 \gamma 2$ receptor subtype shown in transparent mode as seen from the classic perspective.



Figure 54. Steric (left) and electrostatic maps of $\alpha 3 \beta 3 \gamma 2$ receptor subtype shown in transparent mode as seen from the classic perspective rotated 90°.



Figure 55. Steric (left) and electrostatic maps of $\alpha 3 \beta 3 \gamma 2$ receptor subtype shown in line mode as seen from the classic perspective.

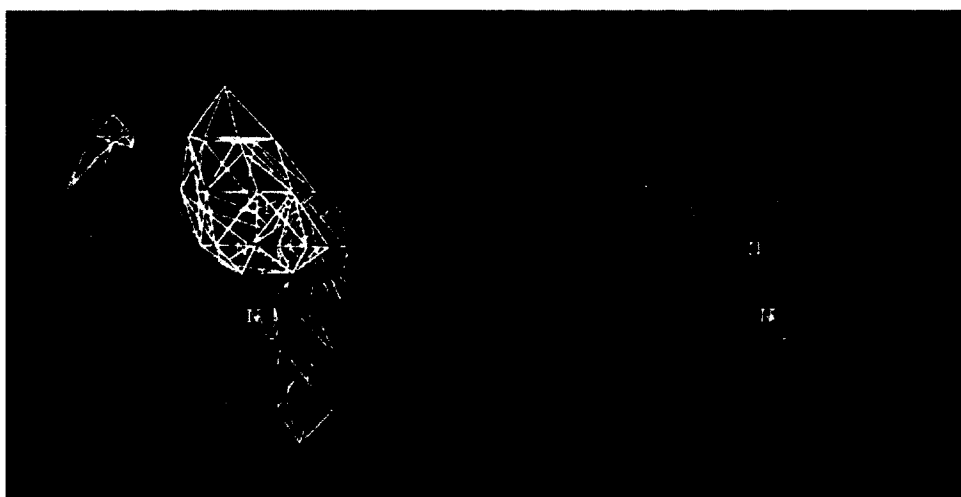


Figure 56. Steric (left) and electrostatic maps of $\alpha 3 \beta 3 \gamma 2$ receptor subtype shown in line mode as seen from the classic perspective rotated 90°.

The $\alpha 5 \beta 3 \gamma 2$ Receptor Subtype

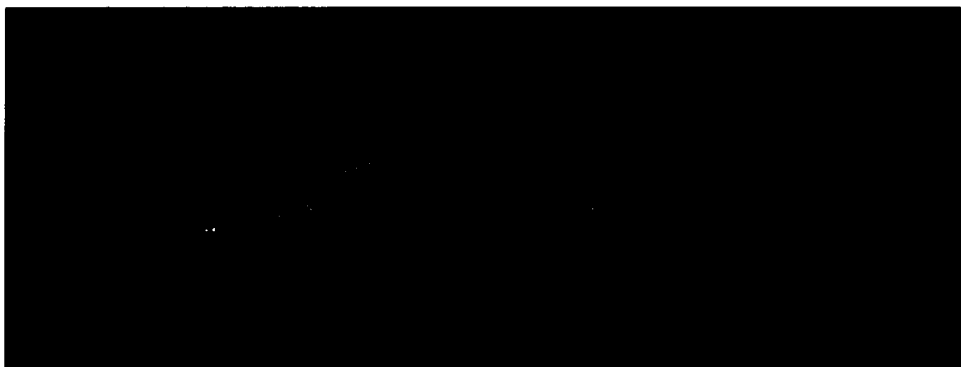


Figure 57. Steric (left) and electrostatic maps of $\alpha 5 \beta 3 \gamma 2$ receptor subtype shown in transparent mode as seen from the classic perspective.



Figure 58. Steric (left) and electrostatic maps of $\alpha 5\beta 3\gamma 2$ receptor subtype shown in transparent mode as seen from the classic perspective rotated 90°.

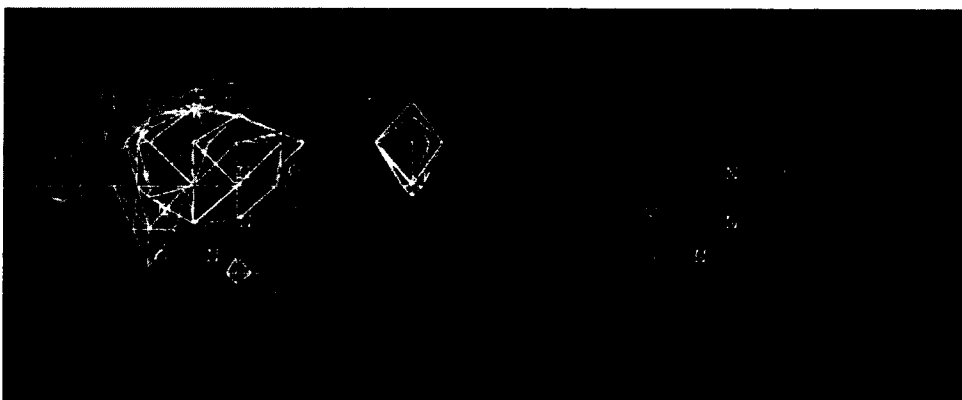


Figure 59. Steric (left) and electrostatic maps of $\alpha 5\beta 3\gamma 2$ receptor subtype shown in line mode as seen from the classic perspective.

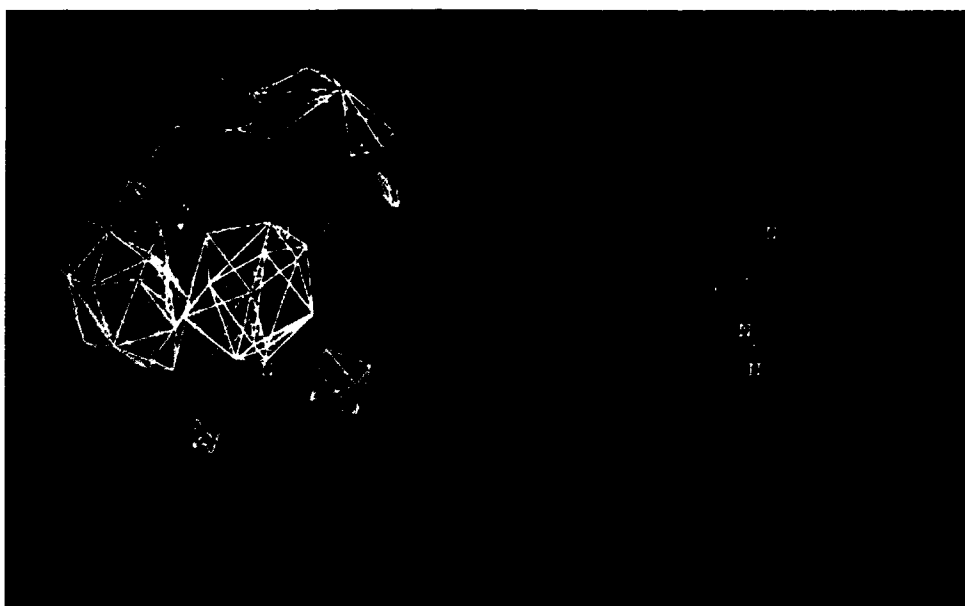


Figure 60. Steric (left) and electrostatic maps of $\alpha 5 \beta 3 \gamma 2$ receptor subtype shown in line mode as seen from the classic perspective rotated 90° .

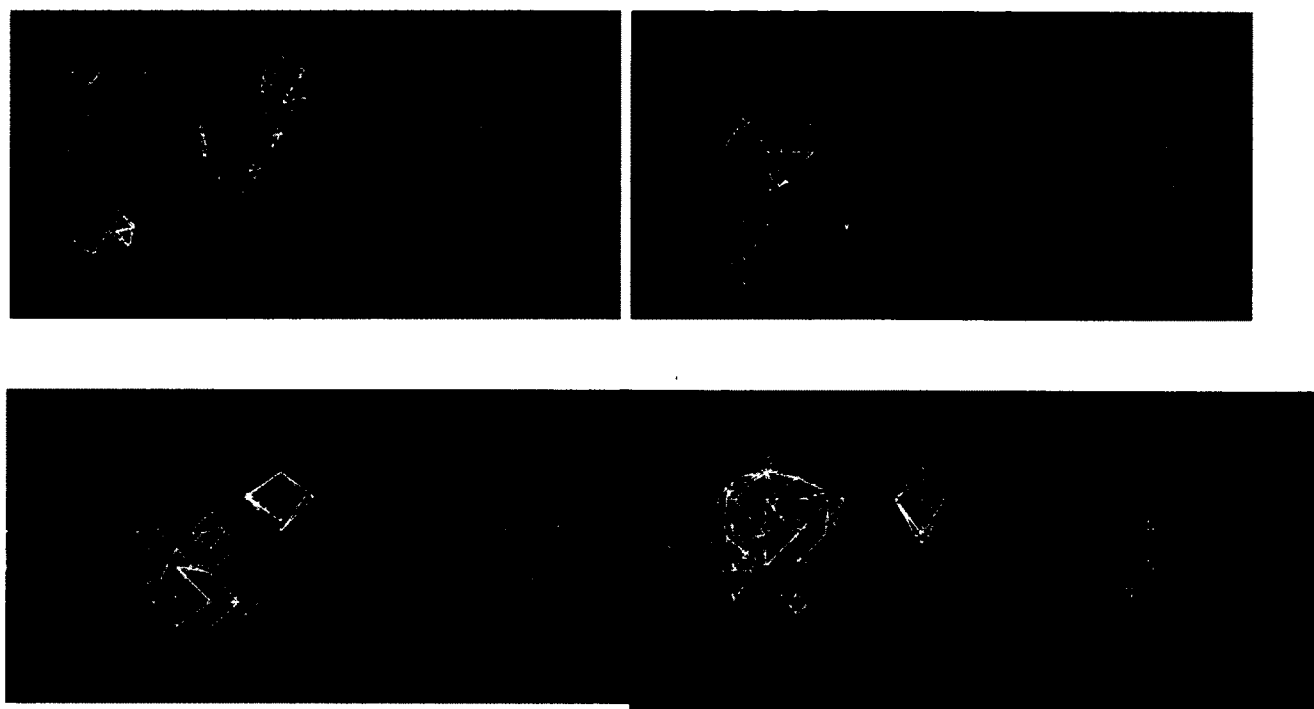


Figure 61. Clockwise from the top left, line maps of the $\alpha 1\beta 3\gamma 2$, $\alpha 2\beta 3\gamma 3$, $\alpha 3\beta 3\gamma 2$, and $\alpha 5\beta 3\gamma 2$ CoMFA.

From the CoMFA maps several observations (Figure 61) can be made. The yellow steric regions near L_3 in the $\alpha 5\beta 3\gamma 2$ map are unique. This illustrates that, in general, benzodiazepines lacking a pendant phenyl are more suited to targeting the alpha 5 subtype. The L_{Di} region of the alpha 1 subtype is most tolerable for compounds with steric interactions in this location with the alpha 3 subtype receptor preferring compounds which have no steric interaction in this location. Negative electrostatics are most preferred by the L_3 pocket of the alpha 2 and alpha 5 receptors. In general, the alpha 1 subtype receptor prefers molecules without a dipole. It should be noted that none of our analogs are ionic in nature and the charges for this model were provided by the Gasteiger-Huckel model. For this reason more emphasis is placed on the steric

relationships which exclude interactions in the pharmacophores. In the future a QSAR study which includes non-binding benzodiazepines in the data set along with activity data will permit the creation of a predictive logarithm which will be very useful in lead targeting.

Comparative Model of the Benzodiazepine Binding Site

Crystallization of GABA(A) receptors thus far has not been accomplished, but the successful structure determination of the water-soluble acetylcholine binding protein (AChBP)²⁶¹ has generated much interest in the GABA(A) receptor community. Although this protein shares only ~ 18 % sequence homology with the extracellular domain of the GABA(A) receptor,²⁶² the structural resemblance has been estimated to be relatively high (60 – 75 %).²⁶² Several comparative modeling studies have used the AChBP structure to derive models of the extracellular domain of GABA(A) receptors.^{40, 263, 264} Following electron cryomicroscopy (cryo-EM) determination of the extracellular and transmembrane domain structure of the nACh receptor, this structure was used as templates for modeling GABA(A) receptors.^{39, 265-267} Sequence homology is so low however, that detailed features of the models are highly uncertain, and the proposed dockings of Bz BS ligands¹⁰⁴⁻¹⁰⁶ have a qualitative character and as of this writing do not sufficiently explain the observed differential effects of ligands interacting with different receptor subtypes. The experimental structure of the nAChR^{268, 269} has provided initial data on how much the fold can vary between members of a family.^{208, 268-270} From this data the extent to which GABA(A) receptor subunits differ from each other in structure can be qualitatively extrapolated, but not predicted in detail.

As mentioned before, the majority of GABA(A) receptors are composed of 1 γ , 2 α and 2 β subunits. Each subunit has per convention a “plus” and a “minus” side (Figure 62). The subunit interfaces consequently consist of the plus and minus sides of neighboring subunits. The modulatory Bz BS is located at the $\alpha^+\gamma$ subunit interface and is larger than, but homologous to the two agonist (GABA) binding sites, which are located at the $\beta^+\alpha$ subunit interfaces.^{268, 269} The absolute subunit configuration for the $\alpha 1\beta 2\gamma 2$ GABA(A) receptor appears to be $\gamma\beta\alpha\beta\alpha$, when viewed counter clockwise (from + to -, Figure 62).²⁶⁰

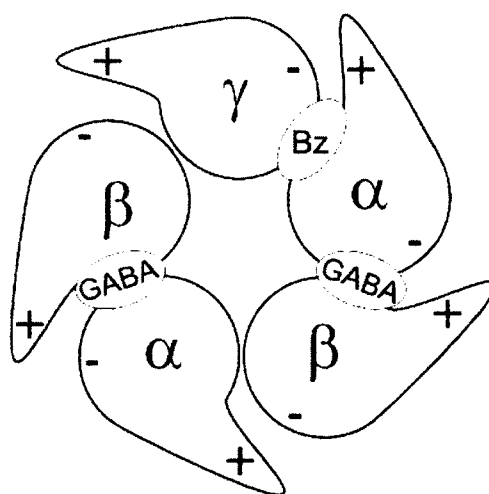


Figure 62. Absolute subunit arrangement of the $\alpha 1\beta 2\gamma 2$ GABA(A) receptor when viewed from the synaptic cleft.

The GABA(A) binding sites are located at the $\beta^+\alpha$ subunit interfaces and the modulatory benzodiazepine binding site is located at the $\alpha^+\gamma$ subunit interface. The part of the schematically drawn subunits marked by the + indicates loop C of the respective subunits (Figure 62).

While the $\gamma 2$ subunit is required for recognition and binding of benzodiazepines as well as many other substance classes that act via the Bz BS,²⁶² it is now clear that sequence variations between different α subunits determine subtype selectivity and efficacy of Bz BS ligands.²⁷¹ The Bz BS has been proposed to consist of three segments provided by the α^+ side, the so-called “loops A, B and C” and by three segments of the γ^- , the so-called “loops D, E and F”.²⁷² These segments were then confirmed by X-ray crystallographic and EM-structures of AChBP²⁷² and the nAChR¹⁷⁴ to form a groove-like pocket at the interface boundary between subunits that appears to be conserved in the entire superfamily. The group at Milwaukee proposed a near planar cleft to represent the BzR binding sites as long ago as the 1980’s by Trudell and Hagen.^{18, 22, 26}

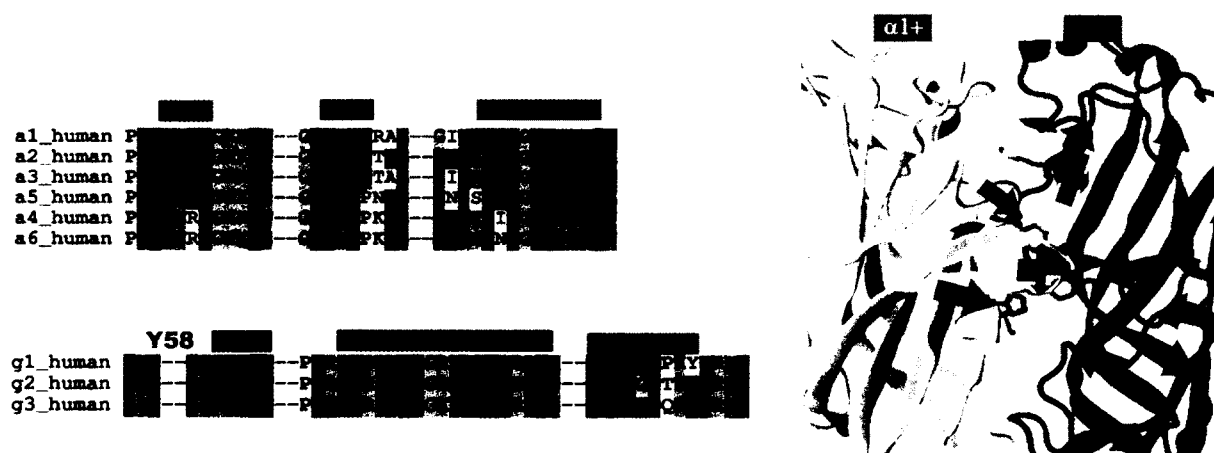


Figure 63. Alignment and homology model depiction of the so called “loops A-F” and flanking regions of the human sequences of the Bz recognition site in different subunits.

The homology model (Figure 64) is as seen from “outside” of the channel mouth, the membrane would be parallel to the top edge of the image. Key residues are shown in stick representation: Loop A His102, loop B Tyr 160 and loop D Phe77.

Even later than the nAChR structure, a series of AChBP crystal structures with co-crystallized ligands appeared.²⁷³ These structures revealed how ligand binding can alter the local conformation of the binding site. Particularly loop C has been found to be a highly mobile sub-domain, with additional and more subtle changes seen along the entire subunit boundary.²⁷⁴ These findings are consistent with the hypothesis that many receptor conformations exist, that are separated by low energy barriers, and can be stabilized by different ligands. Unfortunately, it cannot be decided conclusively at this time *a priori* which of the experimental structures is the “best” template to model a particular receptor/ligand complex. Depending on template and alignment choice, model Bz pockets differ in total volume by as much as 40% and can vary by several angstroms in the distances between key residues in the binding site loops.

Although changes in protein conformation may be minor, it has been demonstrated that they can profoundly affect the efficacy of Bz BS ligands.²⁷⁵ Furthermore, efficacy can vary for the same ligand at different GABA(A) receptor subtypes.³⁸ Since proteins are inherently dynamic and able to sample many conformations, the stabilization of the active state relative to the inactive state has been calculated to be less than 1 kcal/mol.²⁶¹ It is not possible at present to provide absolute assignments of specific side chains to specific descriptors for any particular conformation. This conformational flexibility may imply that residues which satisfy

certain pharmacophoric descriptors can vary, resulting in a “soft” orientation of the pharmacophore in the receptor. Thus, a unified view of a pharmacophore model and a homology derived receptor model will assign large areas of lipophilic interaction to specific regions in the protein, but allow a flexible assignment of specific interactions such as H-bridges or π - π stacking. Further complicating matters is the possibility of waters participating in the binding pocket. This is the reason for the Milwaukee-based pharmacophore/receptor models for drug design have been based on the rigid planar ligands ($K_i = 5\text{nM}$ – 20nM) of Trudell et al.⁴²

Relative Orientation of the Pharmacophore within the Comparative Model

Prior to structure determination of the AChBP, a review was published from Milwaukee, which evaluated results of site-directed mutagenesis and provided insights as to where certain side chains in the Bz BS might be located relative to the pharmacophoric descriptors.^{260, 262, 272} However, with the knowledge gained from recent experimental data and with the aid of our GABA(A) receptor models, built by homology to lymnea AChBP,¹⁹⁵ aplysia AChBP and the nAChR²⁰⁴ an update of the orientation is provided here. An orientation is now proposed which is favored by experimental evidence and allows some degree of conformational flexibility. It can lead to variable assignments for H-bridge interactions, but is based on specific areas of lipophilic interactions that are determined by binding site geometry and hydrogen bonding to certain residues which align “softly” with docked ligands (Figure 67).

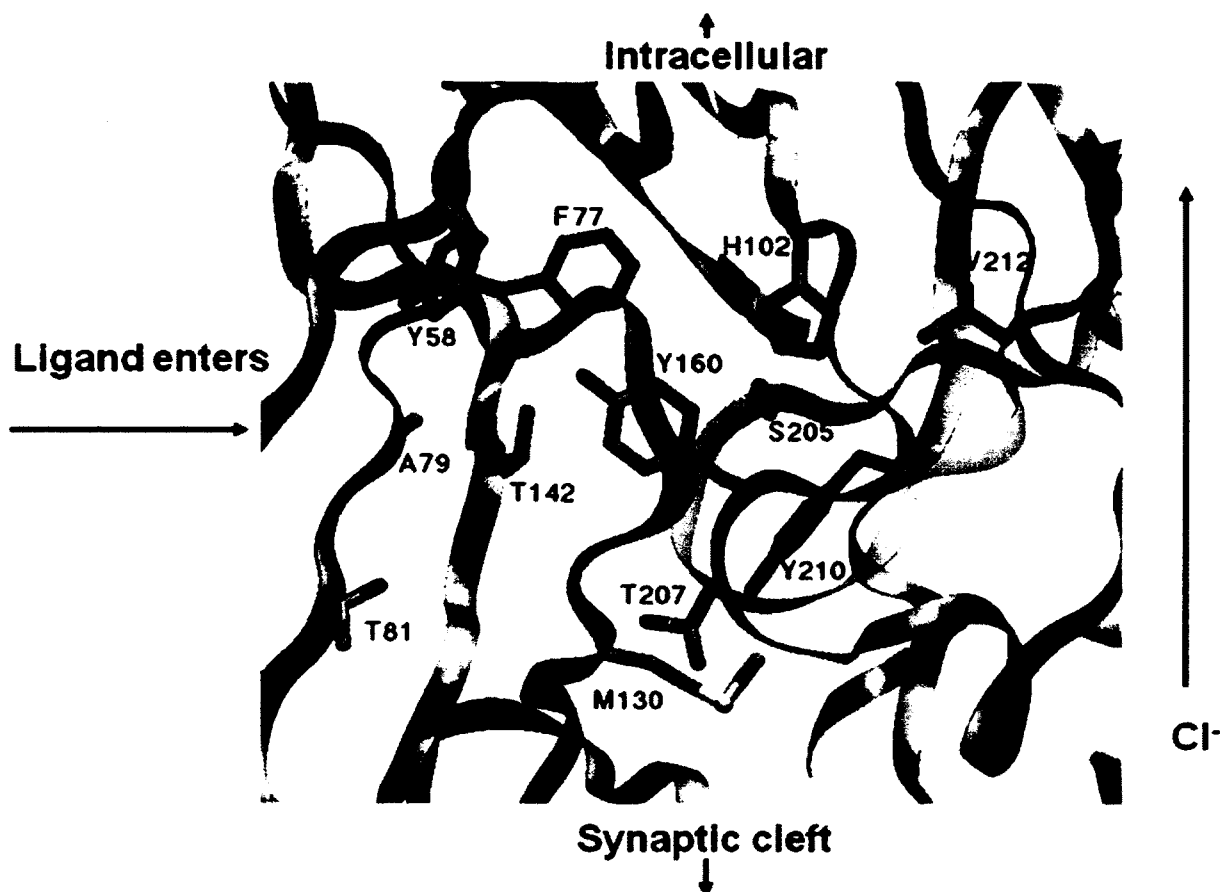


Figure 64. Ribbon illustration of the GABA(A) BzR binding pocket conceived by Clayton et al.^{198, 276,}

277

Combining Homology Model and Experimental Evidence

If the two assignments discussed above are correct, they should be reflected in results of computational ligand docking to homology models of the binding site. Thus, computational docking of diazepam and flumazenil was performed in multiple different models based on different templates²⁷⁴ and the best 100 docking poses per model were collected in a database. A database query was then formulated to search among the (unrefined) docking poses for those with the following properties: The seven membered

ring of diazepam or flumazenil is in the conformation that is assumed to be the active one;^{33, 62, 69, 213} the 7-substituents are near residues $\alpha 1H102/\alpha 1V203/$ and $\alpha 1Y210/\alpha 1V212$ in order to be consistent with the covalent labeling data; the 3' ester group of flumazenil is near residues $\gamma 2A79$ and $\gamma 2T81$. Such a query yields docking poses that are consistent with all covalent labeling studies on the one hand, and with the steric requirements that were found for 3' substituted imidazobenzodiazepines²⁶⁶ on the other hand.

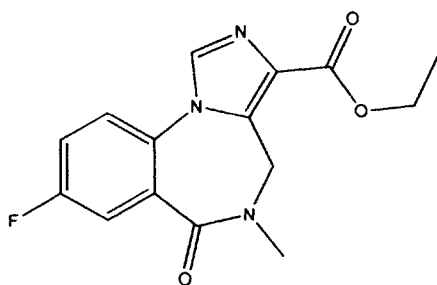


Figure 65. Flumazenil

Such poses were indeed present in the database, and one representative diazepam pose is shown in Figure 66.



Figure 66. Diazepam docking pose in $\alpha 1\gamma 2$. The beta subunit is not in the binding pocket.

In Figure 67, diazepam was rendered space filling, (turquoise: carbon, white: hydrogen, green: halogen, red: oxygen, and blue: nitrogen), the protein as a ribbon, and the key amino acids in stick representation. The insert figure shows the empty pocket in the “upright” position to facilitate orientation in the main figure, where the model has been turned and tilted to bring diazepam approximately into the orientation depicted in the unified pharmacophore model. In this particular docking pose, His102 and Thr207

satisfy H_2 and H_1 , respectively, and His 102, Val 212 and Tyr 210 would be part of the L_2 hydrophobic pocket. This positions 7-substituted reactive analogues such as isothiocyanate **92** into a position where the reactive groups find free access to His102, Tyr 210, Val 212, and Val 203.

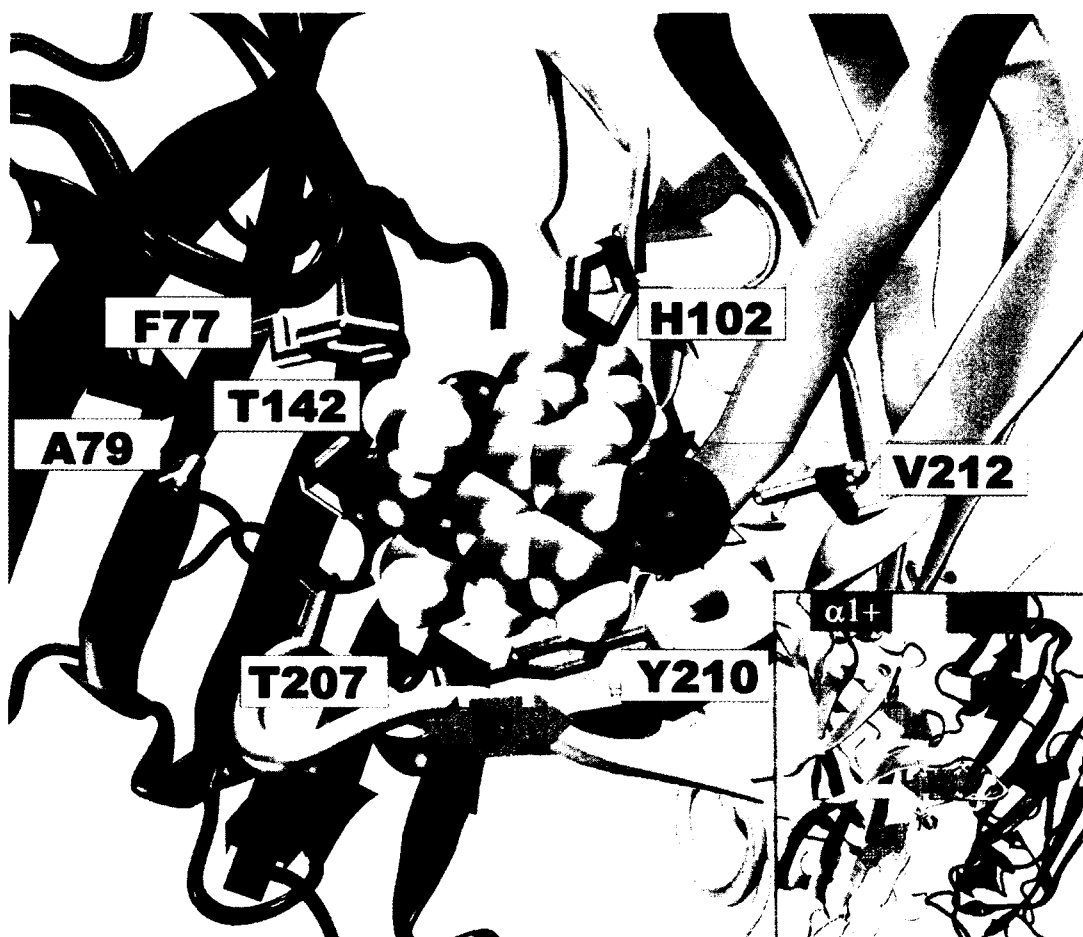
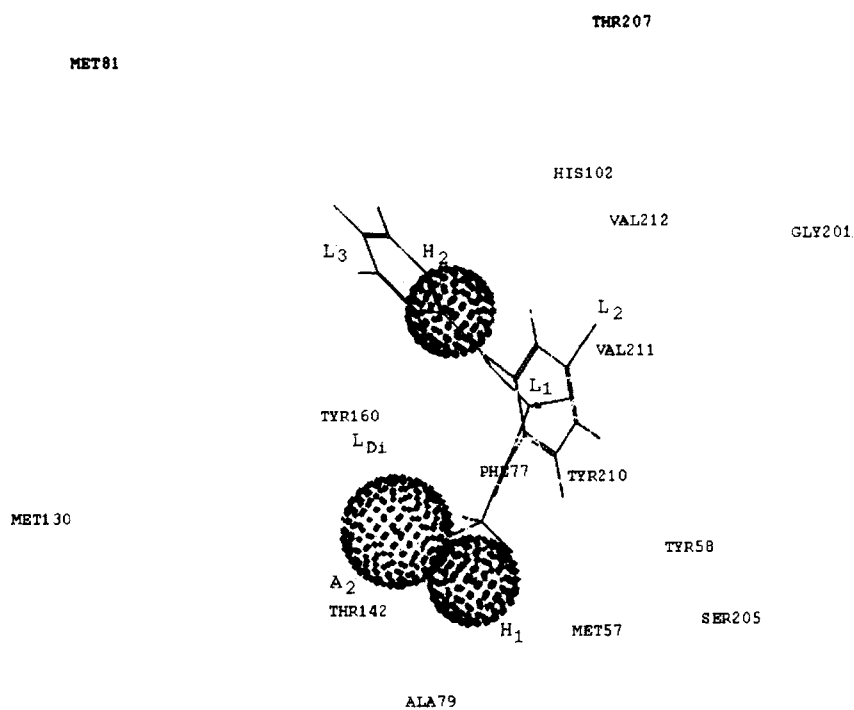
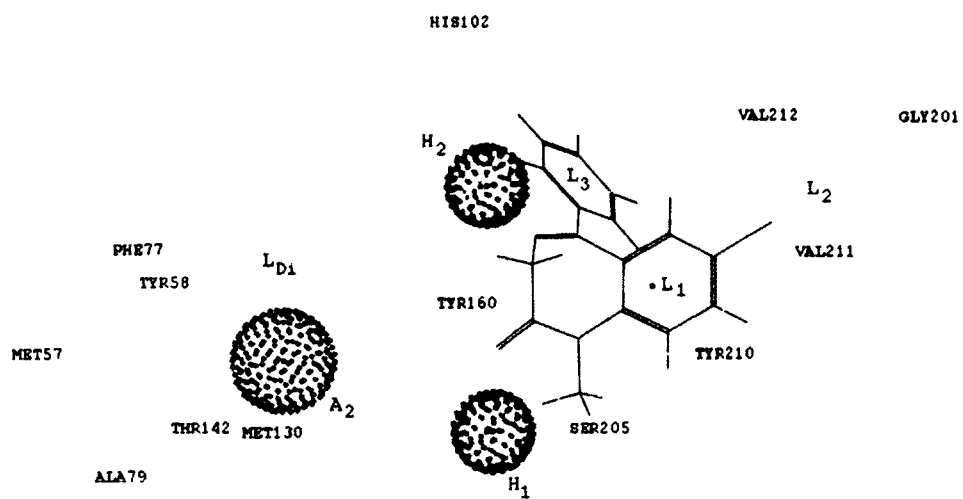


Figure 67. High resolution image of diazepam docking pose in $\alpha 1\gamma 2$ binding pocket

The docking pose in Figure 67 and similar docking poses not only satisfy the two assignments for L_2 and A_2 that are discussed in the sections above, but at the same time position the remaining descriptors as follows: H_1 can be satisfied by appropriate side

chains near the tip of loop C, the L_{DI} region is near the subunit interface, essentially between $\alpha 1$ loop B (Y160) and the $\gamma 2$ region spanned by the interface forming the sheet involving M130, T142 and F77; A_2 can be satisfied by H-bridge accepting sites near $\alpha 1$ Y160, $\gamma 2$ A79, $\gamma 2$ T81, $\gamma 2$ M130 and $\gamma 2$ T142. If these proximity relations that are found in the docking poses are transferred to the unified pharmacophore model, the following residue orientation emerges:



MET81

THR207

Figure 68. Orthogonal views of the location of residues with respect to pharmacophore in the $\alpha 1\beta 3\gamma 2$ BzR binding pocket

The location of important Bz BS residues relative to the pharmacophoric descriptors in two views that correspond to a 90° rotation about L₁, with A₂ in front, as determined by evaluation of experimental data and the comparative model of the $\alpha 1\beta 2\gamma 2$ GABA(A) receptor are illustrated in Figure 67 and 68. The ligand shown is diazepam. Since inverse agonists stabilize protein conformations that vary from the conformations preferred by agonists, it is plausible that more than one side chain could satisfy the same descriptor.

Within the different poses that exhibit this orientation, there is still some degree of variation in structural details. There are several sources for this variability in the computationally derived structures: template and alignment choice, model construction and refinement, as well as docking algorithms contribute to the variability of the poses that are found.

This orientation is also strongly supported by the observation that XLi-093, as aligned in Figure 13 with the docked Ro15-1788 shown above, will be able to thread the portion of the molecule not inside the included volume towards the solvent accessible space through the subunit boundary, but into the extracellular domain.

Agreement between this orientation of the pharmacophore model inside the structural model of the protein with single ligand dockings that have been proposed in the past²⁷⁸ will have to be examined in detail. The overall picture appears to be pointing towards a satisfactory orientation of the pharmacophore model in the pocket, and for those instances where there could be a discrepancy, further experiments will clarify.

Refinement of the predicted protein-ligand complexes with the aid of the unified pharmacophore model is a very promising approach to arrive at 3D structures that are of sufficient accuracy to be used for structure guided drug design. Studies that combine advanced protein modeling techniques with the classical pharmacophore approach are currently underway.



Figure 69. Unified model of the $\alpha 1\gamma 2$ subtype benzodiazepine receptor with diazepam docked in the binding site.

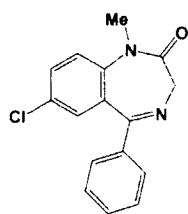
Construction of the Unified Pharmacophore/Receptor Model

More than 150 agonists, antagonists and inverse agonists at the Bz binding site^{43,44} which encompassed 15 structural families were used for generating the unified pharmacophore/receptor model. Although the relative affinities, efficacies and functional effects displayed by various ligands from the same structural class at the diazepam-sensitive and diazepam-insensitive benzodiazepine binding sites were taken into account, the approximate locations of descriptors (hydrogen bond donor sites, hydrogen bond

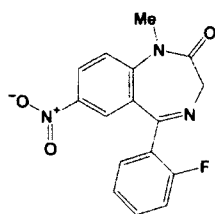
acceptor sites, lipophilic regions, and regions of steric repulsion) were based primarily on *in vitro* binding affinities. Ligands from different structural classes were then superimposed on each other to satisfy the same descriptors, resulting in the unified pharmacophore model. The rigid planar templates ($K_i = 5\text{nM}$ - 20nM) of Trudell were employed to begin this effort.²⁶⁰

The pharmacophore/receptor model consists of two hydrogen bond donating descriptors (H_1 and H_2), one hydrogen bond accepting descriptor (A_2) and one lipophilic descriptor (L_1). In addition to these descriptors, there are lipophilic regions of interaction (L_2 , L_3 , L_4 , and L_{Di}) as well as regions of negative steric repulsion (S_1 , S_2 and S_3). While occupation of L_2 and/or L_3 , and L_4 as well as interactions at H_1 , H_2 , and L_1 are important for positive allosteric modulation, inverse agonists only require interactions with the H_1 , L_1 , and A_2 descriptors of the pharmacophore/receptor model for potent activity *in vivo*.²⁶⁰ The L_3 descriptor is a region of lipophilic interaction, for which the difference between the diazepam sensitive (DS) and the diazepam insensitive (DI) sub-pharmacophore models is most pronounced. Depicted in Figure 30 are the relative locations of the different descriptors and regions of the model. Several classes of ligands for GABA(A) are shown in Table 24.

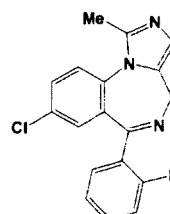
Table 24. Structures of ligands and their modulation at the $\alpha 1$ subtype



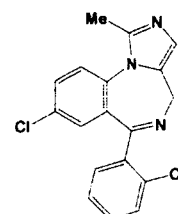
diazepam
agonist



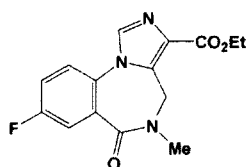
flunitrazepam
agonist



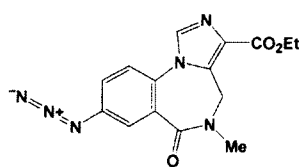
midazolam
agonist



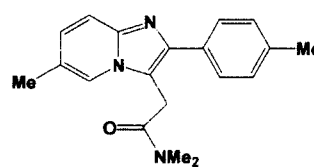
triazolam
agonist



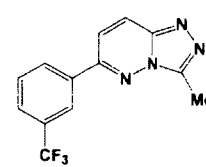
Ro15-1788
antagonist



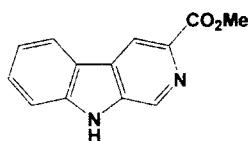
Ro15-4513
inverse agonist



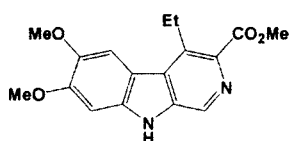
zolpidem
agonist



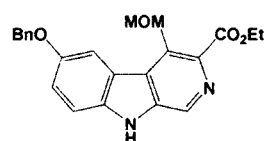
CL-218,872
partial agonist



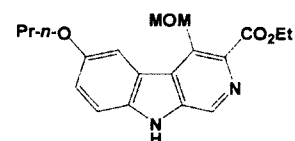
β -CCM
inverse agonist



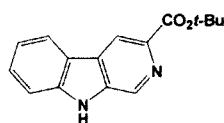
DMCM
inverse agonist



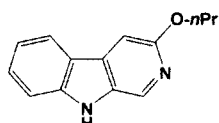
ZK-93423
agonist



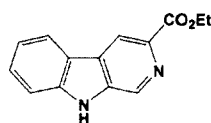
6-PBC
partial agonist



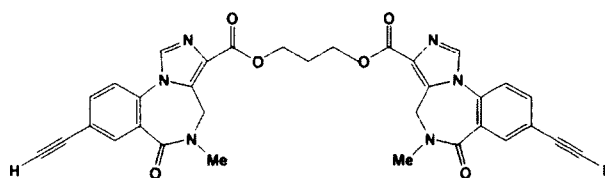
β -CCT
antagonist



3-PBC
antagonist



β -CCE
inverse agonist

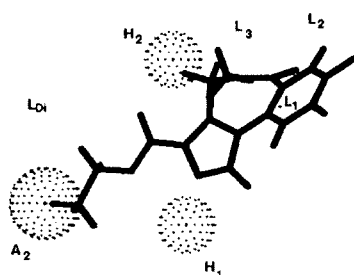


XLi-093

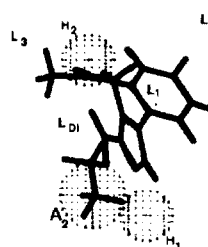
antagonist at $\alpha 5$

The alignments of several Bz BS ligands within this model are shown in Figure

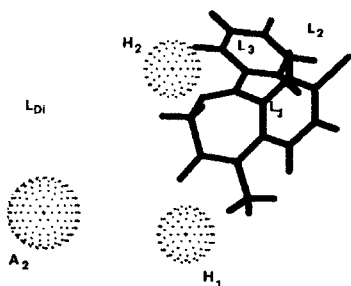
70.



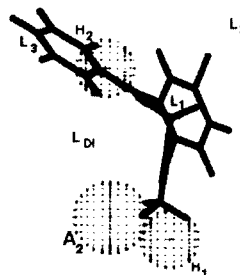
Ro 15-1788



Ro 15-1788 rotated 90°



diazepam



diazepam rotated 90°

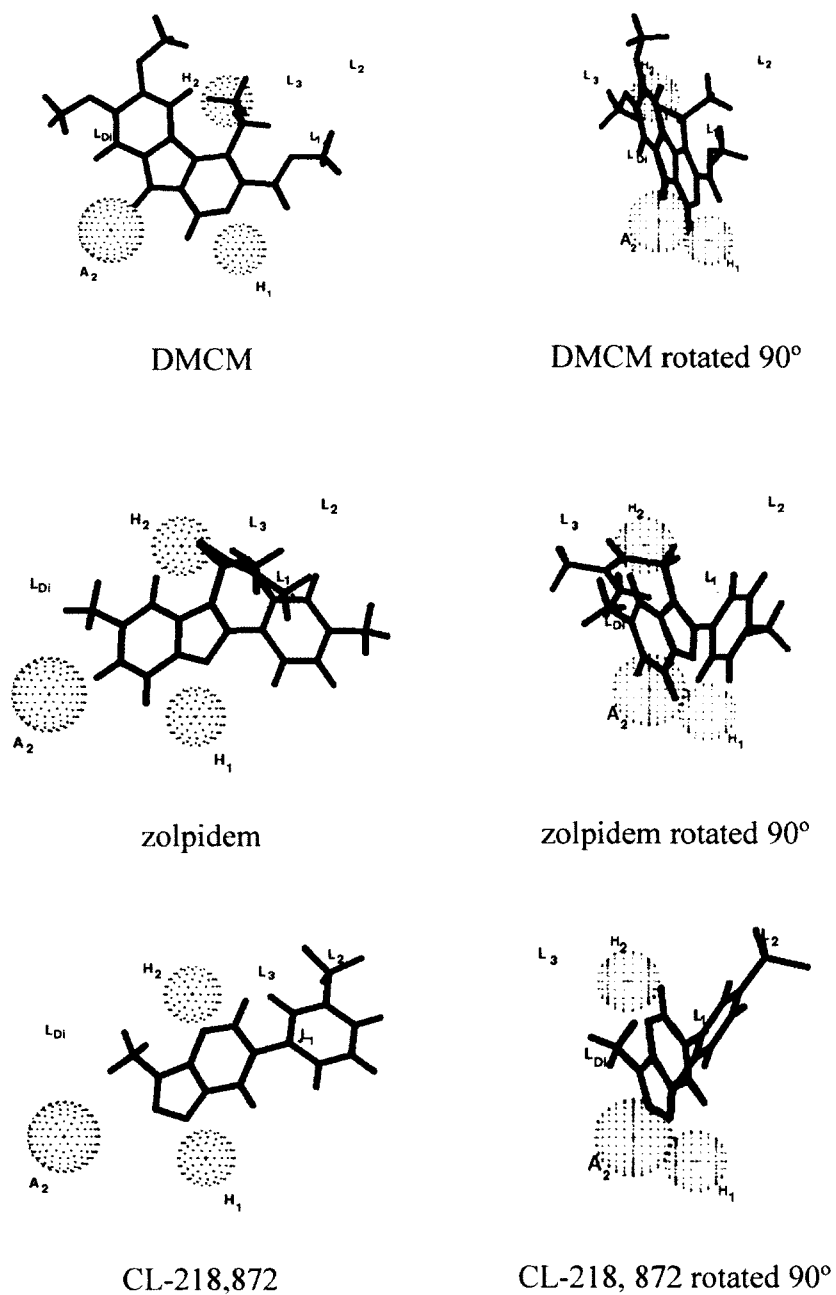


Figure 70. Alignments of several Bz BS ligands within the pharmacophore model.

A unified pharmacophore model incorporating many substance classes that act at the DS and DI benzodiazepine binding sites of GABA(A) receptors has been updated to include new substance classes. Compound development guided by this pharmacophore

model has led to new agents with interesting pharmacological profiles, particularly enhanced preference for $\alpha 2$ or $\alpha 5$ containing GABA(A) receptor subtypes. Based on the evaluation of experimental data and comparative models of the $\alpha 1\beta 2\gamma 2$ GABA(A) receptor, the location of several residues relative to the descriptors of the pharmacophore/receptor model has been proposed. Although no absolute assignments were made regarding which amino acids satisfy the pharmacophoric descriptors, experimental data strongly indicated definite trends with regard to how ligands of varying pharmacological activity are oriented within the receptor. Because the unified pharmacophore/receptor model accounts for the binding and activity profiles at the six GABA(A) receptor subtypes containing any one of the different alpha subunits, the proposed orientation should also be similar within the different models²⁶⁰ of the various receptor subtypes. Information to be immediately gained from these proposed orientations can have far reaching benefits, not only for the rational design of selective ligands and the interpretation of ligand docking results, but also for the identification and evaluation of possible roles certain residues may have within the pocket. As structure determination of the GABA(A) receptor is eagerly awaited, it is hoped that these proposed orientations may be used by others to gain additional insight into the potential mechanisms underlying binding and modulation at the Bz site, all of which will lead to a better understanding of the structure and function of GABA(A) receptors. In the next section the methods used to build the protein model will be explained.

Homology Models of the Benzodiazepine Receptor

The γ -aminobutyric-acid (GABA(A) and GABA_C) pentameric ligand gated ion channels are members of a superfamily of allosteric transmembrane proteins which

includes the nicotinic acetylcholine (nAChR), serotonin 5-HT₃, and glycine receptors. Electrophysiological data on GABA(A) is available but attempts at atomic resolution to acquire structural data have so far been unsuccessful. However, in 2001 Smit²⁶⁰ discovered a homologue of the nACh receptor ligand-binding domain from the snail *Lymnaea stagnalis*. Acetylcholine-binding protein (AChBP) is produced in the glial cells of *Lymnaea stagnalis*. In the synaptic cleft, AChBP modulates synaptic transmission. Subunits of the snail glial cells form a stable homopentamer with conserved N terminal domains. Known agonists and antagonists of nAChRs bind to the homologue. For this reason, it is a valuable template for modeling the N-terminus domains of pentameric ligand gated ion channels.²⁶³

Brejč *et al.* successfully solved the crystal structure of AChBP by X-ray crystallography using weak Pb multiple wavelength anomalous diffraction (MAD) data in two crystal forms.³⁸ The crystals were grown at room temperature using the hanging-drop vapour diffusion technique. The crystal structure revealed a radially symmetric homopentamer with extracellular dimensions of the nicotinic acetylcholine receptor (nAChR) which correlated with measurements taken using electron microscopy.²⁷⁹

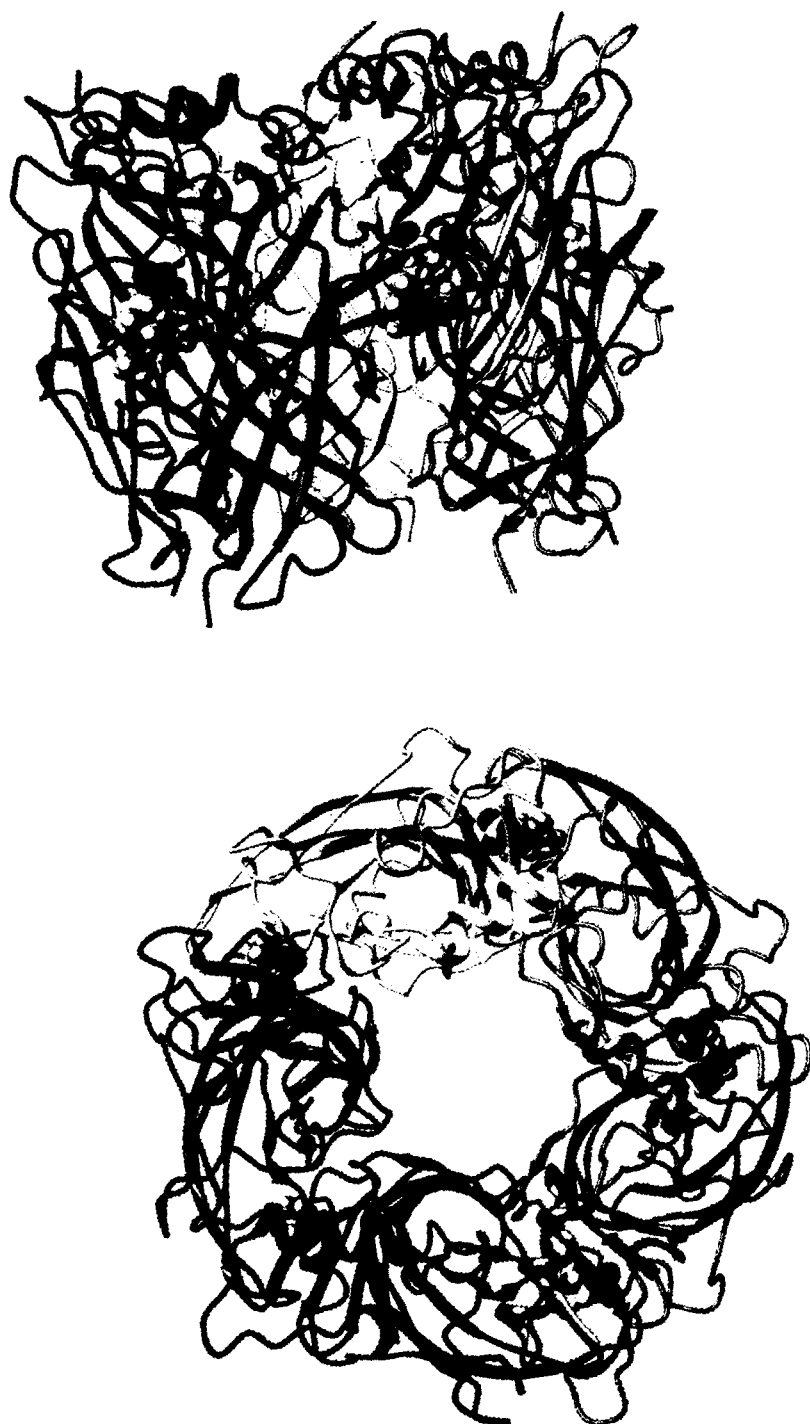


Figure 71. Orthogonal views of the homopentameric acetylcholine binding protein crystallized from *Lymnaea stagnalis*. The subunits have been assigned different colors for clarity

Subunits are homologous and have been colored by chain to distinguish them. In space filling models, HEPES (N-2-hydroxyethylpiperazine-N'-2-ethanesulphonic acid (present during the crystallization process) can be seen bound in the ligand binding site between each subunit interface.²⁸⁰

The N terminus is located at the “mouth” of the ion channel in the synaptic cleft. A molecule of HEPES was present in the acetylcholine binding pocket. This was verified as the residues implicated with agonist binding in nAChR and AChBP were conserved in the receptor. The residues lie in four regions identified as loops A, B, C, and D. Loops A, B, and C are located on what is referred to as the ‘plus’ face while loops D, E, and F lie on the ‘minus’ face (see Figures 72 and 73). In the heteromeric nAChR, agonist binding takes place between the ‘plus’ face of a subunit and the ‘minus’ face of an α or δ subunit. Site directed mutagenesis and radioligand binding assays have established that residues of the GABA(A) receptor involved in ligand binding align with residues in loops A, B, and C of the α subunit and loops D and E of the γ subunit.²⁸⁰

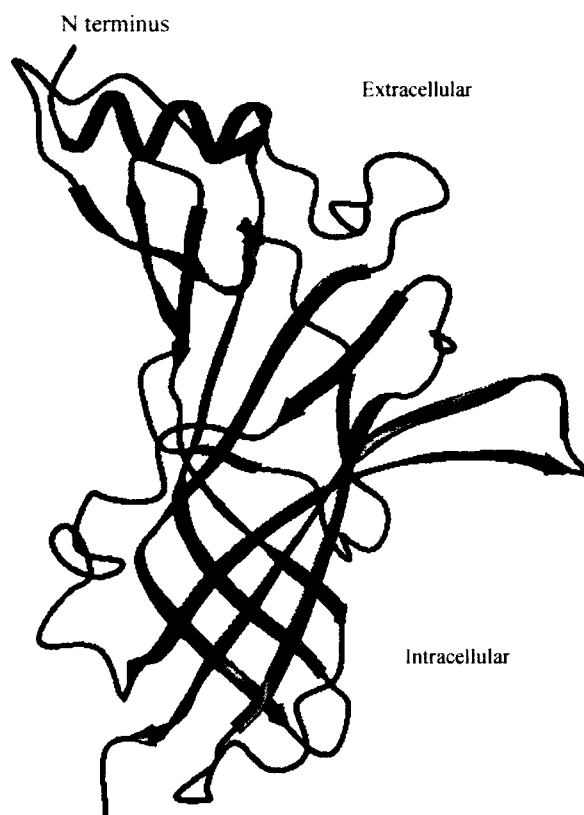


Figure 72. Single subunit of acetylcholine binding protein crystallized from *Lymnaea stagnalis* (side view)

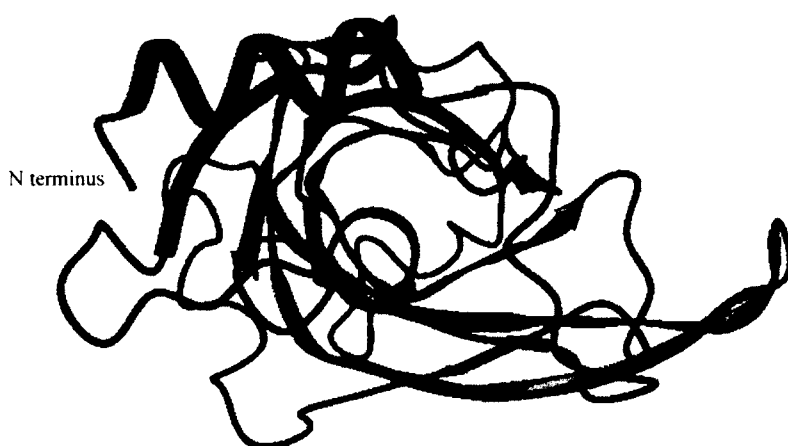


Figure 73. Single subunit of acetylcholine binding protein crystallized from *Lymnaea stagnalis* (top view)

Since the AChBP is a member of the Cys-loop LGIC superfamily, it offers a template for building models of the the ligand binding domains of the Cys-loop superfamily. The AChBP was used to build homology models of the subtypes of the GABA(A) receptors. The ligand binding domains of human GABA(A) receptors ($\alpha 1$, $\alpha 2$, $\alpha 3$, $\alpha 5$, $\beta 2$ and $\gamma 2$) were obtained from the Research Collaboratory for Structural Bioinformatics (RCSB). Originated in 1971 at Brookhaven National Laboratories, this is the home of the Protein Data Bank. The PDB archive is the repository of information about the 3D structures of large biological molecules such as proteins and nucleic acids. With the protein sequences in hand, a critical first step in building a homology model is to align the raw protein sequence with the protein sequence of a target protein or template structure. Alignments are prepared using multiple sequence alignment software for DNA and proteins.³⁸

After calculating the best match for the selected sequences, they are lined up so identities, similarities, and differences can be seen. Programs which perform this include MAFFT, Muscle, Multalin, ClustalW, and BlastAlign (<http://pbil.univ->

lyon1.fr/alignment.html). Templates can also be found by performing a query of the raw protein sequence against the Protein databank. This is performed using the protein database search program, Gapped Blast.³⁸ The report will contain a list of sequences producing significant alignments, PDB code, protein description, a normalized alignment score and an Expect (E) value. In general, a lower E score describes the background noise that exists between sequences. A lower E value correlates to a more significant score. Once a proper alignment of protein sequences was performed, the raw protein sequence was threaded onto the AChBP using Deep View. The crystal structure of the AChBP was downloaded from the Swiss Protein Databank Viewer. Deep View is a Swiss Protein Databank Viewer (<http://ca.expasy.org/spdbv>). Threading is performed after the alignment is complete. Amino acids which have been identified as equivalent between the proteins are “fit”. This is similar, but more precise than the “3 corresponding atoms” technique. Deep View includes a tool, *Magic Fit*,¹⁰ which performs the threading procedure for all residues across a raw sequence and a reference protein. Once the preliminary model has been built, a manual inspection can be performed. Considerations during manual inspection include, identifying areas of low homology, and manually aligning gap regions with loops in the reference protein.²⁸¹ Loop regions which correspond to gaps were in the alignment can be modeled by fitting structures from a loop database. In the current model, loop regions were mapped to a loop database by Cromer et al.^{42, 263}

Upon completion of the preliminary model, the following properties can be studied using Deep View and Sybyl³⁸:

1. Surface hydrophobicity

2. Solvent accessibility of N-glycosylation sites after pentamer assembly
3. Acidic, basic, and non polar maps
4. Sybyl X minimizations
5. Steric clashes
6. RMSD of alpha carbons
7. Location of disulfide bonds

In order to improve the prediction of areas of low homology PHD was utilized by Cromer et al.²⁸²⁻²⁸⁴ PHD or more commonly referred to as PredictProtein is a sequence analysis tool and the prediction of protein structure and function. Protein sequences or alignments are submitted to Columbia University; PredictProtein returns multiple sequence alignments, PROSITE sequence motifs, low-complexity regions (SEG), nuclear localisation signals, regions lacking regular structure (NORS) and predictions of secondary structure, solvent accessibility, globular regions, transmembrane helices, coiled-coil regions, structural switch regions, disulfide-bonds, sub-cellular localization, and functional annotations. Upon request the Rost group will perform fold recognition by prediction-based threading, CHOP domain assignments, predictions of transmembrane strands and inter-residue contacts are also available. PredictProtein is run by Burkhard Rost at Columbia University in New York (www.rostlab.org).²⁸⁵ As an alternative, Swiss Model can be used to model subunit loop regions by searching structures from loop databases.

Once subunits were completed, a pentamer was constructed taking into consideration residues determined experimentally to be present in the allosteric and GABA binding site. On the α subunit, this includes α Tyr160, α Tyr210, γ Phe77, and

α Ser205.^{286, 287} After manually assembling the subunits and comparing an overlay with AChBP, the structure was energy minimized.²⁸⁸

With protein receptor models for $\alpha 1\beta 3\gamma 2$, $\alpha 2\beta 3\gamma 2$, $\alpha 3\beta 3\gamma 2$, and $\alpha 5\beta 3\gamma 2$ completed a truly *unified* pharmacophore model was assembled for each receptor subtype. Using the Tripos Biopolymer software, the pharmacophore was manually aligned into each protein. With mutagenesis data on residue interaction on key ligands, the pharmacophore was carefully adjusted so as to recreate the protein-ligand interactions discussed previously. The protein models below represent the cumulative results of over 20 years of research. The proteins are oriented with the $\gamma 2$ on the left and the α subunit on the right with loop C reaching over the middle to $\gamma 2$. Diazepam has been docked in each receptor and the pharmacophore is visible.

Protein Models of the $\alpha 1\beta 3\gamma 2$, $\alpha 2\beta 3\gamma 2$, $\alpha 3\beta 3\gamma 2$ and $\alpha 5\beta 3\gamma 2$ Subtypes

Presented here are the complete unified protein-pharmacophore models. The Milwaukee-based pharmacophore has been inserted into each of the homology models for the receptor subtypes of the benzodiazepine receptor. The models show the similarities we expected. The two oxygens of serine 206 represent the hydrogen bond acceptor A₂. The hydrogen bond donor, H₁, is due to the hydroxyl group oxygens of Threonine 231 and Tyrosine 234. Threonine 193 is responsible for the H₂ hydrogen bond donor as its hydroxyl group coordinates with lone pairs of ligands. The imidazole ring of histidine 102 coordinates with phenyl rings of ligands through π - π stacking interactions.

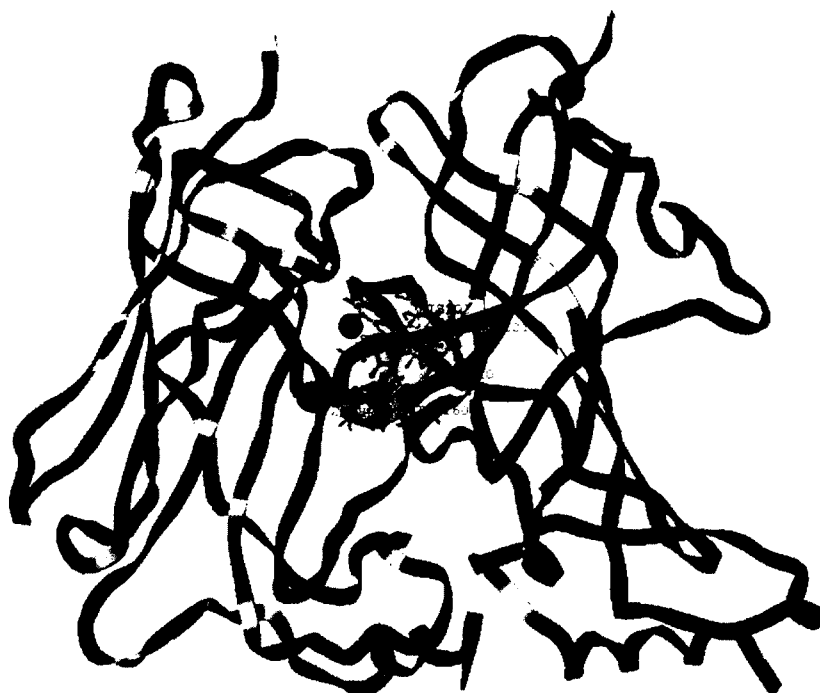


Figure 74. The $\alpha 1\beta 3\gamma 2$ subtype receptor with key residues shown



Figure 75. The benzodiazepine binding site of the $\alpha 1\beta 3\gamma 2$ receptor



Figure 76. The benzodiazepine binding site of the $\alpha 1\beta 3\gamma 2$ receptor rotated 90°



Figure 77. The $\alpha 2\beta 3\gamma 2$ subtype receptor with key residues shown



Figure 78. The benzodiazepine binding site of the $\alpha 2\beta 3\gamma 2$ receptor



Figure 79. The benzodiazepine binding site of the $\alpha 2\beta 3\gamma 2$ receptor rotated 90°



Figure 80. The $\alpha 3\beta 3\gamma 2$ subtype receptor with key residues shown



Figure 81. The benzodiazepine binding site of the $\alpha 3\beta 3\gamma 2$ receptor within the active site



Figure 82. The benzodiazepine binding site of the $\alpha 3\beta 3\gamma 2$ receptor rotated 90°

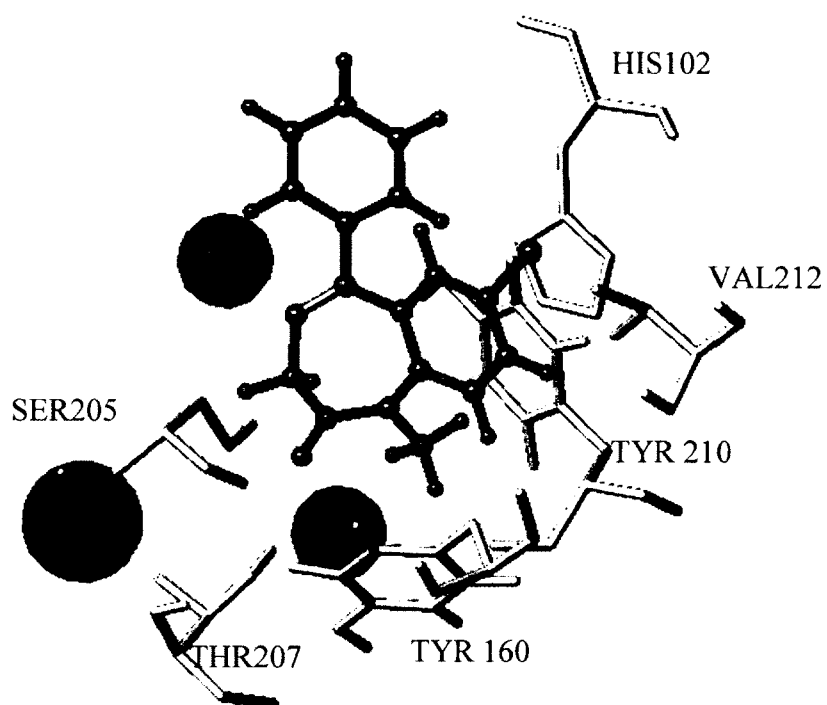


Figure 83. The benzodiazepine binding site of the $\alpha 1\beta 3\gamma 2$ receptor with diazepam in the binding pocket.

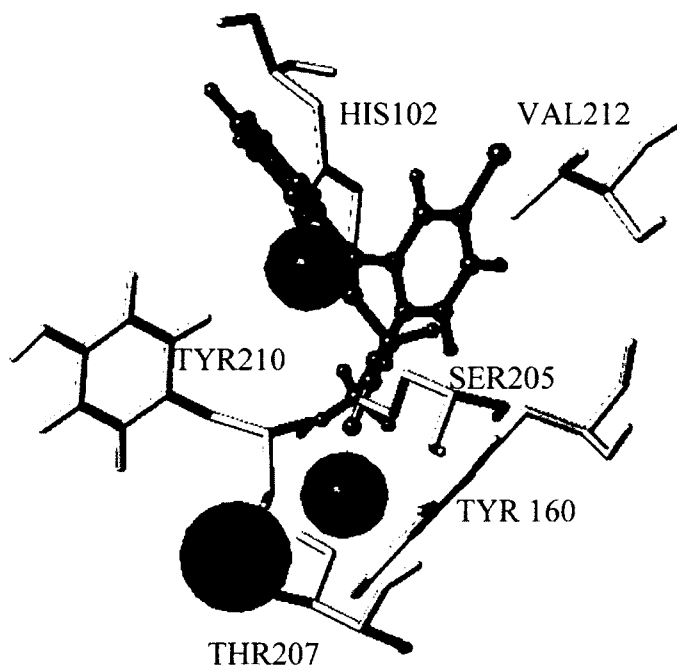


Figure 84. The benzodiazepine binding site of the $\alpha 1\beta 3\gamma 2$ receptor rotated 90° with diazepam in the binding site

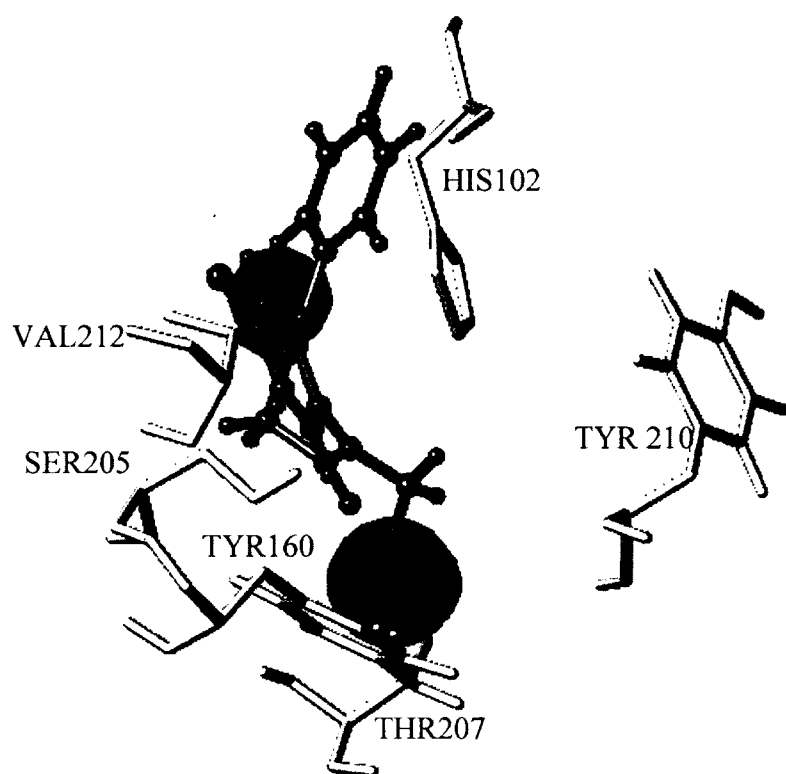


Figure 85. The benzodiazepine binding site of the $\alpha 1\beta 3\gamma 2$ receptor rotated 90° (reverse direction) with diazepam in the binding site



Figure 86. The $\alpha 5 \beta 3 \gamma 2$ subtype receptor with key residues shown with diazepam in the binding site



Figure 87. The benzodiazepine binding site of the $\alpha 5 \beta 3 \gamma 2$ receptor with diazepam in the binding site

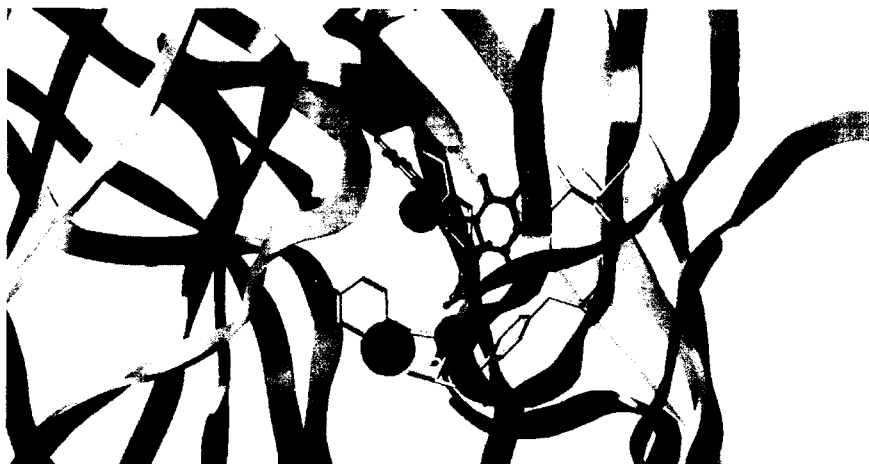


Figure 88. The benzodiazepine binding site of the $\alpha 5\beta 3\gamma 2$ receptor rotated 90° with diazepam in the binding site

From this unified model which was constructed on binding data from hundreds of compounds, included volume analysis, site directed mutagenesis, manual as well as Sybyl Flexidock and AutoDock algorithms, one can now see how any compound will dock in the benzodiazepine binding site of GABA(A) . Presented below is a compound for further research on drug abuse, WYS8.



Figure 89. Flexidock fit of WYS8

Refinement of WYS8 in the unified pharmacophore receptor was completed using FlexiDock. The protein with the pharmacophore set inside the benzodiazepine receptor is displayed with a ligand docked to the pharmacophore. From the compute function, Flexidock is executed. The pocket needs to be defined for Sybyl if it has not already. Pick atoms which are located near the binding site. All atoms within 4 Angstroms will be automatically selected by Sybyl to assist. For Flexidock to work with rigid proteins the following steps must be taken:

1. Water must be removed
2. Select atoms around the binding pocket
3. Add hydrogens
4. Pick 4Å radius to display around binding pocket
5. Have Sybyl add charges if necessary
6. Set rotatable bonds

From these models, the individual pharmacophores, and the compound database the medicinal chemist has a powerful set of tools to determine future ligands to synthesize in order to deliver subtype selective drugs with reduced side effects. New ligands based on this work have been proposed in Part II. For example, knowing how to dock ligands into the pharmacophore, one can begin taking measurements of ligands and residues and analyzing interactions. In the $\alpha 2\beta 2\gamma 2$ Bz receptor His 102 and the phenyl ring of diazepam have a π stacking distance of 4.1 Angstroms. Next we will discuss how one can properly dock ligands into the binding site.

Docking Studies Using AutoDock 4.2

Docking of ligands into the new binding sites of the homology models was also executed using the suite of *Autodock Tools* developed at Scripps Institute.^{289, 290} The general procedure entails preparing *pdb* file formats of the receptor (protein) as well as the ligand. Once these docking grids and docking parameters are set, the docking run will produce multiple potential docking reports. Prior knowledge from SAR studies and mutagenesis studies is then used to select those for a parallel run (clusters) and a final docking prediction is developed.

Preparing the Ligand for Autodock

The ligand is loaded into Autodock as a *pdb* file. Once in *Autodock*, Gasteiger partial charges are determined along with aromatic carbons, rotatable bonds and torsional degrees of freedom. A new “*pdgqt*” file is created which has this information attached to

it. Preparation of the receptor begins with loading it too as a pdb file into Autodock. Water molecules must be removed from the protein if present for *Autodock* processing. If any residues are flexible, these need to be identified in the receptor. Once identified, torsion angles can be assigned. Bonds in side chains can be manually or automatically selected as rotatable, unrotatable, or non-rotatable. *Autodock* needs two files when docking ligands in proteins with flexible residues, a flexible PDBQT file and a Rigid PDBQT file. Before docking can begin the receptor is checked for Gasteiger charges. A map is created which identifies possible hydrogen bonding interactions. Next, a grid box (Figure 90) is constructed around the general vicinity of the receptor if this is known.

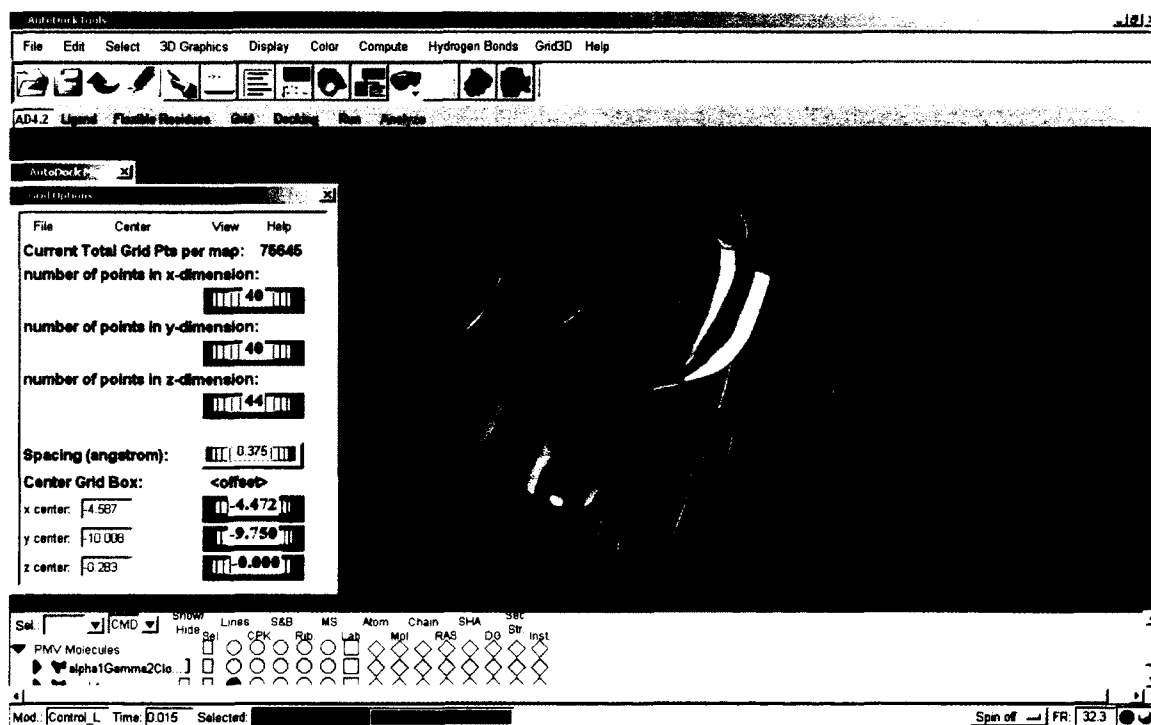


Figure 90. Setting the autogrid in Autodock for the Bz BS protein

With all the appropriate information stored in a parameter file, the docking program will know which map file to use, details about the ligand rules, the potential

presence of flexible residues and which docking algorithm to use. Four different docking algorithms are currently available in AutoDock. Monte Carlo simulated annealing (SA) was used. Briefly, the ligand makes random moves in the receptor and the energy of the new position is compared to the old one. Moves in which the energy is lowered are accepted.

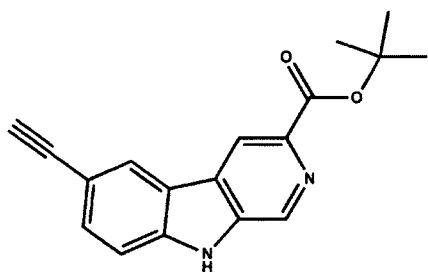


Figure 91. WYS8

Docking WYS8

WYS8 was drawn in ChemDraw Ultra 8.0 (Figure 91). Lone pairs were added and the molecule was minimized in ChemDraw 3D using MM2 to a minimum RMS gradient of 0.100. This was converted to a PDB file to be loaded into AutoDock 4. Upon loading into Autodock, Gasteiger charges were added, 14 non-polar hydrogens were merged, 10 aromatic carbons were identified, 3 rotatable bonds were detected, and TORSDOF was set to 3.

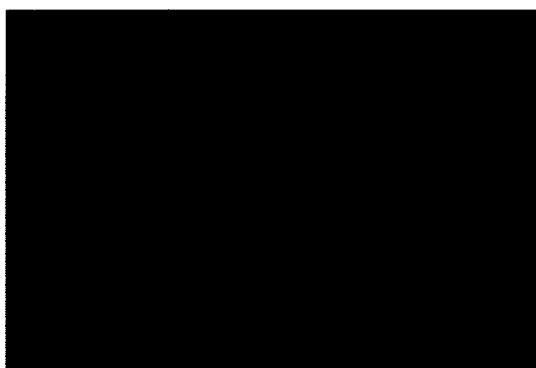


Figure 92. Rotatable bonds are identified along with root atom in ligand WYS8

The root atom with the smallest largest sub-tree (in this case an acetylenic hydrogen) is marked with a green sphere and the root portion (red) is identified. The rotatable bonds are colored green. The receptor was rigid for this analysis.



Figure 93. AutoDock result rendering was performed using Tripos Benchware.

Using Tripos Benchware 3D Explorer 2.6, one of the results was modeled (Figure 93). Key residues were identified and the protein surface five angstroms from the ligand

was mapped showing its lipophilic potential. The results using AutoDock and a rigid protein will be much improved when flexible residues are allowed in the binding pocket along with rotatable bonds. The docking in Figure 89 is preferred when considering the orientation in the Milwaukee-based pharmacophore.

Homology models which have the pharmacophore aligned in the binding pocket have been presented for the $\alpha 1\beta 2\gamma 2$, $\alpha 2\beta 2\gamma 2$, $\alpha 3\beta 2\gamma 2$, and $\alpha 5\beta 2\gamma 2$ GABA(A) receptors. The binding site was constructed in light of years of work including structure-activity-relationships (SAR), site directed mutagenesis, and docking studies of monomer and dimers alike. The $\alpha 4\beta 2\gamma 2$ and $\alpha 6\beta 2\gamma 2$ receptors have not been made as these “diazepam-insensitive” binding sites are not a focus of our research to date. An updated included volume analysis has been presented using ligands from 15 different structural families. The new included volume analyses and the unified pharmacophore protein models will continue to drive the design of novel and selective benzodiazepine receptor ligands. From these new ligands, scientists will increase their understanding of the physiological responses of the specific receptors, the design of pharmaceuticals with reduced side effects, and treatments for schizophrenia, drug addiction and Alzheimer’s disease. The $\alpha 5\beta 2\gamma 2$ receptors are of particular interest because of their concentration in the hippocampus. The discovery of a larger L_3 pocket in the $\alpha 5\beta 2\gamma 2$ receptor versus the other subtypes will provide medicinal chemists with a structural advantage in designing more subtype selective ligands. From the unified pharmacophore protein models presented here, the design of new compounds for the GABA(A) will be more productive than ever.

Future Work

Screening and modeling of more subtype selective ligands will further our current understanding of the benzodiazepine receptor and its function. Continued work on the molecular spreadsheet which will include all the compounds designed in the Milwaukee laboratory as well as other organizations will create a powerful QSAR algorithm for answering the age old question, “What compound should we make next?” This study will need to include all binding and non-binding compounds in order to create a predictive program with a high degree of accuracy (r^2 , q^2) in predicting activity.

Site directed mutagenesis needs to be continued in which receptors of all subtypes are tested to determine how a residues substitution affects each of the subtypes. Such experimentation will shed further light on how ligands are positioned in the binding pocket and what residues they are interacting with. Adding to the new pharmacophore protein alignments which can now be executed, docking runs using *Autodock* in which the residues in the receptor are set to flexible may give further information as to docking preferences of ligands helping to better understand key interactions in each of the different subtypes.

All of these activities have allowed us to develop the current ligands as well as propose next generation ligands, which will be discussed in Part II. The new pharmacophores will aid in furthering our understanding of GABA and in designing better drugs for the CNS until a complete GABA(A) protein receptor ion channel is captured in high resolution.

Part II. Subtype Selective Ligands for $\alpha 5$ GABA(A) /Bz Receptors

Introduction

Senile dementia of the Alzheimer's type (SDAT) accounts for the major portion of all neurodegenerative diseases.²⁸⁹ Within the U.S. alone, about 4 million individuals are afflicted with SDAT, with about 130,000 new cases occurring per year.^{289, 291} Annual costs associated with AD are estimated to exceed \$100 billion.^{289, 290, 292} Epidemiologists expect that by the year 2050 in the more developed world, life expectancies at birth will surpass 80 years of age.^{293, 294} Inevitably, this development will lead to increased numbers of elderly people, from 414 million people over 65 years of age in 2000 to probably 1.4 billion in the year 2050.²⁸⁵ Many of them will be afflicted by dementia, the prevalence of which rises rapidly with very old age. According to a Canadian study, the prevalence of dementia is about 23% in people of the age group, 85-89 years, about 40% in people of the age group, 90-94 years, whereas in people older than 95 years the prevalence of dementia rises to about 58%.^{285, 295} In 2002, the number of individuals suffering from dementia in the more developed world was about 13.5 million cases. This figure is expected to rise to 37 million by the year 2030 and to 105 million worldwide by 2050.²⁸⁹

SDAT and age-related memory decline arises from progressive failure of the cholinergic system, leading to impaired memory and deterioration of other cognitive functions.^{16, 17} Pharmacological treatment for this cognitive decline has primarily focused

on cholinomimetics and cholinesterase inhibitors to mitigate the cholinergic hypofunction. These strategies tend to elicit direct postsynaptic stimulation. The constant tonic neuronal activity which results is unfavorable to normal cognitive processing and seriously undercuts the usefulness of this standard approach.^{16, 17, 296, 297}

A more effective strategy to alleviate memory deficits, attributed to cholinergic hypofunction, would be to enhance cognitive processing by augmenting the impact of acetylcholine (ACh) released from surviving cholinergic neurons on hippocampal pyramidal cells, without disrupting the highly complex transmission patterns inherent to these cortical cholinergic pathways.²⁸⁵ An exciting yet largely underdeveloped therapeutic approach with excellent potential to achieve this outcome is one that would reduce postsynaptic inhibition of cholinergic excitation in the hippocampus via pharmacology.^{285, 298} A rational means to achieve this aim is to influence the functional regulation pathways involved in cognition by manipulating the inhibitory nature of the neurotransmitter GABA.^{299, 300} As mentioned, when GABA binds to the GABA(A) / benzodiazepine receptor, it induces chloride ion (Cl⁻) passage into the neuron, causing hyperpolarization of the surrounding membrane preventing synaptic excitation. GABA's inhibitory effects can be fine-tuned by a variety of substances, including those that specifically bind to the benzodiazepine binding site (BzR) on the GABA(A) receptor.^{299, 300} Appropriate BzR ligands modulate GABA's inhibitory influence on numerous neuronal pathways, including the cholinergic pathways of the basal forebrain that project to the hippocampus.³⁰¹ These cholinergic pathways are important to cognition and are prone to degeneration in SDAT. Although BzR ligands are relatively safe drugs, their downside is due to their broad spectrum of activity and lack of behavioral specificity. Consequently, insight into how BzR ligands elicit their specific physiological effect is

crucial to development of the next generation of behaviorally-specific BzR ligands with reduced side effects.

BzR ligands alone do not activate GABA(A) receptors, but instead act as modulators of GABA's ability to activate this receptor. For example, when cognitive events activate cholinergic excitation in the hippocampus, the GABAergic system is likewise activated to modulate the level of this excitation. In situations where the cholinergic excitation is decreased due to the loss of cholinergic neurons, as in the case of SDAT, the precise reduction in GABAergic inhibition in brain regions where the weakened cholinergic neurons project would selectively augment the functional impact of the ACh released.^{302, 303} It is important to point out that GABAergic neurons remain intact and functional until the very last stages of Alzheimer's disease while cholinergic deficits become more pronounced as the disease progresses.^{303, 304} Consequently, $\alpha 5$ BzR/GABAergic neurons have now become pharmacological targets because these are located almost exclusively in the hippocampus³⁰⁵ and are still functional throughout most stages of the disease. It is well documented that the BzR ligands flunitrazepam and midazolam impair cognition in animal models and humans³⁰⁶ by augmenting GABA-mediated Cl^- flux through the GABA(A) receptor which prevents the induction of Long Term Potentiation (LTP) in rodent hippocampal neurons.^{50, 307} Conversely, BzR ligands that retard GABA-mediated Cl^- passage into the neuron (negative allosteric modulation) potentiates LTP in rodent hippocampal neurons,^{16, 17} which results in improved learning and memory.^{296, 297} Earlier, the therapeutic potential for memory augmentation by BzR ligands has been considered to be limited due to the side effects such as convulsant or proconvulsant activity that occur at slightly higher doses.³⁰⁸ However, new findings

suggest that particular combinations of GABA(A) receptor subunits are intimately associated with cognitive influence.⁶⁴ Although $\alpha 5$ selective inverse agonists from our laboratory^{64, 309, 310} and from the laboratories of others^{50, 307} have been shown to enhance cognition, recently we have developed an $\alpha 5$ subtype selective antagonist which clearly enhances cognition.³¹¹⁻³¹⁴ It has no efficacy at $\alpha 1$ - $\alpha 6$ subtypes; however, binds to the $\alpha 5$ subtype at 15nM and antagonized potently the percent modulation of GABA by diazepam in oocytes.^{17, 315} It was then shown to enhance cognition on the mean delay achieved by C57BL/6J mice under the titrating delayed matching-to-position schedule.³¹⁶ An antagonist at BzR sites would be expected to exhibit no sedative effect, no convulsive, nor any proconvulsive side effects.²⁸⁵

Support for this approach was also derived from the following lines of reasoning:

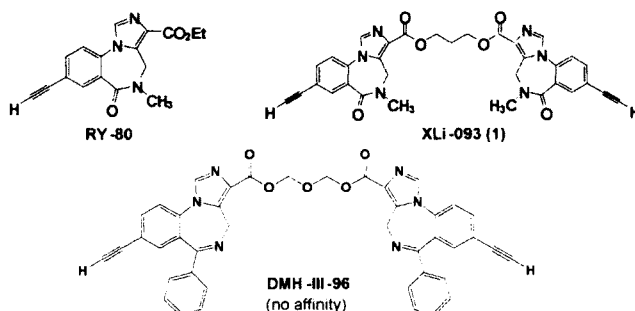
1) While most neurotransmitter systems are degenerating in the SDAT brain, the GABAergic infrastructure is relatively well preserved.^{314, 315} 2) Numerous cognitive deficit models of cholinergic hypofunction, both human and animal, benefit cognitively when GABA activity is reduced.⁵⁰ 3) Beneficial effects of BzR inverse agonists can also be generalized to the aged nervous system, as indicated by their ability to improve working memory performance in memory impaired aged rats.⁵⁰ 4) Lesion studies demonstrate that animals with 50-70% loss of cortical cholinergic fibers exhibit improved cognitive performance from BzR treatment.^{19, 21, 185, 237} As the loss of cholinergic neurons in age associated memory impairment and SDAT is commonly in the 40-70% range^{296, 297, 317} until the very last stage, the effects of BzR inverse agonists on restoring neural transmission in animals with a partial loss of cortical cholinergic inputs suggests

development of specific BzR inverse agonists for the treatment of cognitive decline associated with aging and SDAT.

α 5 Selective Ligands

Interest in BzR/GABA(A) α 5 subtypes has been stimulated recently by the report of Möhler *et. al.*^{16, 17, 296, 297, 317, 318} on α 5 “knockin mice.” In brief, this group has provided strong evidence that hippocampal extrasynaptic α 5 GABA(A) receptors play a critical role in associative learning as mentioned above.¹⁶

Previously, a series of α 5 subtype selective ligands [(RY-023), (RY-024), (RY-079) and (RY-080)] based on the structure of (Ro 15-4513) have been reported from this laboratory,¹⁶ as well as several ligands by McKernan, Attack *et. al.*¹⁷ These ligands are BzR inverse agonists in vivo and a number have been shown to enhance cognition.⁶⁴ One of these ligands was shown by Bailey, Helmstetter *et. al.*⁶⁴ to be important in the acquisition of fear conditioning and has provided further evidence for the involvement of hippocampal GABA(A)/BzR in learning and anxiety.⁶⁴ This is in agreement with the work of DeLorey *et. al.*⁶⁴ in a memory model with a ligand closely related to α 5 subtype selective inverse agonists RY-024 and RY-079.

$\alpha 5$ Selective Antagonist (1)

Ligand	$\alpha 1$	$\alpha 2$	$\alpha 3$	$\alpha 4$	$\alpha 5$	$\alpha 6$
RY-80	28.4	21.4	25.8	5.3	0.49	28.8
XLi-093	>1000	>1000	858	1550	15	>2000

Figure 94. Alpha 5 selective compounds

To enhance the subtype selectivity, the bivalent form of RY-080 was synthesized to provide XLi-093.⁶⁴ The binding affinity of XLi093 *in vitro* was determined on $\alpha 1$ - $\beta 3\gamma 2$ LTK cells and is illustrated in Figure 94. This bivalent ligand bound to $\alpha 5\beta 3\gamma 2$ subtypes with a K_i of 15nM, but exhibited little or no affinity at other BzR/GABA(A) subtypes.³⁰⁹ Since receptor binding studies indicated bivalent ligand XLi-093 bound almost exclusively to the $\alpha 5$ subtype, the effect of this ligand on various GABA(A) receptors expressed in *Xenopus* oocytes was investigated by Sieghart, Fürtmueller, Li and Cook.³⁰⁹ Analysis of the data indicated that XLi093 up to a concentration of 1 μ M did not trigger chloride currents in any one of the GABA(A) subtypes tested. At 1 μ M Xli093 did not modulate GABA induced chloride flux in $\alpha 1\beta 3\gamma 2$, $\alpha 2\beta 3\gamma 2$, or $\alpha 3\beta 3\gamma 2$ receptors, but very slightly inhibited currents in $\alpha 5\beta 3\gamma 2$. At 1uM, (1) only marginally influenced diazepam stimulation of GABA-induced current in $\alpha 1\beta 3\gamma 2$, $\alpha 2\beta 3\gamma 2$ and $\alpha 3\beta 3\gamma 2$ BzR but shifted the diazepam dose response curve to the right in $\alpha 5\beta 3\gamma 2$ receptors in a significant fashion.³⁰⁸ Importantly, bivalent ligand (1) was able to dose

dependently and completely inhibit diazepam-stimulated currents in $\alpha 5\beta 3\gamma 2$ receptors. This was the first subtype selective benzodiazepine receptor site antagonist at $\alpha 5$ receptors. This bivalent ligand (1) provided a lead compound for all of the bivalent ligands in this research.³⁰⁸

Depicted in Figure 95 is Xli093 aligned in the pharmacophore-receptor model of the $\alpha 5\beta 3\gamma 2$ subtype. The fit is excellent.^{66, 308-310} The fit to the pharmacophore-receptor and the binding data indicate that bivalent ligands will bind to BzR subtypes.^{309, 310} As discussed in Part I, it is believed that the dimer enters the binding pocket with one monomeric unit docking while the other monomer tethered by a linker extends out of the protein into the extracellular domain.

In an even more exciting development, Wenger, Li, Cook *et. al.*^{19, 64, 121} have reported preliminary data that the $\alpha 5$ subtype selective antagonist Xli093 does indeed enhance performance under a titrating delayed matching to position schedule of cognition in C57BL/6J mice, as illustrated in Figure 96.^{66, 308-310} This agent does cross the blood brain barrier.

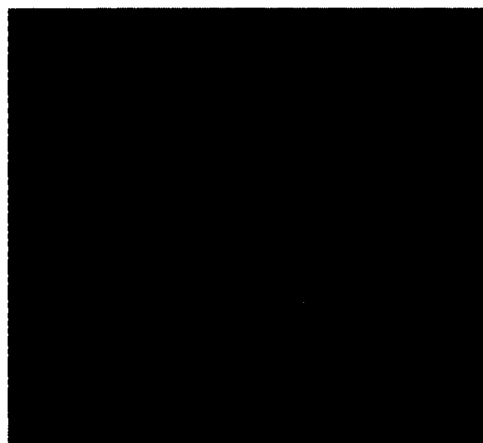


Figure 95. Xli093 aligned in the included volume of the pharmacophore receptor model for the $\alpha 5 \beta 3 \gamma 2$ subtype

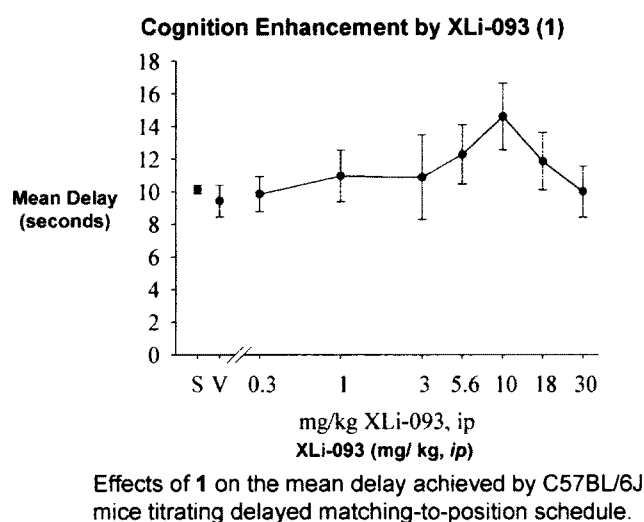


Figure 96. Xli093 in cognition enhancement (Wenger unpublished)

To date, in regard to bivalent ligands, the preferred linkers between the two pharmacophores (see Xli093) have been established as 3 methylene units, 4 methylene units or 5 methylene units. This was established by low temperature NMR experiments, molecular modeling and X-ray crystallography of the ligands in question and will be discussed.³¹⁰

Recently a number of more selective ligands for $\alpha 5\beta 3\gamma 2$ subtypes have been synthesized (See Table 25). Although the basic imidazobenzodiazepine scaffold has been maintained,¹⁷ substituents were varied in regions around the scaffold based on molecular modeling.¹⁶ These are now the most $\alpha 5$ subtype selective ligands ever reported.^{307, 319} Moreover, one can now mix and match the substituents on these ligands to obtain $\alpha 5$ subtype selective agents with 400-1000 fold selectivity for $\alpha 5$ subtypes over the other 5 subtypes. *This is the key to unlocking the true, unequivocal physiological responses mediated by $\alpha 5$ subtypes in regard to cognition, (amnesia), anxiety and convulsions, all of which to some degree, may be influenced by $\alpha 5$ subtypes.* It is clear, in most cases, in the ligands in Table 25 and Table 26, affinity has occurred only at $\alpha 5\beta 3\gamma 2$ subtypes. In addition, since bivalent ligand Xli093 bound very tightly only to $\alpha 5$ BzR subtypes, the functionality present can be incorporated into other bivalent ligands.

From the data in Figure 96 it is clear the $\alpha 5$ antagonist Xli093 has enhanced cognition, moreover, the two acetylenic groups of Xli093 have been reduced to provide ethyl functions.³⁰⁹ This provided a new bivalent ligand (Xli-356) which shows (in oocytes) no activity at $\alpha 1$ subtypes but is a clear inverse agonist at $\alpha 5$ subtypes (Table 21).³⁰ DeLorey has recently shown that Xli-356 does potently reverse scoploamine induced memory deficiencies. This bivalent $\alpha 5$ inverse agonist enhances cognition in agreement with work reported from our laboratory on monovalent inverse agonists RY10¹⁶ and RY 023.¹⁷ In addition Roth *et. al.* has recently determined K_i values for Xli-356 in HEK-T cells [$\alpha 1$ (no affinity); $\alpha 5$ (107 nM)].

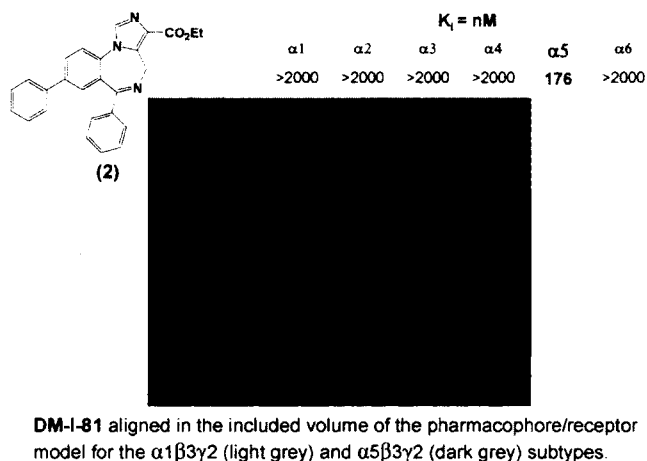


Figure 97. The $\alpha 5$ selective agonist DM-I-81

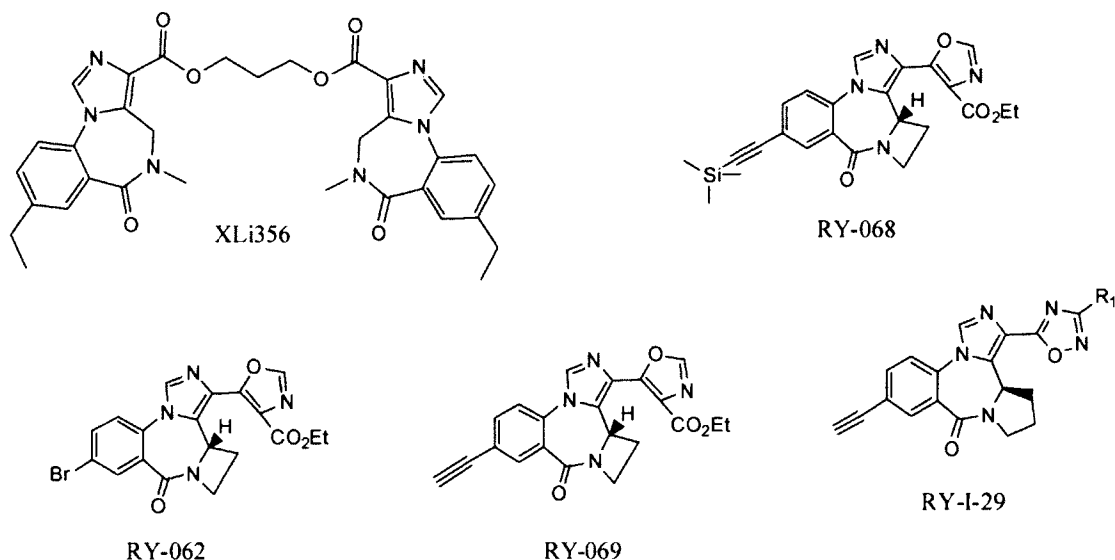
Möhler has proposed that $\alpha 5$ selective inverse agonists or $\alpha 5$ selective agonists might enhance cognition.^{64, 66, 308, 320} This is because of the extrasynaptic pyramidal nature of $\alpha 5\beta 3\gamma 2$ subtypes, located almost exclusively in the hippocampus. Because of this, a new “potential agonist” which binds solely to $\alpha 5\beta 3\gamma 2$ subtypes was designed by computer modeling (See Figure 97). This ligand (DM-I-81) has an agonist framework and binds only to $\alpha 5\beta 3\gamma 2$ subtypes.^{64, 66, 320} The binding potency at $\alpha 5$ subtypes is 174 nM. Additional work on this scaffold was discontinued as it was felt that the bulk of the 8-phenyl moiety was too large to fit into the L_2 pocket potentially.

Chemical structures of compounds 3a-c, 4 (S), 5, and 2 (DM-I-81) are shown. Compound 3a-c is a 4-chloro-2-methyl-1,2,3,4-tetrahydro-1H-benzodiazepine derivative. Compound 4 (S) is a 4-ethynyl-2-methyl-1,2,3,4-tetrahydro-1H-benzodiazepine derivative. Compound 5 is a 4-ethynyl-2-methyl-1,2,3,4-tetrahydro-1H-benzodiazepine derivative. Compound 2 (DM-I-81) is a 4-phenyl-2-methyl-1,2,3,4-tetrahydro-1H-benzodiazepine derivative.

Ligand	R ₁	K _i (nM) ^a					
		α1	α2	α3	α4	α5	α6
3a	CH ₂ OCH ₃	>300	>300	>300	ND	38.8	>300
3b	CH ₂ Cl	>300	>300	>300	ND	28.5	>300
3c	CH ₂ OE _t	>300	>300	>300	ND	82.7	>300
4	CH ₃	>89	>70	>91	ND	3.7	>301
5	CO ₂ Et	>1000	>1000	>1000	>1000	64	>1000
2	CO ₂ Et	>2000	>2000	>2000	>2000	176	>2000

^a Data shown here are the means of two determinations which differed by less than 10%
ND = Not Determined (presumably similar to α6).

Table 26. Binding data of selected imidazobenzodiazepines



Ligand	K_i (nM) ^a					
	$\alpha 1$	$\alpha 2$	$\alpha 3$	$\alpha 4$	$\alpha 5$	$\alpha 6$
XLI356	ND	ND	ND	ND	ND	ND
RY068	>500	877	496	ND	37	>1000
RY062	>1000	>1000	>500	ND	172	>2000
RY069	692	622	506	ND	19	>1000
RY-I-29	>1000	>1000	>1000	ND	157	>1000

^a Data shown here are the means of two determinations which differed by less than 10%
 ND = Not Determined (presumably similar to $\alpha 6$).

In regard to $\alpha 5$ receptor subtype selective ligands, Bailey, Helmstetter *et.al.* have used RY024 to enhance cognition and provide further evidence for the involvement of hippocampal GABA(A) /benzodiazepine receptors in learning and anxiety.^{309, 310} This has been supported by DeLorey *et. al.*, who demonstrated that the closely related $\alpha 5$ inverse agonist RY10 potently reversed scopolamine-induced memory impairment. These $\alpha 5$ inverse agonists provide tools to be used to decipher how GABA(A) receptors

influence contextual memory, an aspect of memory affected in age associated memory impairment and especially in Alzheimer's disease.⁶⁴ In this regard, Savić *et.al.*, have recently employed the $\alpha 1$ preferring ligand BCCt in studies on passive avoidance, which clearly indicated the amnesic effects of midazolam are due to interaction of agonist ligands at $\alpha 5$ in addition to $\alpha 1$ BzR subtypes.

The preferred 3 carbon linkers for BzR/GABA(A) bivalent ligands have been determined^{19, 121, 210, 297} by low temperature NMR studies and X-ray analysis and will be described.^{66, 121, 317, 318}

Molecular modeling was used to generate new lead compounds aimed at the preparation of subtype selective agonists, and inverse agonists of $\alpha 5$ subtypes to study memory and learning as well as amnesia mediated by the hippocampus. All of these compounds have been designed based on the structures of $\alpha 5$ subtype selective ligands prepared in our laboratory³²¹ (see Table 25-26), as well as the binding affinity (15nM)/selectivity of bivalent $\alpha 5$ antagonist XLi093.³²²

Pharmacology

The affinity of all ligands at the 6 major recombinant GABA(A) /BzR subtypes²⁷⁶ was measured by competition for [³H]Ro15-1788 binding to HEK-T cells expressing both human and rat GABA(A) /Bz receptors of composition $\alpha 1\beta 2\gamma 2$ ($\alpha 1$), $\alpha 2\beta 2\gamma 2$ ($\alpha 2$), $\alpha 3\beta 2\gamma 2$ ($\alpha 3$), and $\alpha 5\beta 2\gamma 2$ ($\alpha 5$). It is well known that the $\beta 2$ and $\beta 3$ subunits can be interchanged with no effect on Bz ligand affinity or efficacy.³²³ The $\alpha 4$ and $\alpha 6$ subtypes (diazepam insensitive) were assayed using [³H]-Ro15-4513.³²⁴ This work was done in the laboratory of Bryan Roth⁶⁴ who has already expressed the receptors employing the work of Kucken *et. al.*³²⁵ and Gray *et. al.*⁶⁴ Roth has currently obtained K_i values on more than 125 ligands. In brief, for membrane preparations, the cells were scraped on ice

into 5mL of phosphate buffered saline (pH=7.40) and cells pelleted by centrifugation for 5 min. at 4°C. The pellets were resuspended in 1mL of 50mM Tris-acetate buffer (pH 7.4) and centrifuged at 18,000g for 20 min. Radioligand binding assays were performed in 50mM Tris-acetate buffer (pH 7.4) using 10^{-5} M diazepam for non-specific binding; typically specific binding will represent 90% of total binding. Each pellet was diluted to 6mL and then 100 μ L of membranes was incubated with approximately 1nM final concentration of [3 H]Ro 15-1788 in a total volume of 250 μ L together with serial dilutions of test compound for 90 min. on ice. The membranes were harvested in polyethyleneimine-pretreated Whatman GF/C filters and after drying and addition of scintillation cocktail, counted in a scintillation counter. The counts per minute (cpm) retained on the filters was plotted against log concentration (M) and fitted to one site competition equation to obtain the K_i using Graphpad Prism (V4.0) using the Cheng-Prusoff approximation.⁶⁴

the expression vector pCDM8 or pcDNA1/Amp. After incubation for 24 hr, oocytes were placed in a 50 μ L bath and perfused with modified Barth's medium. From Figure 98, it can be seen that Xli-356 is an inverse agonist selective for the $\alpha 5$ receptor over $\alpha 1$.

Cells were impaled with two 2-3 M Ω electrodes which contain 2MKCl and voltage clamped at a holding potential of -60mV.³²⁶⁻³³⁰ GABA modulators were preapplied for 30 seconds before the addition of GABA, which was coapplied with ligands until a peak response was observed. The highest concentration of DMSO employed in this study perfusing the oocyte was 0.1% which had no effect when applied alone at this concentration.^{16, 331-333}

In regard to cognition, the effect of systemic administration of subtype selective agents on short term memory was determined in white Carneau pigeons by Wenger *et. al.*^{16, 17} Administration of drug was intramuscularly and the titrating matching-to-sample schedule of reinforcement was used.³³⁴ Matching-to-sample is widely used as a measure of short-term memory,³³⁵ and has been shown to be sensitive to the effects of agents to actions at the GABA(A) chloride complex in laboratory animals and humans. Xli-093, the first $\alpha 5$ selective antagonist was shown to enhance cognition in Wenger's laboratory (Figure 96).

Because the hippocampus is involved in the regulation of events underlying learning and memory, $\alpha 5$ subtype selective agents were evaluated for their ability to modulate hippocampal-dependent and hippocampal-independent forms of memory using Pavlovian fear conditioning paradigms^{307, 336-339} with DeLorey.^{307, 336-339} Savic *et. al.* studied selected ligands in the active avoidance acquisition and retention paradigm³³⁹ and passive avoidance task.³⁴⁰

Since the GABAergic system is the major inhibitory neurotransmitter system in the CNS,³⁴¹ it has tremendous therapeutic potential. Alterations in GABA(A) function

from controls are known to occur in anxiety disorders,³⁴² including panic disorder,³⁴³ epilepsy,³⁴⁴ hypersensitive behavior,³⁴⁵ phobias,³⁴⁶ schizophrenia,³⁴⁷ alcoholism,³¹⁰ Angelmans Syndrome³¹⁰ and Rhetts syndrome^{307, 336-339, 342} as well as other diseases.³⁴⁸ Since BzR ligands modulate this system, the design of subtype selective ligands is one way to generate better, safer therapeutic agents.

Synthesis and pharmacological evaluation of these subtype selective agents permitted the assignment of the correct physiological functions to $\alpha 5$ subtypes. This is of special importance here in regard to cognition/amnesia mediated by the hippocampus. It is felt a potential therapeutic agent to improve memory and learning will result from this continued research.

The ligand XLi356 is an inverse agonist in $\alpha 5\beta 3\gamma 2$ oocytes and a weak agonist at $\alpha 1\beta 3\gamma 2$ sites (Figure 98). RY10 behaved as a weak agonist at both $\alpha 1$ and $\alpha 5$ subtypes in oocytes. Therefore, the dimerization of RY10 switches the effect from agonist towards inverse agonist at $\alpha 5\beta 3\gamma 2$ subtypes with a lesser influence (other binding) on $\alpha 1\beta 3\gamma 2$ subtypes.³⁴⁹ The methods used to prepare Xli-356, Xli-093, and RY-10 were reported by Li.³⁵⁰

Correlation of a specific BzR subtype to a specific pharmacological response is crucial for understanding the mechanisms which underlie cognitive deficits but also anxiety disorders,³⁵¹ sleep disorders, convulsions, and will help design selective agents to treat these disease states while being devoid of abuse potential.

History of GABA(A) / Benzodiazepine Receptors

In 1950, Eugene Roberts and Jorge Awapara found large amounts (1mg per gram) of γ -amino butyric acid (GABA) in the mammalian central nervous system.³⁵² Ernst Florey discovered that this GABA acted as an inhibitory neurotransmitter from inhibition studies of the stretch receptor in crayfish.³⁵³ Later, in 1963, Del Castillo demonstrated, through electrophysiological recordings, the application of GABA opens chloride channels in the nerve cells of *Ascaris*.³⁵⁴ This GABA-gated chloride channel is now known as the GABA(A) receptor. Activation of GABA(A) receptors allows chloride ions to enter the nerve cell. The influx of chloride results in hyperpolarization of the cell membrane decreasing the excitability of the cell and is referred to as “hyperpolarizing inhibition.”³⁵⁵

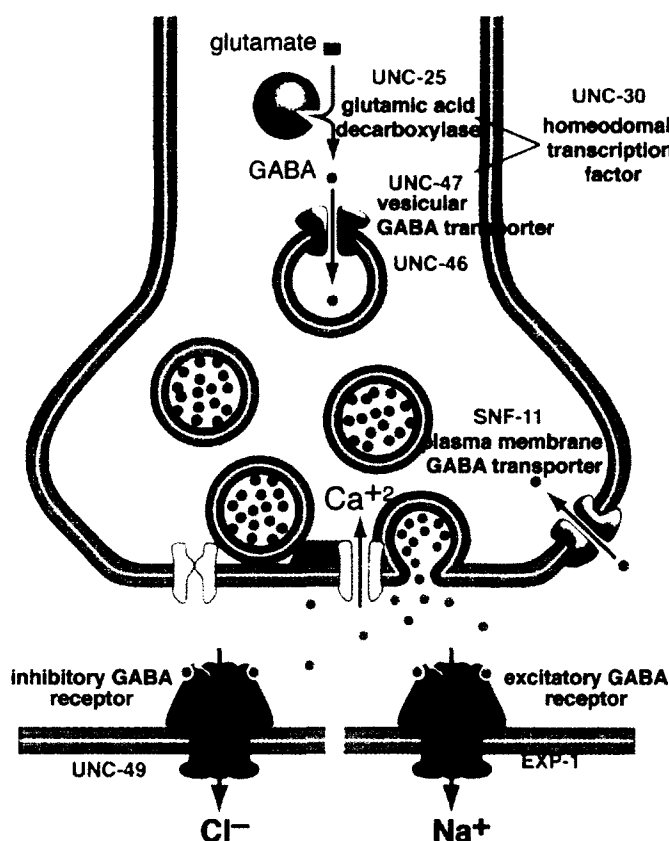


Figure 99. GABA function in *C. elegans*.

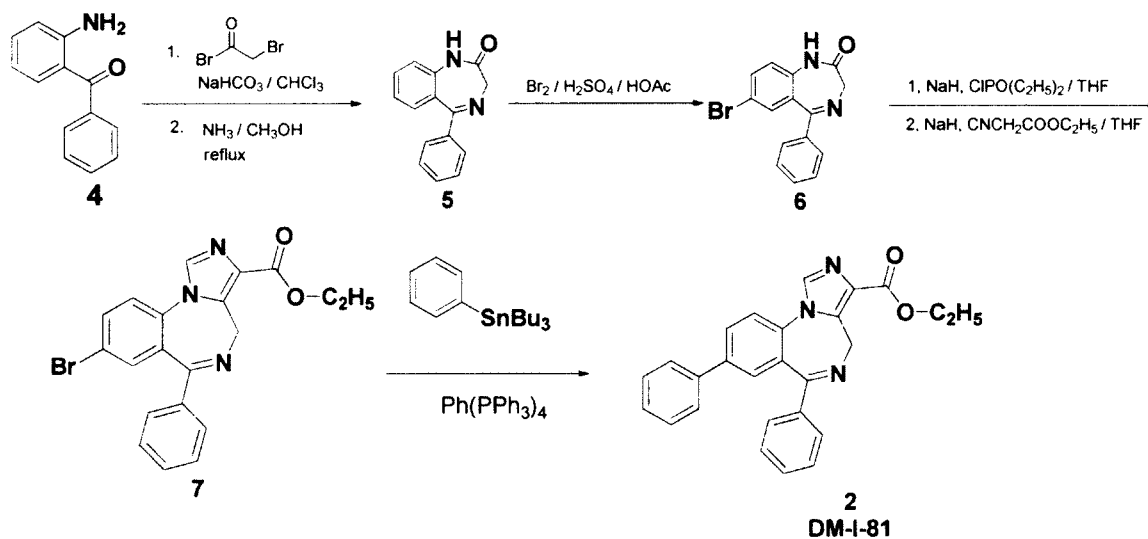
GABA released from presynaptic neurons activates the inhibitory GABA(A) receptor; the influx of chloride ions causes the relaxation of the body muscles. GABA is cleared from the cleft by the plasma membrane transporter, SNF-11 (Figure 99).^{330, 356}

Although benzodiazepines have been approved for use since 1963, it was not until the late seventies that evidence correlated the GABA(A) receptors and benzodiazepines. In 1977, Möhler and Okada,^{357, 358} as well as Squires and Braestrup,³⁵⁸ identified high-affinity binding sites for tritiated diazepam, an early benzodiazepine prescribed primarily to counteract anxiety symptoms. In 1978, Bertilsson, an NIMH (National Institute of Mental Health) researcher, found direct evidence of an interaction of diazepam with the GABA(A) receptor. Using ^{13}C labeled GABA, a decrease in GABA turnover was seen

in rat brain nuclei treated with diazepam (Valium).³⁵⁹ The pharmacological effects of these benzodiazepines include sedation, anxiolytic, anticonvulsant, muscle relaxation, and amnesic properties, as well as some addiction.^{1, 208, 209}

As discussed previously, the lead compounds synthesized in our lab as well as other laboratories resulted in high affinity ligands that have been pooled in a database. The database is an interactive version of Chemdraw/Excel. This interactive database allows one to generate reports based on queries designed by the user and has proven a valuable research tool for querying structural and activity data. Substructure as well as activity searches allow for quick data analysis of our laboratories' library. Primarily, SAR studies quickly help to guide future drug design. This rational approach has led to several compounds with subtype selectivity. The synthesis of key scaffolds will be summarized now.

Synthesis of 8-Substituted imidazobenzodiazepines



Briefly, bromoacetyl bromide is added to 2-aminobenzophenone **4**, followed by treatment with methanol saturated with ammonia under the cooling of an ice-water bath. The benzodiazepine, **5**, is brominated to provide **6**, and reacted with ethyl isocyanoacetate to generate the imidazobenzodiazepine, **7**. The bromide **7** was subjected to a Stille-type coupling to give DM-I-81.²¹⁰ This route can be executed on several hundred gram scale.

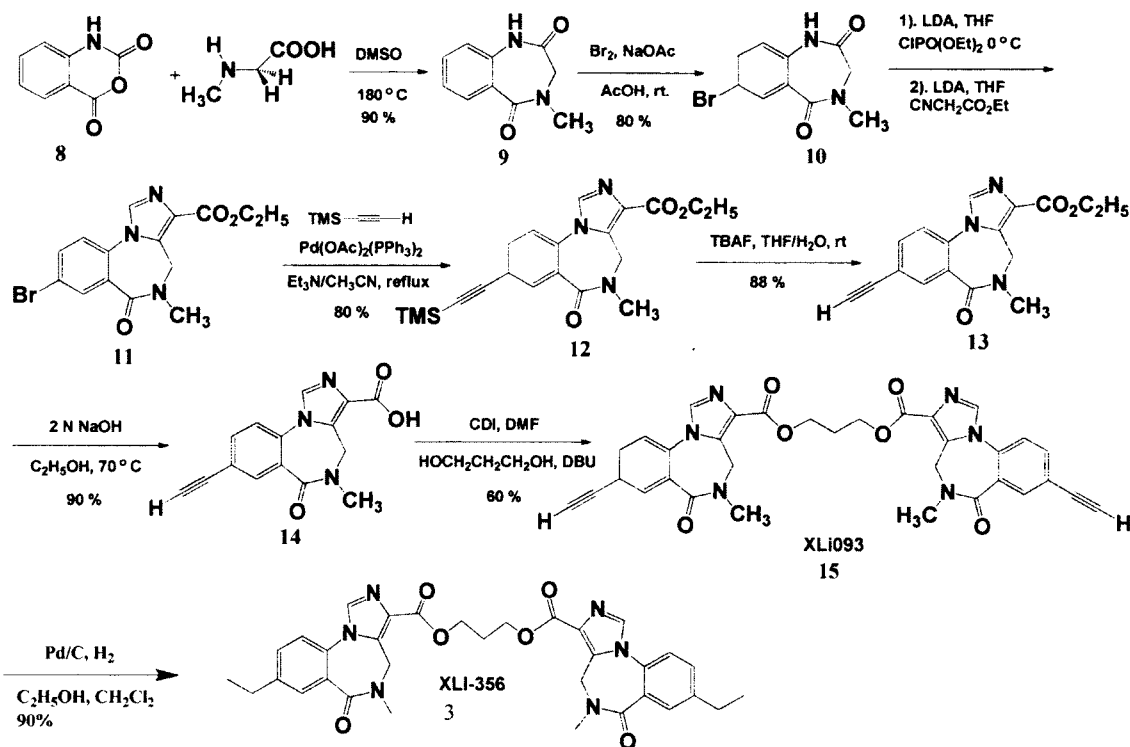


Figure 100. Synthesis of 8-substituted imidazobenzodiazepine bivalent ligands

The benzodiazepine monomers were prepared by the method of Fryer and Gu.¹²¹

²¹⁰ The isatoic anhydride was heated with sarcosine in dimethyl sulfoxide to provide amide **9**. Bromination of **9** in a mixture of acetic acid, bromine, and sodium acetate afforded the corresponding monosubstituted bromide, **10** in good yield. Deprotonation of **10** with lithium diisopropyl amide (LDA) in THF was followed by treatment with diethyl chlorophosphate to provide the intermediate enol phosphate. The enol phosphate was stirred with a solution of ethyl isocyanoacetate and LDA to yield the imidazo congener. A Heck type coupling reaction was employed with the bromide, **11** with bis(acetate)bis(triphenylphosphine)palladium(II) to provide the acetylene **12**. Treatment of **12** with Bu₄NF removed the trimethyl silyl group. Hydrolysis of the ester function of

13 provided the acid **14** in excellent yield and this material was dried scrupulously and subjected to a standard CDI-mediated coupling reaction to furnish bivalent ligand XLi093. The imidazobenzodiazepine diethyl diester XLi356 (**3**) was obtained from XLi093 in high yield *via* catalytic hydrogenation (Pd/C, H₂).

The dimers Xli093 and Xli356 were sent to Case Western Reserve (NIMH supported PDSP program, Roth et al.) for full panel receptor binding and they do not bind to other receptors at levels of concern (Table 27).

Data ("Secondary Binding") are K_i values. K_i values are reported in nanomolar concentration, Case Western Reserve University. Green indicates "Primary Missed" (<50% affinity). (See Appendix for full PDSP screen data)

Table 27. Full panel receptor binding reported for Xli093 and Xli356.

cook code	5ht1a	5ht1b	5ht1d	5ht1e	5ht2a	5ht2b	5ht2c	5ht3	5ht5a	5ht6	5ht7	α 1A	β 1B	α 2A	α 2B
xli093	Repeat														
xli356															
cook code	α 2C	Beta1	Beta2	CB1	CB2	D1	D2	D3	D4	D5	DAT	DOR	H1	H2	H3
xli093															
xli356															
cook code	H4	Imidazole	KOR	M1	M2	M3	M4	M5	MDR	MOR	NET	NMDA	SERT	σ 1	σ 2
xli093															
xli356															

Although Xli093, **27** was found to be an antagonist at the α 5 subtype, Xli356, **3** was found to be a weak agonist. Xli356 was found to reverse scopolamine induced memory deficits in mice. When Xli356 was looked at in audio cued fear conditioning, the results show no activity. This suggests that the effect of Xli356 is selective through α 5 receptors which are abundant in the hippocampus which is highly associated with contextual memory. Audio cued memory instead is amygdala-based, and should not be affected by an α 5 subtype selective compound.^{33, 34, 71, 213}

As illustrated in Figure 101, scopolamine (1 mg/kg) reduced freezing (ie. impairs memory) typically caused by pairing the context (the cage) with a shock. The drug Xli356 when given at 10mg/kg attenuates the impairment of memory returning the freezing to the level that one typically sees the mouse freeze at (ie veh). In audio cued, memory the response was triggered by sound not the context. Xli356 was not able to reverse this type of memory effect which is amygdala driven.

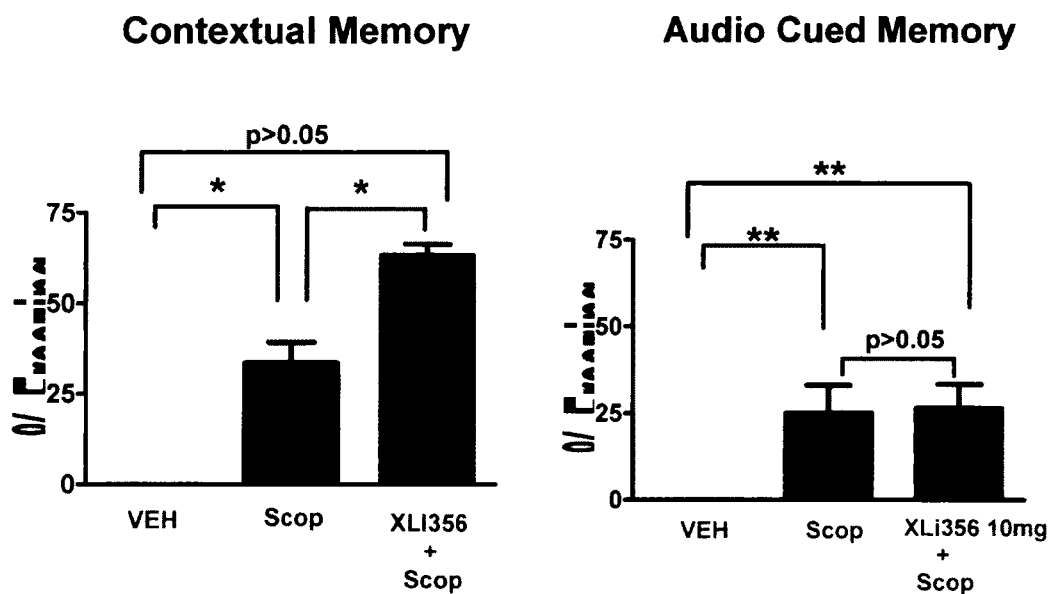


Figure 101. Visual and audio quued data for Xli356

Included Volume Analysis of Ligands Binding to Receptors Containing $\alpha 5$ Subunits

As discussed previously, the benzodiazepine binding site of $\alpha\beta\gamma 2$ GABA(A) receptors is strongly influenced by the type of α subunit present in these receptors as indicated by the existence of ligands exhibiting certain selectivity for receptors containing the respective α subunits.⁴⁶ If subtype selective ligands are then aligned within the pharmacophore model according to the resulting alignment rules,⁴⁷ their included volumes can be constructed and used to compare the topologies of benzodiazepine binding pockets of different receptor subtypes.⁴⁸

For enhanced selectivity at $\alpha 5$, it has been observed that ligands are generally *i*-BZDs and have a lipophilic C(8)-substituent that occupies the L_2 pocket. Based on ligands from various studies, examination of data in Figure 27 and 102 illustrated that the L_2 region was deeper and larger for the $\alpha 2$ and $\alpha 5$ subtypes, respectively, than for the corresponding $\alpha 1$ or $\alpha 6$ subtypes.^{49, 50}

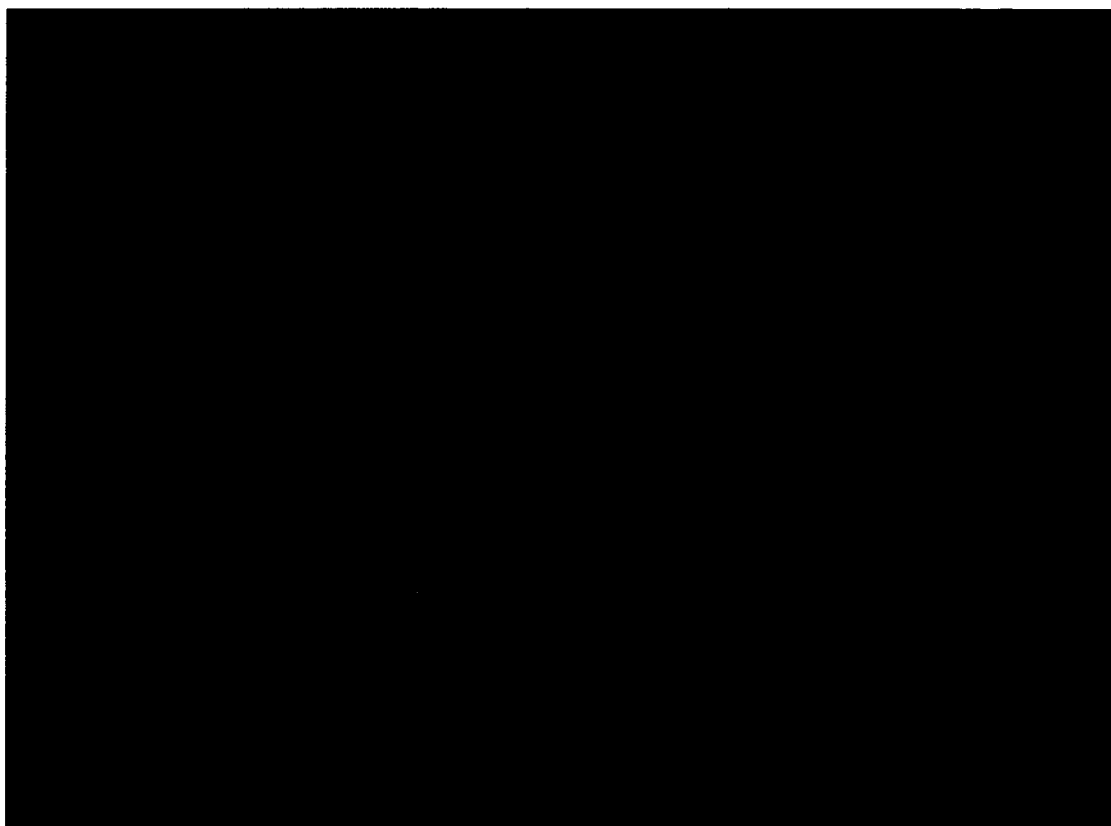


Figure 102. Updates of the $\alpha 5\beta 2\gamma 2$ subtype (solid) overlayed with the previous model (line).

SH-053 Analogs

In extension of this approach using BZ enantiomers, the behavioral activity of three newly-synthesized compounds,⁵¹ functionally selective for α_2 , α_3 and α_5 -containing subtypes of GABA(A) receptors (SH-053-S-CH3 and SH-053-S-CH3-2'F), or essentially selective for α_5 subtypes (SH-053-R-CH3) were examined. Motor influence was tested in the elevated plus maze, spontaneous locomotor activity and rotarod test, which are considered primarily predictive of the anxiolytic, sedative and ataxic influence of BZs, respectively. There was substantially diminished ataxic potential of BZ site agonists devoid of α_1 subunit-mediated effects, with preserved anti-anxiety effects at 30 mg/kg of SH-053-S-CH3 and SH-053-S-CH3-2'F. However, all three ligands, dosed at 30 mg/kg,

decreased spontaneous locomotor activity, suggesting that sedation may be partly dependent on activity mediated by $\alpha 5$ -containing GABA(A) receptors. Such an effect could not have been observed previously, because to date, all apparently non-sedating BZ receptor ligands, which are devoid of activity at $\alpha 1$ -containing GABA(A) receptors, engendered essentially antagonist⁵² or only partial agonist efficacy at $\alpha 5$ -containing GABA(A) receptors.^{49, 50} Therefore, it cannot be ruled out that substantial efficacy at $\alpha 5$ -containing GABA(A) receptors may contribute to sedative effects besides the effects on learning and memory processes.⁴⁶ This is supported by two sets of data which indicate the possibility of substantial motor influence via $\alpha 5$ -GABA(A) receptor modulation: In the spinal cord, somatic and preganglionic motoneurons (lamina IX and lateral cell column) exhibited a moderate to strong staining for the $\alpha 5$ subunit, suggesting a possible influence of receptors containing these subunits in motor behavior.⁵³ In addition, the knock-in mice harboring the $\alpha 5$ subunit insensitive to diazepam are refractory to development of tolerance to the sedative effect of diazepam dosed subchronically. Such a tolerance development might have been caused by a downregulation of receptors containing $\alpha 5$ subunits in the appropriate brain regions of wild-type mice.⁴² These two sets of evidence indicate that the motor influence of $\alpha 5$ -GABA(A) receptor modulation is not necessarily an indirect consequence of the established effects on learning and memory processes.⁶² It has been hypothesized⁶⁶ that locomotor activity changes induced by ligands possessing a substantial $\alpha 5$ -efficacy may be, at least partly, contributed to by modulation at GABA(A) receptors containing the $\alpha 5$ subunit. It, therefore, could be of importance to avoid substantial agonist potentiation of $\alpha 5$ -subunits by candidate anxiolytics, if clinical sedation is to be avoided. Nevertheless, as a caveat

to all studies examining sedation, it should be remembered that a decrease in automatically measured locomotor activity can be due to a variety of causes other than sedation, including the occurrence of stereotypical behavior, motor impairments or pain.^{64, 66} To dissect these overlaps in activity and uncertainties, much is expected from screening of even more selective BZ site ligands in the future.

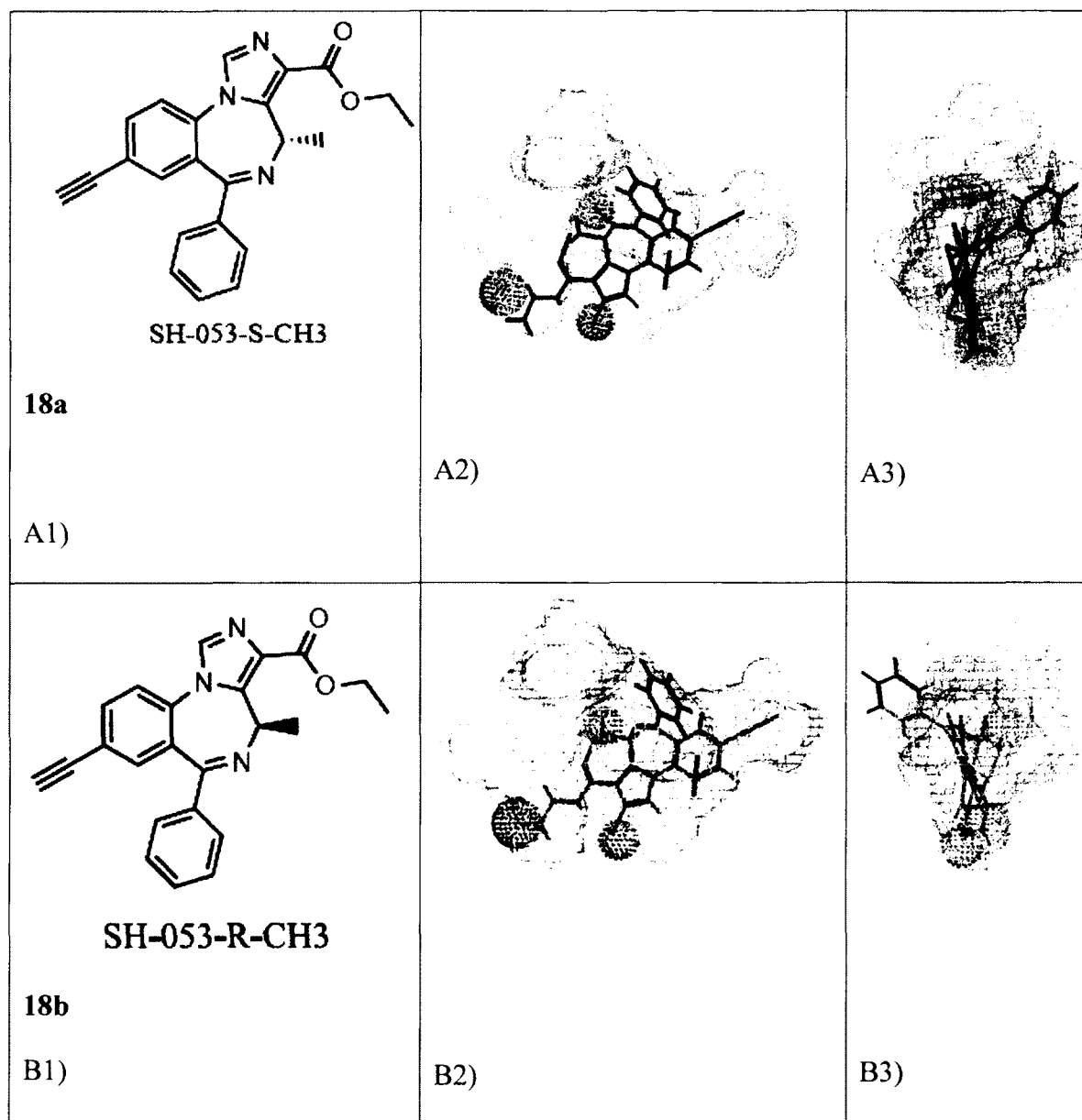


Figure 103. SH053 compounds in the α_2 pharmacophore/receptor model

Structures and conformations of SH-053-S-CH₃ (A1-A3) and SH-053-R-CH₃ (B1-B3) are presented in Figure 103. The molecular modeling was carried out as described in Clayton *et al*, 2007.⁶⁶ SH-053-S-CH₃ fits in the pharmacophore within the included volume of the $\alpha 2$ subtype (A2). A3 is the same image as A2 rotated 90°. It can be clearly seen that this conformer fits within the included volume. SH-053-R-CH₃ fit to the pharmacophore in the included volume of the $\alpha 2$ subtype (B2). B3 is the same image rotated 90°. The R-CH₃ at the prochiral center C4 changes the conformation of the molecule causing the pendant 6-phenyl to stick outside the included volume, consequently this ligand is not efficacious at the $\alpha 2$ subtype. It simply does not interact strongly with $\alpha 1$, $\alpha 2$ or $\alpha 3$ subtypes. However, note that the R-isomer does bind to $\alpha 5$ selectively. It is believed that further enhancement of potency can be achieved using this as a lead compound, by addition of a 2-F' or 2-N' substituent in the pendant phenyl ring at C-6, following the observations of Haefly *et al*.

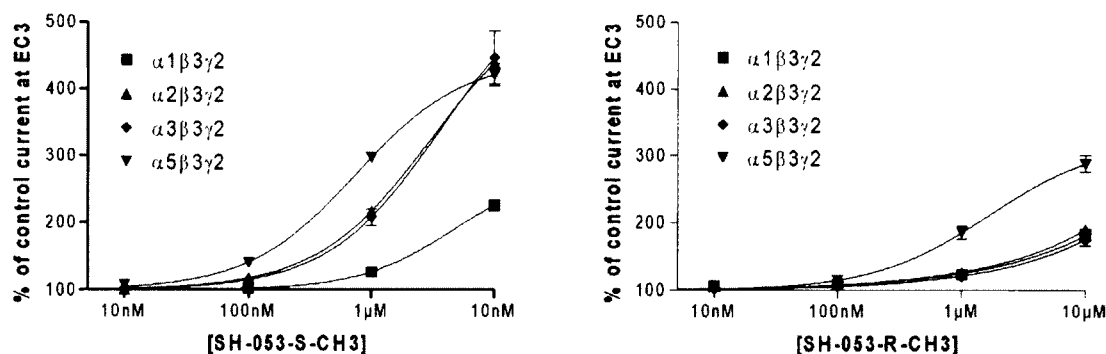
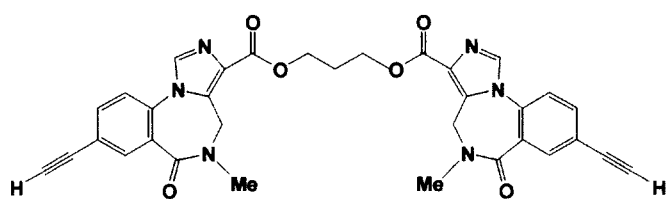
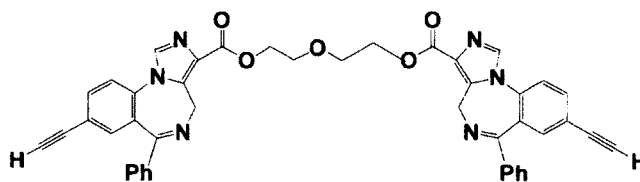


Figure 104. Concentration-effect curves for SH-053-S-CH₃ and SH-053-R-CH₃ on $\alpha 1\beta 3\gamma 2$, $\alpha 2\beta 3\gamma 2$, $\alpha 3\beta 3\gamma 2$, and $\alpha 5\beta 3\gamma 2$ GABA(A) receptors. Data points represent means \pm SEM from at least 4 oocytes from ≥ 2 batches.

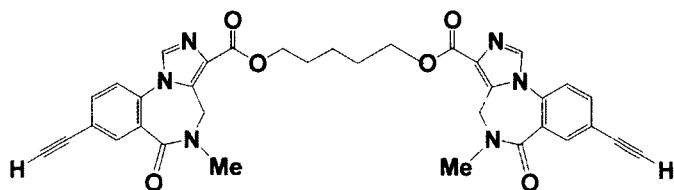
Dimeric Benzodiazepines



XLi-093, **1**



DMH-III-96, **19**



XLi-210, **18**

Table 28. Structures and affinities at the $\alpha\beta\gamma 2$ subtype.^{19,213} NR = not reported; ANT = antagonist; IA = inverse agonist; ND = not determined yet. Activity is defined for receptor subtype listed in bold.

Ligand	K _i (nM)						Activity
	α 1	α 2	α 3	α 4	α 5	α 6	
20 , Ro15-1788	0.8	0.9	1.05	NR	0.6	148	ANT
1 , XLi-093	1000	1000	858	1550	15	2000	ANT
18 , XLi-210	231	661	2666	NR	5.4	54.2	ND
19 , DMH-III-96	460	5000	NR	NR	5000	5000	ND

Design of the bivalent ligand XLi-093 **1** was based on the modeling of the α 5 selective monomer RY-80 **21** in the α 5 pharmacophore model. The ability of this ligand to bind (Table 23) and fit well within the pharmacophore (Figure 105) required the 3-carbon linker to be in a linear (*versus* folded) conformation. This linear conformation of XLi-093 has been confirmed both in the solid phase and in solution (Table 29).^{19, 21} The *J* values calculated from the dihedral angles (*J* = 5.38) were in excellent agreement with those determined from the solution NMR spectrum (*J* = 6.39), as previously mentioned. Because this bivalent ligand is α 5-selective, the enriched selectivity of this dimer and those similar to it, was presumably entropic in nature, as the loss of affinity at the other subtypes was profound.^{16, 187} Future work should include the synthesis of monomeric imidazobenzodiazepine with model (longer) aliphatic alcohol groups in the 3-position to confirm the enriched selectivity is indeed due to an entropic effect, rather than enthalpic.

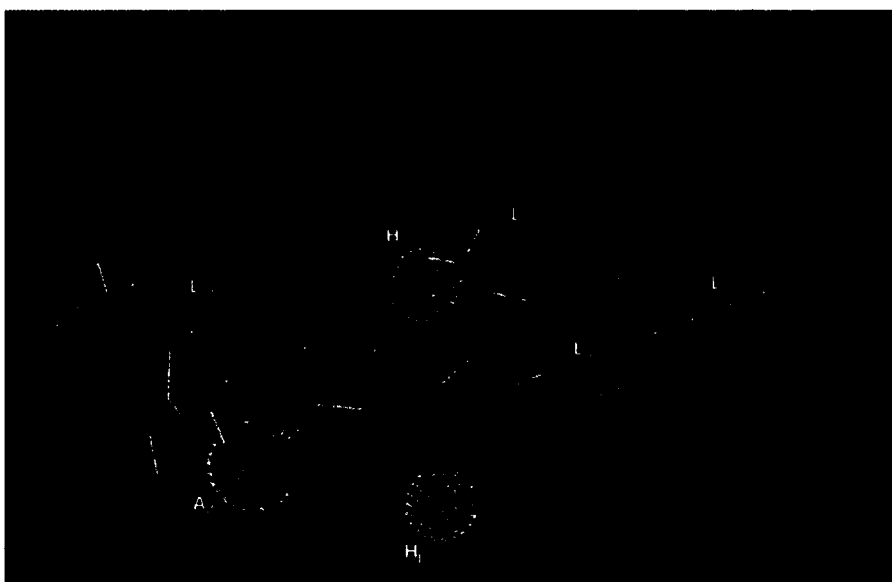


Figure 105. Alignment of XLi-093 **1** (white) and Ro15-1788 **20** (cyan) within the included volume of the $\alpha 5\beta 3\gamma 2$ subtype.

It has been shown *via* crystallographic and solution NMR studies that modification of the aliphatic spacer to a $-\text{CH}_2\text{OCH}_2-$ or a $-(\text{CH}_2)_2\text{O}(\text{CH}_2)_2-$ group, provided a bivalent ligand with a folded conformation (Figure 106).¹⁸⁸ Modeling of this type of ligand (*e.g.* DMH-III-96 **19**, Figure 107) within the $\alpha 5$ pharmacophore model illustrated the inability of bivalent ligands in the folded conformation to bind, presumably, because they are too hindered to access the Bz BS. Current data displaying these trends is shown in Table 29.

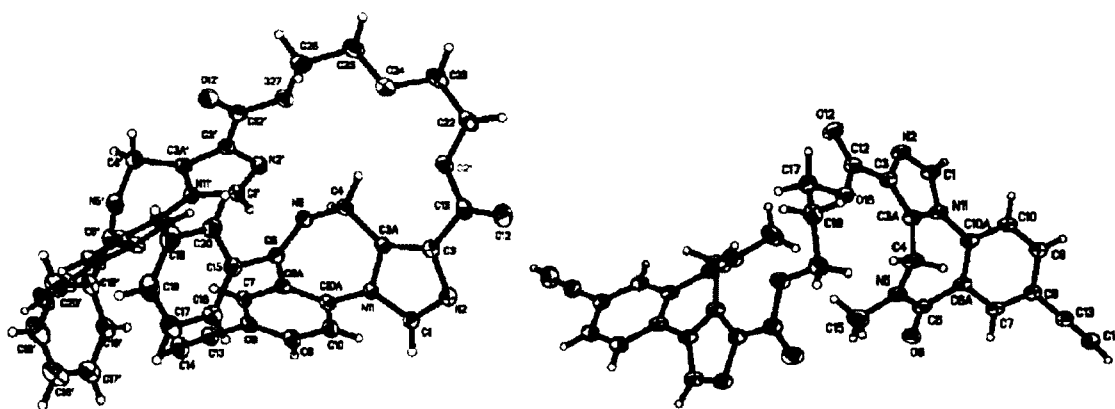


Figure 106. Crystal structures of the linear XLi-093 1 (left) and the folded DMH-III-96 19 (right).

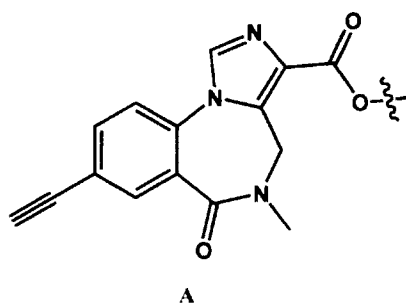


Table 29. The molecular composition and stable conformation of various Bz BS bivalent ligands.

ND = not determined yet.

Ligand	Monounit 1	Monounit 2	Spacer	Conformation in solution	Crystal structure
1, XLi-093	A	A	(CH ₂) ₃	linear	linear
18, XLi -210	A	A	(CH ₂) ₅	linear	ND
22, XLi -347	A	A	(CH ₂) ₂ O(CH ₂) ₂	folded	ND
23, XLi-374	A	A	CH ₂ OCH ₂	folded	ND
19, DMH-III-96	-	-	(CH ₂) ₂ O(CH ₂) ₂	folded	folded

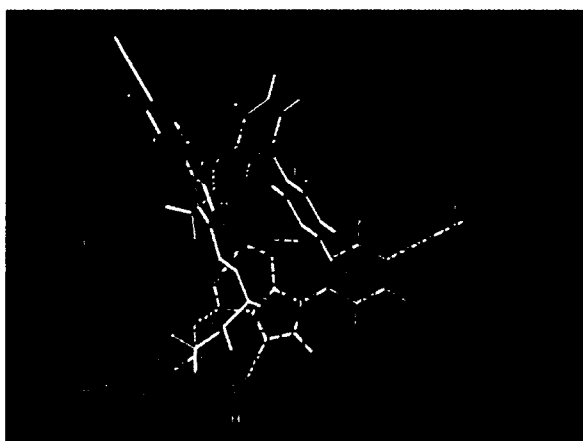


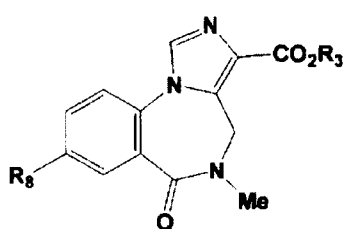
Figure 107. Alignment of DMH-III-96 within the included volume of the $\alpha 5\beta 3\gamma 2$ subtype. It is apparent that the folded conformation prevented it from binding to this GABA(A) subtype.

Although additional experimental data is needed, inspection of the alignment of XLi-093 (Figure 105) and our receptor model indicated the aliphatic linker of these bivalent ligands would thread the second half of the dimer through the L_{D1}/A_2 regions and toward the solvent accessible space outside (extracellular domain) of the receptor.

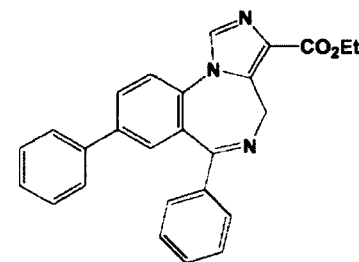
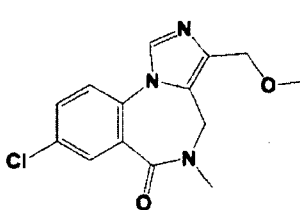
RY-24 and related analogs

Continued interest in the development of $\alpha 5$ selective ligands goes forward in the CNS area for many reasons. From the evaluation of K_i values, it was found that many 8-substituted *i*-BZDs, such as RY-24 **24** and RY-80 **31** and their trimethylsilyl precursors **25** and **26** (Table 30), exhibited a significant degree of binding selectivity at the $\alpha 5$ subtype *in vitro*. This observation was in agreement with the previous hypothesis that correct occupation of the L_2 region can promote $\alpha 5$ selectivity of a ligand.³⁶⁰ Therefore, the efficacy of the $\alpha 5$ -subtype selective ligand RY-24 **24** was evaluated *in vitro*. Recently, it was determined that this ligand was a potent inverse agonist at the $\alpha 5$ subtype with a much weaker efficacy at the other subtypes (Figure 108). These results confirmed previous binding data, which indicated that this ligand was $\alpha 5$ -selective due to the lipophilic C(8)-substituent which fully occupied the L_2 pocket.²¹ The data were also in agreement with previous studies *in vivo*, which indicated that some of these ligands enhanced cognition while other Bz BS ligands were not as effective.¹⁸⁹ Furthermore, ligands devoid of a lipophilic substituent at the C(8) position showed no selectivity for the $\alpha 5$ subtype (Table 30, **28**).

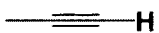
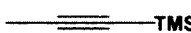
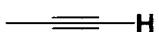

Table 30. Structures and affinities of some $\alpha 5\beta 3\gamma 2$ -subtype selective ligands.



56



DM-I-81, **55**

Ligand	R ₈	R ₃	K _i (nM)				
			α1	α2	α3	α5	α6
24, RY-24		<i>t</i> -Bu	26.9	26.3	18.7	0.4	5.1
25, RY-23		<i>t</i> -Bu	197	143	255	2.61	58.6
13, RY-80		Et	28.4	21.4	25.8	0.49	28.8
26, RY-79		Et	121	142	198	5.0	114
28	H	Et	1.2	2.0	1.1	0.4	> 300
2, DM-I-81	Ph	NA	> 2000	> 2000	> 2000	176	> 2000
56, PWZ-029 ^{111, 190}	Cl	>300	>300	>300	>300	38.8	>300
PWZ-029	Cl	920	ND	ND	ND	30	ND
PWZ-029	Cl	362.4	180.3	328.2	ND	6.185	ND

Inspection of the data in Table 30 revealed some observations worth noting. While the lipophilic substituent at R₈ of RY-24 **24** and RY-80 **31** decreased the affinity for α1, α2 and α3 subtypes, it retained affinity for α5 and actually increased affinity for the α6 subtype. Furthermore, selective affinity of *i*-BZDs at the α5 subtype was independent of the occupation of the L₃ pocket, as illustrated by the *in vitro* data of DM-I-81 **2** (Table 25). This data again supports the importance of the occupation of the lipophilic pocket L₂ for potent selectivity at α5 subtype. However, although 8-pendant phenyl of DM-I-81 was lipophilic and bound to the L₂ pocket, it was abandoned as a lead since its bulk was detrimental to activity and potency was only 176 nM at α5 (weak).

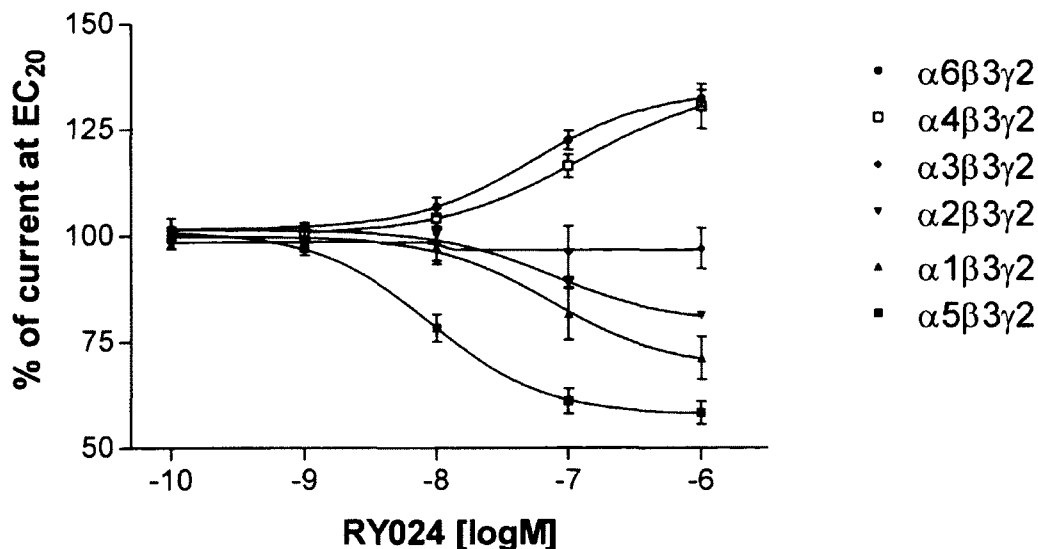


Figure 108. Subtype efficacy of RY-24

As illustrated in Figure 108, dose response curves for RY-24 in oocytes expressed different subunit combinations of GABA(A) receptors. Subtype combinations are indicated in legends. cRNA-injected *Xenopus* oocytes were held at -60 mV under two-electrode voltage clamp. Increasing concentrations of RY-24 were superfused together with a GABA concentration eliciting $\sim 20\%$ of the maximal current amplitude. RY-24 was pre-applied for 30 sec before the addition of GABA, which was co-applied with the drugs until a peak response was observed. Data were normalized for each curve assuming 100% for the response in the absence of RY-24. RY-24 was made up and diluted as a stock solution in DMSO. Final DMSO concentrations perfusing the oocyte were 0.1%. Values are presented as mean \pm SD of at least 4 oocytes from at least 2 batches. From examination of these data (Figure 108) it was clear RY-24 was a potent inverse agonist at $\alpha 5$ subtypes. It was also an inverse agonist at $\alpha 1$ and $\alpha 2$ subtypes, albeit less potent.

This $\alpha 1$ and $\alpha 2$ inverse agonist efficacy is the reason RY-24 also exhibits proconvulsant and convulsant effects in rodents.^{21, 191}

Importantly, however, June *et al.* recently reported the neurobehavioral results of RY-23 and RY-24 in rats. In agreement with previous studies,¹⁶ these $\alpha 5$ selective ligands were highly selective in suppressing ethanol-maintained responding (Figure 109).^{19, 192} As previously stated, the hippocampus contains the greatest concentration of $\alpha 5$ -containing receptors in the CNS,¹⁹³ and it is possible that these hippocampal $\alpha 5$ receptors may regulate alcohol-motivated responding following systemic administration of an $\alpha 5$ -selective agent. Furthermore, RY-24 also antagonized the motor-impairing and sedative effects of ethanol in Long-Evans rats. Combined with additional studies within the ventral pallidum (VP), it has been proposed that the GABAergic systems within the VP and hippocampal pathways may represent new extensions of the mesolimbic ethanol reward circuitry. Although these data do not strongly support a direct role for the modulatory influences of intrinsic efficacy in the behaviors examined, the synthesis of $\alpha 5$ subtype selective ligands provides researchers a unique opportunity to explore the role of this subtype in the neurobehavioral effects of alcohol which is now in progress by Donna Platt at NERPC with PWZ-029.¹⁹⁴ It is clear PWZ-029 reduces alcohol self-administration in monkeys (Platt et al., unpublished results).

Additional behavioral studies of RY-24 were performed by Helmstetter *et al.* and provided further support for the role of the hippocampus in anxiety and learning.^{191, 192} Moreover, the data suggested that Bz binding sites within the hippocampus are important for the acquisition of fear conditioning. Although this subtype selective ligand has been shown to be an inverse agonist at the $\alpha 5$ subtype,^{191, 192} the study suggested that RY-24

may act as an agonist at other alpha subtypes because larger doses of RY-24 were not as anxiogenic as the smaller doses and resulted in decreased learning. Consistent with the studies of Stephens *et al.* using $\alpha 5$ knock-out mice¹⁸ and the efficacy studies of Lüddens, June and Cook *et al.*,^{195, 196} these findings support the concept that the pharmacology observed depends upon the dose, behavioral paradigm employed and subunit composition activated. Ligands such as RY-24 have proven to be valuable in the study of the biochemical and pharmacological properties of GABA(A) receptors and have permitted insight into the role this protein plays in anxiety and learning.

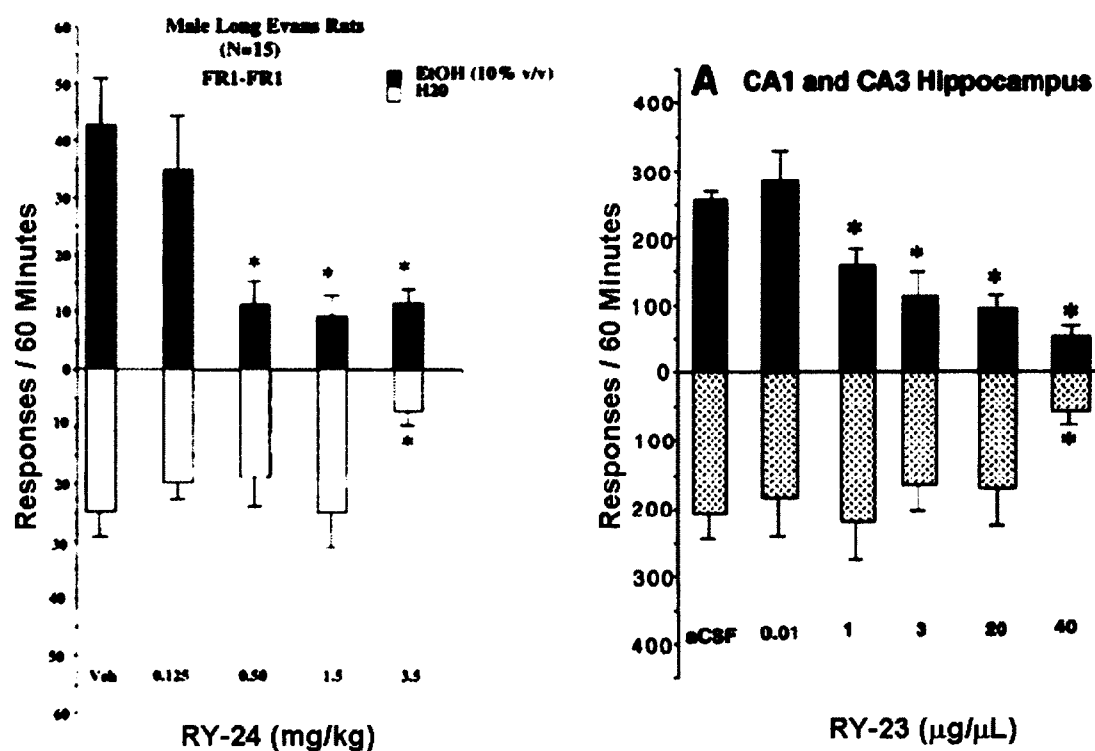


Figure 109. Suppression of alcohol-motivated responding by RY-24 and RY-23.¹⁸⁵

On the left panel of Figure 109, the dose-response of ip administration of RY-24 (0.0–3.5 mg/ kg) and vehicle on responding maintained by ethanol (10 % v/v) (*top panel*) and water (*bottom panel*) in male Long-Evans rats. On the right, the dose-response of unilateral infusions of RY-23 (0.0-40 μ g) into the hippocampus on a concurrent fixed-ratio (FR4) schedule for ethanol (10 % v/v) (*top panel*) and saccharin-maintained (0.025 % v/v) (*bottom panel*). For both studies, $*p \leq 0.05$ versus control condition values was determined using ANOVA and *post hoc* Newman-Keuls test. Each bar represents the mean (\pm SEM) ($n = 15$ for RY-24 and $n = 7$ for RY-23).¹⁸ It is clear both RY-23 and RY-24 reduce alcohol self-administration in rats with very little effect on the saccharin control. This has prompted the work on PWZ-029 by Platt et al. at NERPC since PWZ-029 is a much more selective and safer $\alpha 5$ ligand (neither proconvulsant nor convulsant).

QH-II-066

Due to the pharmacological profile which RY-24 exhibited *in vivo*, the development of additional $\alpha 5$ subtype selective ligands was pursued. Thus, the 7-acetyleno analog of diazepam, QH-ii-066 **29**, was synthesized and was determined also to exhibit a binding and functional selectivity at the $\alpha 5$ subtype over the $\alpha 1$ subtype (Table 26).¹⁸ This was due, presumably, to the full occupation of the L₂ pocket, relative to diazepam (Figure 110). To our knowledge, this was the first agonist ligand to display some $\alpha 5$ selectivity from the 1,4-benzodiazepine family. Importantly, the 7-cyano congener **30** (Table 31) did not potently bind to recombinant receptors of the $\alpha 5$ subtype,

which is in agreement with earlier work of Haefely and Fryer *et al.* on the SAR of 1,4-benzodiazepines.^{361, 362} This cyano ligand also did not exhibit any subtype selectivity, re-emphasizing that occupation of the L₂ region with lipophilic groups is important for α 5 selectivity as well as for high affinity. The selective efficacy of this QH-ii-066 ligand over the α 1 subtype was demonstrated by reversing the convulsant actions of RY-24 **24**, an α 5-selective inverse agonist, in NIH mice.^{363, 364} This ability was not observed at comparable doses for the α 1-selective agonist zolpidem **31**. The acetyleno group of QH-ii-066 increased the occupation of the L₂ region relative to that of diazepam.

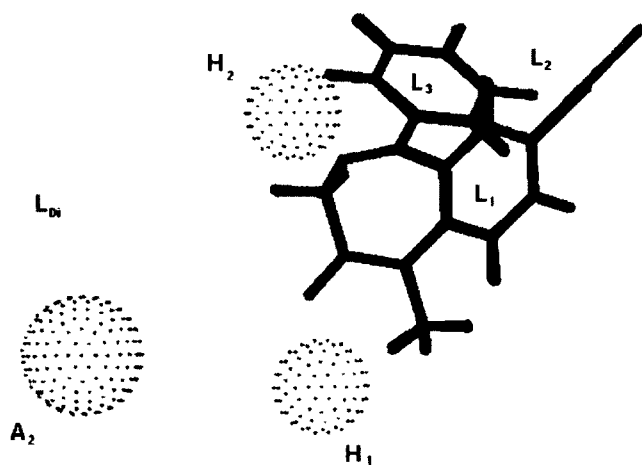
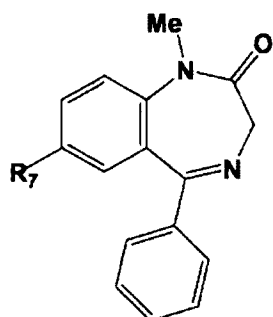


Figure 110. Comparison of non-selective diazepam (black) with the α 5-selective QH-ii-066 (cyan) when aligned within the unified pharmacophore/ receptor model.

Furthermore, Lelas and Cook *et al.* have recently determined that although QH-ii-066 had similar affinity for the DS subtypes in rats, it displayed functional selectivity *in*

vivo, with diazepam-like efficacy at the $\alpha 5$ subtype and partial efficacy at the $\alpha 1$ subtype.³⁶³ The study also indicated that this 7-acetyleno substituted diazepam analog exhibited less potency in protection against ECS-induced seizures relative to diazepam than against PTZ-induced seizures. Hence, the $\alpha 1$ subtype may play a more prominent role in ECS-induced seizures than in PTZ-induced seizures.^{13, 365}

Table 31. Structures and affinities of 1,4-benzodiazepines.



Ligand	R_7	K_i (nM)				
		$\alpha 1$	$\alpha 2$	$\alpha 3$	$\alpha 5$	$\alpha 6$
32 , diazepam	Cl	14	20	15	11	> 3000
29 , QH-ii-066	$\text{—}\equiv\text{—H}$	76.3	42.1	47.4	6.8	> 3000
30	$\text{C}\equiv\text{N}$	320	310	350	265	> 3000

Compound development guided by pharmacophore models has led to new agents with interesting pharmacological profiles, particularly with enhanced preference for $\alpha 2$ or $\alpha 5$ containing Bz GABA(A) receptor subtypes. Based on the evaluation of experimental data and comparative models of the $\alpha 1\beta 2\gamma 2$ GABA(A) receptor, the location of several residues relative to the descriptors of the pharmacophore/receptor model has been proposed. Absolute assignments were made in part I regarding which amino acids satisfy the pharmacophoric descriptors, experimental data strongly indicated definite trends with regard to how ligands of varying pharmacological activity are oriented within the receptor. Future site directed mutagenesis work needs to confirm these assignments and will help improve the $\alpha 5$ model. Information to be immediately gained from this proposed orientation can have far reaching benefits, not only for the rational design of selective ligands and the interpretation of ligand docking results, but also for the identification and evaluation of possible roles certain residues may have within the pocket. Structural determination of the $\alpha 5$ GABA(A) receptor is eagerly awaited. It is hoped that the proposed orientation may be used by others to gain additional insight into the potential mechanisms underlying binding and modulation at the $\alpha 5$ Bz site, all of which will lead to a better understanding of the structure and function of this receptor.

Affect on Passive Avoidance Learning in Rats of a Modest Inverse Agonist (PWZ-029) with Functional Selectivity at GABA(A) Receptors Containing $\alpha 5$ Subunits

It is known that benzodiazepine (BZ) site ligands affect vigilance, anxiety, memory processes, muscle tone somnolence and epileptogenic propensity through modulation of neurotransmission at GABA(A) receptors containing α_1 , α_2 , α_3 or α_5 subunits, and may have numerous experimental and clinical applications. The ability of nonselective BZ site inverse agonists to enhance cognition, documented in animal models and human studies, is clinically not feasible due to potentially unacceptable psychomotor effects. Most investigations to date have proposed the α_1 and/or α_5 subunit-containing GABA(A) receptors as comprising the memory-modulating population of these receptors. The novel ligand PWZ-029, which was synthesized on large scale and characterized electrophysiologically, possesses *in vitro* binding selectivity and moderate inverse agonist functional selectivity at $\alpha 5$ -containing GABA(A) receptors. This ligand has also been examined in rats in the passive and active avoidance, spontaneous locomotor activity, elevated plus maze and grip strength tests, primarily predictive of the effects on the memory acquisition, basal locomotor activity, anxiety level and muscle tone, respectively. The improvement of task learning was detected at the dose of 5 mg/kg in the passive, but not active avoidance test. The inverse agonist PWZ-029 had no effect on anxiety or muscle tone, whereas at higher doses (10 and 20 mg/kg) it decreased

locomotor activity. This effect was antagonized by flumazenil and also by the lower (but not the higher) dose of an agonist (SH-053-R-CH3-2'F) selective for GABA(A) receptors containing the α_5 subunit. The hypolocomotor effect of PWZ-029 was not antagonized by the antagonist β -CCt exhibiting a preferential affinity for α_1 -subunit containing receptors. These data suggest that moderate negative modulation at GABA(A) receptors containing the α_5 subunit is a sufficient condition for eliciting enhanced encoding/consolidation of declarative memory, while the influence of higher doses of modulators at these receptors on motor activity shows an intricate pattern whose relevance and mechanism wait to be defined.

One desirable property in this regard is the pro-mnesic activity of BZ site inverse agonists, repeatedly reported in animal models,¹³ as well as in human volunteers.^{49, 50, 366} However, this desirable effect is confounded by different concomitant psychomotor effects (increased vigilance, anxiogenic and/or proconvulsant state), some of which have been described in memory studies with non-selective inverse agonists in humans, urging their early termination of the studies.^{11, 367} Point mutated mice could not be used to identify the receptor subtypes mediating the promnesic activity of inverse agonists because an unexplained switch to the agonist mode of action occurs when an inverse agonist at wild type diazepam-sensitive recombinant GABA(A) receptors is tested at the respective point-mutated receptors.³⁶⁸ Thus, inverse agonists exerted agonistic-like sedative and anticonvulsant effects in mice with the point-mutated α_1 subunits,³⁶⁹ while corresponding experiments in models of learning and memory were not performed. Nevertheless, behavioral examination of genetically modified animals conducted to date has indicated the α_1 and α_5 subunit-containing GABA(A) receptors comprise the

'memory-modulating' population of these receptors.^{297, 370, 371} It is notable that GABA(A) receptors containing the $\alpha 5$ subunit are abundantly expressed in the hippocampus,³⁷² the structure substantially involved in memory formation.⁷ Recent evidence from animal studies with affinity-selective³⁷³ or efficacy-selective ligands⁴⁶ has confirmed that the $\alpha 5$ subunit was significantly involved in cognition enhancement mediated by the negative modulation of GABA(A) receptor functions. Moreover, it was shown in humans that pre-treatment with an $\alpha 5$ efficacy-selective inverse agonist significantly reduces the amnesic effect of alcohol on learning a word list.³³⁴ However, the affinity- or efficacy-selectivity of the ligands, as well as the diversity of the behavioral tasks used in their characterization to date, were of limited extent, which necessitates screening of newer BZ site negative modulatory ligands, to determine the putative therapeutic role of such compounds in various disorders with diminished cognitive capabilities in humans.^{374, 375}

In this regard, the BZ site ligand PWZ-029 was synthesized (Figure 111) as mentioned. Its efficacy profile was examined by two-electrode voltage clamp experiments in *Xenopus* oocytes expressing recombinant GABA(A) receptor subtypes. The behavioral effects on adult male Wistar rats were evaluated in the passive and active avoidance, spontaneous locomotor activity, elevated plus maze and grip strength tests, primarily predictive of detecting the changes in the memory acquisition, basal locomotor activity, anxiety level and muscle tone, respectively.

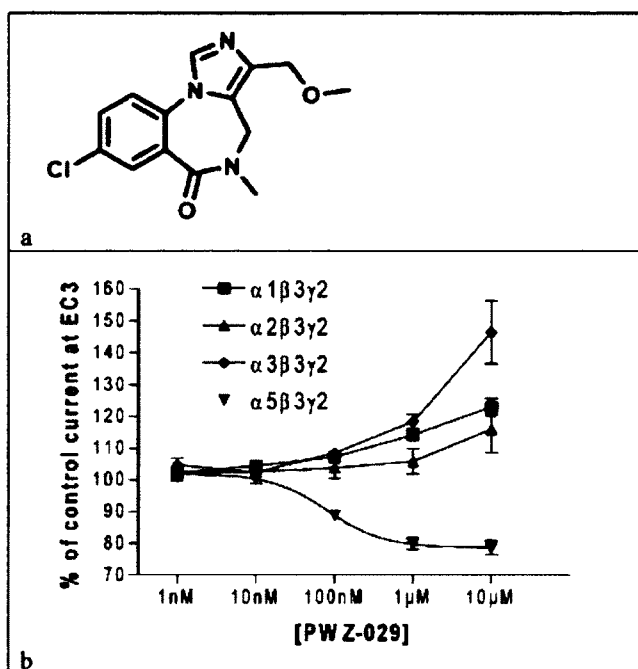


Figure 111. *In vitro* efficacy of PWZ-029 in *Xenopus* oocytes

Concentration-effects curve for modulation of GABA elicited currents by PWZ-029 on *Xenopus* oocytes expressing GABA(A) receptor subtypes $\alpha_1\beta_3\gamma_2$, $\alpha_2\beta_3\gamma_2$, $\alpha_3\beta_3\gamma_2$, and $\alpha_5\beta_3\gamma_2$ is illustrated in Figure 111. Concentrations of GABA that elicit 3% of the maximum GABA-triggered current (EC_3) of the respective cells were applied alone and with various concentrations of PWZ-029. Control currents represent responses in the absence of PWZ-029. Data points represented means \pm SEM from 4 oocytes from ≥ 2 batches. As you can see, 1μM PWZ-029 resulted in $114 \pm 4\%$, $105 \pm 8\%$, $118 \pm 5\%$ and $80 \pm 4\%$ of control current (at GABA EC_3) in $\alpha_1\beta_3\gamma_2$, $\alpha_2\beta_3\gamma_2$, $\alpha_3\beta_3\gamma_2$, and $\alpha_5\beta_3\gamma_2$ receptors,

respectively. All these values except the one for $\alpha_2\beta_3\gamma_2$ receptors were significantly different from that of the respective control currents ($P < 0.01$, student's t-test).

Electrophysiological Experiments

In vitro data for PWZ-029 (Figure 111b) demonstrated that at concentrations up to 1 μM this ligand engendered a significant partial inverse agonist efficacy at the α_5 -containing GABA(A) receptors (reduction of control current by 20%), whereas its activity at the other three types of receptors tended to be weakly and for α_1 - and α_3 -containing receptors significantly in the agonistic direction. Similarly, at 10 μM concentrations PWZ-029 exhibited a weak but significant partial agonistic effect at α_1 - and α_3 -containing receptors. The lower potencies of PWZ-029 for α_1 -, α_2 - and α_3 -subtypes, relative to the α_5 -containing GABA(A) receptors, deduced from the respective efficacy curves, conform with the explicit binding affinity data (Table 27). Hence, PWZ-029 shows a distinct affinity-, potency-, as well as efficacy- selectivity for the α_5 -containing GABA(A) receptors. PWZ-029 exerted negligible activity in 42 other receptor and enzyme assays (See Appendix B. Roth et al., NIMH Psychoactive Drug Screening Program, UNC, unpublished results, available at <https://kiddbdev.med.unc.edu/pdsp>). The *in vitro* concentration-effect curves for SH-053-R-CH3-2'F, the ligand used for interaction studies in the locomotor activity test, showed it is a high-efficacy agonist at the α_5 -containing GABA(A) receptors, with very low efficacies at α_1 , α_2 and α_3 -containing subtypes;^{334, 375} the profile was comparable with that published for its close congener SH-053-R-CH3,³⁶⁸ except for greater potencies and α_5 -efficacy for SH-053-R-CH3-2'F than SH-053-R-CH₃.

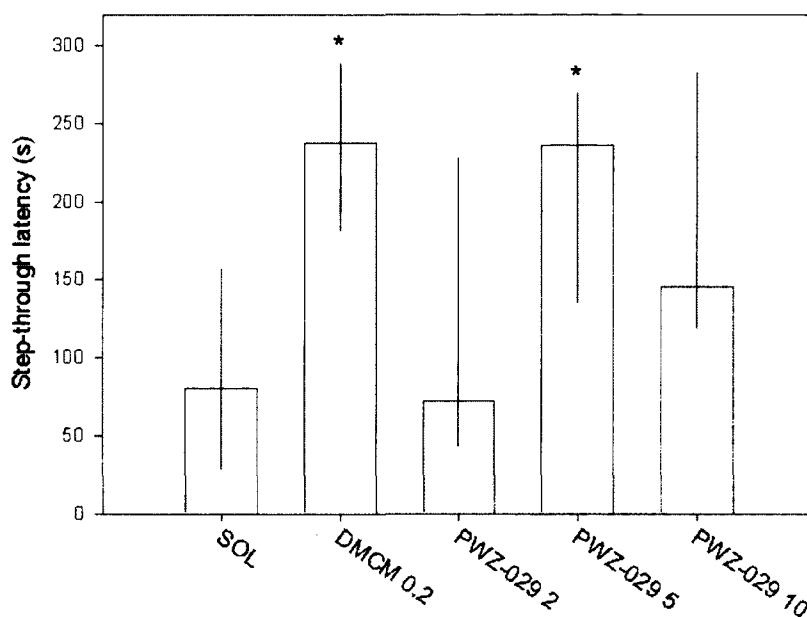


Figure 112. The effects of DMCM (0.2 mg/kg) and PWZ-029 (2, 5 and 10 mg/kg) on retention performance in a passive-avoidance task (* $P < 0.05$ compared to solvent (SOL) group). Number of animals per treatment group: 10.

Table 32. Table 1. PWZ-029 binding affinity (K_i , nM) at human recombinant GABA(A) receptors containing $\beta 3$, $\gamma 2$ and named α subunit, stably expressed in mouse fibroblast L(tk-) cells^a

$\alpha 1$	$\alpha 2$	$\alpha 3$	$\alpha 4$	$\alpha 5$	$\alpha 6$
>300	> 300	> 300	ND	38.8	> 300
920 ^b	ND	ND	ND	30.0 ^b	ND
362.4	180.3	328.2	ND	6.1	ND

^a Affinity was measured using [³H]flumazenil (for $\alpha 1$ -, $\alpha 2$ -, $\alpha 3$ -, and $\alpha 5$ -containing recombinant receptors), and [³H]Ro 15-4513 (for $\alpha 6$ -containing recombinant receptors) as radioligands, according to the method described in Huang et al., 1996. ND – not determined.

^b Recent binding affinity, based on the radioligand binding assay described in Lameh et al., 2001, obtained using the transiently transfected Sf9 insect cell line; data by DeLorey et al., unpublished results.

Passive Avoidance

The acquisition session latencies did not differ significantly irrespective of the treatment administered 15 min before the session (data not shown). The influence of the

pre-acquisition treatment on the retention trial latency was significant [$H(4) = 11.45$, $p = 0.022$]. Subsequent Dunn's test indicated that DMCM (0.2 mg/kg) and PWZ-029 at 5 mg/kg, administered before the acquisition session, significantly increased retention session latency relative to the control group.

Active Avoidance

Figure 120a shows that DMCM (0.1 mg/kg) and PWZ-029 (2-10 mg/kg) did not affect acquisition of avoidance responses on the training day [$F(4, 35) = 0.19$, $p = 0.98$]. Retention AA performance on the second day was significantly altered by the treatment before the acquisition session [$F(4, 35) = 2.82$, $p = 0.039$]; however, DMCM (0.1 mg/kg), but not the PWZ-029, was effective (Dunnett's test) (Figure 113b). Neither of the motor parameters measured (habituation crossings, intertrial crossings) differed significantly on the training or testing day (data not shown).

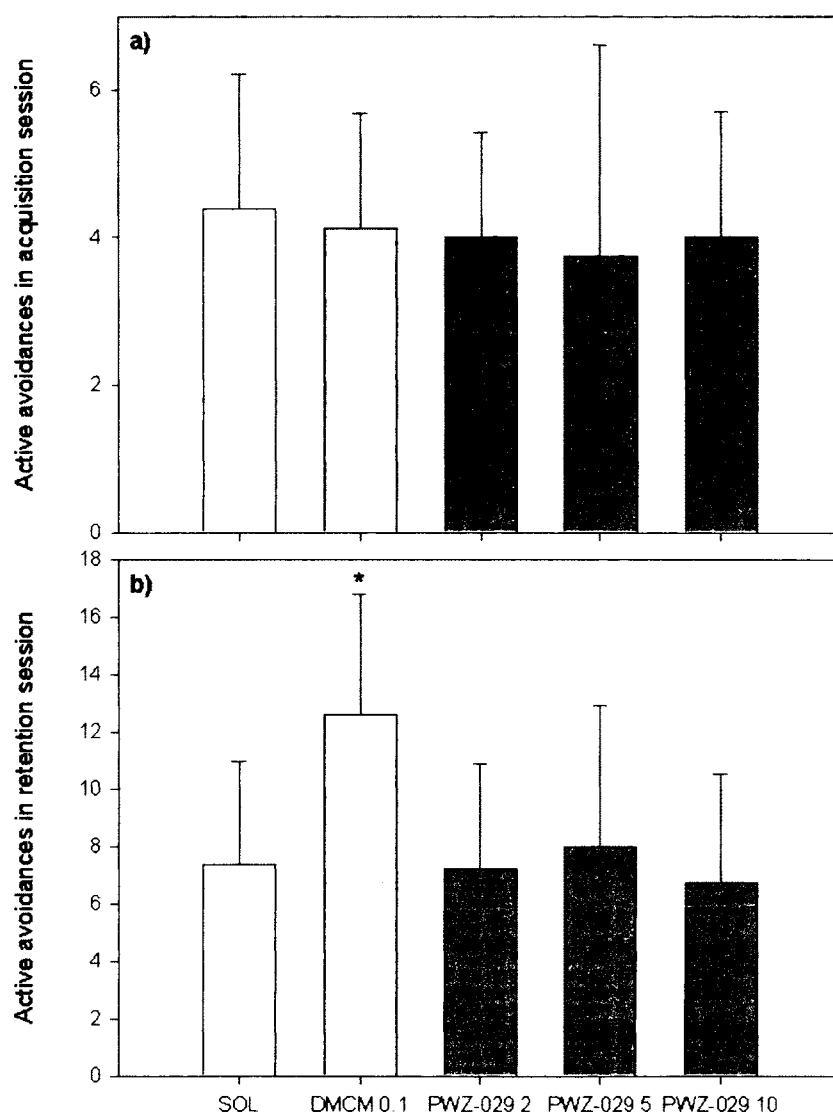


Figure 113. The effects of DMCM (0.2 mg/kg) and PWZ-029 (2, 5 and 10 mg/kg) on acquisition (a) and retention (b) performance in an active-avoidance task (*P<0.05 compared to solvent (SOL) group). Number of animals per treatment group: 8.

Locomotor Activity Assay

Whole Chamber-Activity

An ANOVA showed a significant effect of treatment on total distance travelled during 30 min of monitoring ($F(4,43) = 4.06$, $p = 0.007$) (Figure 114, whole bars). According to Dunnett's test, the two higher doses of PWZ-029 (10 and 20 mg/kg) exerted the activity-decreasing effect related to solvent. When the ANOVA with post hoc analysis was applied on the 5-min intervals of travelled distance (Figure 115), it turned out that locomotor activity was significantly depressed in the time periods 0-10 min (DMCM, 2 mg/kg and PWZ-029, 10 and 20 mg/kg), 10-15 min and 20-25 (PWZ-029, 20 mg/kg). It is notable that in the periods 15-20 min, 20-25 min and 25-30 min the rats treated with DMCM (2 mg/kg) travelled on average for 23%, 21% and 96% greater distance, respectively, than control animals; the difference did not reach statistical significance at either of the periods tested (student's t-test).

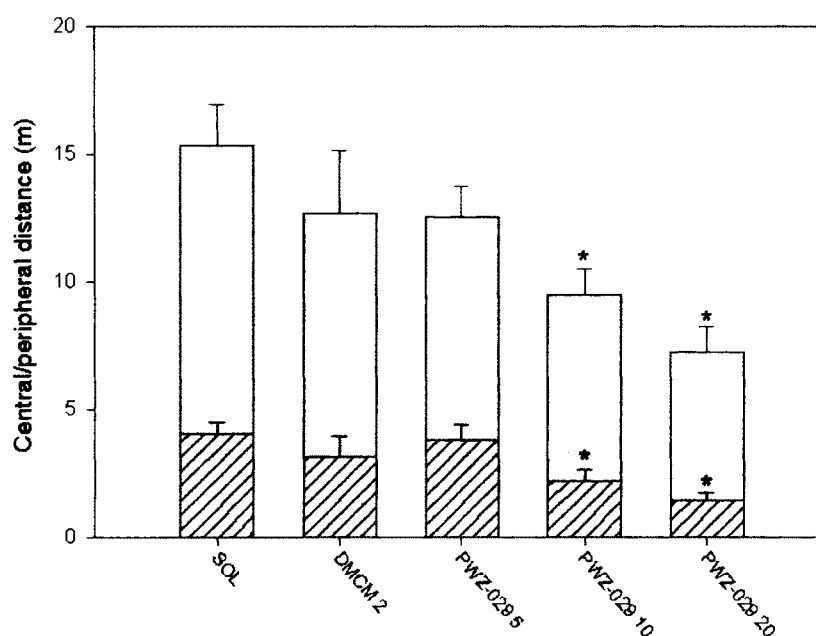


Figure 114. DMCM (2 mg/kg) and PWZ-029 (5,10 and 20 mg/kg)

The effects of DMCM (2 mg/kg) and PWZ-029 (5,10 and 20 mg/kg) on distance travelled in the central (hatched bars) and peripheral (open bars) zone of the activity chamber during 30 min of recording (total activity corresponds to the height of the whole bar). * $P < 0.05$ compared to solvent (SOL) group. Number of animals per treatment group (Figures 114-115) was 10, except for PWZ-029 (8 rats).

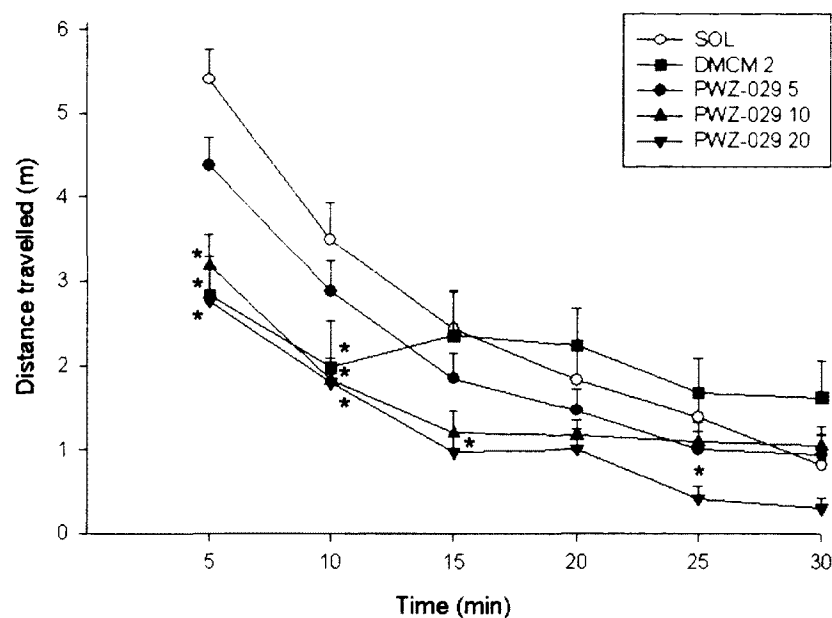


Figure 115. The effects of DMCM (2 mg/kg) and PWZ-020 (5,10 and 20 mg/kg) on the distance travelled in 5-min intervals in the activity assay. * $P < 0.05$ compared to solvent (SOL) group.

Central/Peripheral Distance

An ANOVA showed a significant effect of treatment on distance travelled in the arbitrarily set central parts of the chamber during 30 min of monitoring ($F(4,43) = 4.35$, $p = 0.005$) (Figure 114, hatched bars); the effects of PWZ-029 10 and 20 mg/kg were statistically significant. According to ANOVA, the influence of treatment on activity in peripheral parts of the chamber (Figure 114, open bars) was similar: $F(4,43) = 2.91$, $p = 0.033$; PWZ-029 20 mg/kg significantly decreased activity (Dunnett's test).

Antagonism of the Effect of PWZ-029 (Figure 116)

Both β -CCt (30 mg/kg) and flumazenil (10 mg/kg), the $\alpha 1$ -affinity selective and non-selective antagonist of BZ subtypes, respectively, failed to affect on their own the total distance travelled in the whole chamber, whereas only flumazenil reversed the suppression of locomotion induced by PWZ-029. The $\alpha 5$ -selective agonist SH-053-R-CH3-2'F showed a dose-dependent hypolocomotor influence on rats in the spontaneous locomotor activity assay, with the effective dose of 30 mg/kg (Savić, Furtmüller, Cook, unpublished data). When combined with PWZ-029 20 mg/kg, the dose of 10 mg/kg, but not 20 mg/kg, of SH-053-R-CH3-2'F antagonized the effect of the inverse agonist. There were no significant differences among groups in distances travelled in the central zone of the activity chamber.

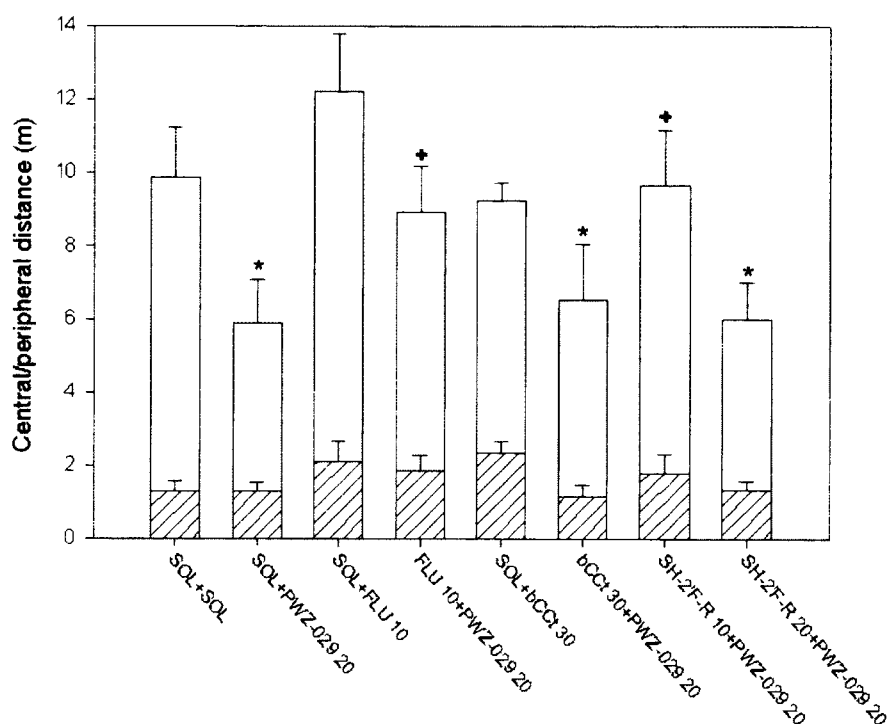


Figure 116. Antagonism of selected ligands (SH = SH-053-)

The influence of addition of the antagonists (flumazenil – FLU and β -CCt – bCCt) and the agonist SH-053-R-CH₃-2'F (SH-2'F-R) on the effect of PWZ-029, administered with solvent (SOL+PWZ-029), on distance travelled in the central (hatched bars) and peripheral (open bars) zone of the activity chamber during 30 minutes of recording (total activity corresponds to the height of the whole bar). * $p < 0.05$ compared to solvent (SOL+SOL) group. + $p < 0.05$ compared to SOL+PWZ-029 group, student's t-test. Number of animals per treatment groups, for SOL+SOL through SH-053-R-CH₃-2'F, respectively, was: 7, 7, 7, 6, 7, 8, 8, 8.

Elevated Plus Maze

Activity-Related Parameters

The influence of treatment on closed arm entries ($F(4,35) = 0.23$, $p=0.922$), total arm entries ($F(4,35) = 1.54$, $p=0.213$) and total distance travelled ($F(4,35) = 1.44$, $p=0.241$) did not reach statistical significance (data not shown).

Anxiety-Related Parameters (Figure 117)

The overall influence of treatment on distance travelled in open arms (Figure 117a) was not significant ($F(4,35) = 2.04$, $p=0.11$). There were significant effects of treatment on the percentage of open arm entries ($F(4,35) = 4.21$, $p=0.007$) (Figure 117b) and percentage of time spent on open arms ($F(4,35) = 3.13$, $p=0.026$) (Figure 117c). In both cases, the effective treatment was DMCM 1.25 mg/kg.

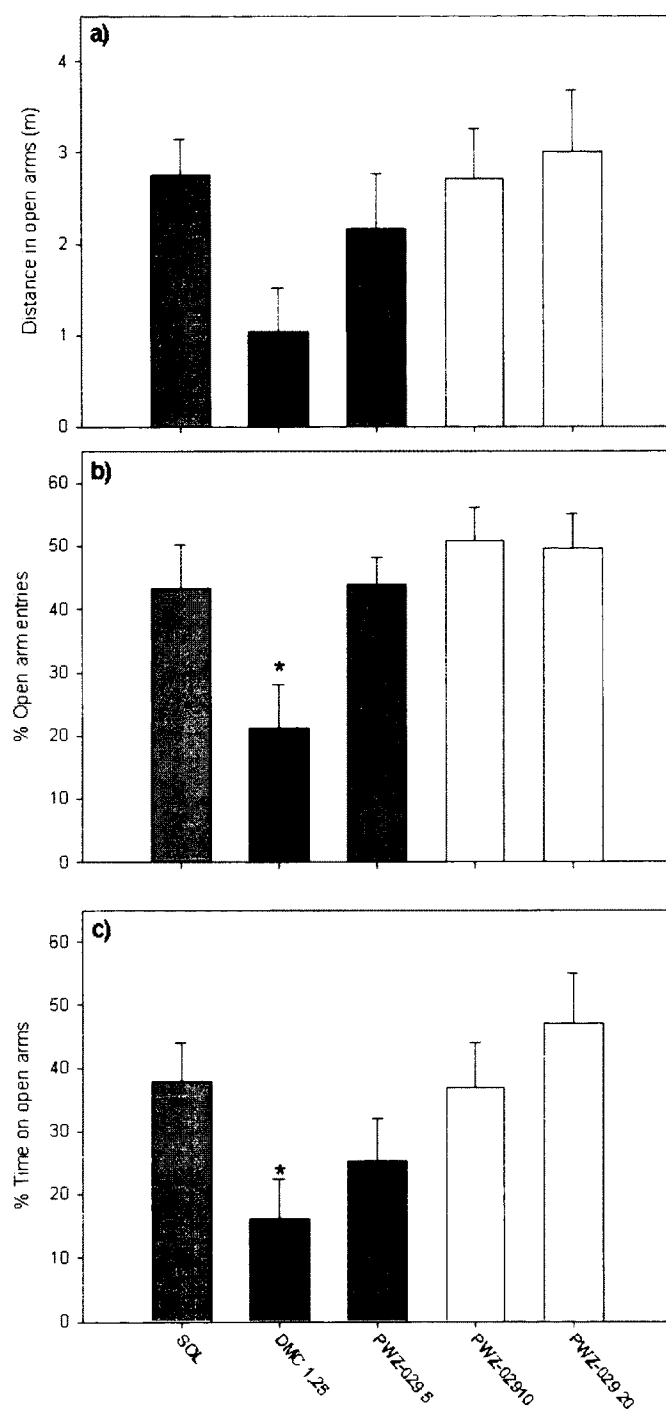


Figure 117. DMCM and PWZ-029 in open arm experiments

The effects of DMCM (1.25 mg/kg) and PWZ-029 (5,10 and 20 mg/kg) on the a) distance travelled on open arms, b) percentage of entries in open arms and c) percentage of time spent on open arms of the EPM. Number of animals per treatment group was 8
*P<0.05 compared to solvent (SOL) group.

Grip Strength Test

According to ANOVA, the overall influence of treatment on grip strength was not significant ($F(4,35) = 2.31$, $p=0.077$). The grip strength (mean \pm SEM) of rats treated with solvent, DMCM 1.25 mg/kg, PWZ-029 5 mg/kg, PWZ-029 10 mg/kg and PWZ-029 20 mg/kg was 505.0 ± 11.4 g, 561.1 ± 29.3 g, 546.5 ± 42.7 g, 468.0 ± 23.3 g, and 467.2 ± 27.1 g, respectively.

The present results demonstrated that PWZ-029, a novel BZ site negative modulator possesses *in vitro* binding selectivity as well as moderate inverse agonist functional selectivity for the $\alpha 5$ -containing GABA(A) receptors, which has translated into the promnesic effect detected in the PA (10 mg/kg), but not AA, learning task in rats. It has been shown that the non-selective inverse agonist DMCM enhances retention performance when administered at a small dose before the acquisition session of the active,³⁷⁶ or passive³⁷⁷ avoidance test, and these findings were replicated as a positive control in the present study. The interactions between DMCM and the antagonists flumazenil and β -CCt have suggested that the α_1 -subunit is substantially involved in processing of both of these memory tasks, whereas the interactions between agonists (midazolam and zolpidem) and antagonists pointed to the importance of some other α -

subunit(s), in addition to the α_1 -subunit, in the passive, but not active avoidance task.⁴⁹

³⁷⁸ **The latter agrees well with the memory-enhancing effect of the α_5 -selective inverse agonist PWZ-029, a ligand largely inactive at α_1 -containing GABA(A) receptors, in the PA task.**

Although seemingly similar, these two tests differ in some important characteristics, including the type of memory assessed and the brain regions involved in memory processing. Namely, the one-trial step-through PA test assesses declarative memory (to the point that terms such as ‘declarative’ or ‘explicit’ can be applied to rodent experiments),³⁷⁹ and for the retention of the task requires the preserved hippocampus.^{367, 380} On the other hand, the two-way AA test is an implicit, i.e. procedural,^{14, 334, 375} hippocampal-independent memory task¹⁴. However, as aversively motivated tests, both ‘measure’ memory of emotionally arousing experiences, and critically involve activity of the amygdala, especially the basolateral amygdala^{11, 367} in which the α_1 subunit is the most abundant of the six α subunits.^{50, 381} It is felt that this fact at least in part explains the uniform involvement of the α_1 subunit-containing GABA(A) receptors in modulation of memory acquisition, found for the present⁴⁹ with DMCM as well as similar, aversively motivated, memory tasks, such as the water-lick suppression test.³⁷¹

Receptors containing the α_5 subunit constitute a modest fraction of BZ-sensitive GABA(A) receptors (approximately 5%), but are substantially expressed in several brain regions, most notably the hippocampus, the olfactory bulb and layers V and VI of the neocortex.³⁸² Studies with untreated mice with the point mutation at the α_5 subunit, which unexpectedly displayed a partial loss, restricted to the hippocampus, of the

expression of this subunit, have indicated the significance of the $\alpha 5$ subunit for learning of certain aversively- as well as appetitively- motivated memory tasks which require temporal integration.³⁸³ On the other hand, in line with the present findings, mice with the deleted $\alpha 5$ subunit did not differ in comparison to the wild-type controls in acquisition of the two-way AA task.³⁸⁴ The results with PWZ-029 in the present memory tests suggest that moderate negative modulation of GABA-ergic transmission mediated by GABA(A) receptors containing the $\alpha 5$ subunit is a sufficient, but possibly not prerequisite condition for eliciting enhanced encoding/consolidation of declarative memory assessed by the PA test.

PWZ-029 had no effect on anxiety-related parameters in the EPM, in agreement with results with the other $\alpha 5$ -selective inverse agonist tested in this model;³⁸⁵ the $\alpha 5$ affinity- selective inverse agonist L-655,708 exerted an unusual U-shaped anxiogenic effect in the murine EPM, but with the use of a non-standard statistical analysis.³⁸⁵ The effect of PWZ-029 on muscle tension measured by the grip strength test also was absent. Hence, its hypolocomotor effect seen in the locomotor activity assay could not be ascribed to any muscle relaxation. Further, there was no hint of convulsive activity in any of the rats treated with PWZ-029 throughout the behavioral studies. This was in agreement with Stables et al. (NINDS) that showed PWZ-029 exhibited weak anticonvulsant activity as well as Rowlett et al. who showed it was a weak anxiolytic in rhesus monkeys (Rowlett, unpublished results). Decreases of locomotor activity may also reflect an increase in emotional reactivity, i.e. anxiety.^{54, 78, 126, 128} However, such an activity was not seen with PWZ-029 in the EPM test, nor was its hypolocomotor effect disproportionately more pronounced in the central, more exposed, and hence 'emotional',

zone of the chamber, but was notably different from standard patterns of activity of a nonselective inverse agonist (i.e. DMCM). Namely, as a rule, when rodents explore a novel environment under the influence of a negative modulator of GABA(A) receptors, locomotor activity is depressed, but usually in a relatively short period of habituation;¹²⁸ afterwards, a type of rebound hyperlocomotion may ensue.^{386, 387} However, as we have concluded from the experiment with DMCM and the α_1 -subunit selective antagonist β -CCt, hyperlocomotion in habituated animals may depend primarily on the negative modulation at α_1 subunit-containing GABA(A) receptors^{297, 369-371} and this was not observed with PWZ-029. Instead, the temporal pattern of the extended motor depression with PWZ-029 (20 mg/kg) was more similar to activity of an agonist, rather than an inverse agonist, and the most parsimonious explanation would be that, at the higher doses, PWZ-029 binds to enough α_1 , α_2 , and α_3 -containing GABA(A) receptors to manifest its slight partial agonistic activity. Nevertheless, the effect of PWZ-029 was mediated by BZ site(s) (antagonism of the effect by flumazenil) other than those at the α_1 -containing GABA(A) receptors (lack of antagonism by β -CCt). Comparative analysis of in vitro affinity and efficacy data of flumazenil and β -CCt⁴⁶ suggests that the principal difference between them lies in activity at α_5 subunit-containing GABA(A) receptors. Namely, flumazenil and β -CCt show qualitatively similar mixed antagonist/agonist efficacy profiles, with the main distinction being at α_5 subunit-containing GABA(A) receptors at which β -CCt is a weak inverse agonist, and flumazenil an antagonist/weak agonist. Moreover, a 150-fold lower affinity of β -CCt for the α_5 over the α_1 Bz subtype of GABA(A) receptors⁴⁹ should plausibly preclude its in vivo binding at α_5 subunit-containing GABA(A) receptors and influencing any effect mediated by them. Hence, it

is hardly conceivable that β -CCt may antagonize the effects of PWZ-029 at these receptors. Similarly, the slight positive modulation at $\alpha 2$ or $\alpha 3$ subunit-containing GABA(A) receptors, also observed at high doses of PWZ-029, could hardly have contributed to its hypolocomotor activity.^{50, 388}

Standard tests of locomotor activity were not usually employed in reported studies with $\alpha 5$ subunit-selective agents by Merck.³⁸⁸ Based on the results with three novel BZ site agonists functionally silent at the $\alpha 1$ subunit, we recently set out the hypothesis that positive modulation at the GABA(A) receptors containing $\alpha 5$ subunits may also contribute to the sedative properties of BZ site agonists.¹³ The finding that SH-053-R-CH₃-2'F at the lower (10 mg/kg), but not higher dose (20 mg/kg), antagonized the hypolocomotor effect of PWZ-029 adds to the notion that there may exist certain discontinuous 'effective windows' of the modulation of locomotion exerted by neurons expressing the $\alpha 5$ -subunit containing GABA(A) receptors. Namely, the maximal level of receptor inhibition obtained with PWZ (80% of the basal GABA effects sustained by the $\alpha 5$ -subunit containing receptors) is clearly different from that present in mice lacking this subunit at all (0% of the basal GABA effects at the affected receptors³⁸⁸) or in mice harboring a point mutation at the $\alpha 5$ subunits (approximately 70% of the basal GABA effects in the hippocampus related to the $\alpha 5$ -subunit containing receptors).³⁸⁹ Nevertheless, the respective locomotor outputs (a decrease with higher doses of PWZ-029, no changes in knockout mice, stimulation/no changes in mice with a point mutation at the $\alpha 5$ subunits) were apparently random in relation to the level of receptor modulation, but certainly dependent on the stress level and experimental settings (cf. an increase of spontaneous locomotor activity in the mice with point-mutated $\alpha 5$ GABA(A)

receptor subunits³⁹⁰ vs. lack of changes^{391, 392}). The present hypothesis of the protean influences of the $\alpha 5$ -subunit containing receptors on locomotion, possibly related to the intricacy of the different processes which are concomitantly modulated by these receptors (such as sensorimotor gating³³⁴ and firing of the layer V pyramidal neurons of the neocortex³³⁴), should be checked through various locomotor tests employing a range of doses of different $\alpha 5$ subunit-selective ligands, both as single treatments and in combination. It is well known that $\alpha 5$ BzR/GABAergic subtypes are located in the dorsal horn of the spinal cord and may be the neurons responsible for any hypolocomotor activity of PWZ-029.

Examination of the present results suggests that the negative modulation engendered by the novel BZ site ligand PWZ-029, which demonstrates binding and functional selectivity for the $\alpha 5$ -containing GABA(A) receptors, may be sufficient to effect enhanced formation of declarative memory. The sedative-like effects, seen at doses higher than those affecting memory formation, reduce the probability of generation of anxiogenic or proconvulsant states. This is important and greatly enhances the clinical potential of these $\alpha 5$ subtype selective negative modulators (inverse agonists). The molecular and neuronal substrates in regard to the role of $\alpha 5$ -subunit containing GABA(A) receptors in control of vigilance, including the proposed phenomenon of the 'on/off switch', may be numerous and wait to be further elucidated. In regard to PWZ-029 it is important to note that neither Stables (NINDS, anticonvulsant activity) nor Rowlett (Rhesus monkeys, anxiolytic) reported any loss of locomotor activity in their strains/species of animals.

Experimental Procedure

Drugs

PWZ-029 (methyl (8-chloro-5,6-dihydro-5-methyl-6-oxo-4H-imidazo [1,5- α] [1,4] benzodiazepin-3-yl)methyl ether), SH-053-R-CH₃-2'F (the (R) stereoisomer of 8-ethynyl-6-(2-fluorophenyl)-4-methyl-4H-2,5,10b-triaza-benzo[e]azulene-3-carboxylic acid ethyl ester) and the preferential α_1 -subunit selective antagonist β -carboline-3-carboxylate-t-butyl ester (β -CCt) were synthesized in Milwaukee. The non-selective antagonist flumazenil was donated from F. Hoffman-La Roche (Basel, Switzerland) and the non-selective inverse agonist DMCM was purchased from Research Biochemicals Incorporated (Natick, MA, USA).

Electrophysiological Experiments (with Sieghart et al.)

The cloning of GABA(A) receptor subunits α_1 , β_3 and γ_2 into pCDM8 expression vectors (Invitrogen, CA) has been described elsewhere.³⁹³ The cDNAs for subunits α_2 , α_3 and α_5 were gifts from P. Malherbe and were subcloned into pCI-vector. After linearizing the cDNA vectors with appropriate restriction endonucleases, capped transcripts were produced using the mMessage mMachine T7 transcription kit (Ambion, TX). The capped transcripts were polyadenylated using yeast poly(A) polymerase (USB, OH) and were diluted and stored in diethylpyrocarbonate-treated water at -70°C . The methods used for isolating, culturing, injecting and defolliculating of the oocytes were identical as described previously.¹¹ Briefly, mature female *Xenopus laevis* (Nasco, WI) were anaesthetized in a bath of ice-cold 0.17 % Tricain (Ethyl-m-aminobenzoate, Sigma, MO) before decapitation and removal of the frogs ovary. Stage 5 to 6 oocytes with the follicle cell layer around them were singled out of the ovary using a platinum

wire loop. Oocytes were stored and incubated at 18°C in modified Barths' Medium (MB, containing 88 mM NaCl, 10 mM HEPES-NaOH (pH 7.4), 2.4 mM NaHCO₃, 1 mM KCl, 0.82 mM MgSO₄, 0.41 mM CaCl₂, 0.34 mM Ca(NO₃)₂) that was supplemented with 100 U/mL penicillin and 100 µg/mL streptomycin. Oocytes with follicle cell layers still around them were injected with a total of 2.25 ng of cRNA. cRNA ratio used was 1:1:5 for the α subunits, β 3 and γ 2, respectively. After injection of cRNA, oocytes were incubated for at least 36 hours before the enveloping follicle cell layers were removed. To this end, oocytes were incubated for 20 minutes at 37°C in MB that contained 1 mg/mL collagenase type IA and 0.1 mg/mL trypsin inhibitor I-S (both Sigma). This was followed by osmotic shrinkage of the oocytes in doubly concentrated MB medium supplied with 4 mM Na-EGTA and manually removing of the follicle cell layer. After peeling off the follicle cell layer, the cells were allowed to recover overnight before being used in the electrophysiological experiments.

For electrophysiological recordings, oocytes were placed on a nylon-grid in a bath of Xenopus Ringer solution (XR, containing 90 mM NaCl, 5 mM HEPES-NaOH (pH 7.4), 1 mM MgCl₂, 1 mM KCl and 1 mM CaCl₂). The oocytes were constantly washed by a flow of 6 mL/min XR which could be switched to XR containing GABA and/or drugs. Drugs were diluted into XR from DMSO-solutions resulting in a final concentration of 0.1 % DMSO perfusing the oocytes. Drugs were preapplied for 30 seconds before the addition of GABA, which was coapplied with the drugs until a peak response was observed. Between two applications, oocytes were washed in XR for up to 15 minutes to ensure full recovery from desensitization. For current measurements the oocytes were impaled with two microelectrodes (2–3 m Ω) which were filled with 2 mM KCl. All recordings were performed at room temperature at a holding potential of –60 mV using a

Warner OC-725C two-electrode voltage clamp (Warner Instruments, Hamden, CT). Data were digitised, recorded and measured using a Digidata 1322A data acquisition system (Axon Instruments, Union City, CA). Results of concentration response experiments were graphed using GraphPad Prism 4.00 (GraphPad Software, San Diego, CA). Data were graphed as mean \pm SEM of at least four oocytes from at least two batches.

Behavioral Experiments (with Savic et al.)

Experiments were carried out on male Wistar rats (Military Farm, Belgrade, Serbia), weighing 220-250 g. All procedures in the study conformed to EEC Directive 86/609 and were approved by the Ethical Committee on Animal Experimentation of the Medical Faculty in Belgrade. The rats were housed in transparent plastic cages, six animals per cage, and had free access to pelleted food and tap water. The temperature of the animal room was $22\pm 1^{\circ}\text{C}$, the relative humidity 40-70%, the illumination 120 lux, and the 12/12 h light/dark period (light on at 6:00 h). All handling and testing took place during the light phase of the diurnal cycle. Throughout the study the animals were used only once, with the exception of the grip strength measurement, which was done immediately after the tracking of behavior on the elevated plus maze. Spontaneous locomotor activity and elevated plus maze behavior were analyzed by the ANY-maze Video Tracking System software (Stoelting Co., Wood Dale, IL, USA). All drugs were dissolved/suspended with the aid of sonication in a solvent containing 85% distilled water, 14% propylene glycol, and 1% Tween 80, and were administered intraperitoneally in a volume of 1 mL/kg, 15 min before behavioral testing (for active and passive avoidance test, before the acquisition session). Time of administration, as well as the

doses of DMCM in various tests were chosen based on our previous studies (Savić et al., 2005a; 2005b; 2006). For interaction studies in the locomotor activity assay, the first treatment indicated in combination was administered into the lower left quadrant of the peritoneum 20 minutes before testing, and the second treatment 5 minutes later into the lower right quadrant of the peritoneum.

Passive Avoidance (PA) Paradigm

The experiments were performed in an adapted Automatic reflex conditioner (Ugo Basile, Milan, Italy, Model 7051), as described earlier.³⁹⁴ In short, the apparatus consisted of a shuttle-box, equipped with a grid floor and divided with a sliding door into a lit and a dark compartment, and a programming unit. The animals were submitted to two, 24 hour – separated sessions. The acquisition session started by placing individual subjects in the illuminated compartment. After 30 seconds, the entrance to the dark compartment was opened, and as soon as the rat had entered it with all four paws, the footshock (2 s, 0.3 mA) was delivered. Immediately afterwards, the rat was returned to its home cage. The same procedure was repeated 24 hours later (retention session), without footshock. A cut-off time of 180 seconds was used on the training day, whereas, on the retention trial, a ceiling of 300 seconds was imposed.

Two-Way Active Avoidance (AA) Paradigm (with Savic et al.)

The AA test was performed in automated two-way shuttle-boxes (Campden Instruments, Sileby, UK), as described earlier.³⁹⁵ In short, the animals were submitted to two, 24-hour separated sessions. Training and test sessions were procedurally identical. Animals were placed singly into the shuttle box and left to freely explore for 15 minutes,

and habituation crossings were automatically counted. Afterward, they received 30 tone foot shock trials. During the first 5 seconds of each trial, a sound signal was presented (broadband noise of 69 dB), allowing the animal to avoid shocks by moving to the other compartment (avoidance response). If the animal did not respond within this period, a foot shock of 0.5 mA (7-s duration) was applied. Crossing to the adjacent compartment during the shock discontinued its delivery. The animal could move freely in the apparatus between trials (18-s intertrial intervals), and the intertrial crossings were automatically counted.

Measurement of Locomotor Activity (with Savic et al.)

Activity of single rats in a clear Plexiglas chamber (40 x 25 x 35 cm) under dim red light (20 lux) was recorded for a total of 30 minutes, without any habituation period, using ANY-maze software (as described above). For purposes of improving data analysis, the central 20% of the chamber (200 cm²) was virtually set as a central zone. The minimum percentage of animal that must have been in the zone for an entry to occur was set at 70%, and 50% of the animal must have remained in the zone for an exit not to occur.

Behavior on the Elevated Plus Maze (EPM) (with Savic et al.)

The apparatus consisted of two open (50 x 10 cm, with a ledge of 0.3 cm) and two enclosed arms (50 x 10 x 40 cm), connected by a junction area (10 x 10 cm). The illumination in the experimental room was 10 lux on the surface of the arms. At the beginning of the experiment, single rats were placed in the center of the maze, facing one of the enclosed arms, and their behavior was recorded for 5 min. An entry into an open or closed arm was scored when 90% of the animal crossed the virtual line separating the central square of the maze from the arm, whereas an exit occurred when more than 90 %

of the animal left the respective arm. After each trial, the maze was cleaned with dry and wet towels.

Grip Strength Test (with Savic et al.)

Muscle strength was assessed by the grip strength meter (Ugo Basile, Milan, Italy, model 47105). When pulled by the tail, the rat grasps the trapeze connected to a force transducer, and the apparatus measures the peak force of experimenter's pull (in g) necessary to overcome the strength of the animal's forelimbs grip. Each animal was given three consecutive trials, and the median value was used for further statistics.

Statistical Analysis

All numerical data presented in the figures were given as the mean \pm SEM, except for results from the PA test (median latency with 25th, 75th interquartile range; data were non-parametric because the procedure involved a cut-off). For electrophysiological data Student's t-test was used for statistical analysis. Data from PA test were assessed by a Kruskal-Wallis non-parametric ANOVA, with post-hoc comparison relative to solvent control by a Dunn's test ($\alpha=0.05$). Data from the AA, EPM, grip strength and activity assay were assessed by a one-way ANOVA. If the ANOVA was significant, each treatment condition was compared with control by a Dunnett's test ($\alpha=0.05$). Where appropriate, the assessment of the antagonist influence on the inverse agonist effect was conducted by a student's t-test. Statistical analyses were performed with ANY-maze Video Tracking System software (Stoelting Co., Wood Dale, IL, USA) and SigmaStat 2.0 (SPSS, Inc., Chicago, IL, USA).

Sedative Influence of α_5 Benzodiazepine Site Agonists on Stereotypical Behavior?

Genetic studies suggest that modulation at the α_1 subunit contributes to much of the adverse effects of BZs, most notably sedation, ataxia and amnesia. Hence, BZ site ligands functionally inactive at GABA(A) receptors containing the α_1 subunit are considered to be promising leads for novel, anxiolytic anxiolytics, devoid of sedative properties. In pursuing this approach, three compounds were examined electrophysiologically to determine the behavioral properties. They were shown to be functionally selective for α_2 , α_3 and α_5 -containing subtypes of GABA(A) receptors (SH-053-S-CH3 and SH-053-S-CH3-2'F), or essentially selective for α_5 subtypes (SH-053-R-CH3). Possible influences on motor function were tested in the elevated plus maze, spontaneous locomotor activity and rotarod test, which are considered primarily predictive of the anxiolytic, sedative and ataxic influence of BZs, respectively. The results confirmed the substantially diminished ataxic potential of BZ site agonists devoid of α_1 subunit-mediated effects, with preserved anti-anxiety effects at 30 mg/kg of SH-053-S-CH3 and SH-053-S-CH3-2'F. However, all three ligands, dosed at 30 mg/kg, decreased spontaneous locomotor activity, suggesting that sedation may be partly dependent on activity mediated by α_5 -containing GABA(A) receptors. As mentioned previously, a small amount of α_5 subtypes are found in the spinal cord consistent with this hypothesis. Hence, it could be of importance to avoid substantial agonist potentiation of α_5 -subunits by candidate anxiolytic anxiolytics, if clinical sedation is to be avoided.

The basic characterization of the diverse pharmacological effects of BZs: anxiolytic, sedative, hypnotic, muscle relaxant, anticonvulsive and amnesic, has been considered to represent one of the major successes of behavioural pharmacology.^{14, 48, 386, 396, 397} In recent years much effort has been expended to improve the understanding of the molecular and neuronal substrates of these effects, with the final goal to clinically separate desired from unwanted side effects.⁴⁸ Among the latter effects, psychomotor and cognitive impairment is common, and more serious neuropsychiatric reactions such as amnesic and aggressive episodes may occur.¹³⁵ BZs act as allosteric modulators of fast inhibitory neurotransmission in the mammalian brain mediated through GABA(A) receptors, which are involved in the regulation of vigilance, anxiety, sleep, muscle tension, epileptogenic activity, and memory functions.^{47, 373, 387, 398} It has been postulated that the four BZ site-building α -subunits, with their distinct patterns of anatomical distribution in the brain, differently participate in the various effects of BZs. Indeed, recent genetic and pharmacological studies pointed to the specific contribution of individual receptor subtypes to the spectrum of behavioral actions of BZ site ligands. Specifically, sedative effects of BZs were principally attributed to α_1 -containing GABA(A) receptor subtypes, anxiolytic actions to the α_2/α_3 -containing receptors, anterograde amnesic effects to the α_1/α_5 -subtypes, anticonvulsant activity partially to the α_1 -containing receptors, and muscle relaxant effects largely due to effects through α_2 -containing receptors, as previously mentioned.^{338, 399} Moreover, it appears that L-838,417, a ligand with zero efficacy at the α_1 -subtype, is unable to engender sedation in rodents^{47, 387} or monkeys,^{20, 48} and similar conclusions were drawn from behavioral experiments with other compounds functionally selective for receptors other than α_1 -

containing receptors such as XHe-II-053 and Hz-166 synthesized in Milwaukee and characterized in rhesus monkeys by Rowlett et al.⁵¹ Since the α_1 -subunit is critically involved in much of the unwanted psychomotor activity of nonselective BZs, " α_1 -neutral" agonists at BZ site are being pursued in the quest for anxiolytic anxiolytics.⁵²

To date, all apparently non-sedating BZ site ligands, which are devoid of activity at α_1 -containing GABA(A) receptors, engendered essentially antagonist^{49, 50} or only partial agonist efficacy at α_5 -containing GABA(A) receptors.³⁷³ Therefore, it cannot be ruled out that substantial efficacy at α_5 -containing GABA(A) receptors may contribute to sedative effects. This is supported by data which indicate the possibility of substantial motor influence by modulation of α_5 subunit-containing GABA(A) receptors. In the spinal cord, somatic and preganglionic motoneurons (lamina IX and lateral cell column) exhibited a moderate to strong staining for the α_5 subunit.^{14, 48} Knock-in mice with the GABA(A) receptor α_5 subunit rendered insensitive to diazepam were refractory to development of tolerance to the sedative effects of diazepam dosed subchronically.^{48, 400} These two sets of evidence indicate that the motor influence of α_5 -GABA(A) receptor modulation, if present, is not necessarily an indirect consequence of the established effects on learning and memory processes.⁴⁰¹ Hence, any activity changes seen with ligands possessing a substantial agonistic efficacy for α_5 subunit-containing GABA(A) receptors may be, at least partly, mediated by such receptors.

To test this hypothesis, we have performed the *in vitro* efficacy measurements and also compared behavioral profiles of three BZ site ligands, functionally selective for α_2 , α_3 and α_5 subtypes of GABA(A) receptors (SH-053-S-CH3 and SH-053-S-CH3-2'F), or

essentially selective for the α_5 subtypes (SH-053-R-CH3), with that of the classical nonselective agonist diazepam. Possible influences on motor function were tested in the elevated plus maze (EPM), spontaneous locomotor activity (SLA) and rotarod test, that are considered primarily predictive of the anxiolytic, sedative and ataxic influence of BZs, respectively.

Drugs

SH-053-S-CH3 and SH-053-R-CH3 (the (S) and (R) stereoisomer, respectively, of 8-ethynyl-4-methyl-6-phenyl-4H-2,5,10b-triaza-benzo[e]azulene-3-carboxylic acid ethyl ester; structures given in Figure 125), as well as SH-053-S-CH3-2'F (the (S) stereoisomer of 8-ethynyl-6- (2-fluorophenyl)-4-methyl- 4H-2,5,10b- triaza-benzo [e] azulene-3-carboxylic acid ethyl ester) were synthesized in Milwaukee. Diazepam for behavioral studies was obtained from Galenika (Belgrade, Serbia).

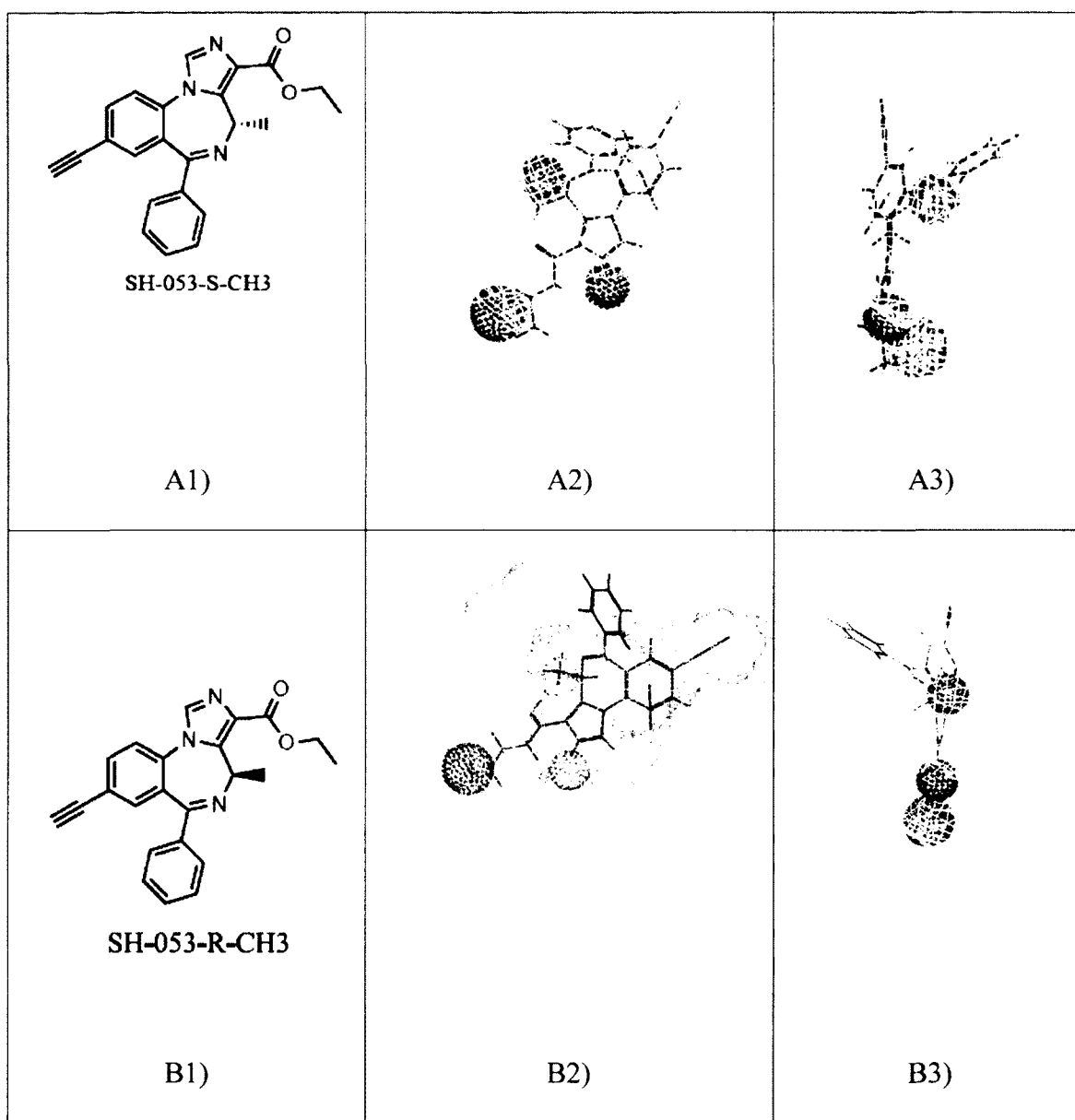


Figure 118. Structures and conformations of SH-053-S-CH3 (A1-A3) and SH-053-R-CH3 (B1-B3) in the included volume of the pharmacophore receptor model for the α_2 subtype.

The molecular modeling was carried out as described in Part I.

Rotarod Performance

Rotarod test (Ugo Basile, Comerio, Italy) measured the capacity of the animal to maintain itself on the rod revolving 10 rpm. During two consecutive days, the rats were

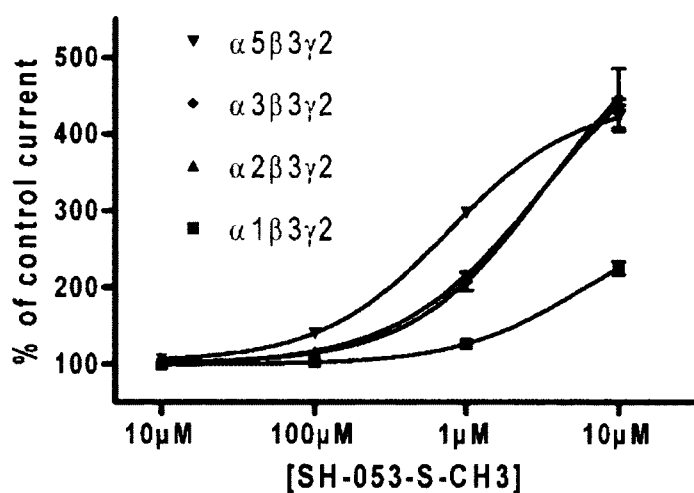
trained to walk on the revolving rod until they could complete three 180 s sessions (each day) without falling off. In the morning of the third day, the final selection was made. Only animals capable of remaining 180 s on the rod, without any fall, were chosen for further testing. Those animals without capability to meet the same criterion when tested 20 minutes after treatment were considered incapacitated.

Statistical Analysis

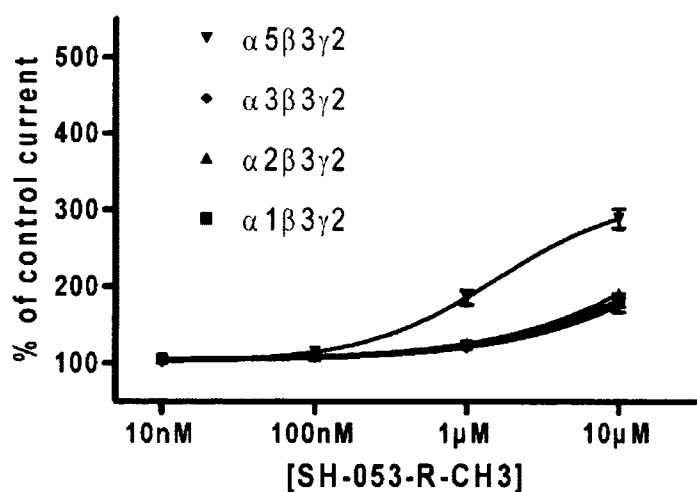
All numerical data presented in the figures were given as the mean \pm SEM. Data from the EPM and activity assay were assessed by a one-way ANOVA. If the ANOVA was significant, each treatment condition was compared with control by a Dunnett's test ($\alpha=0.05$). ED₅₀ value for rotarod incapacitation was calculated by probit analysis according to the method of Litchfield and Wilcoxon. Statistical analyses were performed with ANY-maze Video Tracking System software (Stoelting Co., Wood Dale, IL, USA).

Results

In vitro data for SH-053-S-CH₃ (Figure 119A) and SH-053-R-CH₃ (Figure 119B) demonstrated that at concentrations up to 1 μ M both ligands are high-efficacy agonists at the α 5-containing GABA(A) receptors, with very low efficacies at α 1 containing subtypes. However, while SH-053-S-CH₃ exerted substantial potentiation of an EC₃ GABA response at α 2 and α 3-containing GABA(A) receptors, the influence of SH-053-R-CH₃ at these receptors was comparable to its minor effect at the α 1 subtype (cf. molecular modeling in Figure 118). The in vitro concentration-effects curves for SH-053-S-CH₃-2F³⁹³ were similar to those for SH-053-S-CH₃, but with the higher magnitude of efficacies at the respective α 2, α 3 and α 5 GABA(A) receptor subtypes in the concentration range 0.1-10 μ M as expected from earlier work from Haefley, Fryer and Milwaukee.



A



B

Figure 119. Illustrated here are the concentration-effects curves for SH-053-S-CH3 (A) and SH-053-R-CH3 (B) on $\alpha 1\beta 3\gamma 2$, $\alpha 2\beta 3\gamma 2$, $\alpha 3\beta 3\gamma 2$, and $\alpha 5\beta 3\gamma 2$ GABA(A) receptors, using an EC3 GABA concentration. Data points represent means \pm SEM from at least 4 oocytes from ≥ 2 batches.

Elevated Plus Maze

SH-053-S-CH3

Activity-related parameters (Figure 120)

The influence of treatment on closed arm entries did not reach statistical significance ($F(4,27) = 1.19$, $p=0.337$) (Figure 120a), neither statistical analysis by ANOVA showed a significant effect of treatment on total arm entries ($F(4,27) = 1.72$, $p=0.175$) (Figure 120b) or total distance travelled ($F(4,27) = 1.80$, $p=0.157$) (Figure 120c).

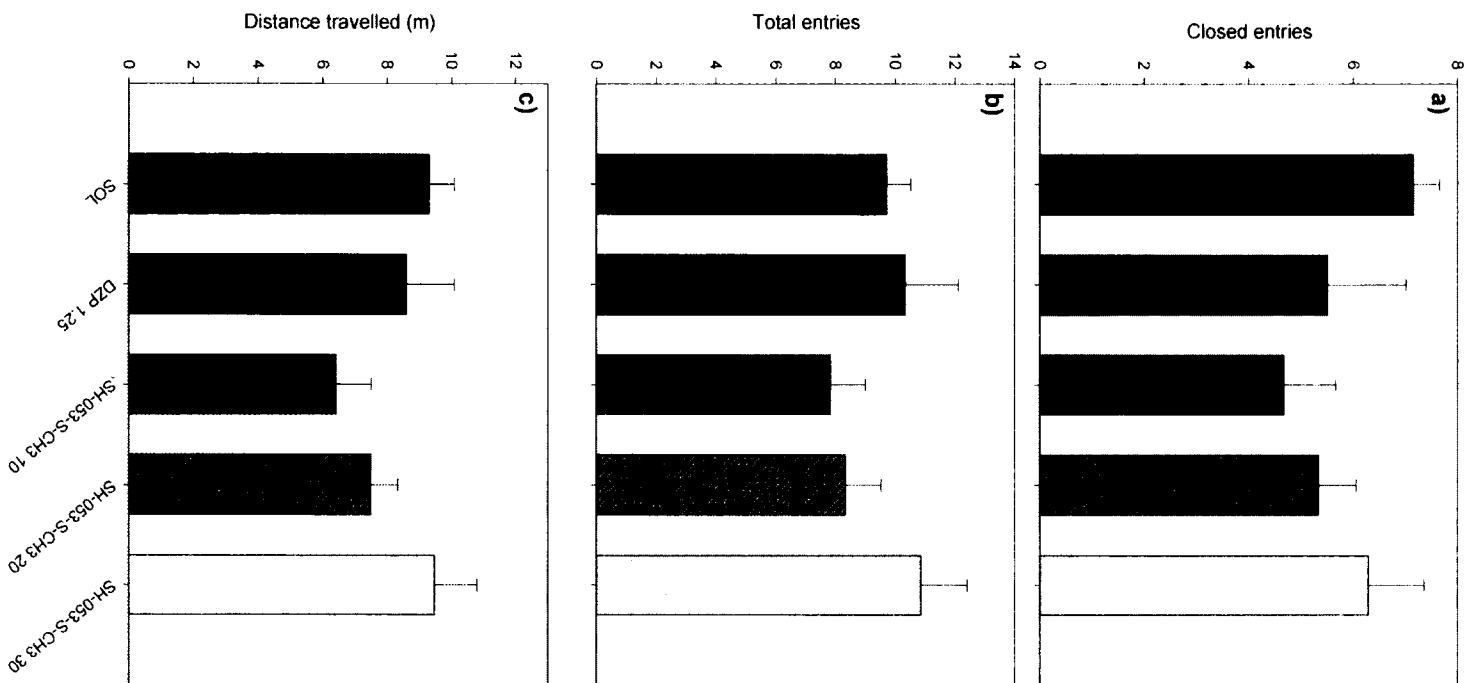


Figure 120. Diazepam (DZP) and SH-053-S-CH3 on closed arm entries and EPM.

Illustrated in Figure 120, the effects of diazepam (1.25 mg/kg) and SH-053-S-CH3 (10, 20 and 30 mg/kg) on the a) closed arm entries, b) total arm entries and c) total distance travelled in the EPM. * $P < 0.05$ compared to solvent (SOL) group. Number of animals per treatment (Figures 127- 128), for SOL through SH-053- S-CH3 30 mg/kg, respectively): 6, 6, 5, 6, 6.

Anxiety-Related Parameters (Figure 121)

There was a close to significant effect of treatment on distance travelled in the open arms ($F(4,27) = 2.37$, $p = 0.078$) (Fig. 121a). The overall influence of treatment on the percentage of open arm entries has reached statistical significance ($F(4,27) = 3.13$, $p = 0.031$) (Fig. 121b), Dunnett's test pointed to the anxiolytic influence of diazepam ($p = 0.038$) and SH-053-S-CH3 dosed at 30 mg/kg ($p = 0.049$). The influence on the percentage of time on open arms also was significant ($F(4,27) = 2.75$, $p = 0.049$) (Figure 121c), but post hoc testing did not detect significant effect of any single treatment.

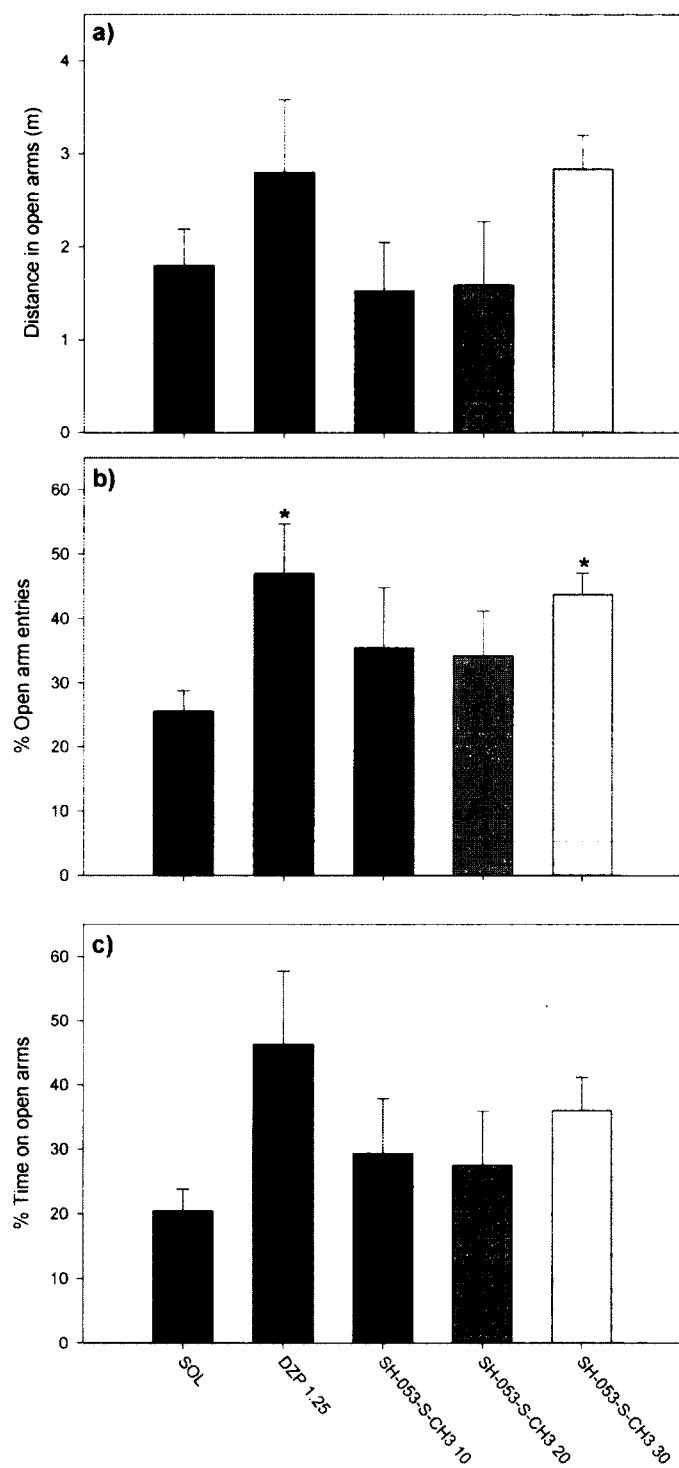


Figure 121. Illustrated here are the effects of diazepam (1.25 mg/kg) and SH-053-S-CH3 (10, 20 and 30 mg/kg) on the a) distance travelled on open arms, b) percentage of entries in open arms and c) percentage of time spent on open arms of the EPM. *P<0.05 compared to solvent (SOL) group.

SH-053-S-CH3-2'F**Activity-related parameters (Figure 122)**

Statistical evaluation by ANOVA did not show significant influences of treatment on closed arm entries (Figure 122a), total arm entries (Figure 122b) or total distance travelled (Figure 122c) [(F(4,45) = 1.29, p=0.290), (F(4,45) = 0.13, p=0.969) and (F(4,45) = 0.25, p=0.911), respectively].

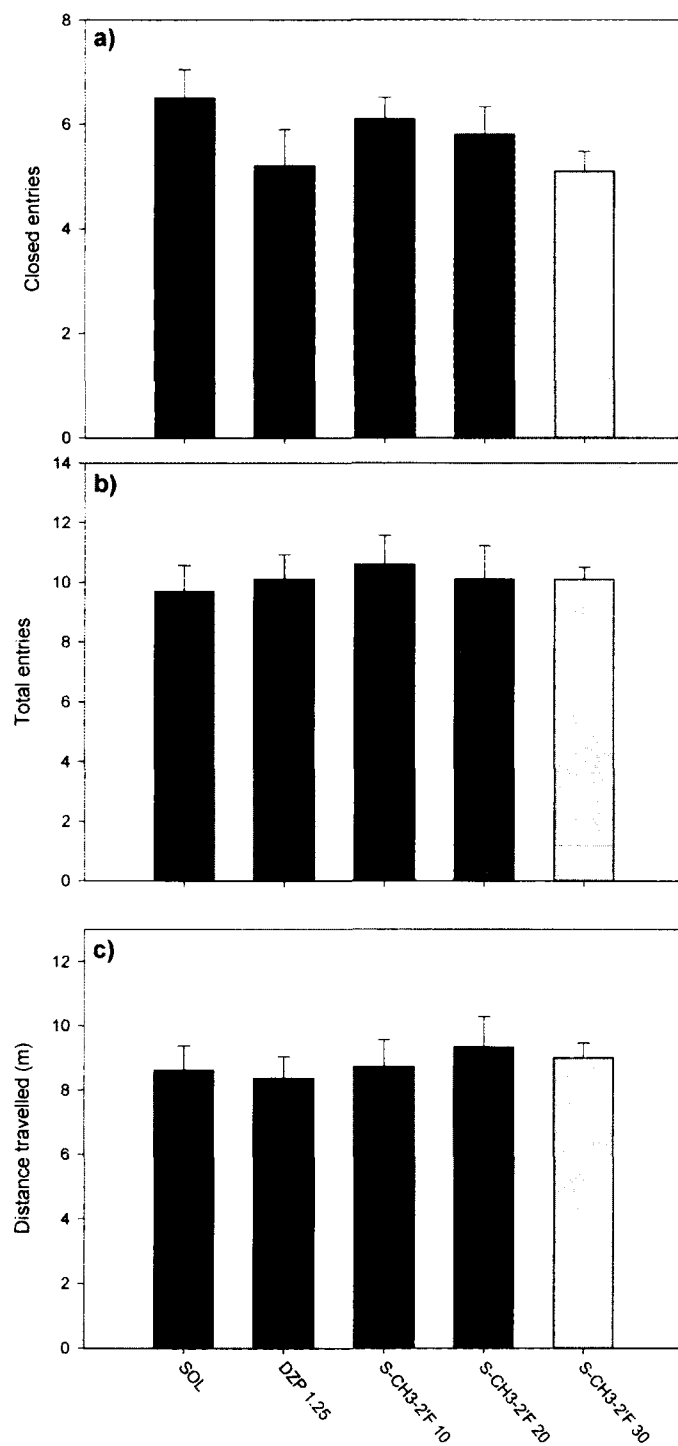


Figure 122. Illustrated here are the effects of diazepam (1.25 mg/kg) and SH-053-S-CH3-2'F (10, 20 and 30 mg/kg, designated as S-CH3-2'F) on the a) closed arm entries, b) total arm entries and c) total

distance travelled in the EPM. Number of animals per treatment (Figure 120-121, for SOL through SH-053-S-CH3-2'F 30 mg/kg) was 10

Anxiety-related parameters (Figure 123)

While the influence of treatment on distance travelled in open arms was not significant ($F(4,45) = 1.92$, $p=0.124$) (Figure 123a), the overall effect on the percentage of open arm entries (Figure 123b) and the percentage of time on open arms (Figure 123c) has reached statistical significance [$F(4,45) = 2.94$, $p=0.031$] and [$F(4,45) = 2.92$, $p=0.031$], respectively]. For both of these parameters, post hoc testing revealed the equivalent influence of diazepam and SH-053-S-CH3 dosed at 30 mg/kg (p values 0.018 for the percentage of open arm entries and 0.017 for the percentage of time on open arms).

SH-053-R-CH3

When tested at doses up to 30 mg/kg, SH-053-R-CH3 failed to induce any significant change of the measured EPM parameters (data not shown). It was not anxiolytic.

Motor Activity Assay

An ANOVA in whole chamber-activity showed a significant effect of treatment on total distance travelled during 45 min of monitoring ($F(4,31) = 3.86$, $p=0.000$) (Figure 131, whole bars). According to Dunnett's test, the activity-decreasing effect of all four tested compounds (diazepam 1.25 mg/kg, SH-053-S-CH3, SH-053-S-CH3-2'F and SH-053-R-CH3 at 30 mg/kg each) appeared to be significant related to solvent. When the ANOVA of travelled distance was developed into 5-min intervals (Figure 132), it turned out that a significant depression of locomotion was effective in the time period 5-20 min (SH-053-S-CH3 (30 mg/kg), SH-053-S-CH3-2'F (30 mg/kg) and SH-053-R-CH3 (30 mg/kg)), whereas diazepam 1.25 mg/kg decreased locomotion in the period 5-15 minutes.

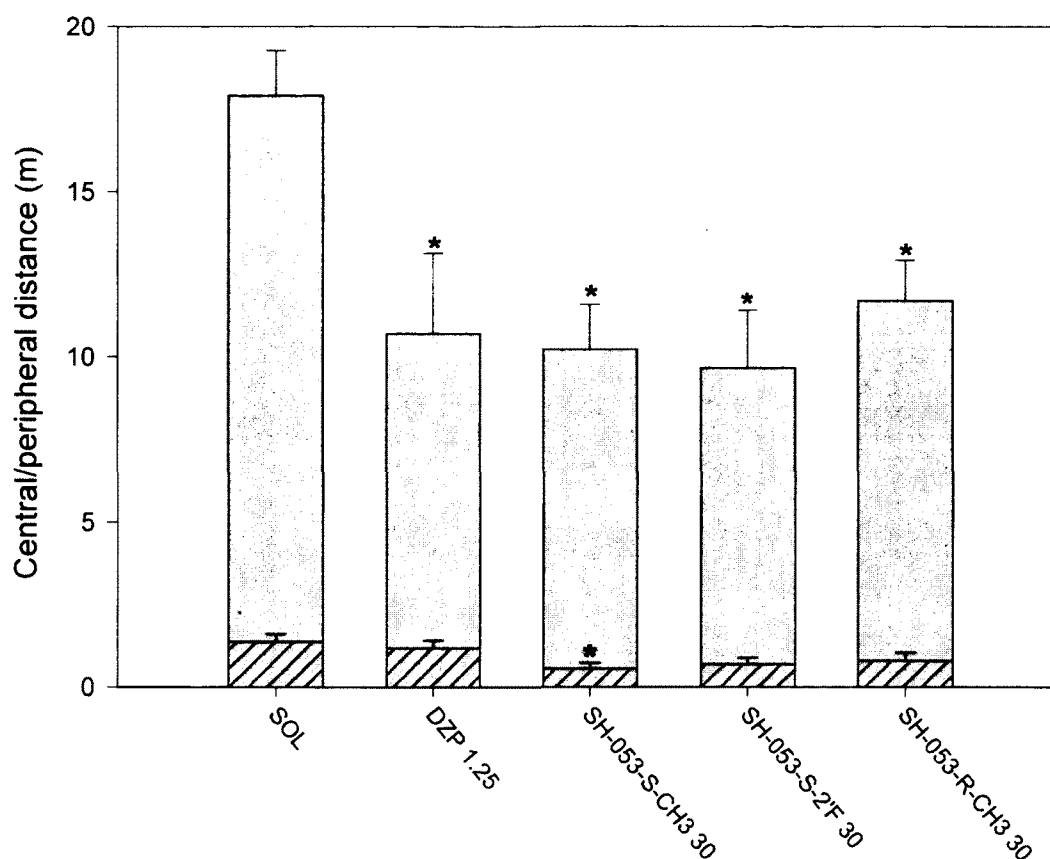


Figure 124. Whole chamber activity

The effects of diazepam (1.25 mg/kg), SH-053-S-CH3 (30 mg/kg), SH-053-S-CH3-2F (30 mg/kg, designated as SH-053-S-2'F) and SH-053-R-CH3 (30 mg/kg) on distance travelled in the central (hatched bars) and peripheral (open bars) zone of the activity chamber during 45 minutes of recording (total activity corresponds to the height of the whole bar). * $P < 0.05$ compared to solvent (SOL) group. Number of animals per treatment group (Figures 124-125) for SOL through SH-053-S-CH3-2'F 30 mg/kg was 8, and 4 for SH-053-R-CH3. Since the P-value was less than 0.05, the null hypothesis can be rejected

and the results are statistically significant.

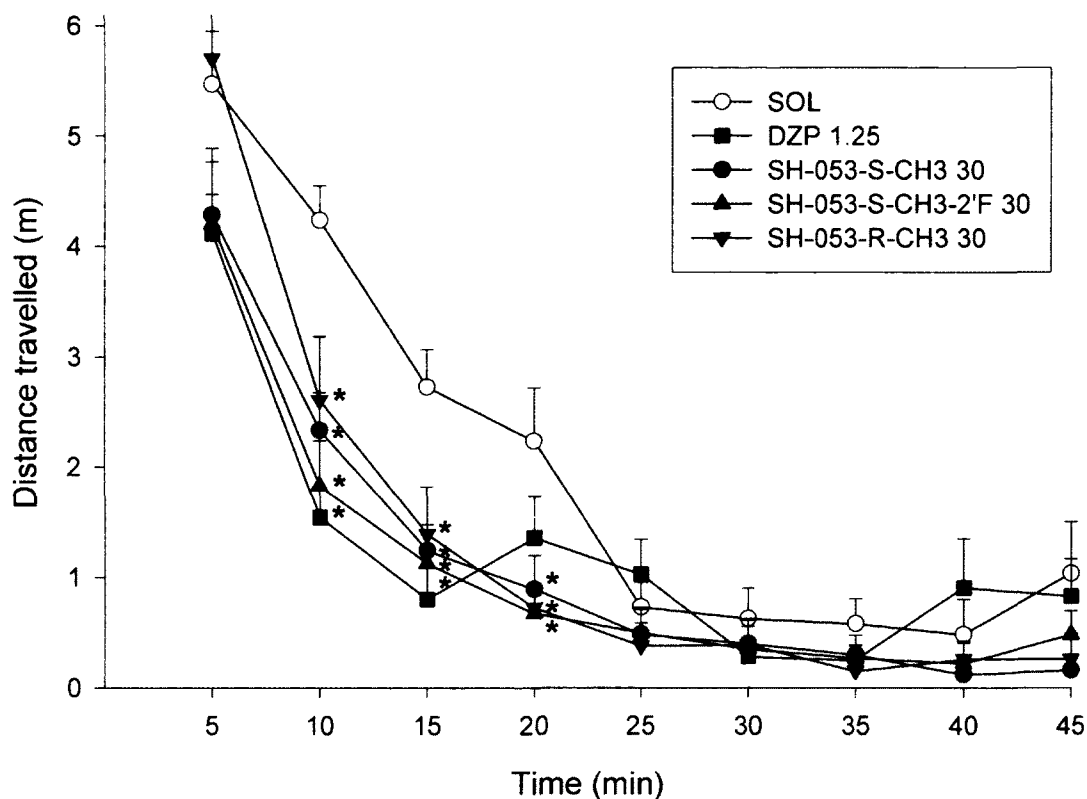


Figure 125. Distance travelled in activity

In Figure 125, the effects of diazepam (1.25 mg/kg), SH-053-S-CH3 (30 mg/kg), SH-053-S-CH3-2'F (30 mg/kg) and SH-053-R-CH3 (30 mg/kg) on the distance travelled in 5-min intervals in the activity assay. *P<0.05 compared to solvent (SOL) group;

Central/Peripheral Distance

An ANOVA showed a significant effect of treatment on distance travelled in the arbitrarily set central parts of the chamber during 45 min of monitoring ($F(4,31) = 2.73$, $p=0.047$) (Figure 124, hatched bars). The respective p values for diazepam 1.25 mg/kg,

SH-053-S-CH3 30 mg/kg, SH-053-S-CH3-2'F 30 mg/kg and SH-053-R-CH3 30 mg/kg were 0.491, 0.029, 0.067 and 0.207, related to solvent. According to ANOVA, the influence of treatment on activity in peripheral parts of the chamber (Figure 124, open bars) was more distinct: $F(4,31) = 3.59$, $p=0.016$; all the four treatments significantly decreased activity when related to control by Dunnett's test.

Rotarod Test

When one monitors the influence on rotarod performance as a quantal phenomenon (i.e. all or none effect), the minimal incapacitating doses of SH-053-S-CH3 and SH-053-S-CH3-2'F were 200 mg/kg for both substances. The median incapacitating doses of diazepam, SH-053-S-CH3 and SH-053-S-CH3-2'F were 2.99 mg/kg, 213.67 mg/kg and 218.80 mg/kg, respectively. Due to the shortage of substance, the median incapacitating dose of SH-053-R-CH3 was not found; at doses up to 100 mg/kg it did not induce any manifest incapacitation in this test.

Discussion

The present experiments demonstrated the anxiolytic potential of two newly-synthesized compounds functionally selective for $\alpha 2$, $\alpha 3$ and $\alpha 5$ -containing GABA(A) receptors, SH-053-S-CH3 and SH-053-S-CH3-2'F, which are mainly devoid of ataxic, but not of sedative actions characteristic of nonselective BZs. Furthermore, a stereoisomer of SH-053-S-CH3 functionally selective for GABA(A) receptors containing the $\alpha 5$ -subunit, SH-053-R-CH3, exerted in the locomotor activity paradigm a significant hypolocomotor effect comparable to diazepam, without observable anti-anxiety or ataxic activity in the EPM and rotarod test, respectively.

These findings were somewhat unexpected, since both, motor incoordination and sedation have been ascribed to the $\alpha 1$ -subunit - mediated action of diazepam.⁴⁰² Hence, either these three compounds were not silent at the $\alpha 1$ -subtype when dosed at 30 mg/kg, or some non- $\alpha 1$ subunits contribute to the hypolocomotor action of BZ site agonists. Although the absence of occupancy data for distinct receptor subtypes precludes drawing firm conclusions, high minimal incapacitating doses of the present functionally selective ligands in the rotarod test could be seen as indirect evidence for lack of involvement of GABA(A) receptors containing the $\alpha 1$ -subunit in behavioral actions of 30 mg/kg doses. Namely, diazepam-induced loss of motor coordination in the rotarod test was linked to the $\alpha 1$ -subunit,⁴⁰³ and the sevenfold differences in effective doses of SH-053-S-CH3 and SH-053-S-CH3-2'F in rotarod vs. SLA test could hardly exist if substantial modulation at $\alpha 1$ -subunit containing GABA(A) receptors were attained already at 30 mg/kg. However, there may exist marked differences in fractional occupancy of GABA(A) receptors containing the $\alpha 1$ -subunit needed for producing behavioral effects of a BZ site agonist in these two tests, meaning that low to moderate modulation at such receptors is sufficient for eliciting sedative, but not rotarod incapacitating action.⁴⁰⁴ Nevertheless, the latter explanation is not highly probable for the ligands tested had very low efficacies at $\alpha 1$ containing subtypes. Namely, even the preferential $\alpha 1$ subunit-selective agonist, zolpidem, does not possess more than 4.3 and 2.5 times greater potency to decrease locomotor activity compared to rotarod impairment in rats and mice, respectively,³⁹⁹ whereas non-subtype-selective agonists, such as diazepam, may be even more potent in exerting rotarod impairment than locomotor hypoactivity.⁴⁰⁵

In its broadest sense, sedation involves decreased psychomotor and cognitive performance, and in most instances it is considered an adverse effect of psychotropic drugs, which should be avoided. In animals, the psychomotor component is most frequently studied,⁴⁰⁶ and measurement of motor activity in rodents represents a standard behavioral assay for testing the sedative potential of drugs.^{403, 404} In fact, sensitivity of preclinical tests for discerning the sedative potential of a drug is of paramount importance; several BZ site partial agonists developed as putative low-sedating anxiolytics have nevertheless appeared to be incapacitating when subsequently tested in humans.⁴⁰⁷ In support of the sensitivity of the standard SLA test used in the present study, Dailly^{20, 387, 408, 409} observed a sedative effect of diazepam (1 mg/kg i.p.) in the actimeter, but not in the light-dark test of anxiety, which also measured locomotor activity of mice. In accordance, SH-053-S-CH₃, SH-053-2'F-S-CH₃ and SH-053-R-CH₃, all dosed at 30 mg/kg, exerted a statistically significant depression of locomotion in the SLA test in our study, while the influence on the standard activity parameters in the EPM (closed arm entries and total distance travelled), if any, was far from significant. It should be emphasized that the hypolocomotor influence in the SLA test is also evident when separately analyzing activity in the peripheral zone of the chamber. Hence, the observed motor depressant effects of the ligands tested were not dependent on central zone activity, which is confounded by influences on emotional reactivity, i.e. anxiety, and could be seen as a pure measure of sedation.⁴⁰⁹ These results further support the routine use of the SLA test³⁸⁷ in efforts to predict clinical sedation.

On the other hand, it is noticeable that standard studies of motor activity, which form the very basis of knowledge of drug effects on behavior,⁴¹⁰ were not employed for characterization of recently reported putative anxiolytic agents.⁴¹⁰ Jennings reported

on an $\alpha 2/\alpha 3$ BZ site selective ligand from the class of imidazo[1,2-b][1,2,4]triazines with anxiolytic activity in the rat EPM test at the dose of 1 mg/kg, which showed no motor incapacitation in the mouse rotarod test at doses up to 30 mg/kg. A close congener of that compound was anxiolytic in the rat EPM test at 3 mg/kg, whereas it showed no significant activity in a surrogate assay of sedation (chain-pulling test in rats) and in the mouse rotarod test when tested in doses up to 10 mg/kg; reportedly, this compound was chosen as a clinical candidate.^{49, 50} Similarly, a 1,2,4-triazolo[4,3-b]pyridazine, TPA023, exerted anxiolytic-like activity in the rat EPM and fear potentiated startle tests at the dose of 1 mg/kg as well as in the assay of conditioned suppression of drinking at 3 mg/kg, whereas, at doses up to 30 mg/kg, it did not significantly affect behavior of rats in the chain pulling test nor rotarod performance of mice.⁵¹ However, the same experimental group, when testing pagoclone, detected sedative action of this BZ site agonist dosed at 1 mg/kg in the chain-pulling test, while already at 0.3 mg/kg in the SLA test.⁵² The very high dose (10 mg/kg) of diazepam used as the active control in the chain-pulling test⁵³ additionally supports the view of superior sensitivity of the standard SLA test.

From these reasons, it was difficult to compare behavioral profiles of the compounds described in the present dissertation with findings from the above cited studies. Evidently, all three newly-synthesized BZ site ligands could have acted through the $\alpha 5$ subtype-containing GABA(A) receptors, one of them (SH-053-R-CH3) as an essentially subtype-selective ligand. There exist data that support the possibility of substantial motor manifestations of $\alpha 5$ -containing GABA(A) receptor modulation, besides the indirect consequences brought on by the effects on learning and memory processes, where pertinent.³⁹⁶ Somatic and preganglionic motoneurons in the spinal cord exhibit a moderate to strong staining for the $\alpha 5$ subunit,²¹ whereas the knock-in mice

harboring the α_5 subunit insensitive to diazepam are refractory to development of tolerance to the sedative effect of diazepam dosed subchronically, presumably due to a down regulation of α_5 subunits in the dentate gyrus.³⁹⁶ Hence, we hypothesize that any locomotor activity changes induced by ligands possessing a substantial α_5 -efficacy may be, at least partly, contributed by modulation at GABA(A) receptors containing this subunit. Nevertheless, as a caveat to all studies examining sedation, it should be remembered that a decrease in automatically measured locomotor activity can be due to a variety of causes other than sedation, including the occurrence of stereotyped behavior, motor impairments or pain.³⁷³ In addition, particular caution is needed when transposing in vitro data to the in vivo conditions. Atack reported³⁷³ on a substantial decrease of the α_5 subtype-binding selectivity of the BZ site inverse agonist RY-080³⁹⁷ when binding was tested in vivo; since RY-080 exerted appreciable inverse agonist efficacy at the α_1 -containing GABA(A) receptors,³⁹⁹ interpretation of behavioral actions of such functionally-nonselective ligands is especially hindered. To dissect these overlaps in activity and uncertainties, much is expected from screening of newer BZ site ligands in the future, which will be still more functionally selective than those presented in this work.

The present results confirm the highly diminished ataxic potential of BZ site agonists devoid of α_1 subunit-mediated effects. Anti-anxiety activity of such ligands remains preserved, whereas the confounding sedation stays observable, and may be partly dependent on the α_5 -containing GABA(A) receptors. Hence, it could be of importance to avoid substantial potentiation through the α_5 -subunits by the candidate anxiolytic agents, if the clinical sedation is to be prevented. However, it is important to note that Fisher, Rowlett et al.⁴¹¹ have recently shown that SH-053-2'F-S-CH₃ is a

nonsedating anxiolytic in rhesus monkeys even dosed to 10 mg/kg while SH-053-2'F-R-CH₃ exerted anxiolytic activity only at much higher doses.⁴¹² In fact Rowlett et al. have shown that in the light-dark box paradigm that SH-053-S-CH₃ is a weak but nonsedating anxiolytic while the R-enantiomer (SH-053-R-CH₃) is devoid of activity at the doses tested (Rowlett et al, unpublished results).

Behavioral Effects Due to Differences in Activity at α_1 Plus α_5 Versus α_2 Plus α_3 Subunits

The affinity and efficacy of four recently-synthesized BZ site ligands: SH-053-2'N, SH-053-S-CH₃-2'F, SH-053-R-CH₃-2'F and JY-XHe-053 were assessed. They were also studied in behavioral tests of spontaneous locomotor activity, elevated plus maze, and water maze in rats, which are considered predictive of, respectively, the sedative, anxiolytic, and amnesic influence of BZs. The novel ligands had moderately low to low affinity and mild to partial agonistic efficacy at GABA(A) receptors containing the α_1 subunit, with variable, but more pronounced efficacy at other BZ-sensitive binding sites. While presumably α_1 receptor-mediated sedative effects of GABA(A) modulation were not fully eliminated with any of the ligands tested, only SH-053-2'N and SH-053-S-CH₃-2'F, both dosed at 30 mg/kg, exerted anxiolytic effects. The lack of clear anxiolytic-like activity of JY-XHe-053, despite its efficacy at α_2 - and α_3 -GABA(A) receptors, may have been partly connected with its preferential affinity at α_5 -GABA(A) receptors coupled with weak agonist activity at α_1 -containing subtypes. Any sedative activity in JY-XHe-053 would have covered up the anxiolytic activity. The

memory impairment in the water-maze experiments, generally reported with BZ site agonists, was completely circumvented with all four ligands. The results suggest that a substantial amount of activity at α_1 GABA(A) receptors is required for effecting spatial learning and memory impairments, while much weaker activity at α_1 - and α_5 -GABA(A) receptors is sufficient for eliciting sedation.

As stated previously, the sedative and ataxic effects of BZs have been attributed to α_1 -containing GABA(A) receptor subtypes, anxiolytic actions to the α_2/α_3 -containing receptors, anterograde amnesic effects to the α_1/α_5 -subtypes, anticonvulsant activity, in part, to all the $\alpha_1/\alpha_2/\alpha_3$ containing receptors, muscle relaxant effects largely to α_2 -subtypes, and tolerance to sedative effects to the coupling of α_1 receptors to α_5 -containing receptors.⁴¹³ If the concept holds true, an ideal anxiolytic, selectively acting through α_2/α_3 -containing receptors, would be devoid of sedative, ataxic, amnesic and tolerance adverse effects. However, despite the notable successes of the studies of several research groups published to date,⁴¹⁴ including the encouraging safety records for an α_2/α_3 -subtype selective partial modulator in healthy volunteers,⁴¹⁵ it appears the ultimate goal of translating breakthroughs in preclinical research into new clinical therapies is still far from realization. An exception to this may be HZ-166. The awareness that a similar conclusion may apply to the whole field of pharmacological modulation of central nervous system disorders^{46, 221, 416} calls for rethinking the clear-cut hypotheses on receptor subtypes and their roles. In this vein, it is interesting to note that some newer BZ binding-site agonists, such as ocinaplon^{417, 418} and DOV 51892,³⁹⁷ were reportedly devoid of overt sedative effects, despite the fact that they did not display compelling subtype selectivity for any of the GABA(A) receptor subtypes.⁴¹⁹

In pursuit of the approach of pharmacological testing of four subtypes of BZ-sensitive GABA(A) receptors to further elucidate their native role, a series of BZ site ligands, presumably inactive/low-activity at α_1 -containing GABA(A) receptors was recently synthesized. Specific portions of the characterization of six of them, with code names SH-053-S-CH₃, SH-053-R-CH₃, SH-053-2'N, JY-XHe-053, SH-053-S-CH₃-2'F and SH-053-R-CH₃-2'F, have been already published.⁴²⁰ The affinity and efficacy data of four of these ligands: SH-053-2'N, SH-053-S-CH₃-2'F, SH-053-R-CH₃-2'F and JY-XHe-053, as well as their behavioral actions in the tests of spontaneous locomotor activity, elevated plus maze and water maze, which are considered primarily predictive of the sedative, anxiolytic, and amnesic influence of BZs, respectively, will be described. Diazepam, a standard non-selective positive allosteric modulator, and zolpidem, a moderately α_1 -subtype selective positive modulator,³⁹⁰ were used as reference ligands, where applicable. The aim of the study was to elucidate whether the expected subtle affinity and efficacy differences at four BZ-sensitive GABA(A) receptor subtypes among the tested BZ-site modulators reflect themselves in dissimilarities in behavioral responses of Wistar rats, with possible implications for further research. Concurrently, the data were to be compared with findings from the knock-in approach^{269, 391} as well as with results from classical studies in the same behavioral tests, investigating antagonism of the effects of non-selective positive modulators (diazepam or midazolam) with the preferential α_1 -subunit affinity-selective antagonist, β -CCt.^{46, 335, 419}

Drugs

The SH-053-2'N (8-ethynyl-6-(2'-pyridine)-4H-2,5,10b-triaza-benzo[e]azulene-3-carboxylic acid ethyl ester), SH-053-S-CH3-2'F and SH-053-R-CH3-2'F (the (S) and (R) stereoisomer, respectively, of 8-ethynyl-6-(2-fluorophenyl)-4-methyl-4H-2,5,10b-triaza-benzo[e]azulene-3-carboxylic acid ethyl ester), as well as JY-XHe-053 (8-ethynyl-6-(2-fluorophenyl)-4H-2,5,10b-triaza-benzo[e]azulene-3-carboxylic acid ethyl ester) were synthesized. Zolpidem for behavioral studies was purchased from Toronto Research Chemicals (North York, Canada), and diazepam was obtained from Galenika (Belgrade, Serbia).

Competition Binding Assays

Competition binding assays were performed in a total volume of 0.5 mL at 4 °C for 1 hour using [³H] flunitrazepam as the radiolabelled ligand. A total of 6 µg of cloned human GABA(A) receptor DNA containing the desired α subtype along with β 2 and γ 2 subunits were used for transfecting the HEK 293T cell line using Fugene 6 (Roche Diagnostic) transfecting reagent. Cells were harvested 48 hrs after transfection, washed with Tris-HCl buffer (pH 7.0) and Tris Acetate buffer (pH 7.4) and the pellets which resulted were stored at -80°C until assayed. On the day of the assay, pellets containing 20-50 µg of GABA(A) receptor protein were resuspended in (50 mM Tris-acetate buffer, pH 7.4 at 4°C) and incubated with the radiolabel as previously described.^{46, 221, 335} Nonspecific binding was defined as radioactivity bound in the presence of 100 µM diazepam and represented less than 20% of total binding. Membranes were harvested

with a Brandel cell harvester followed by three ice-cold washes onto polyethyleneimine-pretreated (0.3%) Whatman GF/C filters. Filters were dried overnight and then soaked in Ecoscint A liquid scintillation cocktail (National Diagnostics; Atlanta, GA). Bound radioactivity was quantified by liquid scintillation counting. Membrane protein concentrations were determined using an assay kit from Bio-Rad (Hercules, CA) with bovine serum albumin as the standard.

Electrophysiological Experiments (with Sieghart et al.)

The cloning of rat GABA(A) receptor subunits $\alpha 1$, $\beta 3$ and $\gamma 2$ into pCDM8 expression vectors (Invitrogen, CA) has been described elsewhere.⁴⁶ The rat cDNAs for subunits $\alpha 2$, $\alpha 3$ and $\alpha 5$ were gifts from P. Malherbe and were subcloned into pCI-vector. After linearizing the cDNA vectors with appropriate restriction endonucleases, capped transcripts were produced using the mMachine T7 transcription kit (Ambion, TX). The capped transcripts were polyadenylated using yeast poly(A) polymerase (USB, OH) and were diluted and stored in diethylpyrocarbonate-treated water at -70°C .

The methods used for isolating, culturing, injecting and defolliculating of the oocytes were identical as described previously.⁴⁶ Briefly, mature female *Xenopus laevis* (Nasco, WI) were anaesthetized in a bath of ice-cold 0.17 % Tricain (Ethyl-m-aminobenzoate, Sigma, MO) before decapitation and removal of the frogs ovary. Stage 5 to 6 oocytes with the follicle cell layer around them were singled out of the ovary using a platinum wire loop. Oocytes were stored and incubated at 18°C in modified Barths' Medium (MB, containing 88 mM NaCl, 10 mM HEPES-NaOH (pH 7.4), 2.4 mM NaHCO_3 , 1 mM KCl,

0.82 mM MgSO_4 , 0.41 mM CaCl_2 , 0.34 mM $\text{Ca}(\text{NO}_3)_2$) with 100 U/mL penicillin and 100 $\mu\text{g/mL}$ streptomycin. Oocytes with follicle cell layers still around them were injected with a total of 2.25 ng of cRNA. The cRNA ratio used was 1:1:5 for the α , $\beta 3$ and $\gamma 2$ subunits, respectively. After injection of cRNA, oocytes were incubated for at least 36 hours before the enveloping follicle cell layers were removed. To this end, oocytes were incubated for 20 minutes at 37°C in MB that contained 1 mg/mL collagenase type IA and 0.1 mg/mL trypsin inhibitor I-S (both Sigma). This was followed by osmotic shrinkage of the oocytes in doubly concentrated MB medium supplied with 4 mM Na-EGTA and manually removing of the follicle cell layer. After peeling off the follicle cell layer, the cells were allowed to recover overnight before being used in electrophysiological experiments.

For electrophysiological recordings, oocytes were placed on a nylon-grid in a bath of Xenopus Ringer solution (XR, containing 90 mM NaCl, 5 mM HEPES-NaOH (pH 7.4), 1 mM MgCl_2 , 1 mM KCl and 1 mM CaCl_2). The oocytes were constantly washed by a flow of 6 mL/min XR which could be switched to XR containing GABA and/or drugs. Drugs were diluted into XR from DMSO solutions which resulted in a final concentration of 0.1 % DMSO perfusing the oocytes. Drugs were preapplied for 30 seconds before the addition of GABA, which was coapplied with the drugs until a peak response was observed. Between two applications, oocytes were washed in XR for up to 15 min to ensure full recovery from desensitization. For current measurements the oocytes were impaled with two microelectrodes (2–3 $\text{m}\Omega$) which were filled with 2 mM KCl. All recordings were performed at room temperature at a holding potential of –60 mV using a Warner OC-725C two-electrode voltage clamp (Warner Instruments, Hamden, CT). Data were digitised, recorded and measured using a Digidata 1322A data acquisition system

(Axon Instruments, Union City, CA). Results of concentration response experiments were graphed using GraphPad Prism 4.00 (GraphPad Software, San Diego, CA). Data were graphed as mean \pm SEM of at least four oocytes from at least two batches.

Behavioral Experiments (with Savic et al.)

Experiments were carried out on male Wistar rats (Military Farm, Belgrade, Serbia), weighing 220-250 g. All procedures in the study conformed to EEC Directive 86/609 and were approved by the Ethical Committee on Animal Experimentation of the Faculty of Pharmacy in Belgrade. The rats were housed in transparent plastic cages, six animals per cage, and had free access to food pellets and tap water. The temperature of the animal room was $22\pm 1^\circ\text{C}$, the relative humidity 40-70%, the illumination 120 lux, and the 12/12 h light/dark period (light on at 6:00 h). All handling and testing took place during the light phase of the diurnal cycle. Separate groups of animals were used for three behavioral paradigms. Care was taken to counterbalance the test order across treatment conditions. The differences in treatments in individual paradigms (*vide infra*) are related to the fact that some pertinent parts of experiments have been done previously.⁴²¹ The behavior was recorded by a ceiling-mounted camera and analyzed by the ANY-maze Video Tracking System software (Stoelting Co., Wood Dale, IL, USA). The drugs were dissolved/suspended with the aid of sonication in a solvent containing 85% distilled water, 14% propylene glycol, and 1% Tween 80, and were administered intraperitoneally in a volume of 2 ml/kg, 20 min before behavioral testing. The selection of dose ranges and the injection-test interval was based on previous experiments,⁴²² as well as on

observations in preliminary experiments, avoiding, where applicable, testing of lower doses in case of lack of the expected behavioral effect at a higher dose.

Measurement of Locomotor Activity

Twenty minutes after receiving the appropriate treatment, single rats were placed in a clear Plexiglas chamber (40 x 25 x 35 cm). Activity under dim red light (20 lux) was recorded for a total of 30 or 45 minutes, without any habituation period, using ANY-maze software. Besides the total distance traveled, behavior was analyzed by dividing the locomotor activity data into 5-minute bins. For purposes of improving data analysis, the central 20% of the chamber (200 cm²) was virtually set as a central zone. An entry into a zone was counted when 70% of the animal's body had crossed the zone border. An exit from the zone was counted when more than 50% of the animal's body had left the zone. Three experiments were performed. In the first study, locomotor influences of SH-053-2'N, dosed at 30 mg/kg, were assessed in comparison with diazepam at 1.25 and 2.5 mg/kg. In the second experiment, the dose response curve for JY-XHe-053 (0; 2.5; 5; 10; 20 and 40 mg/kg), and in the third, for SH-053-R-CH3-2'F (0; 10; 20 and 30 mg/kg, in comparison with 2 mg/kg diazepam), were determined. The characterisation of SH-053-S-CH3-2'F in this test has been published previously.⁴²²

Behavior in the Elevated Plus Maze

The apparatus was constructed of sheet metal, with a black rubber floor. It consisted of a maze elevated to a height of 50 cm with two open (50 x 10 cm) and two enclosed arms (50 x 10 x 40 cm), connected by a junction area (central platform) measured 10 x 10 cm. A ledge of sheet metal (0.3 cm high) surrounding the open arms

was added. The illumination in the experimental room consisted of one red neon tube fixed on the ceiling, giving light intensity of 10 lux on the surface of the closed arms. At the beginning of the experiment, single rats were placed in the center of the maze, facing one of the enclosed arms, and their behavior was recorded for 5 minutes. An entry into an open or closed arm was scored when 90% of the animal crossed the virtual line separating the central square of the maze from the arm, whereas an exit occurred when more than 90% of the animal left the respective arm. After each trial, the maze was cleaned with dry and wet towels.

Three experiments were performed, in which the dose response curves for SH-053-2'N (0; 10; 20 and 30 mg/kg, in comparison with 1.25 mg/kg diazepam), JY-XHe-053 (0; 2.5; 5; 10; 20 and 40 mg/kg), and SH-053-R-CH3-2'F (0; 10; 20 and 30 mg/kg) were determined. The characterisation of SH-053-S-CH3-2'F in this test has been published previously.²²¹

Behavior in the Morris Water Maze

The water maze consisted of a black cylindrical pool (diameter: 200 cm, height: 60 cm), with a uniform inner surface. The pool was filled to a height of 30 cm with 23°C ($\pm 1^\circ\text{C}$) water. The escape platform made of black plastic (15x10 cm) was submerged 2 cm below the water surface. The platform was made invisible to rats by having it painted the same color as the pool wall.^{423, 424} There were many distal cues in the testing room (doors, pipes on the walls and the ceiling, cupboards). An indirect illumination in the experimental room was provided by white neon tubes fixed on the walls near the pool. The rats received the appropriate treatment 20 minutes before a swimming block, each day for 5 consecutive days of spatial acquisition. Each block consisted of 4 trials, lasting a maximum time of 120 seconds, the intertrial interval being 60 seconds. For each trial

the rat was placed in the water facing the pool at one of four pseudorandomly determined starting positions. As during spatial learning the platform was hidden in the middle of the NE quadrant, the four distal start locations were chosen: S, W, NW and SE. Once the rat found and mounted the escape, it was permitted to remain on the platform for 15 seconds. The rat was guided to the platform by the experimenter if it did not locate the escape within 120 seconds. To assess the long-term spatial memory at the end of learning, a probe trial for 60 seconds, with the platform omitted, was given 24 hours after the last acquisition day. The probe trial, starting from the novel, most distant SW location, was performed without any pre-treatment. The tracking software virtually divided the pool into four quadrants, three concentric annuli and a target region consisting of the intersection of the platform quadrant and the platform (middle) annulus, as graphically represented in Savić et al., 2009. The central annulus was set up to 10% of the whole area; the platform annulus equaled 40%, whereas the area of the peripheral annulus was 50% of the whole.

Dependent variables chosen for tracking during the acquisition trials were: latency to platform (time from start to goal), total distance swam (path length), average swim speed and path efficiency (the ratio of the shortest possible path length to actual path length). All these indices are, to a lesser or greater degree, related to goal-directed behavior, i.e. spatial learning.²²¹ As thigmotaxis (the tendency to swim or float near the pool wall) represents a factor which accounts for much of the variance in the water maze performance, and normally weakens during consecutive trials,⁴⁶ we quantified the persistence of the thigmotaxis in the target (NE) quadrant. The loss of thigmotaxis is related to the procedural component of acquisition, and the percent of the distance swam in the target region (away from the wall) of the target quadrant may be seen as a measure

of procedural learning. The indices of memory, assessed during the probe trial, included the distance and time in the platform (target) quadrant, platform ring and target region, as well as the number of entries and distance swam in the area where the platform used to be during training. In addition, the distance swam during 60 seconds in the probe trial was taken as a measure of overall activity, while peripheral ring parameters (distance and time) were connected to the thigmotaxic behavior.

Three experiments in the water maze were performed. In the first study, the dose response curve for the $\alpha 1$ selective agonist zolpidem (0; 0.5; 1 and 2 mg/kg) was found. In the second experiment, water-maze activity of SH-053-2'N, SH-053-S-CH3-2'F and SH-053-R-CH3-2'F, all dosed at 30 mg/kg, was assessed. Finally, the influence of JY-XHe-053 (0; 5; 20 and 40 mg/kg) on the water-maze behavior was determined. From earlier oocyte data from Sieghart et al., it was clear JY-XHe-053 exhibited slightly more agonist efficacy at $\alpha 1$ than did SH-053-2'N and SH-053-S-CH3-2'F.

Statistical Analysis

All numerical data presented in the Figures were given as the mean \pm SEM. For electrophysiological data Student's t-test was used. Data sets were checked for homogeneity of variance and normality prior to analysis by a one-way ANOVA (the activity assay and elevated plus maze), or a two-way ANOVA with repeated measures (the water maze test). Where applicable, Student-Newman-Keuls or Dunnett's test (post hoc comparisons) and analysis of covariance were also used. Statistical analyses were performed with ANY-maze Video Tracking System software (Stoelting Co., Wood Dale, IL, USA) and SigmaStat 2.0 (SPSS, Inc., Chicago, IL, USA).

Competition Binding Assays

In vitro binding data for SH-053-2'N, SH-053-S-CH₃-2'F, SH-053-R-CH₃-2'F and JY-XHe-053, in parallel with those for diazepam and zolpidem, are presented in Table 33. Broadly speaking, these ligands were binding at biologically relevant nanomolar to micromolar affinity to the BZ-sensitive recombinant human GABA(A) receptors, while were devoid of binding and activity in approximately 40 other receptor and enzyme assays (NIMH Psychoactive Drug Screening Program, UNC, available at <https://kidbdev.med.unc.edu/pdsp>). No major selectivity in binding at one over the other receptors was noticed (JY-XHe-053 was the most selective ligand, with approximately 18-fold selectivity for GABA(A) receptors containing the α_5 subunit, while zolpidem exerted an approximately 5-fold selectivity for α_1 -GABA(A) receptors). It is of interest that none of the novel ligands had a relatively high affinity for the α_1 -containing receptors (once more, the highest α_1 -subtype affinity, the K_i of 22 nM, was possessed by JY-XHe-053).

Table 33. Binding affinity at $\alpha\chi\beta 3\gamma 2$ GABA(A) /BZ site subtypes. Measurements were made in duplicate. K_i values are reported in nM.

Compound	$\alpha 1$	$\alpha 2$	$\alpha 3$	$\alpha 4$	$\alpha 5$	$\alpha 6$
diazepam	14	7.8	13.9	ND ^a	13.4	ND ^a
zolpidem	29.6	160	380	ND ^a	10000	ND ^a
SH-053-2'N	300	160	527	ND ^b	82	5000
SH-053-2'N ^c	118	148	365	5000	77	5000
SH-053-R-CH ₃ -2'F	759.1	948.2	768.8	ND ^b	95.2	ND ^b
SH-053-S-CH ₃ -2'F	468.2	33.3	291.5	ND ^b	19.2	5000
JY-XHe-053	22	12.3	34.9	ND ^b	0.7	ND ^b

^a ND, not determined

^b Binding at $\alpha 4$ and $\alpha 6$ subtypes have not been determined, but since the 6-phenyl group is present, the ligand will not bind to $\alpha 4$ and $\alpha 6$ subtypes

^c The second independent set of experiments with SH-053-2'N

Electrophysiological Experiments

The *in vitro* concentration-effect curves for the four novel ligands, in parallel with those for zolpidem and diazepam, are presented in Figure 126, together with explicit data on percent potentiation of a within- and between- day stable EC₃ GABA response at rat recombinant GABA(A) receptors. The efficacy data for SH-053-2'N and JY-XHe-053 have been recently published,^{425, 426} and all data are shown here together for comparison purposes. All four novel ligands exerted the lowest positive modulation at α_1 -containing subtypes of receptors relative to efficacy at the other subtypes. In regard to the other three receptor subtypes, the greatest separation of activity was noticed with SH-053-R-CH3-2'F, which shows relatively low efficacies at α_2 and α_3 , in addition to the α_1 -containing GABA(A) receptors. The other ligands exerted substantial potentiation of an EC₃ GABA response at α_2 and α_3 -containing receptors. At 100 nM concentration, which lies well in the range of typical brain levels of BZ site ligands achievable *in vivo*,³³⁵ this potentiation was slightly above (SH-053-2'N and JY-XHe-053) or slightly below (SH-053-S-CH3-2'F) that one elicited through the α_5 -containing subtypes.

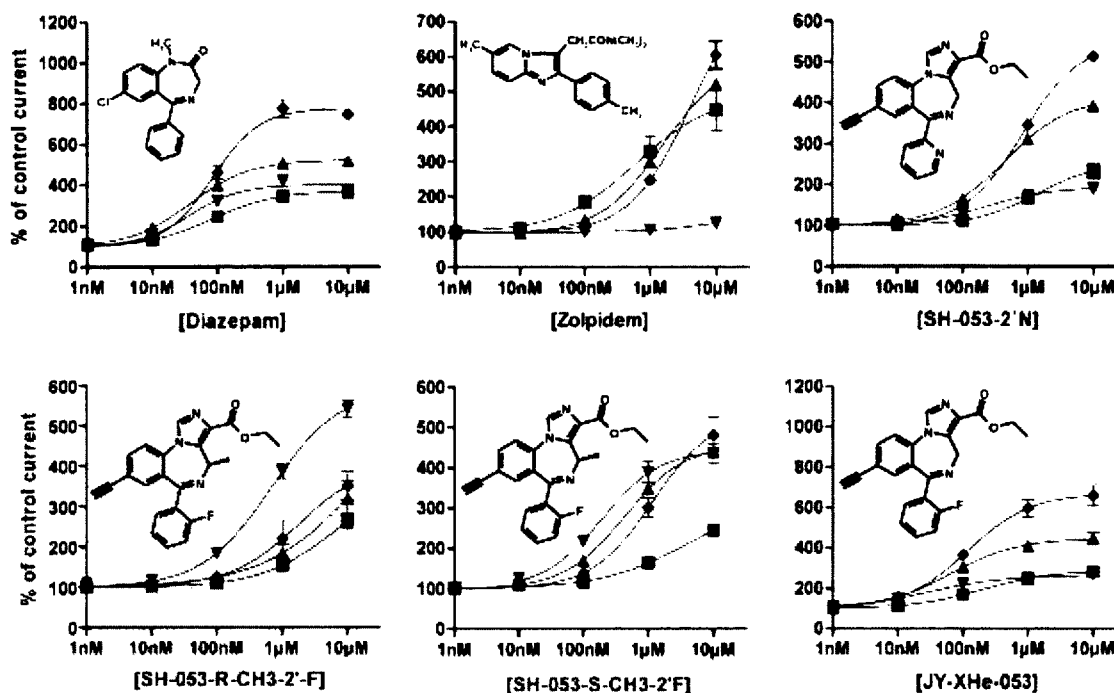


Figure 126. Illustrated here are the concentration-effect curves for diazepam, zolpidem, SH-053-2'N, SH-053-S-CH3-2'F SH-053-R-CH3-2'F and JY-XHe-053 on $\alpha 1\beta 3\gamma 2$ (■), $\alpha 2\beta 3\gamma 2$ (▲), $\alpha 3\beta 3\gamma 2$ (◆), and $\alpha 5\beta 3\gamma 2$ (▼) GABA(A) receptors, using an EC3 GABA concentration. Data points represent means \pm SEM from at least four oocytes from ≥ 2 batches.

As explained in the Results Section, the efficacy data for SH-053-2'N and JY-XHe-053 have been published recently by Rivas.⁴⁶ A concentration of 100 nM of diazepam resulted in $246 \pm 16\%$, $400 \pm 22\%$, $461 \pm 34\%$, and $322 \pm 7\%$ of control current in $\alpha 1\beta 3\gamma 2$, $\alpha 2\beta 3\gamma 2$, $\alpha 3\beta 3\gamma 2$, and $\alpha 5\beta 3\gamma 2$ GABA(A) receptors, respectively. A concentration of 100 nM of zolpidem resulted in $180 \pm 14\%$, $132 \pm 4\%$, $121 \pm 3\%$, and non-significant changes relative to control current in $\alpha 1\beta 3\gamma 2$, $\alpha 2\beta 3\gamma 2$, $\alpha 3\beta 3\gamma 2$, and $\alpha 5\beta 3\gamma 2$ GABA(A) receptors, respectively. A concentration of 100 nM of SH-053-2'N resulted in $113 \pm 2\%$, $165 \pm 2\%$, $149 \pm 3\%$, and $130 \pm 3\%$ of control current in $\alpha 1\beta 3\gamma 2$, $\alpha 2\beta 3\gamma 2$, $\alpha 3\beta 3\gamma 2$, and $\alpha 5\beta 3\gamma 2$ GABA(A) receptors, respectively. A concentration of 100 nM of

SH-053-S-CH3-2'F resulted in non-significant changes relative to control current at $\alpha 1\beta 3\gamma 2$, and $169 \pm 5\%$, $138 \pm 5\%$, and $218 \pm 4\%$ of control current in $\alpha 2\beta 3\gamma 2$, $\alpha 3\beta 3\gamma 2$, and $\alpha 5\beta 3\gamma 2$ GABA(A) receptors, respectively. The effect of $1 \mu\text{M}$ of SH-053-S-CH3-2'F at $\alpha 1\beta 3\gamma 2$ receptors was significant relative to control ($164 \pm 6\%$). A concentration of 100 nM of SH-053-R-CH3-2'F resulted in $111 \pm 2\%$, $124 \pm 9\%$, $125 \pm 8\%$, and $183 \pm 7\%$ of control current in $\alpha 1\beta 3\gamma 2$, $\alpha 2\beta 3\gamma 2$, $\alpha 3\beta 3\gamma 2$, and $\alpha 5\beta 3\gamma 2$ GABA(A) receptors, respectively. A concentration of 100 nM of JY-XHe-053 resulted in $169 \pm 10\%$, $307 \pm 14\%$, $345 \pm 26\%$, and $220 \pm 2\%$ of control current in $\alpha 1\beta 3\gamma 2$, $\alpha 2\beta 3\gamma 2$, $\alpha 3\beta 3\gamma 2$, and $\alpha 5\beta 3\gamma 2$ GABA(A) receptors, respectively. All values given were significantly different from the respective control currents ($p < 0.01$, student's t-test).

Results

Motor Activity Assay

In the experiment with 1.25 and 2.5 mg/kg diazepam and 30 mg/kg SH-053-2'N, ANOVA showed a significant effect of treatment on total distance travelled during 45 min of monitoring ($F(3,27) = 8.33$, $p < 0.001$) (Figure 127, graph a1). According to Dunnett's test, the activity-depressing effect of all three treatments was significant compared with solvent control. The effect was more pronounced in the peripheral zone ($F(3,27) = 8.56$, $p < 0.001$), than in the central zone ($F(3,27) = 4.11$, $p = 0.016$). When the analysis of distance travelled was developed into 5-minute bins (Figure 127, graph b1), it turned out that hypolocomotion was significant during the first 20 minutes of monitoring, and again in the period $30\text{-}35 \text{ min}$, the effect of 30 mg/kg SH-053-2'N being somewhere in the middle between the effects of two tested doses of diazepam.

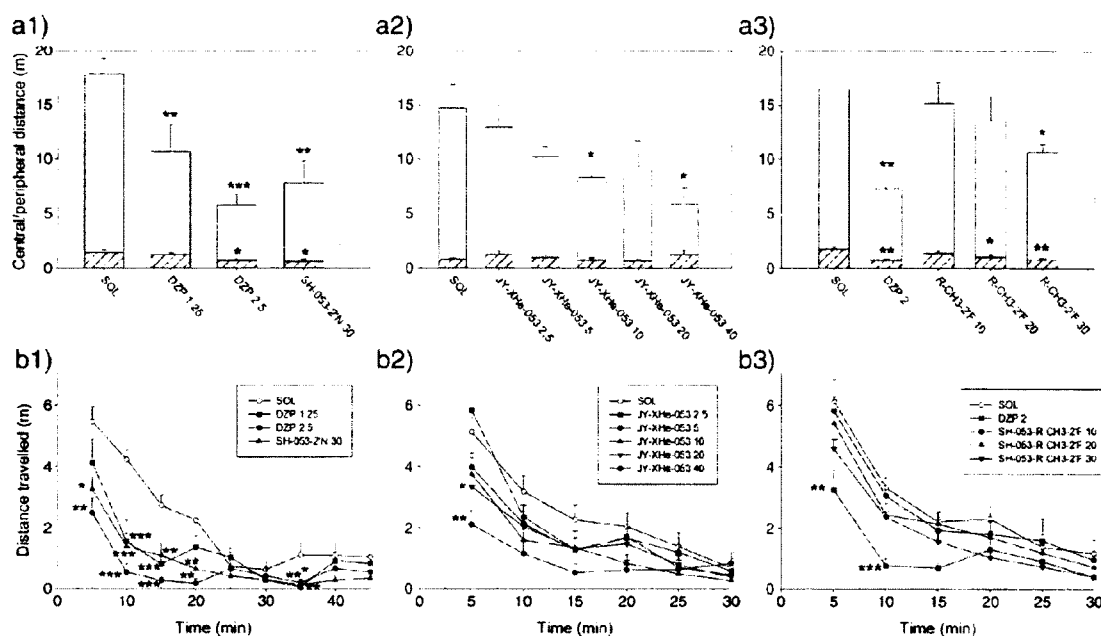


Figure 127. Illustrated here are the effects of diazepam (DZP 1.25 and 2.5 mg/kg) and SH-053-2'N 30 mg/kg (left graphs, a1 and b1), JY-XHe-053 (2.5, 5, 10, 20 and 40 mg/kg) (middle graphs, a2 and b2) and DZP 2 mg/kg and SH-053-R-CH3-2'F (10, 20 and 30 mg/kg) (right graphs, a3 and b3) on distance travelled in the central (hatched bars) and peripheral (open bars) zone of the activity chamber during 45 or 30 minute of recording (total activity corresponds to the height of the whole bar) (upper graphs, a1, a2 and a3) as well as on distance travelled in 5-minute intervals (lower graphs, b1, b2 and b3). *, ** and ***, $P < 0.05$; 0.01 and 0.001, respectively, compared to solvent (SOL) group in each of three experiments. Numbers of animals per treatment group for consecutive groups on each of panels were 8, 8, 7, 8 (left); 8, 6, 6, 8, 8, 6 (middle) and 7, 5, 7, 8, 8 (right).

The dose-response study with JY-XHe-053 showed a significant effect on total locomotor activity during 30 minutes of recording ($F(5,36) = 2.85$, $p = 0.029$) (Figure 127, graph a2). The effective doses of JY-XHe-053 were 10 and 40 mg/kg. The effect on central zone activity was not discernible, while statistical analysis of peripheral zone distance revealed that the three higher doses of JY-XHe-053 were significantly different from control (not shown). The analysis of 5-min bins showed that during the first 5 min of recording the effect of JY-XHe-053 at 20 and 40 mg/kg was significant (Figure 127, graph b2).

In the third experiment, an ANOVA for total distance was also significant ($F(4,30) = 4.50$, $p=0.006$) (Figure 127, graph a3). According to Dunnett's test, 30 mg/kg of SH-053-R-CH3-2'F, besides 2 mg/kg diazepam, significantly depressed locomotion. Notably, central zone activity was affected more profoundly ($F(4,30) = 4.27$, $p=0.007$) than peripheral locomotion ($F(4,30) = 3.74$, $p=0.014$), and SH-053-R-CH3-2'F at 20 and 30 mg/kg decreased central, but not peripheral locomotion. The analysis of 5-minute bins (Figure 134, graph b3) revealed that SH-053-R-CH3-2'F did not significantly decrease locomotion in neither of 6 intervals of recording, far different from diazepam (2 mg/kg), which induced overt sedation during the first 10 min of recording.

A recent study with SH-053-S-CH3-2'F at 30 mg/kg has shown a significant decrease of locomotor activity, which was significantly depressed in the time period 5-20 minutes, and only in the peripheral, but not central, zone.³⁹⁷

Elevated Plus Maze

In regard to influence of SH-053-2'N on activity-related parameters (Figure 128) in the plus maze, the effect of treatment on closed arm entries did not reach statistical significance ($F(4,24) = 2.73$, $p=0.053$) (Figure 128a). However, statistical analysis by ANOVA showed a significant effect of treatment on total arm entries ($F(4,24) = 5.10$, $p=0.004$). Dunnett's test revealed the significant effect of the two higher doses of SH-053-2'N in comparison to solvent group ($p=0.020$ and 0.048 , respectively, Figure 128b). In regard to the total distance travelled, ANOVA pointed to the significant effect of treatment ($F(4,24) = 3.85$, $p=0.015$); however, post hoc test showed that neither of the doses tested was highly different in comparison to the solvent group (Figure 128c).

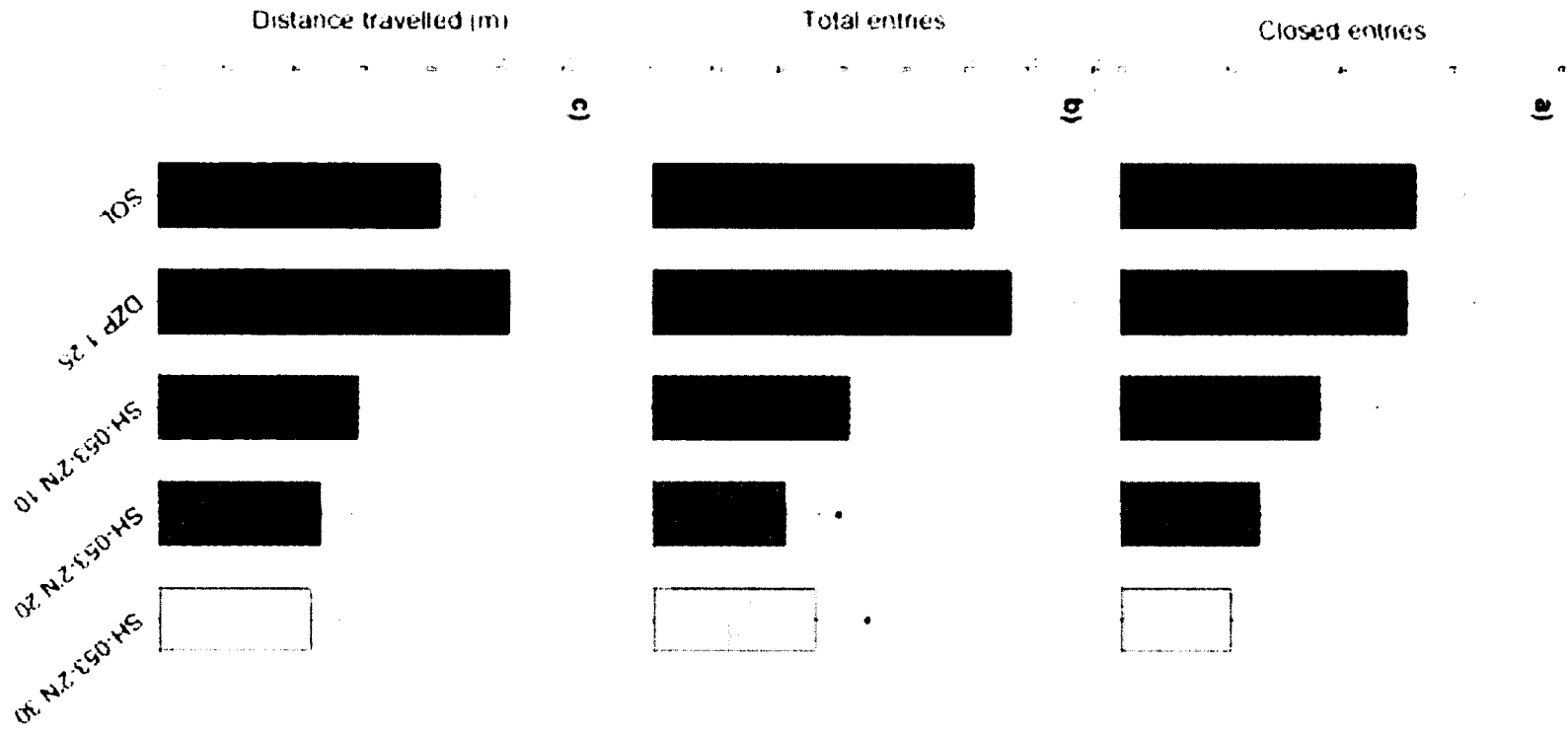


Figure 128. Illustrated here are the effects of diazepam (DZP 1.25 mg/kg) and SH-053-2'N (10, 20 and 30 mg/kg) on the a) closed arm entries, b) total arm entries and c) total distance travelled in the EPM. * $P < 0.05$ compared to solvent (SOL) group. Number of animals per treatment group (Figure 131- 132, for SOL through SH-053-2'N 30 mg/kg, respectively): 6, 6, 5, 6, 6.

The influence of SH-053-2'N on anxiety-related parameters was presented in Figure 129. There was a significant effect of treatment on distance travelled in the open arms ($F(4,24) = 4.45$, $p = 0.008$) (Figure 129a); Dunnett's test showed that the influence of diazepam as a positive control was close to significant ($p = 0.071$ related to control). Although the overall influence of treatment on the percentage of open arm entries had reached statistical significance ($F(4,24) = 2.89$, $p = 0.044$) (Figure 129b), neither of the single doses was significant on its own (post hoc test). The influence on the percentage of time on open arms was significant ($F(4,24) = 5.04$, $p = 0.004$) (Figure 129c), with SH-053-2'N at 30 mg/kg being an effective treatment ($p = 0.045$, Dunnett's test). Because the parameter of total entries could not be seen as a relatively pure index of locomotor activity, i.e. sedation,⁴¹⁹ an analysis of covariance in the anxiety-related parameters using the number of total arm entries as covariate was not necessary.³⁹⁹ However, we opted to conduct a new analysis of anxiety-related parameters, without data for diazepam as positive control. This revealed the preserved significance of effects of SH-053-2'N on the percentage of open arm entries and the percentage of time spent in open arms when an analysis of covariance was performed using the number of closed arm entries as covariate (respective F values: [$F(3,18) = 3.276$, $p = 0.045$] and [$F(3,18) = 6.027$, $p = 0.005$]). This indicates that the anxiolytic-like effects of SH-053-2'N were not directly related with a trend of hypolocomotion in rats treated with this ligand.

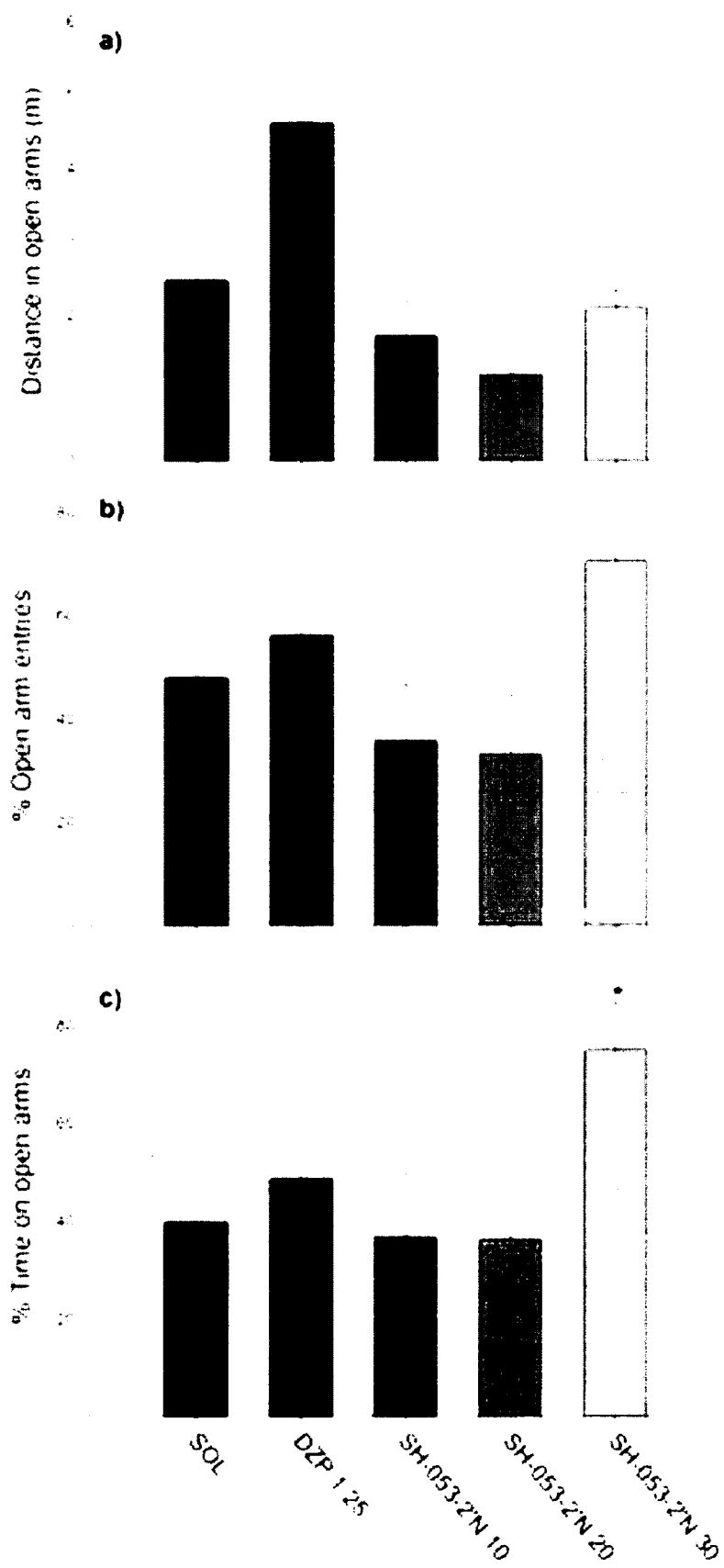


Figure 129. Illustrated here are the effects of diazepam (1.25 mg/kg) and SH-053-2'N (10, 20 and 30 mg/kg) on the a) distance travelled on open arms, b) percentage of entries in open arms and c) percentage of time spent on open arms of the EPM. *P<0.05 compared to solvent (SOL) group.

JY-XHe-053, administered in a wide range of doses, was devoid of significant behavioral activity in the elevated plus maze, when analyzed both, general activity (data not shown) and anxiety-related parameters. In the Figure 130 are presented changes under this treatment of three anxiety-related parameters: distance in open arms (Figure 130a), percent of open arm entries (Figure 130b) and percent of time spent in the open arms (Figure 130c). Despite a hint of an inverted U-shape activity and behavioral disinhibition at 5 mg/kg, discernible changes in behavior were lacking.

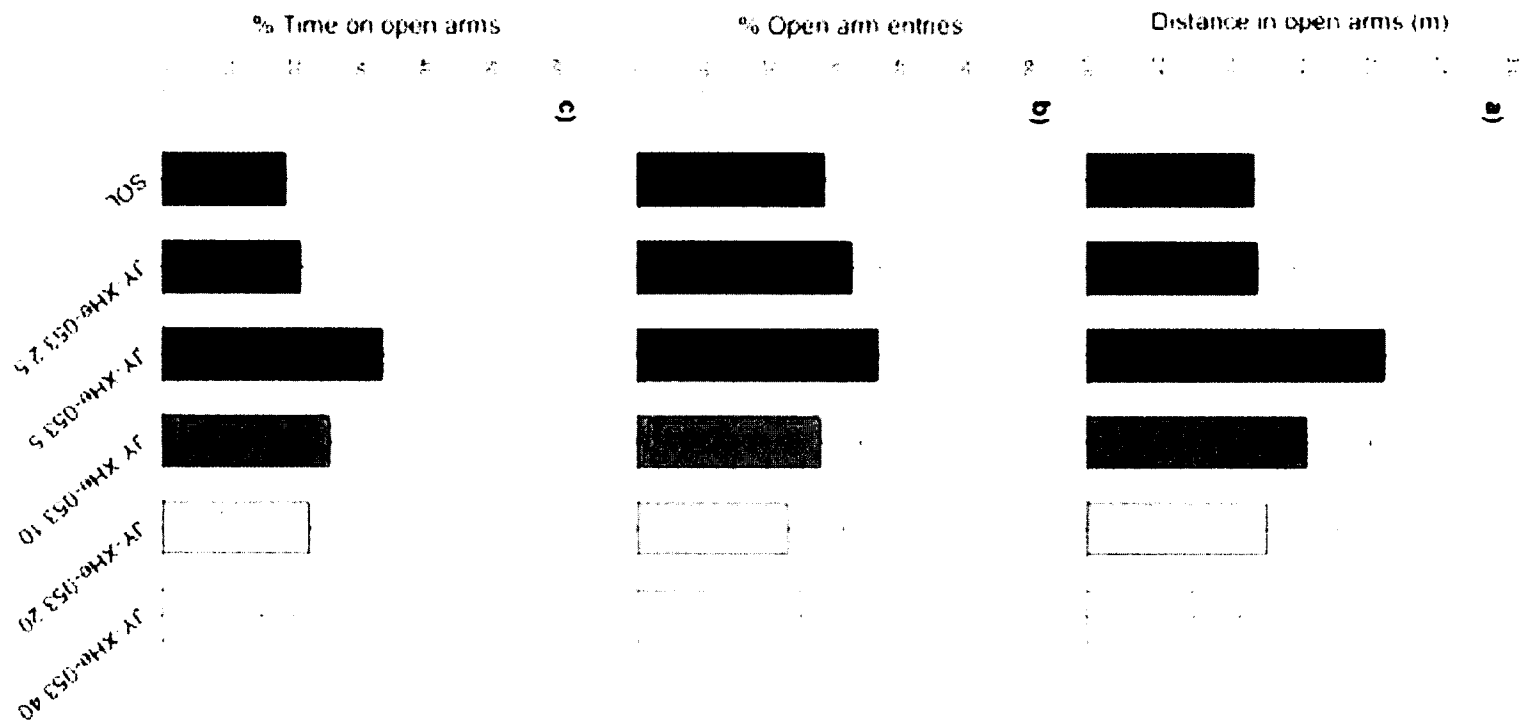


Figure 130. Illustrated here are the influences of JY-XHe-053 (0; 2.5; 5; 10; 20 and 40 mg/kg) on the a) distance traveled on open arms, b) percentage of entries in open arms and c) percentage of time spent on open arms of the EPM. Number of animals per treatment group (for SOL through JY-XHe-053 40 mg/kg) was 7.

The SH-053-R-CH3-2'F in doses up to 30 mg/kg was completely devoid of changes of general activity- or anxiety-related parameters in the elevated plus maze, and hence this set of data was not presented.

Our recent study with SH-053-S-CH3-2'F has shown a significant effect of the 30 mg/kg dose on the percentage of open arm entries and the percentage of time in the open arms, without concomitant effects on general activity-related parameters.^{46-48, 387, 409}

Morris Water Maze

For the dose response study of zolpidem, the factors, treatment and days, but not the interaction treatment x days, were statistically highly significant for the latency to find the platform (treatment effect, $F(3,124) = 21.01$, $p < 0.001$; day effect, $F(4,496) = 42.87$, $p < 0.001$; and treatment x day interaction, $F(12,496) = 1.31$, $p = 0.209$) (shown in Figure 131), the distance swam before finding the platform (treatment effect, $F(3,124) = 4.71$, $p = 0.004$; day effect, $F(4,496) = 32.48$, $p < 0.001$; and treatment x day interaction, $F(12,496) = 1.21$, $p = 0.270$), average swim speed (treatment effect, $F(3,124) = 18.08$, $p < 0.001$; day effect, $F(4,496) = 10.95$, $p < 0.001$; and treatment x day interaction, $F(12,496) = 1.57$, $p = 0.097$) and path efficiency (treatment effect, $F(3,124) = 7.75$, $p < 0.001$; day effect, $F(4,496) = 23.68$, $p < 0.001$; and treatment x day interaction, $F(12,496) = 1.68$, $p = 0.067$). It is worth noting that maximum speed was also significantly different among treatments, but in such a counterintuitive way that zolpidem-treated animals tended to swim the faster (in the maximum) the higher the dose of zolpidem was applied (data not

shown). Significant differences among treatments during training days, obtained by one-way ANOVA applied to that day's latency to find the platform, are presented in Figure 131a. The results of the post hoc analysis of overall influence for the factor treatment are summarized in Table 34. The analysis showed that the lowest tested dose of zolpidem, 0.5 mg/kg, was different related to control, but also that rats treated with higher doses of the drug (1 and 2 mg/kg) were behaviorally impaired related to 0.5 mg/kg zolpidem.

Table 34. Illustrated here is the significant differences among overall influence (averaged for five days of acquisition) on the Morris water maze learning parameters: latency to find the platform (L), distance swam before finding the platform (D), mean swim speed (S) and path efficiency (E) in the dose-response study of zolpidem (ZOL, mg/kg).

	ZOL 0.5	ZOL 1	ZOL 2
Solvent	L: p=0.009 S: p=0.009 E: p=0.010	L: p<0.001 D: p=0.010 S: p<0.001 E: p<0.001	L: p<0.001 D: p=0.004 S: p<0.001 E: p<0.001
ZOL 0.5	-	L: p=0.018 S: p=0.011	L: p<0.001 S: p<0.001
ZOL 1	-	-	L: p=0.014

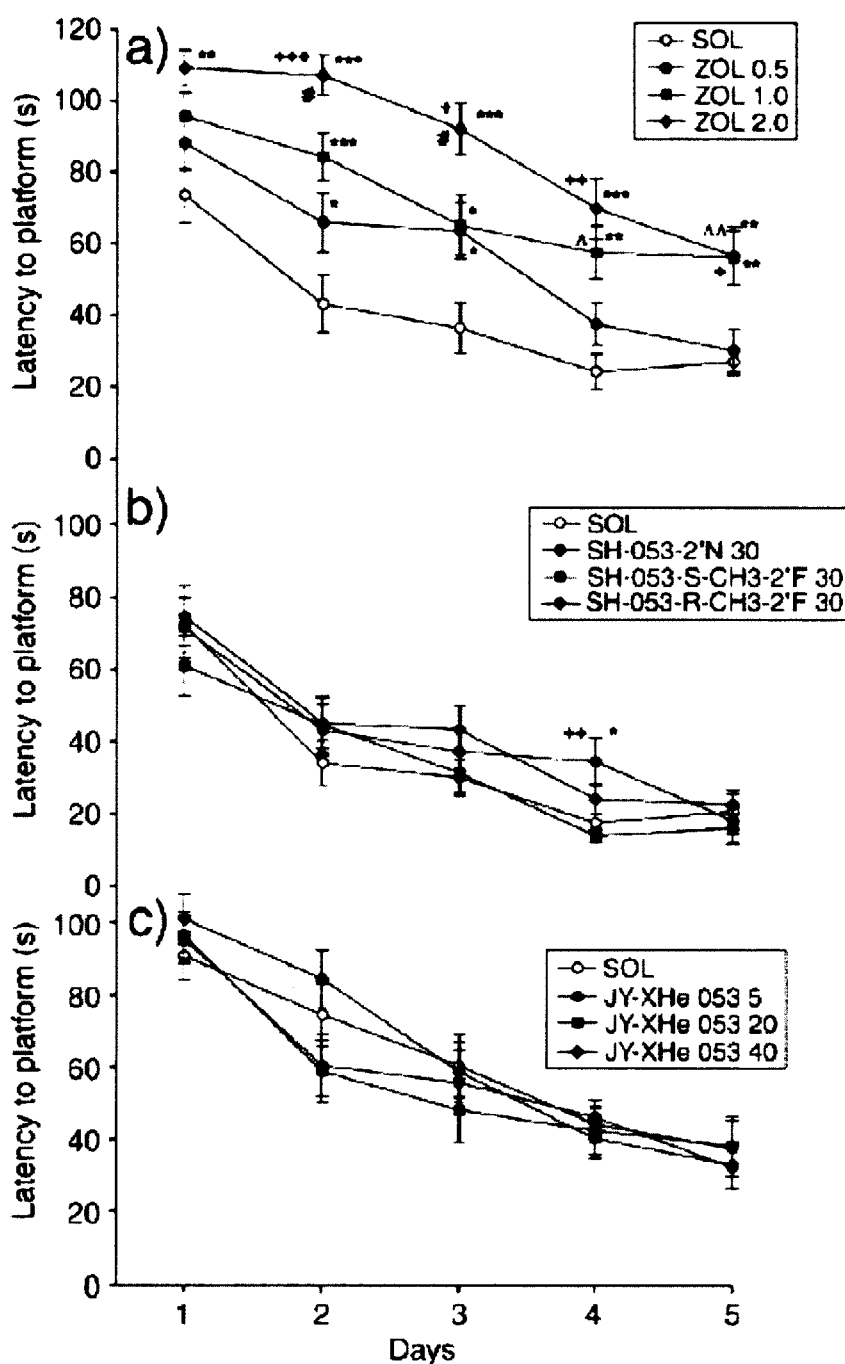


Figure 131. Illustrated here are the effects of a) zolpidem (ZOL 0.5, 1 and 2 mg/kg), b) SH-053-2'N, SH-053-S-CH3-2'F and SH-053-R-CH3-2'F (all dosed at 30 mg/kg) and c) JY-XHe-053 (5; 20 and 40 mg/kg), on latency to platform. **, ***, $P < 0.05$; 0.01 and 0.001, respectively, compared to solvent (SOL) group in each of three experiments. In graph a): +, ++, and +++, $P < 0.05$; 0.01 and 0.001, respectively, compared to ZOL 0.5 group; #, $P < 0.05$ compared to ZOL 1.0 group; ^ and ^^, $P < 0.05$ and 0.01, ZOL 1 group compared to ZOL 0.5 group. In graph b): ++, $P < 0.01$ compared to

SH-053-S-CH3-2'F (30mg) group. Number of animals per each treatment group was 8 in a) and b), and 7 in c).

The results of the probe trial showed an unexpected inconsistency in the data from the control group. Hence, it was decided to perform statistical analysis with zolpidem on its own (Table 35). The incapacitating influence of the previous treatment with zolpidem was discernible during the probe trial as well, when a number of indices of memory were dose-dependently adversely affected (number of entries in platform zone close to significantly, time in the target region significantly). Concomitantly, a significant increase in the peripheral ring distance, i.e. pronounced thigmotaxis, has shown that zolpidem impaired learning the required water maze skills and strategies. The representative parameters of water maze performance in the probe trial of the zolpidem (ZOL) dose-response experiment are illustrated in Table 30. The key to regions used in the analysis is given in Figure 132.

Table 35. Parameters of water maze performance with zolpidem

	ZOL 0.5	ZOL 1.0	ZOL 2.0	ANOVA, F(2,21)	P
Whole water maze parameters					
Distance (m \pm SEM)	10.93 \pm 0.97	11.50 \pm 0.96	12.75 \pm 0.56	1.187	0.325
Platform quadrant (NE) parameters					
Distance (m \pm SEM)	2.41 \pm 0.29	2.18 \pm 0.51	2.22 \pm 0.44	0.083	0.920
Time (s \pm SEM)	11.86 \pm 1.44	9.64 \pm 1.92	9.75 \pm 2.06	0.471	0.631
Peripheral ring parameters					
Distance (m \pm SEM)	4.16 \pm 0.61	6.09 \pm 0.89	7.85 \pm 0.82*	5.564	0.012
Time (s \pm SEM)	33.48 \pm 3.68	39.86 \pm 1.67	42.80 \pm 3.35	2.473	0.109
Platform ring parameters					
Distance (m \pm SEM)	5.27 \pm 0.68	4.48 \pm 0.31	4.00 \pm 0.65	1.247	0.308
Time (s \pm SEM)	21.46 \pm 3.05	17.31 \pm 1.38	14.50 \pm 2.60	2.049	0.154
Target region parameters					
Distance (m \pm SEM)	1.51 \pm 0.27	1.12 \pm 0.14	0.99 \pm 0.22	1.520	0.242
Time (s \pm SEM)	7.26 \pm 1.36	4.03 \pm 0.52*	3.51 \pm 0.76*	4.596	0.022
Platform parameters					
Number of entries (\pm SEM)	1.25 \pm 0.41	0.38 \pm 0.18	0.50 \pm 0.19	2.813	0.083
Distance (m \pm SEM)	0.097 \pm 0.031	0.047 \pm 0.028	0.053 \pm 0.023	0.945	0.405

*, P<0.05 compared to ZOL 0.5 group.

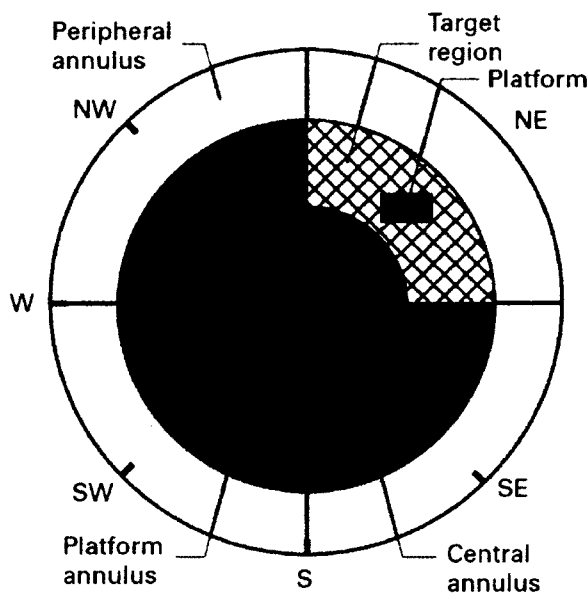


Figure 132. Scheme representing the virtual division of the water maze used in the analysis of rats' performance

In regard to the two other experiments in the water maze, the results were generally dissimilar in relation to those obtained with zolpidem. In the experiment with SH-053-S-CH3-2'F, SH-053-R-CH3-2'F and SH-053-2'N, all dosed at 30 mg/kg, only the factor days, but not the treatment or the interaction treatment x days, was statistically significant for the latency to find the platform (treatment effect, $F(3,124) = 1.40$, $p = 0.248$; day effect, $F(4,496) = 54.45$, $p < 0.001$; and treatment x day interaction, $F(12,496) = 0.84$, $p = 0.611$), the distance swam before finding the platform (treatment effect, $F(3,124) = 0.95$, $p = 0.419$; day effect, $F(4,496) = 41.92$, $p < 0.001$; and treatment x day interaction, $F(12,496) = 0.44$, $p = 0.947$), swim speed (treatment effect, $F(3,124) = 2.24$, $p = 0.087$; day effect, $F(4,496) = 9.13$, $p < 0.001$; and treatment x day interaction, $F(12,496) = 0.96$, $p = 0.489$) and path efficiency (treatment effect, $F(3,124) = 0.32$, $p =$

0.812; day effect, $F(4,496) = 7.90$, $p < 0.001$; and treatment x day interaction, $F(12,496) = 1.31$, $p = 0.207$). Similar results were obtained for the latency to find the platform (treatment effect, $F(3,108) = 0.45$, $p = 0.718$; day effect, $F(4,432) = 90.88$, $p < 0.001$; and treatment x day interaction, $F(12,432) = 1.03$, $p = 0.417$), the distance swam before finding the platform (treatment effect, $F(3,108) = 0.32$, $p = 0.812$; day effect, $F(4,432) = 56.12$, $p < 0.001$; and treatment x day interaction, $F(12,432) = 1.64$, $p = 0.079$), swim speed (treatment effect, $F(3,108) = 1.13$, $p = 0.340$; day effect, $F(4,432) = 7.50$, $p < 0.001$; and treatment x day interaction, $F(12,432) = 1.11$, $p = 0.347$) and path efficiency (treatment effect, $F(3,108) = 0.90$, $p = 0.445$; day effect, $F(4,432) = 28.58$, $p < 0.001$; and treatment x day interaction, $F(12,432) = 1.44$, $p = 0.144$) of rats treated with JY-XHe-053 in the 5 to 40 mg/kg dose range. The graphs representative of the latter two experiments, with latency to find the platform, are given in Figure 131b and 131c, respectively. The one-way ANOVA applied to latency to find the platform showed a significantly longer search time on the fourth day in rats treated with 30 mg/kg SH-053-2'N in comparison with control animals or those treated with 30 mg/kg SH-053-S-CH3-2'F (Figure 131b). However, this result should be seen as an isolated case, since other learning parameters, such as path efficiency presented in Figure 133a, were not affected by SH-053-2'N on either of the learning days. Furthermore, probe trial parameters were close to control throughout the water maze experiments performed with the newly-synthesized ligands. The lack of incapacitating consequences of the previous five-day treatment with SH-053-S-CH3-2'F, SH-053-R-CH3-2'F and SH-053-2'N is illustrated in Figure 133b, with the parameter of platform zone entries during the probe trial presented.

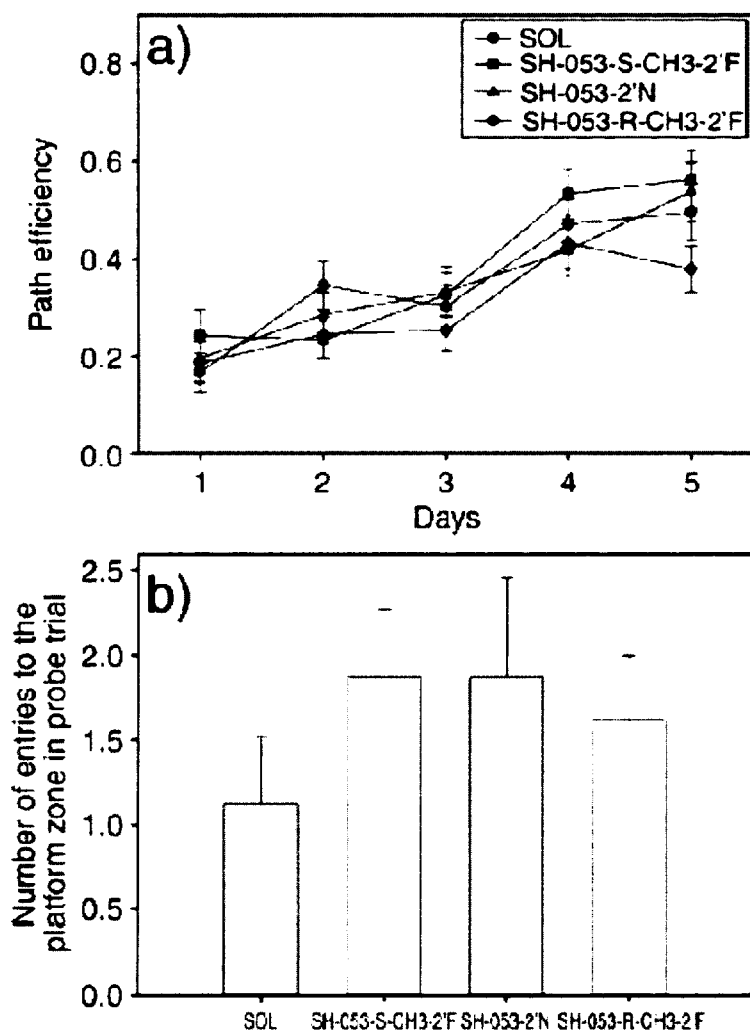


Figure 133. Illustrated here are the effects of SH-053-2'N, SH-053-S-CH3-2'F and SH-053-R-CH3-2'F, all dosed at 30 mg/kg, on a) path efficiency during 5-day acquisition sessions and b) number of entries to the zone of previous days' position of platform in the probe trial.

In Figure 134, the distances the rats swam in the platform quadrant (NE) during acquisition trials are presented alongside the respective distance in the portion of NE quadrant lying in the platform annulus of the maze ("the target region"), for the chosen treatments from three experiments. Providing the rats have no preference for any part of a quadrant, the chance percent of distance swam in the target region would be 40%. The

influence of four novel ligands tested at relatively high doses on this parameter was comparable to control values. On the contrary, the rats treated with 2 mg/kg zolpidem strikingly lacked the preferential activity in that part of the NE quadrant in which finding the platform was possible; even on day 5, only 40.5% of the distance they travelled in the NE quadrant was in the target region.

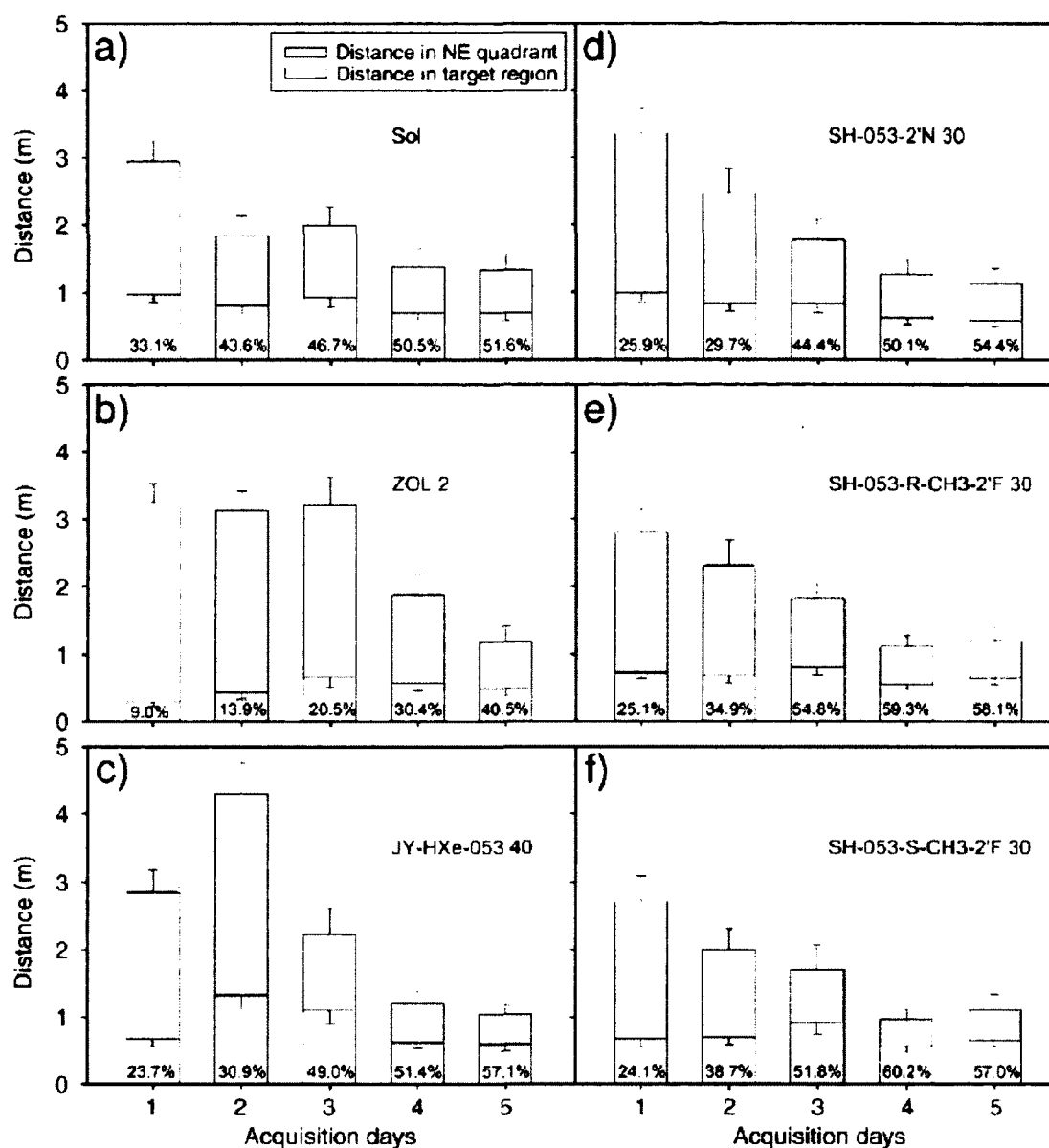


Figure 134. Illustrated here are the effects of b) zolpidem (ZOL 2), c) JY-XHe-053 (30mg), d) SH-053-2'N (30mg), e) SH-053-R-CH3-2'F and f) SH-053-S-CH3-2'F (30mg) (all doses in mg/kg) on the distance rats travelled in the NE quadrant and target region during 5-day acquisition trials in the water maze. The numbers inside the columns are the percent of the distance swam inside the target (NE) quadrant which was travelled in the target region. Control values (SOL) given in a) are taken from the experiment with ZOL. Numbers of animals are as in Figure 128.

Discussion

A substantial body of evidence from both, genetic⁴⁶ and pharmacological studies,¹⁴ supports the search for a new generation of positive allosteric modulators at GABA(A) receptors, which would mostly be devoid of the adverse effects of current BZ drugs. Most notably, GABA(A) receptors which contain the α_1 subunit are believed to be responsible for most of the untoward effects of BZs, and silencing the activity at this subunit has appeared as the most attractive approach.⁴¹⁹ The *in vitro* and *in vivo* pharmacology of a number of novel BZ-site ligands, affinity- and/or efficacy-selective for one, two or three of the subtypes of BZ site, other than that at α_1 -containing GABA(A) receptors, has supported the possibility of obtaining preclinical profiles substantially different from those related to standard BZ drugs.⁴²⁷

The present experiments focused on the recently-synthesized ligands: SH-053-2'N, SH-053-S-CH3-2'F, SH-053-R-CH3-2'F and JY-XHe-053, which as a common trait have moderately low to low affinity and mild to partial agonistic efficacy at α_1 -containing GABA(A) receptors. Positive efficacy is more pronounced at the other BZ-sensitive binding sites in comparison to the α_1 -subtype. These ligands were assessed in a battery of standard behavioral tests, and also compared, where appropriate, with effects of diazepam and zolpidem, a nonselective and relatively α_1 -selective allosteric modulator at BZ site of GABA(A) receptors, respectively. **Putting aside for the moment the subtle differences in the *in vitro* and *in vivo* pharmacology of novel ligands, it was observed that even with ligands that demonstrated efficacy “lower at the α_1 subtypes than at the rest of the subunits”, the sedative-like potential of such GABA(A) modulation was not fully eliminated, while the spatial learning and**

memory impairments, assessed in the water maze and usually seen with BZ site agonists, were completely circumvented; the latter finding represents the single most important result from the present study.

The decreased locomotion induced by all four novel ligands (the effect of 30 mg/kg SH-053-S-CH3-2'F was presented by Savić et al.^{51, 367, 389}) which were tested, may be rationalized in two ways. Firstly, although the lack of occupancy (in vivo potency) data for distinct receptor subtypes precludes drawing firm conclusions about the actual activity at α_1 -containing GABA(A) receptors, which are predominantly involved in the sedative actions of BZs according to genetic⁴⁶ and pharmacological antagonism studies,⁵² it cannot be excluded that, even at presumably low fractional occupancy, moderately low to moderate positive modulation (partial agonism) at these α_1 -receptors may be sufficient for eliciting weak sedation.⁴¹⁹ Secondly, growing neuroanatomical evidence points to the possible role of α_5 -containing GABA(A) receptors in motor control,⁴¹⁹ and Savić recently suggested that any locomotor activity changes induced by ligands possessing a substantial α_5 -agonist efficacy may be contributed by modulation at GABA(A) receptors containing this subunit.⁴²⁸ GABA(A) receptors containing the α_5 -subunit are functionally interrelated in some manner with those containing the α_1 -subunit. Importantly, knock-in mice harboring the α_5 subunit insensitive to diazepam are refractory to development of tolerance to the sedative effects of diazepam dosed subchronically.³⁸⁶ Moreover, the α_5 -subunit affinity- and efficacy-selective antagonist XLi093, at a dose presumably causing a complete antagonism of the effects of diazepam at α_5 -containing GABA(A) receptors, has potentiated sedation induced by diazepam.⁴⁷ Based on these data, we hypothesized further that positive modulation at α_5 GABA(A)

receptors may exert a dual action: to limit sedative effects elicited by supra-physiological stimulation of α_1 -containing receptors (e.g. by full agonists), and, oppositely, to enhance low activation of α_1 GABA(A) receptors (e.g. by partial agonists), and, hence, induce mild sedation.⁴⁶ Such a modulation might be achieved if neurons involved in sedative actions are modulated strongly by α_1 as well as more weakly by α_5 receptors, and if the synapse or neuron mediating the α_1 modulation is at the same time weakly regulated by α_5 receptors. Then low activity at α_1 receptors can overall be enhanced by a direct α_5 receptor activity on the same neuron, but strong α_5 activity would downregulate the strong sedative action of α_1 activity via its indirect effect on the synapse or neuron mediating the α_1 modulation. Such a scenario could, at least partly, explain the unexpected finding that the mice lacking the α_1 -containing GABA(A) receptors (knockout mice) were more sensitive to hypolocomotion and loss of righting reflex induced by diazepam, compared to wild-type controls.⁴⁶ Similarly, tolerance development against the sedative effects of diazepam mediated via α_1 receptors may be explained by upregulation of the putative indirect mechanism of α_5 receptor activity. Further experiments will have to be performed to substantiate this speculation. The roles of these two receptor subtypes in exerting the locomotor effects of the ligands with limited α_1 activity, such as those presented here, may be supplementary and additive: the more avid binding and/or activation at α_5 GABA(A) receptors, the more chance of eliciting sedation. The lack of observable decrease of locomotion with a novel ligand (WYS8) which possesses high affinity and partial agonistic efficacy at α_1 GABA(A)

receptors, but moderately low affinity and partial inverse agonistic efficacy at α_5 GABA(A) receptors (Savić, Sieghart, Cook, unpublished data), supports this notion.

The differences in the capability to induce anxiolytic effects, observed with the ligands evaluated here, are not easily reconciled. Genetic studies have indicated the α_2 subunit was predominantly involved in the anxiolytic-like effects of positive modulation at GABA(A) receptors,^{46, 406} while results with some novel selective ligands pointed to the role of the α_3 subunit, as well.³³⁵ The ligand SH-053-R-CH3-2'F was devoid of anxiolytic potential, in line with results of a congener with a similar profile of α_5 GABA(A) functional selectivity, SH-053-R-CH3.⁴⁶ However, JY-HXe-053, a ligand with relatively high affinity and efficacy at α_2 and α_3 -containing GABA(A) receptors, was devoid of discernible anxiolytic activity, too. When comparing this result with the anxiolytic-like properties of SH-053-2'N and SH-053-S-CH3-2'F⁴²⁹ it was found that JY-HXe-053 has a greater affinity at α_1 -, and especially α_5 -containing GABA(A) receptors, with substantial potentiation at these receptors achieved already at concentration of 100 nM (169% and 220%, respectively). Since JY-HXe-053 has induced a hypolocomotor effect in the SLA at doses (10 mg/kg and above) lower than those observed with SH-053-2'N or SH-053-S-CH3-2'F (30 mg/kg), it is possible that its activity at α_1 and, in parallel, α_5 receptors may have masked the expected anxiolytic-like effects mediated by the other two, α_2 and α_3 -containing, subtypes of GABA(A) receptors. When one compares the in vitro profile of JY-XHe-053 with that of diazepam, it is clear that JY-XHe-053, but not diazepam, exhibits a preferential affinity for α_5 -GABA(A) receptors. The consequent 'priority in activity' at α_5 -GABA(A) receptors may have endowed this population of receptors with a relatively more distinct role in influencing the overall behavior of rats

treated with JY-XHe-053, rather than with diazepam. Finally, it is notable that the hypolocomotor influence of JY-XHe-053 in the SLA test was evident only when analyzing activity in the peripheral, but not in the central zone of the chamber. Hence, the motor depressant effects were not confounded by influence on emotional reactivity, and could be seen as a pure measure of sedation.⁴²⁹ On the contrary, the hypolocomotion induced by SH-053-R-CH3-2'F was due to the inactivity in the central, but not the peripheral zone, which suggests that the sedation-like actions exerted through α_1 and α_5 GABA(A) receptors are qualitatively different.

It has been shown previously that, when observable, the anxiolytic-like effects of zolpidem, the preferential α_1 -subunit selective agonist with intermediate activity at α_2 and α_3 -containing GABA(A) receptors, are statistically dependent on the concomitant decrease of closed arm entries in the elevated plus maze, and hence confounded by general activity changes.⁴²⁹ Analysis of covariance for the current results with SH-053-2'N did not reveal analogous dependence of its anxiolytic-like effects on the concomitant signs of sedation. Nevertheless, it is possible the clinical separation of wanted anxiolytic from unwanted sedative effects would be lower for SH-053-2'N than for SH-053-S-CH3-2'F, having in mind that the latter ligand was devoid of influence on the parameters related to general activity in the elevated plus maze.⁴³⁰

The effects of zolpidem on the acquisition and retention of place learning in the water maze have not been previously assessed. Zolpidem dose-dependently impaired the declarative component of both, learning the task, as assessed by path efficiency, the latency and distance before finding the platform across acquisition trials, and recalling the previous platform position, as assessed by time in the target region during the probe

trial. It also induced a decrease in average swim speed, accompanied by an increase in the maximum swim speed, which may be interpreted as 'bursts' of behavioral disinhibition (activation) interspersed among background sedative effects. By use of the treatment switch, McNamara and Skelton have shown⁴¹⁹ that the reduced swim speed cannot account for deficits in platform localization induced by BZs. Namely, the rats acquiring the task under saline treatment continued to perform normally despite the switch to diazepam, which nonetheless elicited a decrease in swim speed.³⁹⁷ Hence, the data suggest that neither non-specific performance impairment, nor any sensorimotor deficit (according to our preliminary findings with zolpidem in the task of finding the visible platform) was responsible for the observed acquisition deficit.⁴²

Zolpidem also negatively affected the procedural component of the water maze task. Namely, suppression of an instinct to swim thigmotaxically appears to be necessary to effectively accomplish this task,⁴⁶ and zolpidem at 2 mg/kg induced an increase of peripheral annulus, and a decrease of platform annulus parameters throughout the test. It has been recently shown that both, the α_1 -subunit affinity-selective antagonist β -CCt, and the α_5 -subunit affinity- and efficacy-selective antagonist XLi093, may, at least partially, prevent diazepam-induced impairment in the declarative and procedural component of the water maze task; however, the antagonistic effect of β -CCt was manifestly more profound.⁴²⁷ The results show, first, that the effects of zolpidem, a ligand essentially inactive at α_5 GABA(A) receptors, mirror those induced by diazepam, and secondly, that three novel ligands, with moderately low to low activity at α_1 GABA(A) receptors, do not disturb water maze behavior. **The conclusion is straightforward: a substantial amount of activity at α_1 GABA(A) receptors is needed if spatial learning and**

memory incapacitation is to be induced by positive allosteric modulation at BZ site. The positive modulation at α_5 GABA(A) receptors may add to the incapacitating action effected through the α_1 subunit, but is neither necessary (cf. zolpidem), nor sufficient (cf. SH-053-R-CH3-2'F) for spatial cognition impairment in the water maze.

The data and the above conclusions may thus significantly change the common knowledge on the function of individual receptor subtypes.⁴³¹⁻⁴³³ From the data with knock-in mice, it was concluded that sedation is mediated by interaction of diazepam with α_1 receptors. Present and previous data indicate, however, that α_5 receptors may significantly affect the sedative effects of diazepam, as discussed above. Data from knock-in and knock-out mice indicate that α_5 receptors are mainly mediating the effects of diazepam on learning and memory. However, we have discussed above that α_1 receptors might be also important for mediating the incapacitating effects of diazepam on learning and memory. These conclusions do not completely invalidate the previous conclusions from the genetically modified mice, but reflect the more realistic view that more than one GABA(A) receptor subtype is modulating the same behavioral parameter and that depending on which parameter is being investigated; contributions of different receptor subtypes might be more or less strongly involved. We suggest a tentative hypothesis based on the existence of the fine equilibrium between the α_1 - and α_5 -GABA(A) receptors on the one hand, and α_2 - and α_3 -GABA(A) receptors on the other side, in terms of the influence of positive allosteric modulation on the crucial behavioral endpoints of sedation, anxiolysis and amnesia. It is clear that a substantial amount of positive modulation is needed by the α_1 , coordinated in some manner with α_5 -

GABA(A) receptors, if sedation and amnesia are to be elicited, while for the anxiolytic-like actions the $\alpha 2$ and/or $\alpha 3$ GABA(A) receptors must be activated. The other pair of receptors, not primarily involved in mediation of the respective behavioral effect, may counteract, mask or in another way hinder the action of the responsible pair.

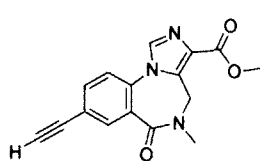
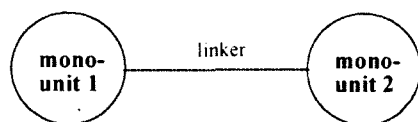
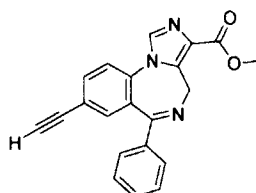
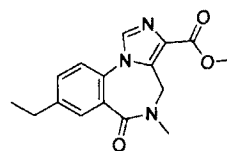
Although the results of these studies suggest a possible role of $\alpha 5$ -containing receptors on motor control, the data is in agreement with earlier oocyte studies from Sieghart et al. and the pharmacophore models and observations discussed in Part I. It was clear JY-XHe-053 exhibited slightly more agonist efficacy at $\alpha 1$ than did SH-053-2'N and SH-053-S-CH3-2'F. These studies are in agreement with the hypothesis proposed in previously^{64, 434} in which a) ligands with an electronegative group in the 2' position on the pendant phenyl position of analogs of XHe-II-053 will interact with the H2 group of the pharmacophore and can enhance binding and b) the selected ligands are selective for $\alpha 2$, $\alpha 3$, and $\alpha 5$ -containing receptors over $\alpha 1$ containing receptors. The lack of memory impairment by SH-053-2'N, SH-053-S-CH3-2'F, SH-053-R-CH3-2'F and JY-XHe-053 is in agreement with previous in vitro binding data which shown that these ligands do not bind potently to the $\alpha 1$ -containing GABA(A) receptor subtypes, which is believed to be responsible for sedation and amnesia. Between the novel positive allosteric modulators presented here and previously,⁶⁴ it appears that SH-053-S-CH3-2'F may possess a pharmacological profile appropriate for further fine tuning, by diminishing the potential of sedation, probably through an additional decrease of activity at $\alpha 1$ - and $\alpha 5$ - GABA(A) receptors. However, besides the in vitro affinity and efficacy data discussed in the present study, a future, more elaborate analysis of the substrate of behavioral effects of BZ site modulators shall take into account target site occupancy,

quantitative neuroanatomical distribution of distinct receptor subtypes (which is very inhomogeneous in the case of BZ-sensitive GABA(A) receptors), differences among animal species and the receptor reserve (if any) of the behavioral effect under investigation.¹²¹

Search for Subtype Selective Ligands for $\alpha 5\beta 3\gamma 2$ Subtypes

In order to further the understanding of the stable conformations of GABA(A) - benzodiazepine receptor bivalent ligands; the conformations of several bivalents were determined by low temperature NMR spectroscopy and confirmed by single crystal X-ray analysis. The stable conformations in solution correlated well with those in the solid state. The linear conformation was important for these dimers to access the binding site and exhibit potent *in vitro* affinity and was illustrated for $\alpha 5$ subtype selective ligands. Bivalent ligands with an oxygen-containing linker folded back upon themselves both in solution and the solid state. Dimers which are folded do not bind to Bz receptors.

Currently, transforming monomers into a bivalent ligand is one of the successful strategies for developing potent ligands with enhanced selectivity.⁴³⁵ Bivalent ligands are defined as compounds which contain two pharmacophores joined through a connecting unit or linker. The general structure for bivalent ligands is described as P-X-P (P: pharmacophore; X: linker) (see Table 36). The proper selection of a suitable linker X is crucial for potent receptor binding.

Table 36. Stable conformations of selected compounds**A****B****C**

Cmpds	Mono unit 1	Mono unit 2	Spanner	Stable Conformation		K _i (αnβ3γ2) = nM					
				X-ray	NMR	α1	α2	α3	α4	α5	α6
21^a	A	-	C ₂ H ₅	-	-	28.4	21.4	25.8	5.3	0.49	2 8.8
1	A	A	(CH ₂) ₃	linear	linear	>1000	>1000	858	1550	15	>2000
18	A	A	(CH ₂) ₅	-	linear	231	661	2666	ND	5.4	54.22
3	C	C	(CH ₂) ₃	-	linear	1852	4703	8545	ND	100.5	5000
32	A	A	CH ₂ OCH ₂	-	folded	3795	2694	1864	ND	76.14	ND
6^a	B	-	C ₂ H ₅	-	-	287	45	96	1504	13.8	1000
19	B	B	(CH ₂) ₂ O(CH ₂) ₂	folded	folded	460	5000	ND	ND	5000	5000
33	B	B	(CH ₂) ₃	linear	linear	236	7.4	272	>5000	194.2	>5000

a: monomer

Recent studies on the binding selectivity of the inverse agonist RY-80 (**31**) indicated preferential binding to α5 BzR/GABA(A) subtypes.⁶⁶ Therefore, the bivalent ligand Xli-093 (**1**) was developed by incorporating the pharmacophore of **31** with a three-carbon linker.⁶⁶ This bivalent ligand exhibited selective affinity for the α5 subtype and behaved as a selective antagonist of the effects of diazepam in oocytes only at the α5 subtype.

Effects at the other three diazepam-sensitive sites were minimal. Encouraged by this, a series of new bivalent ligands were designed and synthesized (Table 36).

It was hoped that these new dimers might exhibit enhanced selectivity and potency at the $\alpha 5$ BzR/GABA(A) subtypes. It was also expected that insertion of an oxygen atom into the linker might increase water solubility and hence enhance molecular hydrophilicity which should play an important role in the pharmacokinetic properties of the ligand.

The nature of the functional groups in a ligand plays an important role in receptor binding, of course, as well as the conformation in solution. The more information about the stable conformation(s) of molecules, the better the understanding of the structure-activity relationships. It was essential from the beginning of the present study to determine the conformation of these bivalent ligands, which contained 3 to 5 atom linkers, since the steric requirements for affinity to the Bz receptor must be satisfied.⁶⁶

In traditional medicinal chemistry, computer assisted molecular modeling programs and X-ray analysis contribute greatly in the search for stable conformations. However, some problems with these methods should not be neglected. Using computer modeling to determine the stable conformation of molecules containing many free rotating bonds, such as those contained in bivalent ligands, is difficult. Although X-ray crystallography is the ultimate arbiter of chemical structure, it has many limitations beyond the obvious need for crystals: it often does not reflect accurately the conformation in solution, nor is it informative regarding conformational equilibria. This information is crucial in drug design. However, NMR spectroscopy is a powerful technique in drug discovery and its role in conformational analysis cannot be surpassed by other spectroscopic methods.^{436, 437}

Herein is described a method utilizing low temperature NMR for the determination of the solution stable conformation of a series of GABA(A) - benzodiazepine bivalent ligands with different monomeric units and linkers. The conformations in solution were determined by NMR spectroscopy and compared with those in the crystal structure. The combination of low temperature NMR and X-ray analysis provided accurate structural information required for understanding structure-activity relationships and drug design. The influence of the molecular structure of the linker on the conformation is also discussed.

Results

Recently it was shown the active dimer **1** existed in a linear conformation in the solid state while dimer **19** with a oxygen containing linker folded back upon itself, as illustrated in Figure 135.⁴³⁸⁻⁴⁴⁰

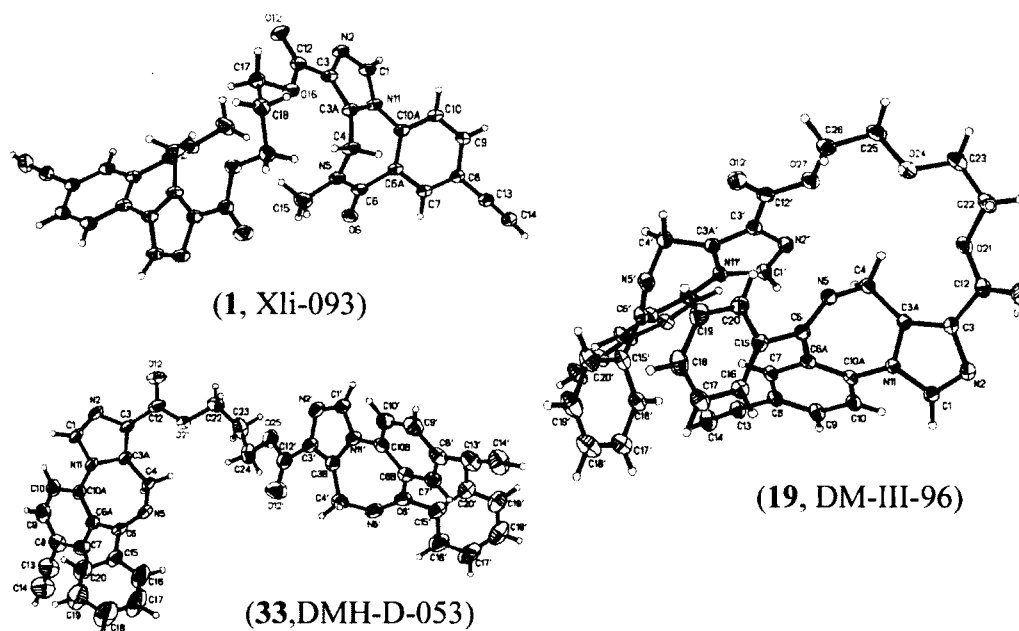


Figure 135. Crystal structures of Xli-093, DMH-D-053, and DM-III-96.

Since the bioactive conformation in solution may or may not parallel that in the crystal structure, the lowest energy solution structure must be established in order to correlate conformation with biological activity. Thus, NMR experiments at variable temperatures were performed and data were collected in different solvents. In methylene chloride or chloroform at room temperature, only a single set of signals was detected for both bivalent ligands **1** and **19**. At low temperature, it was found that the linear dimer **27** exhibited only a small splitting of about 3 Hz for some of the aromatic protons in the ^1H NMR spectra,⁴³⁸⁻⁴⁴² while two clearly separated sets of signals were observed for the folded dimer **19** (Figure 136). For example, as seen in Figure 136 for **19**, the signal of H1 (7.92 ppm at 298 K) was split into two peaks at δ 7.91 and 7.88 ppm, respectively, at 193° K. Similar results were observed in the ^{13}C spectrum where C1 (134.9 ppm at 298°K) split into two signals at 135.3 and 135.4 ppm at 198° K. The doubling of the signals is consistent with disruption of the symmetry between the two domains of the molecule as expected if **19** adopted a static folded structure similar to the crystalline state.

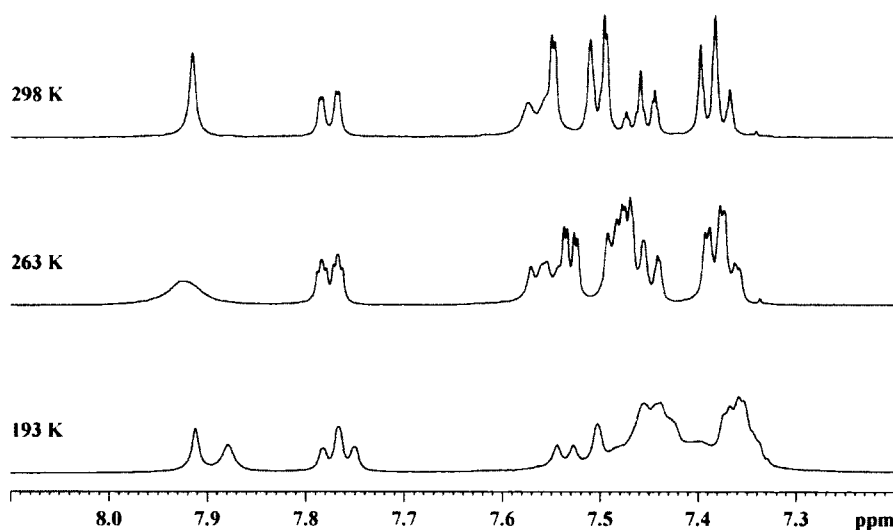


Figure 136. Aromatic region of ^1H NMR spectra of **19** in CD_2Cl_2 at variable temperatures.

However, the possibility could not be ruled out that the split in the signals was caused by slowing a dynamic process within each domain, such as conformational interconversion of the seven-membered ring. In order to investigate this possibility, the NMR spectra of the monomer **6** were run at low temperature as well. At temperatures as low as 173 K only one set of signals was observed in both the ^1H and ^{13}C NMR spectra of **6** (Figure 137).^{437, 443-445} At lower temperatures, however, this was quite different from what was observed for dimer **19** at room temperature; the spectra of **6** and **19** were indistinguishable at 25°C. Moreover, some additional line broadening of some of the aromatic signals was observed at the lowest temperature in both the monomer **6** and in its dimer **19**.

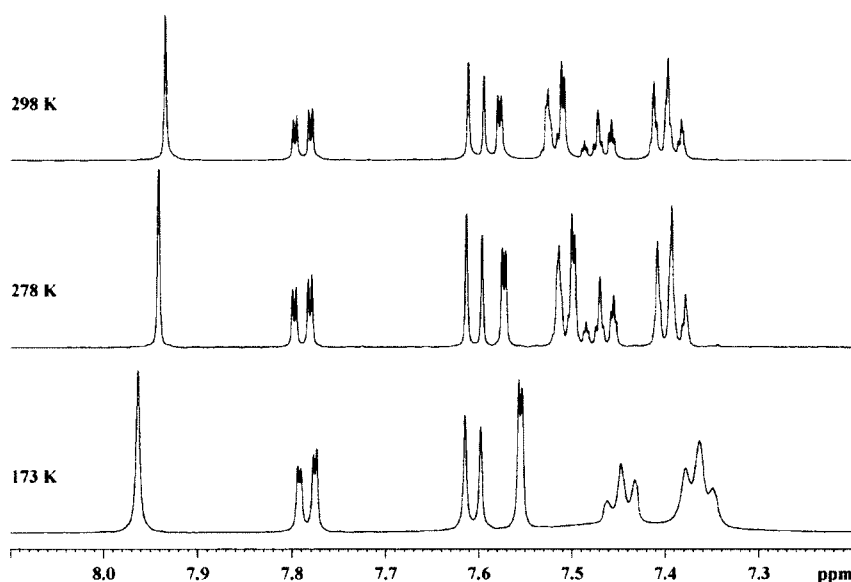


Figure 137. Aromatic region of ^1H NMR spectra of **6** in CD_2Cl_2 at different temperatures.

The analysis of these data indicated that the line broadening at the lowest temperature was due to one of the conformational processes mentioned above, whereas the doubling of the peaks in **19** was caused by the presence of two domains. Certainly an interdomain interaction existed between the two heterocyclic units of **19**, but not in monomer **6**. It was therefore concluded the internal mobility of the molecule decreased when the temperature was lowered which permitted observation of the two sets of signals of **19** on the NMR time scale. It was thus suggested that only when the molecule preferred the folded conformation in solution were two sets of signals observed. The preferred conformations of the molecules in CDCl_3 and CD_2Cl_2 correlated quite well with those observed in the crystal structures (Table 36).

The study was then expanded by varying the nature of the linker and monomer. Dimers **18** and **32** contain the same monomeric unit as **1**, whereas **33** contains an all

carbon linker. It was found that **1**, **3**, **18**, and **33** exhibited only one set of NMR signals at low temperature, whereas the NMR signals of ligands **19** and **32** split into two sets at low temperature. Low temperature NMR studies were performed in CD₂Cl₂. It was concluded that **19** and **32** preferred a folded conformation, while **1**, **3**, **18**, and **33** assumed a linear conformation. These conclusions are supported by a crystal structure obtained for bivalent ligand **33** which indicated **33** was present in a linear conformation in the solid state. These results are illustrated in Table 36.

Since the goal was to design and synthesize bivalent ligands for biological applications in aqueous solution, the question arose: Do the conformations in CDCl₃ or CD₂Cl₂ resemble those in aqueous solution? Attempts to run the NMR experiments in water failed since the ligands were not sufficiently soluble in D₂O. However, the spectra of both the linear and folded dimer **1** and **19** could be carried out in MeOH-*d*₄. The solvating properties of methanol, of course, more closely resemble those of water, and this more closely mimics aqueous physiological condition as well. The conformations of dimers in MeOH-*d*₄ were consistent with conformations in hydrophobic solvents.

Discussion

From the results described above, it is clear that dimers which contain an oxygen atom in the linker tend to adopt a folded conformation. Analysis of these data indicated in the hydrophilic solvent, **19** also had a higher tendency to fold back upon itself than **1**, as it did in the hydrophobic media (Figure 138 and Figure 139). In fact, the tendency of **19** to assume a folded structure appeared to be higher in methanol than in CD₂Cl₂ or CDCl₃, as the free rotation of the molecule was limited (Figure 139). On the other hand, for dimer **27**, which preferred a linear structure in the solid state and in lipophilic

solvents, only one set of signals was observed at room temperature in MeOH- d_4 (Figure 138).

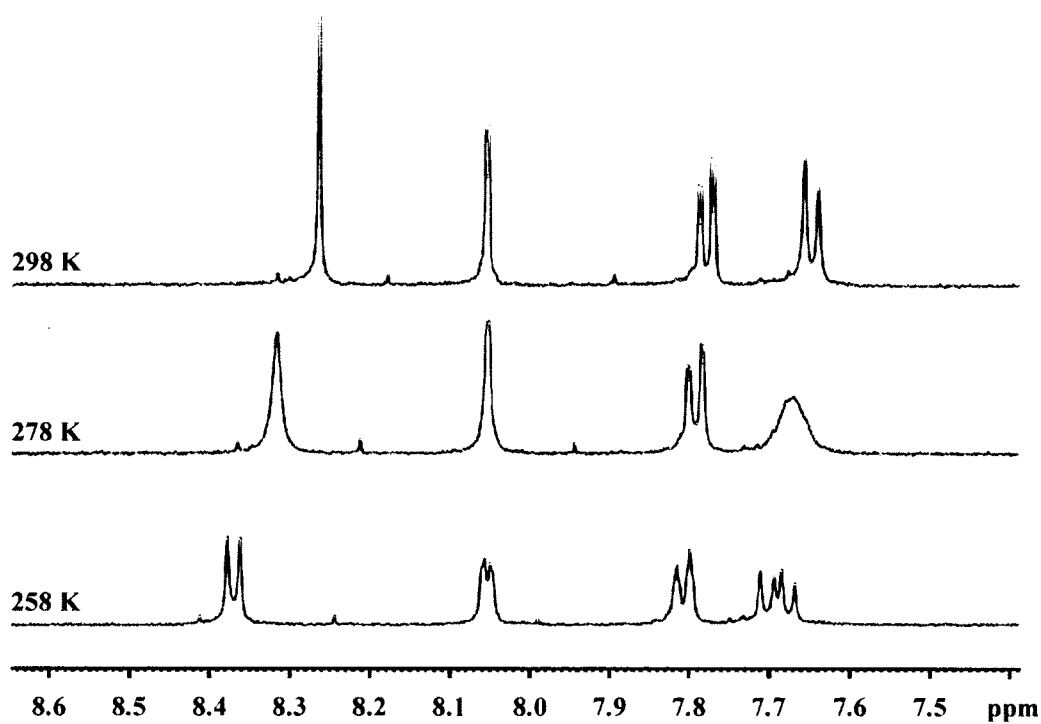


Figure 138. Aromatic region of ^1H NMR spectra of 1 in $\text{MeOH-}d_4$ at different temperatures

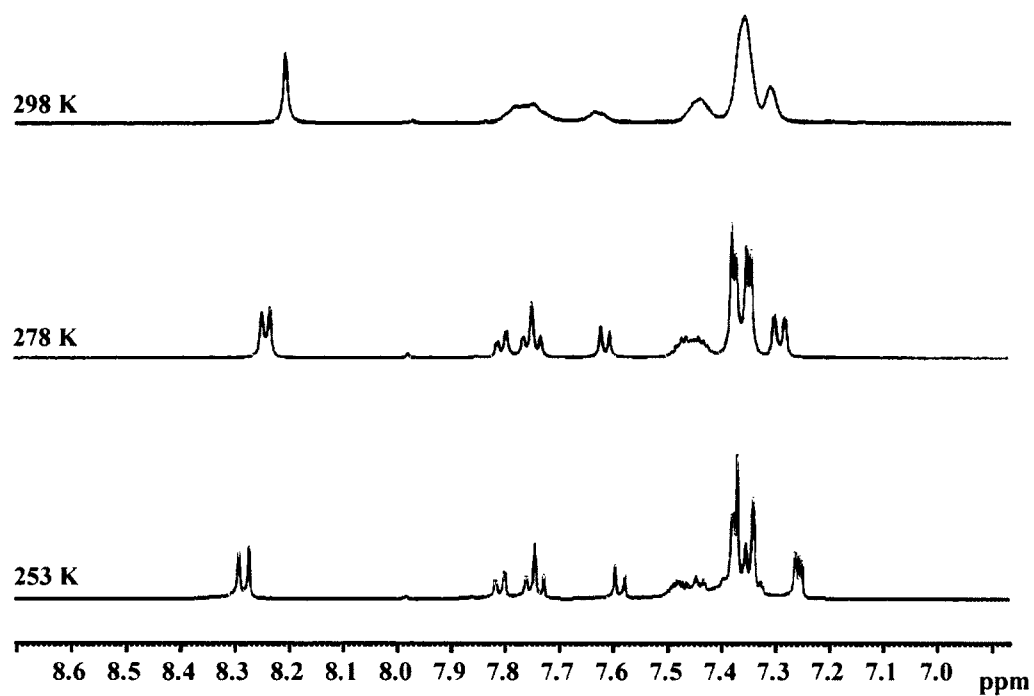


Figure 139. Aromatic region of proton spectra of 19 in MeOH-*d*₄ at different temperatures.

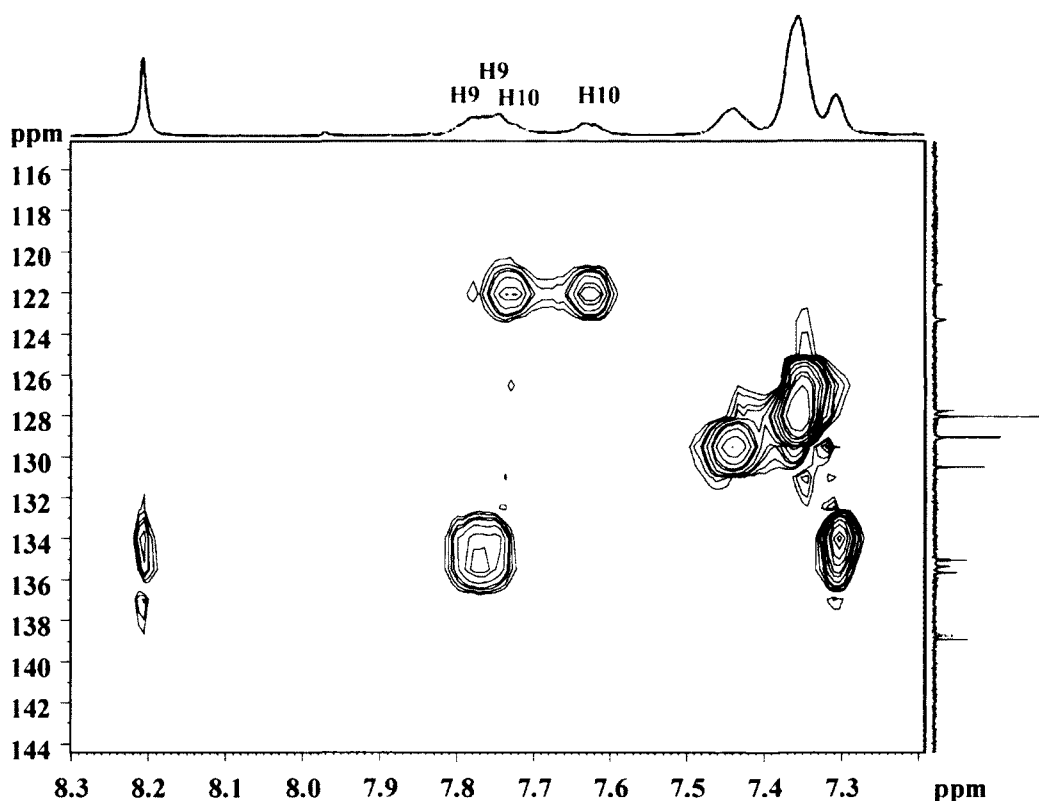


Figure 140. Partial HSQC spectrum of **19** in MeOH-*d*₄ at 298 K.

It is interesting to note that in the preparation of the samples, dimer **1** was less soluble in MeOH-*d*₄ than was **19**. It has been established that ligands are easier to dissolve in a solvent when the ligands surface energy can be minimized. Bivalent ligand **19** was more polar than dimer **1** and has a higher tendency to fold back. Consequently, **19** was presumably, easier to dissolve in methanol because its surface energy was minimized. On the other hand, when ligand **21** was dissolved in a more polar solvent such as methanol, the surface energy may be forced to be minimized.

Since the conformation of molecules **1** and **19** in methanol agree with those in CD₂Cl₂ or CDCl₃, the behavior of these ligands in CD₂Cl₂ or CDCl₃ should reflect those in aqueous solution. The stable conformation of the compounds determined in CD₂Cl₂ or

CDCl_3 were correlated with the newly generated receptor binding data (Table 31). In the pharmacophore/receptor model, the bivalent ligands in the linear conformation align well (Figure 141).

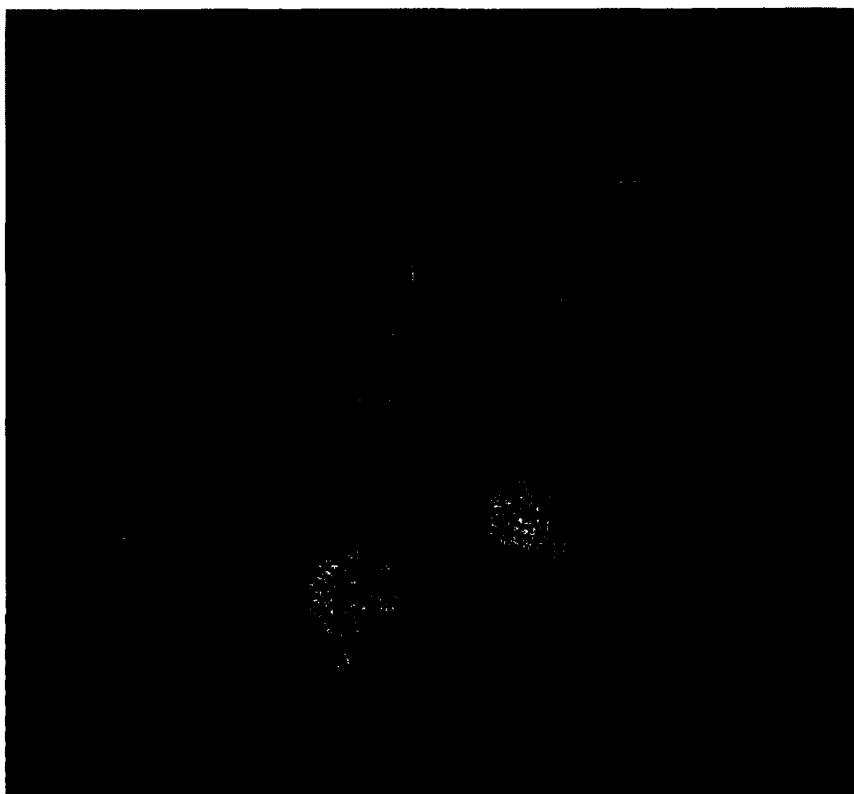


Figure 141. Bivalent ligand **1** (Xli093) aligned in the included volume of the pharmacophore/receptor model for the $\alpha 5\beta 3\gamma 2$ subtype.

Importantly, bivalent ligands **1**, **3**, **18**, and **33** with carbon only linkers preferred the linear conformation as the stable conformation, independent of the number of linker atoms. In contrast, replacing the middle carbon of either linker $(\text{CH}_2)_3$ or $(\text{CH}_2)_5$ with an oxygen atom altered the stable conformation of the molecules **32** and **19** from linear to folded. The only difference between bivalent pairs **1** and **32** with linear and folded conformations as the stable ones, respectively, was the center atom. In compound **1** the middle atom was carbon, while in **32**, oxygen was present. Consequently, it was decided

to focus attention on the conformational difference between carbon and oxygen containing linkers.

It was well-known^{436, 437, 443-445} that the carbon chain in both small molecules and polymers favored the *anti* conformation which results in a linear arrangement of atoms. From examination of the linkers (Figure 142), it was easily seen that linkers **C** and **D** can be regarded as oligomers of oxymethylene (OCH_2)₂ and oxyethylene (OCH_2CH_2)₂.

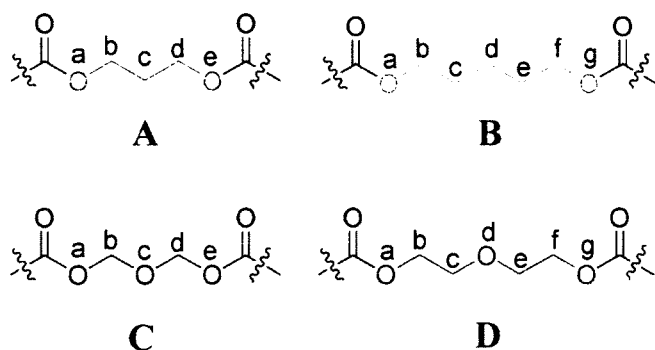


Figure 142. The linkers of the bivalent ligands.

It was well documented that the preference for the *gauche-gauche* conformation^{437, 446, 447} of a simple open-chain acetal such as dimethoxymethane ($\text{CH}_3\text{OCH}_2\text{OCH}_3$) could be predicted on the basis of the anomeric effect and related stereoelectronic effects. In this conformation the polar X–O bonds are favorably oriented such that a lone pair orbital of the oxygen atom was almost antiperiplanar to the X–O bond (Figure 143, lone pair orbital and X–O bond in same color). This permits maximum overlap of the n orbital of the oxygen atom with the σ^* orbital of the X–O bond. This was not possible in the *anti*-

anti or *gauche-trans* conformations and the two rabbit-ear interactions⁴⁴⁸⁻⁴⁵⁰ (Figure 143) engendered by each pair of adjacent oxygen atoms in the *anti-anti* conformer are avoided.

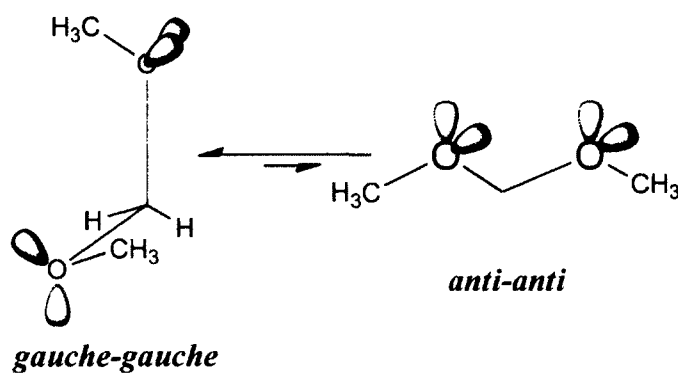


Figure 143. The conformations for dimethoxymethane.

Furthermore, in the related polymer of dimethoxymethane with the two-bond repeating sequence, poly(oxymethylene) (**POM**), the *gauche* conformation was, in fact, markedly preferred over *trans* and the polymer existed in a helical (all *gauche*) conformation⁴⁵¹ rather than in the all-*anti* one.

Similarly, much effort has been spent on the investigation of the conformational characteristics of 1,2-dimethoxyethane (glyme, $\text{CH}_3\text{OCH}_2\text{CH}_2\text{OCH}_3$) as a model molecule for understanding the conformations of poly(oxyethylene) (**POE**). It had long been established that POE chains have a large fraction of bonds in *gauche* conformations and assumed a helical conformation overall.⁴⁵²⁻⁴⁵⁶ It has been proposed that the oxygen

gauche effect⁴³⁷ and 1, 5-CHO interaction⁴⁴³ within the molecule were responsible for the *gauche*-rich conformations.

Based on this pioneering work, the correlation was made that the conformation of the linkers in the bivalents **1**, **3**, **18**, and **33** and **32** and **19** adopt *anti* (**B**), *gauche-gauche* (**C**), *trans-gauche-trans* (**D**) conformations, respectively, regardless of the monomeric units which comprise them. The arrangement in space (disregarding the direction) of every unit in the linkers is depicted in Figure 144. The end-to-end distance of each unit (**C** and **D**) which adopted the *gauche* conformation was shorter than the one in the *anti* conformer. The more units in the linker, the shorter the *gauche* linker. Moreover, it was recognized that the C–O bond length (1.43 Å) is often appreciably shorter than the C–C bond (1.54 Å).³²⁴ Therefore, it was believed that the linkers with the oxygen atom in the middle favored the helical conformation and rendered the two monounits in each dimer sufficiently close to each other with suitable dihedral angles to facilitate the intramolecular lipophilic-lipophilic (aromatic-aromatic) interaction. This was regarded as one of the most important factors to stabilize the folded structure as the preferred conformation.³¹⁰ For these same reasons, bivalent ligands with the linker **B** adopted the linear conformation.

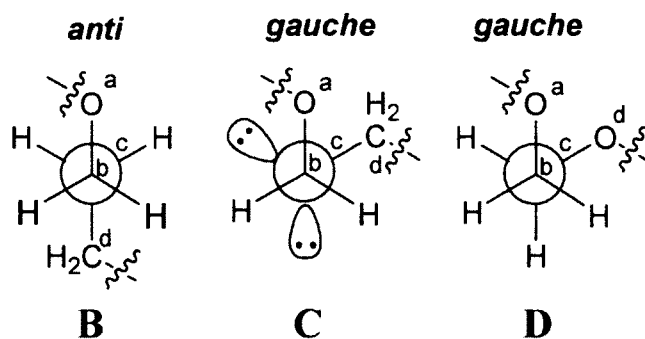


Figure 144. Newman projection for linkers B, C and D.

For the higher analog of **POM** and **POE**, namely, poly(trimethylene oxide) $[(\text{CH}_2)_3\text{O}]_x$ (**POM**₃), *trans-gauche-gauche-trans* was slightly preferred over all-*trans* and *trans-trans-gauche-trans* conformers in the crystalline state.^{215, 457, 458} The preference for the *gauche* state in this case was only 0.2 kcal/mol where as in the **POM** and **POE** examples was 1.5 and 0.4 kcal/mol, respectively.^{19, 360} Since the energy difference between *gauche* and *trans* was low, the linker **A** had more flexibility than the other linkers (**C** and **D**) to rotate freely and less tendency to occur as *gauche*. This could lead to improper end-to-end distances or dihedral angles for the interaction between the aromatic monounits. Hence dimers connected with linker **A** could not be stabilized in the folded conformation even though the same aromatic monounits were contained in the molecules.

Bivalent ligands were evaluated in competition binding assays for specific GABA(A) membrane proteins using [³H] flunitrazepam as the radiolabel. This assay measures the ability of the ligand to displace flunitrazepam. Data is reported as K_i according to the Cheng-Prusoff equation.³⁶⁰ Biological data are presented in Table 36 for dimers synthesized using different spanners (or linkers). The linkers in **19** and **32** contained an

oxygen atom. Compounds **1**, **3**, **18**, and **33** contained all carbon linkers. Binding data indicate decreased affinity when bivalents contain an oxygen atom in the linker. Compounds **1** and **18** showed increased selectivity for the $\alpha 5$ subtype as compared to parent monomer **21**. Compound **32** which was analogous to **1** with the exception of the oxygen atom present in the linker, bound with less affinity at the $\alpha 5$ subtype. Likewise bivalent **33** showed increased selectivity versus monomer **6**. However, the bivalent **19** containing an oxygen atom in the linker did not bind. The data suggests that dimers which contain a single oxygen atom in the linker bind less (decreased affinity) to the Bz receptor. This is due to their propensity to adopt a folded conformation. A strategy to increase hydrophilicity and avoid a folded conformation is to extend the linker length and insert two opposing oxygen atoms. This research is currently underway.

Comparison of the results of low temperature NMR studies to crystal structures has provided enough information to demonstrate that low temperature NMR can be used as a quick method to identify dimeric ligands with a tendency to fold back upon themselves, as compared with those preferring a linear conformation. A correlation with binding data shows that the suitability of a ligand in the $\alpha 5$ BzR/Gabaergic subtype is heavily influenced by its conformation in solution. Variable temperature NMR thus can be used as a tool for screening bivalent ligands for their in vivo suitability. It is also clear the presence of one oxygen atom in the linker was the principle cause for the dimer to fold back onto itself. Ligands which contain two offsetting oxygen atoms in the linker are now under study in our laboratory. Synthesis of bivalents was carried out using the techniques developed by Li.⁴⁵⁹

Chemistry

In brief, isatoic anhydride and sarcosine were heated in DMSO, followed by bromination to provide the bromide . The conversion of bromide into the imidazobenzodiazepine , followed the classic work of Fryer et al. of the Roche group.³⁰² ³⁰³ This bromide was converted into the silyl by a Heck-type coupling reaction^{303, 304} and the silyl group was removed in high yield on treatment with TBAF/H₂O/THF.³⁰⁵ Hydrolysis of the ester function provided the carboxylic acid in excellent yield and this material was subjected to a standard CDI-mediated coupling reaction to furnish bivalent ligand XLi093 **1** in 73.4% yield.

8-Ethynyl-5,6-dihydro-5-methyl-6-oxo-4H-imidazo[1,5-a][1,4]benzodiazepine-3-carboxylic acid **14:** Ethyl 8-ethynyl-5,6- dihydro-5-methyl-6-oxo-4H-imidazo[1,5-a][1,4]benzodiazepine-3-carboxylate (1.5g, 5.3 mmol) was dissolved in EtOH (100 mL), after which aq 2N NaOH (15 mL) was added to the solution. The mixture which resulted was heated at 70 °C for 1 hr. After the mixture was cooled to rt, the EtOH was removed under reduced pressure. Aqueous 2N HCl was added to the residue to bring the pH to approximately 3~4. A precipitate formed and was removed by filtration, washed with water (3 X 50 mL) and dried. The 3-carboxylic acid was obtained as a white solid in 90% yield: mp 315-316 °C; IR (KBr) 3421, 1750, 1640, 1497, 1210 cm⁻¹; ¹H NMR (CD₃OD) δ 3.28 (s, 3H), 3.74 (s, 1H), 4.50 (br, 1H), 5.22 (br, 1H), 7.69 (s, 1H), 7.80 (dd, 1H, J=2.5 Hz, J=10 Hz), 8.20 (s, 1H); MS (EI) m/e (relative intensity) 281 (M⁺, 80), 277 (100), 263 (60), 235 (84), 207 (55). Anal. Calcd for C₁₅H₁₁N₃O₃: C, 64.04; H, 3.94; N, 14.95. Found: C, 64.40; H, 4.12; N, 14.76.

1,3-Bis(8-acetyleno-5,6-dihydro-5-methyl-6-oxo-4H-imidazo[1,5a][1,4]benzodiazepine-3-carboxy) propyl diester 1 (XLi093). To a solution of carbonyl diimidazole (230.3 mg, 0.57 mmol) in anhydrous DMF (5 mL) was added 8-ethynyl-5,6-dihydro-5-methyl-6-oxo-4H-imidazo[1,5-a][1,4]-benzodiazepine-3-carboxylic acid (200 mg, 0.71 mmol). The solution which resulted was stirred for 2 h at rt. Analysis by TLC (silica gel) indicated the absence of starting material. To the solution which resulted was then added 1,3-propanediol (27.1mg, 0.36 mmol) in dry DMF (0.5 mL) and also DBU (114.2 mg, 0.75 mmol) in dry DMF (0.10 mL) at rt. The mixture was stirred at rt for 4.5 h until analysis by TLC (silica gel) indicated the reaction was complete. The reaction mixture was then poured into ice water (30 mL) and extracted with CH₂Cl₂ (3 x 50 mL). The combined organic layer was washed with H₂O (5 x 50 mL), brine and dried (Na₂SO₄). The solvent was removed under reduced pressure and the residue was purified by flash chromatography (silica gel, EtOAc/CH₃OH, 4 : 1) to provide **27** (157 mg) as a white solid in 73.4% yield. **102**: mp >230 °C (Dec.); IR (NaCl) 3247, 1725, 1641, 1359, 1253, 1061 cm⁻¹; ¹H NMR (300 MHz, CDCl₃) δ 2.37(m, 2H), 3.24(s,2H), 3.26 (s, 6H), 4.40(s, 2H), 4.57(t, 4H, J= 6.2Hz), 5.31(br, 2H), 7.41(d., 2H, J=8.3 Hz) 7.72(d,d, 2H, J = 6.43Hz, and J = 1.86Hz), 7.89 (s,2H), 8.19(d, 2H, J = 1.76Hz); ¹³C NMR (75.5 MHz, CDCl₃) δ 26.2, 34.4, 40.7, 60.2, 78.7, 79.7, 120.4, 121.6, 127.1, 127.7, 130.1, 133.4, 134.1, 134.9, 161.3, 164.1; MS (FAB,NBA) *m/e* (relative intensity) 603(M⁺+1, 100). This material was employed for the X-ray crystal structure. It was homogenous in two independent TLC systems [R_f =0.31 in EtOAc/CH₃OH, 4 :1; R_f =0.32 in CH₂Cl₂/CH₃OH, 9 : 1]. Anal. Calcd for C₃₃H₂₆N₆O₆ •2/3 CH₃OH: C, 64.81; H, 4.63; N, 13.47. Found: C, 64.56; H, 4.72; N, 13.76.

1,3-Bis(8-ethyl-5,6-dihydro-5-methyl-6-oxo-4H-imidazo[1,5a][1,4]benzodiazepine-3-carboxy) propyl diester (XLi356): **1,3-Bis(8-**

acetyleno-5,6-dihydro-5-methyl-6-oxo-4H-imidazo[1,5a][1,4]-benzodiazepine-3-carboxy) propyl diester **1** (500 mg, 0.83 mmol) was dissolved in EtOH (150 mL) after which Pd/C (176 mg) was added in solution at rt. The slurry was stirred for 5h under one atmosphere of H₂(bench top, balloon of H₂). The catalyst was removed by filtration and washed with EtOH. The EtOH was removed under reduced pressure to furnish a residue. This material was purified by flash chromatography (silica gel, EtOAc : EtOH/8 : 2) to provide **Xli356** (504 mg, 99%) as white crystals: mp 125-133°C; IR (NaCl) 3407, 2964, 2358, 1725, 1640, 1499 cm⁻¹; ¹H NMR (CDCl₃) δ 1.29 (m, 6H), 2.39(m, 2H), 2.78 (dd, 4H, J=7.5 Hz, 15.1 Hz), 3.26 (s, 6H), 4.48 (br, 2H), 4.56 (t, 4H, J=6.1 Hz, 12.2 Hz), 5.16(br, 2H), 7.33 (d, 2H, J = 8.2Hz), 7.48 (d, 2H, J=1.8 Hz), 7.89 (t, 4H, J=3.2 Hz, 5.3 Hz), 8.15; MS(EI) *m/e* (relative intensity) 611(M⁺+1, 100). Anal. Calcd for C₃₃H₃₄N₆O₆ •2H₂O: C, 61.33; H, 5.92; N, 13.00. Found: C, 61.74; H, 5.91; N, 12.63.

Computational Assessment of Benzodiazepine Influence on Contextual Memory

It has been hypothesized that ligands, acting selectively on GABA(A) receptors containing the $\alpha 5$ subunit, may prove useful in the remediation of age related cognitive loss. Consequently, the chemical determinants of selective binding and subsequent activation of $\alpha 5\beta 2\gamma 2$ GABA(A) receptor subtypes were examined with the aim of gleaning the characteristics important to this selectivity. Ligand-receptor binding and electrophysiological responses were characterized in cells expressing defined GABA(A) receptor isoforms. A 3D-pharmacophore was developed from an initial diverse training set and was used as an initial basis for multivariate discriminant, fragment and 3D-QSAR analyses and used to develop criteria for selection of new compounds that should exhibit

optimal characteristics. The electrostatic potential near the ligands terminal substituents was found to correlate well with a compounds ability to exhibit 100-fold binding selectivity towards the $\alpha_5\beta_2\gamma_2$ versus $\alpha_1\beta_2\gamma_2$ isoforms. Specific chemical properties, such as the Sterimol L parameter and HOMO-LUMO differences of fragments were also found to correlate with a compounds activity. Compounds with promising profiles were further assessed for their ability to attenuate scopolamine-induced impairment of fear conditioned contextual memory in mice. In marked contrast to prior literature reports, the electrophysiological nature of the compounds relative to the $\alpha_5\beta_2\gamma_2$ GABA(A) receptor were found not to be highly predictive of whether the compound was able to attenuate scopolamine induced cognitive impairment in mice. Examples of a weak inverse agonist and antagonists with 100-1000 binding selectivity with respect to $\alpha_5\beta_2\gamma_2$ GABA(A) are shown to have an ability to reverse scopolamine induced cognitive impairment indicating that selective $\alpha_5\beta_2\gamma_2$ GABA(A) antagonists may be effective memory agents lacking sedative, anxiogenic, and/or convulsive side effects.

It has long been known that agonist binding to the benzodiazepine binding site lead to cognitive impairment in both animal and humans.⁴⁶⁰ This impairment is thought to occur by augmentation of GABA-mediated Cl^- flux through the receptor and has been demonstrated to prevent the induction of Long Term Potentiation (LTP) in rodent hippocampal neurons.⁴⁶¹ Conversely, BDZ ligands that attenuate GABA-mediated Cl^- passage into neurons, potentiates LTP in rodent hippocampal neurons⁴⁶² resulting in the facilitation of learning and memory.^{170, 296, 297, 463} However, challenges exist in regard to developing benzodiazepine inverse agonists for therapeutic utilization, including the potential for convulsion, anxiogenesis and hyperactivity. Differing pharmacological

profiles associated with individual GABA(A) receptor isoforms has brought forward the potential to selectively target specific isoforms either through binding selectivity or particular activational profiles. Ligands that behave like an agonist at one behavioral end point and behave qualitatively different (i.e. as an antagonist, inverse agonist or no effect) at another behavioral end point^{48, 395} can often be explained by differences in binding affinities and/or activation profiles of these BDZR ligands at the multiple GABA(A) receptor subtypes throughout the brain. Therefore, this suggests that behavioral influence such as cognitive enhancement may, in principle, be separated within a compound class from undesirable side effects. For example, compounds such as Ro15-1788, R015-4513, ZK-93426 and Ro41-7812 were observed to lack sedative or convulsive properties yet are able to attenuate contextual memory impairment in a mouse model of cholinergic hypofunction.⁴⁶⁴⁻⁴⁶⁶ Interestingly, BDZR ligand antagonist that do not alter the efficacy of GABA, nevertheless possess some degree of intrinsic efficacy.⁵⁰

The association of GABA(A) receptor component composition with observed receptor mediated physiology has been advanced through the use of transgenic mice exhibiting specific point mutations within α subunits leading to altered BDZ ligand binding and activation.⁴⁶⁷ From such efforts, associations have been put forward including the involvement of the $\alpha 1$ subtype in sedative and myorelaxant effects while $\alpha 2$ and $\alpha 3$ subtypes were found to be associated with anxiolytic and anticonvulsant effects.^{19, 21, 121, 468} As stated previously, the $\alpha 5$ subunit, which is primarily expressed in the hippocampus and comprises about 20% of the GABA(A) receptors found there, has been suggested to be involved in associative temporal and spatial memory.^{293, 294} Using transgenic “knockin” mice Crestani et al.,^{299, 312, 314} demonstrated a critical role of

hippocampal extrasynaptic GABA(A) receptors containing the $\alpha 5$ subunit in associative learning. They argue “extrasynaptic $\alpha 5$ subunit containing GABA(A) receptors contribute to the regulation of dendritic excitability of hippocampal pyramidal cells with the efficacy of excitatory inputs, thereby contributing to synaptic plasticity in regulating the temporal association of “threat cues”. Furthermore, Maubach et al.,^{285, 298} hypothesized that a compound with inverse agonism selective for $\alpha 5$ -containing GABA(A) receptors might enhance hippocampally mediated cognitive function. Until recently, only modest progress had been made in the design of receptor-subtype specific ligands, however this is changing with a variety of papers now reporting success in achieving selectivity in the synthesis of BDZ ligands that exhibit 100-fold selectivity for particular GABA(A) receptors isoform.^{315, 316, 461} Unfortunately, BDZ ligands that exhibit true specificity to a single GABA(A) receptor subtype (affinities of a 1000 fold difference between one GABA(A) receptor isoform and all the other isoforms) are to date, not available. This can be achieved by either binding specificity or through activation specificity, in which a compound that does not possess binding specificity but instead elicits specificity through the preferential activation of only one subtype combination. Unfortunately, systematic diversification of a ligand template in order to increase binding selectivity to a particular GABA(A) receptor isoform often results in a deleterious impacts on its activation profile. Therefore, it’s important to understand the links between ligands’ physiochemical features and its binding affinity as well as the nature of the activity manifested at a particular receptor isoform.

Senile dementia of the Alzheimer’s type (SDAT) and age-related memory decline arises from progressive failure of the cholinergic system, leading to impaired memory

and deterioration of other cognitive functions.²⁸⁵ The reduction of postsynaptic inhibition of cholinergic excitation in the hippocampus may attenuate the impact of this process by influencing the functional regulatory pathways involved in cognition by manipulating the inhibitory nature of the neurotransmitter GABA. Interestingly, while most neurotransmitter receptor systems are degenerating in the brains of individuals with SDAT, the GABAergic infrastructure is relatively well preserved including the GABA(A) receptor population that contains the $\alpha 5$ subunit.^{469, 470} Benzodiazepine receptor ligands modulate GABA's regulatory influence on numerous neuronal pathways, including the cholinergic pathways of the basal forebrain that project to the hippocampus. In situations where the cholinergic excitation is lessened due to the loss of cholinergic neurons, as it is in the case of SDAT, precise reduction in GABAergic inhibition in brain regions where the weakened cholinergic neurons project could potentially augment the functional impact of the ACh released.⁴⁷¹ Moreover, numerous cognitive deficit models of cholinergic hypofunction, both human and animal, benefit cognitively when GABA activity is reduced.^{472, 473} Lastly, lesion studies demonstrate that animals with 50-70% loss of cortical cholinergic fibers exhibit improved cognitive performance from BDZ ligand treatment.^{474, 475} As the loss of cholinergic neurons in aging and SDAT is commonly in the 40-70% range⁴⁷⁶⁻⁴⁷⁸ until the very last stage, the effects of BDZR inverse agonists on restoring neural transmission in animals with partial loss of cortical cholinergic inputs suggest development of specific BZD ligands for the treatment of cognitive decline associated with aging and SDAT is warranted.

Large changes in binding and pharmacological activity may be induced by small structural changes to active ligands. This has far reaching consequences in both lead

optimization but also in discovering new leads from pharmacophore based chemical database searches. This is also the basis for the 'latent-hit' phenomena in chemical databases.¹²¹ Therefore, multivariate statistical approaches embodied in QSAR and chemometrics are required to obtain meaningful correlations linking structural variation with changes in pharmacology. This affords one the possibility of detecting subtle patterns modulating either binding/non-binding and/or activation through a particular receptor subtype. However, small changes in a compounds' structural features can also elicit deleterious effects on binding and/or activation at a given GABA(A) receptor isoform. From such approaches there have been numerous instances of success in rational design^{297, 304, 371} including the development of selective COX-2 inhibitors and selective serotonin reuptake inhibitors. Both structure based design⁴⁷⁹ and indirect design^{187, 480} approaches have been employed in guiding chemical transformation of lead compounds initially identified via mass-screening. Several groups have investigated the structural/chemical basis for binding⁴⁷⁷ or activational selectivity of particular GABA(A) receptor subtypes affecting memory.^{231, 267, 274, 481} Both avenues are viable strategies for discovering pharmacological agents that may be palliative for senile dementia of the Alzheimer's type.

Considerable effort has been made in order to develop pharmacophores that characterize the binding of BDZ ligands to their respective binding site between the α and γ subunits of the various GABA(A) receptor isoforms. Our research group has employed hundreds of benzodiazepine site ligands from 10 diverse templates to develop the "Comprehensive pharmacophore". To the point of the present study, several groups of compounds synthesized by this group have proven to be a fruitful testing ground to

elucidate global features that are important for binding selectivity to α_5 -containing GABA(A) receptors, inverse agonism at this receptor subtype and scrutiny as to the importance of inverse agonism at these subtypes upon memory, learning and convulsions.

Other smaller studies include a study of 21 flavanoids⁴⁶¹ and an analysis of BDZR compounds from diverse templates that bind to and activate GABA(A) receptors involved in sedation and anxiolysis.^{476, 480, 482} While past validation efforts involved using these pharmacophores to extract compounds with binding affinity and activity at the behavioral endpoint of interest, the pharmacophores themselves are for the most part 'non-specific'³⁴⁵ in that compounds extracted from chemical database searches bound to and activated multiple GABA(A) receptor isoforms. 3D-QSAR (COMFA and COMSIA) based on these overlap rules in fact results in equivalent statistics for binding models of the ligands regardless of the GABA(A) receptor composition (ie. $\alpha_1\beta\gamma_2$ $\alpha_2\beta\gamma_2$ $\alpha_5\beta\gamma_2$ $\alpha_6\beta\gamma_2$) (D. Harris; unpublished). As pointed out previously, it is important to remember the pharmacophores employed here were developed based on the binding affinity of the rigid ligands designed earlier by Trudell.¹⁸⁷

The core aim of this study was to address the structural/chemical basis for selectively influencing cognition through modulation of α_5 subunit containing GABA(A) receptors. This first step in this process is to understand the structural constraints necessary to elicit both potent and selective binding at GABA(A) receptors that contain the α_5 subunit, closely followed by developing an understanding of how the structural features influence the resulting electrophysiology at α_5 subunit containing GABA(A) receptors. Once this is achieved compounds with favorable profiles can then be further evaluated for cognitive influence in a mouse model of cognitive impairment.

Organization of the Study

In vitro and *in vivo* data from both in-house and literature sources were used to investigate the underlying basis of selective binding and activation of GABA(A) receptors containing the $\alpha 5$ subunit. Previously BDZ ligands were examined for their ability to influence spontaneous locomotor activity and contextual memory in adult C57Bl/6 mice.¹⁹ However, the compounds used in those studies were not selective enough in regards to binding to the $\alpha 5\beta 3\gamma 2$ GABA(A) receptor isoform in order to establish that this receptor isoform is capable of influencing contextual memory on its own at a level that would be considered therapeutically viable. Initial computational work on that original set of compounds (Figure 145) suggested that particular stereoelectronic descriptors (e.g Sterimol L parameter) were discriminants of whether a compound that exhibited reasonable binding affinity to the $\alpha 5\beta 3\gamma 2$ isoform could attenuate scopolamine-induced contextual memory impairment. This served as the initial criteria for selecting additional compounds to be used in the present study. In the current effort *in vitro* binding and electrophysiological assessments of the test set of compounds were used in conjunction with computational methods.¹²¹ Consequently, this enabled one to develop a QSAR representative of selective binding and activation. We then sought to correlate structural, electrostatic, thermodynamic, and electronic properties of both in-house and literature reported compounds of interest with their respective *in vitro* binding affinities and electrophysiological responses in cells only expressing one of the GABA(A) receptor variants. Compounds with desirable profiles were also assessed for their ability to attenuate contextual memory impairment in the previously characterized mouse model.³⁶⁶ The goal was to discover chemical discriminants that favor selective influence over $\alpha 5$ containing GABA(A) receptors in order to test the hypothesis that one

can selectively influence contextual memory via $\alpha 5\beta\gamma 2$ receptors alone. Through this process it was also felt one would limit side effects (ie. sedation, convulsion, etc) that typically arise from non-selective binding of a compound to multiple GABA(A) receptor isoforms. The first step was to compare/contrast initial pharmacophore models previously developed for contextual memory influence and sedation.³⁹⁶ The focus was restricted in the current work to binding affinities associated with just the $\alpha 1\beta\gamma 2$ and $\alpha 5\beta\gamma 2$ receptor isoforms. Pharmacophore definitions were validated by using them to search chemical databases to find ‘hits’ that were then tested for binding to the $\alpha 1\beta\gamma 2$, and/or $\alpha 5\beta\gamma 2$ GABA(A) receptor isoforms expressed individually in cell expression system. Physiochemical properties of compounds from the training set were then evaluated in regards to the requirements of the pharmacophores (alignment rules). Correlations were sought between chemical properties and both binding and activation of the $\alpha 5\beta\gamma 2$ GABA(A) receptor isoforms. This was achieved by multivariate discriminant analysis as well as 3D-QSAR/COMSIA and fragment QSAR approaches in order to identify descriptors that offered discrimination between $\alpha 1\beta\gamma 2$ and $\alpha 5\beta\gamma 2$ receptor isoforms. Through this approach it was determined which chemical features are intimately connected with a compound’s ability to exhibit binding specificity and/or a desirable electrophysiological activation profiles (Figure 145).

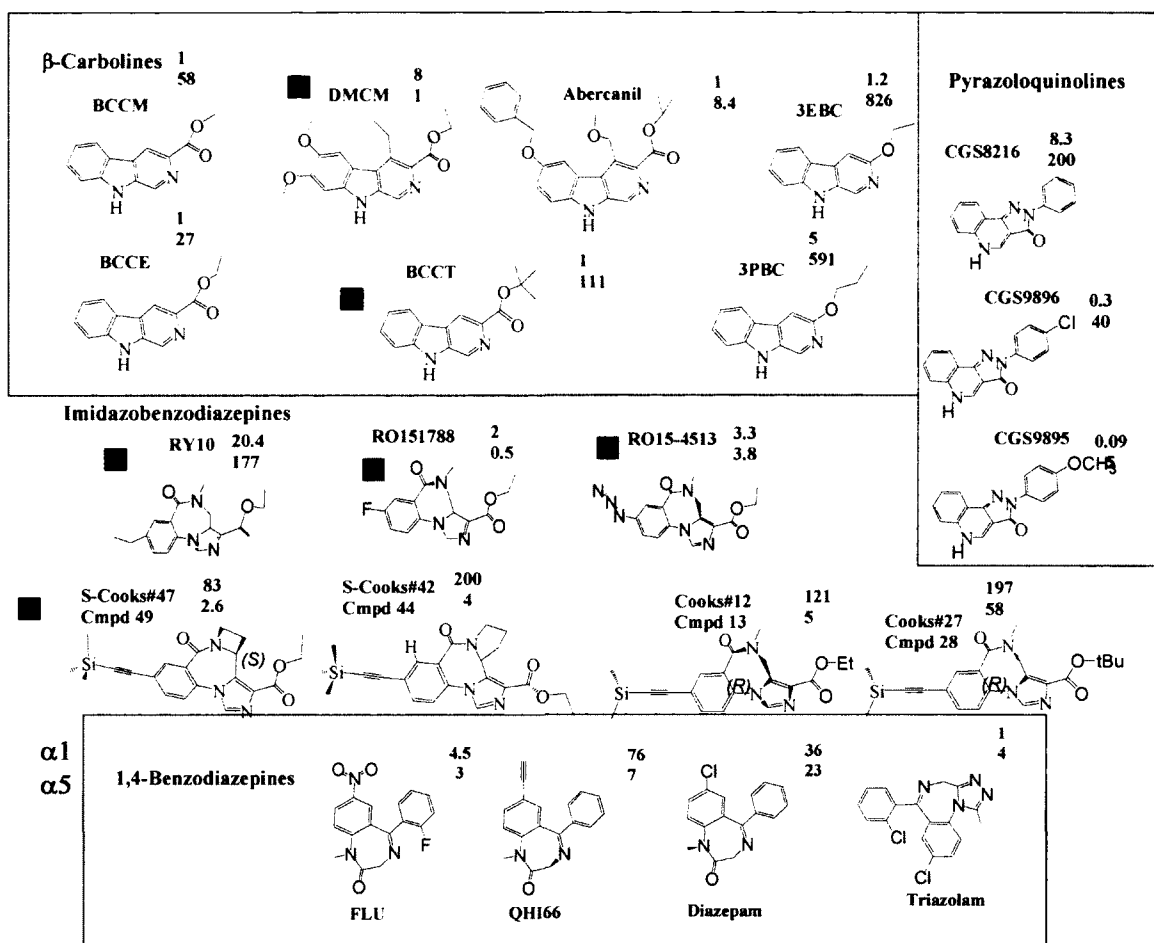


Figure 145. Diverse training set used to develop pharmacophores (overlap rules), COMSIA for binding to $\alpha 1\beta\gamma 2$ and $\alpha 5\beta\gamma 2$ GABA(A) receptor subtypes. S and R refer to the molecular conformation.

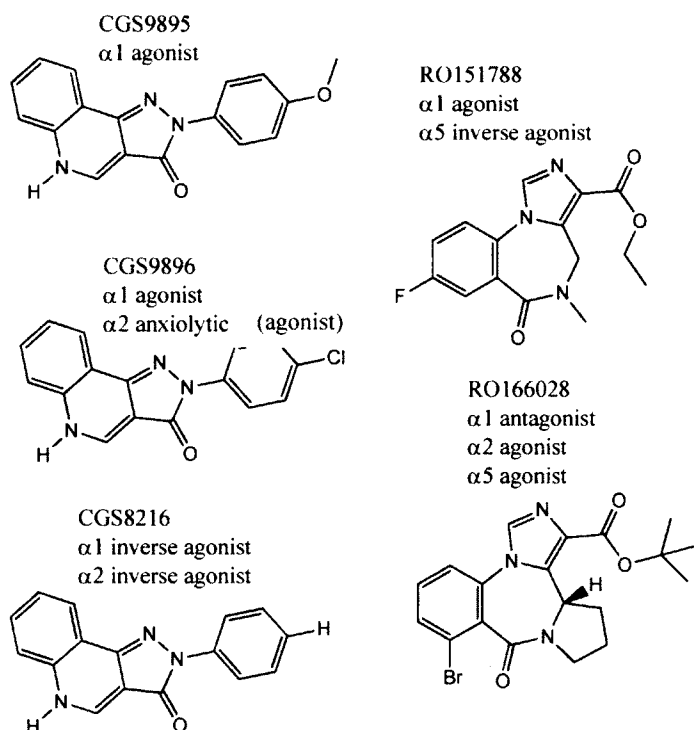


Figure 146. Examples illustrating subtle variations in scaffold substitutions that modulate behavioral profiles of each of the selected benzodiazepine ligands

Binding and Activational Selectivity in the Development of a Palliative Memory Agent.

Most BDZ ligands that bind to GABA(A) receptors do so with a lack of binding specificity. When developing a palliative memory agent, lack of binding or activational selectivity can lead to unacceptable side effects. To demonstrate this point one looked at RY-80, RY-23, and RY-24 (Figure 147) all three are structurally similar BDZ ligands, which exhibit 40-70 fold more selectivity for $\alpha 5\beta\gamma 2$ containing GABA(A) receptor isoforms, over other GABA(A) receptor isoforms.¹⁶ Despite the reasonably good $\alpha 5$

selectivity of these three compounds, they each elicit convulsions at relatively low doses when administered systemically. This somewhat limits their usefulness in thoroughly examining $\alpha 5$ influence over contextual memory as well as potential therapeutic viability. The electrophysiological profile of one of these compounds, RY24 (Fig 147), serves to underscore several aspects that one must be cognizant of in order to employ compounds within this class for palliative treatment of memory deficits. In this example the electrophysiological response of RY24 relative to GABA(A) receptors containing one of the α subunit subtypes (1, 2, 3, 4, 5 and 6) in combination with the $\beta 3$ and $\gamma 2$ subunits GABA(A) receptors expressed in *Xenopus* oocytes is illustrated. At nanomolar concentrations RY-24 modulated GABA-induced currents in an $\alpha 5$ -subtype selective manner. To test for agonistic or inverse agonistic effects, the compound was coapplied with a concentration of GABA that induced approximately 20% of the maximum current amplitude. In GABA(A) receptors containing the $\alpha 1$, $\alpha 2$ and $\alpha 5$ subunits nanomolar concentrations of RY-24 reduced GABA elicited currents in a concentration dependent manner. The EC_{50} for this effect was approximately 10 fold lower for $\alpha 5$ containing receptors than for those containing $\alpha 1$ and $\alpha 2$ (Table 37) receptors. In $\alpha 3$ containing receptors no apparent modulation of GABA elicited currents by RY-24 was seen. However, in these receptors 1 μ M RY-24 reduced the stimulation by 30nM diazepam (284.8 ± 48.7 % at GABA EC_3) by 96.3 ± 4.7 %. In GABA(A) receptors that contain $\alpha 4$ and $\alpha 6$ high nanomolar concentrations of RY-24 weakly stimulated GABA elicited currents (Figure 147). Due to the limited concentration range maximum modulation of GABA elicited currents by RY-24 was estimated by extrapolation (curve-fit by GraphPad Prism) (Table 37). Estimated maximum effect was dependent on the alpha-subunit, with

the $\alpha 5$ subunit showing bigger maximum effects than $\alpha 1$ and $\alpha 2$ ($-40.4 \pm 0.8\%$, $-31.0 \pm 2.5\%$ and $-20.7 \pm 1.2\%$, respectively). In $\alpha 3$ containing receptors, despite obvious binding of the compound (inhibition of diazepam) virtually no effect was seen ($-3.3 \pm 2.1\%$). With this in mind, the electrophysiological profile of RY24 displayed in Figure 147 indicated that the GABA(A) receptor isoforms that contain the $\alpha 1$, $\alpha 2$ or $\alpha 5$ all reduced the relative amplitude of the current elicited by GABA thereby favoring neuronal excitation. The binding affinities of RY24 are relatively high at all the different GABA(A) receptor isoforms with selectivity for the $\alpha 5$ over the other α containing GABA(A) receptor isoforms being in the 10-70 range.¹⁶ Because the $\alpha 1$ (and $\alpha 2$) receptors comprise a large proportion of all the GABA(A) receptors found throughout the brain, the administration of RY-24 would favor an increase in excitatory tone in numerous brain regions (by $\alpha 1$ and $\alpha 2$ subtypes), subsequently resulting in proconvulsant or convulsive behavior. Conversely, by knowing the electrophysiology and binding affinities of RY-24 in regards to the various α subunits, one can hypothesize about the α subunits that are likely to contribute to the convulsant effects of systemically administered RY-24. Furthermore, the $\alpha 1$ subtype has been reported to mediate, in part, the proconvulsant effects of PTZ.⁴⁸³ The relatively high affinity binding of RY-24 at the $\alpha 1$ subtypes would be in line with that observation. As convulsant behavior is generally thought to result from an increase in neuronal excitation, the likely candidates include $\alpha 1$, $\alpha 2$ and $\alpha 5$ containing GABA(A) receptors, which would each attenuate GABA's inhibitory effect in the presence of RY-24 (Fig 154). A similar observation was presented by Attack et al,¹⁸⁸ for RY80 in which they suggest the proconvulsant effects of RY80 cannot be attributed solely to the $\alpha 5$ containing GABA(A) receptor isoform. When, RY-24 is

given systemically to mice it elicits convulsive behavior at a dose as low as 1 mg/kg. Thereby, confounding its evaluation for cognitive influence by systemic administration. However, when Bailey⁴⁶¹ injected RY-24 (1 $\mu\text{g}/\mu\text{l}$) into the hippocampus they observed an increase in Pavlovian fear conditioning over that seen for vehicle alone. No convulsive behavior was noted by this administration route even at a dose of 10 $\mu\text{g}/\mu\text{L}$. Since the expression of α subunits of the GABA(A) receptor is not equal in the hippocampus, with the following order of abundance $\alpha 1 > \alpha 5 > \alpha 2$, $\alpha 4 > \alpha 3$, one can begin to make assumptions as to the α subtype(s) that are potentially involved in the cognitive effects mediated by the hippocampus. Because RY024 exhibited a 60-70 fold higher affinity towards the $\alpha 5$ -containing GABA(A) receptors over the $\alpha 1$ and $\alpha 2$ containing receptors (0.4 nM vs 26-27 nM), the lowest dose would largely affect the $\alpha 5$ -containing GABA(A) receptors with the recruitment of $\alpha 1$ and $\alpha 2$ containing receptors as the dose increases. As can be seen in Figure 147 all three of these receptor isoforms elicit inverse agonism and may be mediating the fear conditioning effect. At the highest dose of 10 $\mu\text{g}/\mu\text{L}$ the $\alpha 4$ -containing receptors, which elicit an agonistic response, could potentially contribute to the decrease in anxiogenic effects observed by Bailey et al.^{297, 484} The $\alpha 3$ receptor is not likely to play a role in this observed behavior because it is not expressed to any appreciable degree in the hippocampus³⁷¹ and is electrophysiologically silent while the $\alpha 6$ subunit was not expressed at all in the hippocampus.

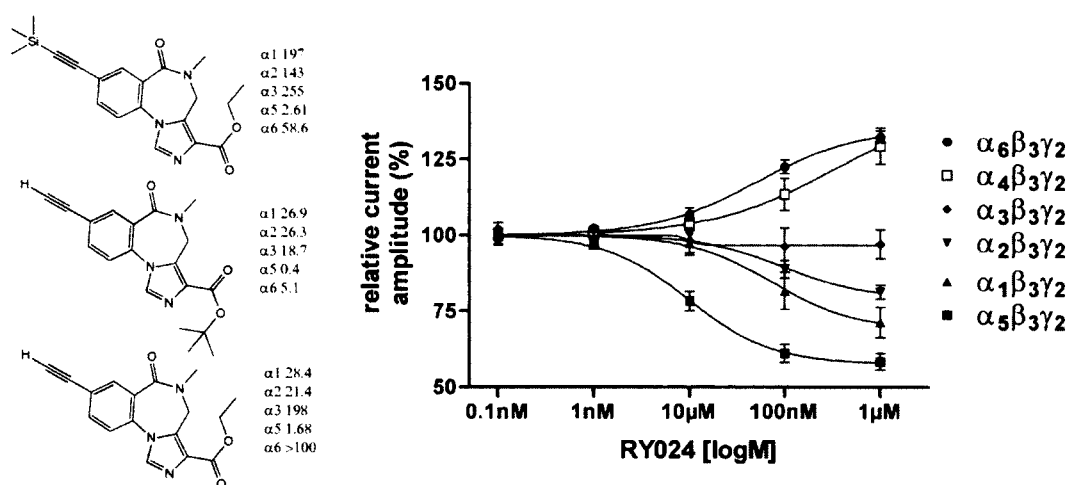


Figure 147. Structures of RY23/RY24/ and RY80 along with the electrophysiological characterization of RY24

Illustrated in Figure 147 are the dose response curves for RY024 in oocytes expressing different subunit combinations of GABA(A) receptors. Subtype combinations are indicated in legends. cRNA-injected *Xenopus* oocytes were held at -60 mV under two-electrode voltage clamp. Increasing concentrations of RY024 were superfused together with a GABA concentration eliciting approximately 20% of the maximal current amplitude. RY024 was preapplied for 30 sec before the addition of GABA, which was coapplied with the drugs until a peak response was observed. Data were normalized for each curve assuming 100% for the response in the absence of RY024. RY024 was made up and diluted as stock solution in DMSO. Final concentrations of DMSO perfusing the oocyte were 0.1%. Values are presented as mean \pm SD of at least four oocytes from at least two batches. Using the two electrode voltage clamp method currents in the μ A range were measured for all subunit combinations in response to application of a saturating concentration of GABA (10 mM). Two electrode voltage clamp experiments were performed to test whether RY-24 triggered chloride currents, modulated GABA-induced

currents or antagonized the effects of benzodiazepines in *Xenopus* oocytes that express GABA(A) receptors. In the absence of GABA, RY-24 at concentrations up to 1 μ M was not able to trigger chloride currents in any of the tested subtypes of the GABA(A) receptor. It was a weak inverse agonist at α 1 and α 2 subtypes and a potent α 5 subtype inverse agonist (negative modulator). Hence, the activity of RY24 is easy to understand. Enhanced cognition seen by Bailey and others is due to negative modulation at the α 5 subtype, while the proconvulsant/convulsant effects are due particularly to negative modulation at α 1 subtypes with some contribution from negative modulation at α 2 subtypes.

Table 37. Concentration-response data for modulation of control GABA EC₂₀ by RY024 in different GABA(A) receptor subtypes

Subtype	EC50 μ M (95% confidence interval)	Estimated maximum modulation \pm SD *	Number of oocytes
α 1 β 3 γ 2	74.4 μ M (38.3 – 144.3)	-31.0 \pm 2.5%	5
α 2 β 3 γ 2	95.5 μ M (59.4 – 153.6)	-20.7 \pm 1.2%	7
α 3 β 3 γ 2		-3.3 \pm 2.1%	5
α 4 β 3 γ 2	324.4 μ M (22.6 – 4651.5)	+43.0 \pm 15.9	8
α 5 β 3 γ 2	9.8 μ M (8.1 – 11.9)	-40.4 \pm 0.8%	8
α 6 β 3 γ 2	51.7 μ M (35.8 – 74.6)	+35.2 \pm 1.5%	7

*estimated by curve-fit (GraphPad Prism)

Because PWZ-029 (related to RY24) was subtype selective only at α 5 receptor subtypes (see **56** below) it was selected for cognitive assessment based on its GABA(A) receptor subtype binding profile and computed properties consistent with discriminant analyses (see section **3D QSAR and Fragment QSAR**). PWZ-029 was not observed to be convulsive up to 30 mg/kg in mice or even at higher doses. In fact, long after the studies in this dissertation were completed PWZ-029 was found to be a weak

anticonvulsant in mice (James Staples, NINDS, unpublished results). It cannot be proconvulsant or convulsant.

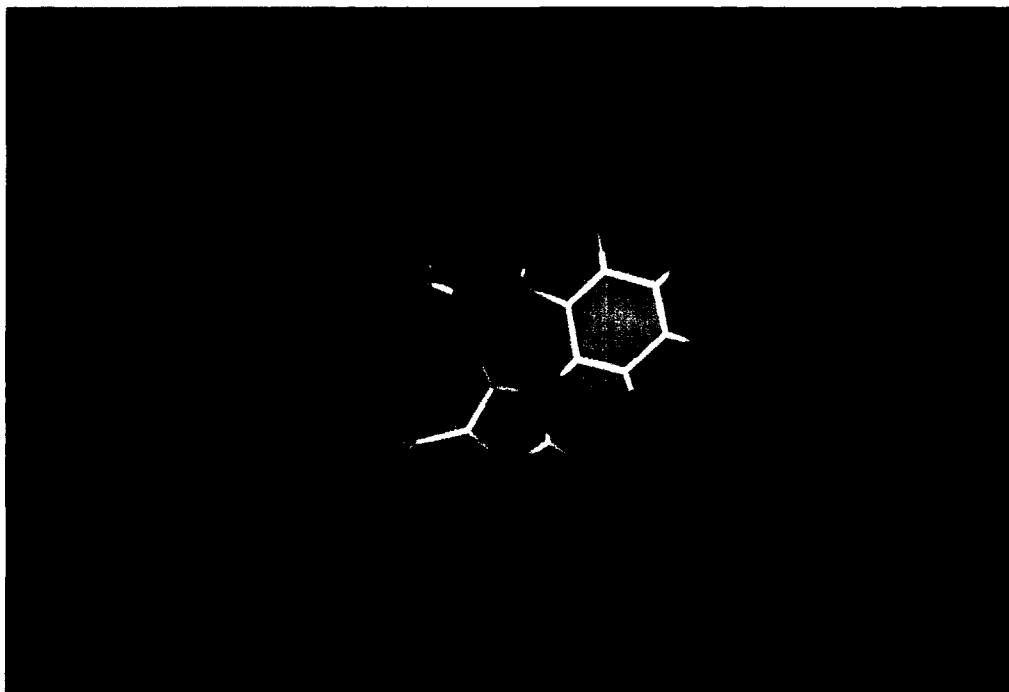


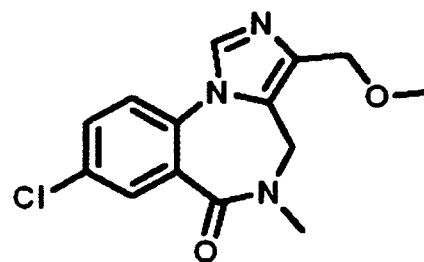
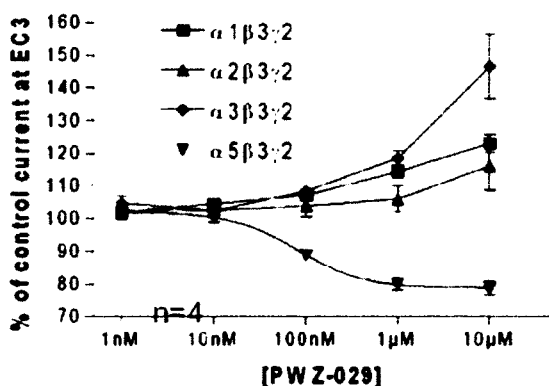
Figure 148. PWZ-029 within the pharmacophore/receptor model for the $\alpha 5\beta 3\gamma 2$ GABA(A) BzR subtype

This observation suggests one of two interpretations, one being that the $\alpha 5$ receptors were not primarily involved in eliciting the convulsive actions of previous compounds or that an overall reduction in the inhibitory tone of the brain via a combination of the $\alpha 1$, $\alpha 2$, $\alpha 3$ and $\alpha 5$ containing GABA(A) receptors could result in a global increase in excitation thereby resulting in a seizure prone brain; that is proconvulsant or convulsant effects in vivo.

Ligand	K_i (nM)					
	$\alpha 1$	$\alpha 2$	$\alpha 3$	$\alpha 4$	$\alpha 5$	$\alpha 6$
56, PWZ-029 ^{187, 461}	>300	>300	>300	>300	38.8	>300
PWZ-029	920	ND	ND	ND	30	ND
PWZ-029	362.4	180.3	328.2	ND	6.185	ND

Either explanation bolsters the concept of potential therapeutic utilization, whether through highly selective binding and/or selective efficacy that is mediated through $\alpha 5$ subunit containing GABA(A) receptors. However, RY10, a similar compound to RY24 with selectivity for the $\alpha 5$ over the other α containing GABA(A) receptors of between 15-120 fold was tested in the concentration range of 0.1-10 μ M on HEK cells expressing the $\alpha 5\beta 2\gamma 2$, RY10 elicited a relatively mild attenuation of GABA-induced Cl^- flux. However, when RY10, a compound from same compound class as RY24, was administered systemically at a dose range of 10-30 mg/kg it lacked convulsive effects and exhibited marginal, yet significant, attenuation of contextual memory impairment in the cognitively impaired mouse model.^{460, 485-487}

**Modulation of EC3 In oocytes currents
By PWZ-029**



Affinity of PWZ for $\alpha x\beta 3\gamma 2$ (x=1-6) benzodiazepine receptor isoforms

	$\alpha 1$	$\alpha 2$	$\alpha 3$	$\alpha 4$	$\alpha 5$	$\alpha 6$
Merck data	>300	>300	>300	ND	38.5	>300
Moltech data	920	ND	ND	ND	30	ND
UNC-Roth data	362.4	180.330	328.2	ND	6.185	ND

Due to the low selectivity of RY10 (see Figure 145 for structures) one can not clearly attribute its cognitive effects mainly to the $\alpha 5$ subunit containing GABA(A) receptors. Another approach to achieving cognitive influence is through functional selectivity, which has been demonstrated with the Merck compound $\alpha 5$ IA, although it is not clear whether there was a fundamental understanding of the molecular facets underlying that functional selectivity.^{187, 461} While $\alpha 5$ IA lacks binding selectivity for the $\alpha 5$ subunit containing GABA(A) receptors over other α subunit isoforms of the GABA(A) receptor, it exhibits only marginal electrophysiological effects at GABA(A) receptor isoforms containing the $\alpha 1$, $\alpha 2$ or $\alpha 3$ with about a 30-40% reduction in the GABA-induced current amplitude only occurring at GABA(A) receptor isoforms that contain the $\alpha 5$ subunit. Compound $\alpha 5$ IA was also observed to enhance performance in rats in the Morris water maze, a spatial memory test with some overlap with contextual memory, both are likely mediated by GABA(A) receptors containing the $\alpha 5$ subunit.⁴⁸⁸ PWZ-029, like $\alpha 5$ IA, is an inverse agonist at the $\alpha 5$ subunit, however unlike $\alpha 5$ IA, PWZ-029 does not bind to $\alpha 1$, $\alpha 2$, and $\alpha 3$ subtypes.

Validation of 3D Pharmacophore for Sedation and Contextual Memory Endpoints by 3D-Database Search and Testing (Harris, Delorey, Clayton et al.)

Harris and Delorey developed a pharmacophore independently of the Milwaukee group for contextual memory and sedation endpoints centered on diverse sets of nonselective ligands based on 1,4-benzodiazepines, imidazobenzodiazepines, imidazopyridines, β -carbolines, pyrazoloquinolines, imidazoquinolines, imidazopyrimidines, and imidazothienodiazepines classes which have been characterized in relation to sedation (influence on spontaneous locomotor activity) and attenuation of scopolamine-induced contextual memory impairment.⁴⁸⁹ This set was dominantly comprised of benzodiazepine ligands that lacked selectivity to the benzodiazepine binding sites found on the various GABA(A) receptor isoforms. Using such ligands allowed one to first determine core features common to numerous classes of benzodiazepine ligands that mediate their behavioral effects through various GABA(A) receptors isoforms. Depicted in Figure 145 are a diverse set of compounds along with their binding affinities at the $\alpha 1\beta 2\gamma 2$, and $\alpha 5\beta 2\gamma 2$ GABA(A) receptor isoforms. As is typical for most benzodiazepines, subtle structural changes to pendant groups attached to particular scaffolds/templates resulted in significant variations in binding profiles relative to the different GABA(A) receptor isoforms. Moreover, as demonstrated in Figure 146, small structural/chemical variations can drastically alter the observed behavioral pharmacology for a given compound template e.g. the CGS series in this Figure illustrates how permutation of a -H, to a -OCH₃ or -Cl group dramatically alters the pharmacological profile of the pyrizoquinolines (CGS8216, CGS9896, and CGS9895). While changes in the -(CH₂)_n- bridgehead and terminus of classic

imidazobenzodiazepines alters the activity profiles, as illustrated by Ro15-1788 and Ro16-6028 as well.⁴⁸⁹

Distance No's	Sedation	Memory
1-2	4.9±1.1	3.2±1.7
1-3	5.6±1.8	3.5±1.0
1-4	4.4±1.1	6.9±0.7
1-5	2.3±0.9	
2-3	4.5±1.2	5.2±1.2
2-4	4.7±1.2	8.9±1.4
2-5	3.1±1.3	
3-4	5.1±1.1	4.9±0.0
3-5	3.0±0.8	
4-5	7.8±1.3	

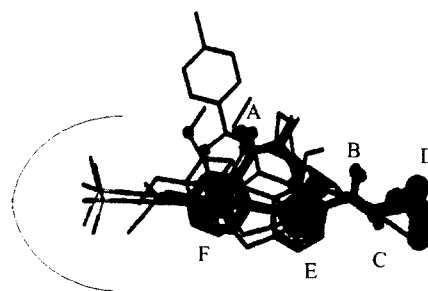
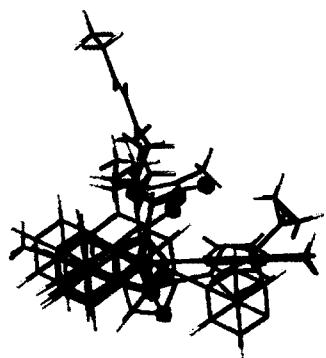
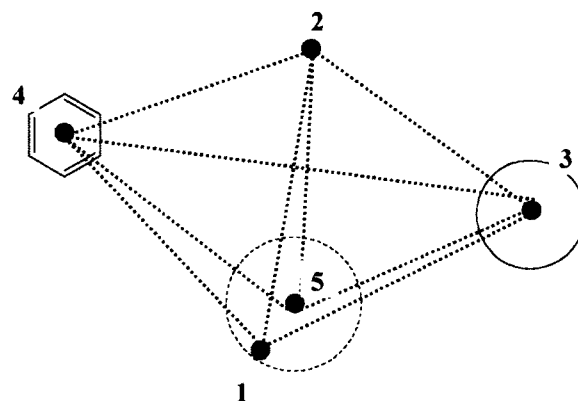


Figure 149. Harris pharmacophore. The inset table displays the distances between the pharmacophore points (1,2 = hydrogen bond acceptor, 3 = hydrophobic terminus, 4 = aliphatic/aromatic centroid with LUMO, 5 = ring system containing hydrogen bond acceptor) identified in benzodiazepines binding to and activating GABA(A) receptor subtypes associated with sedation and memory. In the upper right panel is a graphical depiction of 3D pharmacophore points for compounds having at the sedation and memory endpoints corresponding to the table in the upper left. Lower left and right panels show the overlap of several compounds complying with the sedation and memory pharmacophores, respectively, illustrating some of the commonalities: green spheres represent hydrogen bond acceptors, red spheres represent the polar core ring system, purple ring centroid represents the aromatic ring, LUMO center, blue sphere represents the hydrophobic group at one end of the ligands.

Not surprisingly pharmacophores derived from non-selective compounds that were active at both the sedation and contextual memory endpoints exhibit similar

distance (pharmacophore) metrics. The pharmacophores depicted in Figure 149 were derived by: 1) development of conformational libraries based on nested rotation of all rotatable bonds in compounds previously examined for influence on sedation or contextual memory ⁴⁸⁹ 2) the examination of whether a common set of inter-pharmacophore point distances is/are present for at least 1-conformation of each ligand, between all compounds in the training set using a 2 Å distance criteria and the lowest 10 kcal/mol energy conformer. Illustrated in Figure 150, is a small subset of compounds that were extracted from the Maybridge Chemical database by employing the distance metrics representing the distances between the pharmacophore entities established for the contextual memory pharmacophore. Several of these compounds: 1) were found to exhibit sub-micromolar binding affinities at $\alpha 1\beta 2\gamma 2$ and/or $\alpha 5\beta 2\gamma 2$ GABA(A) receptor isoforms and could be considered lead compounds for further refinement, 2) two of these compounds were able to influence spontaneous locomotor activity. These results illustrate that the contextual memory pharmacophore can serve to increase the likelihood of identifying compounds from a chemical database that are capable of binding to $\alpha 1\beta 2\gamma 2$, and/or $\alpha 5\beta 2\gamma 2$ receptor isoforms and therefore ‘enrich’ the number of compounds extracted that bind to GABA(A) receptors. However, the Harris model itself does not encode sufficient information by itself to identify $\alpha 5$ subtype selective compounds from a binding or activational perspective. Rather the development of this pharmacophore served as a basis for overlapping structural features prior to performing 3D-QSAR (COMSIA) computations and serves to select a particular set of conformations to be used in computing the Fragment QSAR. It is these QSARs, rather than the initial pharmacophore, that will actually provide the insights that will eventually aid in the

understanding of what is required to achieve the desired selectivity in the Harris model derived from the Milwaukee-based library of compounds.

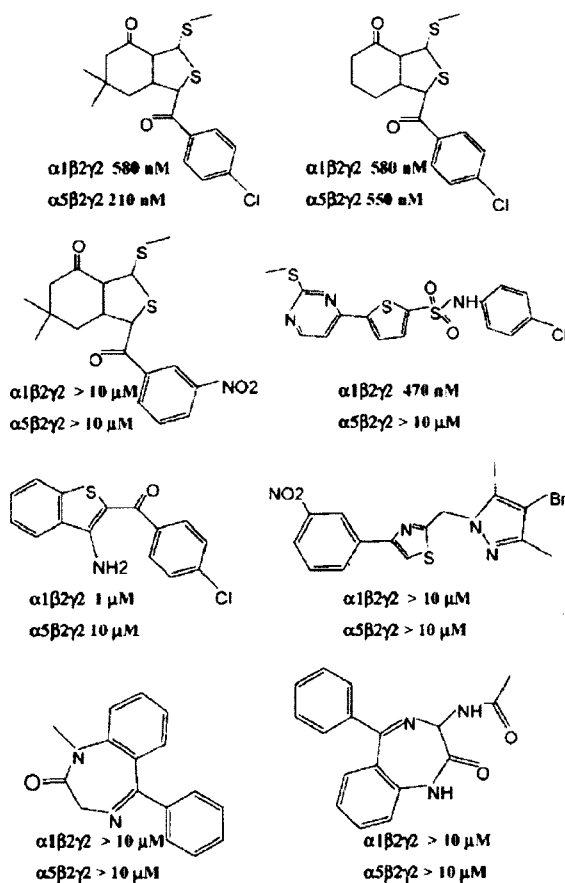
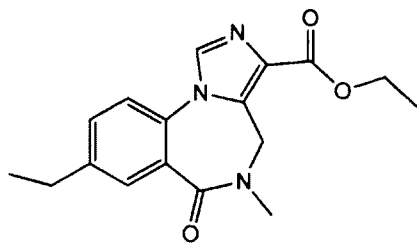


Figure 150. Selected structures retrieved from pharmacophore directed searches of the Maybridge Chemical Database with indicated binding affinities (IC_{50} , [H^3]Ro15-4513 competition in a cell based binding assay, see Methods Section) to GABA(A) receptors with either the $\alpha 1\beta 2\gamma 2$ or $\alpha 5\beta 2\gamma 2$ stoichiometry.

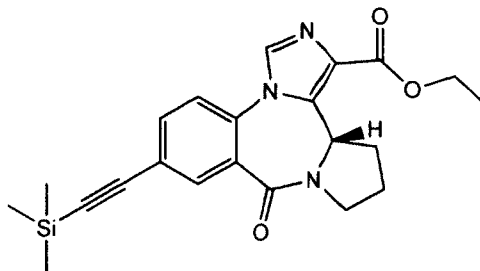
3D-QSAR (COMSIA) Models of $\alpha 5\beta 2\gamma 2$ and $\alpha 1\beta 2\gamma 2$ Receptor Isoforms.

Displayed in Figure 151 is the use of the above mentioned overlap rule, to develop 3D-QSAR models based on the experimental binding data, which in turn provided a modest predictivity when diverse templates were used.¹⁸⁷ Moreover, given that it was developed from a set of non-selective compounds, the same overlap rule gives rise to predictive 3D-QSARs for both $\alpha 5\beta 2\gamma 2$ and $\alpha 1\beta 2\gamma 2$ receptor combinations. Illustrated in figure 151 is the predictive q^2 for $\alpha 1\beta 2\gamma 2$ binding to be 0.43 and a non-crossvalidated r^2 of 0.99 with a standard error of 0.50 while shown in Figure 152, using the same overlap rule, contains a model for $\alpha 5\beta 2\gamma 2$ binding with a $q^2=0.41$, $q^2=0.99$ and a standard error of 0.52. The order of magnitude of q^2 values are reflective of the typical predictivity for 3D-QSAR models developed from the use of compounds from diverse templates such as those depicted in Figure 145. ***The expectation value of q^2 for such models involving a diverse training set is typically on the order of 0.3.***¹²¹ Such QSAR's can be used to predict order of magnitude binding affinities as displayed in the histogram in the lower panel of Figure 158 showing both the predicted and actual K_d s (in nM). The 3D-QSAR (COMSIA) for compounds that bind nonspecifically to $\alpha 1\beta 2\gamma 2$ and $\alpha 5\beta 2\gamma 2$ would indicate comparable contributions of hydrophobic, electrostatic and steric COMSIA fields as indicated by the magnitude of the fractions, which reflect the relative contributions to the COMSIA regression equation, as reported in Table 38. The inset colored molecule in Figure 152 is of RY-023 and shows how variations in the electrostatic (red/blue) components explain variations in the compounds binding affinity. The ester functional group is included in the region where modulation of charge affecting electrostatics would affect the binding affinity. While the use of a diverse training set is useful for developing a model capable of providing predictions of binding affinities of

diverse compounds, one loses information as to what features are most important to binding selectivity when employing such an approach.^{121, 170}



RY-10



Cmpd 44

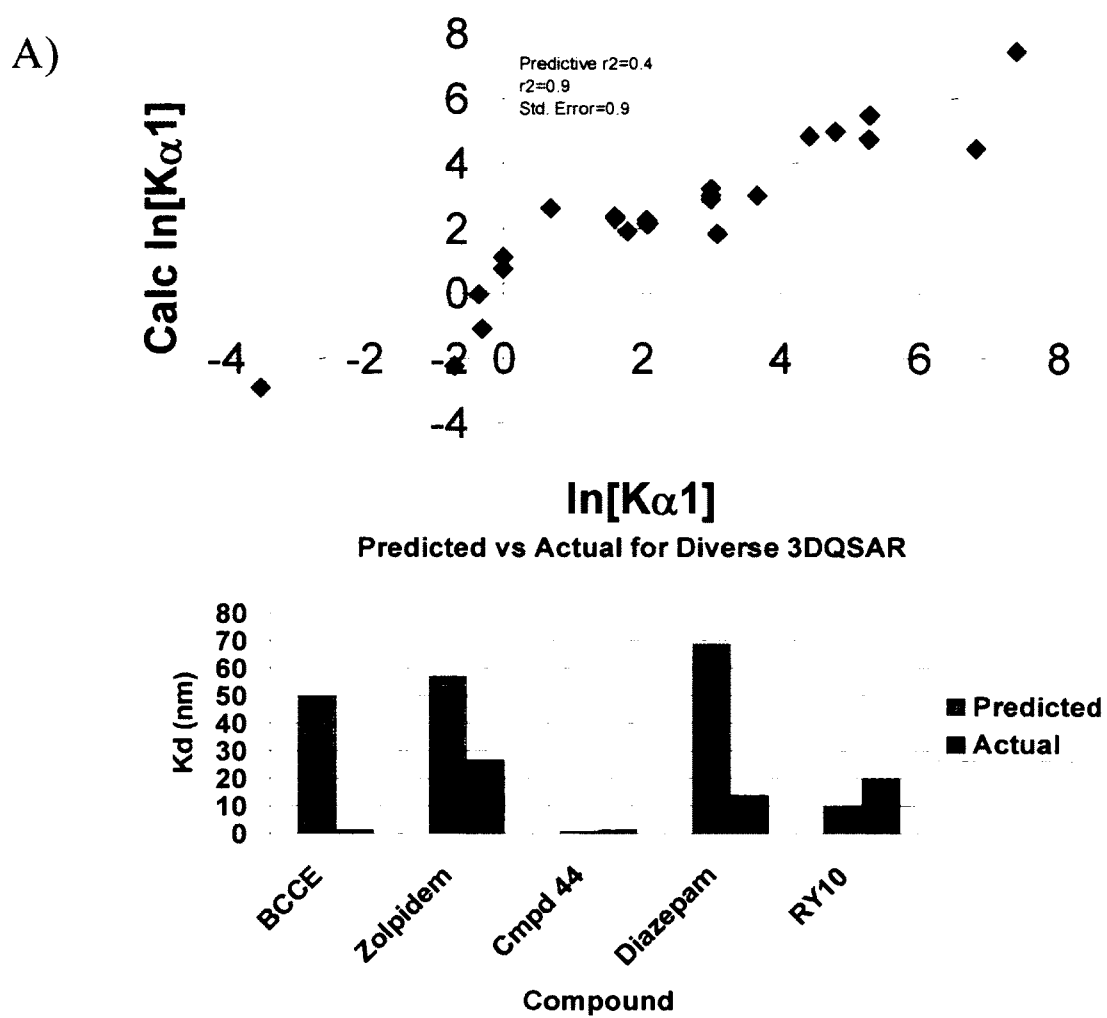


Figure 151. COMSIA based on overlap rules and observed binding affinities for BZD training set ligands at $\alpha 1\beta 2\gamma 2$ subunits.

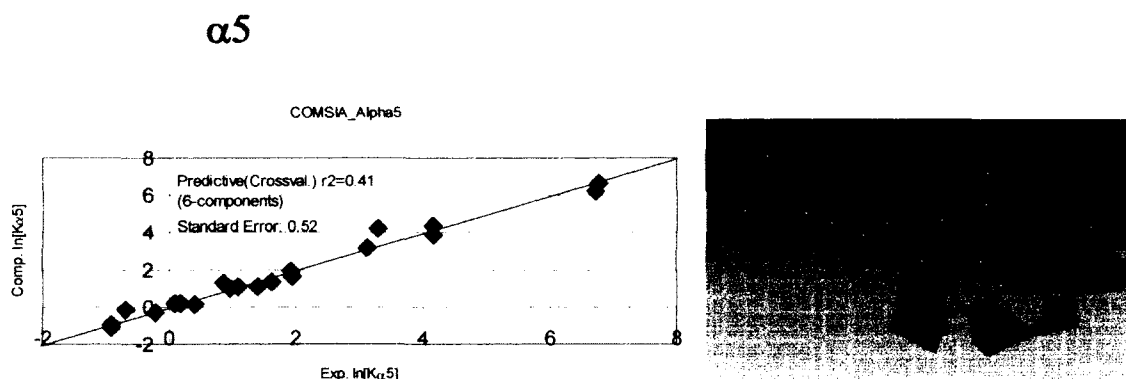


Figure 152. COMSIA model predictive of compounds binding to the $\alpha 5\beta 2\gamma 2$ GABA(A) receptor isoform.

Table 38. Normalization coefficients and fractions of the components in the COMSIA analyses for A, a diverse training set of benzodiazepines and B, a homogenous set consisting of imidazobenzodiazepines^a

A		$\alpha 5\beta 2\gamma 2$		$\alpha 1\beta 2\gamma 2$	
component		norm coeff	fraction	norm coeff	fraction
electrostatic		1.48	0.35	1.14	0.29
steric		1.13	0.27	0.99	0.26
hydrophobic		1.63	0.38	1.63	0.45

B		homogenous set of imidazobenzodiazepines ^a			
component		norm coeff	fraction	norm coeff	fraction
electrostatic		0.12	0.041	1.14	0.256
steric		1.04	0.35	1.15	0.29
hydrophobic		1.81	0.61	1.73	0.44

^a RY-10, RY-024, RY-066, RY-080, Ro15-1788, Ro15-4513, PWZ-029, PWZ-031, PWZ-035A, and compd 44.

We therefore next took a subset of 10 imidazobenzodiazepines that were more homogenous in order to analyze what characteristics lead to more selective binding in regards to the $\alpha 5\beta 2\gamma 2$ receptor isoform. The analysis which resulted gave a $q^2=0.94$, $R^2=0.99$ and a standard error of 0.09. While an analysis based on a narrow compound class such as this has limited predictivity for templates other than imidazobenzodiazepines, it does provide a means to examine the relative importance of particular components in regards to influencing the modulation of binding affinities. For example, the lower portion of Table 38 provides an analysis of the importance of the contribution (fraction) of the electrostatic component in explaining the variations in the experimental binding affinity. The value of the electrostatic component was found to be 0.041, which is minor compared to the contributions of the hydrophobic and steric components, which were 0.61 and 0.35, respectively. Given that the more restrictive COMSIA model is suggestive of a discriminating factor for binding involving electrostatic factors we undertook a quantum mechanical study of this series to probe the underlying electrostatic potential surfaces. This information was then incorporated with the volumes of the fragments in a fragment QSAR for binding thereby providing an independent cross-check on the information gleaned from the COMSIA analysis.

Fragment QSAR: Facets Effecting Differential Binding Between $\alpha 1\beta 2\gamma 2$ and $\alpha 5\beta 2\gamma 2$ GABA(A) Receptor Isoforms.

We next sought to scrutinize the robustness of the conclusions deduced in the COMSIA analysis by performing an analysis via a fragment QSAR approach. While 3D-QSAR often provides some clues as to variations in binding and/or activity with differences in molecular/grid based fields, the results are often sensitive to how the

compounds are aligned/overlapped. In principle, one should obtain similar conclusions about what is important from a fragment QSAR analysis as one does from COMSIA analysis from an analysis of the whole ligand if you are using a set of ligands based on a shared template (see Figure 153). The idea behind this additional analysis is illustrated through the four panels depicted in Figure 154, which displayed the computed molecular electrostatic potential (MEP) surfaces computed on top of the van der Waals surface of the ligands. Below each panel are listed the binding affinities at the $\alpha 5\beta 2\gamma 2$ and $\alpha 1\beta 2\gamma 2$ GABA(A) receptor isoforms. In the present example we are computing the MEP for the whole molecule, rather than just the fragments/substitutions to the core template. Note that the effect of the substitution of the ethyl ester moiety in Ro15-1310 by successively less polar fragments (moving clockwise in the figure) to $-\text{CH}_2\text{OCH}_3$, $-(\text{C}=\text{O})\text{CH}_2\text{CH}_2\text{CH}_2\text{CH}_3$, and finally $-\text{CH}_2\text{CH}_2\text{CH}_2\text{CH}_2\text{CH}_3$ does not provide a simple explanation as to the importance of electrostatic versus steric properties independent of each other. From this, one can deduce that the changes in the electrostatic potential surface minimum, close to the benzodiazepine ring $-\text{N}-$, is only slightly altered by the changes in the fragment a few angstroms away (i.e. there are changes, but there small). The changes in the second electrostatic minimum, closest to the fragment, are more pronounced. Note that as one proceeds clockwise from Ro15-1310 to PWZ-029 to compounds **32** and **40**, the binding affinities to $\alpha 5\beta 2\gamma 2$ and $\alpha 1\beta 2\gamma 2$ both drop, but that the binding affinity to $\alpha 1\beta 2\gamma 2$ drops more rapidly than for $\alpha 5\beta 2\gamma 2$ and appears to have an apparent correlation to the changes in the presence/absence and depth of the second electrostatic minimum proximate to the changing fragment. This analysis was performed after the quantitative fragment analysis, discussed below, and reveals in hindsight, the

chemical picture behind the following analysis. The pattern is not apparent from staring at the MEP'S computed for all the compounds shown in Figure 153. Illustrated in Figure 155 is the fragment QSAR analyses for binding affinities as a function of the electrostatic potential minimum, computed for the fragment itself, the fragment volume and fragment hydropobicity. The analysis of the compounds in terms of these variables results in r^2 values of 0.84 and 0.94 for binding models for $\alpha 5\beta 2\gamma 2$ and $\alpha 1\beta 2\gamma 2$, respectively. The QSAR equations highlighted in the figure indicated, analogous to the COMSIA analyses, that while the electrostatic component is finite for both $\alpha 5\beta 2\gamma 2$ and $\alpha 1\beta 2\gamma 2$ receptor subtype binding models that it is more important for $\alpha 1\beta 2\gamma 2$ than $\alpha 5\beta 2\gamma 2$. Therefore while, selectivity is enhanced by reduction in the polar components in the fragment, it takes place at the expense of reduced binding affinity to $\alpha 5\beta 2\gamma 2$ receptor subtypes. The fragment QSAR analysis for binding have statistical significant with $F_{3,7}$ values for the analysis are 12.0 and 36.1, which indicates that the regressions in terms of the variables indicated are significant at the 99% confidence level.⁴⁹⁰

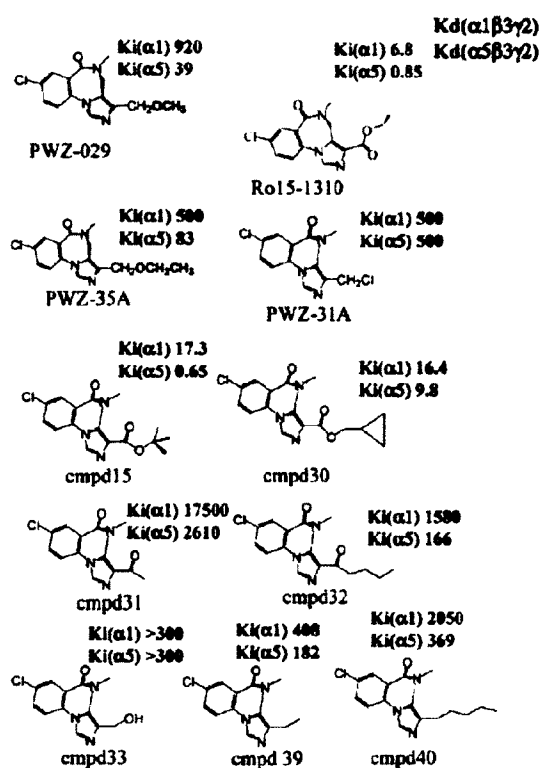


Figure 153. Selected benzodiazepines employed in the fragment QSAR analyses for $\alpha 1\beta 3\gamma 2$ and $\alpha 5\beta 3\gamma 2$ binding

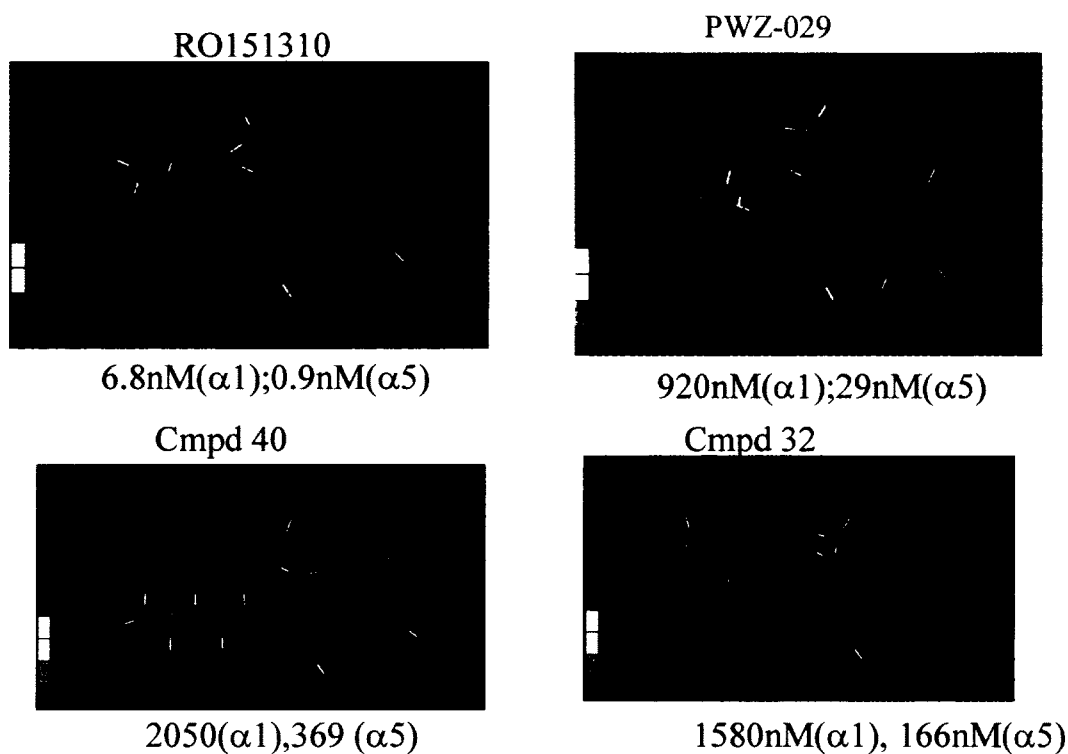


Figure 154. Computed electrostatic potentials (computed using density function theory (B3LYP/6-3G**) evaluated on the van der Waals surfaces of compounds showing selectivity of binding to $\alpha 5\beta 3\gamma 2$ versus $\alpha 1\beta 3\gamma 2$

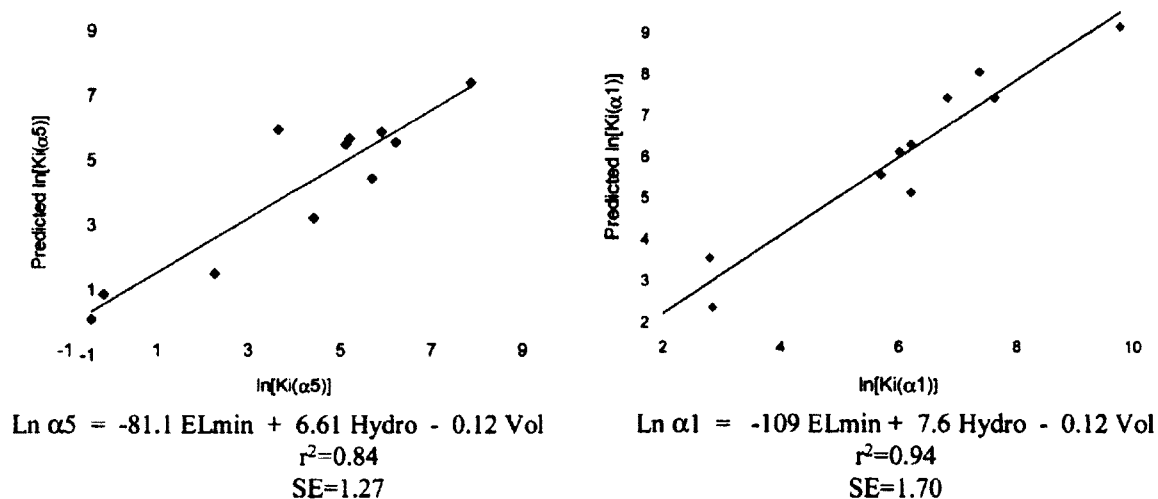


Figure 155. Fragment QSAR for the binding of compounds in figure 145 to $\alpha 5\beta 3\gamma 2$ (left) and $\alpha 1\beta 3\gamma 2$ (right) receptor isoforms, illustrating, via the derived QSAR relations at the bottom of the figures,

that the electrostatic contributions (EL min) are more important for ligand binding to the $\alpha 5\beta 3\gamma 2$ receptor isoform than to the $\alpha 1\beta 3\gamma 2$ isoform, as indicated by the larger magnitude of the coefficient of the electrostatic term for the $\alpha 5\beta 3\gamma 2$ isoform compared to that for the $\alpha 1\beta 3\gamma 2$ isoform. SE = standard error.

The pharmacophore depicted in Figure 149 created from information derived from compounds that exhibited activity at the contextual memory endpoint, revealed commonalities in the ligands capable of binding to and activating $\alpha 1\beta 2\gamma 2$ receptors, in other words the core features are in common and have similar distance relationships.⁴⁹¹ Most of the training set compounds, illustrated in Figure 145, have an ester moiety at one end of the ligand that appears to be essential to cause substantial binding affinities to the GABA(A) receptors associated with sedation and contextual memory effects. However, the results above show that the elimination of this hydrogen bond acceptor nevertheless resulted in a substantial binding affinity to the $\alpha 5\beta 2\gamma 2$ receptor subtype (see PWZ-029), but with lesser binding affinities to other subtypes. This indicated that one of the pharmacophore points indicated in Figure 149 is not essential in order to elicit substantial binding affinity to the $\alpha 5\beta 2\gamma 2$ isoform. However, it is not yet clear whether the inclusion of such a polar hydrogen bond accepting group at this location might not lead to an increase in the binding affinity by an order of magnitude. The compounds PWZ-029, PWZ-31A, and PWZ-35A in Figure 153, originally reported by Huang et al.,⁴⁶¹ were reported only as having binding affinities of greater than 300 nM. Recently, binding assays were performed (see methods) in order to establish a more accurate value for compound **34**. A binding affinity of 920 nM to $\alpha 1\beta 2\gamma 2$ and 8 μ M to $\alpha 6\beta 2\gamma 2$ GABA(A) receptor isoforms compared to the binding affinity of this compound at $\alpha 5\beta 2\gamma 2$ of 39 nM

(compound **34**/ PWZ-029).⁴⁹² By all indications the elimination of the ester moiety from the 1,4-BDZ template offered discrimination between $\alpha 1\beta 2\gamma 2/\alpha 6\beta 2\gamma 2$ and $\alpha 5\beta 2\gamma 2$ receptor compositions. The extra hydrogen bond acceptor was virtually a requirement for binding to $\alpha 1\beta 2\gamma 2/\alpha 6\beta 2\gamma 2$ BzR but not $\alpha 5\beta 2\gamma 2$ isoforms. The pharmacological activities of these compounds will be further addressed below.

GABA(A) receptors containing $\alpha 1\beta 2\gamma 2$, $\alpha 2\beta 2\gamma 2$ and $\alpha 5\beta 2\gamma 2$ subunit compositions are believed to be associated with sedative, anxiolytic, and memory effects, respectively.

⁴⁶¹ Given the 70% sequence identity between α subunits, this implied that small differences in the BZD ligand binding site, situated at the interface between the α_x and γ_2 subunits, were responsible for large changes in binding and activation. Renard and coworkers illustrated this principle in site directed mutagenesis studies on $\alpha 5\beta 2\gamma 2$ subunits wherein they introduced $\alpha 5$ -P162T, $\alpha 5$ -E200G, and $\alpha 5$ -T204S mutations.⁴⁹³⁻⁴⁹⁵ The authors of that study argued that the first two mutations appeared to alter the binding pocket conformation whereas $\alpha 5$ -T204S appeared to better allow the formation of a hydrogen bond with a proton acceptor in zolpidem. The $\alpha 5$ -T204S mutation itself seemed to confer $\alpha 1$ -like binding properties for zolpidem in a receptor subtype that was essentially $\alpha 5$ in character in that it changed the binding affinity of zolpidem from >10000 nM to ~300nM. Clearly fine tuning of the hydrogen bonding complementarity of ligand and receptor is a significant modulator of binding subtype selectivity for ligands binding to $\alpha 5\beta 2\gamma 2$ subunits.

Computational Assessment of Molecular Properties Correlated with Electrophysiological Response

After examination of the molecular properties that provide insight into binding discrimination between $\alpha 5\beta 2\gamma 2$ and $\alpha 1\beta 2\gamma 2$ receptor isoforms one next sought to determine what molecular properties (cf. Table 39) were correlated with the electrophysiological response and attenuation of scopolamine induced contextual memory impairment from an earlier study.⁴⁹⁶ The early assessment of fear conditioned contextual memory response used sterimol descriptors,⁴⁹² polar and nonpolar volumes, hydrophobicities, free energies of solvation, electronic properties (HOMO, LUMO energetics), and solvent accessible surface areas in a discriminant variable test of the ability to affect fear conditioned contextual memory results.^{296, 297} These preliminary analyses indicated that the longest dimension of the ligands was able to discriminate between compounds that were able to attenuate scopolamine-induced contextual memory impairment from those that were not. This provided the working rationale to select an initial set of compounds for electrophysiological evaluation in regards to $\alpha 5\beta 2\gamma 2$ activation. Information was also supplemented from data on other compounds reported in the literature. COMSIA and fragment QSAR analyses of the electrophysiological data of compounds were used to determine molecular descriptors that correlated with the electrophysiological response at the $\alpha 5\beta xy 2$ subtype to see to what extent these descriptors correlated with descriptors derived from the analysis of the behavioral data set.

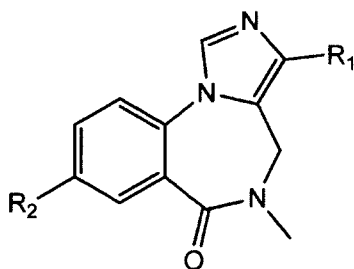


Table 39. Fragment properties for the imidazobenzodiazepines shown in Figure 153.

	ln(Ea5+100)	R ₁	L1	B1	(H-L)1	HYD1	R ₂	L2	B2	(H-L)2	(HYD)2
RY10	4.52	-CO ₂ Et	7.81	3.09	-12.46	0.06	-CH ₂ CH ₃	5.44	2.64	-15.86	1.30
RO151788	4.56	-CO ₂ Et	7.81	3.09	-12.46	0.06	-F	3.29	1.30	-20.78	3.77
RO166028	4.97	-CO ₂ Et	7.81	3.09	-12.46	0.06	-H	3.02	1.17	-19.89	0.66
RO154513	4.58	-CO ₂ Et	7.81	3.09	-12.46	0.06	-N ₃	5.71	2.25	-10.38	-2.45
PWZ-29A	4.26	-CH ₂ OCH ₃	6.44	2.75	-13.65	0.28	-Cl	4.22	1.77	-14.20	0.66
RY24	4.09	-CO ₂ tBu	7.73	3.87	-12.58	0.81	-CCH	5.69	1.76	-13.53	1.78
RY23	3.69	-CO ₂ tBu	7.73	3.87	-12.58	0.81	-CCSi(CH ₃) ₃	7.87	4.16	-12.79	2.83
PWZ-31A	4.55	-CH ₂ Cl	5.29	2.82	-12.92	0.99	-Cl	4.22	1.77	-14.20	0.66
PWZ-35A	4.60	-CH ₂ OCH ₂ CH ₃	7.65	2.69	-13.42	0.67	-Cl	4.22	1.77	-14.20	0.66
RY66/CMPD	4.42	-CO ₂ Et	7.81	3.09	-12.46	0.06	-CCSi(CH ₃) ₃	7.87	4.16	-12.79	2.83
47											
RY80	4.10	-CO ₂ Et	7.81	3.09	-12.46	0.06	-CCH	5.69	1.76	-13.53	1.78

COMSIA analyses

Illustrated in Figure 156 are compounds are overlapped using the pharmacophore in Figure 149. Table 39 lists the results of a comparative molecular similarity index (COMSIA) analysis applied to electrophysiological data and employing steric, hydrophobic, and electrostatic COMSIA fields which surrounded the overlapped ligands (see Methods). In this type of analysis each of the physiochemical descriptors are given a gaussian weighted functional form and then similarity indices are computed between the training set compounds and a probe atom.^{296, 297} In Figure 153 are the structures of the ligands and the electrophysiological results at 1uM. The analysis provided a modestly predictive result with a q² (predictive r²) of 0.35 and an r² of 0.99 (Figure 157). The weighting of the COMISIA descriptors in this analysis indicated that steric and hydrophobic components between the ligands are key factors in explaining the differences in their electrophysiological activities at the $\alpha 5\beta 2\gamma 2$ GABA(A) receptor

subtype. These initial results supported a correlation between substitutions altering the length of the ligands and the ligands activity, initially deduced from examination of the behavioral results.

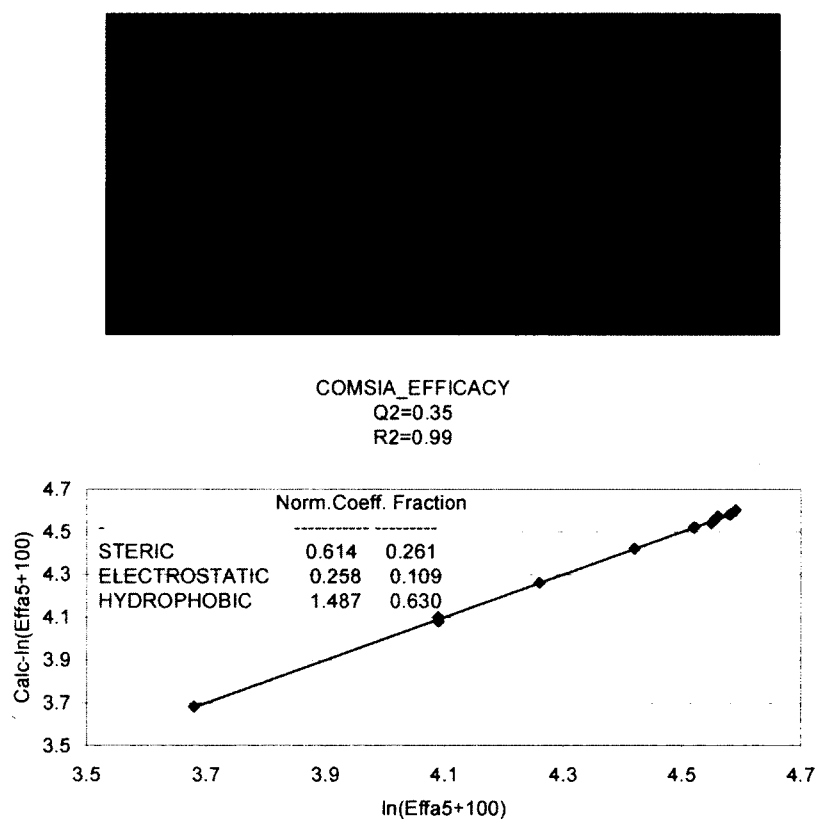


Figure 156. COMSIA analyses (bottom) for the electrophysiological responses ($\ln[E(\alpha 5) + 100]$) of the imidazobenzodiazepines from Figure 153 relative to the $\alpha 5\beta 3\gamma 2$ GABA(A) receptor isoform. The molecular superposition used to perform the COMSIA is shown (above). This COMSIA analyses highlights the importance of steric and hydrophobic features in explaining variations in the electrophysiological response: ($\ln[E(\alpha 5) + 100]$) at $\alpha 5\beta 3\gamma 2$ in that these coefficients (0.3 steric/0.06 hydrophobic) are significantly larger than the electrostatic components (0.1 electrostatic).

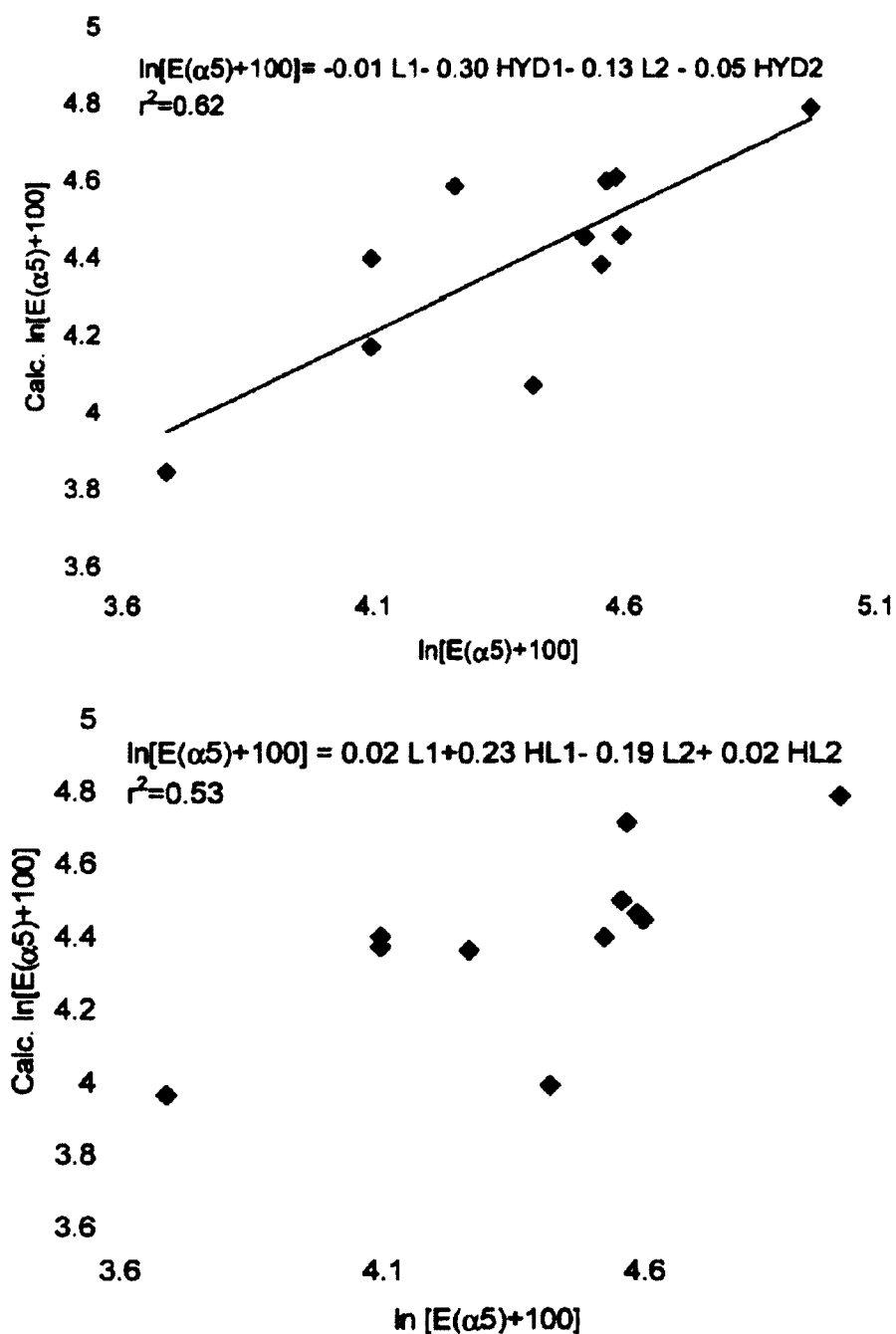


Figure 157. Fragment QSAR analyses of selected properties of the substituents on the common imidazobenzodiazepine template in Table 39. The coefficients of the terms in the QSAR equations indicate the correlations of the magnitude of the fragment Sterimol L (L1 and L2), HOMO-LUMO (HL1 and HL2), and hydrophobicities (HYD1 and HYD2) of the terminal substituents with the resulting electrophysiological response. The finding of significant QSAR coefficients for the fragment Sterimol L values of the second substituents (Table 39) is consistent with the initial notion derived from COMSIA analyses (see A) that ligand length is correlated with electrophysiological response.

COMSIA analysis exhibits strong sensitivities to the overlap criteria applied to the compound set. Therefore, one took steps to independently verify that variations, which resulted in a change in the longest dimension of the ligands, which was correlated with the electrophysiological response seen in the $\alpha 5\beta 2\gamma 2$ receptor subtype. The results in Figure 157 are the results of a fragment QSAR analysis in which variations in the electrophysiological response were modeled in terms of the length of the ‘fragment’ substitutions at either end of the ligand template along with a second variable: HOMO-LUMO energy differences. A comparable analysis could be found using group-hydrophobicity^{296, 297} as the 2nd parameter (results not shown). Both results indicated a reasonable correlation, $r^2=0.53$ for Sterimol L/HOMO-LUMO^{296, 297, 497} and $r^2=0.63$ for Sterimol L/hydrophobicity in regard to the electrophysiological response. The statistical importance, however, was not as great as in the binding fragment QSAR in that the significance was only at the 80% confidence interval (compared to the 99% confidence interval seen with the binding analysis).

In order to further validate the importance of the variables identified using our small test set, one sought to examine a larger published test set. For this a test set of ligands derived from studies by Chambers and coworkers was chosen.⁶⁴ The structures of these ligands and their electrophysiological response are shown in Table 40. If there are particular molecular descriptors that correlate with electrophysiological effects at the $\alpha 5\beta 2\gamma 2$ GABA(A) receptor isoform they should correlate with activation independent of the core template. Illustrated in Figure 158 is an overlap at pharmacophore points for RY10 with the test set published by Chambers and coworkers^{297, 484} in the upper panel

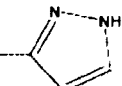
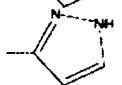
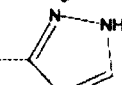
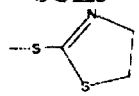
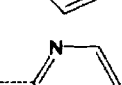
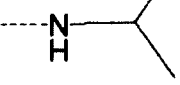
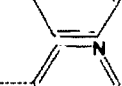
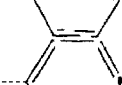
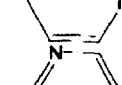
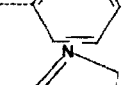
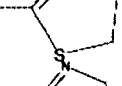
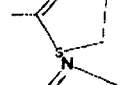
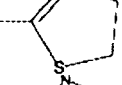
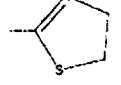

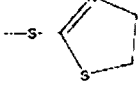
and Ro15-4513 with compound **43** (below). These overlaps make obvious correspondences between polar functional groups as well as hydrophobic/steric features in the two compound sets. Given that the same overlap rule applies, we probed whether the same sets of molecular features found to be important for imidazobenzodiazepines in Table 40 also are explanatory descriptors of the electrophysiological response of the compounds studied by Chambers and coworkers (Table 40). The fragment QSAR (Figure 159) was performed using the properties shown in Table 39 for just the L1/L2 (Sterimol L value for the R1 and R2 substituent) variable set, which had an $r^2=0.5$, an F value of 3.5, and a standard error of 0.2. When the analysis was performed in terms of L1/(HOMO-LUMO)-1 and L2/(HOMO-LUMO)2 one found an r^2 of 0.5, an F value of 1.5 and a standard error of 0.2. These independent results further verify the importance of the fragment length and HOMO-LUMO of the terminal substituents. Note that this test set, like our own, highlights the subtlety of minor size changes of substituents and their electronic effects. Moreover, compounds **43** and **44** of this set differ only in the insertion of an extra $-(CH_2)-$ /methylenic fragment and yet this alteration changes the electrophysiological response at α_5 containing receptors from -38 to $+25$. Demonstrated in Figure 160 is the level of discrimination of inverse agonists from antagonists in this set based on the HOMO-LUMO energy differences. This independently verifies the importance of electronic factors in discriminating subtle differences in electrophysiological responses.

Illustrated in Table 40 are fragments and selected fragment properties for a series of 6,7-dihydro-2-benzothiophen-4(5H)-ones L, B1, Sterimol and electronic HOMO-

LUMO (HLn) parameters used in a fragment QSAR for direct comparison with results for the imidazobenzodiazepines shown in Table 39.

Table 40. (Above) Structures with binding affinities (top number) and efficacies (bottom number) of compounds studied by Chambers et. al.⁴⁹⁸⁻⁵⁰¹ (Below) Fragments and selected fragment properties for a series of 6,7-dihydro-2-benzothiophen-4(5H)-ones L, B1, Sterimol and electronic HOMO-LUMO (HLn) parameters used in a fragment QSAR for direct comparison with results for the imidazobenzodiazepines shown in Table 39.

			Ki ($\alpha 5$) nM	
			$\epsilon(\alpha 5)$	
45	#26	#39	1.2	1.2
5.1	1	2.2	1.2	1.2
3	32	24	1.2	1.2
			1.2	1.2
#11	#37	#13	1.6	1.6
1.1	3	1.6	1.6	1.6
1	6	2	1.6	1.6
			1.6	1.6
#11	#37	#13	1.6	1.6
1.1	3	1.6	1.6	1.6
1	6	2	1.6	1.6
			1.6	1.6
#11	#37	#13	1.6	1.6
1.1	3	1.6	1.6	1.6
1	6	2	1.6	1.6
			1.6	1.6
#11	#37	#13	1.6	1.6
1.1	3	1.6	1.6	1.6
1	6	2	1.6	1.6
			1.6	1.6
#11	#37	#13	1.6	1.6
1.1	3	1.6	1.6	1.6
1	6	2	1.6	1.6
			1.6	1.6
#11	#37	#13	1.6	1.6
1.1	3	1.6	1.6	1.6
1	6	2	1.6	1.6
			1.6	1.6
#11	#37	#13	1.6	1.6
1.1	3	1.6	1.6	1.6
1	6	2	1.6	1.6
			1.6	1.6
#11	#37	#13	1.6	1.6
1.1	3	1.6	1.6	1.6
1	6	2	1.6	1.6
			1.6	1.6
#11	#37	#13	1.6	1.6
1.1	3	1.6	1.6	1.6
1	6	2	1.6	1.6
			1.6	1.6
#11	#37	#13	1.6	1.6
1.1	3	1.6	1.6	1.6
1	6	2	1.6	1.6
			1.6	1.6
#11	#37	#13	1.6	1.6
1.1	3	1.6	1.6	1.6
1	6	2	1.6	1.6
			1.6	1.6
#11	#37	#13	1.6	1.6
1.1	3	1.6	1.6	1.6
1	6	2	1.6	1.6
			1.6	1.6
#11	#37	#13	1.6	1.6
1.1	3	1.6	1.6	1.6
1	6	2	1.6	1.6
			1.6	1.6
#11	#37	#13	1.6	1.6
1.1	3	1.6	1.6	1.6
1	6	2	1.6	1.6
			1.6	1.6
#11	#37	#13	1.6	1.6
1.1	3	1.6	1.6	1.6
1	6	2	1.6	1.6
			1.6	1.6
#11	#37	#13	1.6	1.6
1.1	3	1.6	1.6	1.6
1	6	2	1.6	1.6
			1.6	1.6
#11	#37	#13	1.6	1.6
1.1	3	1.6	1.6	1.6
1	6	2	1.6	1.6
			1.6	1.6
#11	#37	#13	1.6	1.6
1.1	3	1.6	1.6	1.6
1	6	2	1.6	1.6
			1.6	1.6
#11	#37	#13	1.6	1.6
1.1	3	1.6	1.6	1.6
1	6	2	1.6	1.6
			1.6	1.6
#11	#37	#13	1.6	1.6
1.1	3	1.6	1.6	1.6
1	6	2	1.6	1.6
			1.6	1.6
#11	#37	#13	1.6	1.6
1.1	3	1.6	1.6	1.6
1	6	2	1.6	1.6
			1.6	1.6
#11	#37	#13	1.6	1.6
1.1	3	1.6	1.6	1.6
1	6	2	1.6	1.6
			1.6	1.6
#11	#37	#13	1.6	1.6
1.1	3	1.6	1.6	1.6
1	6	2	1.6	1.6
			1.6	1.6
#11	#37	#13	1.6	1.6
1.1	3	1.6	1.6	1.6
1	6	2	1.6	1.6
			1.6	1.6
#11	#37	#13	1.6	1.6
1.1	3	1.6	1.6	1.6
1	6	2	1.6	1.6
			1.6	1.6
#11	#37	#13	1.6	1.6
1.1	3	1.6	1.6	1.6
1	6	2	1.6	1.6
			1.6	1.6
#11	#37	#13	1.6	1.6
1.1	3	1.6	1.6	1.6
1	6	2	1.6	1.6
			1.6	1.6
#11	#37	#13	1.6	1.6
1.1	3	1.6	1.6	1.6
1	6	2	1.6	1.6
			1.6	1.6
#11	#37	#13	1.6	1.6
1.1	3	1.6	1.6	1.6
1	6	2	1.6	1.6
			1.6	1.6
#11	#37	#13	1.6	1.6
1.1	3	1.6	1.6	1.6
1	6	2	1.6	1.6
			1.6	1.6
#11	#37	#13	1.6	1.6
1.1	3	1.6	1.6	1.6
1	6	2	1.6	1.6
			1.6	1.6
#11	#37	#13	1.6	1.6
1.1	3	1.6	1.6	1.6
1	6	2	1.6	1.6
			1.6	1.6
#11	#37	#13	1.6	1.6
1.1	3	1.6	1.6	1.6
1	6	2	1.6	1.6
			1.6	1.6
#11	#37	#13	1.6	1.6
1.1	3	1.6	1.6	1.6
1	6	2	1.6	1.6
			1.6	1.6
#11	#37	#13	1.6	1.6
1.1	3	1.6	1.6	1.6
1	6	2	1.6	1.6
			1.6	1.6
#11	#37	#13	1.6	1.6
1.1	3	1.6	1.6	1.6
1	6	2	1.6	1.6
			1.6	1.6
#11	#37	#13	1.6	1.6
1.1	3	1.6	1.6	1.6
1	6	2	1.6	1.6
			1.6	1.6
#11	#37	#13	1.6	1.6
1.1	3	1.6	1.6	1.6
1	6	2	1.6	1.6
			1.6	1.6
#11	#37	#13	1.6	1.6
1.1	3	1.6	1.6	1.6
1	6	2	1.6	1.6
			1.6	1.6
#11	#37	#13	1.6	1.6
1.1	3	1.6	1.6	1.6
1	6	2	1.6	1.6
			1.6	1.6
#11	#37	#13	1.6	1.6
1.1	3	1.6	1.6	1.6
1	6	2	1.6	1.6
			1.6	1.6
#11	#37	#13	1.6	1.6
1.1	3	1.6	1.6	1.6
1	6	2	1.6	1.6
			1.6	1.6
#11	#37	#13	1.6	1.6
1.1	3	1.6	1.6	1.6
1	6	2	1.6	1.6
			1.6	1.6
#11	#37	#13	1.6	1.6
1.1	3	1.6	1.6	1.6
1	6	2	1.6	1.6
			1.6	1.6
#11	#37	#13	1.6	1.6
1.1	3	1.6	1.6	1.6
1	6	2	1.6	1.6
			1.6	1.6
#11	#37	#13	1.6	1.6
1.1	3	1.6	1.6	1.6
1	6	2	1.6	1.6
			1.6	1.6
#11	#37	#13	1.6	1.6
1.1	3	1.6	1.6	1.6
1	6	2	1.6	1.6
			1.6	1.6
#11	#37	#13	1.6	1.6
1.1	3	1.6	1.6	1.6
1	6	2	1.6	1.6
			1.6	1.6
#11	#37	#13	1.6	1.6
1.1	3	1.6	1.6	1.6
1	6	2	1.6	1.6
			1.6	1.6
#11	#37	#13	1.6	1.6
1.1	3	1.6	1.6	1.6
1	6	2	1.6	1.6
			1.6	1.6
#11	#37	#13	1.6	1.6
1.1	3	1.6	1.6	1.6
1	6	2	1.6	1.6
			1.6	1.6
#11	#37	#13	1.6	1.6
1.1	3	1.6	1.6	1.6
1	6	2	1.6	1.6
			1.6	1.6
#11	#37	#13	1.6	1.6
1.1	3	1.6	1.6	1.6
1	6	2	1.6	1.6
			1.6	1.6
#11	#37	#13	1.6	1.6
1.1	3	1.6	1.6	1.6
1	6	2	1.6	1.6
			1.6	1.6
#11	#37	#13	1.6	1.6
1.1	3	1.6	1.6	1.6
1	6	2	1.6	1.6
			1.6	1.6
#11	#37	#13	1.6	1.6
1.1	3	1.6	1.6	1.6
1	6	2	1.6	1.6
			1.6	1.6
#11	#37	#13	1.6	1.6
1.1	3	1.6	1.6	1.6
1	6	2	1.6	1.6
			1.6	1.6
#11	#37	#13	1.6	1.6
1.1	3	1.6	1.6	1.6
1	6	2	1.6	1.6
			1.6	1.6
#11	#37	#13	1.6	1.6
1.1	3	1.6	1.6	1.6
1	6	2	1.6	1.6
			1.6	1.6
#11	#37	#13	1.6	1.6
1.1	3	1.6	1.6	1.6
1	6	2	1.6	1.6
			1.6	1.6
#11	#37	#13	1.6	1.6
1.1	3	1.6	1.6	1.6
1	6	2	1.6	1.6
			1.6	1.6
#11	#37	#13	1.6	1.6
1.1	3	1.6	1.6	1.6
1	6	2	1.6	1.6
			1.6	1.6
#11	#37	#13	1.6	1.6
1.1	3	1.6	1.6	1.6
1	6	2	1.6	1.6
			1.6	1.6
#11	#37	#13	1.6	1.6
1.1	3	1.6	1.6	1.6
1	6	2	1.6	1.6
			1.6	1.6
#11	#37	#13	1.6	1.6
1.1	3	1.6	1.6	1.6
1	6	2	1.6	1.6
			1.6	1.6
#11	#37	#13	1.6	1.6
1.1	3	1.6	1.6	1.6
1	6	2	1.6	1.6

No.	R1	R2	B5	A5	L1	B1-1	HL1	L-2	B1-2	HL2
			5.2	-3	6.64	3.37	-10.4	5.53	2.67	-9.4
5		SCH ₃								
14			1.4	-7	6.64	3.37	-10.4	8.01	3.36	-8.6
20			3.9	-2	6.64	3.37	-10.4	6.66	3.37	-13.3
26		SCH ₃	1.7	-38	7.24	3.34	-10.2	5.53	2.67	-9.4
27		SCH ₃	5.8	-40	7.24	3.34	-10.2	5.53	2.67	-9.4
28		SCH ₃	9.1	-20	7.24	3.34	-10.2	5.53	2.67	-9.4
34		SCH ₃	0.5	-39	7.24	3.34	-10.2	7.82	2.59	-9.2
39		SCH ₂ CH ₂ OH	2.2	-24	6.98	3.50	-9.6	5.53	2.67	-9.4
43		SCH ₃	1.6	-38	6.98	3.50	-9.6	7.82	2.59	-9.2
44		SCH ₂ CH ₂ OH	4.7	+25	6.98	3.50	-9.6	8.22	3.82	-9.3
45		SCH ₂ CH ₂ CH ₂ OH								
			1.4	-5	6.98	3.50	-9.6	8.01	3.36	-8.6

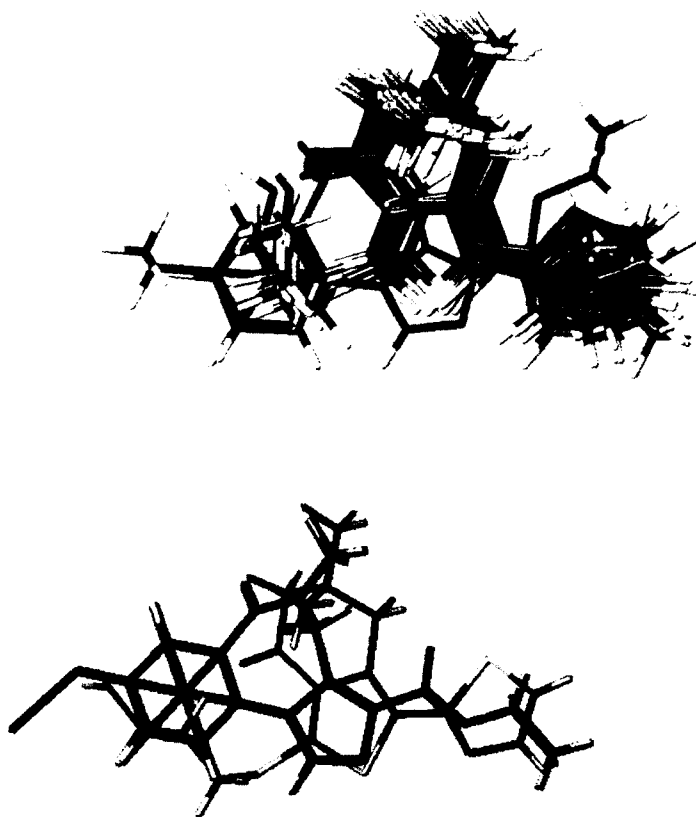


Figure 158. Overlap of ligands studied by Chambers and coworkers with RY10 (above) and Ro15-4513 (below). Note the spatial correspondence of polar (red O/blue N/yellow S atoms) and hydrophobic (grey C/white H) regions.

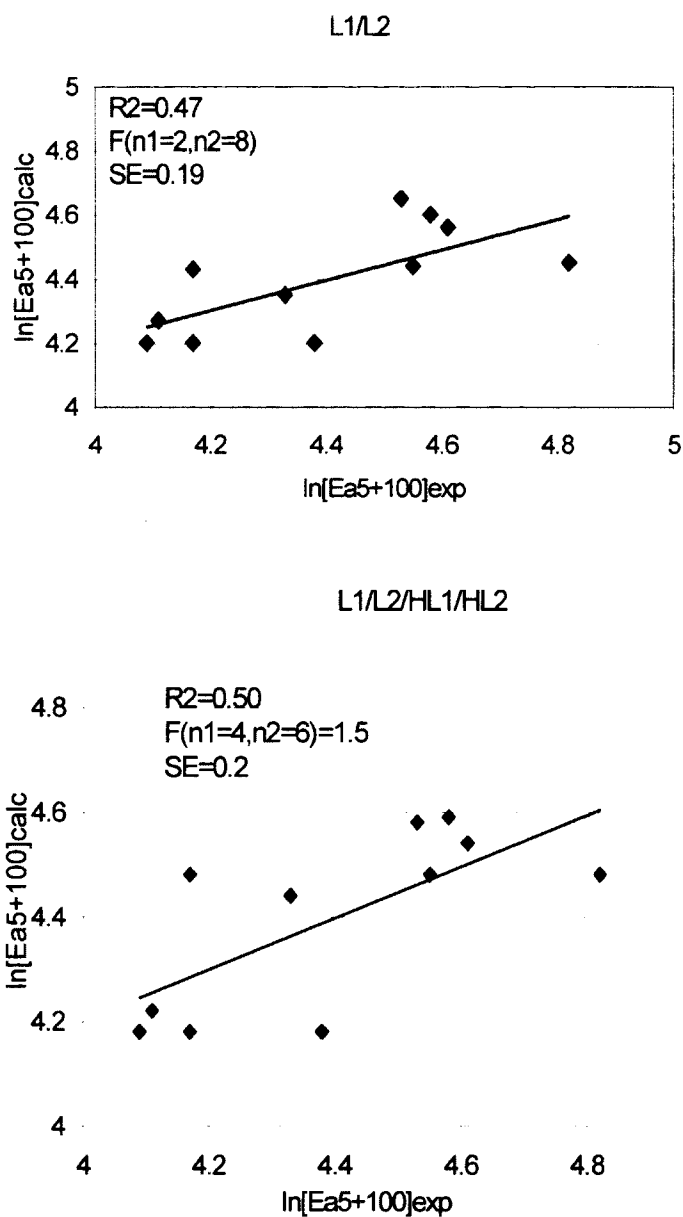


Figure 159. Fragment QSAR for binding at $\alpha 5\beta 3\gamma 2$ with electrophysiological response ($\ln[E(\alpha 5)+100]=0.73 L1+0.22 L2$ (upper panel) and $\ln[E(\alpha 5)+100]=0.66 L1+0.21 HL1+0.09 L2+0.04 HL2$) (lower panel) where HL1 and HL2 are the HOMO-LUMO energy differences for the substituents identified in Table 40.

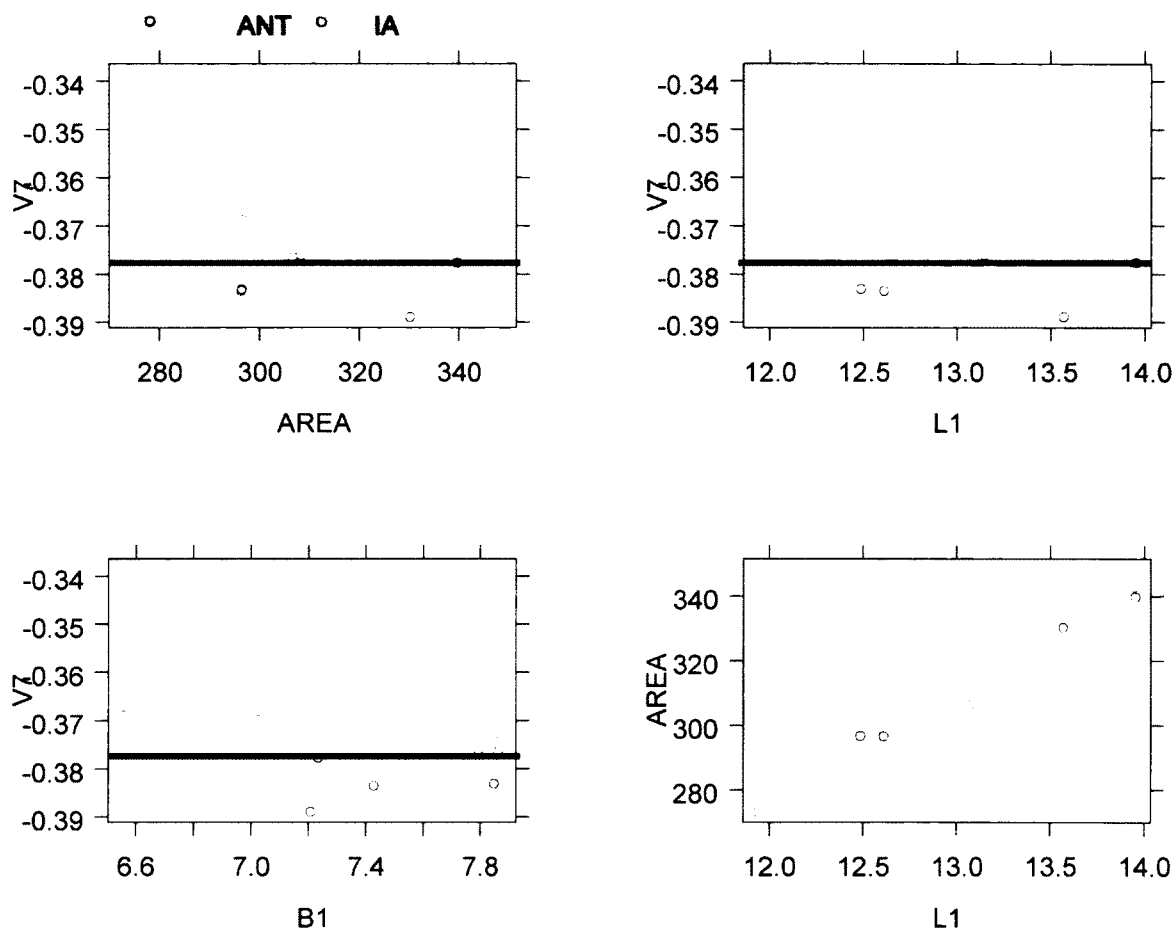


Figure 160. HOMO-LUMO energy differences between inverse agonists and antagonists.

In Figure 158, the overlap of ligands studied by Chambers and coworkers⁴⁶ with RY10 and Ro15-4513 is illustrated. Note the spatial correspondence of polar and hydrophobic regions. In Table 40, the structures and binding affinities of compounds studied by Chambers *et. al.* is presented. Fragment QSAR for binding at $\alpha 5\beta 2\gamma 2$ left panel and multivariate discriminant analysis (whole ligands) are shown in Figure 158. The variable $V7=E(\text{HOMO})-E(\text{LUMO})$ calculated is presented in Figure 160.

$\alpha 5\beta 2\gamma 2$ BzR/GABA(A)ergic Subtype Selective Bivalent Antagonists Reverse Scopolomine Induced Cognitive Impairment.

Earlier the profile of RY-80 as a selective ligand for $\alpha 5$ subtypes based on a 1,4-benzodiazepine template was discussed. However, it was also an inverse agonist at $\alpha 1$ and $\alpha 2$ receptor subtypes and was therefore proconvulsant/convulsant. In marked contrast, when RY80 was made into the bivalent molecule BiRY80 (created by linking together two molecules of RY80 at C-3 via a 3 carbon linker to the ester function), Figure 161 it exhibited a selectivity for the $\alpha 5\beta 2\gamma 2$ isoform with binding affinities of 70-150 fold higher than for binding at other GABA(A) receptors.⁴⁶ A variety of reports have suggested the achievement of subtype selectivity, however, few have achieved this level of discrimination.⁴⁶ This synthetic effort was successful in that it also reduced the convulsive potential of the new ligand compared to RY80 (unpublished data).

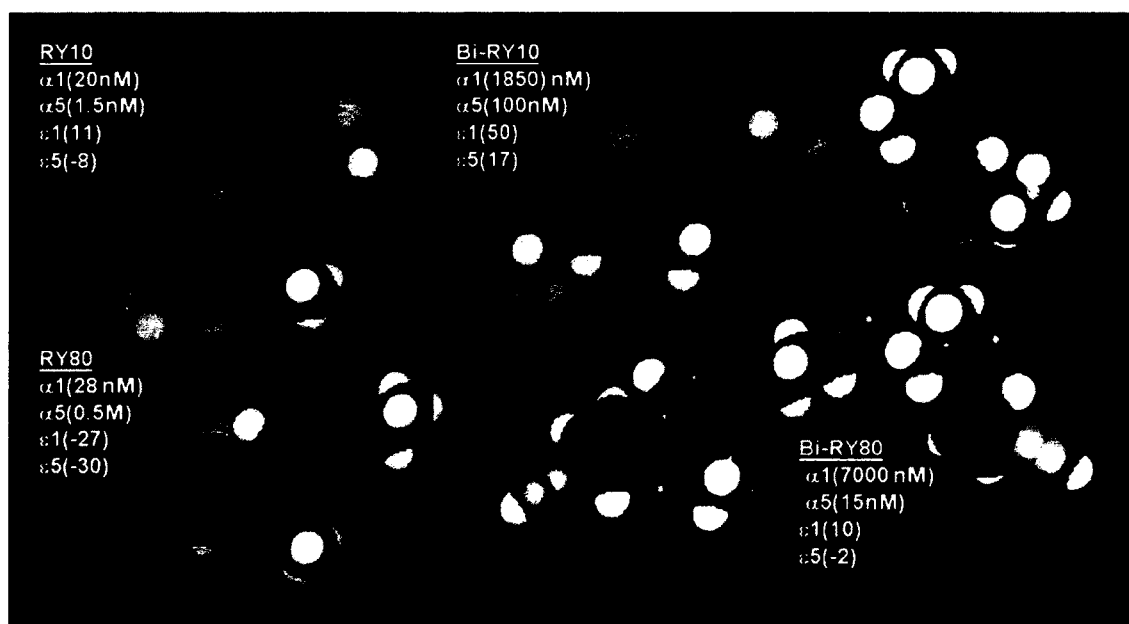


Figure 161. Van der Waal representations of compounds RY80, RY10 and their respective bivalent compounds BiRY80 and BiRY10

The binding affinities at the GABA(A) receptor isoforms that contain either the $\alpha 1$ or $\alpha 5$ subunits in combination with $\beta 3$ and $\gamma 2$ subunits is presented along with van der Waals radii in Figure 161. The bottom two numbers represent the electrophysiological values determined in the presence of the EC_{20} of GABA at a 1 μ M concentration of the ligand being tested.

However, the robust 30% attenuation of GABA mediated Cl^- currents through $\alpha 5$ subunit containing GABA(A) receptors observed with RY80 was also diminished with BiRY80, which behaved more like an antagonist. Given that both RY80 and BiRY80 effectively compete off the radioactive Ro15-4513 ligand suggest subtle facets that alter either BiRY80's binding orientation or its modulation of receptor conformation which leads to an alteration of the pharmacological activity profile. Given the antagonistic

outcome of BiRY80 in regards to electrophysiological measurements this compound was expected to lack effects on attenuating cognitive impairment in our mouse model. However, this proved not be the case as BiRY80 was found to significantly attenuate scopolamine-induced contextual memory impairment in a mouse model used for Alzheimer's early screening of ligands (Figure 162). We also saw a similar effect with BiRY10 (a bivalent molecule made by connecting two molecules of RY10 via their ester groups) (Figure 162). In a similar fashion to BIRY80, BIRY10 led to an increase in the selectivity of binding for the $\alpha 5\beta 2\gamma 2$ GABA(A) receptor isoform resulting in about a 20-80 fold selectivity for $\alpha 5$ subunit containing GABA(A) receptors over other isoforms. Like BiRY80, BiRY10 was also able to reverse scopolamine induced contextual memory (Figure 162). In order to determine if the cognitive effects may have been produced by interacting with another receptor class this compound was further screened for effects on other receptor classes in the NIH Case Western Reserve Drug Screening Program and found to be without appreciable binding to other major classes of receptors. Therefore, one is left with the observation that highly selective antagonists of $\alpha 5$ subunit containing GABA(A) receptors are able to influence contextual memory. This in itself is not a new observation as the classic BZD antagonist Ro15-1788 (flumazenil), with high affinity binding towards most GABA(A) receptor isoforms, has also been consistently reported to exhibit effects by itself, both clinically and electrophysiologically. However, depending on the screen the effects of Ro15-1788 have been agonist sometimes, antagonist sometimes and inverse agonist at times.⁴⁸⁹

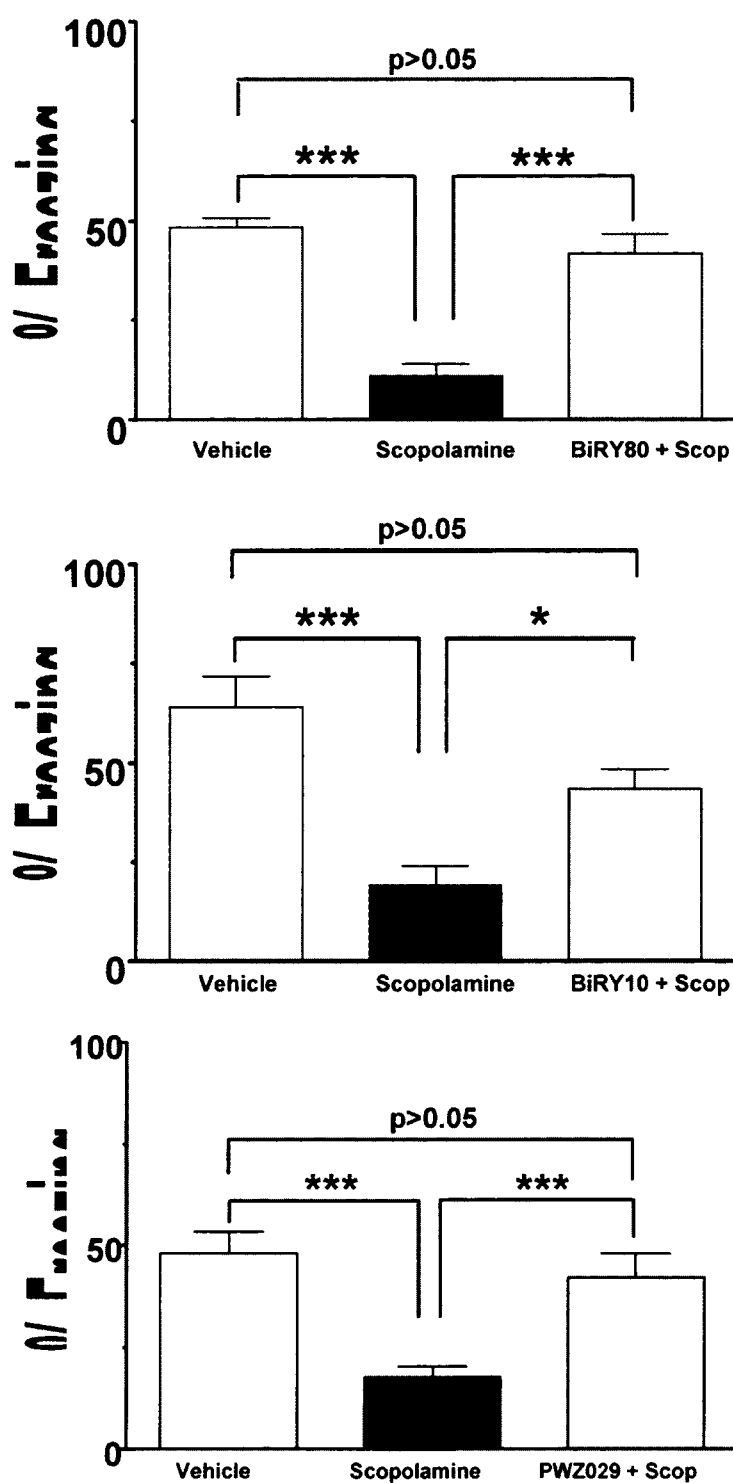


Figure 162. Pavlovian fear conditioned contextual memory. Each mouse was injected ip with either vehicle (0.9% saline containing 2.5% encapsin), 1.5 mg/kg scopolamine, or 1.5 mg/kg scopolamine + drug (top) 10 mg/kg BiRY80 or (center) 10 mg/kg BiRY10 or (bottom) 10

mg/kg PWZ-029. Twenty minutes after injection mice were fear conditioned to the context and tested 24 hours later, well after the drugs and scopolamine have cleared. A reduction in freezing, as observed in mice that received scopolamine alone, is reflective of a low level of contextual memory. Each drug, tested in the absence of scopolamine, was found not to differ significantly from vehicle administered alone; * $p < 0.05$, data not shown; * $p < 0.001$. $N = 12$ male C57BL/6J mice per vehicle or drug. This is an important set of results.**

Finally, the selective $\alpha 5$ isoform agonist, SH-053-R-CH3,^{296, 297} was also assessed in mice in order to ascertain whether it is able to impair contextual memory in the absence of scopolamine. SH-053-R-CH3 (30 mg/kg) was indeed able to impair contextual memory in the absence of scopolamine (Figure 163), thereby providing further “proof of principle” that compounds displaying selective influence on $\alpha 5$ isoforms, whether by potentiation or attenuation of GABA’s effect on $\alpha 5$ isoforms, lead to significant effects on contextual memory. In stark contrast to the findings of Savic et al.,³⁷¹ one did not observe a significant reduction ($p = 0.284$) in locomotion between mice given either 30 mg/kg SH- 053-R-CH3 or vehicle during a 40 min post injection observation period, as measured by automated assessment of spontaneous locomotor activity (1026 ± 57 versus 770 ± 210 , respectively). In addition, chamber circumnavigation was also assessed during the initial 4 minute exploration phase of the fear conditioning protocol prior to shock delivery and no significant difference ($p = 0.63$) in this locomotor parameter between mice receiving SH-053-R-CH3 or vehicle (data not shown) was found. In a similar fashion, Savic et al.,¹²³ did not observe a change in distance traveled between mice receiving SH-053-R-CH3 or vehicle when evaluated in the elevated plus maze protocol. It was beyond the scope of this study to systematically investigate the affects of structural substitutions on the imidazobenzodiazepine template that would lead to robust electrophysiological agonism at $\alpha 5\beta\gamma 2$ GABA(A) receptor

isoforms. However, if one were to juxtapose the structures of the majority of imidazobenzodiazepines in this study (e.g., see Figure 153) with SH-053-RCH3 and Ro16-6028, both robust electrophysiological agonists of $\alpha 5$ isoforms, one quickly discerns that both compounds involve structural changes in a region outside of our present pharmacophore, which was primarily designed to aid in predicting inverse agonism.

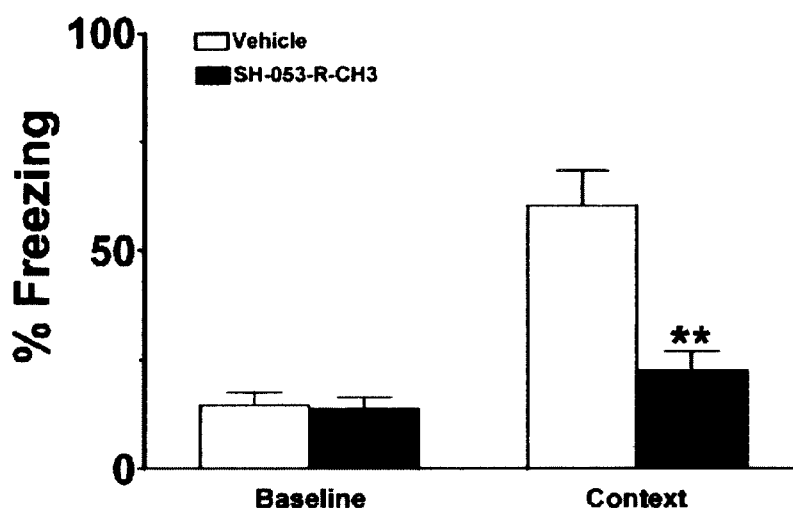


Figure 163. 30 mg/kg SH-053-R-CH3 in the absence of scopolamine.

Further confirmation that the activity of Xli356 (BiRY10) was hippocampal-driven was the observation that in audio cued memory experiments there was no increase in freezing (see Audio Cued data for Xli356 in the Appendix).

Whereas at the dosages used of either BiRY80 or BiRY10, they would not be expected to attenuate GABA influence on Cl flux, the interpretation of such results are not clear and again raises the question, “Is there the presence of an endogenous modulation of the BDZ site that is being antagonized by these bivalent molecules?” Over the years many investigators have attempted to identify a natural ligand for this site with results heavily debated. This potential endogenous modulator, termed endozepine (endogenous BDZ-like compounds), has been suggested as being involved in reducing anxiety, seizure thresholds and muscle relaxation as well as modulating vigilance.⁵⁰² There also exists the possibility that a metabolite of BiRY80 is acting perhaps more like an inverse agonist *in vivo* than would be expected from antagonistic results seen in the *in vitro* electrophysiological studies of BiRY80.

Xli356 and PWZ-029 PDSP data

Reports from Roth at NIMH Psychoactive Drug Screening Program (PDSP) at the University of North Carolina Chapel Hill Medical School have shown PWZ-029 and Xli356 (BiRY10) were quite clean BzR ligands (Figure 164). Examination of the binding affinity of Xli356 and PWZ-029 in a battery of receptors indicated both bound to benzodiazepine receptors but did not potently bind to other receptors run to date. Receptors in the PDSP screen include cannabinoids, histamines, prostoglandins, glutamate, Ca⁺ channel, transporters, adrenergic, acetylcholine, dopamine, serotonin, opiates, and others (See Appendix for complete PDSP data and code numbers).

NOTE: Data on this page ("Secondary Binding") are K_i values.
 K_i values are reported in nanomolar concentration.
 To view the experiment error, source, species, concentration, etc, click on the result

Legend:		Secondary Approved						
CMPD	PI	5ht1a	5ht1b	5ht1d	5ht1e	5ht2a	5ht2b	5ht2c
1693	Cook							
3173	Cook							
CMPD	Beta1	Beta2	Beta3	BZP (a1)	BZP (a2)	BZP (a3)	BZP (a5)	BZP (a6)
1693								
3173								
CMPD	5ht3	5ht5a	5ht6	5ht7	A2	A2B2	A2B4	A3B2
1693								
3173								
CMPD	DOR	EP1	EP2	EP3	EP4	GabaA	GabaB	H1
1693								
3173								
CMPD	H3	H4	HERG	Midazolam	KA-R*	KOR	M1	M2
1693						6.118.00		
3173								
CMPD	M4	M5	MDR 1	mGluR1a	mGluR2	mGluR4	mGluR5	mGluR5_Cloned
1693								
3173								
CMPD	mGluR6	MOR	A-Chan	NET	NK-1	NK-2	NK-3	NMDA/MK801
1693								
3173								
CMPD	PKCa	PKCb	PKCd	PKCe	PKCg	SERT	Sigma 1	Sigma 2
1693								
3173								
CMPD	A4B2	A4B2**	A4B4	Alpha1A	Alpha1B	Alpha2A	Alpha2B	Alpha2C
1693								
3173								
CMPD	Ca+Channel	CB1	CB2	D1	D2	D3	D4	D5
1693								
3173								
CMPD	V2	V3	VMAT1	VMAT2				
1693								
3173								

1693	xdl356
3173	pwz-029

Figure 164. BzR ligands binding to other receptors. Data represent mean % inhibition (N = 4 determinations) for compounds tested at receptor subtypes.

Numerous papers have reported the cognitive influence, attenuating or potentiating, that benzodiazepine ligands elicit. However, due to potential side effects (ie. convulsive or proconvulsive tendencies of the inverse agonists) therapeutic viability has been questioned. As more subtype selective BZD ligands are beginning to turn up in the literature, one is able to begin the process of determining if there are isoforms of the GABA(A) receptors

that contribute to cognitive effects separate of convulsive potential. With this goal in mind, pharmacophores were initially developed based on a set of nonselective ligands with high binding affinities to GABA(A) receptor subtypes at $\alpha 1\beta 2\gamma 2$ and $\alpha 5\beta 2\gamma 2$. The pharmacophores were used to search chemical databases. A selected set of “hits” were tested for binding affinities to GABA(A) receptors with $\alpha 1\beta 2\gamma 2$ and $\alpha 5\beta 2\gamma 2$ subtype compositions and several of these hits demonstrated sub μ M binding affinities (ranging from 200 nM to 1 μ M). A set of imidazobenzodiazepines displaying a higher degree of selectivity towards the $\alpha 5$ subunit containing isoforms over $\alpha 1$ subunit containing isoforms were then analyzed in order to glean principles underlying binding selectivity towards $\alpha 5\beta 2\gamma 2$ relative to $\alpha 1\beta 2\gamma 2$ GABA(A) isoforms. Examination of computed molecular electrostatic potential surfaces, fragment QSAR, and COMSIA analyses for this series independently revealed the greater importance of one of the hydrogen bond acceptor pharmacophore points for binding to the $\alpha 1\beta 2\gamma 2$ isoform relative than to the $\alpha 5\beta 2\gamma 2$ isoform. The early chemometric analysis of the effects of benzodiazepine ligands on the reversal of scopolamine induced memory deficit indicated the ligands with a sterimol L parameter <14 did not reverse effects of scopolamine. COMSIA and fragment QSAR indicated the importance of the size of the terminal substituents on the imidazobenzodiazepine template and HOMO-LUMO (fragment) energy difference to be correlated with the electrophysiological response at $\alpha 5\beta 2\gamma 2$. If such discriminants of activation are to be meaningful they should apply to other training sets. For this reason we examined the compounds published by Chambers and coworkers^{503, 504} and found the same fragment/substituent properties to be correlated with the electrophysiological response at $\alpha 5\beta 2\gamma 2$. In agreement with our computational assessments one was able to

demonstrate the cognitive influence of several BZD ligands that exhibited reasonable selectivity towards GABA(A) receptor isoforms containing the $\alpha 5$ subunit over other α subunits. Analysis of the the data supported the notion that selective binding to and/or activation of GABA(A) receptors that contain the $\alpha 5$ subunit may prove valuable in addressing potential treatment regimes for memory loss, which result from cholinergic mechanisms.

Further investigations found that compound PWZ-029, which exhibited reasonable binding selectivity toward GABA(A) receptors containing the $\alpha 5$ subunit and possessed a favorable electrophysiological profile, was able to attenuate scopolamine induced contextual memory impairment in mice. In a similar fashion, Dawson et al.,⁵⁰⁵ demonstrated that compound $\alpha 5$ IA, which also selectively decreased GABA-induced activation of $\alpha 5$ isoforms was able to enhance rat performance in the Morris water maze, a spatial memory task sharing similarities with contextual memory tasks. Therefore, one is left with the conclusion that selective attenuation of the activational influence of GABA (either by binding or efficacy) on GABA(A) receptors that contain the $\alpha 5$ subunit may prove valuable in addressing conditions that result in contextual/spatial memory impairment. The additional observation that compound SH-053-R-CH3, which selectively potentiates GABA's influence on GABA(A) receptors containing the $\alpha 5$ subunit, impairs contextual memory further supports the "proof of principle" that $\alpha 5$ subunit containing GABA_A receptor isoforms can be selectively exploited in order to influence processes involved in contextual memory. PWZ-029, **56**, enhanced cognition specifically and demonstrated a weak anxiolytic effect⁵⁰⁶ using rhesus monkeys in the conflict model and

weak anticonvulsant activity in rodents.⁴⁸⁸ **The ligand, PWZ-029 enhances memory but cannot possibly be proconvulsant nor convulsant.**

Given the electrophysiological profiles of the two bivalent compounds in relationship to their cognitive effects poses some intriguing questions into the nature of the molecular mechanisms by which these compounds are influencing contextual memory.

The electrophysiological profiles of the bivalent compound BiRY-080, an $\alpha 5$ selective antagonist, when juxtaposed with its ability to attenuate scopolamine-induced contextual memory impairment, raises intriguing questions into the nature of the molecular mechanism by which a compound such as this is able to influence contextual memory. One observed that the ability of $\alpha 5$ selective antagonists and weak inverse agonists to affect memory was dependent on ligand size (Sterimol L parameter). These results are not unlike other nonclassical inhibition patterns, where the ability to inhibit appears to correlate better with ligand size rather than affinity.^{391, 392} While beyond the scope of this dissertation, these results suggest that either (1) the earlier hypotheses of endogenous ligand displacement by an antagonist, in this case only requiring antagonism of $\alpha 5$ subunit containing GABA(A) receptor isoforms, is sufficient for behavioral alteration; (2) alternatively, an additional GABA(A) receptor isoform (i.e., $\alpha 4\beta 3\gamma$),^{46, 64} not originally expected to have an effect, is mitigating the observed effects. Our results lend support toward the notion that compounds that selectively influence $\alpha 5\beta \gamma 2$ GABA(A) receptors, whether by inverse agonism, antagonism, or agonism, are each capable of modulating

contextual memory; the former two ligands enhance cognition, the former two ligands enhance cognition, the later decreases it.

Preparation of Cloned mRNA

Cloning of GABA(A) receptor subunits $\alpha 1$, $\beta 3$ and $\gamma 2$ into pCDM8 expression vectors (Invitrogen, CA) for these studies has been described elsewhere.⁵⁰⁷ The GABA(A) receptor subunit $\alpha 4$ was cloned in an analogous way. The cDNAs for subunits $\alpha 2$, $\alpha 3$ and $\alpha 5$ were gifts from P. Malherbe and were subcloned into pCI-vector. The cDNA for subunit $\alpha 6$ was a gift from P. Seeburg and was subcloned into the vector pGEM-3Z (Promega). After linearizing the cDNA vectors with appropriate restriction endonucleases, capped transcripts were produced using the mMessage mMachine T7 transcription kit (Ambion, TX). The capped transcripts were polyadenylated using yeast poly(A) polymerase (USB, OH) and were diluted and stored in diethylpyrocarbonate-treated water at -70°C .^{187, 480}

Functional Expression of GABA(A) Receptors

The methods used for isolating, culturing, injecting and defolliculating of the oocytes were identical with those described by E. Sigel.^{187, 480} Mature female *Xenopus laevis* (Nasco, WI) were anaesthetized in a bath of ice-cold 0.17 % Tricain (Ethyl-m-aminobenzoate, Sigma, MO) before decapitation and removal of the frogs ovary. Stage 5 to 6 oocytes with the follicle cell layer around them were singled out of the ovary using a platinum wire loop. Oocytes were stored and incubated at 18°C in modified Barths' Medium (MB, containing 88 mM NaCl, 10 mM HEPES-NaOH (pH 7.4), 2.4 mM NaHCO_3 , 1 mM KCl, 0.82 mM MgSO_4 , 0.41 mM CaCl_2 , 0.34 mM $\text{Ca}(\text{NO}_3)_2$) that was

supplemented with 100 U/mL penicillin and 100 µg/ml streptomycin. Oocytes with follicle cell layers still around them were injected with 50 nL of an aqueous solution of cRNA. This solution contained the transcripts for the different alpha subunits and the beta 3 subunit at a concentration of 0.0065 ng/nL as well as the transcript for the gamma 2 subunit at 0.032 ng/nL. After injection of cRNA, oocytes were incubated for at least 36 hours before the enveloping follicle cell layers were removed. To this end, oocytes were incubated for 20 min at 37°C in MB that contained 1 mg/mL collagenase type IA and 0.1 mg/ml trypsin inhibitor I-S (both Sigma). This was followed by osmotic shrinkage of the oocytes in doubly concentrated MB medium supplied with 4 mM Na-EGTA. Finally, the oocytes were transferred to a culture dish containing MB and were gently pushed away from the follicle cell layer which stuck to the surface of the dish. After removing of the follicle cell layer, oocytes were allowed to recover for at least four hours before being used in electrophysiological experiments.

Electrophysiological Experiments with Sieghart et al.⁵⁰⁸

For electrophysiological recordings, oocytes were placed on a nylon-grid in a bath of *Xenopus* Ringer solution (XR, containing 90 mM NaCl, 5 mM HEPES-NaOH (pH 7.4), 1 mM MgCl₂, 1 mM KCl and 1 mM CaCl₂). The oocytes were constantly washed by a flow of 6 mL/min XR which could be switched to XR containing GABA and/or drugs. Drugs were diluted into XR from DMSO-solutions resulting in a final concentration of 0.1 % DMSO perfusing the oocytes. Drugs were pre-applied for 30 sec before the addition of GABA, which was coapplied with the drugs until a peak response was observed. Between two applications, oocytes were washed in XR for up to 15 minutes to ensure full recovery from desensitization. For current measurements the oocytes were impaled with two microelectrodes (2–3 mΩ), which were filled with 2 mM KCl. All

recordings were performed at room temperature at a holding potential of -60 mV using a Warner OC-725C two-electrode voltage clamp (Warner Instruments, Hamden, CT) or a Dagan CA-1B Oocyte Clamp (Dagan Corporation, Minneapolis, MN). Data were digitised, recorded and measured using a Digidata 1322A data acquisition system (Axon Instruments, Union City, CA). Results of concentration response experiments were fitted using GraphPad Prism 3.00 (GraphPad Software, San Diego, CA). The equation used for fitting concentration response curves was $Y = \text{Bottom} + (\text{Top} - \text{Bottom}) / (1 + 10^{-(X - \text{LogEC}_{50})})$; X represents the logarithm of concentration, Y represents the response; Y starts at Bottom and goes to Top with a sigmoid shape.

In vivo Assessments

Male C57Bl/6 mice were obtained from Charles Rivers Laboratories (Holister, CA) at 6 weeks of age. Mice used in fear conditioning were between 7 and 12 weeks of age. Animals were housed eight to a cage in rooms with a normal 12-h light/12-h dark cycle lights on 700–1900 hr with free access to food and water. Tests were conducted during the light phase between 1300 and 1700 h with a 30-min acclimation period in the testing room prior to drug or vehicle administration. All animal protocols used in this study conform to the guidelines determined by the National Institute of Health, Office for Protection from Research Risks and are approved by the Animal Care and Use Committee of the Palo Alto Veterans Administration Medical Center, Palo Alto, CA, USA.

Pavlovian Fear Conditioning

Before testing each day, the mice were moved to a holding room and allowed to acclimate for at least 30 minutes. Each mouse received an i.p. injection of one of the following: vehicle, benzodiazepine binding site ligand 2–30 mg/kg, scopolamine 1 mg/kg, scopolamine 1 mg/kg combined with one of the benzodiazepine binding site ligands 2–30 mg/kg. The dose level chosen for each compound was one that neither

elicited convulsions nor impaired locomotion. Twenty minutes after injection, the mice were placed individually in one of four identical experimental chambers (Med Associates, St. Albans, VT) that had been scented with 0.3% ammonium hydroxide solution before testing. Chambers were back-lit with fluorescent light with a white noise generator providing 70 dB of background noise. After 4 minutes in the chamber, mice were exposed to a loud tone 85 dB, 2.9 kHz for 32 sec with the last 3 seconds coupled with a 0.75-mA scrambled footshock. This procedure was repeated for a total of three episodes with a 1 minute period separating each episode. One minute after the final footshock, the mice were returned to their home cages. Twenty-four hours later, contextual memory was assessed by placing the mice back into the freshly re-scented 0.3% ammonium hydroxide conditioning chambers in which they were trained, for a 4 minute test period in the absence of footshock. Conditioned fear to the context was assessed by measuring the freezing response according to the methods of Fanselow and Bolles.⁵⁰⁹ Freezing was defined as the absence of all visible movements of the body aside from those necessitated by respiration. Scoring was done using the FreezeScan (Clever Systems Inc., Reston, VA). These data were transformed to a percentage of total observations. Data were analyzed by one-way analysis of variance ANOVA using GraphPad PRISM 2.01 (GraphPad Software). Separate treatment effects between groups were analyzed post hoc using Dunnett's or Bonferroni's multiple comparisons.

Conformational Libraries for Pharmacophore/Overlap Rule Development.

Conformational libraries were developed using a nested rotation approach wherein the energy was evaluated by varying each of the rotatable bonds by 30°, constraining their values at this geometry, and then energy minimizing (using Conjugate Gradients)

the remainder of the structure until the RMS changes in the gradient were smaller than 0.01. All force field parameters used were from the Quanta/CHARMM (Chemistry at Harvard Macromolecular Mechanics) force field. The net atomic charges used, based on parameterization in this program, were also consistent with the fact that all of the compounds are neutral. The initial structures were then energy minimized using 200 steps of steepest descents followed by 2000 - 3000 steps of conjugate gradients or until the RMS changes in the gradient were smaller than 0.01 Å. A long 90 Å potential truncation was used to minimize effects on structure due to potential truncation via a switching function.

Initial Pharmacophore Development

MOLMOD developed in the laboratory of Harris and Delorey⁵¹⁰ was used to develop 3D pharmacophores from input of conformational libraries for each of the ligands, independent distance criteria for conformational clustering and pharmacophore distance-criteria, a trial pharmacophore definition in terms of a set of ligand or receptor based pharmacophore points [including hydrogen bond donor/acceptor, hydrophobic centers, centroids of ring systems or functional groups, and/or user-defined classes based on user-defined property definitions] and an energy window criteria for consideration of ligand conformers. The program first performs conformational clustering and determines if there is at least one conformer from each ligand in the training set in the energy-windows specified that has the same 3D distance metrics within the 'tolerances' specified by the user. The program allows for difference 'tolerances' for each pharmacophore point to allow for conformational/sterically allowed variation in particular regions. If the 3D-distance metrics between pharmacophore points is the same at least one conformation of

each ligand and the pharmacophore distance metrics are reported and the ligands superimposed via a quaternion/least squares procedure for those conformers complying with the pharmacophore. The latter superposition(s) may then be used in 3D-QSAR applications and properties evaluated for those conformers that comply with the pharmacophore for use in multivariate statistical analysis to ascertain the determinants of recognition or activation.

Validation of Overlap Rules/Pharmacophores Via Database Searches

The overlap rules were input to SYBYL/UNITY as sets of hydrogen bond acceptors and centroids. Databases were searched using a distance window of ± 2 angstroms. In particular, Unity, Chapman & Hall, and Maybridge databases were searched for two distinct purposes: 1) to ensure compounds with known GABA(A) receptor binding and activation were retrieved,⁵¹¹ and 2) to extract new compounds for binding, electrophysiological, and behavioral assessment.

Quantum Chemical Evaluation of Properties in Conformations Complying with Pharmacophores for Use in QSAR

Following development of the initial pharmacophores the properties of all compounds were evaluated in their conformations complying with the pharmacophore definition and were evaluated using a combination of semi-empirical quantum mechanics and a MOPAC-7 AM1 Hamiltonian⁵¹² density functional theory as incorporated in Gaussian⁵¹² and Jaguar (Schrödinger, Portland, OR). This included both whole molecule properties as well as those of 'fragments' corresponding to substituent replacements on particular templates. In an effort to understand the SAR of these substitutions we computed: (i) frontier orbital energetics (HOMO/LUMO/HOMO-LUMO), (ii) Sterimol

parameters, (iii) group hydrophobicities, (iv) volumes, (v) areas, (vi) solvent-accessible surface areas, (vii) polar and nonpolar volumes, (viii) globularities, (ix) electrostatic potentials on the van der Waals surface using MOPAC-AM-derived properties developed by the in-house program GRAPHIA and (x) solvation energies. In the case of fragment properties, the substituents were 'capped' with H's prior to calculation of properties.

Fragment and 3D-QSAR Analyses

Both the TRIPOS QSAR module as well as MS-EXCEL were used to form multivariate QSAR analyses for both binding and electrophysiological response as a function of substitutions. The TRIPOS COMSIA module (Tripos QSAR (St. Louis, MO)) was used to perform molecular similarity index analysis (CoMSIA) employing field descriptors around ligands superimposed using MOLMOD.

Molecular Modeling, Synthesis, and Pharmacological Studies of Some Tetracyclic 1,3-Diazepinium Chlorides (with Grant et al.)

Seven new 1, 3-diazepinium chlorides exhibiting structural similarities to the 1,4-benzodiazepines were synthesized Grant et al.⁵¹³⁻⁵¹⁸ and evaluated in the Milwaukee based pharmacophoric model. In a Hippocratic screen using mice, three of these salts, 3-methoxy-6-oxo-7,13-dihydro-6*H*-benzofuro[2,3-*e*]pyrido[1,2-*a*][1,3]diazepin-12-ium chloride **8a**, 3-methoxy-9-methyl-6-oxo-7,13-dihydro-6*H*-benzofuro[2,3-*e*]pyrido[1,2-*a*][1,3]diazepin-12-ium chloride **8c**, and 3-methoxy-11-methyl-6-oxo-7,13-dihydro-6*H*-benzofuro[2,3-*e*]pyrido[1,2-*a*][1,3]diazepin-12-ium chloride **8e**, were examined for their effect on the central nervous system, and their activities compared to that of diazepam. On their own, salts **8a**, **8c**, and **8e** solicited no sedative effects on the behaviour of the animals. However, they elicited significant effects in combination with diazepam on diazepam-induced activities such as decreased motor activity, ataxia and loss of righting reflex. Compounds **8a** and **8c** were fitted into the pharmacophore/receptor model developed by Clayton in Milwaukee with interactions at the L₁, H₁ and A₂ sites indicating that they are potential inverse agonists of the Bz receptor. The compounds displayed some affinity for the $\alpha 1$ isoform of the GABA(A) /BzR (L_{D1} interaction) but were nonselective for $\alpha 5$ (no L₂ interaction). Results of binding affinity studies showed that compound **8a** is mildly selective for the $\alpha 1$ receptor although not very potent ($K_i = 746.5$ nM). The significant potentiation of diazepam-induced ataxia and decreased motor activity by compounds **8a** and **8c** in the Hippocratic screen may be associated with $\alpha 1$ activity. However, this is preliminary data. Experimentation to confirm this needs to be

PART I. UNIFIED PHARMACOPHORE PROTEIN MODELS OF THE
BENZODIAZEPINE RECEPTOR SUBTYPES
PART II. SUBTYPE SELECTIVE LIGANDS FOR $\alpha 5$ GABA(A) /BZ RECEPTORS
VOLUME II

by

Terrill S. Clayton

A Dissertation Submitted in
Partial Fulfillment of the
Requirements for the Degree of

Doctor of Philosophy
in Chemistry

at

The University of Wisconsin-Milwaukee

December 2011

done on other receptor systems (for example cholinergic, ganglionic, and adrenergic receptors).

Other benzodiazepine analogues such as, the 1,3- 2,3- and 1,5-Bzs are known but have received much less attention in comparison to the 1,4-Bzs. Several of the 2,3- and 1,5-Bz analogues have displayed pharmacological activities similar to those of the 1,4-Bzs, while a few 1,3-Bzs, which were synthesized as part of a drug development program for new psychotic drugs, have exhibited antidepressant activity comparable to that of the classic tricyclic antidepressant amitriptyline.⁵¹⁹⁻⁵²²

In 1997, Jackson and Williams⁵¹² reported the synthesis of the pyridinium bromide **1** - a 1,3-diazepinium salt- from the readily available 7-hydroxy-4-methylcoumarin. Structural comparison of compound **1** with the well known 1,4-Bzs is shown in Figure 165.

Both have a 7-membered heterocyclic ring fused to an aromatic ring, but the nitrogen atoms of the heterocyclic rings are in different relative positions. The 4,5-double bond of the 1,4-Bz is β - to the amide functionality and has an aryl moiety attached whereas in salt **1**, the double bond is part of an α,β -unsaturated amide and the aryl substituent is rigidly fixed by a fused furan ring.

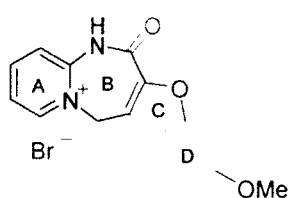
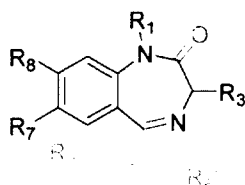
**1****1,4-Benzodiazepines**

Figure 165. Comparison of the structure of 1,3-diazepinium bromide to 1,4-benzodiazepines

Since tetracyclic 1,3-diazepinium bromide (**1**) displays some resemblance to the 1,4-Bzs,⁵²³ Grant and Jackson proposed to synthesize analogues of this type with a view to conducting pharmacological studies to evaluate these compounds as potential therapeutic agents.

Bromides are not ideal for pharmacological studies since they are toxic to the body.⁵¹² Iodides also have chronic effects and are unsuitable here.^{33, 34, 71, 74} Chlorides, on the other hand, are non-toxic and found naturally in the body and were therefore used in their studies.

Outlined here are the reports on pharmacological studies (Hippocratic screen)⁴² and molecular modeling of some tetracyclic 1,3-diazepinium chlorides of type **8**. The 1,3-diazepinium compounds were fitted into the pharmacophore/receptor model for GABA(A) /BzR subtypes and observed for selectivity towards any of the BzR subtypes at Milwaukee. The results were then correlated with those of the pharmacological screen (see Appendix for Chemistry).

Pharmacology

Pharmacological assessment of the 1,3-diazepinium chlorides was done using the Hippocratic screen.⁴² Of the seven salts prepared, only salts **8a**, **8c** and **8e** were tested since they were more soluble in the sample vehicle.⁵²⁴ The observed activities of the chlorides were compared with those of diazepam.

Animals

Albino male and female mice, aged 7-8 weeks with a weight of 16–25 g were obtained from the Animal House of the University of the West Indies, Mona. The animals were provided with food and water *ad libitum*. The studies were performed according to protocols approved by the Faculty of Medicinal Sciences/University Hospital of the West Indies Ethics Committee.

Preparation of Drug Samples

Diazepam was dissolved in corn oil (5 mg/mL) and compounds **8a**, **8c** and **8e** were dissolved in distilled water (2 mg/ mL).

Hippocratic Screen 1

Mice were randomly assigned to six groups with six animals in each group. Animals in groups one (C1) and two (C2) were administered distilled water and corn oil respectively. Group three (DZ1) was administered the diazepam solution and groups four to six administered solutions of **8a**, **8c**, and **8e**, respectively. All administrations were done by intraperitoneal ip injection at a dosage volume of 0.2 mL/10 g of body weight. The grouping and dosing of the animals was done independent of the observer, hence all observations were made without prejudice. Activities measured in the Hippocratic screen include: decreased motor activity, ataxia, loss of righting reflex, analgesia, anesthesia, pinnal reflex, loss of screen grip, paralysis, respiratory rate, tremor and startle reaction.

All observations were made at +5, 10, 15, 30, 45, 60, 90 and 120 minutes, then 24 and 48 hours from the time of injection and the activities were rated as -, ±, +, ++, +++ or +++++, in all cases, - represented no change compared to the control animals.

Hippocratic Screen 2

In a second set of experiments, the animals were divided into four groups of six. Distilled water was given 15 minutes prior to administering diazepam to animals in group one (DZ2) and the remaining groups two to four (**8a**+DZ, **8c**+DZ and **8e**+DZ) were administered salts **8a**, **8c** and **8e**, respectively, 15 minutes before diazepam. All administrations were done by IP injection at a dosage volume of 0.2 mL/10 g of body weight. All observations are unbiased. Activities measured and assigned ratings were the same as in Hippocratic Screen 1. All observations are made at +5, 10, 15, 30, 45, 60, 90 and 120 minutes, then 24 and 48 hours from the time of diazepam injection.

Statistical Analysis

The ratings: -, ±, +, ++, +++ or ++++ were quantified to 5, 4, 3, 2, 1 or 0 respectively. Statistical analysis of the data was performed using SPSS version 12.0 and consisted of General Linear Model (Repeated Measures) with Dunnett t (2-sided) Post Hoc test, the Kruskal-Wallis test followed by the Mann-Whitney test. Differences were considered statistically significant when associated with a probability level of less than 0.05.

Hippocratic Screen 1

Diazepam significantly induced decreased motor activity, ataxia, loss of righting reflex and screen grip within 10 minutes of administration to the animals ($p < 0.01$). The effects of diazepam persisted for more than 2 hours, but activities were restored within 24 hours. These results confirm the CNS sedative activity of diazepam in the Hippocratic screen. Diazepam, however, had no influence on the animals' pinnal reflex, respiratory rate or analgesic and anesthetic response. It also produced no paralysis or tremor and did

not significantly affect the startle reaction of the animals. Compounds **8a**, **8c** and **8e** were found to have no significant effect on the behaviour of the animals.

Hippocratic Screen 2

The 1,3-diazepinium chlorides (**8a**, **8b** and **8c**) had some significant effects on the animals' response to diazepam. Activities affected include decreased motor activity, ataxia, righting and pinna reflex.

Decreased Motor Activity

Salts **8a** and **8c** potentiated the decrease in motor activity produced by diazepam by shortening the time taken to reach maximum efficacy for 10 to 15 minutes ($p < 0.01$ and 0.05 respectively, Figure 166). Salt **8e** attenuated the animals' response to diazepam-induced decreased motor activity ($p < 0.05$) which persisted for over 2 hours ($p < 0.01$). Ligand **8c** potentiated diazepam-induced decreased motor activity ($p < 0.01$) and caused it to persist for more than 24 hours ($p < 0.01$) but less than 48 hours. Ligand **8c** also significantly increased the maximum efficacy induced by diazepam ($p < 0.05$).

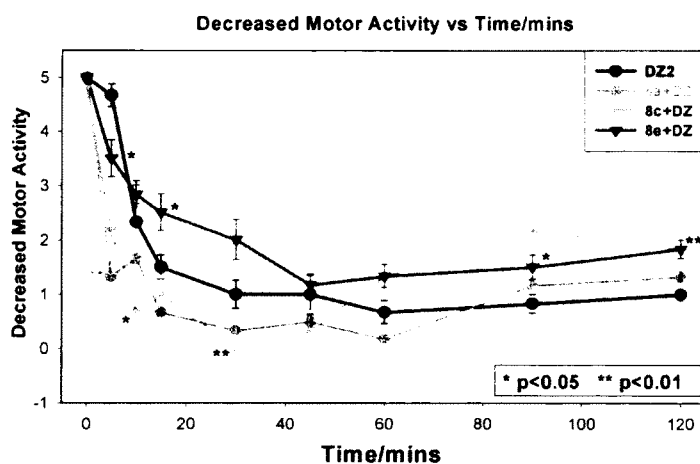


Figure 166. Effects of **8a**, **8c** and **8e** on diazepam-induced decreased motor activity in mice.

Ataxia

Salt **8a** enhanced the onset of ataxia induced by diazepam to within 5 minutes ($p < 0.05$) and augmented the maximum of diazepam-induced ataxic effect ($p < 0.05$). However, **8e** retards the onset of the ataxia to greater than 15 minutes ($p < 0.05$) but does not interfere with the maximum induced ataxic effect of diazepam (Figure 167). Ligand **8c** also produced a significant increase in the maximum of the diazepam-induced ataxic effect ($p < 0.001$) (Figure 167). Both salts **8a** and **8c** potentiated the efficacy of diazepam ($p < 0.01$ and $p < 0.05$ respectively).

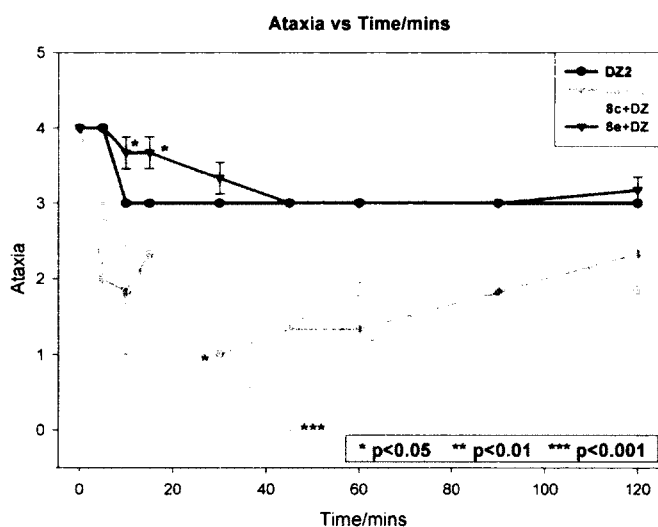


Figure 167. Effects of **8a**, **8c** and **8e** on diazepam-induced ataxia in mice.

Loss of Righting Reflex

Salts **8a**, **8c** and **8e** did not significantly affect the onset nor the overall efficacy of diazepam-induced loss of righting reflex, however, **8c** attenuated the effect caused by diazepam at times greater than 1 hour after diazepam was administered ($p < 0.01$) (Figure

168). None of the compounds prolonged the loss of righting reflex induced by diazepam for more than 2 hours.

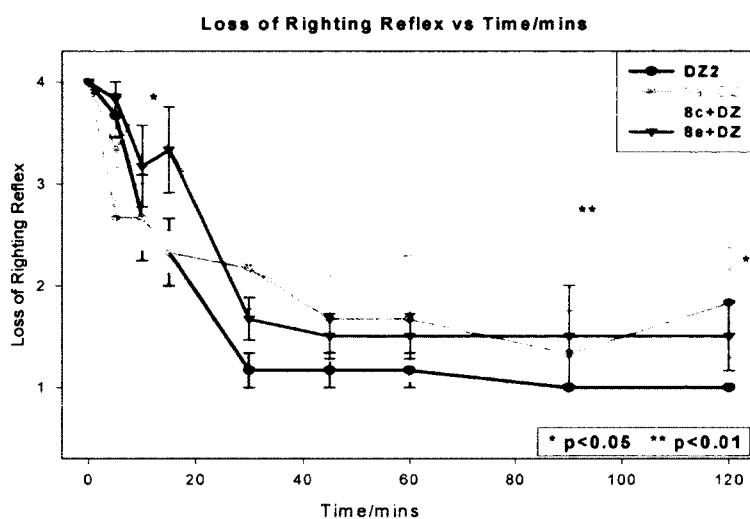


Figure 168. Effects on 8a, 8c, and 8e on diazepam-induced loss of righting reflex in mice.

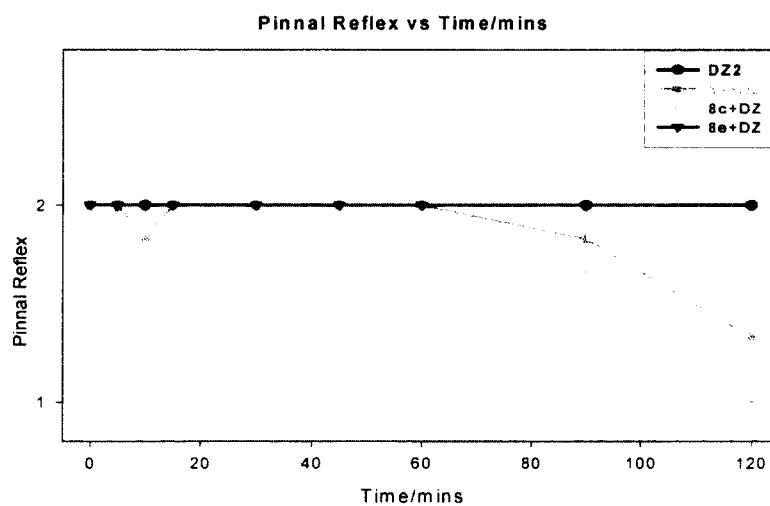


Figure 169. Effects of 8a, 8c and 8e on pinnal reflex in mice when treated with diazepam.

Pinnal Reflex

The dose of diazepam did not affect the pinnal reflex in mice (Figure 169). However, **8a** produced an overall reduction in the efficacy of diazepam on pinnal reflex in mice ($p < 0.01$). Salts **8c** and **8e** had no effect on the activity of diazepam towards pinnal reflex (Figure 169).

The effect of diazepam on the animals with respect to screen grip, respiratory rate, analgesia, anesthesia, paralysis, tremor and startle reaction was not significantly affected by 1,3-diazepinium chlorides **8a**, **8c** and **8e**.

The 1,3-diazepinium chlorides (**8a**, **8c** and **8e**), on their own, had no effect on the behaviour of the animals but elicited significant effects on diazepam-induced decreased motor activity, ataxia and loss of righting reflex. This suggests that the chlorides may either be binding to specific sites on the GABA(A) /BzR and influencing the CNS depressant or sedative activity of diazepam or be undergoing a synergistic effect with the diazepam.

Chlorides **8a** and **8c** potentiated the maximum decreased motor activity and disrupted coordinated movement (ataxia) caused by diazepam. This indicates that they are diazepam agonists. In particular, chloride **8a** enhanced the onset of these activities which means that it promotes the binding of diazepam more readily. However, chloride **8c** inhibited the loss of righting reflex, caused by diazepam, after 1 hour which suggests antagonist or inverse agonist effects over time. The chlorides did not significantly alter

loss of screen grip, thus indicating no effect on the muscle skeletal activity of diazepam on the animals. Chloride **8c** also decreased the efficacy of pinnal reflex in the animals thereby indicating some CNS depressant activity.

Chloride **8e** attenuated the diazepam-induced decreased motor activity and ataxia. This suggests that **8e** either blocks the diazepam binding site or binds at another site and inhibits the binding of diazepam to its receptor site. Chloride **8e** neither affects loss of righting reflex caused by diazepam nor pinnal reflex in the animals. Chloride **8e** appears to be an antagonist of diazepam in this screen.

Molecular Modeling

Alignment of compounds **8a** and **8c** within the pharmacophore/receptor model for the $\alpha 1\beta 3\gamma 2$ subtype is shown in Figures 170 and 171 respectively. The centroid of ring D in **8a** and **8c** is overlapped with the lipophilic region L_1 . The lone pair of electrons of the C6 amide carbonyl oxygen is hydrogen-bonded to H_1 of the receptor (bond length of 1.84 Å and bond angle of C=O– H_1 is 135°). There was also potential hydrogen bonding between the lone pair of electrons of the furan oxygen (O5) and the H_1 site giving rise to a 3-centered hydrogen bond interaction with the C6 carbonyl oxygen, H_1 and O5 (C=O– H_1 –O5). The N7 proton interacts with the A_2 site (bond length of 1.84 Å and bond angle of N7–H– A_2 is 180°). Although **8a** and **8c** are aligned similarly into the model, **8a** fits better as the methyl substituent at position 9 on ring A of **8c** sticks out into the extracellular region (Figure 171b).

When compared to diazepam, it is clearly seen that **8a** and **8c** did not occupy the L_2 nor L_3 regions of the pharmacophore/receptor model (Figure 172). Also, there was no lone pair of electrons available on the iminium ion at the junction of rings A and B for interaction with the H_2 descriptor. Compounds **8a** and **8c** are, therefore, not expected to

be full agonists like diazepam, since they do not have the required interactions in the model for positive allosteric modulation of the Bz receptor.

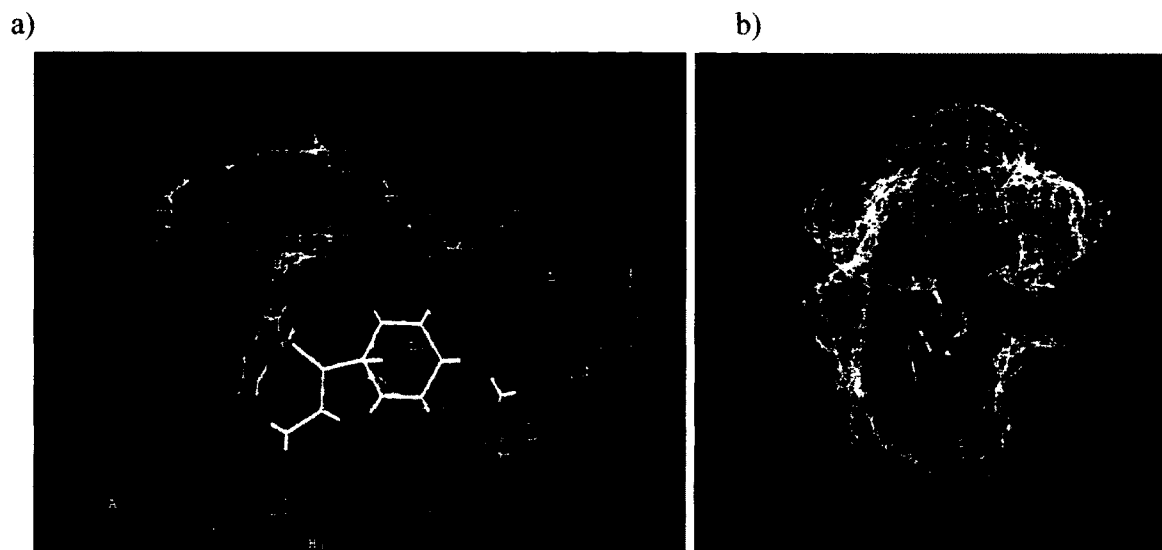


Figure 170. a) Alignment of 1,3-diazepinium chloride 8a within the pharmacophore/receptor model for the $\alpha 1\beta 3\gamma 2$ GABA(A) /BzR subtype; b) Alignment of 8a in the model rotated 90°.

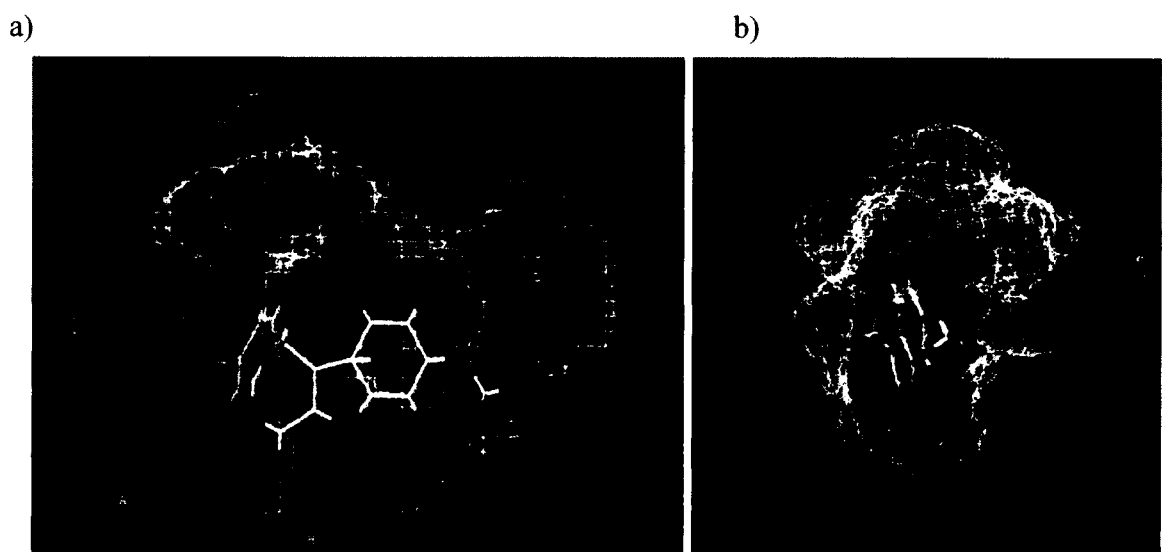


Figure 171. a) Alignment of 1,3-diazepinium chloride 8c within the pharmacophore/receptor model for the $\alpha 1\beta 3\gamma 2$ GABA(A) /BzR subtype; b) Alignment of 8c in the model rotated to 90° showing methyl group on ring A sticking out into the extracellular region.

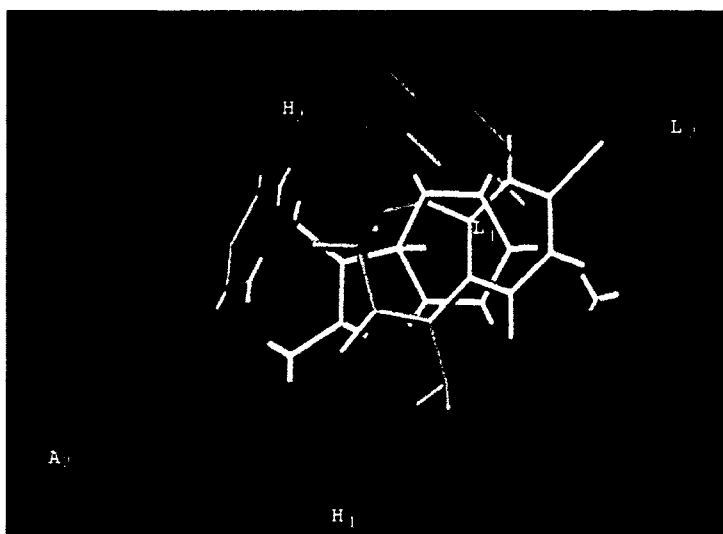


Figure 172. 1,3-Diazepinium chloride **8a** overlaid with diazepam (yellow) in the pharmacophore/receptor model.

On the other hand, **8a** and **8c** are potential Bz receptor inverse agonists or antagonists since they have interactions at the L_1 , H_1 and A_2 sites. 3-Methoxy-11-methyl-6-oxo-7,13-dihydro-6*H*-benzofuro[2,3-*e*]pyrido[1,2-*a*][1,3]diazepin-12-ium chloride, **8e** exhibited some inverse agonist activities in the Hippocratic screen and although it was not fitted into the pharmacophore model, it was expected to align in similar fashion to **8a** and **8c**.

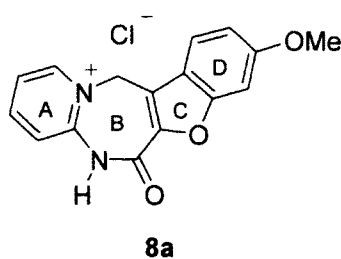
The lack of occupation of the L_2 lipophilic region by **8a** and **8c** implies that they have no affinity for the $\alpha 5$ isoform.⁵¹⁰ However, there may be some $\alpha 1$ activity as there appears to be some occupation of the L_{Di} region of the receptor by ring A of **8a** and **8c**.

The β -carbolines generally display some selectivity at the $\alpha 1$ -containing receptor subtypes which, based on experimental evidence, is due to occupation of the L_{Di} site of

the molecules in the receptor model.⁴¹⁹ Inverse agonist methyl-6,7-dimethoxy-4-ethyl- β -carboline-3-carboxylate (DMCM) occupies the L_{Di} region of the pharmacophore model and has a high affinity ($K_i = 5.7$ nM) for the $\alpha 1\beta 3\gamma 2$ -subtype.^{64, 78, 121}

In the Hippocratic screen, both **8a** and **8c** produced significant potentiation of diazepam-induced ataxia and decreased motor activity. These effects could be associated with $\alpha 1$ activity. Binding affinity studies showed that compound **8a** exhibited poor affinity at the $\alpha 1$, $\alpha 2$, $\alpha 3$ and $\alpha 5$ receptor subtypes (Table 41). Compound **8a**, however, shows very slight selectivity at the $\alpha 1$ -containing receptor subtype ($K_i = 746.5$ nM) and therefore, could be used for the design of a next generation ligand, once its clear that **8a-8c** do not bind to other types of receptors.

Table 41. Affinity of 3-methoxy-6-oxo-7,13-dihydro-6*H*-benzofuro[2,3-*e*]pyrido[1,2-*a*][1,3]diazepin-12-ium chloride, **8a**, for $\alpha x\beta 3\gamma 2$ ($x = 1-6$) BzR isoforms.



Ligand	K_i (nM)					
	$\alpha 1$	$\alpha 2$	$\alpha 3$	$\alpha 4$	$\alpha 5$	$\alpha 6$
8a	746.5	8081	1543	ND	2364	ND

(ND = NOT DETERMINED)

Primary binding experiments in the PDSP (see Appendix) also revealed that compound **8a** inhibited norepinephrine and serotonin transporters with a mean % inhibition of 81.3 and 62.5%, respectively (significant inhibition is considered > 50%). By inhibiting these transporters compound **8a** would prevent the reuptake of the neurotransmitters and cause prolonged neuronal activity. This is a characteristic feature of many antidepressant drugs. Some of these antidepressants also exhibit anticholinergic activity which can lead to ataxia.^{525, 526}

In summary, seven new tetracyclic 1,3-diazepinium chlorides with structural similarities to the 1,4-Bzs were synthesized *via* intramolecular cyclization of the respective allyl chlorides.^{64, 128} Three of these chlorides (**8a**, **8c** and **8e**) were evaluated in a Hippocratic screen and their activities compared to diazepam. On their own, compounds **8a**, **8c** and **8e** had no notable effect on the behaviour of the animals (mice) but, they significantly affected diazepam-induced ataxia, decreased motor activity, righting and pinnal reflex. Compounds **8a** and **8c** exhibited CNS depressant-like effects since they enhanced these diazepam-induced activities, while **8e** attenuated these activities and therefore displayed antagonist or antidepressant-like effects (other receptors). Compounds **8a** and **8c** were aligned into the pharmacophore/receptor with interactions at the L₁, H₁ and A₂ sites and some occupation of the L_{Di} region of the model. These results indicate that the compounds are potential inverse agonists/antagonists with possible $\alpha 1$ selectivity. Binding affinity studies confirmed that there is very slight selectivity of compound **8a** for the $\alpha 1$ subtype but the compound is not very potent (K_i = 746.5 nM). Hence, the potentiation of diazepam-induced ataxia and decreased motor activity by compounds **8a** and **8c** in the Hippocratic screen may have resulted from $\alpha 1$ associated effects but it is difficult to confirm since they bound to other

receptors. Compound **8a** may also display antidepressant activity since it significantly inhibited the norepinephrine and serotonin transporters (> 50%). Certainly, the modeling here indicates that **8a-8c** could bind to BzR receptors, but they lack the required functionality at specific descriptors necessary for potent BzR mediated response (see Figure 172).

The Role of $\alpha 1$ and $\alpha 5$ containing GABA(A) Receptors in Mediating Diazepam Effects on Spontaneous Locomotor Activity and Water Maze Learning and Memory in Rats

The clinical use of benzodiazepines (BZs) is hampered by sedation and cognitive deterioration. Although genetic and pharmacological studies suggest that α_1 - and α_5 -containing GABA(A) receptors mediate and/or modulate these effects, their molecular substrate is not fully elucidated. By the use of two selective ligands: the α_1 -subunit affinity-selective antagonist β -CCt, and the α_5 -subunit affinity- and efficacy-selective antagonist XLi093, Savic et al.⁴¹⁹ examined the mechanisms of behavioral effects of diazepam in the tests of spontaneous locomotor activity and water maze acquisition and recall, the two paradigms indicative of sedative and cognition-impairing effects of BZs, respectively. The locomotor activity decreasing propensity of diazepam (significant at 1.5 and 5 mg/kg) was antagonized by β -CCt (5 and 15 mg/kg), while it tended to be potentiated by XLi093 in doses of 10, and especially 20 mg/kg. Diazepam decreased acquisition and recall in the water maze, with a minimum effective dose of 1.5 mg/kg. Both antagonists reversed the thigmotaxis induced by 2 mg/kg diazepam throughout the test, which suggests that both GABA(A) receptor subtypes participate in BZ effects on

the procedural component of the task. Diazepam-induced impairment in the declarative component of the task, as assessed by path efficiency, the latency and distance before finding the platform across acquisition trials, and also by the spatial parameters in the probe trial was partially prevented by both 15 mg/kg β -CCt and 10 mg/kg XLi093. **Combining a BZ with β -CCt results in the near to control level of performance of a cognitive task, without sedation, and may be worthy of testing on human subjects.**

The aim was to elucidate, by the use of two selective ligands: the preferential α_1 -subunit affinity-selective antagonist β -CCt, and the α_5 -subunit affinity- and efficacy-selective antagonist XLi093, to what extent GABA(A) receptors containing α_1 and α_5 subunits contribute to the well-established behavioral effects of diazepam in the tests of spontaneous locomotor activity and water maze acquisition and recall, the two paradigms mainly, but not exclusively, indicative of sedative and spatial cognition impairing effects of classical BZs, respectively. The selectivity of β -CCt and XLi093 has been confirmed in *in vitro* experiments of affinity and efficacy at recombinant GABA(A) receptors,⁴²¹ as well as in *in vivo* studies of inhibition of [³H] flumazenil binding in distinct brain regions, which differ in the GABA(A) receptor subtype expression.⁴²²

Drugs

XLi093 (4H-imidazo[1,5-a][1,4]benzodiazepine-3-carboxylic acid, 8-ethynyl-5,6-dihydro-5-methyl-6-oxo-, 1,3-propanediyl ester), the α_5 -subunit affinity- and efficacy-selective antagonist, and β -CCt (t-butyl- β -carboline-3-carboxylate), the preferential α_1 -subunit affinity-selective antagonist were synthesized as described in detail previously.⁵²⁷ Diazepam was obtained from Galenika (Belgrade, Serbia).

Behavioral Experiments by Savic et al.^{429, 528}

Experiments were carried out on male Wistar rats (Military Farm, Belgrade, Serbia), weighing 220-250 g. All procedures in the study conformed to EEC Directive 86/609 and were approved by the Ethical Committee on Animal Experimentation of the Faculty of Pharmacy in Belgrade. The rats were housed in transparent plastic cages, six animals per cage, and had free access to pelleted food and tap water. The temperature of the animal room was $22 \pm 1^\circ\text{C}$, the relative humidity 40-70%, the illumination 120 lux, and the 12/12 h light/dark period (light on at 6:00 h). All handling and testing took place during the light phase of the diurnal cycle. Separate groups of animals were used for two behavioral paradigms. The behavior was recorded by a ceiling-mounted camera and analyzed by the ANY-maze Video Tracking System software (Stoelting Co., Wood Dale, IL, USA). The drugs were dissolved/suspended with the aid of sonication in a solvent containing 85% distilled water, 14% propylene glycol, and 1% Tween 80, and were administered in a total volume of 2 ml/kg, 20 min before behavioral testing. The first treatment indicated in combination was administered into the lower right quadrant of the peritoneum, and the second treatment immediately afterwards into the lower left quadrant of the peritoneum.

Measurement of Locomotor Activity

Twenty minutes after receiving the appropriate treatment, single rats were placed in a clear Plexiglas chamber (40 x 25 x 35 cm). Activity under dim red light (20 lux) was recorded for a total of 30 minutes, without any habituation period, using ANY-maze software. Besides the total distance travelled, behavior was analyzed by dividing the locomotor activity data into 5 minute bins.

Two experiments were performed. In the first one, the dose response curve for diazepam (0; 0.5; 1.5 and 5.0 mg/kg) was determined. In the second study, the design included the factors agonist (the same doses of diazepam as those used in the dose-response study) and antagonists (β -CCt at 0; 5 and 15 mg/kg, and XLi093 at 0; 10 and 20 mg/kg), thus generating 20 experimental groups in total.

Behavior in the Morris Water Maze

The water maze consisted of a black cylindrical pool (diameter: 200 cm, height: 60 cm), with a uniform inner surface. The pool was filled to a height of 30 cm with 23°C ($\pm 1^\circ\text{C}$) water. The escape platform of black plastic (15x10 cm) was submerged 2 cm below the water surface. The platform was made invisible to rats by having it painted the same color as the pool wall.⁵²⁹ There were many distal cues in the testing room (doors, pipes on the walls and the ceiling, cupboards, a camera suspended above the centre of the maze). An indirect illumination in the experimental room was provided by white neon tubes fixed on the walls (Figure 173).

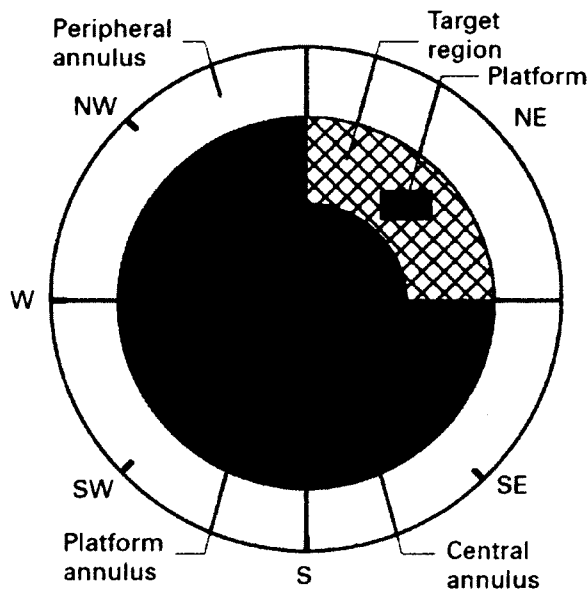


Figure 173. The scheme representing the virtual division of the water maze used in the analysis of rats' performance.

The rats received the appropriate treatment 20 minutes before a swimming block, each day for 5 consecutive days of spatial acquisition. Each block consisted of 4 trials, lasting a maximum time of 120 seconds, the intertrial interval being 60 seconds. For each trial the rat was placed in the water facing the pool at one of four pseudorandomly determined starting positions. As during spatial learning the platform was hidden in the middle of the NE quadrant, the four distal start locations were chosen: S, W, NW and SE (Figure 173). Once the rat found and mounted the escape, it was permitted to remain on the platform for 15 s. The rat was guided to the platform by the experimenter if it did not locate the escape within 120 s. To assess the long-term spatial memory at the end of learning, a probe trial for 60 s, with the platform omitted, was given 24 h after the last acquisition day. The probe trial, starting from the novel, most distant SW location (in

order to ensure that any spatial bias is a consequence of the spatial memory of escape location, rather than of a specific swim strategy⁴²² was performed without any pre-treatment. A drug-free probe trial⁴²² was chosen because diazepam impairs acquisition, but not retrieval of place preference in the water maze,⁴¹⁹ and confounding effects of possible sensorimotor, i.e. non-cognitive actions of treatment on recall performance were avoided by such a protocol. The tracking software virtually divided the pool into four quadrants, three concentric annuli and a target region consisting of the intersection of the platform quadrant and the platform annulus (Figure 173). Similarly to the approach used by Cain,^{46, 48, 52, 366} the central annulus was set up to 10% of the whole area; the platform annulus equaled 40%, whereas the area of the peripheral annulus was 50% of the whole.

Dependent variables chosen for tracking during the acquisition trials were: latency to platform (time from start to goal), total distance swam (path length), average swim speed and path efficiency (the ratio of the shortest possible path length to actual path length). All these indices are, to a lesser or greater degree, related to goal-directed behavior, i.e. spatial learning.⁴¹⁹ As thigmotaxis (the tendency to swim or float near the pool wall) represents a factor which accounts for much of the variance in the water maze performance, and normally weakens during consecutive trials,^{48, 366} we quantified the persistence of the thigmotaxis in the target (NE) quadrant. The loss of thigmotaxis is related to the procedural component of acquisition, and the percent of the distance swam in the target region (away from the wall) of the target quadrant may be seen as a measure of procedural learning.

The indices of memory, assessed during the probe trial, included the distance and time in the platform (target) quadrant, platform ring and target region, as well as the number of entries and distance swam in the area where the platform used to be during

training (Figure 173). In addition, the distance swam during 60 sec in the probe trial was taken as a measure of overall activity, while peripheral ring parameters (distance and time) were connected to the thigmotaxic behavior.

Three experiments in the water maze were performed. In the first study, the dose response curve for diazepam (0; 1; 1.5; 2 and 5 mg/kg) was determined. In the second experiment, the influences of β -CCt (5 and 15 mg/kg) and XLi093 (10 and 20 mg/kg) on the effects of 1.5 mg/kg diazepam (the minimal effective dose from the dose-response study) were assessed. The inclusion of the groups treated by the antagonists without diazepam would have made the experiment overly long, on each of five training days. In preliminary experiments with the current protocol, the lack of behavioral activity was observed at the higher doses of β -CCt and XLi093 used here (15 mg/kg and 20 mg/kg, respectively). In the third water maze experiment, the capability of β -CCt (15 mg/kg) and XLi093 (10 mg/kg) to antagonize the behavioral effects of a higher dose of diazepam (2 mg/kg) was assessed.

Statistical Analysis

All numerical data presented in the Figures were given as the mean \pm SEM. Data from the activity assay were assessed by a one-way or two-way ANOVA, whereas the results from the water maze test were analyzed using a two-way ANOVA with repeated measures. Post hoc comparisons, where applicable, were performed using Student-Newman-Keuls or Dunnett's test. Statistical analyses were performed with ANY-maze Video Tracking System software (Stoelting Co., Wood Dale, IL, USA).

Results

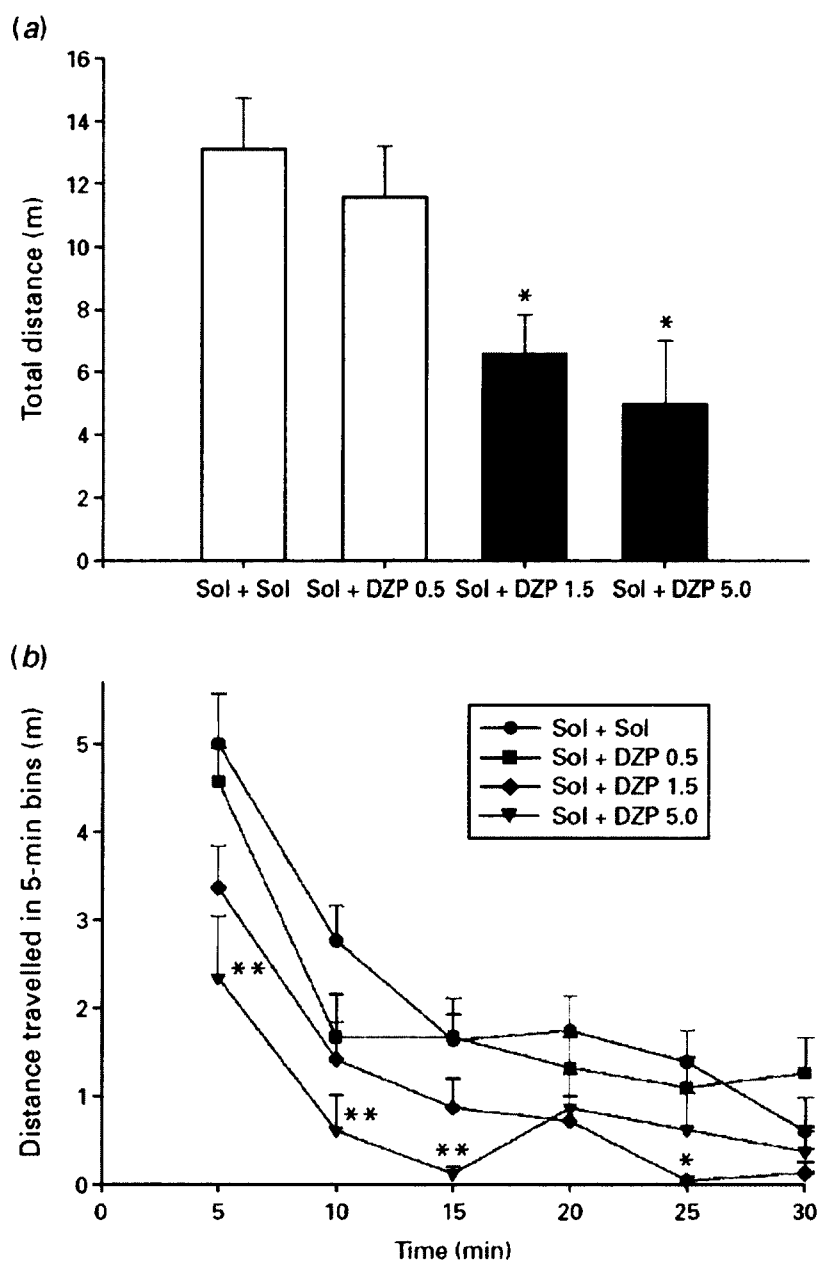


Figure 174. The effects of diazepam (Sol+DZP 0.5, 1.5 and 5.0 mg/kg) on total distance (a) and distance travelled in 5-min intervals (b). * $p < 0.05$ compared to solvent (Sol+Sol) group; ** $p < 0.01$ compared to solvent. Animals per treatment ($n=8$).

Motor Activity Assay

An ANOVA showed a significant effect of diazepam treatment on total distance travelled during 30 minutes of monitoring ($F(3,28) = 5.63$, $p=0.004$) (Figure 174a). According to Dunnett's test, the activity-depressing effect of two higher doses of diazepam was significant compared with solvent control. When the analysis of distance travelled was developed into 5 minute intervals (Figure 174b), it turned out that diazepam at 5 mg/kg highly significantly decreased locomotion in the period 0-15 minutes, whereas the dose of 1.5 mg/kg was effective in the period 20-25 minutes.

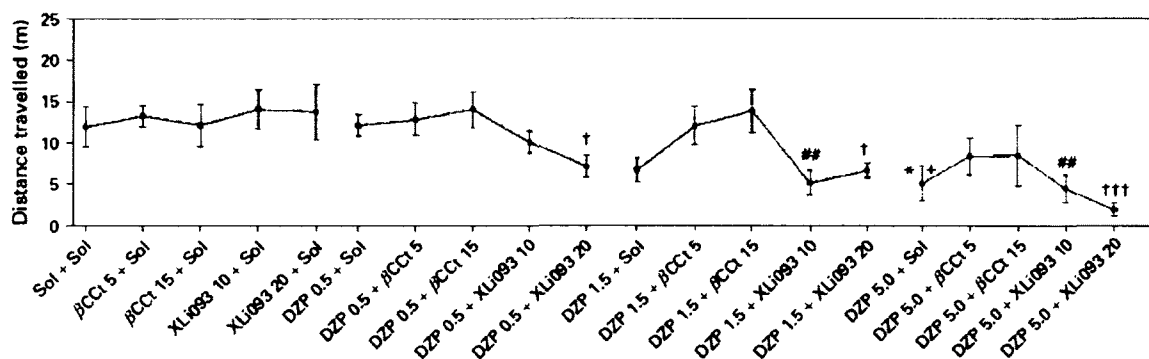


Figure 175. The effect of combinations of drugs.

The effects of combinations of diazepam (DZP), at doses of 0, 0.5, 1.5 and 5.0 mg/kg, and the antagonists b-CCt (0, 5, 15 mg/kg) and XLi93 (0, 10, 20 mg/kg), on total distance travelled in the spontaneous locomotor activity test (Figure 175). * $p<0.05$, compared to solvent (Sol+Sol) group; + $p<0.05$ compared to DZP 0.5+Sol group; ## $p<0.01$ compared to XLi93 10+Sol group; † $p<0.05$, ††† $p<0.001$ compared to XLi93 20+Sol group. Animals per treatment ($n=6$).

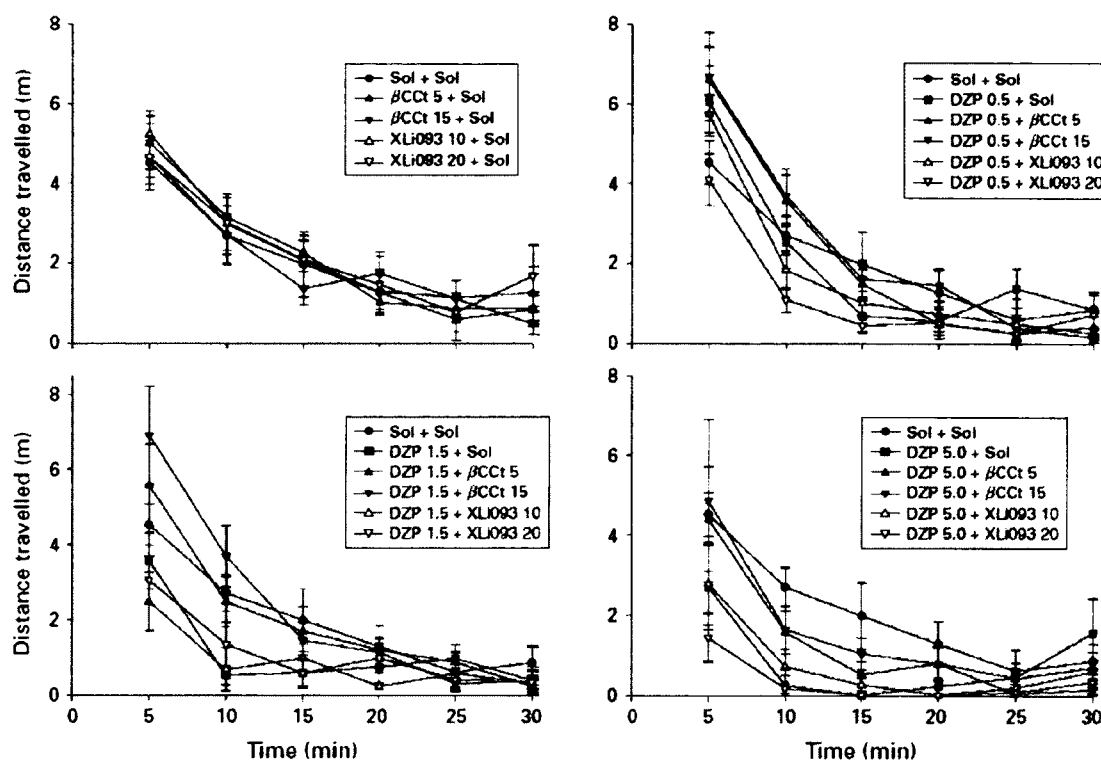


Figure 176. Mean distance travelled in successive 5-min blocks for groups

On the other hand, while devoid of discernible activity of their own, β -CCt and XLI093 exerted differential effects on the hypolocomotor effect of diazepam (Figure 176). Their influences were evaluated by separate statistical analyses. A two-way ANOVA for the analysis of the influence of β -CCt has shown a significant effect of the dose of diazepam ($F(3,71) = 3.95$, $p=0.012$), whereas the dose of the antagonist as a factor, as well as the agonist x antagonist interaction did not reach significance ($F(2,60) = 2.30$, $p=0.109$, and $F(6,71) = 0.49$, $p=0.811$, respectively). Post hoc Student-Newman-Keuls method revealed that the existing significant differences between the levels of diazepam itself (5 mg/kg vs. 0 mg/kg and 5 mg/kg vs. 0.5 mg/kg) disappeared when

multiple comparisons were made within the 5 mg/kg β -CCt dose (respective p values 0.419 and 0.339), as well as within the 15 mg/kg β -CCt level (respective p values 0.251 and 0.302). When analyzing the overall influence of XLi093 as an antagonist, there was a significant effect of the dose of diazepam ($F(3,71) = 15.323$, $p < 0.001$), whereas the dose of XLi093 as a factor, as well as the agonist x antagonist interaction were insignificant ($F(2,60) = 0.806$, $p = 0.451$, and $F(6,71) = 0.846$, $p = 0.540$, respectively). Oppositely to the antagonism exerted by β -CCt, post hoc analysis revealed that the existing effects of diazepam (5 mg/kg vs. 0 mg/kg, $p = 0.027$, and 5 mg/kg vs. 0.5 mg/kg, $p = 0.041$) were potentiated by XLi093 (Figure 175). Namely, comparisons within the 10 mg/kg XLi093 level have shown highly significant differences in the effects of 1.5 mg/kg and 5 mg/kg doses of diazepam versus the effect of the antagonist itself (p values of 0.003 in both cases), whereas within the dose of 20 mg/kg XLi093, all three levels of diazepam (0.5; 1.5 and 5 mg/kg) were statistically different from the antagonist (respective p values: 0.013, 0.002 and below 0.001). Similar conclusions can be reached while statistically analyzing (not shown) the data obtained by dividing the locomotor activity into 5 minute bins (Figure 176). As a rule, locomotor activity of animals treated with a combination of diazepam and β -CCt, irrespective of the doses employed, was near to, or slightly above, the control value, whereas XLi093, especially at the higher dose, tended to deepen, or unveil, the sedation induced by diazepam.

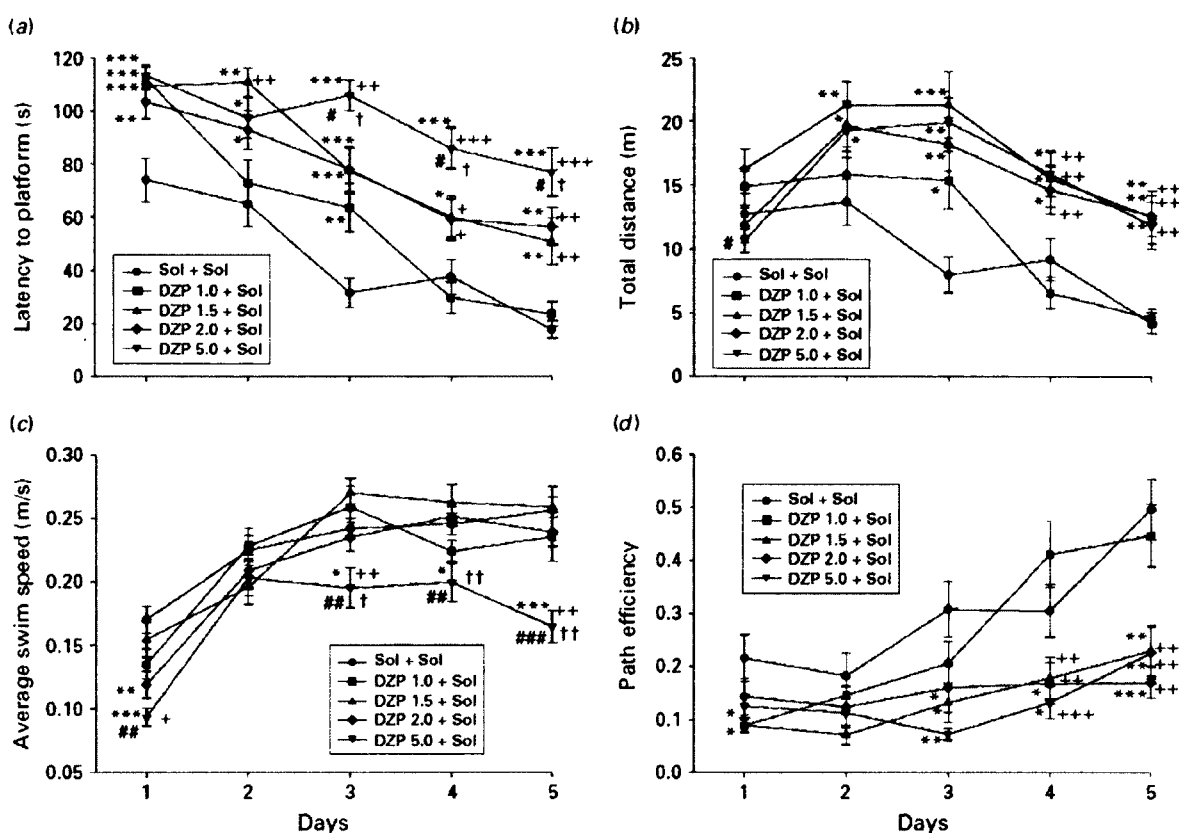


Figure 177. Latency to platform data

The effects of diazepam 1.0, 1.5, 2.0 and 5.0 mg/kg (DZP 1.0+Sol to DZP 5.0+Sol) on (a) latency to platform, (b) total distance, (c) average swim speed and (d) path efficiency of rats during 5 d acquisition trials in the water maze is illustrated in Figure 177. * p<0.05, ** p<0.01, *** p<0.001 compared to solvent (Sol+Sol) group; +p<0.05, ++ p<0.01, +++ p<0.001 compared to DZP 1.0+Sol group; # p<0.05, ## p<0.01, ### p<0.001 compared to DZP 1.5+Sol group; † p<0.05, †† p<0.01 compared to DZP 2.0+Sol group. Animals per treatment (n=7).

Morris Water Maze

For the dose response study of diazepam, the factors treatment and days, as well as the interaction treatment x days, were statistically highly significant for the latency to find the platform, the distance swam before finding the platform, swim speed and path efficiency; significant differences among treatments during training days are presented in Table 42. The results of the post hoc analysis for the factor treatment are summarized in Table 43. The analysis showed that the lowest effective dose of diazepam was 1.5 mg/kg.

Illustrated in Table 42 are the significant differences among overall influences (averaged for five days of acquisition) on the water maze learning parameters: latency to find the platform (L), distance swam before finding the platform (D), mean swim speed (S) and path efficiency (E) in the dose-response study of diazepam (DZP mg/kg).

Table 42. Differences among influence of diazepam on water maze learning

	DZP 1.0 + Sol	DZP 1.5 + Sol	DZP 2.0 + Sol	DZP 5.0 + Sol
Sol + Sol	L: $p = 0.004$	L: $p < 0.001$ D: $p < 0.001$ E: $p < 0.001$	L: $p < 0.001$ D: $p = 0.001$ E: $p < 0.001$	L: $p < 0.001$ D: $p = 0.002$ S: $p < 0.001$ E: $p < 0.001$
DZP 1.0 + Sol		L: $p < 0.001$ D: $p = 0.002$ E: $p = 0.001$	L: $p = 0.001$ D: $p = 0.014$ E: $p = 0.001$	L: $p < 0.001$ D: $p = 0.030$ S: $p < 0.001$ E: $p = 0.001$
DZP 1.5 + Sol				L: $p = 0.007$ S: $p < 0.001$
DZP 2.0 + Sol				L: $p = 0.002$ S: $p < 0.001$

Sol, Solvent.

Table 43 illustrates the representative parameters of water maze performance in the probe trial of the diazepam (DZP mg/kg) dose-response experiment. The key to regions used in the analysis is given in Figure 173. *,** and ***, $P < 0.05$; 0.01 and 0.001,

38), has confirmed that learning the required water maze skills and strategies was impaired under diazepam.

Based on the dose response study presented here, Savic performed a further experiment in which two doses of each of the antagonists tested in the locomotor activity assay were combined with 1.5 mg/kg diazepam.⁵²⁶ However, in this experiment, the effect of diazepam did not reach significance compared with control for any of the learning measures calculated. A two-way ANOVA with repeated measures for this antagonism study revealed significant variability in regard to latencies to find the platform (treatment effect, $F(5,138) = 6.59$, $p < 0.001$; day effect, $F(4,552) = 50.39$, $p < 0.001$; and treatment x day interaction, $F(20,552) = 1.80$, $p = 0.018$) and path efficiencies across the five days (treatment effect, $F(5,138) = 4.67$, $p = 0.001$; day effect, $F(4,552) = 17.61$, $p < 0.001$; and treatment x day interaction, $F(20,552) = 1.88$, $p = 0.012$). The respective significant differences among treatments during days are presented in Figures 178a and 178d. The factors, but not the interaction, also reached significance when swim distances (Figure 178b) and average swim speed (Figure 178c) were analyzed (treatment effect, $F(5,138) = 5.42$, $p < 0.001$; day effect, $F(4,552) = 34.27$, $p < 0.001$, and treatment x day interaction, $F(20,552) = 1.50$, $p = 0.075$, and treatment effect, $F(5,138) = 5.02$, $p < 0.001$; day effect, $F(4,552) = 21.08$, $p < 0.001$, and treatment x day interaction, $F(20,552) = 1.22$, $p = 0.233$, respectively). Having in mind especially the latency to platform (Figure 178a), it appears that antagonism of the effects of diazepam at GABA(A) receptors containing $\alpha 5$ subunits (1.5 mg/kg diazepam + 10 mg/kg XLi093) may enhance acquisition in the earliest stages of spatial learning, while addition of a higher dose of the antagonist (1.5 mg/kg diazepam + 20 mg/kg XLi093) may even impair the later phases of learning. Throughout the acquisition trials there were no discernible effects of adding

β CCt, at either dose, to diazepam. In the probe trial, the significant differences in dependent measures of performance were generally absent, probably due to the lack of clear behavioral activity of the dose used of diazepam, and these data are not presented.

Finally, the results of the experiment with a higher effective dose of diazepam (2 mg/kg), on its own and in combination with 10 mg/kg XLi093 and 15 mg/kg β CCt, are shown in Figures 179 and 180, and Tables 44 and 45. A two-way ANOVA with repeated measures of latencies to find the platform across the five days (Figure 179a) revealed the following results: treatment effect, $F(3,100) = 11.65$, $p < 0.001$; day effect, $F(4,400) = 56.74$, $p < 0.001$; and treatment x day interaction, $F(12,400) = 0.96$, $p = 0.484$. Similar tendencies were evident when swim distances (Figure 186b) and path efficiencies (Figure 179d) were analyzed (treatment effect, $F(3,100) = 6.34$, $p = 0.001$; day effect, $F(4,400) = 28.17$, $p < 0.001$; and treatment x day interaction, $F(12,400) = 1.46$, $p = 0.135$, and treatment effect, $F(3,100) = 5.98$, $p = 0.001$; day effect, $F(4,400) = 27.68$, $p < 0.001$; and treatment x day interaction, $F(12,400) = 1.03$, $p = 0.422$, respectively). The interaction only reached significance when swim speed was analyzed: treatment effect, $F(3,100) = 6.29$, $p = 0.001$; day effect, $F(4,400) = 14.03$, $p < 0.001$; and treatment x day interaction, $F(12,400) = 1.92$, $p = 0.031$, and significant differences among treatments during days are given in Figure 179c. As treatment as factor was statistically significant for all four learning parameters illustrated, the respective significances for single treatments are shown in the Table 39. β CCt (15 mg/kg) completely prevented acquisition-impairing actions of diazepam administered at the dose of 2 mg/kg, whereas addition of XLi093 (10 mg/kg) was effective in this sense for all parameters considered, with the exception of the mean swim speed (Table 45). It is noteworthy to point out that statistical analysis

revealed no overall significant difference in maximum speed among treatments; moreover, on the first day, the rats treated with diazepam were even faster, in maximum, than control ones (1.16 ± 0.44 m/s vs. 0.78 ± 0.14 m/s), which is a hint of transient behavioral disinhibition.

In Figure 180, the distances the rats swam in the platform quadrant (NE) during acquisition trials are presented alongside the respective distance in the portion of the NE quadrant lying in the platform annulus of the maze (“the target region”). The rats treated with 2 mg/kg diazepam strikingly lacked the preferential activity in that part of the NE quadrant in which platform finding was possible; even on day 5, only 49.4% of the distance they travelled in NE quadrant was in the target region; the respective values for control, 2 mg/kg diazepam+15 mg/kg β CCt and 2 mg/kg diazepam+10 mg/kg XLi093 groups were 75.4%, 82.9% and 69.8%.

In Table 41, a number of parameters calculated from the probe trial performance in the antagonism study with 2 mg/kg diazepam are presented. The total distance swam was not different, and also there were not significant differences among groups in distance and time spent in the platform quadrant. On the other hand, the animals treated for 5 days with diazepam exerted a strong bias towards the peripheral annulus, which was reversed by both antagonists. Concomitantly, previous treatment with diazepam resulted in significant avoidance of platform annulus, which was also antagonized by both, β CCt (15 mg/kg) and XLi093 (10 mg/kg). The changes of these two parameters are indicative of influences on previous days’ behavioral strategies of learning, i.e. the procedural component of water maze spatial memory. There were no significant difference in the target region activity, whereas diazepam treatment tended to decrease platform site entries and significantly decreased the distance in the platform position. The latter effect,

indicative of influence on the declarative spatial component of memory, was attenuated, but not reversed, by both antagonists.

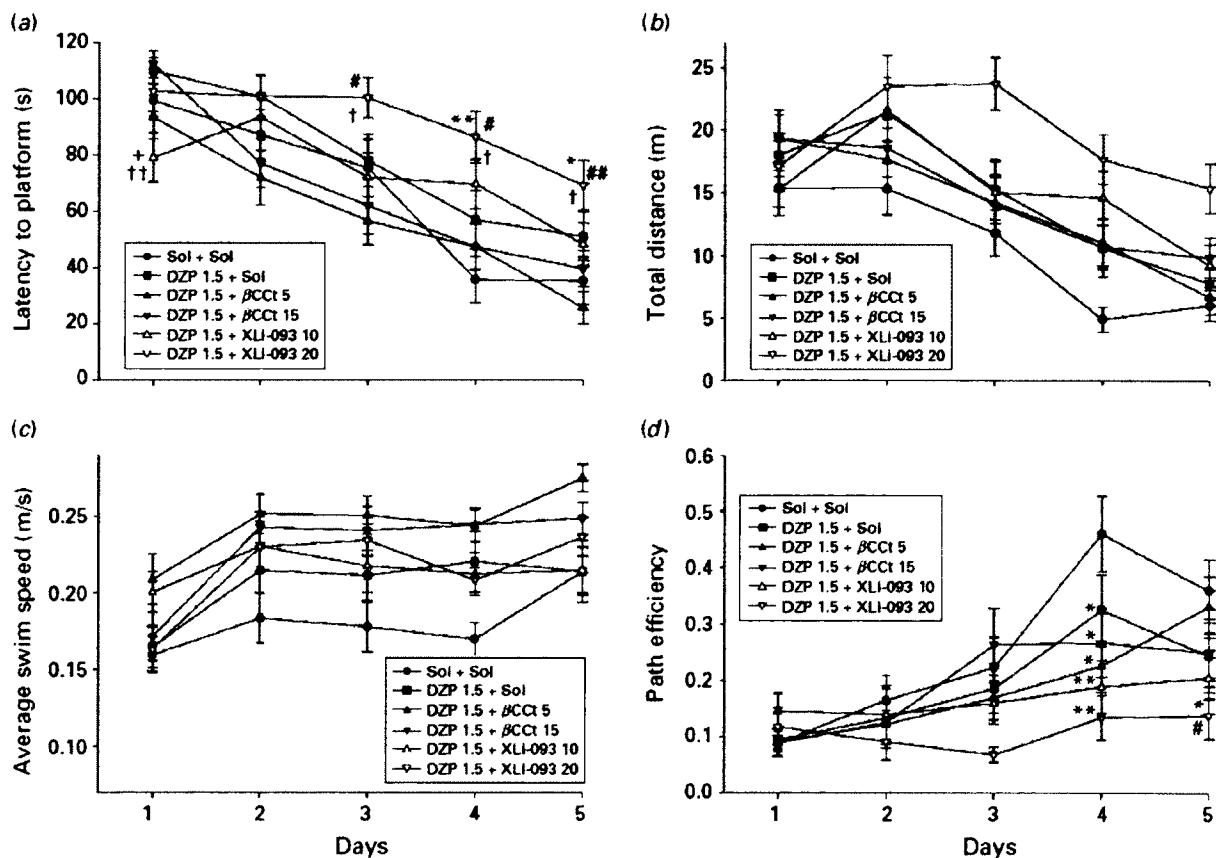


Figure 178. Acquisition trials in the water maze.

Illustrated in Figure 174 are the effects of diazepam (DZP 1.5+Sol), diazepam and b-CCt (DZP 1.5+b-CCt 5 and DZP 1.5+b-CCt 15) and diazepam and XLI093 (DZP 1.5+XLI093 10 and DZP 1.5+XLI093 20) (all doses in mg/kg) on (a) latency to platform, (b) total distance, (c) average swim speed and (d) path efficiency of rats during 5 d acquisition trials in the water maze. * $p < 0.05$, ** $p < 0.01$ compared to solvent (Sol+Sol) group; + $p < 0.05$ compared to DZP 1.0+Sol group; # $p < 0.05$, ## $p < 0.01$ compared to DZP 1.5+b-CCt 5 group; † $p < 0.05$, †† $p < 0.01$ compared to DZP 1.5+b-CCt 15 group. The

animals per treatment group (n=6).

The α_1 - and α_5 -containing GABA(A) receptors have been repeatedly implicated, to a different degree, in mediation or modulation of widely known sedative and amnesic effects of agonists at BZ-sensitive GABA(A) receptors.⁴⁶ The present experiments, using the selective antagonists at the BZ sites of α_1 - and α_5 -containing GABA(A) receptors, demonstrated that the activity-decreasing propensity of diazepam, as a measure of sedation, is the consequence of its binding at α_1 -containing GABA(A) receptors, whereas spatial learning and memory deficits induced by diazepam are related to action at both of these receptor populations (α_1 and α_5).^{530, 531}

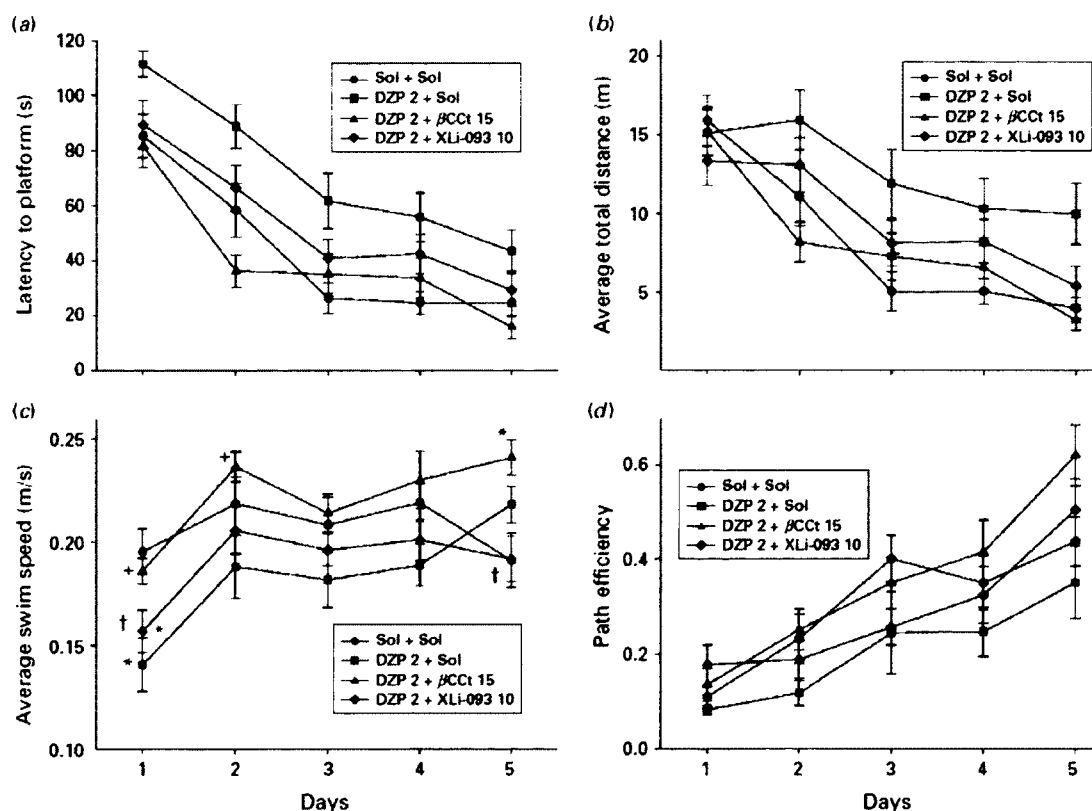


Figure 179. Acquisition trials in the Morris water maze

Illustrated in Figure 179 are the effects of diazepam (DZP 2+Sol), diazepam and b-CCt (DZP 2+b-CCt 15) and diazepam and XLi093 (DZP 2+XLi093 10) (all doses in mg/kg) on (a) latency to platform, (b) average total distance, (c) average swim speed and (d) path efficiency of rats during 5 d acquisition trials in the water maze. * $p < 0.05$ compared to solvent (Sol+Sol) group; + $p < 0.05$ compared to DZP 2+Sol group; † $p < 0.05$ compared to DZP 2+b-CCt 15 group. The animals per treatment group, for Sol+Sol to DZP 2+XLi093 10 (n=6, 6, 7, 7, respectively).

The findings in the motor activity assay on the predominant role of α_1 GABA(A) receptors are in accordance with genetic studies.⁵¹ What appears to be the most surprising result of this part of study, combining diazepam with XLi093, especially with the higher (20 mg/kg) of the two tested doses of the antagonist, potentiated sedation induced by diazepam. The 20 mg/kg dose of XLi093 presumably caused a complete antagonism of the effects of diazepam at α_5 -containing GABA(A) receptors (cf. occupancy of about 65% of α_5 GABA(A) receptors in mice at 10 mg/kg of XLi093 in Shinday et al.^{367, 389}). We have recently put forward the hypothesis that locomotor activity changes induced by ligands possessing a substantial α_5 -efficacy may be, at least partly, contributed to by modulation at GABA(A) receptors containing the α_5 subunit.⁵¹ It appears that the role of positive modulation at α_5 GABA(A) receptors depends on the concomitant activity at α_1 -containing GABA(A) receptors. Moreover, α_5 GABA(A) receptors may exert a dual control on the state of vigilance: to limit sedative effects elicited by supra-physiological stimulation of α_1 -containing receptors, and, oppositely, to enhance basal/endogenous activation of α_1 GABA(A) receptors, and, hence, induce mild sedation. Three sets of data may indirectly support the notion of the modulatory role of

this population of receptors. Firstly, it is notable that α_5 -containing GABA(A) receptors are at least moderately present in both regions believed to be involved in the sedative properties of GABA(A) receptor activators,⁵³² ventral horn of the spinal cord,⁵² and pyramidal neurons of the neocortex, especially the layer V.^{529, 533} Secondly, there is a conspicuous association between α_1 and α_5 subunits: the co-localization within individual neurons,⁵² and even within the single GABA(A) receptor.⁴²⁹ Thirdly, the knock-in mice harboring the α_5 subunit insensitive to diazepam are refractory to development of tolerance to the α_1 -mediated sedative effect of diazepam dosed subchronically.³³⁴ Finally, Mohler, Rudolph and others have shown that the tolerances to some of the effects of diazepam are due to the coupling of α_1 receptors to α_5 receptors; one is down-regulated while the other is upregulated on chronic dosing of diazepam.

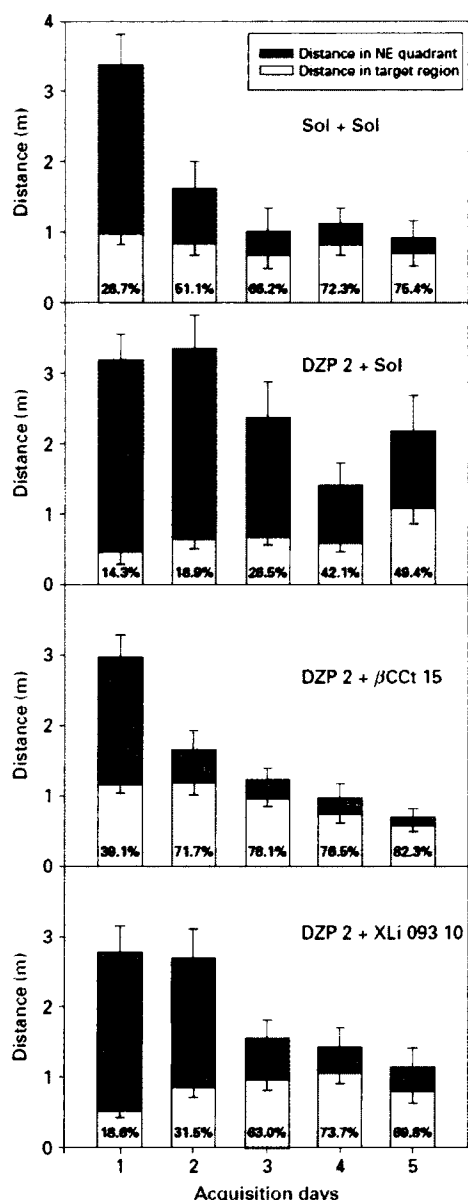


Figure 180. Distance data during 5 day acquisition trials in the water maze.

Illustrated in Figure 180 are the effects of (a) solvent (Sol+Sol) ; (b) diazepam (DZP 2+Sol), (c) diazepam and b-CCt (DZP 2+b-CCt 15) and (d) diazepam and XLi093 (DZP 2+XLi093 10) (all doses in mg/kg) on the distance rats travelled in the SE quadrant and target region during 5 d acquisition trials in the water maze. The numbers inside the

columns are the percent of the distance swam inside the target (NE) quadrant which was travelled in the target region.

The effects of diazepam on the acquisition and retention of place learning in the water maze have been previously assessed in two settings, similar but not identical to the present procedure.³³⁴ The lowest dose effective in our experiment (1.5 mg/kg) lies between those found by Arolfo and Brioni (1.0 mg/kg) and Cain (3.0 mg/kg diazepam). However, the antagonism study showed that the 1.5 mg/kg dosage level was a borderline dose of diazepam, unreliable in affecting rats' behavior under the conditions used in the current water maze protocol. Nevertheless, in such settings, an impairment of the later phases of water maze learning produced by the combination of diazepam (1.5 mg/kg) and the higher dose of XLi093 (20 mg/kg) was revealed. We hypothesize that this finding may be connected with the profound sedation observed with the same combination in the procedure measuring locomotor activity. Namely, it is possible that the supposed complete antagonism at α_5 -containing GABA(A) receptors forestalls development of tolerance to sedation and/or decreased vigilance, and hence impairs learning; this question could be partly resolved with the further studies of repeated dosing of diazepam and XLi093 in the locomotor activity test.³⁷⁵

In the antagonism study with 2.0 mg/kg diazepam, both antagonists tended to reverse its effects, which may be seen as corroborating previous conclusions that the water maze acquisition impairment is not due to the sedative effect of diazepam.^{334, 335} The fact that rats treated with a combination of diazepam 2 mg/kg + β -CCt 15 mg/kg were even faster swimmers, in overall, than both, the group treated with diazepam and the group treated with combination diazepam 2 mg/kg + XLi093 10 mg/kg, replicates our previous finding with the combination midazolam 2 mg/kg + β -CCt 30 mg/kg, which

potentiated intertrial crossings during acquisition sessions of the active avoidance paradigm.³⁷⁹ In regard to the cognitive function-related parameters, β -CCt antagonized the inhibitory effect of midazolam on procedural memory tested through active avoidance retention,⁵³⁴ and attenuated the deteriorating effect of the BZ on declarative memory in passive avoidance paradigm.⁵³⁵ In the anxiety-related paradigms (elevated plus maze and acquisition session of active avoidance), the potentiation of the anti-anxiety action of midazolam was observed.⁵²⁹ As the emotionally arousing experiences tend to be well remembered,⁵²⁹ it is widely accepted that suppression of arousal and anxiety by BZs may impair some aspects of cognitive functioning.⁴²⁹ However, the present water maze results, together with the previous findings, dismiss the suggestion⁵³⁴ that the diazepam-induced place learning impairment may be mainly related to its anxiolytic properties. Despite the fact that the anti-anxiety effect of diazepam may have only been preserved or potentiated, not abolished, by β -CCt, the overall performance during 5 acquisition days was at least equal to that of the control group. **The present and previous results suggest that combining a Bz with β -CCt may result in the near to control level of performance of a cognitive task, without sedation, but with highly desirable preserved anti-anxiety activity.**

Illustrated in Table 44 are the significant differences among overall influence (averaged for five days of acquisition) of the tested treatments (mg/kg) on the water maze learning parameters: latency to find the platform (L), distance swam before finding the platform (D), mean swim speed (S) and path efficiency (E).

Table 44. Differences on influences on water maze learning

	Sol + Sol	DZP 2 + β CCt 15	DZP 2 + XLi093 10
DZP 2 + Sol	L: $p < 0.001$ D: $p = 0.001$ E: $p = 0.024$	L: $p < 0.001$ D: $p = 0.001$ S: $p = 0.001$ E: $p < 0.001$	L: $p = 0.002$ D: $p = 0.011$ E: $p = 0.025$
DZP 2 + XLi093 10		S: $p = 0.005$	

DZP, Diazepam; Sol, solvent.

Illustrated in Table 45 are the representative parameters of water maze performance in the probe trial. The key to regions used in the analysis is given in Figure 180. * $P < 0.05$ compared to solvent (SOL + SOL) group; ** $P < 0.01$ compared to solvent; + $P < 0.05$ compared to diazepam 2 mg/kg group (DZP 2 + SOL); ++ $P < 0.01$ compared to DZP 2 mg/kg group.

Table 45. Parameters of water maze performance in the probe trial

	Sol + Sol	DZP 2 + Sol	DZP 2 + β CCt 15	DZP 2 + XLi093 20	ANOVA, <i>F</i>	<i>p</i>
Whole water maze parameters						
Distance (m)	10.74 \pm 1.62	11.74 \pm 0.40	12.45 \pm 0.58	11.43 \pm 0.96	0.531	0.67
Platform quadrant (NE) parameters						
Distance (m)	2.11 \pm 0.48	2.39 \pm 0.28	1.72 \pm 0.47	1.65 \pm 0.29	0.522	0.52
Time (s)	10.50 \pm 2.05	11.98 \pm 1.59	7.33 \pm 2.13	9.31 \pm 2.06	0.971	0.42
Peripheral ring parameters						
Distance (m)	3.80 \pm 0.99	7.86 \pm 0.84**	5.16 \pm 0.60 [†]	5.11 \pm 0.61 [†]	4.77	0.010
Time (s)	29.45 \pm 4.18	44.82 \pm 2.39**	29.19 \pm 2.81 ^{††}	32.20 \pm 2.42 ^{††}	5.81	0.004
Platform ring parameters						
Distance (m)	6.26 \pm 0.91	2.98 \pm 0.55*	6.03 \pm 0.50 [†]	5.08 \pm 0.71 [†]	4.62	0.012
Time (s)	27.05 \pm 3.19	11.75 \pm 2.32**	25.87 \pm 1.98 ^{††}	22.31 \pm 2.29 ^{††}	7.66	0.001
Target region parameters						
Distance (m)	1.48 \pm 0.44	0.78 \pm 0.26	1.06 \pm 0.22	1.12 \pm 0.27	0.86	0.48
Time (s)	5.63 \pm 1.82	3.20 \pm 1.09	3.94 \pm 1.05	4.79 \pm 1.24	0.61	0.62
Platform parameters						
No. of entries	1.33 \pm 0.49	0.17 \pm 0.17	0.57 \pm 0.20	0.86 \pm 0.26	2.52	0.084
Distance (m)	0.146 \pm 0.051	0.007 \pm 0.007*	0.051 \pm 0.019	0.076 \pm 0.034	3.11	0.047

DZP, Diazepam; Sol, solvent.

Values are mean \pm S.E.M.

DZP, β CCt, XLi093 treatments in mg/kg.

* $p < 0.05$ compared to solvent (Sol + Sol) group; ** $p < 0.01$ compared to solvent; [†] $p < 0.05$ compared to DZP 2 mg/kg group (DZP 2 + Sol); ^{††} $p < 0.01$ compared to DZP 2 mg/kg group.

On the other hand, Cain⁴²⁹ suggested that the acquisition deficits may result from the sensorimotor disturbances that diazepam causes. Namely, the author found that non-spatial pretraining without pretreatment eliminated swimming in the periphery of the pool, platform deflections and swimovers, and resulted in the normal, rapid acquisition of the water maze task under diazepam.⁵²⁹ Nevertheless, McNamara and Skelton⁵³⁶ found that treatment with diazepam after the rats acquired the location of the platform did not affect further water maze activity, while it did impair finding of the newly-located platform. Bearing in mind the interaction between arousal, cognitive function and anxiety,⁴³⁰ it is difficult to say that the present results support the view of either pure learning-impairing^{430, 537} or non-selective incapacitating⁴²² effects of diazepam as the

explanation for its effects on spatial learning. Both types of influence may be partly operating in the learning impairment induced by diazepam in the Morris water maze.

The results from the probe trial show that the platform quadrant parameters are not a reliable measure of spatial memory influence of the doses used of diazepam.⁵³⁶ As an example, the rats treated during previous days with 2.0 mg/kg diazepam spent three quarters of the probe trial time in balanced circling throughout the peripheral annulus, and it was not possible to detect any lack of preference for the target quadrant during the resting 15 seconds. Suppression of an instinct to swim thigmotactically appears to be necessary to effectively accomplish the maze task.³⁶⁷ β -CCt as well as XLi093 reversed both, the increase of peripheral annulus, and decrease of platform annulus parameters, induced by 2 mg/kg diazepam. The results from the recall trial as well as from acquisition trials suggest that it is sufficient to antagonize the activity of diazepam at either α_1 - or α_5 -containing GABA(A) receptors in order to forestall its influence on learning the required water maze skills and strategies, i.e. procedural components of this memory task.⁴⁹

Despite the expected relatively low control group activity in the platform zone on its own,⁴⁹ the anterograde amnesic influence of previous treatment with 2 mg/kg diazepam still reached statistical significance, and was only partially prevented by both antagonists used, i.e., they attenuated, but not antagonized, the spatial memory deficit. In fact, the parameters related to the previous platform location in the probe trial are the only ones in the antagonism study with 2 mg/kg diazepam which did not tend to be at least a bit more preserved in combination with β -CCt than with XLi093. The water maze is usually seen as a hippocampal-dependent memory model,^{430, 537} and abundant staining in the rat hippocampus was shown for the α_1 - as well as α_5 -subunit.⁵³⁸ There are several

experimental findings related to the role of the α_5 -subunit in spatial memory. Thus, the α_5 -knock-out mice, compared to the wild-type animals, performed significantly better in a working memory protocol of the water maze,^{367, 389} while an inverse agonist selective for GABA(A) receptors containing α_5 subunits facilitated the acquisition and recall of rats in a similar protocol of working memory.⁵³⁴ The present protocol enabled the long-term consolidation of spatial memory to happen, so that it can be hypothesized that potentiation of inhibitory transmission at both, the α_5 - and α_1 -containing GABA(A) receptors contributes in an interactive way to impairment in the declarative spatial component of the task.³³⁴ It is conceivable that besides the hippocampus, with its crucial role in long-term spatial memory,^{334, 335, 375} the α_1 - and α_5 -containing GABA(A) receptors in neocortex²¹⁷ may be of significance for spatial memory deficits induced by diazepam.

Curran concluded that sedative effects of benzodiazepines in humans are much more easily reversed than amnesic effects;⁴² a similar conclusion may have been applied to rats' behavior in the active avoidance task^{416, 488} and to a certain degree to the present results. It appears that the procedural component (strategy learning) of the water maze learning deficit induced by diazepam is more prone to reversion by α_1 - and α_5 -subtype selective antagonists, the role of α_1 -containing GABA(A) receptors being more salient, while the declarative spatial memory component of learning deficit is less prone to attenuation by antagonists, and may be more related to α_5 -containing GABA(A) receptors. **Bearing in mind the previous results with the combination of a non-selective BZ site agonist and the α_1 selective antagonist β -CCt,^{218, 539} it appears that behavioral effects of such a polypharmacy approach may be highly attractive. In the**

quest for anxiolytics, such a combination may be worth testing on human subjects, and it could be especially useful in treating those forms of emotional disorders which are accompanied by psychomotor slowing.

Where To Go From Here- Next Generation Ligands

Although one of the goals of my research in drug design is 400 fold selectivity of GABA(A) ergic $\alpha 5\beta 3\gamma 2$ subtypes over sedating, ataxic $\alpha 1\beta 3\gamma 2$ subtypes, subtype selectivity of >1000 fold is desirable. Since $\alpha 1$ GABA(A) ergic subtypes are principally responsible for the sedative, ataxic and amnesic properties of benzodiazepine receptor ligands,⁶⁴ poor affinity and/or efficacy at these $\alpha 1$ subtypes are a requirement here for ligands. Based on molecular modeling⁵²⁶ and the cognition enhancement activity of lead BzR ligand PWZ-029,⁴² a series of new $\alpha 5$ subtype selective ligands have been designed. As depicted in Table 46, PWZ-029, YT-II-76, YT-I-78, JY-I-03, SH-I-75, JY-I-10, and Xli-093 have been synthesized on 30 milligram scale and the K_i 's determined by our collaborators at UNC (B. Roth and Dr. Samarpan Majumder). The type of chemistry necessary to prepare such ligands has been reported in preliminary form in patents.⁵³⁹ Although PWZ-029 is only 60 fold more selective for $\alpha 5$ subtypes over $\alpha 1$ subtypes, the subtype selective efficacy (see oocyte data, Figure 193) of this ligand was extremely high. However, the subtype selectivity ($\alpha 5$ vs. $\alpha 1$) for most of the ligands in Table 46 is even better [B. Roth, J. Cook, et al., unpublished results, K_i 's in nM, YT-II-76 (2370 fold), YT-I-38 (236 fold), JY-I-03 (200 fold), SH-I-75 (8000 fold), JY-I-10 (400 fold), Xli-093 (65 fold)] and provides support for both the modeling and the medicinal chemistry strategy. Although the bivalent lead is only 65 fold more selective, this ligand has been shown to be the first $\alpha 5$ subtype selective antagonist both *in vitro*⁴² and *in vivo*.⁵²⁶ For the first time, a subtype selective antagonist (Xli-093), active *in vivo*,

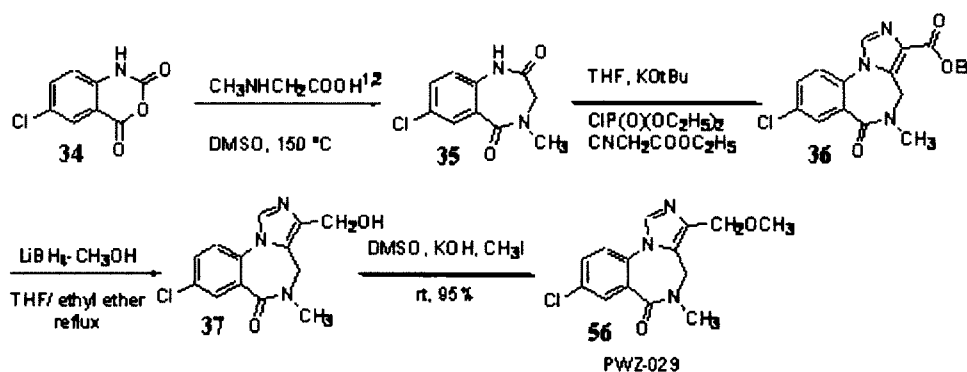
at $\alpha 5$ GABA(A) ergic Bz receptors is in hand which can be employed to confirm biology mediated via $\alpha 5$ subtypes. Moreover, (see oocyte profile), the R-enantiomer (SH-I-75) is about 8000 fold selective for $\alpha 5$ subtypes over $\alpha 1$ receptors and is an agonist at $\alpha 5$ BzR providing another selective tool to confirm data resulting from this research. It is a positive control and should be amnesic. Moreover, it would be expected to reverse the effects of ligands such as PWZ-029 in the cognition models providing both face and construct validity to this approach.

Because $\alpha 5$ BzR GABA(A) ergic subtypes are found primarily in the hippocampus, these are the subtypes of interest.⁵²⁶ The synthesis of 5-10 grams of lead ligands PWZ-029 , Xli-093, and agonist SH-I-75 has been carried out for studies in rodents. This can be followed by the synthesis of 40-100 mgs of the PWZ-029 analogs in Scheme 2 and finally approximately 1 to 2 grams of the other $\alpha 5$ subtype selective ligands in Table 46 (for studies in mice) will be completed. The analogs in Scheme 2 can be synthesized on small scale in order to search for more subtype selective analogs of PWZ-029. The new analogs should be prepared on small scale for receptor binding, and the best of these tested for functional efficacy in oocytes. Synthesis of existing analogs in Schemes 1, 3, 4, 5, and 6 on gram scale for rodent and primate studies, as well as the new analogs (Scheme 2) on 40-100 milligram scale provides a two-pronged attack toward clinical agents for treatment of age associated memory deficits and Alzheimer's disease.

The synthesis of these ligands is based upon previous chemistry in Milwaukee and the precedents are fully cited at the bottom of each scheme. The steps in the route have been carried out previously and reported.^{416, 488, 526}

Illustrated in Scheme 2 are the new PWZ-029 analogs. In the upper left hand corner is YT-I-76 (**5**) recently shown to be 2360 times more selective for the desired $\alpha 5$ subtypes over the undesired $\alpha 1$ subtypes. In brief, the PWZ-intermediate **3**, from Scheme 1, can be converted into the new PWZ-analogs **5**, **6**, and **7** via known, cited chemistry. The fluoro analogs **6**, **7**, **9**, and **11** provide enhanced metabolic stability, but still interact with the $\alpha 5$ receptor isoform in the same fashion as the $R\text{-CH}_2\text{OCH}_3$ group of PWZ-029.⁵⁴⁰ These analogs have been modeled and fit the included volume well.

Scheme 1



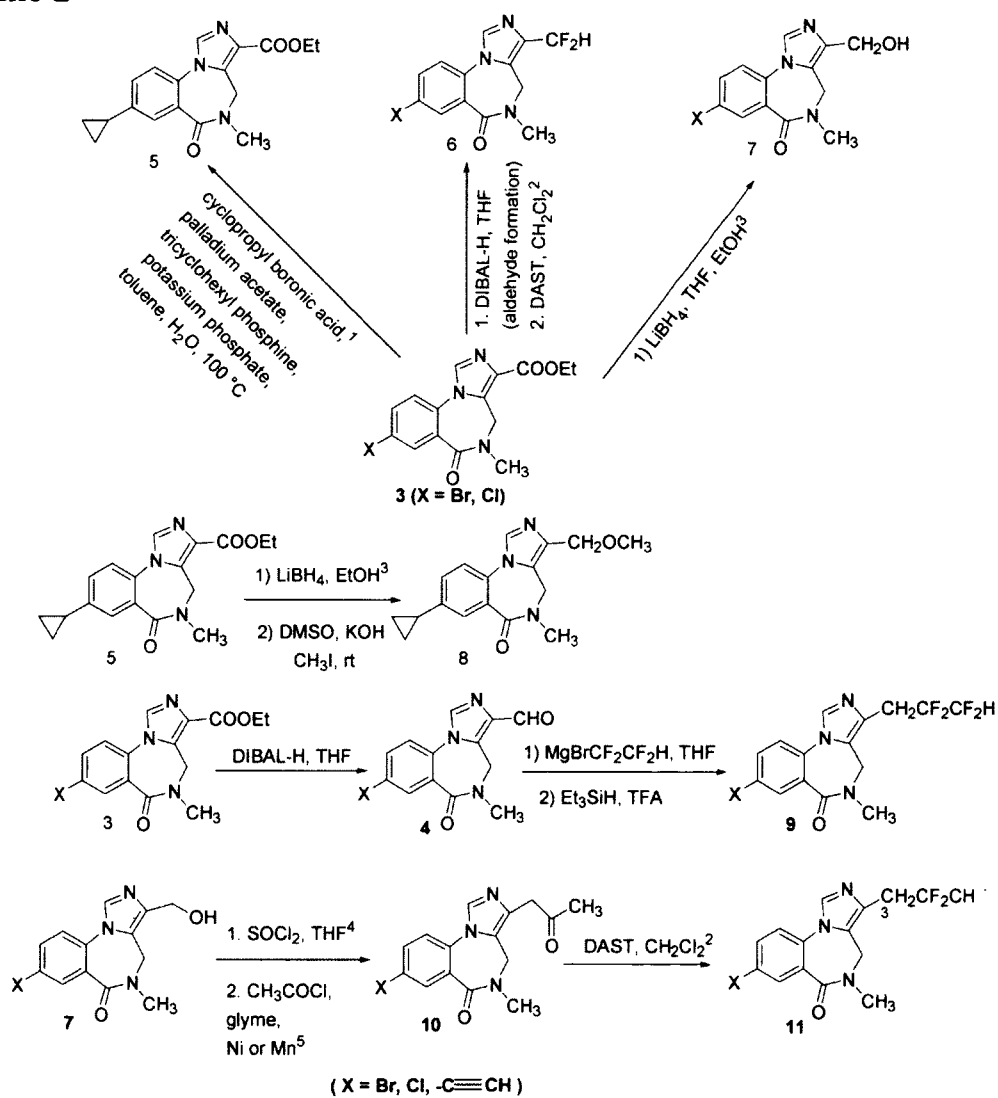
1. Zhang, P.; Zhang, W.; Liu, R.; Harris, B.; Skolnick, P.; Cook, J. M. Synthesis of Novel Imidazobenzodiazepines as Probes of the Pharmacophore for "Diazepam-Insensitive" GABA_A Receptors. *J. Med. Chem.* 1995, 38, 1679-1688.
2. Cook, James M.; Han, Dongmei; Clayton, Terry. Imidazobenzodiazepines as gabaergic agents to treat memory deficits and their preparation. U.S. Pat. Appl. Publ. (2006), 82pp. CODEN: USXXCO US 2006258643 A1 20061116 CAN 145: 505485 AN 2006:1204617 CAP LUS

In Scheme 2 is illustrated the synthesis of a hybrid analog (see **8**) of PWZ-029 (**56**) and the cyclopropyl substituted subtype selective ligand (**5**). Reduction of YT-II-76 (**5**) with lithium borohydride, followed by the standard methylation with methyl iodide will provide hybrid ligand **8**. The synthesis of the fluoro analogs will be carried out employing the usual DAST-mediated fluorination process. All of these analogs **5**, **6**, **7**, **8**, **9**, **10**, and **11** will be prepared as mentioned, on 40-100 milligram scale for receptor binding and functional oocyte efficacy (on the most $\alpha 5$ subtype selective ligands). Since drug design is an iterative process, the molecular modeling and analog improvement must await some *in vitro* and *in vivo* data in order to improve subtype selectivity, bioavailability, and metabolic stability (fluoro analogs).

The synthesis of the first $\alpha 5$ subtype selective antagonist^{416, 488, 526} is illustrated in Scheme 3. At least 1-5 grams of Xli-093 and the closely related bivalent ligand Xli-210 have been prepared. The antagonist, Xli-093 is a key tool with which to establish face and construct validity. It is the only $\alpha 5$ subtype selective antagonist whose antagonist activity at $\alpha 5$ subtypes *in vivo* mirrors that reported *in vitro*.⁵⁴¹ Certainly Xli-093 is a critical tool in this study and Xli-210 might be even better. This remains to be established in future research.

Depicted in Table 46 is the structure and $\alpha 5$ subtype selectivity of three new ligands recently developed. Illustrated in Scheme 5 is a hybrid ligand (YT-TC-3) between active inverse agonist PWZ-029 and $\alpha 5$ subtype selective antagonist Xli-093. Since PWZ-029 and Xli-093 are active in rodents ip, it is clear these types of ligands cross the blood brain barrier.⁶⁴

Scheme 2



1. Wallace, D.J.; Chen, C. Cyclopropylboronic acid: synthesis and Suzuki cross-coupling reactions. *Tetrahedron Lett.* **2002**, *43*, 6987.
2. (a) Bombrun, Agnes; Gerber, Patrick; Casi, Giulio; Terradillos, Olivier; Antonsson, Bruno; Halazy, Serge. 3,6-Dibromocarbazole Piperazine Derivatives of 2-propanol as First Inhibitors of Cytochrome c Release via Bax Channel Modulation. *J. Med. Chem.* **2003**, *46*, 4365. (b) Caldwell, Charles; Chapman, Kevin; Hale, Jeffrey; Kim, Dooseop; Lynch, Christopher; Maccoss, Malcolm; Mills, Sander G.; Rosauer, Keith; Willoughby, Christopher; Berk, Scott. Preparation of Pyrrolidine Derivatives as Modulators of Chemokine Receptor Activity. WO patent 2000059503 (2000) A1 20001012 CAN 133:296375.
3. Cook, James M.; Han, Dongmei; Clayton, Terry. Imidazobenzodiazepines as gabaergic agents to treat memory deficits and their preparation. U.S. Pat. Appl. Publ. (2006), 62pp. CODEN: USXXCO US 2006258643 A1 20061116 CAN 145: 505485 AN 2006:1204617 CAPLUS
4. Zhang, Puwen; Zhang, Weijiang; Liu, Ruiyan; Harris, Bradford; Skolnick, Phil; Cook, James M. Synthesis of Novel Imidazobenzodiazepines as Probes of the Pharmacophore for "Diazepam-Insensitive" GABA(A) receptors. *J. Med. Chem.* **1995**, *38*(10), 1679.
5. (a) Inaba, Shinichi; Rieke, Reuben D. Metallic nickel: A Coupling Reagent of Benzyl Halides and Acyl Halides to Yield Benzyl Ketones. *Tetrahedron Lett.* **1983**, *24*(24), 2451. (b) Inaba, Shinichi; Rieke, Reuben D. Metallic Nickel-Mediated Synthesis of Ketones by the Reaction of Benzylic, Allylic, Vinylic, and Pentafluorophenyl Halides with Acid Halides. *J. Org. Chem.* **1985**, *50*(9), 1373. (c) Suh, YoungSung; Lee, Jun-sik; Kim, Seoung-Hoi; Rieke, Reuben D. Direct Preparation of Benzylic Manganese Reagents from Benzyl Halides, Sulfonates, and Phosphates and their Reactions: Applications in Organic Synthesis. *J. Organomet. Chem.* **2003**, *684*(1-2), 20.

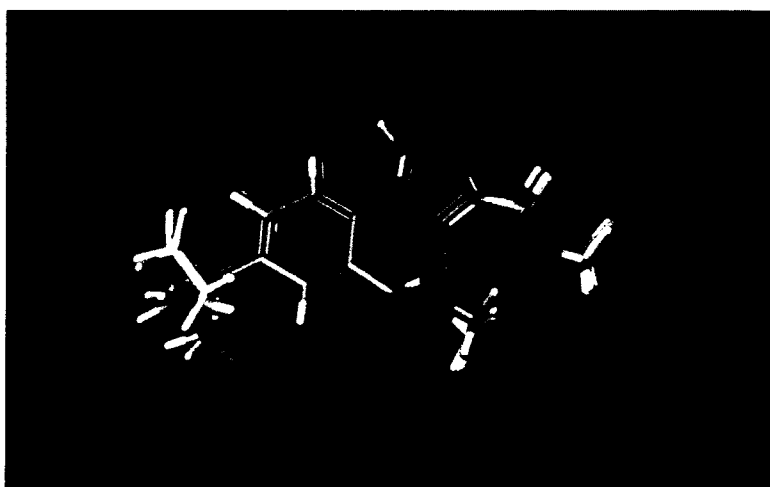
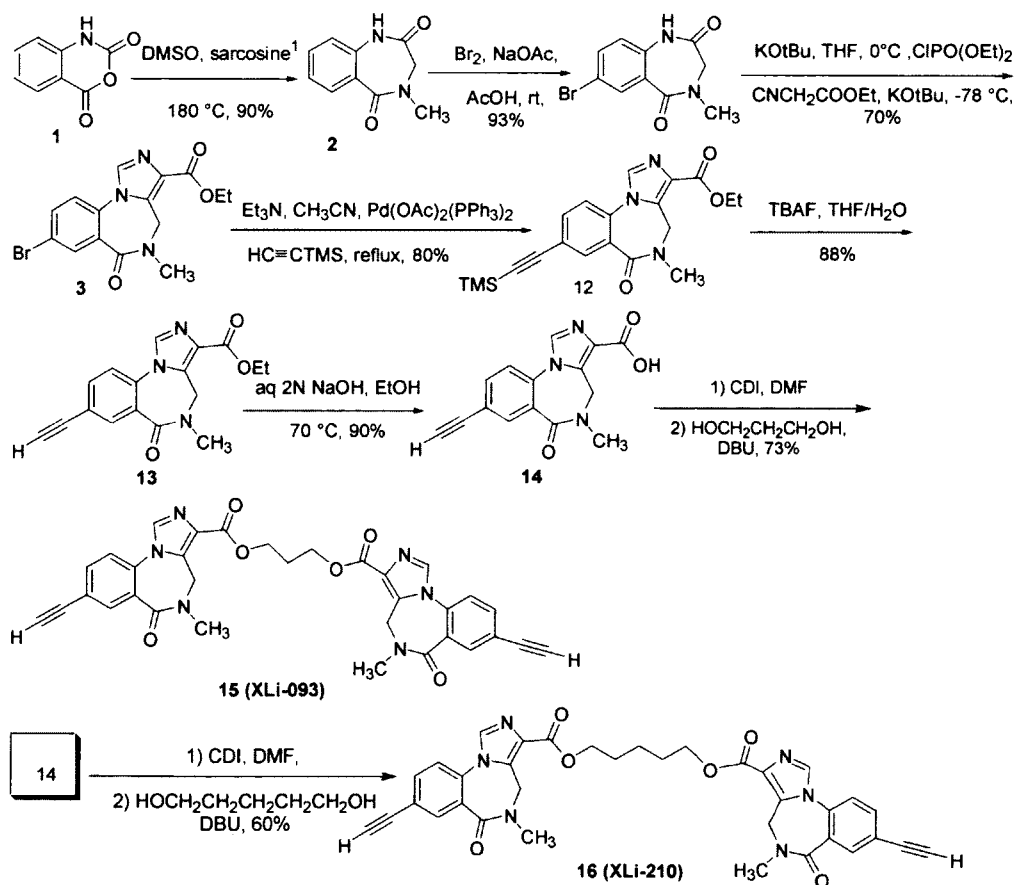


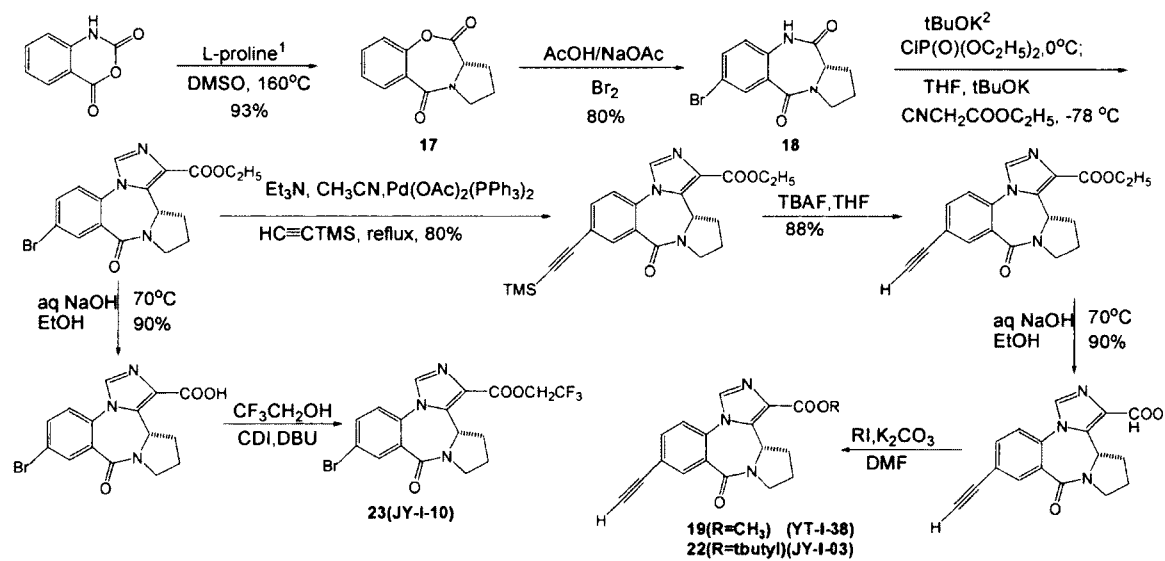
Figure 181. Overlay of cyclopropyl analogs of PWZ-029

Scheme 3

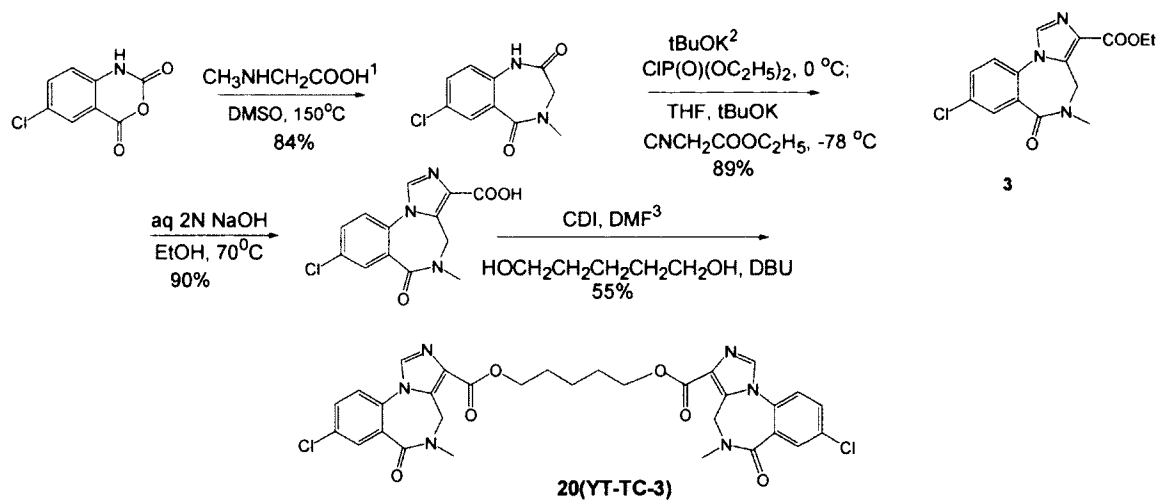


1. Xiaoyan Li, Hui Cao, Chunchun Zhang, Roman Furtmueller, Karoline Fuchs, Sigismund Huck, Werner Sieghart, Jeffrey Deschamps, James M Cook, Synthesis, in Vitro Affinity and Efficacy of a Bis 8- Ethynyl-4H-imidazo [1,5a]-[1,4] benzodiazepine Analogue, the first Bivalent $\alpha 5$ Subtype Selective BzR/GABA_A Antagonist. J.Med.Chem. 2003 46, 5567-5570

Scheme 4

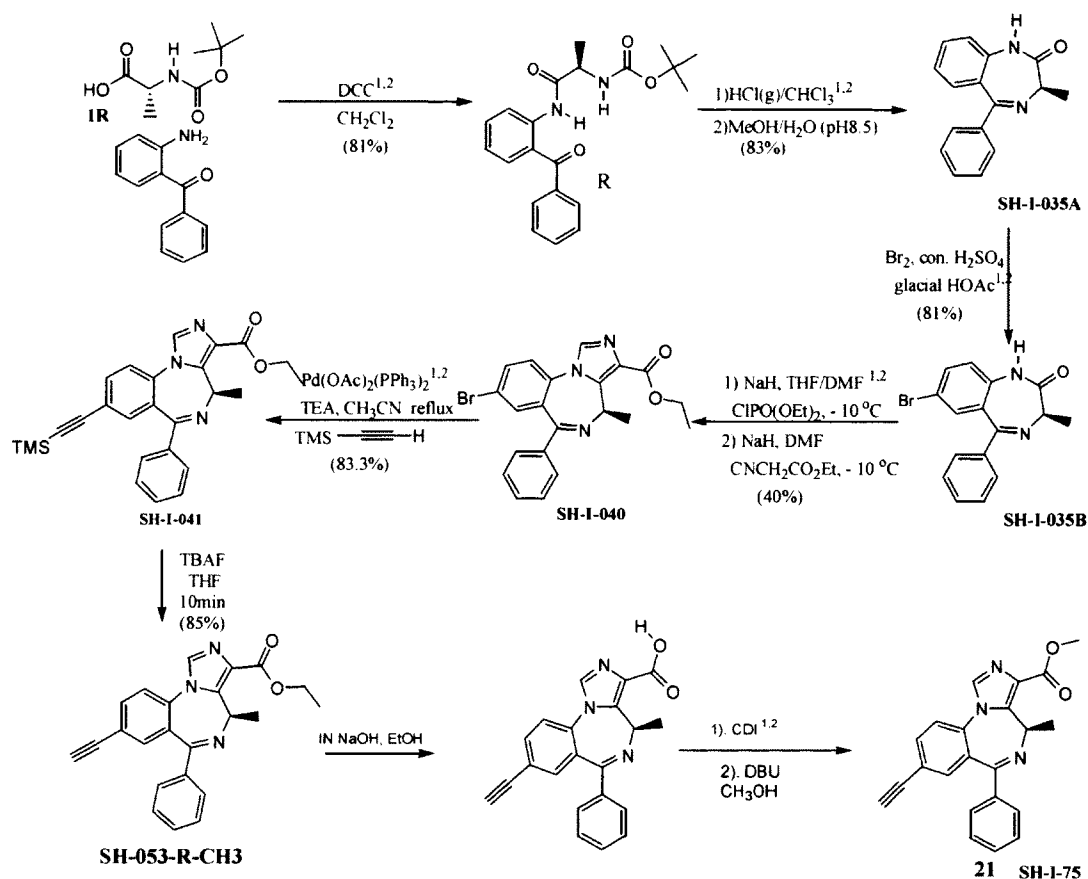


Scheme 5



1. Zhang, P.; Zhang, W.; Liu, R.; Harris, B.; Skolnick, P.; Cook, J. M. Synthesis of Novel Imidazobenzodiazepines as Probes of the Pharmacophore for "Diazepam-Insensitive" GABAA Receptors. *J. Med. Chem.* 1995, 38, 1679-1688.
2. Yang, J.; Teng, Y.; Ara, S.; Rallapalli, S. and Cook J. M. An Improved Procedure for the Synthesis of Imidazo[1,5-a][1,4]benzodiazepines. *Synthesis*, Manuscript accepted, 2009
3. Li, X.; Yin, W.; Sarma, P.V.; Zhou, H.; Ma, J.; Cook, J. M. Synthesis, in Vitro Affinity, and Efficacy of a Bis 8-Ethynyl-4H-imidazo[1,5a]-[1,4]benzodiazepine Analogue, the First Bivalent 5 Subtype Selective BzR/GABAA Antagonist. *J. Med. Chem.*, 2003, 46, 5567-5570

Scheme 6



1. Shengming Huang. Synthesis of Optically Active Subtype Selective Benzodiazepine Receptor Ligands. Univ. of Wisconsin, Milwaukee, PhD Thesis, Milwaukee, WI, USA., 2007
2. Miroslav M Savić, Shengming Huang, Roman Furtmüller, Terry Clayton, Sigismund Huck, Dragan I Obradović, Nenad D Ugrešić, Werner Sieghart, Dubravko R Bokonić, James M Cook. Are GABA_A Receptors Containing $\alpha 5$ Subunits Contributing to the Sedative Properties of Benzodiazepine Site Agonists? *Neuropsychopharmacology*, 2008, 33, 332-339.

The chemistry used to design fluoro analogs of PWZ-029 can be adapted to design ligands of XHE-053 with less potential for metabolism by esterases. Fluorines in place of the carbonyl group satisfy current included volumes and electronegativity requirements of the Milwaukee-based pharmacophore receptor model. The covalent

radius of a hydrogen is 37 pm whereas a fluorine is 71 pm, whereas an oxygen atom with lone pairs (carbonyl) is 57 pm (picometers).

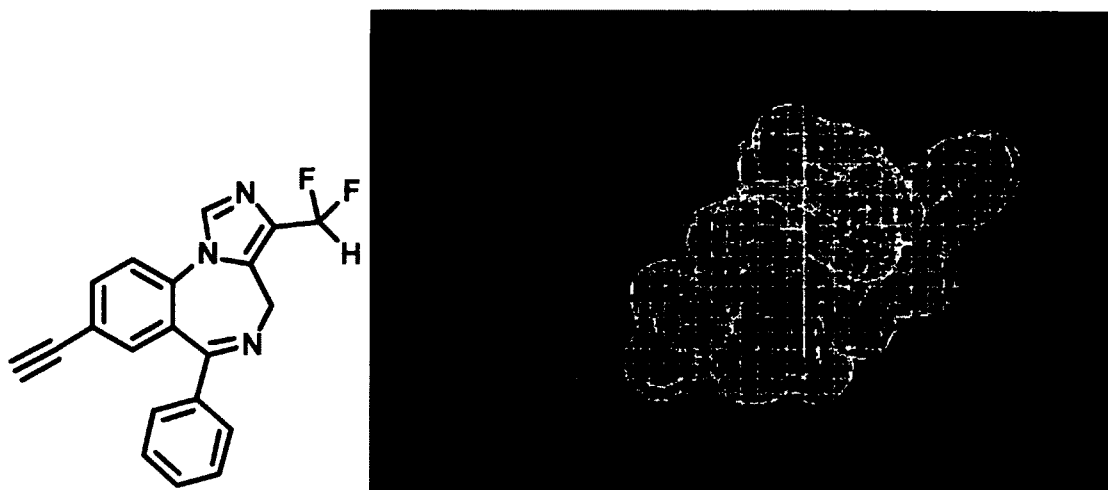


Figure 182. Fluoro analogs of the XHe-II-053

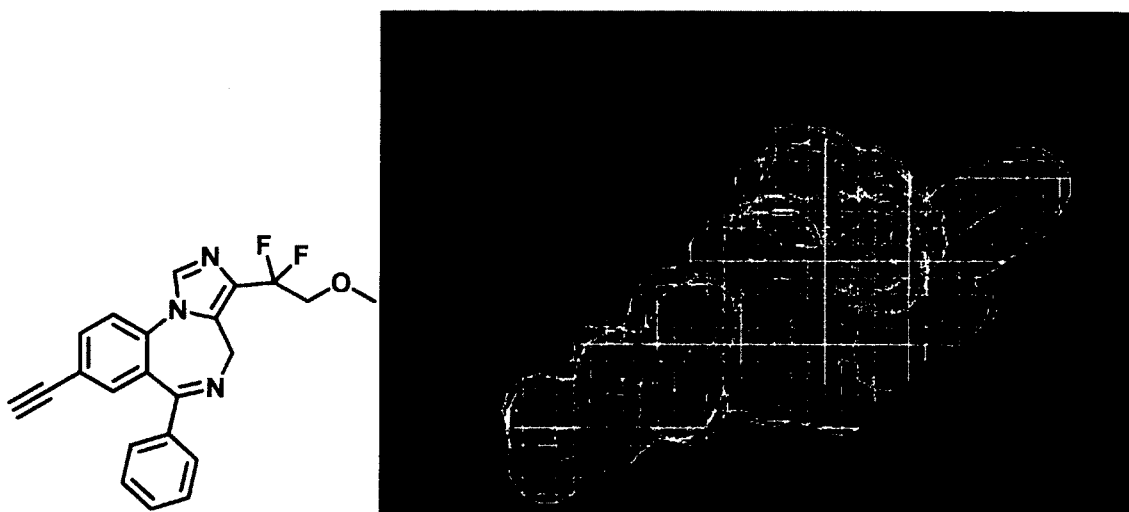
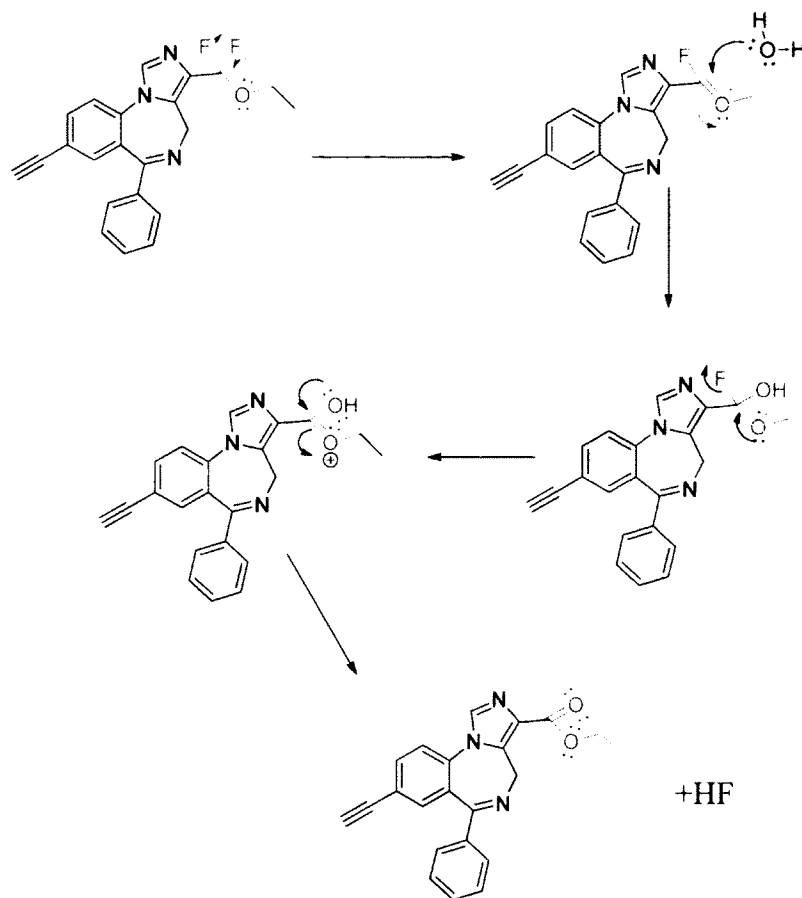


Figure 183. Alkyl ether fluoro analogs of XHe-II-053

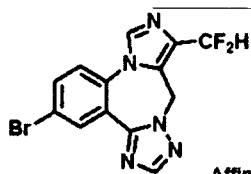
Again, molecular modeling of a methyl ether fluoro analog of XHe-II-053 appears reasonable. Due to known binding, the methyl ether which appears exposed in the Figure is not expected to be a problem.

Due to the concern that fluoro ethers would auto hydrolyze to form hydrofluoric acid by way of the mechanism shown below, these types have not been made.



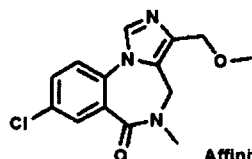
This approach is in agreement by a recent compounds patented by Roche.⁶⁴ Several new analogs have been proposed and docked in the Milwaukee based pharmacophore.

PWZ-029 and Roche Cmpd 7



Affinity for $\alpha\beta\gamma 2$ ($x = 1-6$) benzodiazepine receptor isoforms

	Alpha 1	Alpha 2	Alpha 3	Alpha 4	Alpha 5	Alpha 6
Roche	174.3	185.4	79.6	ND	4.6	ND



Affinity of PWZ-029 for $\alpha\beta\gamma 2$ ($x = 1-6$) benzodiazepine receptor isoforms

	Alpha 1	Alpha 2	Alpha 3	Alpha 4	Alpha 5	Alpha 6
Merck	>300	>300	>300	ND	38.5	>300
Moltech	920	ND	ND	ND	30	ND
UNC-Roth	362.4	180.330	328.2	ND	6.185	ND

Figure 184. Binding data for PWZ-029 and Roche Compound 7.

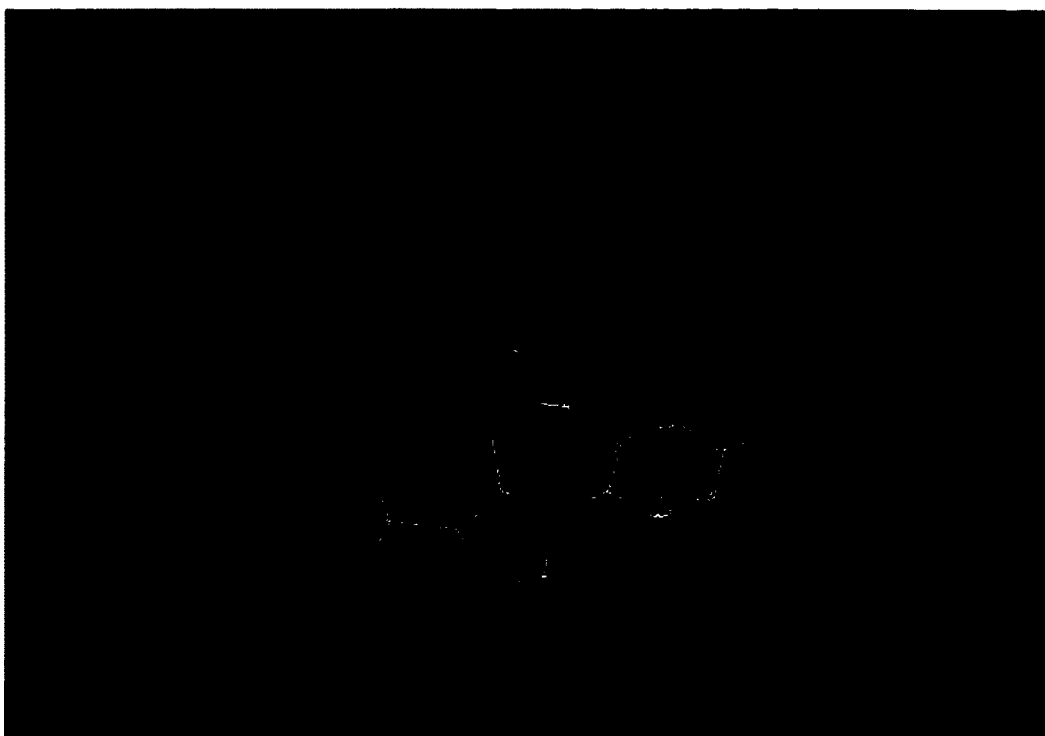


Figure 185. Roche Compound 7 docked in the pharmacophore of the $\alpha 5 \beta 3 \gamma 2$ receptor subtype

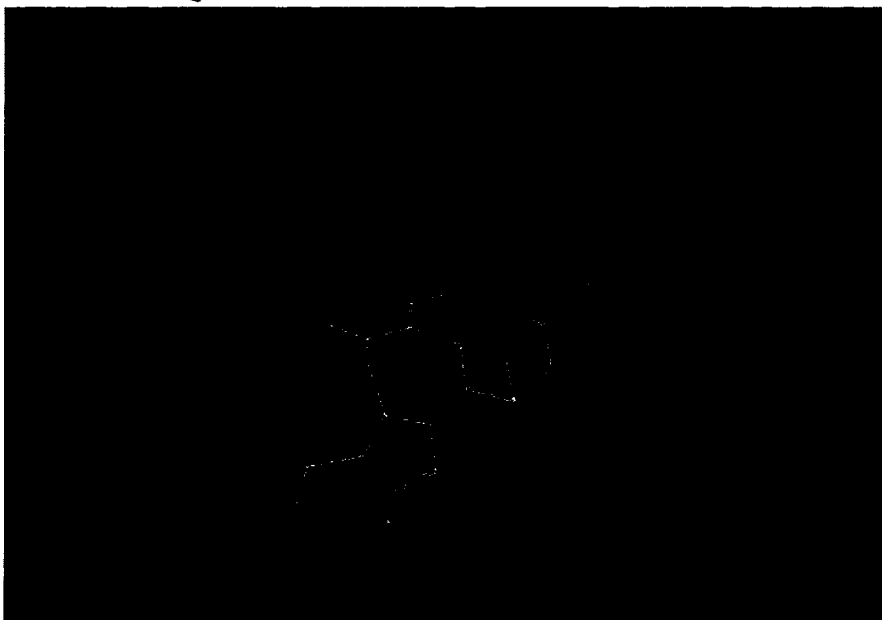
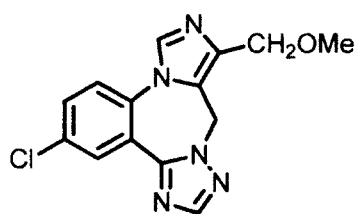


Figure 186. Proposed analog of PWZ-029

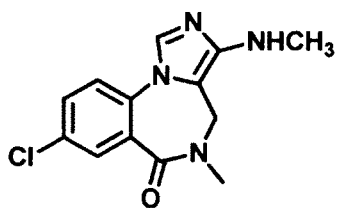
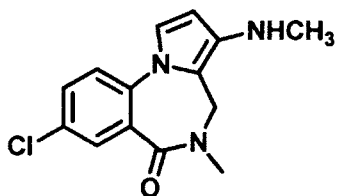




Figure 187. Proposed analog of PWZ-029.



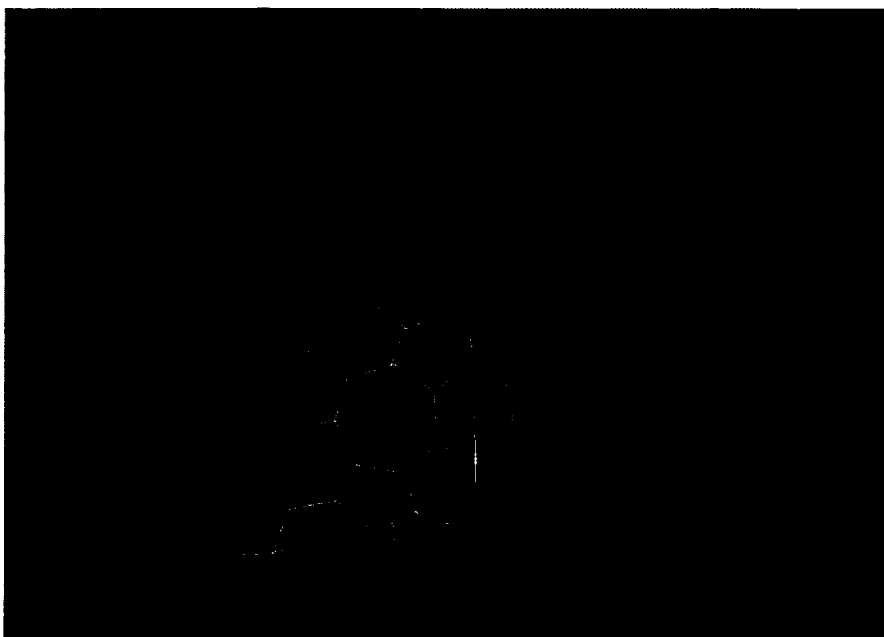
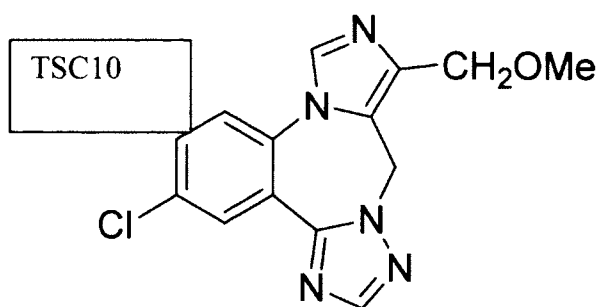
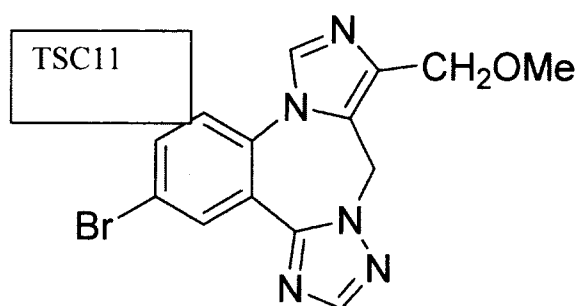


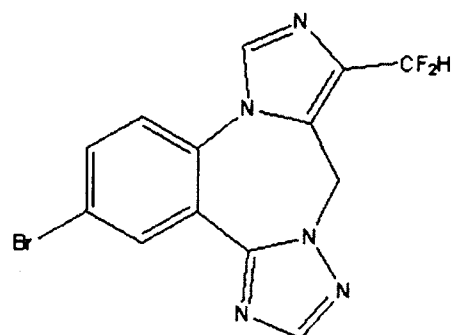
Figure 188. Proposed amine analog of PWZ-029



Log P: 1.7
CLogP: 1.45903

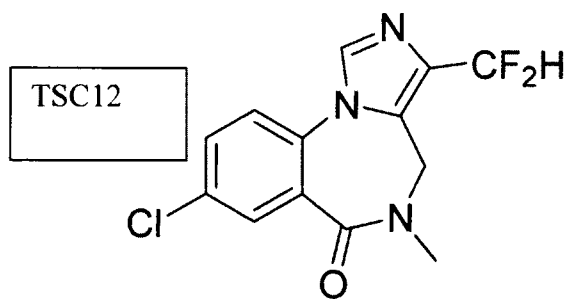


Log P: 1.97
CLogP: 1.60903

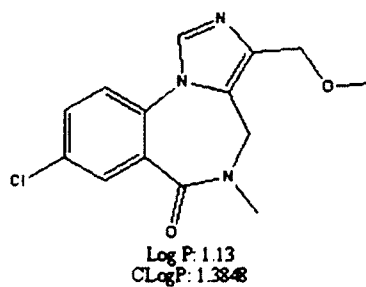


Log P: 2.45
CLogP: 1.88603

Roche compound



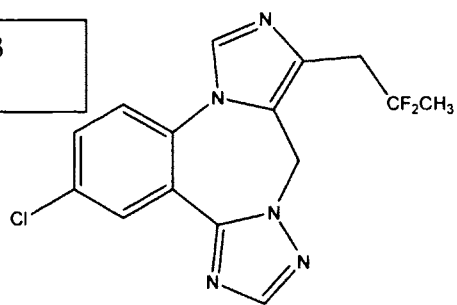
Log P: 1.61
CLogP: 1.6618



Log P: 1.13
CLogP: 1.3848

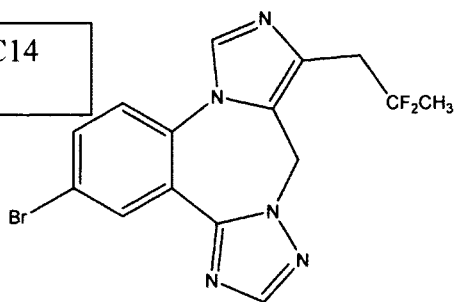
PWZ-029

TSC13

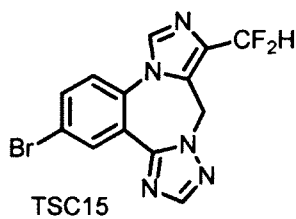


Log P: 2.81
CLogP: 2.01403

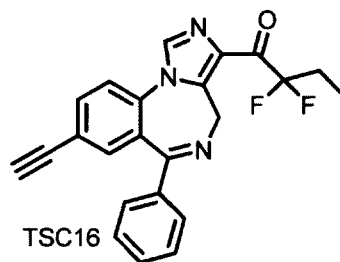
TSC14



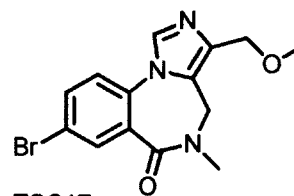
Log P: 3.08
CLogP: 2.16403



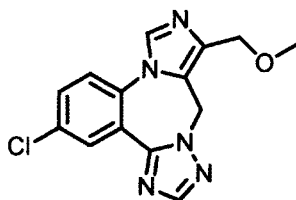
TSC15



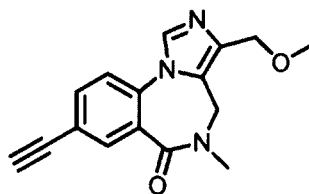
TSC16



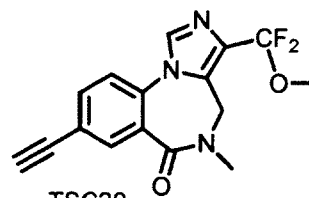
TSC17



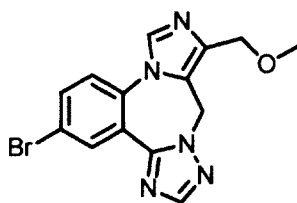
TSC18



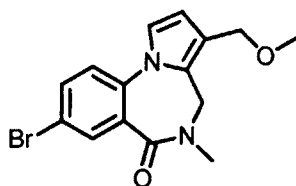
TSC19



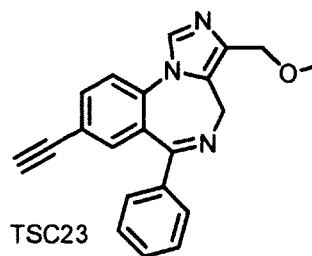
TSC20



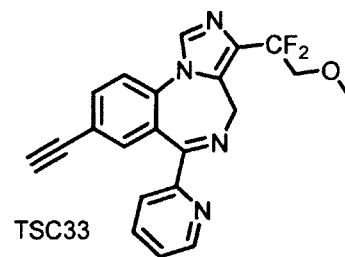
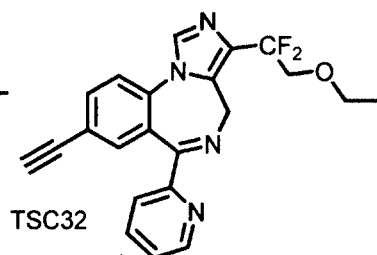
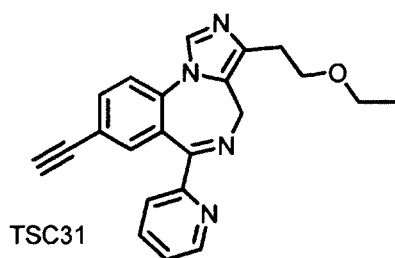
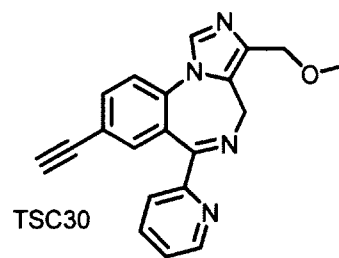
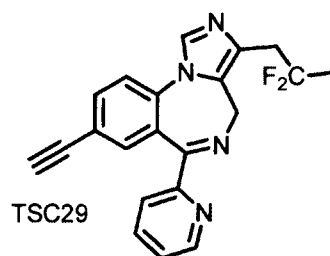
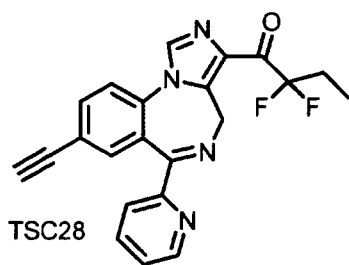
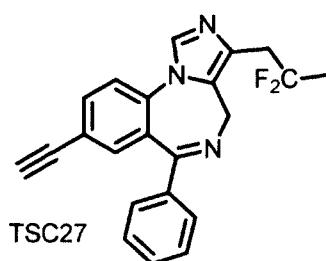
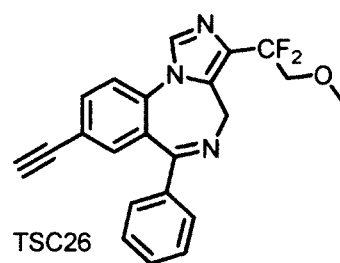
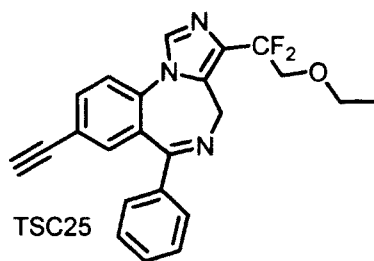
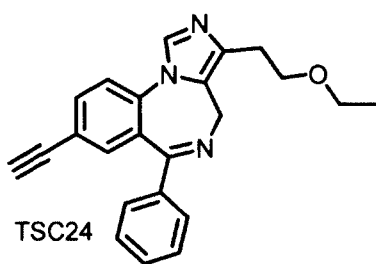
TSC21



TSC22



TSC23



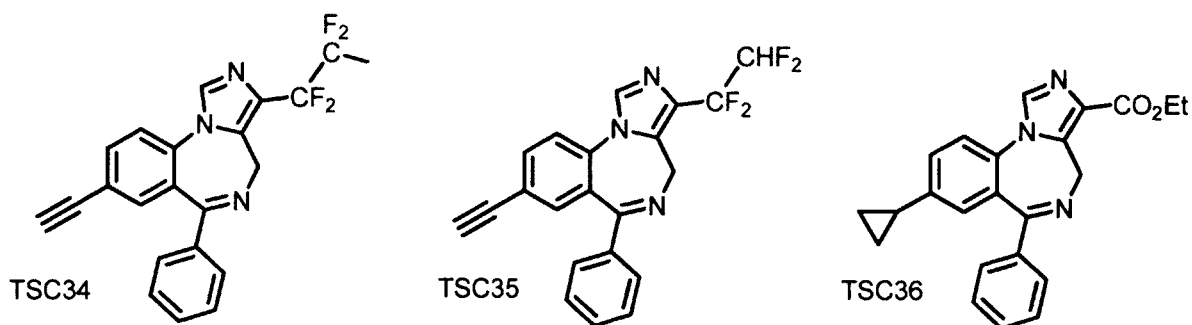
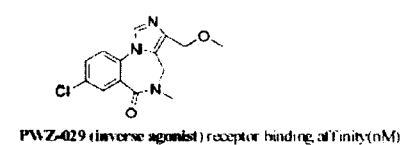
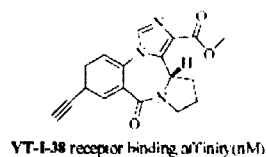


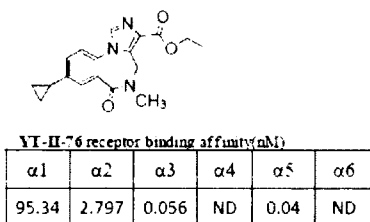
Table 46. Alpha 5 GABA(A) ergic Subtype Selective Ligands



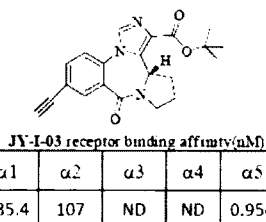
$\alpha 1$	$\alpha 2$	$\alpha 3$	$\alpha 4$	$\alpha 5$	$\alpha 6$
>300	>300	>300	ND	38.5	>300
362.4	180.3	328.2	ND	6.185	ND
920	ND	ND	ND	30	ND



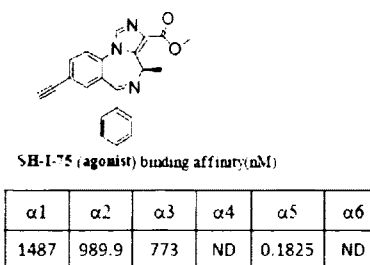
$\alpha 1$	$\alpha 2$	$\alpha 3$	$\alpha 4$	$\alpha 5$	$\alpha 6$
945.9	326.8	245.9	ND	4.07	ND



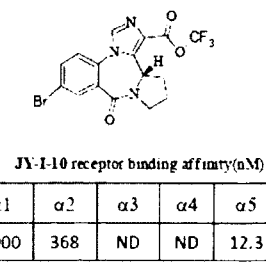
$\alpha 1$	$\alpha 2$	$\alpha 3$	$\alpha 4$	$\alpha 5$	$\alpha 6$
95.34	2.797	0.056	ND	0.04	ND



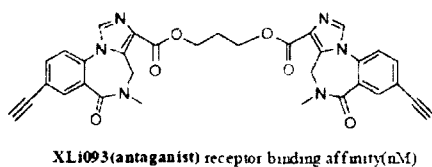
$\alpha 1$	$\alpha 2$	$\alpha 3$	$\alpha 4$	$\alpha 5$	$\alpha 6$
185.4	107	ND	ND	0.954	3.34



$\alpha 1$	$\alpha 2$	$\alpha 3$	$\alpha 4$	$\alpha 5$	$\alpha 6$
1487	989.9	773	ND	0.1825	ND



$\alpha 1$	$\alpha 2$	$\alpha 3$	$\alpha 4$	$\alpha 5$	$\alpha 6$
5000	368	ND	ND	12.3	23

**XL1093 (antagonist) receptor binding affinity (nM)**

$\alpha 1$	$\alpha 2$	$\alpha 3$	$\alpha 4$	$\alpha 5$	$\alpha 6$
1000	1000	858	1550	15	2000

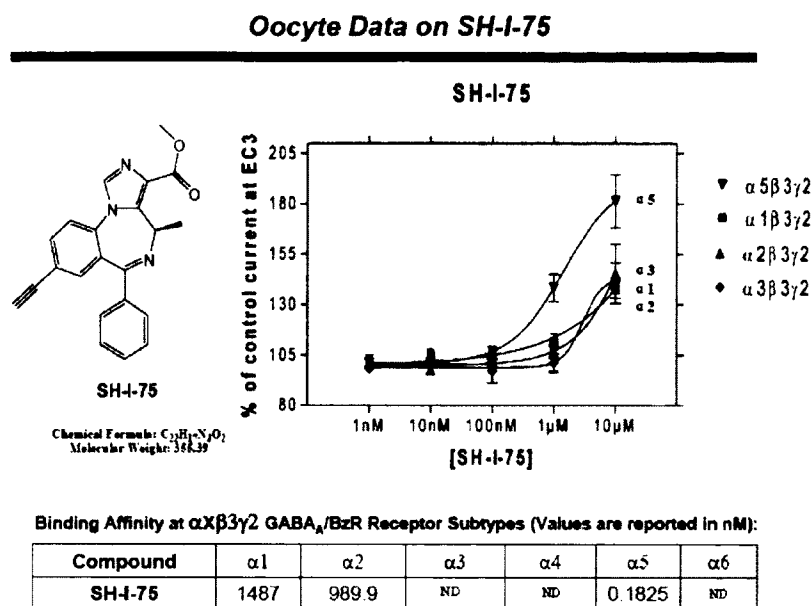


Figure 189. Control compound SH-I-75

Examination of the data at the bottom of Table 41 clearly illustrates SH-I-75 (**21**) is the most potent (>2000 fold selective) $\alpha 5$ subtype selective agonist ever prepared. Its functional efficacy and selectivity render it the perfect positive control for this work. The ligand **21** should have properties exactly opposite that of PWZ-029. It is believed; ligand **21** will cause amnesia, will antagonize the effects of PWZ-029 and again lend face and construct validity to this research. Positive controls and an $\alpha 5$ antagonist render this a very strong approach to hippocampal-mediated drug design in regard to the development

of agents to treat cognition deficits in Alzheimer's and related age-associated memory deficits.

Again, it is known from previous work⁵²⁶ that ligands **4** and **15** are active i.p. *in vivo* and ligands closely related in structure to SH-I-75 (**21**) are orally active in rodents (Stables, J.; NINDS; anticonvulsant screening program).⁵²⁶ These $\alpha 5$ subtype selective analogs cross the blood brain barrier.

Biology

Diazepam significantly impairs performance in a holeboard memory task, in which mice learned the location of 4 baited holes (out of 16 possible) over the course of 4 trials. This performance impairment suggests a diazepam-induced working memory deficit. The novel antagonist XLi-093 showed appreciable selectivity for the $\alpha 5$ GABA(A) receptor *in vivo*, consistent with previous finding *in vitro*.⁵⁴ The memory-impairing effects of diazepam were blocked (Figure 190) by a dose of Xli093 (3.0 mg/kg) that occupied ~66% of $\alpha 5$ GABA(A) binding sites but < 25% (non-significant) of $\alpha 1$ GABA(A) and $\alpha 2/3$ GABA(A) binding sites (Figure 198).⁴⁸⁸ Memory impairment measured via the holeboard task occurred at a dose of diazepam that resulted in a relatively high degree of $\alpha 5$ GABA(A) binding site occupancy (64%). Interestingly, even at a saturating dose of diazepam (10 mg/kg), Xli093 was still able to block diazepam's memory impairing effects. The data suggests $\alpha 5$ GABA(A) receptors play an important role in diazepam-induced memory impairments. Identification of compounds with reduced $\alpha 5$ GABA(A) activity may result in nonsedating-anxiolytics ($\alpha 2/\alpha 3$ mediated) that lack memory-impairing effects of classical benzodiazepines.⁴¹⁶

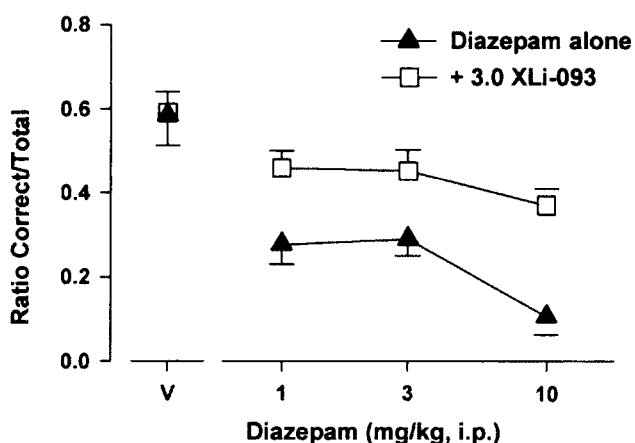


Figure 190. Reversal of Diazepam-induced memory deficit

XLi-093 (3.0 mg/kg) blocked the DZ-induced suppression of performance ratio on the holeboard task. Note that XLi-093 showed no effect when administered with vehicle. Percent of $\alpha 5$ GABA(A) binding sites occupied by XLi-093 and DZ at doses used in the behavioral studies: $n=8$.

In vivo binding studies (Figure 191) with XLi-093 showed negligible occupancy of $\alpha 1$ GABA(A) and $\alpha 2/3$ GABA(A) binding sites; however, occupancy of $\alpha 5$ GABA(A) binding sites was significant at 1.0 mg/kg and above.

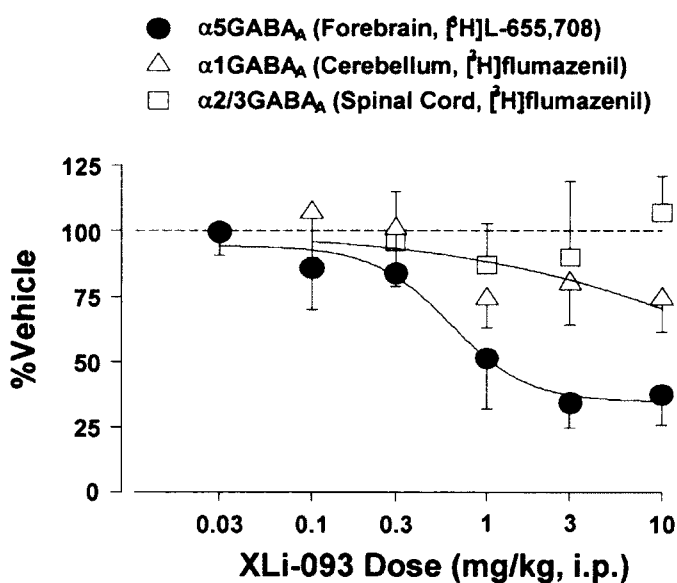


Figure 191. In vivo binding assay of Xli-093

To determine the binding site occupancy at $\alpha 1$ and $\alpha 2/3$ GABA(A) receptors, mice were injected with [3 H]flumazenil ([3 H]FLZ) (1.5 μ Ci/mouse, i.v.) (Figure 191). Pretreatments of 30 minutes included: DZ (0.3-10.0 mg/kg, i.p.), XLi-093 (0.03-10.0 mg/kg, i.p.), flunitrazepam (30.0mg/kg, i.p., used to determine non-specific binding). Mice were sacrificed 3 min after i.v. injection of tritiated ligand. Cerebellum and spinal cord were quickly removed, homogenized, and stored in ScintiSafe. All samples were processed with a Packard 1900CA liquid scintillation analyzer. For binding site occupancy at $\alpha 5$ GABA(A) receptors, methods followed those above using [3 H]L655,708 (1.5 μ Ci/mouse, i.v.). Non-specific binding was determined using

bretazenil (5.6 mg/kg, i.p.). Mice were sacrificed 1 min after injection with tritiated ligand and the forebrain was quickly removed and prepared as described above.

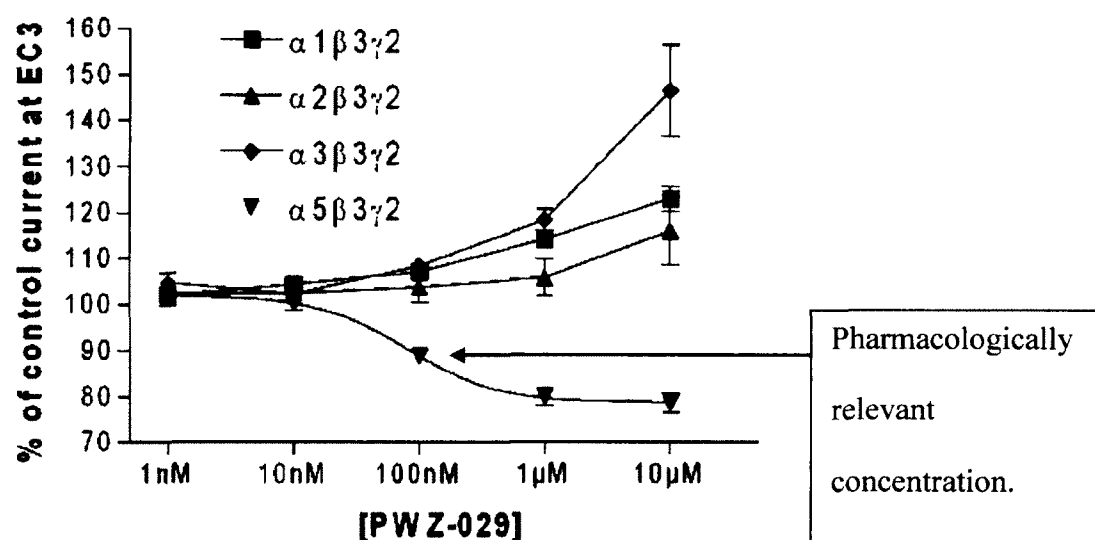
The ability of a novel $\alpha 5$ GABA(A) subtype selective antagonist, Xli-093(Xli; 0.3-10.0mg/kg), to occupy $\alpha 5$ GABA(A) receptors *in vivo* binding (*in vivo* [3 H]L-655,708 binding) has also been evaluated (Figure 192). Based on percent binding occupancy, we assessed the ability of a range of Xli-093 doses to reverse impairments induced by the minimal effective dose of DZ (3.0 mg/kg). Xli-093 reversed DZ-induced impairments at doses of 1.0 and 3.0 mg/kg, which occupied ~50-65% of [3 H]L-655,708 binding. In contrast, these doses resulted in only ~20% occupancy of $\alpha 1$ GABA(A) and $\alpha 2/3$ GABA(A) receptors in cerebellum and spinal cord, respectively (determined by *in vivo* [3 H]flumazenil binding). These findings are consistent with a key role for $\alpha 5$ GABA(A) receptors in BZ-induced impairments in learning and memory.

Ligand (Dose, ip)	% $\alpha 5$ GABA(A) Occupancy
Xli093 (3.0)	65.8
DZ (1.0)	63.8
DZ (3.0)	83.5
DZ (10.0)	99

Figure 192. $\alpha 5$ GABA(A) occupancy in the brain⁴¹⁶

Illustrated in Figure 192 are the percent of $\alpha 5$ GABA(A) binding sites occupied by XLi-093 and DZ at doses used in the behavioral studies.

The novel ligand PWZ-029, which we synthesized and characterized electrophysiologically, possesses *in vitro* binding selectivity and moderate inverse agonist functional selectivity at $\alpha 5$ -containing GABA(A) receptors (Figure 193).



	Alpha 1	Alpha 2	Alpha 3	Alpha 4	Alpha 5	Alpha 6
Merck	>300	>300	>300	ND	38.5	>300
Moltech	920	ND	ND	ND	30	ND
UNC-Roth	362.4	180.330	328.2	ND	6.185	ND

Figure 193. Oocyte and binding data for PWZ-029 by Sieghart et al.⁴¹⁶

Illustrated in Figure 193 are the concentration–effects curve for modulation of GABA(A) elicited currents by PWZ-029 on *Xenopus* oocytes expressing GABA(A) receptor subtypes $\alpha 1\beta 3\gamma 2$, $\alpha 2\beta 3\gamma 2$, $\alpha 3\beta 3\gamma 2$, and $\alpha 5\beta 3\gamma 2$. Concentrations of GABA(A) that elicit 3% of the maximum GABA(A) -triggered current of the respective cells were applied alone and with various concentrations of PWZ-029. Control currents represent responses in the absence of PWZ-029. Data points represent means \pm SEM from 4 oocytes from ≥ 2 batches. The 1 μ M PWZ-029 resulted in 114 \pm 4%, 105 \pm 8%, 118 \pm 5% and 80 \pm 4% of control current (at GABA(A) EC₃) in $\alpha 1\beta 3\gamma 2$, $\alpha 2\beta 3\gamma 2$, $\alpha 3\beta 3\gamma 2$, and $\alpha 5\beta 3\gamma 2$ receptors, respectively. All these values except the one for $\alpha 2\beta 3\gamma 2$ receptors were significantly different from that of the respective control currents ($p < 0.01$, Student's t-test). Note that 100 nM is the pharmacologically relevant concentration.

$\alpha 5\beta 2\gamma 2$ Selective Ligands Attenuate Scopolamine Induced Contextual Memory Impairment.

The new analogs of PWZ-029 are of strong interest due to the recent contextual memory impairment data wherein doses of scopolamine decreased memory while the $\alpha 5$ ligand reversed this. PWZ-029 was assessed for its ability to attenuate scopolamine-induced impairment of Pavlovian fear conditioned contextual memory in mice. PWZ-029 possesses reasonable selectivity towards $\alpha 5$ subunit containing GABA(A) receptor isoforms (Figure 193).⁴²⁰

SH-I-075 will be of special interest to future research as it exhibits selective agonism towards the $\alpha 5\beta 3\gamma 2$ GABA(A) receptor isoform as determined by

electrophysiological recordings (Table 41). This compound will serve to support the "proof of principle" that compounds selective for $\alpha 5$ subunit containing GABA(A) receptor isoforms can be exploited in order to influence contextual memory. PWZ-029 was selected for contextual memory assessment based on its GABA(A) receptor binding profile and its electrophysiological effect. In addition, it was without convulsive effect up to a dose of 30 mg/kg with no locomotor effects in mice up to 10 mg/kg. PWZ-029 administered i.p. at a dose of 10 mg/kg was able to robustly attenuate the scopolamine-induced impairment of contextual memory (Figure 194). In addition, PWZ-029 was screened for effects on a series of common receptor classes in the NIH Case Western Reserve Drug Screening Program and found to be without appreciable binding to other major classes of receptors (B. Roth et al, NIMH Psychoactive Drug Screening Program, UNC, unpublished results, available at <https://kidbdev.med.unc.edu/pdsp> or see Appendix).

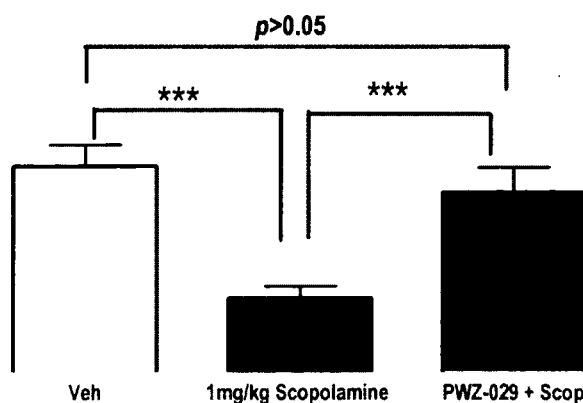


Figure 194. Fear conditioned contextual memory

This ligand has also been examined in rats in the passive and active avoidance test, spontaneous locomotor activity, elevated plus maze and grip strength tests, primarily predictive of the effects on the memory acquisition, basal locomotor activity, anxiety level and muscle tone, respectively. The improvement of task learning was detected at the dose of 5 mg/kg in the passive avoidance task (Figure 195). The passive avoidance task is a one trial fear-motivated avoidance task in which the mouse learns to refrain from stepping through a door to an apparently safer but previously punished dark compartment. The latency to refrain from crossing into the punished compartment serves as an index of the ability to avoid, and allows memory to be assessed. PWZ-029 at 5 mg/kg, administered before the acquisition session, significantly increased retention session latency relative to the control group.^{46, 64, 542, 543}

The inverse agonist PWZ-029 had no effect on anxiety or muscle tone, whereas at higher doses (10 and 20 mg/kg) it decreased locomotor activity. This effect was antagonized by flumazenil and also by the lower (but not the higher) dose of an agonist (SH-053-R-CH3-2'F) selective for GABA(A) receptors containing the $\alpha 5$ subunit. The hypolocomotor effect of PWZ-029 was not antagonized by the antagonist β CCt which exhibits a preferential affinity for $\alpha 1$ -subunit-containing receptors. These data suggest that moderate negative modulation at GABA(A) receptors containing the $\alpha 5$ subunit is a sufficient condition for eliciting enhanced encoding/consolidation of declarative memory, while the influence of higher doses of modulators at these receptors on motor activity shows an intricate pattern whose relevance and mechanism await to be defined.^{42, 64, 390.}

⁵⁴²⁻⁵⁴⁴ In fact, in the conflict paradigm in Rowlett's lab in rhesus monkeys, PWZ-029 was a weak anxiolytic, with no sedation observed in either the suppressed or nonsuppressed portion of the test. Recently, Stables et al. at NINDS has shown PWZ-029 to be a weak anticonvulsant with no effect on locomotor activity. Consequently, this partial $\alpha 5$ inverse agonist cannot be proconvulsant nor convulsant.

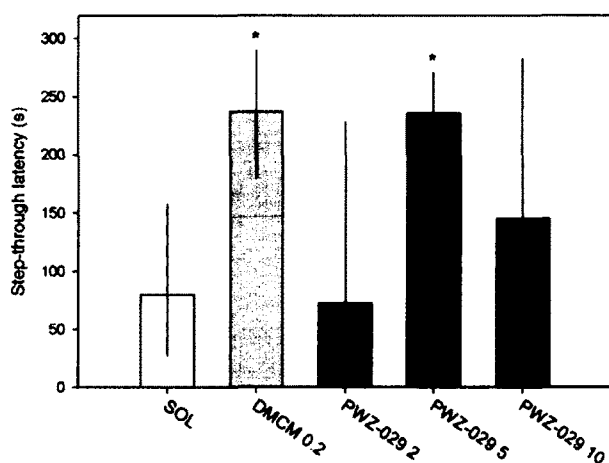


Figure 195. Passive avoidance task^{64, 542-544}

The effects of DMCM (0.2 mg/kg) and PWZ-029 (2, 5 and 10 mg/kg) on retention performance in a passive avoidance task (* $p < 0.05$ compared to solvent (SOL) group) as illustrated in Figure 195. Number of animals per treatment group : 10.

Experimental

Competition Binding Assays

Competition binding assays were performed in a total volume of 0.5 mL at 4°C for 1 hour using [³H] flunitrazepam as the radiolabel. For these binding assays, 20-50 µg of membrane protein harvested with hypotonic buffer (50 mM Tris-acetate pH 7.4 at 4 degree) was incubated with the radiolabel as previously described.^{46, 64} Nonspecific binding was defined as radioactivity bound in the presence of 100 µM diazepam and represented less than 20% of total binding. Membranes were harvested with a Brandel cell harvester followed by three ice-cold washes onto polyethyleneimine-pretreated (0.3%) Whatman GF/C filters. Filters were dried overnight and then soaked in Ecoscint A liquid scintillation cocktail (National Diagnostics; Atlanta, GA). Bound radioactivity was quantified by liquid scintillation counting. Membrane protein concentrations were determined using an assay kit from Bio-Rad (Hercules, CA) with bovine serum albumin as the standard.

Preparation of Cloned mRNA (with Dr. R. Furtmüller, Dr. Ramerstorfer and Dr. W. Sieghart).^{545, 546}

Cloning of GABA(A) receptor subunits $\alpha 1$, $\beta 3$ and $\gamma 2$ into pCDM8 expression vectors (Invitrogen, CA) has been described elsewhere.^{46, 64} The GABA(A) receptor $\alpha 4$ subunit was cloned in an analogous way. The cDNAs for subunits $\alpha 2$, $\alpha 3$ and $\alpha 5$ were gifts from P. Malherbe and were subcloned into a pCI-vector. The cDNA for the $\alpha 6$ subunit was a gift from P. Seeburg and was subcloned into the vector pGEM-3Z (Promega). After linearizing the cDNA vectors with appropriate restriction

endonucleases, capped transcripts were produced using the mMessage mMachine T7 transcription kit (Ambion, TX). The capped transcripts were polyadenylated using yeast poly (A) polymerase (USB, OH) and were diluted and stored in diethylpyrocarbonate-treated water at -70°C .^{46, 64}

Functional Expression of GABA(A) Receptors (with Dr. R. Furtmüller, Dr. Ramerstorfer and Dr. W. Sieghart).^{36, 37}

The methods used for isolating, culturing, injecting and defolliculating the oocytes were identical with those described by E. Sigel.⁴⁶ Mature female *Xenopus laevis* (Nasco, WI) were anaesthetized in a bath of ice-cold 0.17 % Tricain (Ethyl-m-aminobenzoate, Sigma, MO) before decapitation and removal of the frog ovary. Stage 5 to 6 oocytes with the follicle cell layer around them were singled out of the ovary using a platinum wire loop. Oocytes were stored and incubated at 18°C in modified Barths medium (MB, containing 88 mM NaCl, 10 mM HEPES-NaOH (pH 7.4), 2.4 mM NaHCO_3 , 1 mM KCl, 0.82 mM MgSO_4 , 0.41mM CaCl_2 , 0.34 mM $\text{Ca}(\text{NO}_3)_2$) that was supplemented with 100 Units/mL penicillin and 100 $\mu\text{g}/\text{mL}$ streptomycin. Oocytes with follicle cell layers still around them were injected with 50 nL of an aqueous solution of the cRNA. This solution contained the transcripts for the different alpha subunits and the beta 3 subunit at a concentration of 0.0065 ng/nL as well as the transcript for the gamma 2 subunit at 0.032 ng/nL. After injection of the cRNA, oocytes were incubated for at least 36 h before the enveloping follicle cell layers were removed.

To this end, oocytes were incubated for 20 minutes at 37 °C in MB that contained 1 mg/mL collagenase type IA and 0.1 mg/mL trypsin inhibitor I-S (both Sigma). This was followed by osmotic shrinkage of the oocytes in doubly concentrated MB medium supplied with 4 mM Na-EGTA. Finally, the oocytes were transferred to a culture dish containing MB and were gently pushed away from the follicle cell layer which stuck to the surface of the dish. After removal of the follicle cell layer, oocytes were allowed to recover for at least 4 h before being used in electrophysiological experiments.^{457, 547}

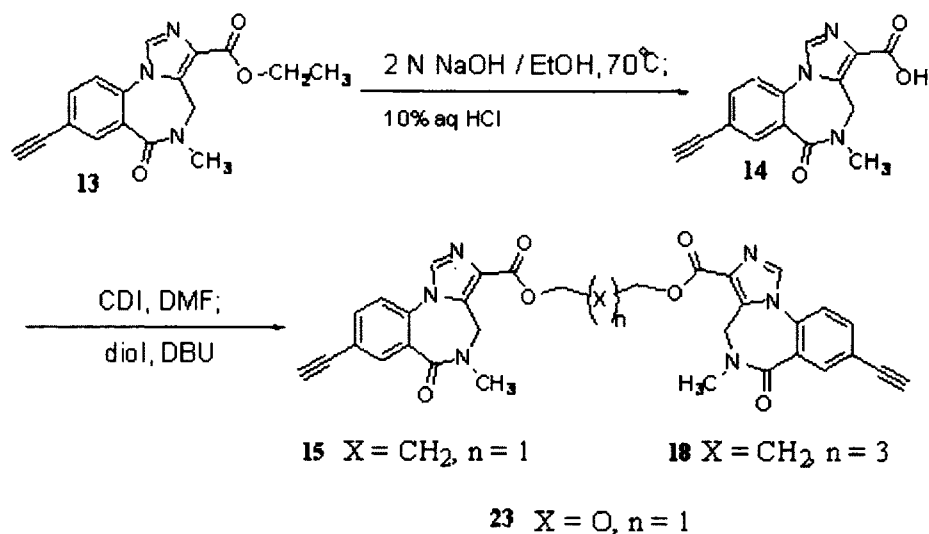
Electrophysiological Experiments (with Dr. R. Furtmüller, Dr Ramerstorfer and Dr. W. Sieghart).^{64, 310}

For electrophysiological recordings, oocytes were placed on a nylon-grid in a bath of *Xenopus* Ringer solution (XR, containing 90 mM NaCl, 5 mM HEPES NaOH (pH 7.4), 1 mM MgCl₂, 1 mM KCl and 1 mM CaCl₂). The oocytes were constantly washed by a flow of 6 mL/min XR which could be switched to XR containing GABA and/or drugs. Drugs were diluted into XR from DMSO solutions resulting in a final concentration of 0.1 % DMSO perfusing the oocytes. Drugs were preapplied for 30 seconds before the addition of GABA, which was coapplied with the drugs until a peak response was observed. Between two applications, oocytes were washed in XR for up to 15 minutes to ensure full recovery from desensitization. For current measurements the oocytes were impaled with two microelectrodes (2–3 mΩ) which were filled with 2 mM KCl.

All recordings were performed at room temperature (rt) at a holding potential of –60 mV using a Warner OC-725C two-electrode voltage clamp (Warner Instruments, Hamden, CT).^{357, 547} Data were digitized, recorded and measured using a Digidata 1322A data acquisition system (Axon Instruments, Union City, CA). Results of concentration response experiments were fitted using GraphPad Prism 3.00 (GraphPad Software, San Diego, CA). The equation used for fitting concentration response curves was $Y = \text{Bottom} + (\text{Top} - \text{Bottom}) / (1 + 10^{((\text{LogEC50} - X) * \text{HillSlope}))}$; X represents the logarithm of concentration, Y represents the response; Y starts at Bottom and goes to Top with a sigmoid shape. This is identical to the "four parameter logistic equation."^{548, 549}

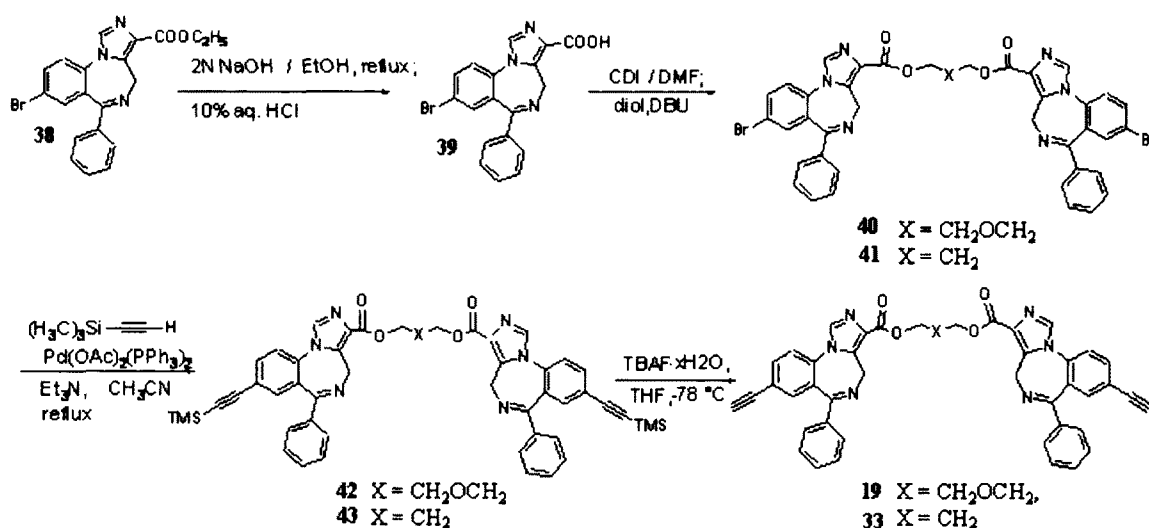
Synthesis of Bivalents

Inverse agonist **13** was synthesized via the reported procedure.⁴²⁰ Hydrolysis of the ester function of **13** provided the acid **14** in excellent yield and this material was subjected to a standard CDI-mediated coupling reaction to furnish bivalent ligands **15**, **18**, and **23** in 60% yield (Scheme 7).³⁹⁶

Scheme 7. Synthesis of bivalent analogs of Xli-093.

The acid **39**, obtained from the ester **38**, which was available from the literature,³²⁴ was stirred with CDI in DMF, followed by stirring with the required diol and DBU to provide bromide dimers **40** or **41**, respectively. They were converted into the trimethylsilylacetylenyl **42** or **43**, respectively under standard conditions (Pd-mediated, Heck-type coupling).⁵⁵⁰ The bisacetylene **19** or **33** (individually) was easily obtained by treatment of the trimethylsilyl ligand **42** or **43** with fluoride anion, as shown in Scheme II.

Scheme II. Synthesis of bivalent analogues of DMH-D-053.



Materials and General Instrumentation

Chemicals were purchased from Aldrich Chemical Co. or Tokyo Chemical Industries and were used without further purification except where otherwise noted. Anhydrous THF was distilled from sodium/benzophenone ketyl. TLC analyses were carried out on Merck Kieselgel 60 F₂₅₄, and flash column chromatography was performed on silica gel 60b purchased from E. M. Laboratories. Melting points were taken on a Thomas-Hoover melting point apparatus or an Electrothermal Model IA8100 digital melting point apparatus and are reported uncorrected. NMR spectra were recorded on a Bruker 300 or 500 MHz multiple-probe spectrometer. Infrared spectra were recorded on a Nicolet DX FTIR BX V5.07 spectrometer or a Mattson Polaris IR-10400 instrument. Low-resolution mass spectral data (EI/CI) were obtained on a Hewlett-Packard 5985B GC-mass spectrometer, while high resolution mass spectral data were taken on a VG

autospectrometer (Double Focusing High Resolution GC/Mass Spectrometer, UK). Microanalyses were performed on a CE Elantech EA1110 elemental analyzer.

Competition Binding Assays

Competition binding assays were performed in a total volume of 0.5 mL at 4°C for 1 hour using [^3H] flunitrazepam as the radioligand. For these binding assays, 20-50 mg of membrane protein harvested with hypotonic buffer (50 mM Tris-acetate pH 7.4 at 4 degree) was incubated with the radiolabel as previously described.⁵¹² Nonspecific binding was defined as radioactivity bound in the presence of 100 μM diazepam and represented less than 20% of total binding. Membranes were harvested with a Brandel cell harvester followed by three ice-cold washes onto polyethyleneimine-pretreated (0.3%) Whatman GF/C filters. Filters were dried overnight and then soaked in Ecoscint A liquid scintillation cocktail (National Diagnostics; Atlanta, GA). Bound radioactivity was quantified by liquid scintillation counting. Membrane protein concentrations were determined using an assay kit from Bio-Rad (Hercules, CA) with bovine serum albumin as the standard.

Radioligand Binding Assays (Drs. McKernan and Atack)⁵⁵¹

In brief, the affinity of compounds for human recombinant GABA(A) receptors was measured by competition binding using 0.5 nM [^3H]flunitrazepam. Transfected HEK cells (beta2 gamma2 and desired alpha subtype) were harvested into phosphate-buffered saline, centrifuged at 3,000 g and stored at -70°C until required. On the day of the assay, pellets were thawed and re-suspended in sufficient volume of 50 mM Tris/acetate (pH 7.4 at 4°C) to give a total binding of approximately 1500-2000 dpm. Non-specific binding was defined in the presence of 100 mM (final concentration) diazepam. Test compounds were dissolved in DMSO at a concentration of 10 mM and diluted in assay buffer to give

an appropriate concentration range in the assay, such that the final DMSO concentration in the assay was always less than 1%. Total assay volume was 0.5 mL and assays were carried out in 96-well plates and incubation time started by the addition of 0.1 mL of re-suspended cell membranes. Following incubation for 1 hour at 4°C, assays were terminated by filtration through GF/B filters, washed with 10 mL ice cold buffer, dried and then counted using a liquid scintillation counter. The percentage inhibition of [³H] flunitrazepam binding, the IC₅₀ and the K_i values were calculated using the Activity Base Software Package (ID Business Solutions, Guildford, UK) according to the Cheng-Prusoff equation.^{552, 553}

1,3-Bis(8-acetyleno-5,6-dihydro-5-methyl-6-oxo-4H-imidazo[1,5a][1,4]benzodiazepine-3-carboxy) propyl diester 1 (XLi093) (Procedure A). To a solution of carbonyl diimidazole (230.3 mg, 0.57 mmol) in anhydrous DMF (5 mL) was added 8-ethynyl-5,6-dihydro-5-methyl-6-oxo-4Himidazo[1,5-a][1,4]-benzodiazepine-3-carboxylic acid **14** (200 mg, 0.71 mmol). The solution which resulted was stirred for 2 h at rt. Analysis by TLC (silica gel) indicated the absence of starting material. To the solution which resulted was then added 1,3-propanediol (27.1 mg, 0.36 mmol) in dry DMF (0.5 mL) and also DBU (114.2 mg, 0.75 mmol) in dry DMF (0.10 mL) at rt. The mixture was stirred at rt for 4.5 h until analysis by TLC (silica gel) indicated the reaction was complete. The reaction mixture was then poured into ice water (30 mL) and extracted with CH₂Cl₂ (3 x 50 mL). The combined organic layer was washed with H₂O (5 x 50 mL), brine and dried (Na₂SO₄). The solvent was removed under reduced pressure and the residue was purified by flash chromatography (silica gel, EtOAc/CH₃OH, 4 : 1) to provide **1** (157 mg) as a white solid in 73.4% yield. **1**: mp >230° C (dec.); IR (NaCl) 3247, 1725, 1641, 1359, 1253, 1061 cm⁻¹; H NMR (300

MHz, CDCl₃) δ 2.37(m, 2H), 3.24(s, 2H), 3.26 (s, 6H), 4.40(s, 2H), 4.57(t, 4H, J=6.2Hz), 5.31(br, 2H), 7.41(d, 2H, J=8.3 Hz) 7.72(d, d, 2H, J = 6.43Hz, and J = 1.86Hz), 7.89 (s, 2H), 8.19(d, 2H, J = 1.76Hz); ¹³C NMR (75.5 MHz, CDCl₃) δ 26.2, 34.4, 40.7, 60.2, 78.7, 79.7, 120.4, 121.6, 127.1, 127.7, 130.1, 133.4, 134.1, 134.9, 161.3, 164.1; MS (FAB, NBA) *m/e* (relative intensity) 603(M⁺+1, 100). This material was employed for the X-ray crystal structure. It was homogenous in two independent TLC systems [*R_f* = 0.31 in EtOAc/CH₃OH, 4 : 1; *R_f* = 0.32 in CH₂Cl₂/CH₃OH, 9 : 1]. Anal. Calcd for C₃₃H₂₆N₆O₆ · 2/3 CH₃OH: C, 64.81; H, 4.63; N, 13.47. Found: C, 64.56; H, 4.72; N, 13.76.

1,5-Bis(8-acetyleno-5,6-dihydro-5-methyl-6-oxo-4H-imidazo[1,5a][1,4]benzodiazepine-3-carboxy) pentyl diester 18 (XLi210). Ligand **18** was prepared by following the procedure above with acid **14** by replacing the 1,3-propanediol with 1,5-pentanediol to provide **18** as a white solid in 89.2% yield. **18**: mp 132-138°C; IR (KBr) 3422, 3280, 2931, 1714, 1635, 1487, 1249, 1064 cm⁻¹; ¹H NMR (500 MHz, CDCl₃) δ 1.90(m, 4H), 3.24(s, 6H), 3.52 (s, 2H), 4.39(s, 8H), 5.29(s, 2H), 7.36(dd, 2H, J=8.1Hz, 16Hz), 7.70(m, 2H) 7.70(m, 2H), 7.86 (s, 2H), 8.18(s, 2H); MS (FAB, NBA) *m/e* (relative intensity) 631(M⁺+1, 13). Anal. Calcd for C₃₅H₃₀N₆O₆ · 5/3 H₂O: C, 63.61; H, 4.83; N, 12.72. Found: C, 63.16; H, 4.72; N, 13.06.

1,3-Bis(8-ethyl-5,6-dihydro-5-methyl-6-oxo-4H-imidazo[1,5a][1,4]benzodiazepine-3-carboxy) propyl diester 3 (XLi356): 1,3-Bis(8-acetyleno-5,6-dihydro-5-methyl-6-oxo-4H-imidazo[1,5a][1,4]-benzodiazepine-3-carboxy) propyl diester **1** (500 mg, 0.83 mmol) was dissolved in EtOH (150 mL) after

which Pd/C (176 mg) was added in solution at rt. The slurry was stirred for 5h under one atmosphere of H₂(bench top, balloon of H₂). The catalyst was removed by filtration and washed with EtOH. The EtOH was removed under reduced pressure to furnish a residue. This material was purified by flash chromatography (silica gel, EtOAc : EtOH/8 : 2) to provide **3** (504 mg, 99%) as white crystals: mp 125-133°C; IR (NaCl) 3407, 2964, 2358, 1725, 1640, 1499 cm⁻¹; ¹H NMR (CDCl₃) δ 1.29 (m, 6H), 2.39(m, 2H), 2.78 (dd, 4H, J=7.5 Hz, 15.1 Hz), 3.26 (s, 6H), 4.48 (br, 2H), 4.56 (t, 4H, J=6.1 Hz, 12.2 Hz), 5.16(br, 2H), 7.33 (d, 2H, J = 8.2Hz), 7.48 (d, 2H, J=1.8 Hz), 7.89 (t, 4H, J=3.2 Hz, 5.3 Hz), 8.15; MS(EI) *m/e* (relative intensity) 611(M⁺+1, 100). Anal. Calcd for C₃₃H₃₄N₆O₆ • 2H₂O: C, 61.33; H, 5.92; N, 13.00. Found: C, 61.74; H, 5.91; N, 12.63.

Bis(8-acetyleno-5,6-dihydro-5-methyl-6-oxo-4H-imidazo[1,5a][1,4]benzodiazepine-3-carboxy) dimethyl glycol diester 23 (XLi374). Ligand **23** was prepared by following the procedure for **1** and acid **14**, by replacing 1,3-propanediol with methylene glycol to afford dimer **23** (80% yield): mp >220 °C (dec.); IR (KBr) 3419, 3237, 2910, 1714, 1635, 1561, 1498 cm⁻¹; ¹H NMR (500 MHz, CD₂Cl₂) δ d 3.18(s, 6H), 3.31(s,2H), 4.37 (br, 2H), 5.29(br, 2H), 5.74 (s, 4H), 7.40(d, 2H, J=8.1 Hz), 7.74(dd, 2H, J=1.6Hz and J=8.2Hz), 7.90 (s, 2H), 8.15 (s, 2H); MS(FAB,NBA) *m/e* (relative intensity) 605(M⁺+1, 100). Anal. Calcd for C₃₂H₂₄N₆O₇ • 3/2 CH₃COOC₂H₅: C, 61.99; H, 4.93; N, 11.41. Found: C, 61.36; H, 4.52; N, 11.96.

8-Bromo-6-phenyl-4H-benzo[f]imidazo[1,5-a][1,4]diazepine-3-carboxylic acid 39.

The ester **38** (2g) was dissolved in EtOH (50 mL) and aq sodium hydroxide (10 mL, 2N) was added to the solution. The mixture was heated to reflux for 0.5 hour. After the EtOH was removed under reduced pressure, the solution was allowed to cool. The pH value was

adjusted to 4 by adding 10% aq HCl dropwise. The mixture was filtered and the solid was washed with water and ethyl ether. The solid was dried to provide **39** (1.8g, 96.6%): mp >250 °C; IR (KBr) 3450 (b), 2844, 1707, 1615, 1493, 1166, 700 cm^{-1} ; ^1H NMR (300 MHz, DMSO- d_6) δ 4.14 (d, 1H, $J=12.6\text{Hz}$), 5.79 (d, 1H, $J=12.6\text{Hz}$), 7.41-7.54 (m, 6H), 7.88 (d, 1H, $J=8.7\text{Hz}$), 8.03 (dd, 1H, $J=8.7\text{Hz}$, $J=2.1\text{Hz}$), 8.47 (s, 1H); MS (EI) m/e (rel intensity) 381 (M^+ , 20), 383 (19). This material was used directly in the next experiment.

1, 3-Bis(8-bromo-6-phenyl-4H-benzo[f]imidazo[1,5-a][1,4]diazepine-3-carboxy) propyl diester 41 (DMH-D-070).

(Procedure B) The carboxylic acid **39** (2 g, 5.2 mmol) was dissolved in DMF (20mL), after which CDI (1.02 g, 6.3 mmol) was added at rt and the mixture was stirred for 2 h. Then 1,3-propanediol (0.19 mL, 2.6 mmol) and DBU (0.78 mL, 5.2 mmol) were added to the mixture and stirring continued overnight. The reaction solution was then cooled with an ice-water bath, after which water was added to precipitate a solid. This material was purified further by flash chromatography on silica gel (gradient elution, EtOAc:EtOH 20:1, 15:1, 10:1) to provide the bisbromide **41** (DMH-D-070) as a white solid (1.3 g, 61.9%): mp 187.5-189 °C; IR (KBr) 3112, 2968, 1708, 1610, 1559, 1491, 1269, 1160, 1123, 1073 cm^{-1} ; ^1H NMR (300 MHz, CDCl_3) δ 2.35 (m, 2H), 4.08 (d, 2H, $J=12.6\text{Hz}$), 4.55 (m, 4H), 6.05 (d, 2H, $J=12.6\text{Hz}$), 7.37-7.53 (m, 12H), 7.6 (d, 2H, $J=2.1\text{Hz}$), 7.81 (dd, 2H, $J=2.1\text{Hz}$, 8.6 Hz), 7.93 (s, 2H); ^{13}C NMR (75.5 MHz, CDCl_3) δ 28.2, 44.9, 61.4, 120.7, 124.2, 128.3, 129.0, 129.3, 129.6, 130.6, 134.1, 134.4, 134.7, 135.0, 138.9, 138.9, 162.6, 167.9; MS (FAB, NBA) m/e (rel intensity) 803 (M^++1 , 15); Anal. Calcd. For $\text{C}_{39}\text{H}_{28}\text{N}_6\text{O}_4\text{Br}_2$: C, 58.23; H, 3.51; N, 10.45. Found: C, 57.92; H, 3.43; N, 10.29.

1,3-Bis(8-trimethylsilylacetylenyl-6-phenyl-4H-benzo[f]imidazo[1,5-a][1,4]-

diazepine-3-carboxy) propyl diester 43 (DMH-D-048). (Procedure C). To a suspension of bisbromide **41** (1.005 g, 1.25 mmol) in acetonitrile (50 mL) and triethylamine (65 mL), was added bis(triphenylphosphine)-palladium (II) acetate (0.15 g, 0.2 mmol). The solution which resulted was degassed and trimethylsilylacetylene (0.7 mL, 5 mmol) was added after which it was degassed again (argon followed by vacuum). The mixture was heated to reflux and stirring maintained overnight. After removal of the solvent under reduced pressure, the residue was dissolved in CH_2Cl_2 and washed with water. 3-Mercaptopropyl functionalized silica gel (0.6g) was added into the organic layer and stirring continued for 1 hour. The silica gel/Pd complex was removed by filtration and the filtrate was concentrated under reduced pressure. The residue was purified by flash column chromatography on silica gel (gradient elution, EtOAc:EtOH 20:1, 15:1, 10:1) to furnish the bistrimethylsilyl dimer **43** (DMH-D-048, 680 mg, 60.8%) as a white solid: mp 169-172 °C; IR (KBr) 3449, 2950, 1725, 1720, 1715, 1496, 1250, 1160, 1080, 847 cm^{-1} ; ^1H NMR (300 MHz, CDCl_3) δ 0.25 (s, 18H), 2.35 (m, 2H), 4.05 (d, 2H, $J=12.6\text{Hz}$), 4.55 (m, 4H), 6.02 (d, 2H, $J=12.6\text{Hz}$), 7.37-7.55 (m, 14H), 7.75 (dd, 2H, $J=1.8\text{Hz}$, 8.4Hz), 7.94 (s, 2H); ^{13}C NMR (75.5 MHz, CDCl_3) δ -0.3, 28.3, 44.9, 61.4, 97.4, 102.3, 122.4, 122.6, 128.0, 128.3, 129.0, 129.4, 130.5, 134.1, 134.9, 135.1, 139.0, 139.2, 139.2, 162.6, 168.5; MS (FAB, NBA) m/e (rel intensity) 839 ($\text{M}^+ + 1$, 100); Anal. Calcd. For $\text{C}_{49}\text{H}_{46}\text{N}_6\text{O}_4\text{Si}_2$: C, 70.14; H, 5.53; N, 10.02. Found: C, 69.97; H, 5.35; N, 9.77.

1,3-Bis(8-acetylenyl-6-phenyl-4H-benzo[f]imidazo[1,5-a][1,4]diazepine-3-carboxy)propyl diester 33 (DMH-D-053). A solution of bistrimethylsilyl dimer **43** (330 mg, 0.4 mmol) in THF (70 mL) was stirred with tetrabutylammonium fluoride hydrate (250 mg, 0.96 mmol) at -78°C for 5 min. After this, H_2O (35 mL) was added to the

solution to quench the reaction and stirring continued at low temperature for one half hour. The solution was extracted with EtOAc (3x100 mL), and the organic layer was washed with water. After removal of the solvent under reduced pressure, ethyl ether was added to the residue to precipitate a solid. The mixture was filtered and the solid was washed with CH₂Cl₂-Et₂O (ca 1:15) to provide the bisacetylenyl dimer **33** (DMH-D-053, 220 mg, 80%) as a yellow solid which crystallizes in CH₂Cl₂: mp 172-175 °C; IR (KBr) 3450, 3280, 2950, 1720, 1715, 1495, 1250, 1120, 1050 cm⁻¹; ¹H NMR (300 MHz, CDCl₃) δ 2.35 (m, 2H), 3.18 (s, 2H), 4.08 (d, 2H, J=12.3Hz), 4.56 (m, 4H), 6.04 (d, 2H, J=12.6Hz), 7.36-7.59 (m, 14H), 7.78 (dd, 2H, J=8.4Hz, 1.7Hz), 7.95 (s, 2H); ¹³C NMR (75.5 MHz, CDCl₃) δ 28.8, 45.4, 61.9, 80.2, 81.3, 121.4, 122.7, 128.1, 128.3, 129.0, 129.3, 130.5, 134.2, 135.2, 135.3, 135.6, 138.9, 139.2, 162.6, 168.5; MS (FAB, NBA) *m/e* (rel intensity) 695 (M⁺+1, 100). Anal. Calcd. For C₄₃H₃₀N₆O₄•¼CH₂Cl₂: C, 72.63; H, 4.30; N, 11.75. Found: C, 72.36; H, 4.27; N, 11.36.

Bis(8-bromo-6-phenyl-4H-benzo[f]imidazo[1,5-a][1,4]diazepine-3-carboxy) diethylene glycol diester 40(DM-III-93). Ligand **40** was prepared from acid **39**, under the same conditions employed in procedure B, by replacing 1,3-propanediol with diethylene glycol to yield a yellow solid (93.7%) **40**: mp 165-168°C; IR (KBr) 3060, 2956, 1725, 1610, 1558, 1491, 1267, 1161, 1123, 1074 cm⁻¹; ¹H NMR (300 MHz, CDCl₃) δ 3.93 (t, 4H, J=4.8 Hz), 4.06 (d, 2H, J=12.6Hz), 4.54 (m, 4H), 6.05 (d, 2H, J=12.6Hz), 7.39-7.50 (m, 12H), 7.57 (d, 2H, J=2.7Hz), 7.80 (dd, 2H, J=2.1Hz, 8.4 Hz), 7.90 (s, 2H); ¹³C NMR (75.5 MHz, CDCl₃) δ 44.9, 63.6, 69.0, 120.7, 124.2, 128.3, 129.0, 129.3, 129.6, 130.6, 134.1, 134.4, 134.6, 135.0, 138.9, 139.0, 162.5, 167.9; MS (FAB,

NBA) m/e (rel intensity) 833 ($M^+ + 1$, 5). Anal. Calcd. For $C_{40}H_{30}Br_2N_6O_5 \cdot 0.15CHCl_3$: C, 56.72; H, 3.57; N, 9.88. Found: C, 56.61; H, 3.55; N, 9.92.

Bis(8-trimethylsilylacetylenyl-6-phenyl-4H-benzo[f]imidazo[1,5-a][1,4]diazepine-3-carboxy) diethylene glycol diester 14 (DM-III-94).

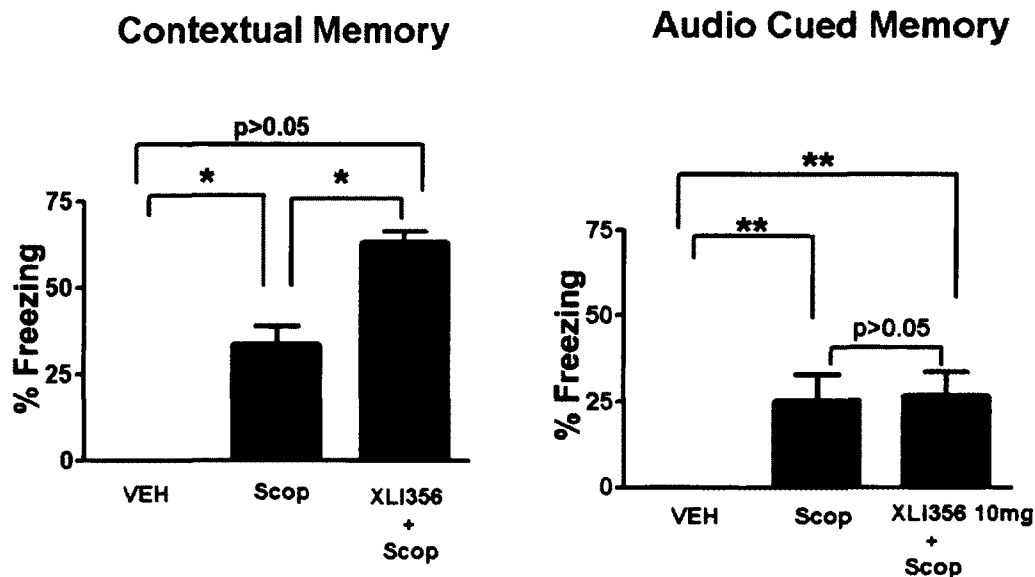
Ligand **42** was prepared from dibromide **40**, under the same conditions employed in Procedure C by replacing 1,3-propanediol with diethylene glycol to produce a yellow solid (49.5%) **42**: mp 205-208°C; IR (KBr) 3433, 2960, 1730, 1700, 1612, 1493, 1255, 1169, 1120, 1071, 847 cm^{-1} ; 1H NMR (300 MHz, $CDCl_3$) δ 0.25 (s, 18H), 3.93 (t, 4H, $J=5.4Hz$), 4.04 (d, 2H, $J=12.6Hz$), 4.55 (m, 4H), 6.04 (d, 2H, $J=12.6Hz$), 7.37-7.53 (m, 14H), 7.74 (dd, 2H, $J=1.2Hz$, 8.4Hz), 7.91 (s, 2H); ^{13}C NMR (75.5 MHz, $CDCl_3$) δ -0.3, 45.0, 63.6, 69.0, 97.5, 102.4, 122.5, 122.7, 128.1, 128.3, 129.0, 129.4, 130.5, 134.2, 135.0, 135.1, 135.2, 139.1, 139.3, 162.7, 168.6; MS (FAB, NBA) m/e (rel intensity) 869 ($M^+ + 1$, 100). Anal. Calcd. For $C_{50}H_{48}N_6O_5Si_2 \cdot \frac{1}{4}H_2O$: C, 68.81; H, 5.60; N, 9.62. Found: C, 68.88; H, 5.66; N, 9.51.

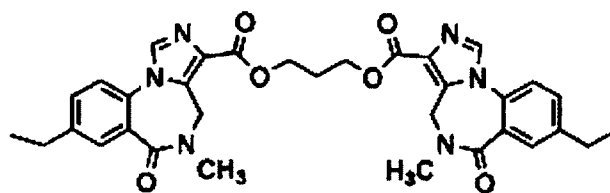
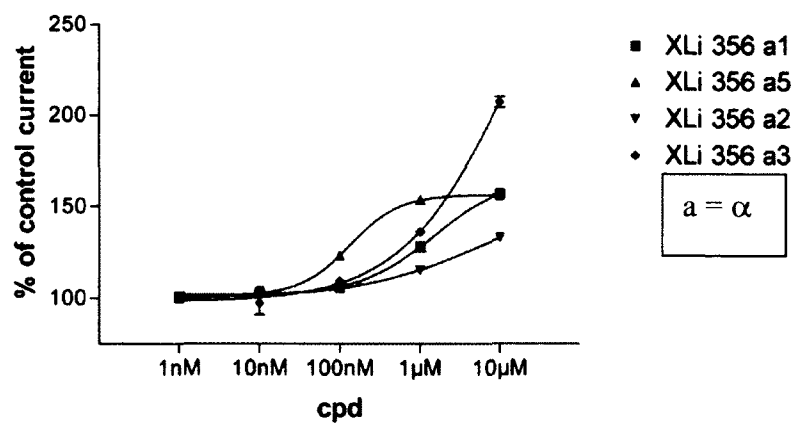
Bis(8-acetylenyl-6-phenyl-4H-benzo[f]imidazo[1,5-a][1,4]diazepine-3-carboxy) diethylene glycol diester 19 (DM-III-96). Ligand **19** was prepared from diester **42**, under the same conditions employed in procedure B, by replacing 1,3-propanediol with diethylene glycol to provide a yellow solid (81.6%) **19**: mp 173-177°C; IR (KBr) 3432, 3280, 1720, 1715, 1496, 1254, 1175, 1120, 1074 cm^{-1} ; 1H NMR (300 MHz, $CDCl_3$) δ 3.12 (s, 2H), 3.93 (t, 4H, $J=4.5Hz$), 4.06 (d, 2H, $J=12.6Hz$), 4.55 (m, 4H), 6.05 (d, 2H, $J=12.6Hz$), 7.38-7.56 (m, 14H), 7.75 (dd, 2H, $J=8.4Hz$, 1.8Hz), 7.91 (s, 2H); ^{13}C NMR (75.5 MHz, $CDCl_3$) δ 45.0, 63.6, 69.0, 79.8, 81.3, 121.3, 122.7, 128.1, 128.3, 129.0,

129.3, 130.5, 134.2, 135.2, 135.3, 135.6, 139.0, 139.1, 162.6, 168.4; MS (FAB, NBA) m/e (rel intensity) 725 ($M+1$, 63). Anal. Calcd. For $C_{44}H_{32}N_6O_5 \cdot \frac{1}{4}EtOAc \cdot \frac{1}{2}H_2O$: C, 69.89; H, 4.82; N, 10.87. Found: C, 70.12; H, 4.45; N, 10.58.

X-ray Crystallographic Data. Crystallographic data (excluding structure factors) for the structures in this thesis have been deposited with the Cambridge Crystallographic Data Centre as supplementary publication nos. 687205(DMH-D-053), 222395(Xli093), and 222396(DM-III-96). Copies of the data can be obtained, free of charge, on application to CCDC, 12 Union Road, Cambridge CB2 1EZ, UK, (fax: +44-(0)1223-336033 or email: deposit@ccdc.cam.ac.uk).

Audio Cued Data for Xli356





(XLI-356) receptor binding (nM)

$\alpha 1$	$\alpha 2$	$\alpha 3$	$\alpha 4$	$\alpha 5$	$\alpha 6$
2383	5980	>2000	5000	<u>107</u>	5000

References

1. Sieghart, W.; Ernst, M., Heterogeneity of GABA(A) receptors: revived interest in the development of subtype-selective drugs. *Curr. Med. Chem.: Cent. Nerv. Syst. Agents* **2005**, 5, (3), 217-242.
2. Bowser, D. N.; Wagner, D. A.; Czajkowski, C.; Cromer, B. A.; Parker, M. W.; Wallace, R. H.; Harkin, L. A.; Mulley, J. C.; Marini, C.; Berkovic, S. F.; Williams, D. A.; Jones, M. V.; Petrou, S., Altered kinetics and benzodiazepine sensitivity of a GABA(A) receptor subunit mutation [γ 2(R43Q)] found in human epilepsy. *Proc. Natl. Acad. Sci. U.S.A.* **2002**, 99, (23), 15170-15175.
3. Bateson, A. N., The benzodiazepine site of the GABA(A) receptor: An old target with new potential? *Sleep Medicine* **2004**, 5, (Suppl. 1), S9-S15.
4. Otani, K.; Ujike, H.; Tanaka, Y.; Morita, Y.; Katsu, T.; Nomura, A.; Uchida, N.; Hamamura, T.; Fujiwara, Y.; Kuroda, S., The GABA type A receptor alpha 5 subunit gene is associated with bipolar I disorder. *Neuroscience Letters* **2005**, 381, (1-2), 108-113.
5. Dean, B.; Scarr, E.; McLeod, M., Changes in hippocampal GABA(A) receptor subunit composition in bipolar I disorder. *Brain Res. Mol. Brain Res.* **2005**, 138, 145-155.
6. Guidotti, A.; Auta, J.; Davis, J. M.; Dong, E. B.; Grayson, D. R.; Veldic, M.; Zhang, X. Q.; Costa, E., GABAergic dysfunction in schizophrenia: new treatment strategies on the horizon. *Psychopharmacology* **2005**, 180, (2), 191-205.
7. Maubach, K., GABA(A) receptor subtype selective cognition enhancers. *Drug Targets-CNS & Neuro. Disorders* **2003**, 2, 233-239.
8. Burt, D. R.; Kamatchi, G. L., GABA(A) receptor subtypes - from pharmacology to molecular biology. *FASEB* **1991**, 5, (14), 2916-2923.
9. Keramidas, A.; Moorhouse, A.; Schofield, P. C.; Barry, P., Ligand-gated ion channels: mechanisms underlying ion selectivity. *Progress Biophys. Mol. Biol.* **2004**, 86, 161-204.
10. Cromer, B., unpublished work. **2009**.
11. Sieghart, W.; Sperk, G., Subunit composition, distribution and function of GABA(A) receptor subtypes. *Curr. Top. Med. Chem.* **2002**, 2, 795-816.
12. Kralic, J. E.; Korpi, E. R.; O'Buckley, T. K.; Homanics, G. E.; Morrow, A. L., Molecular and pharmacological characterization of GABA(A) receptor α 1 subunit knockout mice. *J. Pharmacol. Exp. Ther.* **2002**, 302, (3), 1037-1045.
13. Crestani, F.; Assandri, R.; Tauber, M.; Martin, J.; Rudolph, U., Contribution of the α 1-GABA(A) receptor subtype to the pharmacological actions of benzodiazepine site inverse agonists. *Neuropharmacology* **2002**, 43, 679-684.

14. Rudolph, U.; Crestani, F.; Benke, D.; Brunig, I.; Benson, J. A.; Fritschy, J. M.; Martin, J. R.; Bluethmann, H.; Möhler, H., GABA(A) -receptor subtype-specificity of benzodiazepine actions. *Nature* **1999**, 401, (6755), 796-800.
15. Collinson, N.; Cothliff, R.; Rosahl, T.; Sur, C.; Kuenzi, F. M.; Howell, O.; Seabrook, G.; Atack, J.; McKernan, R.; Dawson, G. R.; Whiting, P., Role of the alpha 5 subunit of GABA(A) receptor in learning and memory. *Eur. J. Neurosci.* **2000**, 12, (Suppl. 11), 171.
16. Bailey, D. J.; Tetzlaff, J. E.; Cook, J. M.; He, X. H.; Helmstetter, F. J., Effects of hippocampal injections of a novel ligand selective for the $\alpha 5\beta 2\gamma 2$ subunits of the GABA/benzodiazepine receptor on Pavlovian conditioning. *Neurobiol. Learn. Mem.* **2002**, 78, (1), 1-10.
17. DeLorey, T. M.; Lin, R. C.; McBrad, B.; He, X. H.; Cook, J. M.; Lameh, J.; Loew, G. H., Influence of benzodiazepine binding site ligands on fear-conditioned contextual memory. *Eur. J. Pharmacol.* **2001**, 426, (1-2), 45-54.
18. Lelas, S.; Rohrbach, K.; Glick, S. D.; Zeller, K.; Bourin, C.; Sieracki, K.; Bertekap, R.; Chen, J.; Cook, C. M.; Helmstetter, F. J.; Li, X. H.; Westphal, R.; Lindner, M.; Tertyshnikova, S.; Cook, J.; McElroy, J. F., *In vivo* and *in vitro* profiles of the GABA(A) / $\alpha 5$ -preferring agonist QH-ii-066 and the non-selective agonist diazepam. *manuscript in preparation*.
19. Liu, R. Y.; Hu, R. J.; Zhang, P. W.; Skolnick, P.; Cook, J. M., Synthesis and pharmacological properties of novel 8-substituted imidazobenzodiazepines: High-affinity, selective probes for $\alpha 5$ -containing GABA(A) receptors. *J. Med. Chem.* **1996**, 39, (9), 1928-1934.
20. Griebel, G.; Perrault, G.; Simiand, J.; Cohen, C.; Granger, P.; Decobert, M.; Francon, D.; Avenet, P.; Depoortere, H.; Tan, S.; Oblin, A.; Schoemaker, H.; Evanno, Y.; Sevrin, M.; George, P.; Scatton, B., SL651498: An anxiolytic compound with functional selectivity for $\alpha 2$ - and $\alpha 3$ -containing γ -aminobutyric acid(A) (GABA(A)) receptors. *J. Pharmacol. Exp. Ther.* **2001**, 298, (2), 753-768.
21. Liu, R. Y.; Zhang, P. W.; McKernan, R. M.; Wafford, K.; Cook, J. M., Synthesis of novel imidazobenzodiazepines selective for the $\alpha 5\beta 2\gamma 2$ (Bz5) GABA(A) / benzodiazepine receptor subtype. *Med. Chem. Res.* **1995**, 5, (9), 700-709.
22. Minier, F.; Sigel, E., Positioning of the α -subunit isoforms confers a functional signature to γ -aminobutyric acid type A receptors. *Proc. Natl. Acad. Sci. U.S.A.* **2004**, 101, (20), 7769-7774.
23. Wafford, K. A.; Macaulay, A. J.; Fradley, R.; O'Meara, G. F.; Reynolds, D. S.; Rosahl, T. W., Differentiating the role of γ -aminobutyric acid type A (GABA(A)) receptor subtypes. *Biochem. Soc. Trans.* **2004**, 32, 553-556.

24. Casula, M. A.; Bromidge, F. A.; Pillai, G. V.; Wingrove, P. B.; Martin, K.; Maubach, K.; Seabrook, G. R.; Whiting, P. J.; Hadingham, K. L., Identification of amino acid residues responsible for the $\alpha 5$ subunit binding selectivity of L-655,708, a benzodiazepine binding site ligand at the GABA(A) receptor. *J. Neurochem.* **2001**, 77, (2), 445-451.
25. Wafford, K. A.; Whiting, P. J.; Kemp, J. A., Differences in affinity and efficacy of benzodiazepine receptor ligands at recombinant gamma-aminobutyric acid(A) receptor subtypes. *Mol. Pharmacol.* **1993**, 43, (2), 240-244.
26. Atack, J. R., The benzodiazepine binding site of GABA(A) receptors as a target for the development of novel anxiolytics. *Expert Opin. Invest. Drugs* **2005**, 14, (5), 601-618.
27. Möhler, H.; Rudolph, U.; McKernan, R. at ACNP Meeting.
28. Study, R. E. B., J.L., Diazepam and (–)-pentobarbital: fluctuation analysis reveals different mechanisms for potentiation of gamma-aminobutyric acid responses in cultured central neurons. *Proc. Natl. Acad. Sci. U.S.A.* **1981**, 78, (11), 7180-7184.
29. Rogers, C.; Twyman, R. E.; MacDonald, R. L., Benzodiazepine and beta-carboline regulation of single GABA(A) receptor channels of mouse spinal neurons in culture. *J. Physiol. (London)* **1994**, 475, 69-82.
30. Kash, T. L.; Jenkins, A.; Kelley, J. C.; Trudell, J.; Harrison, N. L., Coupling of agonist binding to channel gating in the GABA(A) receptor. *Nature* **2003**, 421, 272-275.
31. Rüsch, D.; Forman, S. A., Classic benzodiazepines modulate the open-close equilibrium in $\alpha 1\beta 2\gamma 2$ γ -aminobutyric acid type A receptors. *Anesthesiology* **2005**, 102, 783-792.
32. Baur, R.; Sigel, E., Benzodiazepines affect channel opening of GABA(A) receptors induced by either agonist binding site. *Mol. Pharmacol.* **2005**, 67, (4), 1005-1008.
33. Zhang, W.; Koehler, K. F.; Zhang, P.; Cook, J. M., Development of a comprehensive pharmacophore model for the benzodiazepine receptor. *Drug Des. Discov.* **1995**, 12, (3), 193-248.
34. Zhang, W.; Diaz-Arauzo, H.; Allen, M. S.; Koehler, K. F.; Cook, J. M., *Chemical and computer assisted development of the inclusive pharmacophore of benzodiazepine receptors, in Studies in Medicinal Chemistry, M.I., Choudhary, Editor. Harwood Academic Publishers: 1996; p 303.*
35. Sigel, E.; Schaerer, M. T.; Buhr, A.; Baur, R., The benzodiazepine binding pocket of recombinant $\alpha 1\beta 2\gamma 2$ γ -aminobutyric acid(A) receptors: Relative

- orientation of ligands and amino acid side chains. *Mol. Pharmacol.* **1998**, 54, (6), 1097-1105.
36. Dunn, S. M. J.; Davies, M.; Muntoni, A. L.; Lambert, J. J., Mutagenesis of the rat $\alpha 1$ subunit of the γ -aminobutyric Acid(A) receptor reveals the importance of residue 101 in determining the allosteric effects of benzodiazepine site ligands. *Mol. Pharmacol.* **1999**, 56, (4), 768-774.
 37. Davies, M.; Bateson, A. N.; Dunn, S. M. J., Structural requirements for ligand interactions at the benzodiazepine recognition site of the GABA(A) receptor. *J. Neurochem.* **1998**, 70, (5), 2188-2194.
 38. Cromer, B.; Morton, C.; Parker, M. W., Cromer's model, anxiety of GABA(A) receptor structure relieved by AChBP. *Trends Biochem. Sci.* **2002**, 27, 280-287.
 39. Ernst, M.; Brauchart, D.; Boresch, S.; Sieghart, W., Comparative modeling of GABA(A) receptors: Limits, insights, future developments. *Neuroscience* **2003**, 119, (4), 933-943.
 40. Sigel, E., Mapping of the benzodiazepine recognition site on GABA(A) receptors. *Curr. Top. Med. Chem.* **2002**, 2, 833-840.
 41. Drover, D. R., Comparative pharmacokinetics and pharmacodynamics of short-acting hypnotosedatives - Zaleplon, zolpidem and zopiclone. *Clin. Pharmacokin.* **2004**, 43, (4), 227-238.
 42. Clayton, T.; Chen, J. L.; Ernst, M.; Richter, L.; Cromer, B. A.; Morton, H. N.; Kaczorowski, C. C.; Helmstetter, F. J.; Furtmuller, R.; Ecker, G.; Parker, M. W.; Sieghart, W.; Cook, J. M., Analysis of the benzodiazepine binding site on γ -aminobutyric acid(A) receptors: correlation of experimental data with pharmacophore and comparative models. *Curr. Med. Chem.* **2007**, 14, (26), 2755-2775.
 43. Noble, S.; Langtry, H. D.; Lamb, H. M., Zopiclone - An update of its pharmacology, clinical efficacy and tolerability in the treatment of insomnia. *Drugs* **1998**, 55, (2), 277-302.
 44. Jerussic, T. unpublished results, **2006**.
 45. Mohler, H., Molecular regulation of cognitive functions and developmental plasticity: impact of GABA(A) receptors. *J Neurochem* **2007**, 102, 1-12.
 46. Savic, M. M.; Huang, S.; Furtmueller, R.; Clayton, T.; Huck, S.; Obradovic, D. I.; Ugresic, N. D.; Sieghart, W.; Bokonjic, D. R.; Cook, J., Are GABA(A) receptors containing $[\alpha]5$ subunits contributing to the sedative properties of benzodiazepine site agonists? *Neuropsychopharmacology* **2008**, 33, 332-339.

47. Dias, R.; Sheppard, W. F. A.; Fradley, R. L.; Garrett, E. M.; Stanley, J. L.; Tye, S. J.; Goodacre, S.; Lincoln, R. J.; Cook, S. M.; Conley, R.; Hallett, D.; Humphries, A. C.; Thompson, S. A.; Wafford, K. A.; Street, L. J.; Castro, J. L.; Whiting, P. J.; Rosahl, T. W.; Attack, J. R.; McKernan, R. M.; Dawson, G. R.; Reynolds, D. S., Evidence for a significant role of alpha 3-containing GABA(A) receptors in mediating the anxiolytic effects of benzodiazepines. *J. Neurosci.* **2005**, 25, (46), 10682-10688.
48. McKernan, R. M.; Rosahl, T. W.; Reynolds, D. S.; Sur, C.; Wafford, K. A.; Attack, J. R.; Farrar, S.; Myers, J.; Cook, G.; Ferris, P.; Garrett, L.; Bristow, L.; Marshall, G.; Macaulay, A.; Brown, N.; Howell, O.; Moore, K. W.; Carling, R. W.; Street, L. J.; Castro, J. L.; Ragan, C. I.; Dawson, G. R.; Whiting, P. J., Sedative but not anxiolytic properties of benzodiazepines are mediated by the GABA(A) receptor alpha(1) subtype. *Nat. Neurosci.* **2000**, 3, (6), 587-592.
49. Collinson, N.; Kuenzi, F. M.; Jarolimek, W.; Maubach, K. A.; Cothliff, R.; Sur, C.; Smith, A.; Otu, F. M.; Howell, O.; Attack, J. R.; McKernan, R. M.; Seabrook, G. R.; Dawson, G. R.; Whiting, P. J.; Rosahl, T. W., Enhanced learning and memory and altered GABAergic synaptic transmission in mice lacking the alpha 5 subunit of the GABA(A) receptor. *J. Neurosci.* **2002**, 22, (13), 5572-5580.
50. Crestani, F.; Keist, R.; Fritschy, J.; Benke, D.; Vogt, K. E.; Prut, L., Trace fear conditioning involves hippocampal alpha5 GABA(A) receptors. *Proc. Natl. Acad. Sci. U.S.A.* **2002**, 99, 8980-8985.
51. Bohlhalter, S.; Weinmann, O.; Möhler, H.; Fritschy, J. M., Laminar compartmentalization of GABA(A)-receptor subtypes in the spinal cord: An immunohistochemical study. *J. Neurosci.* **1996**, 16, (1), 283-297.
52. van Rijnsoever, C.; Tauber, M.; Choulli, M. K.; Keist, R.; Rudolph, U.; Möhler, H.; Fritschy, J. M.; Crestani, F., Requirement of alpha(5)-GABA(A) receptors for the development of tolerance to the sedative action of diazepam in mice. *J. Neurosci.* **2004**, 24, (30), 6785-6790.
53. Porsolt, R. D.; McArthur, R. A.; Lenegre, A., *Psychotropic screening procedures*. Elsevier: New York, **1993**; Vol. 10, p 23-51.
54. Sieghart, W. Unpublished results, **2009**.
55. Wang, Q.; Han, Y.; Xue, H., Ligands of the GABA(A) receptor benzodiazepine binding site. *CNS Drug Rev.* **1999**, 5, 125-144.
56. Miksiek, R., Commonly occurring plant flavonoids have estrogenic activity. *Mol. Pharmacol.* **1993**, 44, 37-43.
57. Häberlein, H.; Tschiersch, K. P.; Schäfer, H. L., Flavonoids from *Leptospermum-Scoparium* with affinity to the benzodiazepine receptor

characterized by structure-activity-relationships and in-vivo studies of a plant-extract. *Pharmazie* **1994**, *49*, (12), 912-922.

58. Huang, X. Q.; Liu, T.; Gu, J. D.; Luo, X. M.; Ji, R. Y.; Cao, Y.; Xue, H.; Wong, J. T. F.; Wong, B. L.; Pei, G.; Jiang, H. L.; Chen, K. X., 3D-QSAR model of flavonoids binding at benzodiazepine site in GABA(A) receptors. *J. Med. Chem.* **2001**, *44*, (12), 1883-1891.
59. Marder, M.; Estiu, G.; Blanch, L. B.; Viola, H.; Wasowski, C.; Medina, J. H.; Paladini, A. C., Molecular modeling and QSAR analysis of the interaction of flavone derivatives with the benzodiazepine binding site of the GABA(A) receptor complex. *Bioorg. Med. Chem.* **2001**, *9*, (2), 323-335.
60. Yu, J.; Cook, J. unpublished results, **1999**.
61. Costanzo, A.; Guerrini, G.; Ciciani, G.; Bruni, F.; Costagli, C.; Selleri, S.; Besnard, F.; Costa, B.; Martini, C.; Malmberg-Aiello, P., Benzodiazepine receptor ligands. 7. Synthesis and pharmacological evaluation of new 3-esters of the 8-chloropyrazolo[5,1-c][1,2,4]benzotriazine 5-oxide. 3-(2-thienylmethoxycarbonyl) derivative: An anxiolytic agent in rodents. *J. Med. Chem.* **2002**, *45*, (26), 5710-5720.
62. Wong, G.; Koehler, K. F.; Skolnick, P.; Gu, Z. Q.; Ananthan, S.; Schönholzer, P.; Hunkeler, W.; Zhang, W. J.; Cook, J. M., Synthetic and computer-assisted analysis of the structural requirements for selective, high-affinity ligand-binding to diazepam-insensitive benzodiazepine receptors. *J. Med. Chem.* **1993**, *36*, (13), 1820-1830.
63. Yin, W. Y.; Sarma, P.; Han, J.; Chen, J. L.; Cook, J. M., Synthesis of bivalent ligands of beta-carboline-3-carboxylates via a palladium-catalyzed homocoupling process. *Tetrahedron Lett.* **2005**, *46*, (37), 6363-6368.
64. Li, X. Y.; Cao, H.; Zhang, C. C.; Furtmueller, R.; Fuchs, K.; Huck, S.; Sieghart, W.; Deschamps, J.; Cook, J. M., Synthesis, in vitro affinity, and efficacy of a bis 8-ethynyl-4H-imidazo[1,5a]-[1,4]benzodiazepine analogue, the first bivalent alpha 5 subtype selective BzR/GABA(A) antagonist. *J. Med. Chem.* **2003**, *46*, (26), 5567-5570.
65. Choudhary, M. S.; Craigo, S.; Roth, B. L., Identification of receptor domains that modify ligand binding to 5-hydroxytryptamine₂ and 5-hydroxytryptamine_{1c} serotonin receptors. *Mol. Pharmacol.* **1992**, *42*, 627-633.
66. Han, D. M.; Forsterling, F. H.; Li, X. Y.; Deschamps, J. R.; Cao, H.; Cook, J. M., Determination of the stable conformation of GABA(A)-benzodiazepine receptor bivalent ligands by low temperature NMR and X-ray analysis. *Bioorg. Med. Chem. Lett.* **2004**, *14*, (6), 1465-1469.

67. Ferretti, V.; Gilli, P.; Borea, P. A., Structural features controlling the binding of beta-carbolines to the benzodiazepine receptor. *Acta Crystallogr., Sect. B: Struct. Sci.* **2004**, 60, 481-489.
68. Allen, M. S.; Tan, Y. C.; Trudell, M. L.; Narayanan, K.; Schindler, L.; Martin, M. J.; Schultz, C. A.; Hagen, T. J.; Koehler, K. F.; Codding, P.; Skolnick, P.; Cook, J., Synthetic and computer-assisted analyses of the pharmacophore for the benzodiazepine receptor inverse agonist site. *J. Med. Chem.* **1990**, 33, 2343-2357.
69. Allen, M. S.; Laloggia, A. J.; Dorn, L. J.; Martin, M. J.; Constantino, G.; Hagen, T. J.; Koehler, K. F.; Skolnick, P.; Cook, J. M., Predictive binding of β -carboline inverse agonists and antagonists via the CoMFA/GOLPF approach. *J. Med. Chem.* **1992**, 35, 4001-4010.
70. Codding, M. G.; Roszak, A. W.; Szkaradzinska, M. B.; Cook, J. M.; Aha, L. J., *Modeling of the benzodiazepine receptor using structural and theoretical characterization of novel beta-carbolines*, . Elsevier Science Publishers: Amsterdam, **1989**; p 109.
71. Huang, Q.; Cox, E. D.; Gan, T.; Ma, C. R.; Bennett, D. W.; Mckernan, R. M.; Cook, J. M., Studies of molecular pharmacophore/receptor models for GABA(A) /benzodiazepine receptor subtypes: Binding affinities of substituted β -carbolines at recombinant $\alpha 1\beta 3\gamma 2$ subtypes and quantitative structure-activity relationship studies *via* a Comparative Molecular Field Analysis. *Drug. Des. Discov.* **1999**, 16, 55-76.
72. Codding, P. W., and Muir, A.K.S., Molecular-structure of Ro15-1788 and a model for the binding of benzodiazepine receptor ligands-structural identification of common features in antagonists. *Mol. Pharmacol.* **1985**, 28, 178.
73. Cox, E. D.; Diaz-Arauzo, H.; Huang, Q.; Reddy, M. S.; Harris, B.; Mckernan, R. M.; Skolnick, P.; Cook, J. M., Synthesis and evaluation of analogues of the partial agonist 6-(propyloxy)-4-(methoxymethyl)-beta-carboline-3-carboxylic acid ethyl ester (6-PBC) and the full agonist 6-(benzyloxy)-4-(methoxymethyl)-beta-carboline-3-carboxylic acid ethyl ester (Zk 93423) at wild type and recombinant GABA(A) receptors. *J. Med. Chem.* **1998**, 41, 2537-2552.
74. Diaz-Arauzo, H.; Evoniuk, G.; Skolnick, P.; Cook, J., The agonist pharmacophore of the benzodiazepine receptor. Synthesis of a selective anticonvulsant/anxiolytic. *J. Med. Chem.* **1991**, 34, 1754-1756.
75. Diaz-Arauzo, H.; Koehler, K. F.; Hagen, T. J.; Cook, J. M., Synthetic and computer-assisted analysis of the pharmacophore for agonists at benzodiazepine receptors. *Life Sci.* **1991**, 49, (3), 207-216.
76. Yin, W.; Majumder, S.; Clayton, T.; Petrou, S.; VanLinn, M. L.; Namjoshi, O. A.; Ma, C. R.; Cromer, B.; Roth, B. L.; Platt, D. M.; Cook, J. M., Design,

- synthesis, and subtype selectivity of 3,6-disubstituted β -carbolines at Bz/GABA(A)ergic receptors. SAR and studies directed toward agents for treatment of alcohol abuse. *Bioorg. Med. Chem.* **2010**, 1, (18), 7548-64.
77. Cook, J. M.; Van Linn, M. L.; Yin, W. Preparation of aza-beta-carbolines and methods of using same for treatment of chemical addiction, anhedonia, and anxiety. WO 2009143445 A1, 20090522., **2009**.
 78. June, H. L.; Foster, K. L.; McKay, P. F.; Seyoum, R.; Woods, J. E.; Harvey, S. C.; Eiler, W. J. A.; Grey, C.; Carroll, M. R.; McCane, S.; Jones, C. M.; Yin, W. Y.; Mason, D.; Cummings, R.; Garcia, M.; Ma, C. R.; Sarma, P.; Cook, J. M.; Skolnick, P., The reinforcing properties of alcohol are mediated by GABA(A1) receptors in the ventral pallidum. *Neuropsychopharmacology* **2003**, 28, (12), 2124-2137.
 79. Harvey, S. C.; Foster, K. L.; McKay, P. F.; Carroll, M. R.; Seyoum, R.; Woods, J. E.; Grey, C.; Jones, C. M.; McCane, S.; Cummings, R.; Mason, D.; Ma, C. R.; Cook, J. M.; June, H. L., The GABA(A) receptor alpha(1) subtype in the ventral pallidum regulates alcohol-seeking behaviors. *J. Neurosci.* **2002**, 22, (9), 3765-3775.
 80. Weerts, E. M. presented at the CPDD meeting, **2005**.
 81. Kessler, R. C.; Frank, R. G., The impact of psychiatric disorders on work loss days. *Psychiatric Medicine* **1997**, 27, 861-873.
 82. O'Malley, S. S.; Jaffe, A. J.; Chang, G.; Schottenfeld, R. S.; Meyer, R. E.; Rounsaville, B., Naltrexone and coping skills therapy for alcohol dependence: A controlled study. *Arch. Gen. Psychiatry* **1992**, 49, 881-889.
 83. Volpicelli, J. R.; Alterman, A. I.; Hayashida, M.; O'Brien, C. P., Naltrexone and the treatment of alcohol abuse. *Arch. Gen. Psychiatry* **1992**, 49, 876-880.
 84. Kranzler, H. R., Pharmacotherapy of alcoholism: Gaps in knowledge and opportunities for research. *Alcohol* **2000**, 35, 537-547.
 85. Spanagel, R.; Zieglgansberger, W., Anti-craving compounds for ethanol: New pharmacological tool to study addictive processes. *Trends Pharmacol. Sci.* **1997**, 18.
 86. Cloninger, C. R., Neurogenetic adaptive mechanisms in alcoholism. *Science* **1987**, 236, 410-416.
 87. Li, T.-K., Pharmacogenetics of responses to alcohol and genes that influence alcohol drinking. *J. Stud. Alcohol* **2000**, 61, 5-12.
 88. Li, T.-K.; Crabb, D. W.; Lumeng, L., *Neuropharmacology of Ethanol*. Birkhauser: Boston, **1991**; p p 107-124.
 89. Johnson, B. A.; Ait-Daoud, N., Neuropharmacological treatments for alcoholism: scientific basis and clinical findings. *Psychopharmacology* **2000**, 149, 327-344.

90. Koob, G. F.; Roberts, A. J.; Schulteis, G. e. a., Neurocircuitry targets in ethanol reward and dependence. *Alcohol Clin. Exp. Res.* **1998**, *22*, 3-9.
91. June, H. L.; Cason, C. R.; Cheatham, G.; Liu, R. Y.; Gan, T.; Cook, J. M., GABA(A)-benzodiazepine receptors in the striatum are involved in the sedation produced by a moderate, but not an intoxicating ethanol dose in out-bred Wistar rats. *Brain Res.* **1998**, *794*, (1), 103-118.
92. McBride, W.; J.; Li, T., Animal models of alcoholism: Neurobiology of high alcohol-drinking behavior in rodents. *Critical Reviews in Neurobiology* **1998**, *12*, 339-369.
93. Allain, H.; Belliard, S.; Decertaines, J.; Bentueferrer, D.; Bureau, M.; Lacroix, P., Potential biological targets for anti-Alzheimer drugs. *Dementia* **1993**, *4*, 347-352.
94. Heimer, L.; Alheid, G. F., *The basal forebrain: anatomy and function*. Plenum Press: New York, **1991**; p p 1-42.
95. Heimer, L.; Zahm, D. S.; Churchill, P.; Kalivas, W., Specificity in the projection patterns of accumbal core and shell in the rat. *Neurosci.* **1991**, *41*, 89-125.
96. Criswell, H. E.; Simson, P. E.; Duncan, G. E.; Mc Cown, T. J.; Herbert, J. S.; Morrow, L., Molecular basis for regionally specific action of ethanol on γ -aminobutyric acid (A) receptors: Generalization to other ligand-gated Ion channels. *J. Pharmacol. Exper. Ther.* **1993**, *267*, 522-527.
97. Criswell, H. E.; Simson, P. E.; Knapp, D. J.; Devaud, L. L.; Mc Cown, T. J.; Duncan, G. E., Effect of zolpidem on γ -aminobutyric acid (GABA)-induced inhibition predicts the interaction of ethanol with GABA on individual neurons in several rat brain regions. *J. Pharmacol. Exper. Ther.* **1995**, *273*, 525-536.
98. June, H. L.; Zuccarelli, D.; Torres, L.; Craig, K. S.; DeLong, J.; Allen, A.; Braun, M. R.; Cason, C. R.; Murphy, J. M., High-affinity benzodiazepine antagonists reduce responding maintained by ethanol presentation in ethanol-preferring rats. *J. Pharmacol. Exp. Ther.* **1998**, *284*, (3), 1006-1014.
99. June, H. L.; Harvey, S. C.; Foster, K. L.; McKay, P. F.; Cummings, R.; Garcia, M.; Mason, D.; Grey, C.; McCane, S.; Williams, L. S.; Johnson, T. B.; He, X. H.; Rock, S.; Cook, J. M., GABA(A) receptors containing alpha 5 subunits in the CA1 and CA3 hippocampal fields regulate ethanol-motivated behaviors: An extended ethanol reward circuitry. *J. Neurosci.* **2001**, *21*, 2166-2177.
100. Hyytia, P.; Koob, G. F., GABA(A) receptor antagonism in the extended amygdala decreases ethanol self-administration in rats. *Eur. J. Pharmacol.* **1995**, *283*, 151-159.

101. Nowak, K. L.; McBride, W. J.; Lumeng, L.; Li, T.-K.; Murphy, J. M., Blocking GABA(A) receptors in the anterior ventral tegmental area attenuates ethanol intake of the alcohol-preferring P rat. *Psychopharmacol.* **1998**, 139, 108-116.
102. Nauta, H. J.; Smith, G. P.; Faull, R. L. M.; Domesick, V. B., Efferent connections and nigral afferents of the nucleus accumbens septi in the rat. *Neurosci.* **1978**, 3.
103. Zahm, D. S.; Heimer, L., Ventral striatopallidal parts of the basal ganglia in the rat: I. Neurochemical compartmentation as reflected by the distributions of neurotensin and substance P immunoreactivity. *J. Comp. Neurology* **1988**, 272, 516-535.
104. Groenwegen, H. J.; Berende, H. W., Organization of the output of the ventral striatopallidal system in the rat: Ventral pallidal efferents. *Neurosci.* **1993**, 57, 113-142.
105. Churchill, L.; Kalivas, P. W., A topographical organized GABA projection from the ventral pallidum to the nucleus accumbens in the rat. *J. Comp. Neurology* **1994**, 345, 579-595.
106. Kuo, H.; Chang, H. T., Ventral-pallidostriatal pathway in the rat brain: A light electron microscopic study. *J. Comp. Neurol.* **1992**, 321, 626-636.
107. Morgenson, G. J.; Nielson, M., Evidence that an accumbens to subpallidal GABAergic projection contributes to locomotor activity. *Brain Res. Bulletin* **1983**, 11, 309-314.
108. Fritschy, J. M.; Mohler, H., GABA(A) -receptor heterogeneity in the adult-rat brain: differential regional and cellular-distribution of 7 major subunits. *J. Comp. Neurol.* **1995**, 359, (1), 154-194.
109. Turner, J. D.; Bodewitz, G.; Thompson, C. L.; Stephenson, F. A., *Anxiolytic beta carbolines: from molecular biology to the clinic*. Springer-Verlag: New York, **1993**; p p 29-49.
110. Churchill, L.; Bourdelais, A.; Austin, M. C.; Lolait, S. J.; Mahan, L. C.; O'Carroll, A. M.; Kalivas, P. W., GABA(A) receptors containing alpha 1 and beta 2 subunits are mainly localized on neurons in the ventral pallidum. *Synapse* **1991**, 8, (2), 75-85.
111. Wisden, W.; Laurie, D. J.; Monyer, H.; Seeburg, P. H., The distribution of 13-Gaba-A receptor subunit messenger-RNAs in the rat-brain. 1. Telencephalon, Diencephalon, Mesencephalon. *J. Neurosci.* **1992**, 12, (3), 1040-1062.
112. Duncan, G. E.; Breese, G. R.; Criswell, H. E.; McCown, T. J.; Herbert, J. S.; Devaud, L. L.; Morrow, A. L., Distribution of [3H] zolpidem binding sites in relation to messenger RNA encoding the alpha 1, beta 2 and gamma 2 subunits of GABA(A) receptors in rat brain. *Neurosci.* **1995**, 64, 1113-1128.

113. Napier, T. C.; Chrobak, J. J., Evaluation of ventral pallidal dopamine receptor activation in behaving rats. *Neuroreport* **1992**, 3, 609-611.
114. Hubner, C. B.; Koob, G. F., GABA(A) receptor antagonism in the extended amygdala decreases ethanol self-administration in rats. *Eur. J. Pharmacol.* **1995**, 283, 151-159.
115. Gong, W.; Justice, J. B., Dissociation of locomotor and conditioned place preference responses following manipulation of GABA-A and AMPA receptors in ventral pallidum. *Prog. Neuropsychopharmacol. Bio. Psych.* **1997**, 21, 839-852.
116. Gong, W.; Neill, D., Place preference conditioning and locomotor activation induced by local injection of psychostimulants into ventral pallidum. *Brain Res.* **1996**, 707, 64-74.
117. Cicero, T. J., *Biochemistry and Pharmacology of Ethanol*. Plenum Press: New York, **1979**; Vol. 2, p p 533-560.
118. Lumeng, L.; Murphy, J. M.; McBride, W. J.; Li, T.-K., *Genetic Influences on alcohol preference in animals*. Oxford University Press: New York, **1995**; p p 165-201.
119. June, H. L.; Eggers, M. W.; Warren-Reese, C.; DeLong, J.; Ricks-Cord, A.; Durr, L. F.; Cason, C. R., The effects of the novel benzodiazepine receptor inverse agonist Ru 34000 on ethanol-maintained behaviors. *Eur. J. Pharmacol.* **1998**, 350, (2-3), 151-158.
120. June, H. L.; Torres, L.; Cason, C. R.; Hwang, B. H.; Braun, M. R.; Murphy, J. M., The novel benzodiazepine inverse agonist RO19-4603 antagonizes ethanol motivated behaviors: neuropharmacological studies. *Brain Res.* **1998**, 784, 256-275.
121. Huang, Q.; He, X. H.; Ma, C. R.; Liu, R. Y.; Yu, S.; Dayer, C. A.; Wenger, G. R.; McKernan, R.; Cook, J. M., Pharmacophore/receptor models for GABA(A) /BzR subtypes ($\alpha 1\beta 3\gamma 2$, $\alpha 5\beta 3\gamma 2$, and $\alpha 6\beta 3\gamma 2$) via a comprehensive ligand-mapping approach. *J. Med. Chem.* **2000**, 43, (1), 71-95.
122. Carroll, M.; Woods II, J. E.; Seyoum, R. A.; June, H. L., The role of the GABA(A) $\alpha 1$ subunit in mediating the sedative and anxiolytic properties of benzodiazepines. *Alcohol Clin Exp Res* **2001**, 25, (12A).
123. Rowlett, J. K., unpublished results. **2010**.
124. Carroll, M.; Woods II, J. E.; Seyoum, R. A.; June, H. L., The role of the GABA(A) $\alpha 1$ subunit in mediating the sedative and anxiolytic properties of benzodiazepines. *Alcohol Clin. Exp. Res.* **2001**, 25.
125. Foster, K. L.; McKay, P. F.; Seyoum, R.; Milbourne, D.; Yin, W.; Sarma, P. V. V. S.; Cook, J. M.; June, H. L., GABA(A) and opioid receptors of the central

nucleus of the amygdala selectively regulate ethanol-maintained behaviors.

Neuropsychopharmacol. **2004**, 29, (2), 269-284.

126. June, H. L.; Cook, J. M.; Ma, C. R. Methods for reducing alcohol cravings in chronic alcoholics. US Patent 2003/0176456, **2003**.

127. Araki, T.; Tohyama, M., Region-specific expression of GABA(A) receptor alpha 3 and alpha 4 subunits mRNAs in the rat brain. *Mol. Brain Res.* **1992**, 12, 295-314.

128. Cox, E. D.; Hagen, T. J.; McKernan, R. M.; Cook, J. M., Bz(1) receptor subtype specific ligands. Synthesis and biological properties of BCCt, a Bz(1) receptor subtype specific antagonist. *Med. Chem. Res.* **1995**, 5, (9), 710-718.

129. Griebel, G.; Perrault, G.; Letang, V.; Grainger, P.; Avenet, P.; Schoemaker, H., New evidence that the pharmacological effects of benzodiazepine receptor ligands can be associated with activities at different BZ (α) receptor subtypes. *Psychopharmacol.* **1999**, 146, 205-213.

130. Carroll, M. E.; Carmona, G.; May, S., Modifying drug-reinforced behavior by altering the economic conditions of the drug and the drug reinforcer. *J. Exp. Anal. Behav.* **1991**, 18, 361-376.

131. Paronis, C. A.; Cox, E. D.; Cook, J. M.; Bergman, J., Different types of GABA(A) receptors may mediate the anticonflict and response rate-decreasing effects of zaleplon, zolpidem, and midazolam in squirrel monkeys. *Psychopharmacol.* **2001**, 156, 461-468.

132. Rowlett, J. K.; Tornatzky, W.; Cook, J. M.; Ma, C. R.; Miczek, K. A., Zolpidem, triazolam, and diazepam decrease distress vocalizations in mouse pups: Differential antagonism by flumazenil and β -carboline-3-carboxylate-t-butyl ester (β CCt). *J. Pharmacol. Exp. Ther.* **2001**, 297, 247-253.

133. Shannon, H. E.; Guzman, F.; Cook, J. M., β -Carboline-3-carboxylate-t-butyl ester: a selective BZ1 benzodiazepine receptor antagonist. *Life Sci.* **1984**, 35, 2227-2236.

134. Rowlett, J. K.; Spealman, R. D.; Lelas, S.; Cook, J. M.; Yin, W. Y., Discriminative stimulus effects of zolpidem in squirrel monkeys: role of GABA(A)/(alpha 1) receptors. *Psychopharmacol.* **2003**, 165, 209-215.

135. Rowlett, J. K.; Cook, J. M.; Duke, A. N.; Platt, D. M., Selective antagonism of GABA(A) receptor subtypes: An in vivo approach to exploring the therapeutic and side effects of benzodiazepine-type drugs. *CNS Spectrums* **2005**, 10, (1), 40-48.

136. Allen, M. S.; Laloggia, A. J.; Dorn, L. J.; Martin, M. J.; Constantino, G.; Hagen, T. J.; Koehler, K. F.; Skolnick, P.; Cook, J., Predictive binding of β -carboline inverse agonists and antagonists via the CoMFA/GOLPF approach. *J. Med. Chem.* **1992**, 35, 4001-4010.

137. Cain, M.; Weber, R. W.; Guzman, F.; Cook, J. M.; Barker, S. A.; Rice, K. C.; Crawley, J. N.; Paul, S. M.; Skolnick, P., β -Carbolines: Synthesis and neurochemical and pharmacological actions on brain benzodiazepine receptors. *J. Med. Chem.* **1982**, 25, 1081-1091.
138. Hagen, T. J.; Skolnick, P.; Cook, J. M., Synthesis of 6-substituted β -carbolines that behave as benzodiazepine receptor antagonists or inverse agonists *J. Med. Chem.* **1987**, 30, 750-753.
139. Cook, J. M.; Diaz-Arauzo, H.; Allen, M. S., Inverse agonists, probes to study the structure, topology and function of the benzodiazepine receptor. *NIDA Res. Monogr.* **1990**, 133-139.
140. Schweri, M.; Cain, M.; Cook, J. M.; Paul, S.; Skolnick, P., Blockade of 3-carbomethoxy- β -carboline induced seizures by diazepam and the benzodiazepine antagonists, Ro 15-1788 and CGS 8216. *Pharmacol. Biochem. Behav.* **1982**, 17, 457-460.
141. Fryer, R. I.; Cook, C.; Gilman, N. W.; Walser, A., Conformational shifts at the benzodiazepine receptor related to the binding of agonists, antagonists and inverse agonists. *Life Sci.* **1986**, 39, 1947-1957.
142. Trullas, R.; Ginter, H.; Jackson, B.; Skolnick, P.; Allen, M. S.; Hagen, T. J.; Cook, J. M., 3-Ethoxy- β -carboline: a high affinity benzodiazepine receptor ligand with partial inverse agonist properties. *Life Sci.* **1988**, 43, 1193-1197.
143. Ninan, P. T.; Insel, T. M.; Cohen, R. M.; Cook, J. M.; Skolnick, P.; Paul, S. M., Benzodiazepine receptor-mediated experimental "anxiety" in primates. *Sci.* **1982**, 218, 1332-1334.
144. Mendelson, W. B.; Cain, M.; Cook, J. M.; Paul, S. M.; Skolnick, P., A benzodiazepine receptor antagonist decreases sleep and reverses the hypnotic actions of flurazepam. *Sci.* **1983**, 219, 414-416.
145. Hagen, T. J.; Guzman, F.; Schultz, C.; Cook, J. M.; Shannon, H. E., Synthesis of 3,6-disubstituted β -carbolines which possess either benzodiazepine antagonist or agonist activity. *Heterocycles* **1986**, 24, 2845-2855.
146. Allen, M. S.; Hagen, T. J.; Trudell, M. L.; Coddington, P.; Skolnick, P.; Cook, J. M., Synthesis of novel 3-substituted β -carbolines as benzodiazepine receptor ligands: probing the benzodiazepine receptor pharmacophore. *J. Med. Chem.* **1988**, 31, 1854.
147. Diaz-Arauzo, H.; Evoniuk, G. E.; Skolnick, P.; Cook, J. M., The agonist pharmacophore of the benzodiazepine receptor. Synthesis of a selective anticonvulsant/anxiolytic *J. Med. Chem.* **1991**, 34, 1754-1756.

148. Wafford, K. A.; Bain, C. J.; Whiting, P. J.; Kemp, J. A., Functional comparison of the role of γ subunits in recombinant human γ -aminobutyric acid(A)/benzodiazepine receptors. *Mol. Pharmacol.* **1993**, *44*, 437-442.
149. Braestrup, C.; Nielsen, M., GABA reduces binding of 3H-methyl β -carboline-3-carboxylate to brain benzodiazepine receptors. *Nature* **1981**, *294*, 472-474.
150. Venault, P.; Chapouthier, G.; de-Carvalho, L. P.; Simiand, J.; Morre, M.; Dodd, R. H.; Rossier, J., Benzodiazepine impairs and β -carboline enhances performance in learning and memory tasks. *Nature* **1986**, *321*, 864-866.
151. Lippke, K. P.; Schunack, W. G.; Wenning, W.; Müller, W. E., β -Carbolines as benzodiazepine receptor ligands. 1. Synthesis and benzodiazepine receptor interaction of esters of β -carboline-3-carboxylic acid. *J. Med. Chem.* **1983**, *26*, 499-503.
152. Corda, M. G.; Blaker, W. D.; Mendelson, W. B.; Guidotti, A.; Costa, E., β -Carbolines enhance shock-induced suppression of drinking in rats. *Proc. Natl. Acad. Sci. USA* **1983**, *80*, 2072-2076.
153. Havoundjian, H.; Reed, G. F.; Paul, S. M.; Skolnick, P., Protection against the lethal effects of pentobarbital in mice by a benzodiazepine receptor inverse agonist, 6,7-dimethoxy-4-ethyl-3-carbomethoxy- β -carboline. *J. Clin. Invest.* **1987**, *79*, 473-477.
154. Hadingham, K. L.; Wingrove, P.; Le-Bourdellès, B.; Palmer, K. J.; Ragan, C. I.; Whiting, P. J., Cloning of cDNA sequences encoding human α_2 and α_3 γ -aminobutyric acid(A) receptor subunits and characterization of the benzodiazepine pharmacology of recombinant α_1 -, α_2 -, α_3 -, and α_5 -containing human γ -aminobutyric acid(A) receptors. *Mol. Pharmacol.* **1993**, *43*, 970-975.
155. Sanger, D. J.; Benavides, J.; Perrault, G.; Morel, E.; Cohen, C.; Joly, D.; Zivkovic, B., Recent developments in the behavioral pharmacology of benzodiazepine-(omega) receptors - Evidence for the functional-significance of receptor subtypes. *Neurosci. Biobehav. Rev.* **1994**, *18*, (3), 355-372.
156. Braestrup, C.; Nielsen, M.; Olsen, R., Urinary and brain β -carboline-3-carboxylates as potent inhibitors of brain benzodiazepine receptors. *Proc. Natl. Acad. Sci. USA* **1980**, *77*, 2288-2292.
157. Nielsen, M.; Braestrup, C., Ethyl β -carboline-3-carboxylate shows differential benzodiazepine receptor interaction. *Nature* **1980**, *286*, 606-607.
158. Yin, W.; Sarma, P. V. V. S.; Ma, J.; Han, D.; Chen, J. L.; Cook, J. M., Synthesis of bivalent ligands of β -carboline-3-carboxylates via a palladium-catalyzed homocoupling process. *Tetrahedron Lett.* **2005**, *46*, (37), 6363-6368.

159. Portoghese, P. S., From models to molecules: Opioid receptor dimers, bivalent ligands, and selective opioid receptor probes. *J. Med. Chem.* **2001**, *44*, (14), 2259-2269.
160. Portoghese, P. S.; Lin, C. E.; Farouq, F.; Takemori, A. E., Structure-activity relationship of N17'-substituted norbinaltorphimine congeners - role of the N17' basic group in the interaction with a putative address subsite on the kappa-opioid receptor. *J. Med. Chem.* **1994**, *37*, (10), 1495-1500.
161. Halazy, S., G-protein coupled receptors bivalent ligands and drug design. *Expert Opinion on Therapeutic Patents* **1999**, *9*, (4), 431-446.
162. Barnard, E.; Skolnick, P.; Olsen, R.; Möhler, H.; Sieghart, W.; Biggio, G.; Braestrup, C.; Bateson, A.; Langer, S., International union of pharmacology. XV. Subtypes of γ -aminobutyric acid_(A) receptors: classification on the basis of subunit structure and function. *J. Pharmacol. Exp. Ther. (Pharmacol. Rev.)* **1998**, *50*, 291-313.
163. June, H. L., Sr.; Foster, K. L.; Eiler, W. J. A. I.; Goergen, J.; Cook, J. B.; Johnson, N.; Mensah-Zoe, B.; Simmons, J. O.; June, H. L., Jr.; Yin, W.; Cook, J. M.; Homanics, G. E., Dopamine and benzodiazepine-dependent mechanisms regulate the EtOH-enhanced locomotor stimulation in the GABA_(A) α_1 subunit null mutant mice. *Neuropsychopharmacol.* **2007**, *32*, (1), 137-152.
164. Bell, R. L.; A., Z.; Lumeng, L.; Murphy, J. M.; McBride, W. J., The alcohol-preferring P rat and animal models of excessive alcohol drinking. *Addict. Biol.* **2006**, *11*, 270-288.
165. Koob, G. F., A Role for GABA Mechanisms in the Motivational Effects of Alcohol *Biochem Pharmacol.* **2004**, *68*, (8), 1515-1525 (review and references therein).
166. Trudell, J. R., Unique assignment of inter-subunit association in GABA(A) $\alpha_1\beta_3\gamma_2$ receptors determined by molecular modeling. *Biochim. Biophys. Acta* **2002**, *1565*, 91-96.
167. Ma, C. Part one, Efficient asymmetric synthesis of ring-A substituted tryptophans : synthesis of 6-methoxy-(D)-tryptophan required for the total synthesis of ring-A oxygenated indole alkaloids. Part two, Syntheses of selective ligands for GABA(A) /benzodiazepine receptor subtypes Ph. D. Thesis, University of Wisconsin -Milwaukee, Milwaukee, WI, **2000**.
168. Lüddens, H.; Korpi, E. R.; Seeburg, P. H., GABA(A) /benzodiazepine receptor heterogeneity: neurophysiological implications. *Neuropharmacol.* **1995**, *34*, (3), 245-254, Review.
169. Huang, Q.; Zhang, W. J.; Liu, R. Y.; McKernan, R. M.; Cook, J. M., Benzo-fused benzodiazepines employed as topological probes for the study of benzodiazepine receptor subtypes. *Med. Chem. Res.* **1996**, *6*, (6), 384-391.

170. Huang, Q.; Liu, R. Y.; Zhang, P. W.; He, X. H.; McKernan, R.; Gan, T.; Bennett, D. W.; Cook, J. M., Predictive models for GABA(A)/benzodiazepine receptor subtypes: Studies of quantitative structure-activity relationships for imidazobenzodiazepines at five recombinant GABA(A)/benzodiazepine receptor subtypes [$\alpha \times \beta 3 \gamma 2$ ($x = 1-3, 5$, and 6)] via comparative molecular field analysis. *J. Med.Chem.* **1998**, *41*, (21), 4130-4142.
171. He, X. H.; Huang, Q.; Ma, C. R.; Yu, S.; McKernan, R.; Cook, J., Pharmacophore/receptor models for GABA(A) /BzR $\alpha 2 \beta 3 \gamma 2$, $\alpha 3 \beta 3 \gamma 3$, and $\alpha 4 \beta 3 \gamma 2$ recombinant subtypes. Included volume analysis and comparison to $\alpha 1 \beta 3 \gamma 2$, $\alpha 5 \beta 3 \gamma 2$ and $\alpha 6 \beta 3 \gamma 2$ subtypes *Drug Des. Discov.* **2000**, *17*, 131-171.
172. Arnold, K.; Bordoli, L.; Kopp, J.; Schwede, T., The SWISS-MODEL Workspace: A web-based environment for protein structure homology modeling. *Bioinformatics* **2006**, *22*, 195-201.
173. Buhr, A.; Baur, R.; Sigel, E., Subtle changes in residue 77 of the gamma subunit of alpha 1 beta 2 gamma 2 GABA(A) receptors drastically alter the affinity for ligands of the benzodiazepine binding site. *J. Biol. Chem.* **1997**, *272*, (18), 11799-11804.
174. Mihic, S. J.; Whiting, P.; Klein, R. L.; Wafford, K.; Harris, R. A., A single amino acid of the human γ -aminobutyric acid type A receptor $\gamma 2$ subunit determines benzodiazepine efficacy. *J. Biol. Chem.* **1994**, *269*, 32768-32773.
175. Buhr, A.; Schaerer, M. T.; Baur, R.; Sigel, E., Residues at positions 206 and 209 of the $\alpha 1$ subunit of gamma-aminobutyric acid(A) receptors influence affinities for benzodiazepine binding site ligands. *Mol. Pharmacol.* **1997**, *52*, 676-682.
176. Buhr, A.; Sigel, E., A point mutation in the gamma(2) subunit of gamma-aminobutyric acid type A receptors results in altered benzodiazepine binding site specificity. *Proc. Natl. Acad. Sci. U.S.A.* **1997**, *94*, 8824-8829.
177. Sigel, E.; Schaerer, M. T.; Buhr, A.; Baur, R., The benzodiazepine binding pocket of recombinant $\alpha 1 \beta 2 \gamma 2$ γ -aminobutyric acid(A) receptors: Relative orientation of ligands and amino acid side chains. *Mol. Pharmacol.* **1998**, *54*, 1097-1105.
178. Braestrup, C.; Honore, T.; Nielsen, M. C.; Peterson, E. N.; Jensen, L. H., Ligands for benzodiazepine receptors with positive and negative efficacy. *Biochem. Pharmacol.* **1984**, *33*, 859-862.
179. Lawson, J.; Uyeno, E. T.; Nienow, J.; Loew, G. H.; Toll, L., Structure-activity studies of β -carboline analogs. *Life Sci.* **1984**, *34*, 2007-2013.
180. Ramachandran, P. V.; Teodorovic, A. V.; Brown, H. C., Chiral synthesis *via* organoboranes. 38. Selective reductions. 48. Asymmetric reduction of trifluoro-

methyl ketones by B-chlorodiisopinocampheylborane in high enantiomeric purity. *Tetrahedron* **1993**, 49, 1725-1738.

181. Hanzawa, Y.; Kawagoe, K.; Ito, M.; Kobayashi, Y., Kinetic resolution of (E)-[(fluoroalkyl)vinyl]carbinol derivatives by asymmetric epoxidation with titanium-tartrate catalysts. *Chem. Pharm. Bull.* **1987**, 35, 1633-1636.

182. Liu, R.; Zhang, P.; Gan, T.; Mckernan, R. M.; Cook, J. M., Evidence for the conservation of conformational topography at five major GABA_A/benzodiazepine receptor subsites. Potent affinities of the (S)-enantiomers of framework-constrained 4,5-substituted pyrroloimidazobenzodiazepines. *Med. Chem. Res.* **1997**, 7, 25-35.

183. Rowlett, J. K.; Spealman, R. D.; Lelas, S.; Cook, J. M.; Yin, W. Y., Discriminative stimulus effects of zolpidem in squirrel monkeys: role of GABA(A)/(alpha 1) receptors. *Psychopharmacology* **2003**, 165, (3), 209-215.

184. Ator, N. A., Contributions of GABA(A) receptor subtype selectivity to abuse liability and dependence potential of pharmacological treatments for anxiety and sleep disorders. *Cns Spectrums* **2005**, 10, (1), 31-39.

185. Skolnick, P.; Hu, R. J.; Cook, C. M.; Hurt, S. D.; Trometer, J. D.; Lu, R. Y.; Huang, Q.; Cook, J. M., [H-3]RY 80: A high-affinity, selective ligand for gamma-aminobutyric acid(A) receptors containing alpha-5 subunits. *J. Pharmacol. Exp. Ther.* **1997**, 283, (2), 488-493.

186. Zhang, P. W., Synthesis of novel imidazobenzodiazepines as probes of the pharmacophore for "diazepam-insensitive" GABA(A) receptors. *J. Med. Chem.* **1995**, 38, 1679-1688.

187. Harris, D. L.; DeLorey, T. M.; He, X. H.; Cook, J. M.; Loew, G. H., Determinants of recognition of ligands binding to benzodiazepine receptor/GABA(A) receptors initiating sedation. *Eur. J. Pharmacol.* **2000**, 401, (3), 271-287.

188. Roth, B., unpublished results. In 2006.

189. Kelly, M. D.; Smith, A.; Banks, G.; Wingrove, P.; Whiting, P. W.; Atack, J.; Seabrook, G. R.; Maubach, K. A., Role of the histidine residue at position 105 in the human $\alpha 5$ containing GABA(A) receptor on the affinity and efficacy of benzodiazepine site ligands. *Br. J. Pharmacol.* **2002**, 135, (1), 248-256.

190. Turner, D.; Sapp, D.; Olsen, R. W., The benzodiazepine/ alcohol antagonist Ro15-4513: binding to a GABA(A) receptor subtype that is insensitive to diazepam. *J. Pharmacol. Exp. Ther.* **1991**, 257, 1236-1242.

191. McKay, P. F.; Foster, K. L.; Mason, D.; Cummings, R.; Garcia, M.; Williams, L. S.; Grey, C.; McCane, S.; He, X. H.; Cook, J. M.; June, H. L., A high affinity ligand for GABA(A)-receptor containing alpha(5) subunit antagonizes

- ethanol's neurobehavioral effects in Long-Evans rats. *Psychopharmacology* **2004**, 172, (4), 455-462.
192. June, H. L.; Harvey, S. C.; Foster, K. L.; McKay, P. F.; Cummings, R.; Garcia, M.; Mason, D.; Grey, C.; McCane, S.; Williams, L. S.; Johnson, T. B.; He, X. H.; Rock, S.; Cook, J. M., GABA(A) receptors containing alpha 5 subunits in the CA1 and CA3 hippocampal fields regulate ethanol-motivated behaviors: An extended ethanol reward circuitry. *J. Neurosci.* **2001**, 21, (6), 2166-2177.
193. Stephens, D. N.; Pistovcakova, J.; Worthing, L.; Atack, J. R.; Dawson, G. R., Role of GABA(A) alpha 5-containing receptors in ethanol reward: The effects of targeted gene deletion, and a selective inverse agonist. *Eur. J. Pharmacol.* **2005**, 526, (1-3), 240-250.
194. Lüddens, H.; June, H. L.; Cook, J., β -CCT produces agonist and antagonist effects in the *in vivo* HEK cells assay. **(In preparation)**.
195. Haefely, W., Kyburz, E., Gerecke, M., and Mohler, H. , *Recent Advances in the Molecular Pharmacology of Benzodiazepine Receptors and in the Structure-Activity Relationships of their Agonists and Antagonists*. Academic Press: New York, **1985**; Vol. 99, p 165-322.
196. Fryer, R. I., *Comprehensive Medicinal Chemistry*. Pergamon Press: Oxford, **1989**; Vol. 99, p 539-566.
197. CambridgeSoft, *Chem & Bio Draw 12.0*. **2010**.
198. Sawyer, G. W.; Chiara, D. C.; Olsen, R. W.; Cohen, J. B., Identification of the bovine gamma-aminobutyric acid type A receptor alpha subunit residues photolabeled by the imidazobenzodiazepine [^3H] Ro15-4513. *J. Biol. Chem.* **2002**, 277, (51), 50036-50045.
199. Colquhoun, D., Binding, gating, affinity and efficacy: The interpretation of structure-activity relationships for agonists and of the effects of mutating receptors. *Br. J. Pharmacol.* **1998**, 125, 923-947.
200. Smith, G. B.; Olsen, R. W., Deduction of amino acid residues in the GABA(A) receptor α subunits photoaffinity labeled with the benzodiazepine flunitrazepam. *Neuropharmacology* **2000**, 39, (1), 55-64.
201. McKernan, R.; Farrar, S.; Collins, I.; Emms, F.; Asuni, A.; Quirk, K.; Broughton, H. B., Photoaffinity labeling of the benzodiazepine binding site of $\alpha 1\beta 3\gamma 2$ γ -aminobutyric acid A receptors with flunitrazepam identifies a subset of ligands that interact directly with His102 of the α subunit and predicts orientation of these within the benzodiazepine pharmacophore. *Mol. Pharmacol.* **1998**, 54, 33-43.

202. Berezhnoy, D.; Nyfeler, Y.; Gonthier, A.; Schwob, H.; Goeldner, M.; Sigel, E., On the benzodiazepine binding pocket in GABA(A) receptors. *J. Biol. Chem.* **2004**, 279, (5), 3160-3168.
203. Duncalfe, L.; Carpenter, M.; Smillie, L.; Martin, I. L.; Dunn, S. L., The major site of photoaffinity labeling of the GABA(A) receptor by [³H]flunitrazepam is histidine 102 of the subunit. *J. Biol. Chem.* **1996**, 271, 9209-9214.
204. Kucken, A. M.; Teissere, J. A.; Seffinga-Clark, J.; Wagner, D. A.; Czajkowski, C., Structural requirements for imidazobenzodiazepines binding to GABA(A) receptors. *Mol. Pharmacol.* **2003**, 63, 289-296.
205. Tan, K. R.; Gonthier, A.; Baur, R.; Ernst, M.; Goeldner, M.; Sigel, E., Proximity-accelerated chemical coupling reaction in the benzodiazepine binding site of GABA(A) receptors: Superposition of different allosteric modulators. *J. Biol. Chem.* **2007**.
206. Teissere, J. A.; Czajkowski, C., A β -strand in the $\gamma 2$ subunit lines the benzodiazepine binding site of the GABA(A) receptor: Structural rearrangements detected during channel gating. *J. Neurosci.* **2001**, 21, 4977-4986.
207. Ogris, W.; Poltl, A.; Hauer, B.; Ernst, M.; Oberto, A.; Wulff, P.; Hoger, H.; Wisden, W.; Sieghart, W., Affinity of various benzodiazepine site ligands in mice with a point mutation in the GABA(A) receptor gamma 2 subunit. *Biochem. Pharmacol.* **2004**, 68, (8), 1621-1629.
208. Sieghart, W., Structure and pharmacology of gamma-aminobutyric acid(A) receptor subtypes. *Pharmacol. Rev.* **1995**, 47, (2), 181-234.
209. Hevers, W.; Luddens, H., The diversity of GABA(A) receptors - Pharmacological and electrophysiological properties of GABA(A) channel subtypes. *Mol. Neurobiol.* **1998**, 18, (1), 35-86.
210. He, X. B.; Huang, Q.; Ma, C. R.; Yu, S.; McKernan, R.; Cook, J., Pharmacophore/receptor models for GABA(A) /BzR $\alpha 2\beta 3\gamma 2$, $\alpha 3\beta 3\gamma 3$, and $\alpha 4\beta 3\gamma 2$ recombinant subtypes. Included volume analysis and comparison to $\alpha 1\beta 3\gamma 2$, $\alpha 5\beta 3\gamma 2$ and $\alpha 6\beta 3\gamma 2$ subtypes *Drug Des. Discov.* **2000**, 17, 131-171.
211. Hadingham, K. L.; Wingrove, P. B.; Wafford, K. A.; Bain, C.; Kemp, J. A.; Palmer, K. J.; Wilson, A. W.; Wilcox, A. S.; Sikela, J. M.; Ragan, C. I.; Whiting, P. J., Role of the beta-subunit in determining the pharmacology of human gamma-aminobutyric-acid type-a receptors. *Mol. Pharmacol.* **1993**, 44, (6), 1211-1218.
212. Barnard, E. A., Receptor classes and the transmitter-gated ion channels. *Trends Biochem. Sci.* **1992**, 17, (10), 368-374.

213. Zhang, P. W.; Zhang, W. J.; Liu, R. Y.; Harris, B.; Skolnick, P.; Cook, J. M., Synthesis and SAR study of novel imidazobenzodiazepines at 'diazepam-insensitive' benzodiazepine receptors. *J. Med. Chem.* **1995**, 38, (10), 1679-1688.
214. Wafford, K. A.; Thompson, S. A.; Thomas, D.; Sikela, J.; Wilcox, A. S.; Whiting, P. J., Functional characterization of human gamma-aminobutyric acid(A) receptors containing the alpha 4 subunit. *Mol. Pharmacol.* **1996**, 50, (3), 670-678.
215. Fryer, R. I.; Gu, Z. Q.; Wang, C. G., Synthesis of novel, substituted 4H-imidazo[1,5-a][1,4]benzodiazepines. *J. Heterocycl Chem* **1991**, 28, (7), 1661-1669.
216. Fryer, R. I.; Zhang, P.; Rios, R.; Gu, Z. Q.; Basile, A. S.; Skolnick, P., Structure-activity relationship studies at the benzodiazepine receptor (Bzr) - a comparison of the substituent effects of pyrazoloquinolinone analogs. *J. Med. Chem.* **1993**, 36, (11), 1669-1673.
217. Platt, D. M.; Rowlett, J. K.; Spealman, R. D.; Cook, J.; Ma, C. R., Selective antagonism of the ataxic effects of zolpidem and triazolam by the GABA(A)/alpha(1)-preferring antagonist beta-CCt in squirrel monkeys. *Psychopharmacology* **2002**, 164, (2), 151-159.
218. Cook, J. M.; Q., H.; X., H.; Li, X.; Yu, J.; Han, D.; Lelas, S.; McElroy, J. F. Anxiolytic agents with reduced sedative and ataxic effects. US Patent 7119196 B2. **2006**.
219. Rivas, F.; Edwanker, C., Antiseizure Activity of Novel γ -Aminobutyric Acid (A) Receptor Subtype-Selective Benzodiazepine Analogs in Mice and Rat Models. *J. Med. Chem.* **2009**, 52, (7), 1795-1798.
220. Cook, J. M.; Zhao, H.; Huang, S.; Sarma, P. S.; Zhang, C. C. Stereospecific anxiolytic and anticonvulsant agents with reduced muscle-relaxant, sedative-hypnotic and ataxic effects. US Patent 2006004945, **2007**.
221. Rivas, F.; Edwanker, C., Antiseizure activity of novel γ -aminobutyric acid (A) receptor subtype-selective benzodiazepine analogs in mice and rat models. *J. Med. Chem.* **2009**, 52, (7), 1795-1798.
222. Villar, H. O., Davies, M.F., Loew, G.H., and Maguire, P.A., *Life Sci.* **1991**, 48, 593.
223. Villar, H. O.; Uyeno, E. T.; Toll, L.; Polgar, W.; Davies, M. F.; Loew, G. H., Molecular determinants of benzodiazepine receptor affinities and anticonvulsant activities. *Mol. Pharmacol.* **1989**, 36, (4), 589-600.
224. Crippen, G. M., Distance geometry analysis of the benzodiazepine binding site. *Mol. Pharm.* **1981**, 22, 11.

225. Ghose, A. K.; Crippen, G. M., Modeling the benzodiazepine receptor binding site by the general three-dimensional structure-directed quantitative structure-activity relationship method REMOTEDISC. *Mol. Pharm.* **1990**, 28, 178.
226. Muir, A. K. S.; Coddington, P. W., Structure activity studies of beta-carbolines. 3. Crystal and molecular-structures of methyl beta-carboline-3-carboxylate. *Can. J. Chem.* **1985**, 63, 2752.
227. Borea, P. A.; Gilli, G.; Bertolasi, V.; Ferretti, V., Stereochemical features controlling binding and intrinsic activity properties of benzodiazepine-receptor ligands. *Mol. Pharmacol.* **1987**, 31, (4), 334-344.
228. Tebib, S.; Bourguignon, J. J.; Wermuth, C. G., The active analog approach applied to the pharmacophore identification of benzodiazepine receptor ligands. *J. Comput. Aided Mol. Des.* **1987**, 1, 153.
229. Gardner, C. R., A review of recently-developed ligands for neuronal benzodiazepine receptors and their pharmacological activities. *Neuro-Psychopharmacol. & Biol. Psychiat.* **1992**, 16, 755.
230. Martin, M. J.; Trudell, M. L.; Arauzo, H. D.; Allen, M. S.; Laloggia, A. J.; Li, D.; Schultz, C. A.; Tan, Y. C.; Bi, Y. Z.; Narayanan, K.; Dorn, L. J.; Koehler, K. F.; Skolnick, P.; Cook, J. M., Molecular yardsticks - rigid probes to define the spatial dimensions of the benzodiazepine receptor-binding site. *J. Med. Chem.* **1992**, 35, (22), 4105-4117.
231. Trudell, M. L.; Lifer, S. L.; Tan, Y. C.; Martin, M. J.; Deng, L.; Skolnick, P.; Cook, J. M., Synthesis of substituted 7,12-dihydropyrido[3,2-B-5,4-B']diindoles - rigid planar benzodiazepine receptor ligands with inverse agonist/antagonist properties. *J. Med. Chem.* **1990**, 33, (9), 2412-2420.
232. Narayanan, K.; Cook, J. M., Probing the Dimensions of the Benzodiazepine Receptor Inverse Agonist Site. *Heterocycles* **1990**, 31, 203.
233. Hollinshead, S. P.; Trudell, M. L.; Skolnick, P.; Cook, J. M., Structural requirements for agonist actions at the benzodiazepine receptor - studies with analogs of 6-(benzyloxy)-4-(methoxymethyl)-beta-carboline-3-carboxylic acid ethyl-ester. *J. Med. Chem.* **1990**, 33, (3), 1062-1069.
234. Cook, J. M.; Diaz-Arauzo, H.; Allen, M. S. In *Inverse agonists: probes to study the structure, topology and function of the benzodiazepine receptor*, National Institute on Drug Abuse Research Monograph, Proceedings of the 51st Annual Scientific Meeting **1991**; Harris, L. S., Ed. The College on Problems of Drug Dependence: 1991; p p. 133.
235. Zhang, W. J.; Koehler, K. F.; Harris, B.; Skolnick, P.; Cook, J. M., Synthesis of benzo-fused benzodiazepines employed as probes of the agonist pharmacophore of benzodiazepine receptors. *J Med Chem* **1994**, 37, (6), 745-757.

236. Trullas, R.; Ginter, H.; Jackson, B.; Skolnick, P.; Allen, M. S.; Hagen, T. J.; Cook, J. M., 3-Ethoxy-beta-carboline: a high affinity benzodiazepine receptor ligand with partial inverse agonist properties. *Life Sci.* **1988**, 43, 1193.
237. Liu, R. Y.; Zhang, P. W.; Gan, T.; McKernan, R. M.; Cook, J. M., Evidence for the conservation of conformational topography at five major GABA(A)/benzodiazepine receptor subsites. Potent affinities of the (S)-enantiomers of framework-constrained 4,5-substituted pyrroloimidazobenzodiazepines. *Med. Chem. Res.* **1997**, 7, (1), 25-35.
238. Yu, S.; He, X. H.; Ma, C. R.; McKernan, R.; Cook, J. M., Studies in search of $\alpha 2$ selective ligands for GABA(A) /BzR receptor subtypes. Part I. Evidence for the conservation of pharmacophoric descriptors for DS subtypes. *Med. Chem. Res.* **1999**, 9, (3), 186-202.
239. Arbilla, S.; Depoortere, H.; George, P.; Langer, S. Z., Pharmacological profile of the imidazopyridine zolpidem at benzodiazepine receptors and electrocorticogram in rats. *Naunyn-Schmiedebergs Archives of Pharmacology* **1985**, 330.
240. Bertolasi, V., Feretti, V., Gilli, G., and Borea, P.A., Stereochemistry of benzodiazepine-receptor ligands .1. Structure of methyl beta-carboline-3-carboxylate (beta-CCM), C₁₃H₁₀N₂O₂. *Acta Crystallogr. Sect. C Cryst. Struct. Commun.* **1984**, 40, 1981.
241. Camerman, A., Camerman, N., Stereochemical basis of anticonvulsant drug action. 2. Molecular structure of diazepam *J. Am. Chem. Soc.* **1972**, 94, 268.
242. Ferretti, V., Bertolasi, V., Gilli, G., and Borea, P.A., Structures of two 2-arylpyrazolo[4,3-c]quinolin-3-ones: CGS8216, C₁₆H₁₁N₃O, and CGS9896, C₁₆H₁₀CIN₃O. *Acta Crystallogr. Sect. C Cryst. Struct. Commun.* **1985**, C41, 107.
243. Hempel, A.; Camerman, N.; Camerman, A., Benzodiazepine stereochemistry - Crystal-structures of the diazepam antagonist Ro-15-1788 and the anomalous benzodiazepine Ro-5-4864. *Can. J. Chem.* **1987**, 65, (7), 1608-1612.
244. Neidle, S.; Webster, G. D.; Jones, G. B.; Thurston, D. E., Structures of 2 DNA minor-groove binders, based on pyrrolo[2,1-C][1,4]-benzodiazepines. *Acta Crystallogr. Sect. C Cryst. Struct. Commun.* **1991**, 47, 2678-2680.
245. Halgren, T. A., Merck molecular force field .5. Extension of MMFF94 Using experimental data, additional computational data, and empirical rules. *J. Comput. Chem.* **1996**, 17, (5-6), 616-641.
246. Halgren, T. A., Merck molecular force field .3. Molecular geometries and vibrational frequencies for MMFF94. *J. Comput. Chem.* **1996**, 17, (5-6), 553-586.

247. Halgren, T. A., Merck molecular force field .2. MMFF94 Van der Waals and electrostatic parameters for intermolecular interactions. *J. Comput. Chem.* **1996**, 17, (5-6), 520-552.
248. Halgren, T. A., Merck molecular force field .1. Basis, form, scope, parameterization, and performance of MMFF94. *J. Comput. Chem.* **1996**, 17, (5-6), 490-519.
249. Halgren, T. A.; Nachbar, R. B., Merck molecular force field .4. Conformational energies and geometries for MMFF94. *J. Comput. Chem.* **1996**, 17, (5-6), 587-615.
250. Mohamadi, F.; Richards, N. G. J.; Guida, W. C.; Liskamp, R.; Lipton, M.; Caufield, C.; Chang, G.; Hendrickson, T.; Still, W. C., Macromodel - An integrated software system for modeling organic and bioorganic molecules using molecular mechanics. *J. Comput. Chem.* **1990**, 11, (4), 440-467.
251. *Gaussian92*, Gaussian, Inc., Carnegie Office Park, Bldg.6: Pittsburgh, PA.
252. *Gaussian94*, Gaussian, Inc., Carnegie Office Park, Bldg. 6 15106: Pittsburgh, PA.
253. Andzelm, J., Klobukowski, M., and Radzio-Andzelm, E., Compact contracted Gaussian-type basis-sets for halogen atoms- basis-set superposition effects on molecular properties. *J. Comput. Chem.* **1984**, 5, 146.
254. McGrath, M. P.; Radom, L., Extension of Gaussian-1 (G1) theory to bromine-containing molecules. *J. Chem. Phys.* **1991**, 94, (1), 511-516.
255. Glukhovtsev, M. N.; Pross, A.; McGrath, M. P.; Radom, L., Extension of Gaussian-2 (G2) theory to bromine- and iodine-containing molecules: Use of effective core potentials. *J. Chem. Phys.* **1996**, 104, (9), 3407.
256. Glukhovtsev, M. N.; Pross, A.; McGrath, M. P.; Radom, L., Extension of Gaussian-2 (G2) theory to bromine-containing and iodine-containing molecules - use of effective core potentials. *J. Chem. Phys.* **1995**, 103, (5), 1878-1885.
257. Benavides, J.; Peny, B.; Dubois, A.; Perrault, G.; Morel, E.; Zivkovic, B.; Scatton, B., In vivo interaction of zolpidem with central benzodiazepine (Bzd) binding-sites (as sabeled by [H-3]Ro-15-1788) in the mouse-brain - preferential affinity of zolpidem for the omega-1 (Bzd1) subtype. *J. Pharmacol. Exp. Ther.* **1988**, 245, (3), 1033-1041.
258. *Sybyl6.5*, Tripos, Inc., 1699 S. Hanley Road: St. Louis, MO, 63144.
259. Carlier, P. R.; Zhao, H.; DeGuzman, J.; Lam, P. C. H., Enantioselective synthesis of "quaternary" 1,4-benzodiazepin-2-one scaffolds via memory of chirality. *J. Am. Chem. Soc.* **2003**, 125, (38), 11482-11483.

260. Brejc, K.; van Dijk, W.; Klassen, R.; Schuurmans, M.; van Der Oost, J.; Smit, A. B.; Sixma, T., Crystal structure of ACh-binding protein reveals the ligand-binding domain of nicotinic receptors. *Nature* **2001**, 411, 269-276.
261. Ernst, M.; Bruckner, S.; Boresch, S.; Sieghart, W., Comparative models of GABA(A) receptor extracellular and transmembrane domains: Important insights in pharmacology and function. *Mol. Pharmacol.* **2005**, 68, (5), 1291-1300.
262. Unwin, N., Refined structure of the nicotinic acetylcholine receptor at 4Å resolution. *J. Mol. Biol.* **2005**, 346, (4), 967-89.
263. Sigel, E.; Buhr, A., The benzodiazepine binding site of GABA(A) receptors. *Trends Pharmacol. Sci.* **1997**, 18, (11), 425-429.
264. Baumann, S. W.; Baur, R.; Sigel, E., Forced subunit assembly in $\alpha 1\beta 2\gamma 2$ GABA(A) receptors. *J. Biol. Chem.* **2002**, 277, (48), 46020-46025.
265. Neish, C. S.; Martin, I. L.; Davies, M.; Henderson, R. M.; Edwardson, J. M., Atomic force microscopy of ionotropic receptors bearing subunit-specific tags provides a method for determining receptor architecture. *Nanotechnol.* **2003**, 14, (8), 864-872.
266. Chou, K. C., Modelling extracellular domains of GABA-A receptors: subtypes 1, 2, 3, and 5. *Biochem. Biophys. Res. Commun.* **2004**, 316, (3), 636-642.
267. Trudell, J. R., Unique assignment of inter-subunit association in GABA(Alpha) alpha 1 beta 3 gamma 2 receptors determined by molecular modeling. *Biochim. Biophys. Acta* **2002**, 1565, (1), 91-96.
268. Buhr, A.; Baur, R.; Malherbe, P.; Sigel, E., Point mutations of the alpha 1 beta 2 gamma 2 gamma-aminobutyric acid(A) receptor affecting modulation of the channel by ligands of the benzodiazepine binding site. *Mol. Pharmacol.* **1996**, 49, (6), 1080-1084.
269. Sigel, E.; Baur, R.; Trube, G.; Möhler, H.; Malherbe, P., The effect of subunit composition of rat-brain GABA-A receptors on channel function. *Neuron* **1990**, 5, 703-711.
270. Khom, S.; Baburin, I.; Timin, E. N.; Hohaus, A.; Sieghart, W.; Hering, S., Pharmacological properties of GABA(A) receptors containing gamma 1 subunits. *Mol. Pharmacol.* **2006**, 69, (2), 640-649.
271. Hagen, T. J. I. The synthesis of benzodiazepine receptor antagonists and inverse agonists. II. The total synthesis of the cytotoxic indole alkaloid: 1 methoxy canthine 6 one. PhD Thesis. University of Wisconsin, Milwaukee, Milwaukee, **1988**.
272. Hansen, S. B.; Sulzenbacher, G.; Huxford, T.; Marchot, P.; Taylor, P.; Bourne, Y., Structures of *Aplysia* AChBP complexes with nicotinic agonists and

- antagonists reveal distinctive binding interfaces and conformations. *Embo J* **2005**, 24, (20), 3635-46.
273. Downing, S.; Lee, Y. F.; Farb, D. H.; Gibbs, T. T., Benzodiazepine modulation of partial agonist efficacy and spontaneously active GABA(A) receptors supports an allosteric model of modulation. *Br. J. Pharmacol.* **2005**, 145, 894-906.
274. Trudell, M. L. I. The synthesis and study of the pharmacologic activity of 7,12 dihydropyrido[3,2 b:5,4 b']diindoles. A novel class of rigid, planar benzodiazepine receptor ligands. II. The total synthesis of the indole alkaloid, (\pm) suaveoline. PhD Thesis. University of Wisconsin - Milwaukee, Milwaukee, **1989**.
275. He, X. H.; Zhang, C. C.; Cook, J. M., Model of the BzR binding site: Correlation of data from site-directed mutagenesis and the pharmacophore/receptor model. *Med. Chem. Res.* **2001**, 10, (5), 269-308.
276. Kucken, A. M.; Wagner, D. A.; Ward, P. R.; Teissere, J. A.; Boileau, A. J.; Czajkowski, C., Identification of benzodiazepine binding site residues in the gamma 2 subunit of the gamma-aminobutyric acid(A) receptor. *Mol. Pharmacol.* **2000**, 57, (5), 932-939.
277. Sancar, F.; Ericksen, S. S.; Kucken, A. M.; Teissere, J. A.; Czajkowski, C., Structural determinants for high-affinity zolpidem binding to GABA(A) receptors. *Mol. Pharmacol.* **2007**, 71, (1), 38-46.
278. Smit, A. B., A glia-derived acetylcholine-binding protein that modulates synaptic transmission. *Nature* **2001**, 411, (261-268).
279. Arnold, K.; Bordoli, L.; Kopp, J.; Schwede, T., The SWISS-MODEL Workspace: A web-based environment for homology modelling. *Bioinformatics* **2006**, 22, 195-201.
280. Guex, N.; Peitsch, M. C., SWISS-MODEL and the Swiss-PdbViewer: An environment for comparative protein modeling. *Electrophoresis* **1997**, 18, 2714-2723.
281. Rost, B.; Yachdav, G.; Liu, L., The PredictProtein server. *Nucleic Acids Research* **2004**, 32 (suppl 2), W321-W326.
282. Goodsell, D. S.; Olson, A. J., Automated docking of substrates to proteins by simulated annealing. *Proteins: Structure, Function, and Genetics* **1990**, 8, 195-202.
283. Morris, G. M.; Goodsell, D. S.; Halliday, R. S.; Huey, R.; Hart, W. E.; Belew, R. K.; Olson, A. J., Automated docking using Lamarckian genetic algorithm and an empirical binding free energy function. *J. Comp. Chem* **1998**, 19, 1639-1662.

284. Morris, G. M.; Goodsell, D. S.; Huey, R.; Olson, A. J., Distributed automated docking of flexible ligands to proteins: parallel applications of AutoDock 2.4. *J. Computer-Aided Molecular Design* **1996**, 10, 293-304.
285. Sarter, M.; Bruno, J. P., Trans-synaptic stimulation of cortical acetylcholine and enhancement of attentional functions: A rational approach for the development of cognition enhancers. *Behavioural Brain Research* **1997**, 83, (1-2), 7-14.
286. Small, G. W., Diagnosis and treatment of Alzheimer disease and related disorders. Consensus statement of the American Association of Geriatric Psychiatry, The Alzheimer's Association and the American Geriatric Society. *JAMA* **1997**, 278, 1363-71.
287. Anger, W. K., Animal test systems to study behavioral dysfunctions of neurodegenerative disorders. *Neurotoxicology* **1991**, 12, 403-13.
288. Ernst, R. L.; Hay, J. W.; Fenn, C.; Tinklenberg, J.; Yesavage, J. A., Cognitive function and the costs of Alzheimer's disease. An exploratory study. *Arch. Neurol.* **1997**, 54, 687-93.
289. Froestl, W., Introduction to receptors in aging diseases: GABA(A) receptors. *Med. Chem. Res.* **2004**, 13, (1-2), 99-102.
290. Katzman, R.; Fox, P., *The World-Wide Impact of Dementia: Projections of Prevalence and Costs*. Springer-Verlag: New York, **2000**; p 1-17.
291. Ebly, E.; Parhad, I.; Hogan, D.; Fung, T., Prevalence and types of dementia in the very old - Results from the Canadian study of health and aging. *Neurology* **1994**, 44, 1593-1600.
292. CIA World Factbook (from <http://mrdownling.com/800life.html>).
293. Whitehouse, P., The cholinergic deficit in Alzheimer's disease. *J Clin Psychiatry* **1998**, 59 Suppl 13, 19-22.
294. Perry, E.; Johnson, M.; Kerwin, J.; Piggott, M.; Court, J.; Shaw, P.; Ince, P.; Brown, A.; Perry, R., Convergent cholinergic activities in aging and Alzheimer's disease. *Neurobiol Aging* **1992**, 13, 393-400.
295. Sarter, M.; Bruno, J. P., Cognitive functions of the cortical arch: lessons from studies on the trans-synaptic modulation of activated efflux. *Trends Neurosci.* **1994**, 17, 217-21.
296. Chambers, M. S.; Atack, J. R.; Bromidge, F. A.; Broughton, H. B.; Cook, S.; Dawson, G. R.; Hobbs, S. C.; Maubach, K. A.; Reeve, A. J.; Seabrook, G. R.; Wafford, K.; MacLeod, A. M., 6,7-Dihydro-2-benzothiophen-4(5H)-ones: A novel class of GABA-A alpha 5 receptor inverse agonists. *J. Med. Chem.* **2002**, 45, (6), 1176-1179.

297. Chambers, M. S.; Atack, J. R.; Broughton, H. B.; Collinson, N.; Cook, S.; Dawson, G. R.; Hobbs, S. C.; Marshall, G.; Maubach, K. A.; Pillai, G. V.; Reeve, A. J.; MacLeod, A. M., Identification of a novel, selective GABA(A) α 5 receptor inverse agonist which enhances cognition. *J. Med. Chem.* **2003**, 46, (11), 2227-2240.
298. Abe, K.; Takeyama, C.; Yoshimura, K., Effects of S-8510, a novel benzodiazepine receptor partial inverse agonist, on basal forebrain lesioning-induced dysfunction in rats. *Eur J Pharmacol* **1998**, 24, 145-52.
299. Howell, O.; Atack, J. R.; Dewar, D.; McKernan, R. M.; Sur, C., Density and pharmacology of α 5 subunit-containing GABA(A) receptors are preserved in hippocampus of Alzheimer's disease patients. *Neuroscience* **2000**, 98, (4), 669-675.
300. Quirk, K.; Blurton, P.; Fletcher, S.; Leeson, P.; Tang, F.; Mellilo, D.; Ragan, C. I.; McKernan, R. M., [H-3]L-655,708, a novel ligand selective for the benzodiazepine site of GABA(A) receptors which contain the α 5 subunit. *Neuropharmacology* **1996**, 35, (9-10), 1331-1335.
301. Costa, E.; Guidotti, A., Benzodiazepines on trial: A research strategy for their rehabilitation. *Trends Pharmacol. Sci.* **1996**, 17, (5), 192-200.
302. Evans, M. S.; Viola-McCabe, K. E., Midazolam inhibits long-term potentiation through modulation of GABA(A) receptors. *Neuropharmacology* **1996**, 35, (3), 347-57.
303. Seabrook, G. R.; Easter, A.; Dawson, G. R.; Bowery, B. J., Modulation of long-term potentiation in CA1 region of mouse hippocampal brain slices by GABA(A) receptor benzodiazepine site ligands. *Neuropharmacology* **1997**, 36, (6), 823-30.
304. Kawasaki, K.; Eigyo, M.; Ikeda, M.; Kihara, T.; Koike, K.; Matsushita, A.; Murata, S.; Shiomi, T.; Takada, S.; Yasui, M., A novel benzodiazepine inverse agonist, S-8510, as a cognitive enhancer. *Prog Neuropsychopharmacol Biol Psychiatry* **1996**, 20, (8), 1413-25.
305. Duka, T.; Dorrow, R., *Human experimental psycho-pharmacology of benzodiazepine receptor inverse agonists and antagonists*. Wiley-Liss: New York, **1995**; p 243-270.
306. Potier, M. C.; Decarvalho, L. P.; Dodd, R. H.; Besselievre, R.; Rossier, J., In Vivo binding of beta-carbolines in mice: regional differences and correlation of occupancy to pharmacological effects. *Mol. Pharm.* **1988**, 34, 124-8.
307. Mohler, H.; Fritschy, J. M.; Crestani, F.; Hensch, T.; Rudolph, U., Specific GABA(A) circuits in brain development and therapy. *Biochem. Pharmacol.* **2004**, 68, (8), 1685-1690.

308. Yin, W.; Rivas, F.; Furtmueller, R.; Li, X.; Sieghart, W.; Wenger, G. R.; Cook, J. M., Synthesis, in-vitro affinity and efficacy of the first bivalent alpha 5 subtype selective BzR/GABA(A) antagonist. *Neuroscience Meeting*, San Diego, CA, 2004.
309. Zhang, C. C. Structure activity relationships and cytotoxic activity of analogs of tryprostatin A and B. Preparation of irreversible inhibitors for studies of mechanism and action. II. Pharmacophore receptor models of GABA(A)/BzR. University of Wisconsin, Milwaukee, 2004.
310. Li, X. Synthesis of selective ligands for GABA(A) /benzodiazepine receptors. PhD Thesis. University of Wisconsin-Milwaukee, Milwaukee, 2004.
311. Meyer, M.; Koeppe, R. A.; Frey, K. A.; Foster, N. L.; Kuhl, D. E., Positron emission tomography measures of benzodiazepine binding in Alzheimers-disease. *Archives of Neurology* **1995**, 52, (3), 314-317.
312. Mizukami, K.; Ikonovic, M. D.; Grayson, D. R.; Rubin, R. T.; Warde, D.; Sheffield, R.; Hamilton, R. L.; Davies, P.; Armstrong, D. M., Immunohistochemical study of GABA(A) receptor beta2/3 subunits in the hippocampal formation of aged brains with Alzheimer-related neuropathologic changes. *Experimental Neurology* **1997**, 147, 333-45.
313. Lowe, S. L.; Francis, P. T.; Procter, A. W.; Palmer, A. M.; Davison, A. N.; Bowen, D. M., Gamma-aminobutyric acid concentration in brain tissue at two stages of Alzheimer's disease. *Brain* **1988**, 111, 785-99.
314. Nagga, K.; Bogdanovic, N.; Marcusson, J., GABA transporters (GAT-1) in Alzheimer's disease. *J Neural Transm* **1999**, 106, 1141-9.
315. Flood, J. F.; Harris, F. J.; Morley, J. E., Age-related changes in hippocampal drug facilitation of memory processing in SAMP8 mice. *Neurobiol Aging* **1996**, 17, (1), 15-24.
316. Forster, M. J.; Prather, P. L.; Patel, S. R.; Lal, H., The benzodiazepine receptor inverse agonist RO 15-3505 reverses recent memory deficits in aged mice. *Pharmacology Biochemistry and Behavior* **1995**, 51, 557-60.
317. Sur, C.; Quirk, K.; Dewar, D.; Atack, J.; McKernan, R., Rat and human hippocampal alpha 5 subunit-containing gamma-aminobutyric acid(A) receptors have alpha 5 beta 3 gamma 2 pharmacological characteristics. *Mol. Pharmacol.* **1998**, 54, (5), 928-933.
318. Sarter, M., Taking stock of cognition enhancers. *Trends Pharmacol. Sci.* **1991**, 12, 456-461.
319. Mohler, H., GABA(A) Receptors in cellular and network excitability. *12th Neuropharmacology Conference*, Sheraton World Resort, Orlando, FL, 2002.

320. Han, D.; Forsterling, F. H.; Li, X.; Deschamps, J.; Cao, H.; Cook, J. M., Study of the structure activity relationships of GABA(A)-benzodiazepine receptor ligands by low temperature NMR spectroscopy and X-ray analysis. *227th ACS National Meeting*, Anaheim, CA, 2004.
321. Li, X. Y.; Ma, C. R.; He, X. H.; Yu, J. M.; Han, D. M.; Zhang, C. C.; Atack, J. R.; Cook, J. M., Studies in search of diazepam-insensitive subtype selective agents for GABA(A)/Bz receptors. *Med. Chem. Res.* **2003**, 11, (9), 504-537.
322. Roth, B. L.; Baner, K.; Westkaemper, R.; Siebert, D.; Rice, K. C.; Steinberg, S.; Ernsberger, P.; Rothman, R. G., Salvinorin: A potent naturally occurring nonnitrogenous kappa opioid selective agonist. *Proc. Natl. Acad. Sci.* **2002**, 99, (11934-11939).
323. Gray, J. A.; Compton-Toth, B. A.; Roth, B. L., Identification of two serine residues essential for agonist-induced 5-HT_{2A} receptor desensitization. *Biochemistry* **2003**, 42, 10853-10862.
324. Cheng, Y., Prusoff, W.H., Relationship between inhibition constant (K_i) and concentration of inhibitor which causes 50 per cent inhibition (I_{50}) of an enzymatic-reaction. *Biochem. Pharmacol.* **1973**, 22, 3099-3108.
325. Johnstone, T. B. C.; Hogenkamp, D. J.; Coyne, L.; Su, J. P.; Halliwell, R. F.; Tran, M. B.; Yoshimura, R. F.; Li, W. Y.; Wang, J.; Gee, K. W., Modifying Quinolone antibiotics yields new anxiolytics. *Nature* **2004**, 10, 31-32.
326. Wenger, G. R.; Wright, D., Disruption of performance under titrating matching to sample schedule of reinforcement by drugs of abuse. *J. Pharmacol. Exp. Ther.* **1990**, 254, 258-269.
327. Mello, N. K., The effect of alcohol on short-term memory in rhesus monkeys. *Psychopharm. Bull.* **1971**, 8, 20-22.
328. Davis, M., The Role of the amygdala in fear-potentiated startle: implications for animal models of anxiety. *Trends Pharmacol. Sci.* **1992**, 13, 35-41.
329. LeDoux, J. E., Emotion: clues from the brain. *Ann. Rev. of Psychol* **1995**, 46, 209-235.
330. Lister, R. G., The amnesic action of benzodiazepines in man. *neurosci. Biobehav.* **1985**, 9, 87-94.
331. Tershner, S. A.; Helmstetter, F. J., Injections of corticotropin-releasing factor into the periaqueductal gray enhance Pavlovian fear conditioning. *Psychobiology* **1996**, 24, 49-56.
332. Bailey, D. J.; Kim, J.; Sun, W.; Thompson, R. F.; Helmstetter, F. J., Acquisition of fear conditioning in rats requires the synthesis of mRNA in the amygdala. *Behav. Neurosci.* **1999**, 113, 275-282.

333. Knight, D.; Smith, C.; Stein, E.; Helmstetter, F. J., Functional MRI of human Pavlovian fear conditioning: patterns of activation as a function of learning. *Neuroreport* **1999**, 10, 3665-3670.
334. Savic, M. M.; Obradovic, D. I.; Ugresic, N. D.; Cook, J. M.; Sarma, P.; Bokonjic, D. R., Bidirectional effects of benzodiazepine binding site ligands on active avoidance acquisition and retention: differential antagonism by flumazenil and beta-CCt. *Psychopharmacology* **2005**, 180, (3), 455-465.
335. Savic, M. M.; Obradovic, D. I.; Ugresic, N. D.; Cook, J. M.; Yin, W. Y.; Bokonjic, D. R., Bidirectional effects of benzodiazepine binding site ligands in the elevated plus-maze: differential antagonism by flumazenil and beta-CCt. *Pharmacology Biochemistry and Behavior* **2004**, 79, (2), 279-290.
336. Atack, J., Anxiolytic compounds acting at the GABA(A) receptor benzodiazepine binding site. *CNS Neur. Dis.* **2003**, 2, 213-232.
337. Greenberg, P. E.; Sisitsky, T.; Kessler, R. C.; Finkelstein, S. N.; Berndt, E. R.; Davidson, J. R. T.; Ballenger, J. C.; Fyer, A. J., The economic burden of anxiety disorders in the 1990's. *J. Clin. Psychiatry* **1999**, 60, 427-435.
338. Basile, A. S.; Lippa, A. S.; Skolnick, P., Anxiolytic compounds: can less be more? *Eur. J. Pharmacol.* **2004**, 500, (1-3), 441-451.
339. Goddard, A.; Mason, G. F.; Rothman, D.; Behar, K.; Petroff, O.; Krystal, J. H., Family psychopathology and magnitude of reductions in occipital cortex GABA levels in panic disorder. *Neuropsychopharm.* **2004**, 29, 639-40.
340. Baneijee, P. K.; Tillakaratne, N.; Brailowsky, S.; Olsen, R. W.; Tobin, A. J.; Snead, O. C., Alterations in GABA(A) receptor alpha1 and alpha4 subunit mRNA levels in thalamic relay nuclei following absence-like seizures in rats. *Exp. Neurology* **1998**, 154, 213-223.
341. Homanics, G. E.; DeLorey, T. M.; Firestone, L. L.; Quinlan, J. J.; Handforth, A.; Harrison, N. L.; Krasowski, M. D.; Rick, C. E. M.; Korpi, E. R.; Makela, R.; Brilliant, M. H.; Hagiwara, N.; Ferguson, C.; Snyder, K.; Olsen, R. W., Mice devoid of gamma-aminobutyrate type A receptor beta 3 subunit have epilepsy, cleft palate, and hypersensitive behavior. *Proc. Natl. Acad. Sci. U.S.A.* **1997**, 94, (8), 4143-4148.
342. Crestani, F.; Matthias, L.; Baer, K.; Essrich, C.; Benke, D.; Laurent, J.; Belzung, C.; Fritschy, J. M.; Luschen, B.; Mohler, H., Decreased GABA(A)-receptor clustering results in enhanced anxiety and a bias for threat cues. *Nature* **1999**, 2, 833-839.
343. Benes, F. M.; Wickramasinghe, R.; Vincent, S. L.; Khan, Y.; Todtenkopf, M., Uncoupling of GABA(A) and benzodiazepine receptor binding activity in the

- hippocampal formation of schizophrenic brain. *Brain Research* **1997**, 755, (1), 121-129.
344. Mahmoudi, M.; Kang, M. H.; Tillakaratne, N.; Tobin, A. J.; Olsen, R. W., Chronic intermittent ethanol treatment in rats increases GABA(A) receptor alpha 4-subunit expression: Possible relevance to alcohol dependence. *J. Neurochem.* **1997**, 68, (6), 2485-2492.
345. DeLorey, T. M.; Handforth, A.; Anagnostaras, S. G.; Homanics, G. E.; Minassian, B. A.; Asatourian, A.; Fanselow, M. S.; Delgado-Escueta, A.; Ellison, G. D.; Olsen, R. W., Mice lacking the beta3 subunit of the GABA(A) receptor have the epilepsy phenotype and many of the behavioral characteristics of Angelman syndrome. *J Neurosci* **1998**, 18, (20), 8505-14.
346. Blue, M.; Sakkubai, N.; Johnston, M., Altered development of glutamate and GABA receptors in the basal ganglia of girls with Rhetts Syndrome. *Exp. Neurology* **1999**, (156), 345-352.
347. Leshner, A., Drug abuse and mental disorders: comorbidity is reality. *NIDA Notes* **1999**, 14, 3-4.
348. Roberts, E., *Adventures with GABA: Fifty Years On*. In *GABA in the nervous system: the view at fifty years*. Lippincott Williams & Wilkins: Philadelphia, **2000**.
349. Bazemore, A. W.; Elliott, K. A. C.; Florey, E., Isolation of factor I. *J. Neurochem.* **1957**, 1, 334-339.
350. Del Castillo, J.; Morales, T.; Sanchez, V., Action of piperazine on the neuromuscular system of *Ascaris lumbricoides*. *Nature* **1963**, 200, 706-707.
351. Jorgensen, E. M., GABA. In *GABA Wormbook*, Community, T. C. e. R., Ed. WormBook, doi/10.1895/wormbook.1.14.1, <http://www.wormbook.org>; 2005.
352. Schuske, K.; Beg, A. A., The GABA nervous system in *C. elegans*. *Trends Neurosci* **2004**, 27, 407-414.
353. Möhler, H.; Okada, T., Benzodiazepine receptor: demonstration in the central nervous system. *Science* **1977**, 198, 849.
354. Squires, R. F.; Braestrup, C., Benzodiazepine receptors in rat brain. *Nature* **1977**, 266, 732-734.
355. Bertilsson, L., Mechanism of action of benzodiazepines - the GABA hypothesis *Acta Psychiatr Scand Suppl* **1978**, 274, 19-26.
356. Squires, R., *GABA and Benzodiazepine Receptors*. CRC Press: Boca Raton, Florida, **1988**; Vol. 1-2.
357. Sternbach, L. H.; Fryer, R.I.; Metlesics, W.; Reeder, E.; Sach, G.; Saucy, G., and Stempel, A., Quinazolines and 1,4-benzodiazepines. VI. Halo-, methyl-, and methoxy-substituted 1,3,-dihydro-5-phenyl-2H-1,4-benzodiazepin-2-ones. *J. Org. Chem.* **1962**, 27, (11), 3788-3796.

358. Gu, Z. Q.; Wong, G.; Dominguez, C.; Decosta, B. R.; Rice, K. C.; Skolnick, P., Synthesis and evaluation of imidazo[1,5-a][1,4]benzodiazepine esters with high affinities and selectivities at diazepam-insensitive benzodiazepine receptors. *J. Med. Chem.* **1993**, 36, (8), 1001-1006.
359. Delorey, T. M. Unpublished data. **2005**.
360. Skolnick, P.; Hu, R. J.; Cook, C. M.; Hurt, S. D.; Trometer, J. D.; Liu, R.; Huang, Q.; Cook, J. M., [³H]RY-80: A high affinity, selective ligand for GABA(A) receptors containing $\alpha 5$ subunits. *J. Pharmacol. Exp. Ther.* **1997**, 283, 488-495.
361. Venault, P.; Chapouthier, G.; de Carvalho, L. P.; Simiand, J.; Morre, M.; Dodd, R. H.; Rossier, J., *Nature* **1986**, 321, 864-866.
362. Jensen, L. H.; Stephens, D. N.; Sarter, M.; Petersen, E., Bidirectional effects of beta-carbolines and benzodiazepines on cognitive processes. *Brain Res. Bull.* **1987**, 9, 359-364.
363. Dorow, R.; Horowitz, B.; Paschelke, G.; Amin, M., Severe anxiety induced by FG 7142, a beta-carboline ligand for benzodiazepine receptors. *Lancet* **1983**, 2, 98-9.
364. Duka, T.; Ott, H.; Rohloff, A.; Voet, B., The effects of a benzodiazepine receptor antagonist beta-carboline ZK-93426 on scopolamine-induced impairment on attention, memory and psychomotor skills. *Psychopharmacology* **1996**, 123, 361-373.
365. Benson, J. A.; Low, K.; Keist, R.; Mohler, H.; Rudolph, U., Pharmacology of recombinant gamma-aminobutyric acid(A) receptors rendered diazepam-insensitive by point-mutated alpha-subunits. *FEBS Lett.* **1998**, 431, (3), 400-404.
366. Rudolph, U.; Crestani, F.; Benke, D.; Brunig, I.; Benson, J. A.; Fritschy, J. M.; Martin, J. R.; Bluethmann, H.; Mohler, H., Benzodiazepine actions mediated by specific gamma-aminobutyric acid(A) receptor subtypes. *Nature* **1999**, 401, (6755), 796-800.
367. Pirker, S.; Schwarzer, C.; Wieselthaler, A.; Sieghart, W.; Sperk, G., GABA(A) receptors: Immunocytochemical distribution of 13 subunits in the adult rat brain. *Neuroscience* **2000**, 101, (4), 815-850.
368. Izquierdo, I.; Medina, J. H.; Vianna, M. R.; Izquierdo, L. A.; Barros, D. M., Separate mechanisms for short-and long-term memory. *Behav. Brain Res* **1999**, 103, 1-11.
369. Atack, J.; Bayley, P. J.; Seabrook, G.; Wafford, K. A.; McKernan, R.; Dawson, G. R., L-655,708 enhances cognition in rats but is not proconvulsant at a dose selective for alpha5-containing GABA(A) receptors. *Neuropharmacology* **2006**, 51, 1023-1029.

370. Collinson, N.; Atack, J.; Laughton, D. L.; Dawson, G. R.; Stephens, D. N., An inverse agonist selective for alpha5 subunit containing GABA(A) receptors improves encoding and recall but not consolidation in the Morris water maze. *Psychopharmacology* **2006**, 188, 619-628.
371. Dawson, G. R.; Maubach, K. A.; Collinson, N.; Cobain, M.; Everitt, B. J.; MacLeod, A. M.; Choudhury, H. I.; McDonald, L. M.; Pillai, G.; Rycroft, W.; Smith, A. J.; Sternfeld, F.; Tattersall, F. D.; Wafford, K. A.; Reynolds, D. S.; Seabrook, G. R.; Atack, J. R., An inverse agonist selective for alpha 5 subunit-containing GABA(A) receptors enhances cognition. *J. Pharmacol. Exp. Ther.* **2006**, 316, (3), 1335-1345.
372. Nutt, D.; Besson, M.; Wilson, S. J.; Dawson, G. R.; Lingford-Hughes, A., Blockade of alcohol's amnestic activity in humans by an alpha5 subtype benzodiazepine receptor inverse agonist. *Neuropharmacology* **2007**, 53, 810-820.
373. Fisher, B. D.; Licata, S. C.; Zhou, H.; Edwankar, R.; Wang, Z.; Huang, S.; HE, X.; Yu, J.; Cook, J. M.; Furtmueller, R.; Sieghart, W.; Roth, B. L.; Majumder, S.; Rowlett, J. K., Anxiolytic-like effect of 8-acetylene imidazobenzodiazepines in a rhesus monkey conflict procedure. *Neuropharmacology* **2010**, 59, 612-618.
374. File, S. E.; Pellow, S., Low and high doses of benzodiazepine receptor inverse agonists respectively improve and impair performance in passive avoidance but do not affect habituation. *Behav. Brain Res* **1988**, 30, 31-36.
375. Savic, M. M.; Obradovic, D. I.; Ugresic, N. D.; Cook, J. M.; Yin, W. Y.; Bokonjic, D. R., Bidirectional effects of benzodiazepine binding site ligands in the passive avoidance task: differential antagonism by flumazenil and beta-CCt. *Behavioural Brain Research* **2005**, 158, (2), 293-300.
376. Izquierdo, I.; Medina, J. H., Memory formation: the sequence of biochemical events in the hippocampus and its connection to activity in other brain structures. *Neurobiol. Learn. Mem.* **1997**, 68, 285-316.
377. Squire, L. R., Memory and the hippocampus- a synthesis from findings with rats, monkeys, and humans. *Psychol. Rev.* **1992**, 99, 195-231.
378. Gray, J. A.; McNaughton, N., Comparison between the behavioral affects of septal and hippocampal lesions: A review. *Neurosci. Biobehav.* **1983**, Rev. 7, 119-188.
379. McGaugh, J. L., The amygdala modulates the consolidation of memories of emotionally arousing experiences. *Annu. Rev. Neurosci.* **2004**, 27, 1-28.
380. Fujimura, J.; Nagano, M.; Suzuki, H., Differential expression of GABA(A) receptor subunits in the distinct nuclei of the rat amygdala. *Molecular Brain Research* **2005**, 138, (1), 17-23.

381. Yee, B. K.; Hauser, J.; Dolgov, V. V.; Keist, R.; Mohler, H.; Rudolph, U.; Feldon, J., GABA receptors containing the alpha5 subunit mediate the trace effect in aversive and appetitive conditioning and extinction of conditioned fear. *Eur. J. Neurosci.* **2004**, 20, 1928-1936.
382. Navarro, J. F.; Buron, E.; Martin-Lopez, M., Anxiogenic-like activity of L-655,708, a selective ligand for the benzodiazepine site of GABA(A) receptors which contain the alpha-5 subunit, in the elevated plus-maze test. *Progress in Neuro-Psychopharmacology & Biological Psychiatry* **2002**, 26, (7-8), 1389-1392.
383. Atack, J. R.; Hutson, P. H.; Collinson, N.; Marshall, G.; Bentley, G.; Moyes, C.; Cook, S. M.; Collins, I.; Wafford, K.; McKernan, R. M.; Dawson, G. R., Anxiogenic properties of an inverse agonist selective for alpha 3 subunit-containing GABA(A) receptors. *Br. J. Pharmacol.* **2005**, 144, (3), 357-366.
384. Jaskiw, G. E.; Lipska, B. K.; Weinberger, D. R., The anxiogenic beta-carboline FG-7142 inhibits locomotor exploration similarly in postweaning and adult rats. *Neurosci. Lett.* **2003**, 346, 5-8.
385. Savic, M. M.; Obradovic, D. I.; Ugresic, N. D.; Cook, J. M.; Yin, W.; Van Linn, M.; Bokonic, D. R., Benzodiazepine site inverse agonists and locomotor activity in rats: bimodal and biphasic influence. *Pharmacol. Biochem. Behav.* **2006**, 84, 35-42.
386. Low, K.; Crestani, F.; Keist, R.; Benke, D.; Brunig, I.; Benson, J., Molecular and neuronal substrate for the selective attenuation of anxiety. *Science* **2000**, 290, 131-134.
387. Atack, J. R.; Wafford, K. A.; Tye, S. J.; Cook, S. M.; Sohal, B.; Pike, A.; Sur, C.; Melillo, D.; Bristow, L.; Bromidge, F.; Ragan, I.; Kerby, J.; Street, L.; Carling, R.; Castro, J. L.; Whiting, P.; Dawson, G. R.; McKernan, R. M., TPA023 [7-(1,1-dimethylethyl)-6-(2-ethyl-2H-1,2,4-triazol-3-ylmethoxy)-3-(2-fluorophenyl)-1,2,4-triazolo[4,3-b]pyridazine], an agonist selective for alpha 2-and alpha 3-containing GABA(A) receptors, is a nonsedating anxiolytic in rodents and primates. *J. Pharmacol. Exp. Ther.* **2006**, 316, (1), 410-422.
388. Hauser, J.; Rudolph, U.; Keist, R.; Mohler, H.; Feldon, J.; Yee, B. K., Hippocampal alpha 5 subunit-containing GABA(A) receptors modulate the expression of prepulse inhibition. *Molecular Psychiatry* **2005**, 10, (2), 201-207.
389. Yamada, J.; Furukawa, K.; Ueno, S.; Yamamoto, S.; Fukuda, A., Molecular basis for the GABA(A) receptor-mediated tonic inhibition in rat somatosensory cortex. *Cereb. Cortex* **2007**, 17, (1782-1787).
390. Fuchs, K.; Zezula, J.; Slany, A.; Sieghart, W., Endogenous [H-3] Flunitrazepam binding in human embryonic kidney-cell line-293. *Eur. J. Pharmacol.-Mol. Pharmacol. Section* **1995**, 289, (1), 87-95.

391. Sigel, E., Properties of single sodium channels translated by *Xenopus* oocytes after injection with messenger ribonucleic acid. *J. Physiol.* **1987**, 386, 73-90.
392. Sigel, E.; Baur, R.; Trube, G.; Mohler, H.; Malherbe, P., The effect of subunit composition of rat brain GABA(A) receptors on channel function. *Neuron* **1990**, 5, (5), 703-11.
393. Sanger, D. J.; Morel, E.; Perrault, G., Comparison of the pharmacological profiles of the hypnotic drugs, zaleplon and zolpidem. *Eur J Pharmacol* **1996**, 313, 35-42.
394. Lader, M., Limitations on the use of benzodiazepines in anxiety and insomnia: are they justified? *Eur Neuropsychopharmacol* **1999**, 9, (Suppl 6), S399-405.
395. Rudolph, U.; Mohler, H., Analysis of GABA(A) receptor function and dissection of the pharmacology of benzodiazepines and general anesthetics through mouse genetics. *Annual Review of Pharmacology and Toxicology* **2004**, 44, 475-498.
396. Atack, J.; Bayley, P. J.; Fletcher, S. R.; McKernan, R.; Wafford, K. A.; Dawson, G. R., The proconvulsant effects of the GABA(A) $\alpha 5$ subtype selective compound RY-080 may not be $\alpha 5$ -mediated. *Eur J Pharmacol* **2006**, 548, 77-82.
397. Rudolph, U.; Mohler, H., GABA-based therapeutic approaches: GABA(A) receptor subtype functions. *Current Opinion in Pharmacology* **2006**, 6, (1), 18-23.
398. Licata, S. C.; Platt, D. M.; Cook, J. M.; Sarma, P. S.; Griebel, G.; Rowlett, J. K., Contribution of GABA(A) receptor subtypes to the anxiolytic-like, motor, and discriminative stimulus effects of benzodiazepines: studies with the functionally selective ligand SL651498 [6-fluoro-9-methyl-2-phenyl-4-(pyrrolidin-1-yl-carbonyl)-2,9-dihydro-1H-pyridol[3,4-b]indol-1-one]. *J. Pharmacol. Exp. Ther.* **2005**, 313, 1118-1125.
399. Whiting, P. J., GABA-A receptors: a viable target for novel anxiolytics? *Current Opinion in Pharmacology* **2006**, 6, (1), 24-29.
400. Crestani, F.; Martin, J. R.; Mohler, H.; Rudolph, U., Resolving differences in GABA(A) receptor mutant mouse studies. *Nat. Neurosci.* **2000**, 3, 1059.
401. Facklam, M.; Schoch, P.; Bonetti, E. P.; Jenck, F.; Martin, J. R.; Moreau, J., Relationship between benzodiazepine receptor occupancy and functional effects in vivo of four ligands of differing intrinsic efficacies. *J. Pharmacol. Exp. Ther.* **1992**, 261, 1113-21.

402. Savic, M. M.; Obradovic, D. I.; Ugresic, N. D.; Bokonic, D. R., The influence of diazepam on atropine reversal of behavioural impairment in dichlorvos-treated rats. *Pharmacol. Toxicol.* **2003**, 93, 211-218.
403. Bourin, M.; Briley, M., Sedation, an unpleasant, undesirable and potentially dangerous side-effect of many psychotropic drugs. *Hum. Psychopharmacol.* **2004**, 19, 135-139.
404. Vogel, H., *Drug discovery and evaluation*. Springer: Berlin, **2002**.
405. Dailly, E.; Hascoet, M.; Colombel, M. C.; Joliet, P.; Bourin, M., Relationship between cerebral pharmacokinetics and anxiolytic activity of diazepam and its active metabolites after a single intraperitoneal administration of diazepam in mice. *Hum. Psychopharmacol.* **2002**, 17, 239-245.
406. Savic, M. M.; Obradovic, D. I.; Ugresic, N. D.; Cook, J. M.; Yin, W.; Van Linn, M., Benzodiazepine site inverse agonists and locomotor activity in rats: bimodal and biphasic influence. *Pharmacol. Biochem. Behav.* **2006**, 84, 35-42.
407. Kelley, A. E., Locomotor activity and exploration. In *Techniques in the behavioral and neural sciences. vol. 10. Methods in behavioral pharmacology*, van Haaren, F., Ed. Elsevier: New York, **1993**; Vol. 10, pp 499-518.
408. Jennings, A. S. R.; Lewis, R. T.; Russell, M. G. N.; Hallett, D. J.; Street, L. J.; Castro, J. L.; Attack, J. R.; Cook, S. M.; Lincoln, R.; Stanley, J.; Smith, A. J.; Reynolds, D. S.; Sohal, B.; Pike, A.; Marshall, G. R.; Wafford, K. A.; Sheppard, W. F. A.; Tye, S. J., Imidazo[1,2-b][1,2,4]triazines as $\alpha 2/\alpha 3$ subtype selective GABA(A) agonists for the treatment of anxiety. *Bioorg. Med. Chem. Lett.* **2006**, 16, (6), 1477-1480.
409. Russell, M. G. N.; Carling, R. W.; Street, L. J.; Hallett, D. J.; Goodacre, S.; Mezzogori, E.; Reader, M.; Cook, S. M.; Bromidge, F. A.; Newman, R.; Smith, A. J.; Wafford, K. A.; Marshall, G. R.; Reynolds, D. S.; Dias, R.; Ferris, P.; Stanley, J.; Lincoln, R.; Tye, S. J.; Sheppard, W. F. A.; Sohal, B.; Pike, A.; Dominguez, M.; Attack, J. R.; Castro, J. L., Discovery of imidazo[1,2-b][1,2,4]triazines as GABA(A) $\alpha 2/3$ subtype selective agonists for the treatment of anxiety. *J. Med. Chem.* **2006**, 49, (4), 1235-1238.
410. Attack, J.; Pike, A.; Marshall, G.; Stanley, J.; Lincoln, R.; Cook, S. M., The in vivo properties of pagoclone in rat are most likely mediated by 5'-hydroxy pagoclone. *Neuropharmacology* **2006**, 50, 677-689.
411. de Haas, S. L.; de Visser, S. J.; van der Post, J. P.; de Smet, M.; Schoemaker, R. C.; Rijnbeek, B., Pharmacodynamic and pharmacokinetic effects of TPA023, a GABA(A) $\alpha 2/3$ subtype selective agonist, compared to lorazepam and placebo in healthy volunteers. *J Psychopharmacol* **2007**, 21, 374-83.

412. Markou, A.; Chiamulera, C.; Geyer, M. A.; Tricklebank, M.; Steckler, T., Removing obstacles in neuroscience drug discovery: the future path for animal models. *Neuropsychopharmacol* **2009**, *34*, 74-89.
413. Lippa, A.; Czobor, P.; Stark, J.; Beer, B.; Kostakis, E.; Gravielle, M.; Bandyopadhyay, S.; Russek, S. J.; Gibbs, T. T.; Farb, D. H.; Skolnick, P., Selective anxiolysis produced by ocinaplon, a GABA(A) receptor modulator. *Proc. Natl. Acad. Sci. U.S.A.* **2005**, *102*, (20), 7380-7385.
414. Popik, P.; Kostakis, E.; Krawczyk, M.; Nowak, G.; Szewczyk, B.; Krieter, P., The anxiolytic agent 7-(2-chloropyridin-4-yl)pyrazolo-[1,5-a]-pyrimidin-3-yl(pyridin-2-yl)methanone (DOV 51892) is more efficacious than diazepam at enhancing GABA-gated currents at $\alpha 1$ subunit containing GABA(A) receptors. *J Pharmacol Exp Ther* **2006**, *319*, 1244-52.
415. Berezhnoy, D.; Gravielle, M.; Downing, S.; Kostakis, E.; Basile, A. S.; Skolnick, P., Pharmacological Properties of DOV 315,090, an ocinaplon metabolite. *Pharmacol.* **2008**, *8*, 11.
416. Savic, M. M.; Clayton, T.; Furtmueller, R.; Gavrilovic, I.; Samardzic, J.; Savic, S.; Huck, S.; Sieghart, W.; Cook, J. M., PWZ-029, a compound with moderate inverse agonist functional selectivity at GABA-A receptors containing $\alpha 5$ subunits, improves passive, but not active, avoidance learning in rats. *Brain Res.* **2008**, *1208*, (1), 150-159.
417. Hadingham, K. L.; Wingrove, P.; Lebourdelles, B.; Palmer, K. J.; Ragan, C. I.; Whiting, P. J., Cloning of c-dna sequences encoding human α -2 and α -3 gamma-aminobutyric acid(A) receptor subunits and characterization of the benzodiazepine pharmacology of recombinant α -1-containing, α -2-containing, α -3-containing, and α -5-containing human gamma-aminobutyric Acid(a) receptors. *Mol. Pharmacol.* **1993**, *43*, (6), 970-975.
418. Sanna, E.; Busonero, F.; Talani, G.; Carta, M.; Massa, F.; Peis, M.; Maciocco, E.; Biggio, G., Comparison of the effects of zaleplon, zolpidem, and triazolam at various GABA(A) receptor subtypes. *Eur. J. Pharmacol.* **2002**, *451*, (2), 103-110.
419. Savic, M. M.; Milinkovic, M. M.; Rallapalli, S.; Clayton, T. S.; Joksimovic, S. M.; Van Linn, M., The differential role of $\alpha 1$ - and $\alpha 5$ -containing GABA(A) receptors in mediating diazepam effects on spontaneous locomotor activity and water-maze learning and memory in rats. *Int J Neuropsychopharmacol* **2009**, *12*, 1179-93.
420. Choudhary, M. S., Craig, S., Roth, B.L., Identification of receptor domains that modify ligand binding to 5-hydroxytryptamine 2 and 5-hydroxytryptamine 1c serotonin receptors. *Mol. Pharmacol.* **1992**, *42*, (4), 627-633.

421. Terry, J. A. V., *Spatial navigation (water maze) tasks*. . CRC Press: Boca Raton, **2000**; p 153-166.
422. Vorhees, C. V.; Williams, M. T., Morris water maze: procedures for assessing spatial and related forms of learning and memory. *Nat Protoc* **2006**, 1, 848-58.
423. Pike, A.; Cook, S. M.; Watt, A. P.; Scott-Stevens, P.; Rosahl, T.; McKernan, R., Contribution of specific binding to the central benzodiazepine site to the brain concentrations of two novel benzodiazepine site ligands. *Biopharm Drug Dispos* **2007**, 28, 275-82.
424. Wang, J.; Shen, X.; Fenyk-Melody, J.; Pivnichny, J. V.; Tong, X., Simple and sensitive liquid chromatography/tandem mass spectroscopy method for determination of diazepam and its major metabolites in rat cerebrospinal fluid. *Rapid Commun Mass Spectrom* **2003**, 17, 519-25.
425. Rodgers, R. J.; Johnson, N. J., Factor analysis of spatiotemporal and ethological measures in the murine elevated plus-maze test of anxiety. *Pharmacol Biochem Behav* **1995**, 52, 297-303.
426. Cruz, A. P.; Frei, F.; Graeff, F. G., Ethopharmacological analysis of rat behavior on the elevated plus maze. *Pharmacol Biochem Behav* **1994**, 49, (171-6).
427. Grimwood, S.; Hartig, W., Target site occupancy: Emerging generalizations from clinical and preclinical studies. *Pharmacol. Ther* **2009**, 122, 281-301.
428. Kralic, J. E.; O'Buckley, T. K.; Khisti, R. T.; Hodge, C. W.; Homanics, G. E.; Morrow, A. L., GABA(A) receptor alpha-1 subunit deletion alters receptor subtype assembly, pharmacological and behavioral responses to benzodiazepines and zolpidem. *Neuropharmacology* **2002**, 43, (4), 685-694.
429. McNamara, R. K.; Skelton, R. W., Diazepam impairs acquisition but not performance in the Morris water maze. *Pharmacol Biochem Behav* **1991**, 38, 651-8.
430. Cain, D. P., Testing the NMDA, long-term potentiation, and cholinergic hypotheses of spatial learning. *Neurosci Biobehav Rev* **1998**, 22, 181-93.
431. Erez, M.; Takemori, A. E.; Portoghese, P. S., Narcotic antagonist potency of bivalent ligands which contain β -naltrexamine. *J. Med. Chem.* **1982**, 25, 847-849.
432. Portoghese, P. S.; Larson, D. L.; Yim, C. B.; Sayre, L. M.; Ronsisvalle, G.; Lipkowski, A. W.; Takemori, A. E.; Rice, K. C.; Tam, S. W., Stereostructure-activity relationship of opioid agonist and antagonist bivalent ligands. Evidence for bridging between vicinal opioid receptors. *J. Med. Chem.* **1985**, 28, 1140-1141.
433. Portoghese, P. S.; Larson, D. L.; Sayre, L. M.; Yim, C. B.; Ronsisvalle, G.; Tam, S. W.; Takemori, A. E., Opioid agonist and antagonist bivalent ligands. The

relationship between spacer length and selectivity at multiple opioid receptors. *J. Med. Chem.* **1986**, 29, 1855-1861.

434. Roth, B. unpublished results, **2006**.

435. *Burger's Medicinal Chemistry & Drug Discovery*. 6 ed.; John Wiley & Sons Inc.: **2003**; Vol. 1.

436. Eliel, E. L.; Wilen, S. H., *Stereochemistry of Organic Compounds*. Wiley-Interscience: New York, **1994**.

437. Flory, P. J., *Statistical Mechanics of Chain Molecules*. Interscience Publishers: New York, **1968**.

438. Lemieux, R. U., *Molecular Rearrangement*. Interscience Publishers: New York, **1964**.

439. Eliel, E. L., Conformational analysis in saturated heterocyclic compounds. *Acc. Chem. Res.* **1970**, 3, 1-8.

440. Graczyk, P. P.; Mikolajczyk, M., *Topics in Stereochemistry*. John Wiley & Sons: New York, **1994**; Vol. 21.

441. Hutchins, R. O.; Kopp, L. D.; Eliel, E. L., Repulsion of syn-axial electron pairs. The rabbit-ear effect. *J. Am. Chem. Soc.* **1968**, 90, 7174-7175.

442. Eliel, E. L.; Giza, C. A., Conformational analysis. XVII. 2-Alkoxy- and 2-alkylthiotetrahydropyrans and 2-alkoxy-1,3-dioxanes. Anomeric effect. *J. Org. Chem.* **1968**, 33, 3754-3758.

443. Uchida, T.; Kurita, Y.; Kubo, M., The dipole moments and the structures of polyoxymethylene dimethyl ethers. *J. Polym. Sci.* **1956**, 19, 365-372.

444. Abe, A.; Mark, J. E., Conformational energies and the random-coil dimensions and dipole moments of the polyoxides $\text{CH}_3\text{O}[(\text{CH}_2)_y\text{O}]_x\text{CH}_3$. *J. Am. Chem. Soc.* **1976**, 98, 6468-6476.

445. Ohsaku, M., Electronic Structures and Conformations of Polyoxymethylene and Polyoxyethylene. *Macromolecules* **1978**, 11, 970-976.

446. Wolfe, S., Gauche effect. Stereochemical consequences of adjacent electron pairs and polar bonds. *Acc. Chem. Res.* **1972**, 5, 102-111.

447. Jaffe, R. J.; Smith, G. D.; Yoon, D. Y., Conformation of 1,2-dimethoxyethane from ab initio electronic structure calculations. *Phys. Chem.* **1993**, 97, 12745-12751.

448. Bultinck, P.; Van Alsenoy, C.; Goeminne, A., Theoretical conformational analysis of 1,3-dimethoxypropane and 14-crown-4: importance of stabilizing intramolecular interactions. *J. Phys. Chem.* **2001**, 105, 9203-9210.

449. Bultinck, P.; Goeminne, A.; Van de Vondel, D., Ab initio and molecular mechanics study of 1,2-dimethoxyethane and 12-crown-4. *J. Mol. Struct.* **1999**, 467, 211.

450. Glendening, E. D.; Feller, D.; Thompson, M. A., An ab initio investigation of the structure and alkali metal cation selectivity of 18-crown-6. *J. Am. Chem. Soc.* **1994**, 116, 10657-10669.
451. Glasstone, S.; Laidler, K. J.; Eyring, H., *The Theory of Rate Processes*. McGraw-Hill: New York, **1941**.
452. Azumaya, I.; Uchida, I.; Kato, T.; Yokoyama, A.; Tanatani, A.; Takayanagi, H.; Yokozawa, T., Aromatic-aromatic-interaction array communication. *Angew. Chem. Int. Ed.* **2004**, 43, 1360-1363.
453. Rashkin, M. J.; Waters, M. L., Unexpected substituent effects in offset π - π stacked interactions in water. *J. Am. Chem. Soc.* **2002**, 124, 1860-1861.
454. Tsuzuki, S.; Honda, K.; Uchimaru, T.; Mikami, M.; Tanabe, K., Origin of attraction and directionality of the π/π interaction: Model chemistry calculations of benzene dimer interaction. *J. Am. Chem. Soc.* **2002**, 124, 104-112.
455. Hobza, P.; Selzle, H. L.; Schlag, E. W., Potential energy surface of the benzene dimer: ab initio theoretical study. *J. Am. Chem. Soc.* **1994**, 116, 3500-3506.
456. Burley, S. K.; Petsko, G. A., Aromatic-aromatic interaction: A mechanism of protein structure stabilization. *Sci.* **1985**, 229, 23-28.
457. Fryer, R. I.; Schmidt, R.A.; Sternbach, L.H., Quinazoines + 1,4-benzodiazepines. 17. Synthesis of 1,3-dihydro-5-pyridyl-2H-1,4-benzodiazepine derivatives. *J. Pharm. Sci.* **1964**, 53, 264-268.
458. Fryer, R. I.; Zhang, P.; Lin, K.-Y.; Upasani, R. B.; Wong, G.; Skolnick, P., Conformational similarity of diazepam-sensitive and -insensitive benzodiazepine receptors determined by chiral pyrroloimidazobenzodiazepines. *Med. Chem. Res.* **1993**, 3, 183-191.
459. Costa, E.; Guidotti, A., Benzodiazepines on trial: a research strategy for their rehabilitation. *Trends Pharmacol Sci* **1996**, 17, (5), 192-200.
460. Chen, S. W.; Chen, H. A.; Davies, M. F.; Loew, G. H., Putative benzodiazepine partial agonists demonstrate receptor heterogeneity. *Pharmacol Biochem. Behav.* **1996**, 53, (1), 87-97.
461. DeLorey, T.; Lin, R.; McBrady, B.; He, X.; Cook, J.; Lamah, J.; Loew, G., Attenuation of scopolamine-induced impairment of fear conditioned contextual memory by ligands that bind to the benzodiazepine site on the GABA(A) receptor. *Eur J Pharmacol* **2001**, 426, 45-54.
462. Malizia, A. L.; Nutt, D. J., The effects of flumazenil in neuropsychiatric disorders. *Clin Neuropharmacol* **1995**, 18, (3), 215-32.
463. He, X.; Huang, Q.; Ma, C.; Yu, S.; McKernan, R.; Cook, J. M., Pharmacophore/receptor models for GABA(A)/BzR $\alpha 2\beta 3\gamma 2$, $\alpha 3\beta 3\gamma 2$ and $\alpha 4\beta 3\gamma 2$ recombinant subtypes. Included

- volume analysis and comparison to $\alpha 1\beta 3\gamma 2$, $\alpha 5\beta 3\gamma 2$, and $\alpha 6\beta 3\gamma 2$ subtypes. *Drug Des Discov* **2000**, 17, (2), 131-71.
464. McKernan, R. M.; Whiting, P. J., Which GABA(A) -receptor subtypes really occur in the brain? *Trends Neurosci.* **1996**, 19, (4), 139-43.
465. Mohler, H., GABA(A) receptor diversity and pharmacology. *Cell Tissue Res* **2006**, 326, (2), 505-16.
466. Quirk, K.; Gillard, N. P.; Ragan, C. I.; Whiting, P. J.; McKernan, R. M., γ -aminobutyric acid type A receptors in rat brain can contain both $\gamma 2$ and $\gamma 3$ subunits, but $\gamma 1$ does not exist in combination with another γ subunit. *Molecular Pharmacology* **1991**, 45, 1061-1070.
467. Maubach, K., GABA(A) receptor subtype selective cognition enhancers. *Curr Drug Targets CNS Neurol Disord* **2003**, 2, (4), 233-9.
468. Carling, R. W.; Moore, K. W.; Street, L. J.; Wild, D.; Isted, C.; Leeson, P. D.; Thomas, S.; O'Connor, D.; McKernan, R. M.; Quirk, K.; Cook, S. M.; Atack, J. R.; Wafford, K. A.; Thompson, S. A.; Dawson, G. R.; Ferris, P.; Castro, J. L., 3-Phenyl-6-(2-pyridyl)methoxy-1,2,4-triazolo[3,4-a]phthalazines and analogues: high-affinity gamma-aminobutyric acid-A benzodiazepine receptor ligands with $\alpha 2$, $\alpha 3$, and $\alpha 5$ -subtype binding selectivity over $\alpha 1$. *J Med Chem* **2004**, 47, (7), 1807-22.
469. Lehericy, S.; Hirsch, E.; Cervera-Pierot, P.; Hersh, L.; Bakchine, S.; Piette, F.; Duyckaerts, C.; Hauw, J.; Javoy-Agid, F.; Agid, Y., Heterogeneity and selectivity of the degeneration of cholinergic neurons in the basal forebrain of patients with Alzheimer's disease. *J Comp Neurol* **1993**, 330, 15-31.
470. Geula, C.; Mesulam, M., Systematic regional variations in the loss of cortical cholinergic fibers in Alzheimer's disease. *Cereb Cortex* **1996**, 6, 165-77.
471. Mestres, J.; Veeneman, G. H., Identification of "latent hits" in compound screening collections. *J Med Chem* **2003**, 46, (16), 3441-4.
472. Kubinyi, H., Strategies and recent technologies in drug discovery. *Pharmazie* **1995**, 50, (10), 647-62.
473. Flower, D. R., *Drug Design: Cutting Edge Approaches*. Royal Society of Chemistry: Cambridge, U.K., **2003**.
474. Antonini, I.; Polucci, P.; Magnano, A.; Cacciamani, D.; Konieczny, M. T.; Paradziej-Lukowicz, J.; Martelli, S., Rational design, synthesis and biological evaluation of thiadiazinoacridines: a new class of antitumor agents. *Bioorg Med Chem* **2003**, 11, (3), 399-405.
475. Wlodawer, A., Rational approach to AIDS drug design through structural biology. *Annu Rev Med* **2002**, 53, 595-614.

476. Barreca, M. L.; Gitto, R.; Quartarone, S.; De Luca, L.; De Sarro, G.; Chimirri, A., Pharmacophore modeling as an efficient tool in the discovery of novel noncompetitive AMPA receptor antagonists. *J Chem Inf Comput Sci* **2003**, 43, (2), 651-655.
477. Filizola, M.; Harris, D. L.; Loew, G. H., Development of 3D pharmacophore for non-specific ligand recognition of α_1 , α_2 , α_5 , and α_6 containing GABA(A) /benzodiazepine receptors. *Bioorg. Med. Chem.* **2000**, 8, 1799-1807.
478. Huang, P.; Loew, G. H.; Funamizu, H.; Mimura, M.; Ishiyama, N.; Hayashida, M.; Okuno, T.; Shimada, O.; Okuyama, A.; Ikegami, S.; Nakano, J.; Inoguchi, K., Rational design, discovery, and synthesis of a novel series of potent growth hormone secretagogues. *J Med Chem* **2001**, 44, (24), 4082-91.
479. Dekermendjian, K.; Kahnberg, P.; Witt, M.-R.; Sterner, O.; Nielsen, M.; Liljefors, T., Structure-activity relationships and molecular modeling analysis of flavanoids binding to the benzodiazepine site of the rat brain GABA(A) receptor complex. *J. Med. Chem.* **1999**, 42, 4343-4350.
480. Harris, D. L.; Loew, G. H., Development and assessment of a 3D pharmacophore for ligand recognition of BDZR/GABA(A) receptors initiating the anxiolytic response. *Bioorg. Med. Chem.* **2000**, 8, 2527-2538.
481. Trudell, M. L.; Basile, A. S.; Shannon, H. E.; Skolnick, P.; Cook, J. M., Synthesis of 7,12-dihydropyrido[3,4-B-5,4-B']diindoles - a novel class of rigid, planar benzodiazepine receptor ligands. *J. Med. Chem.* **1987**, 30, (3), 456-458.
482. Filizola, M.; Harris, D. L.; Loew, G. H., Benzodiazepine-induced hyperphagia: Development of a 3D pharmacophore by computational methods. *J. Biomol. Struct. & Design* **2000**, 17, 1-10.
483. Pirker, S.; Schwarzer, C.; Wieselthaler, A.; Sieghart, W.; Sperk, G., GABA(A) receptors: immunocytochemical distribution of 13 subunits in the adult rat brain. *Neuroscience* **2000**, 101, (4), 815-50.
484. Albaugh, P. A.; Marshall, L.; Gregory, J.; White, G.; Hutchison, A.; Ross, P. C.; Gallagher, D. W.; Tallman, J. F.; Crago, M.; Cassella, J. V., Synthesis and biological evaluation of 7,8,9,10-tetrahydroimidazo[1,2-c]pyrido[3,4-e]pyrimidin-5(6H)-ones as functionally selective ligands of the benzodiazepine receptor site on the GABA(A) receptor. *J Med Chem* **2002**, 45, (23), 5043-51.
485. Bennett, D. A., Pharmacology of the pyrazolo-type compounds: agonist, antagonist and inverse agonist actions. *Physiol Behav* **1987**, 41, (3), 241-5.
486. Davies, M. F.; Onaivi, E. S.; Chen, S. W.; Maguire, P. A.; Tsai, N. F.; Loew, G. H., Evidence for central benzodiazepine receptor heterogeneity from behavior tests. *Pharmacol. Biochem. Behav.* **1994**, 49, (1), 47-56.

487. File, S. E., Proconvulsant action of CGS 8216. *Neurosci Lett* **1983**, 35, (3), 317-20.
488. Harris, D. L.; Clayton, T.; Cook, J. M.; Peyman, S.; Halliwell, R. F.; Furtmueller, R.; Huck, S.; Sieghart, W.; Delorey, T. M., Selective influence on contextual memory: physiochemical properties associated with selectivity of benzodiazepine ligands at GABA(A) receptors containing the alpha5 subunit. *J. Med. Chem.* **2008**, 51, (13), 3788-3803.
489. Delorey, T. M. **2006**.
490. Mohler, H.; Crestani, F.; Rudolph, U., GABA(A)-receptor subtypes: a new pharmacology. *Curr Opin Pharmacol* **2001**, 1, (1), 22-5.
491. Renard, S.; Olivier, A.; Granger, P.; Avenet, P.; Graham, D.; Sevrin, M.; George, P.; Besnard, F., Structural elements of the gamma-aminobutyric acid type A receptor conferring subtype selectivity for benzodiazepine site ligands. *J Biol Chem* **1999**, 274, (19), 13370-4.
492. Verloop, A.; Hoogenstraaten, W.; Tipker, J., *Development and Application of New Substituent Parameters in Drug Design*. Academic Press: New York, **1976**.
493. Klebe, G.; Abraham, U., Comparative molecular similarity index analysis (CoMSIA) to study hydrogen-bonding properties and to score combinatorial libraries. *J Comput Aided Mol Des* **1999**, 13, (1), 1-10.
494. Klebe, G.; Abraham, U.; Meitzner, T., Molecular similarity indices in a comparative analysis (CoMSIA) of drug molecules to correlate and predict their biological activity. *J. Med. Chem.* **1994**, 37, 4130-4136.
495. Kubinyi, H.; Hamprecht, F. A.; Mietzner, T., Three-dimensional quantitative similarity-activity relationships (3D QSiAR) from SEAL similarity matrices. *J Med Chem* **1998**, 41, (14), 2553-64.
496. Kantola, A.; Villar, H. O.; Loew, G. H., Atom based parameterization of a conformationally dependent hydrophobic index. *J. Comput. Chem.* **1991**, 12, 681-689.
497. Chambers, M. S.; Atack, J. R.; Carling, R. W.; Collinson, N.; Cook, S. M.; Dawson, G. R.; Ferris, P.; Hobbs, S. C.; O'Connor, D.; Marshall, G.; Rycroft, W.; Macleod, A. M., An orally bioavailable, functionally selective inverse agonist at the benzodiazepine site of GABA(A) alpha5 receptors with cognition enhancing properties. *J Med Chem* **2004**, 47, (24), 5829-32.
498. Asproni, B.; Talani, G.; Busonero, F.; Pau, A.; Sanna, S.; Cerri, R.; Mascia, M. P.; Sanna, E.; Biggio, G., Synthesis, structure-activity relationships at the GABA(A) receptor in rat brain, and differential electrophysiological profile at the recombinant human GABA(A) receptor of a series of substituted 1,2-diphenylimidazoles. *J. Med. Chem.* **2005**, 48, (7), 2638-2645.

499. File, S. E., The contribution of behavioral-studies to the neuropharmacology of anxiety. *Neuropharmacology* **1987**, 26, (7B), 877-886.
500. File, S. E.; Baldwin, H. A., Effects of beta-carbolines in animal-models of anxiety. *Brain Research Bulletin* **1987**, 19, (3), 293-299.
501. File, S. E.; Dingemanse, J.; Friedman, H. L.; Greenblatt, D. J., Chronic treatment with Ro 15-1788 distinguishes between its benzodiazepine antagonist, agonist and inverse agonist properties. *Psychopharmacology* **1986**, 89, (1), 113-7.
502. Stables, J. P.; personal communication; at NINDS: 2007.
503. Cheng, D.; Harris, D. L.; Reed, J. R.; Backes, W. L., Inhibition of CYP2B4 by 2-ethynylnaphthalene: evidence for the cobinding of substrate and inhibitor within the active site. *Arch. Biochem. Biophys.* **2007**, 468, 174-182.
504. Cheng, D.; Reed, J. R.; Harris, D. L.; Backes, W. L., Inhibition of CYP2B4 by the mechanism-based inhibitor 2ethynylnaphthalene: inhibitory potential of 2EN is dependent on the size of the substrate. *Arch. Biochem. Biophys.* **2007**, 462, 28-37.
505. Hanchar, H. J.; Chutsrinopkun, P.; Meera, P.; Supavilai, P.; Sieghart, W.; Wallner, M.; Olsen, R. W., Ethanol potently and competitively inhibits binding of the alcohol antagonist Ro15-4513 to $\alpha 4/6\beta 3\gamma$ GABA(A) receptors. *Proc. Natl. Acad. Sci.* **2006**, 103, 8546-8551.
506. Fuchs, K.; Zezula, J.; Slany, A.; Sieghart, W., Endogenous [3H]flunitrazepam binding in human embryonic kidney cell line 293. *Eur J Pharmacol* **1995**, 289, (1), 87-95.
507. Fanselow, M. S.; Bolles, R. C., Naloxone and shock-elicited freezing in the rat. *J Comparative Phys Psy* **1979**, 93, 736-744.
508. Stewart, J. J. P., MOPAC: A Semiempirical molecular orbital program. *J. Comp Aided Mol. Des.* **1990**, 4, 1-105.
509. Frisch, M. J.; Trucks, G. W.; Schlegel, H. B.; Scuseria, G. E.; Robb, M. A.; Cheeseman, J. R.; Zakrzewski, V. G.; J. A. Montgomery, J.; Stratmann, R. E.; Burant, J. C.; Dapprich, S.; Millam, J. M.; Daniels, A. D.; Kudin, K. N.; Strain, M. C.; Farkas, O.; Tomasi, J.; Barone, V.; Cossi, M.; Cammi, R.; Mennucci, B.; Pomelli, C.; Adamo, C.; Clifford, S.; Ochterski, J.; Petersson, G. A.; Ayala, P. Y.; Cui, Q.; Morokuma, K.; Malick, D. K.; Rabuck, A. D.; Raghavachari, K.; Foresman, J. B.; Cioslowski, J.; Ortiz, J. V.; Stefanov, B. B.; Liu, G.; Liashenko, A.; Piskorz, P.; Komaromi, I.; Gomperts, R.; Martin, R. L.; Fox, D. J.; Keith, T.; Al-Laham, M. A.; Peng, C. Y.; Nanayakkara, A.; Gonzalez, C.; M. Challacombe; Gill, P. M. W.; Johnson, B.; Chen, W.; Wong, M. W.; Andres, J. L.; Gonzale, C.; Head-Gordon, M.; Replogle, E. S.; Pople, J. A. *Gaussian98*, **1998**.

510. Grant, J. A.; Bonnick, T.; Gossel-Williams, M.; Clayton, T.; Cook, J. M.; Jackson, Y., Synthesis, pharmacological studies and molecular modeling of some tetracyclic 1,3-diazepinium chlorides. *Bioorg. Med. Chem.* **2010**, 18, (2), 909-21.
511. Martin, L. L.; Geyer, H. M.; Crichlow, C. A.; Dekow, F. W.; Ellis, D. B.; Kruse, H.; Setescak, L. L.; Worm, M., (+-)-4-Aryl-4,5-dihydro-3H-1,3-benzodiazepines. 1. Synthesis and evaluation of (+-)-4,5-dihydro-2,3-dimethyl-4-phenyl-3H-1,3-benzodiazepine and analogs as potential antidepressant agents. *J. Med. Chem.* **1982**, 25, 340.
512. Jackson, Y.; Williams, M., Heterocycles from 2-Aminopyridine and Derivatives of 3-Methylbenzofuran-2-carboxylic Acid. *Heterocycles* **1997**, 45, 787.
513. Bagajewicz, M. J.; Levin, R. R.; Welsh, C. T.; Schartz-Bloom, R. D., *Levine's Pharmacology: Drug Action and Reactions*. Taylor and Francis: Oxon, **2005**; p 252.
514. Loeber, J. G.; Franken, M. A. M.; Van Leewen, F. X. R., Effect of sodium bromide on endocrine parameters in the rat as studied by immunocytochemistry and radioimmunoassay. *Food Chem Toxicol* **1983**, 21, 391.
515. Van Leewen, F. X. R.; Den Tonkelaar, E. M.; Van Logten, M., Toxicity of sodium bromide in rats: effects on endocrine system and reproduction. *J. Food Chem Toxicol* **1983**, 21, 383.
516. Van Leewen, F. X. R.; Sangster, B., *CRC Crit. Rev. Toxicol.* **1987**, 18, 189.
517. Ewing, J. A.; Grant, W., The bromide hazard. *South Med J* **1965**, 58, 148.
518. Pavelka, S., Metabolism of Bromide and Its Interference with the Metabolism of Iodine. *Physiol. Res.* **2004**, 53, (Suppl 1), S81.
519. Cameron, A. T.; Hollenberg, M. S., The relative toxicity of the halides and certain other anions. *J. Gen. Physiol.* **1922**, 411.
520. Andes, E., Two meteorites of unusually short cosmic-ray exposure age. *Science* **1962**, 138, 431.
521. Sadhu, D. P., Vitamin A, iodide and thyrotropic hormone content of the anterior pituitary. *Am. J. Physiol.* **1948**, 152, 263.
522. Markou, K. B.; Paraskevopoulou, P.; Karaikos, K. S.; Makri, M.; Georgopoulos, N. A.; Iconomou, G.; Mengreli, C.; Vagenakis, A. G., Hyperthyrotropinemia during iodide administration in normal children and in children born with neonatal transient hypothyroidism *J. Clin. Endocr. and Metab.* **2003**, 88, 617.
523. Malone, M. H.; Robichaud, R. C., A hippocratic screen for pure or crude drug materials. *Lloydia* **1962**, 25, 320.
524. Rang, H. P.; Dale, M. M.; Ritter, J. M.; Gardner, P., *Pharmacology*. Churchill and Livingstone: New York, **2003**; p 671.

525. Griebel, G.; Perrault, G.; Letang, V.; Granger, P.; Avenet, P.; Schoemaker, H.; Sanger, D. J., New evidence that the pharmacological effects of benzodiazepine receptor ligands can be associated with activities at different BZ (omega) receptor subtypes. *Psychopharmacology* **1999**, 146, (2), 205-213.
526. Shinday, N.; Rowlett, J. K.; Cook, J. M., The selective $\alpha 5$ GABA(A) receptor antagonist XLi-093 reverses diazepam-induced memory deficits in the holeboard task at *Society for Neuroscience*, Washington D.C., 2008.
527. McNamara, R. K.; Skelton, R. W., Benzodiazepine receptor antagonists flumazenil and CGS 8216 and inverse-agonist b-CCM enhance spatial learning in the rat: Dissociation from anxiogenic actions. *Psychobiology* **1993**, 21, 101-108.
528. Anand, N.; Saraf, M. K.; Prabhakar, S., Sustained inhibition of brotizolam induced anterograde amnesia by norharmane and retrograde amnesia by L-glutamic acid in mice. *Behavioural Brain Research* **2007**, 182, 12-20.
529. Cain, D. P., Prior non-spatial pretraining eliminates sensorimotor disturbances and impairments in water maze learning caused by diazepam. *Psychopharmacology* **1997**, 130, 313-319.
530. Hentschke, H.; Schwarz, C.; Antkowiak, B., Neocortex is the major target of sedative concentrations of volatile anaesthetics: strong depression of firing rates and increase of GABA(A) receptor-mediated inhibition. *Eur. J. Neurosci.* **2005**, 21, (1), 93-102.
531. Kiehn, O., Locomotor circuits in the mammalian spinal cord. *Annual Review of Neuroscience* **2006**, 29, 279-306.
532. Araujo, F.; Ruano, D.; Vitorica, J., Native gamma-aminobutyric acid type A receptors from rat hippocampus, containing both alpha 1 and alpha 5 subunits, exhibit a single benzodiazepine binding site with alpha 5 pharmacological properties. *J. Pharmacol. Exp. Ther.* **1999**, 290, (3), 989-997.
533. Brioni, J. D.; Arolfo, M. P.; Jerusalinsky, D.; Medina, J. H.; Izquierdo, I., The effect of flumazenil on acquisition, retention, and retrieval of spatial information *Behavioral and Neural Biology* **1991**, 56, (3), 329-335.
534. Curran, H. V., Benzodiazepines, memory and mood: a review. *Psychopharmacology* **1991**, 105, 1-8.
535. Zanolli, A.; Arban, R.; Perazzolo, M.; Giusti, P., Diazepam impairs place learning in native but not in maze-experienced rats in the Morris water maze. *Psychopharmacology* **1994**, 115, 73-78.
536. Gerlai, R., Behavioral tests of hippocampal function: simple paradigms complex problems. *Behavioural Brain Research* **2001**, 125, 269-277.
537. Rossato, J. I.; Zinn, C. G.; Furini, C.; Bevilaqua, L. R.; Medina, J. H.; Cammarota, M.; Izquierdo, I., A link between the hippocampal and the striatal

- memory systems of the brain. *Anais de Academia Brasileira de Ciencias* **2006**, 78, 515-523.
538. Bird, C. M.; Burgess, N., The hippocampus and memory: insights from spatial processing. *Nature Reviews Neuroscience* **2008**, 9, 182-194.
539. Cook, J. M.; Han, D.; Clayton, T. GABAergic agents to treat memory deficits. US Patent 2006/0258643 A1. **2006**.
540. Knust, H. Substituted Imidazol [1,5-]Triazolo[1,5-D][Benzodiazepine Derivatives. US Patent 7514426 B2 **2009**.
541. Rivas, F.; Stables, J. P.; Cook, J. M., in press. *J. Med. Chem.* **in press**, **2009**.
542. El Hadri, A.; Abouabdellah, A.; Thomet, U.; Baur, R.; Furttmuller, R.; Sigel, E.; Sieghart, W.; Dodd, R. H., N-substituted 4-amino-3,3-dipropyl-2(3H)-furanones: New positive allosteric modulators of the GABA(A) receptor sharing electrophysiological properties with the anticonvulsant loreclezole. *J. Med. Chem.* **2002**, 45, (13), 2824-2831.
543. Sieghart, W., Pharmacology of Benzodiazepine Receptors - an Update. *J Psych Neurosci* **1994**, 19, (1), 24-29.
544. Schreibmayer, W.; Hester, H.; Dascal, N., Voltage clamping of *Xenopus laevis* oocytes utilizing agarose-cushion electrodes. *N. Pflugers Arch.: European J Phys* **1994**, 46, 453-458.
545. Sigel, E.; Baur, R., Allosteric modulation by benzodiazepine receptor ligands of the GABA(A) receptor channel expressed in *Xenopus* oocytes. *J. Neurosci.* **1988**, 8, 289-295.
546. Sigel, E.; Minier, F., The *Xenopus* oocyte: System for the study of functional expression and modulation of proteins. *Molecular Nutrition & Food Research* **2005**, 49, (3), 228-234.
547. Wong, G.; Skolnick, P., High-Affinity Ligands for Diazepam-Insensitive Benzodiazepine Receptors. *Eur. J. Pharmacol.-Mol. Pharmacol. Section* **1992**, 225, (1), 63-68.
548. Austin, W. B.; Bilow, N.; Kelleghan, W. J.; Lau, K. S. Y., Facile synthesis of ethynylated benzoic acid derivatives and aromatic compounds via ethynyltrimethylsilane. *J. Org. Chem.* **1981**, 46, 2280-2286.
549. Heck, R. F., *Palladium Reagents in Organic Synthesis*; Academic Press. Academic Press: Orlando, **1985**.
550. Buckingham, J., *Dictionary of Organic Compounds*. Chapman and Hall: New York, **1982**; Vol. 2, p 1585.
551. Jackson, Y.; Marriott, K. C., A Novel. photochemical route to dibenzonaphthyrones. *Heterocycles* **2002**, 57, 1897.

552. Yonovich-Weiss, M.; Sasson, Y., Synthesis of primary alkyl bromides. *Synthesis* **1984**, 34.
553. Sasson, Y.; Weiss, M.; Loupy, A.; Bram, G.; Pardo, C., Bromide–chloride exchange between alkyl halides and metal halide salts under phase transfer conditions. *J. Chem. Soc. Chem. Comm.* **1986**, 371, 1250.
554. Yamazaki, H.; Dokoshi, W.; Kibayashi, C., Total Synthesis of (-)-stelllettamide B and determination of its absolute stereochemistry. *Org. Lett.* **2001**, 3, 193.
555. Yu, J.; Wang, T.; Liu, X.; Deschamps, J.; Flippen-Anderson, J.; Liao, X.; Cook, J. M., General approach for the synthesis of Sarpagine indole alkaloids. Enantiospecific total synthesis of (+)-Velloimine, (+)-Normacusine B, (-)-alkaloid Q3, (-)-Panarine, (+)-Na-methylvellosimine, and (+)-Na-methyl-16-epipericyclivine. *J. Org. Chem.* **2003**, 68, 7565.

Appendix I. Key Amino Acid Sequences

Data Table 1. Amino acid sequence of the alpha subunit of the acetylcholine receptor in the *lymnaea stagnalis* (Great Pond Snail)

>sp|P58154|ACHP_LYMST Acetylcholine-binding protein OS=Lymnaea stagnalis PE=1 SV=1
 MRRNIFCLACLWIVQACLSLDRADILYNIRQTSRPDVIPTQRDRPVAVSVSLKFINILEV
 NEITNEVDVVFQQTTWSDRTLAWNSSHSPDQVSVPISSLWVPDLAAAYNAISKPEVLTPQ
 LARVSDGEVLYMPSIRQRFSCDVSGVDTESGATCRIKIGSWTHHSREISVDPTTENSDD
 SEYFSQYSRFEILDVTQKKNSVTYSCCPEAYEDVEVSLNFRKKGRSEIL

Data Table 2. Amino acid sequence of the alpha subunit of the acetylcholine receptor in the *Torpedo californica* (Pacific Electric Ray)

>sp|P02710|ACHA_TORCA Acetylcholine receptor subunit alpha OS=Torpedo californica GN=CHRNA1 PE=1
 SV=1
 MILCSYWHVGLVLLLFSCCGLVLGSEHETRLVANLLENYNKVIRPVEHHTHFVDITVGLQ
 LIQLISVDEVNQIVETNVRLRQQWIDVRLRWNPADYGGIKKIRLPSSDDVWLPLDLVLYNNA
 DGDFAIHVMTKLLLDYTGKIMWTTPAIFKSYCEIIVTHFPFDQQNCTMKLGIWTYDGTKV
 SISPESDRPDLSTFMESGEWVMKDYRGWKHWVYYTCCPDTPYLDITYHFIMQRIPLYFVV
 NVIIPCLLSFLTGLVFYLPDTSGEKMTLSISVLLSLTVFLLVIVELIPSTSSAVPLIGK
 YMLFTMIFVISSIIITVVVINTHHRSPSTHTMPQWVRKIFIDTIPNVMFFSTMKRASKEK
 QENKIFADDIDISDISGKQVTGEVIFQTPLIKNPDVKSAIEGVKYIAEHMKSDEESSNAA
 EEWKYVAMVIDHILLCVFMLICHGTVSVFAGRLIELSQEG

Data Table 3. Amino acid sequence of the alpha 1 subunit of the rat GABA(A) receptor

>sp|P62813|GBRA1_RAT Gamma-aminobutyric acid receptor subunit alpha-1 OS=Rattus norvegicus
 GN=Gabra1 PE=1 SV=1
 MKKSRGLSDYLWAWTLILSTLSGRSYGQPSQDELKDNTTVFTRILDRLLDGYDNRLRPGL

GERVTEVKTDIFVTSFGPVSDDHMEYTDVFFRQSWKDERLKFKGPMTVLRLNNLMASKI
 WTPDTFFHNGKKSVAHNMTMPNKLLRITEDGTLLYTMRLTVRAECPMHLEDFPMDAHACP
 LKFGSYAYTRAENVVYEWTPARSVVVAEDGSRLNQYDLLGQTVDSGIVQSSTGEYVVM
 THFHLKRKIGYFVIQTYLPCIMTVILSQVSFWLNRESVPARTVFGVTTVLTMTTLLSISAR
 NSLPKVAYATAMDWFIAVCYAFVFSALIEFATVNYFTKRGYAWDGKSVVPEKPKKVKDPL
 IKKNNTYAPTATSYTPNLARGDPGLATIAKSATIEPKVKPETKPPEPKKTFNSVSKIDR
 LSRIAFPLLFGIFNLVYWATYLNREPQLKAPTPHQ

Data Table 4. Amino acid sequence of the gamma 2 subunit of the rat GABA(A) receptor

>sp|P18508|GBRG2_RAT Gamma-aminobutyric acid receptor subunit gamma-2 OS=Rattus norvegicus
 GN=Gabrg2 PE=1 SV=1

MSSPNTWSTGSTVYSPVFSQKMTLWILLLLSLYPGFTSQKSDDDYEDYASNKTWVLTPKV
 PEGDVTILNLLLEGYDNKLRPDIGVKPTLIHTDMYVNSIGPVNAINMEYTIDIFFAQTW
 YDRRLKFNSTIKVLRNLSNMVGKIWIPDTFFRNSKKADAHWITTPNRMLRIWNDGRVLYT
 LRLTIDAEQQLQHNFPMDHSCPLEFSSYGYPREEIVYQWKRSSVEVGDTRSWRLYQFS
 FVGLRNTTEVVKTTSGDYVVMVSVYFDLSRRMGYFTIQTYIPCTLIVLSWVSFWINKDAV
 PARTSLGITTTLTMTTLLSTIARKSLPKVSYVTAMDLFVSVCFIFVFSALVEYGLTHYFVS
 NRKPSKDKDKKKKNPAPTIDIRPRSATIQMNNATHLQERDEEYGYECLDGKDCASFFCCF
 EDCRTGAWRHGRIHIRIAKMDSYARIFFPTAFCLFNLVYWVSYYLYL

Data Table 5. Amino acid sequence of the alpha 1 subunit of the human GABA(A) receptor

>sp|P14867|GBRA1_HUMAN Gamma-aminobutyric acid receptor subunit alpha-1 OS=Homo sapiens
 GN=GABRA1 PE=1 SV=3

MRKSPGLSDCLWAWILLSTLTGRSYGQPSLQDELKDNTTVFTRILDRLLDGYDNRLRPG
 LGERVTEVKTDIFVTSFGPVSDDHMEYTDVFFRQSWKDERLKFKGPMTVLRLNNLMASK
 IWTPDTFFHNGKKSVAHNMTMPNKLLRITEDGTLLYTMRLTVRAECPMHLEDFPMDAHAC
 PLKFGSYAYTRAENVVYEWTPARSVVVAEDGSRLNQYDLLGQTVDSGIVQSSTGEYVVM
 TTHFHLKRKIGYFVIQTYLPCIMTVILSQVSFWLNRESVPARTVFGVTTVLTMTTLLSISA

RNSLPKVAYATAMDWFIACVAFVFSALIEFATVNYFTKRGYAWDGKSVVPEKPKKVKDP
 LIKKNNITYAPTATSYPNLRGDPGLATIAKSATIEPKVKPETKPPEPKKTFNSVSKID
 RLSRIAFPLLFGIFNLVYWATYLNREPQLKAPTPHQ

Data Table 6. Amino acid sequence of the gamma 2 subunit of the human GABA(A) receptor

>sp|P18507|GBRG2_HUMAN Gamma-aminobutyric acid receptor subunit gamma-2 OS=Homo sapiens
 GN=GABRG2 PE=1 SV=2

MSSPNIWSTGSSVYSTPVFSQKMTVWILLLLSLYPGFTSQKSDDDYEDYASNKTWVLTPK
 VPEGDVTVILNNLLEGYDNKLRPDIGVKPTLIHTDMYVNSIGPVNAINMEYTIIDIFFAQT
 WYDRRLKFNSTIKVLRNLSNMVGKIWIPDTFFRNSKKADAHWITTPNRMLRIWNDGRVLY
 TLRLTIDAECQLQLHNFPMDEHSCPLEFSSYGYPREEIVYQWKRSSVEVGDTRSWRLYQF
 SFVGLRNTTEVVKTTSGDYVVMMSVYFDLSRRMGYFTIQTYIPCTLIVVLSWVSFWINKDA
 VPARTSLGITTVLMTTLSTIARKSLPKVSYVTAMDLFVSVCFIFVFSALVEYGTLLHYFV
 SNRKPSKDKDKKKKNPAPTIDIRPRSATIQMNNATHLQERDEEYGYECLDGKDCASFFCC
 FEDCRTGAWRHGRIHIRIAKMDSYARIFFPTAFCLFNLVYWVSYYLYL

Data Table 7. Amino acid sequence of the Beta 2 Subunit of the Human GABA(A) Receptor

>sp|P47870|GBRB2_HUMAN Gamma-aminobutyric acid receptor subunit beta-2 OS=Homo sapiens
 GN=GABRB2 PE=1 SV=1

MWRVRKRGYFGIWSFPLIIAAVCAQSVNDPSNMSLVKETVDRLKGYDIRLRPDFGGPPV
 AVGMNIDIASIDMVSEVNMDYTLTMYFQQAWRDKRLSYNVIPLNLTLNDRVADQLWVPDT
 YFLNDKKSFVHGVTVKNRMIRLHPDGTVLYGLRITTTAACMMDLRRYPLDEQNCTLEIES
 YGYTTDDIEFYWRGDDNAVTVTKIELPQFSIVDYKLITKKVVVFSTGSYPRLSLSFKLKR
 NIGYFILQTYMPSILITLSWVSFWINYDASAARVALGITTVLMTTINTHLRETLPKIP
 YVKAIDMYLMGCFVVFMALLEYALVNYIFFGRGPQRQKKA AEKAASANNEKMRLDVNKM
 DPHENILLSTLEIKNEMATSEAVMGLGDPRSTMLAYDASSIQYRKAGLPRHSFGRNALER
 HVAQKKSRLLRRRASQLKITIPDLTDVNAIDRWSRIFFPVVFSFFNIVYWLYYVN

Appendix II.

Data Table 8. Coordinates of the Pharmacophore

REMARK File generated by Swiss-PdbViewer 4.00b0

REMARK <http://www.expasy.org/spdbv/>

HETATM 1 * hip 0 2.246 2.113 1.413 0.00100.00

HETATM 2 O hip 0 -5.691 -0.267 -4.151 0.00100.00

HETATM 3 H1 hip 0 0.742 3.154 -3.474 0.00100.00

HETATM 4 H2 hip 0 -2.472 -1.062 0.681 0.00100.00

SPDBVT 1.0000000000 0.0000000000 0.0000000000

SPDBVT 0.0000000000 1.0000000000 0.0000000000

SPDBVT 0.0000000000 0.0000000000 1.0000000000

SPDBVT 0.0000000000 0.0000000000 0.0000000000

SPDBVT 0.0000000000 0.0000000000 0.0000000000

SPDBVV default;

SPDBVV 15.426431672954 1678.699418606842 20.000000000000

SPDBVV 0.4758893755 0.5102135228 -0.7163877885

SPDBVV 0.3084772896 0.6659613576 0.6792181034

SPDBVV 0.8236328455 -0.5442220423 0.1595346499

SPDBVV -1.7224999666 1.0460000038 -1.3689999580

SPDBVV 0.0000000000 0.0000000000 0.0000000000

SPDBVf 27

SPDBVi 1.00 1.00 1.00

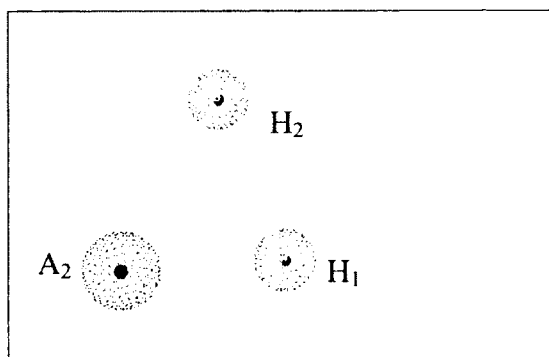
SPDBVb 0.00 0.00 0.20

SPDBVg 64

SPDBVi 1 1 1 0 1 1 1 1 0 1 0 0 1 0 0

SPDBVp 0

END



Appendix III. Pharmacology

Extraction of Diazepam from Valium® Tablets (5 mg)

Valium® tablets (5×5 mg), contributed by the University Health Centre, U.W.I., Mona, were crushed with a mortar and pestle then placed in a 50 mL round bottom flask fitted with reflux condenser and calcium chloride guard tube. Chloroform (25 mL) was added and the mixture heated at reflux for 2 hours with stirring. The mixture was then filtered and the chloroform evaporated under vacuum to give diazepam (23 mg, 92%) as pale yellow crystals; mp 129–132 °C, [lit.⁵¹² 125–126 °C (acetone/ petroleum ether)]; $^1\text{H-NMR}$ δ = 3.42 (s, 3H, -NCH₃), 3.80 (d, J = 11 Hz, 1H, H-3), 4.86 (d, J = 11 Hz, 1H, H-3), 7.33 (m, 2H, H-3' and H-5'), 7.45 (m, 2H, H-2' and H-6'), 7.51 (dd, J = 1 and 7 Hz, 1H, H-8), 7.55 (m, 1H, H-4'), 7.62 (d, J = 1 Hz 1H, H-6), 7.64 ppm (d, J = 7 Hz 1H, H-9); $^{13}\text{C-NMR}$ δ = 35.2, 57.4, 122.9, 128.9, 129.7, 129.9, 130.3, 130.5, 131.1, 131.8, 138.6, 143.0, 169.3, 170.3 ppm.

Hippocratic Screen Activities

The following activities were measured in the Hippocratic screen:

- a) **Decreased motor activity** – spontaneous movement of the animals: \pm , is quiet but moves spontaneously; +, does not move spontaneously but moves rapidly when

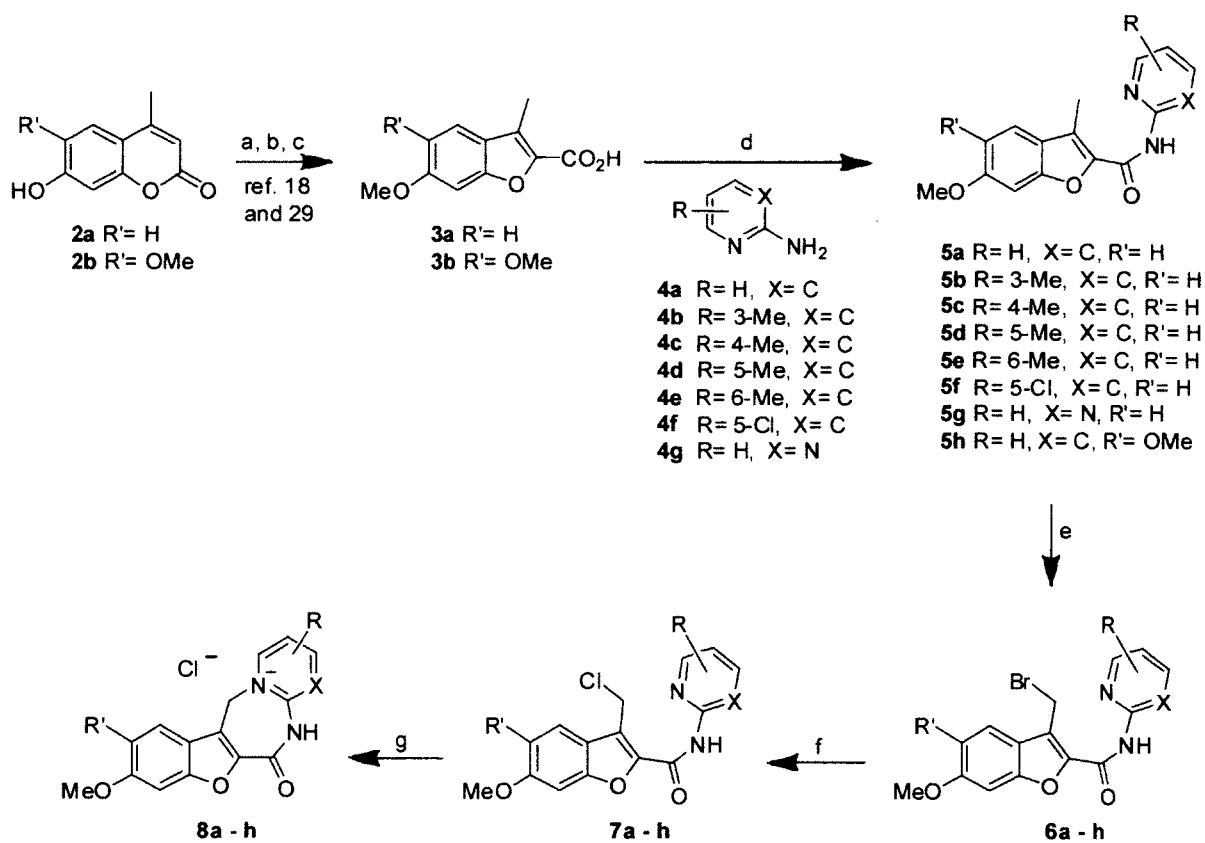
handled; ++, moves slowly when handled; +++, moves very sluggishly when handled; +++++, does not move at all when handled.

- b) **Ataxia** – coordinated movement of the animals: +, shows slight incoordination; ++, has difficulty walking in a straight line but its course is true; +++, cannot walk in a straight line and its course is erratic; +++++, cannot walk on any course.
- c) **Loss of righting reflex** – the animals' response when placed on their sides or back: +, can be placed on one side; ++, can be placed on either side equally well; +++, can be placed on back as well as both sides; +++++, cannot get up from back position on its own.
- d) **Analgesia** – animals' response to pain inflicted across the instep and toes: ±, sluggish response with vocalization and or attempts to bite or escape; +, no vocalization nor attempts to bite or escape but does attempt to calmly withdraw foot; ++, no response
- e) **Anesthesia** – animals' response when a hypodermic needle is pressed to foot pad: ±, a sluggish response; +, no response to needle pressure; ++, no response to needle penetration.
- f) **Pinnal reflex** – the animals' response to a gentle touch with a probe (brush bristle) into the ear canal: ±, sluggish response; +, no response
- g) **Loss of screen grip** – animals' ability to remain on a wire screen when tilted at 45 – 180° or gently shaken in a horizontal plane when inverted: ±, unequivocal loss; +, falls at first shake when screen is inverted; ++, falls when screen is inverted; +++, falls at 90°, +++++, falls at 45°.
- h) **Paralysis** – animals were inspected for signs of paralysis in forelegs, hind legs and neck: ±, unequivocal; +, complete.

- i) **Respiratory rate** – animals' rate of breathing per minute compared to the period before the animal is tested: +, 10 % change; ++, 20 % change; +++, 40 % change; +++++, 80 % change.
- j) **Tremor** – animals were observed for any signs of abnormal or excessive shaking: \pm , unequivocal presence; +, definite but periodically; ++, continuous; +++, convulsions.
- k) **Startle reaction** – The animals' response when the observation rink was sharply slapped with a flat metal object: \pm , a mild startle; +, animal visibly jerks; ++, animal jerks, jumps and attempts to escape; +++, animal goes into convulsions.

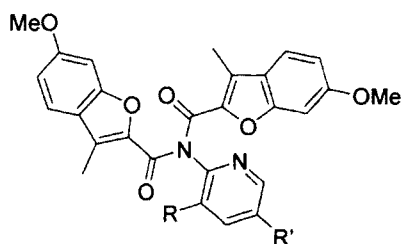
Appendix IV. Tetracyclic 1,3-Diazepinium Chemistry (with Grant et al.)

In the synthetic pathway outlined by Jackson and Williams,⁵⁵⁴ tetracyclic 1,3-diazepinium bromide **1** was prepared by intramolecular cyclization of bromomethyl amide **6a** which readily occurred in refluxing acetone. Amide **6a** was obtained from 7-hydroxy-4-methylcoumarin (**2**) as shown in Scheme 1. It was proposed that this synthetic route could be modified to produce the required 1,3-diazepinium chlorides by cyclization of the respective chloromethyl amides (Scheme 1) or by ion exchange of the 1,3-diazepinium bromides (Scheme 2).



Scheme 1. Reagents and conditions: (ai) **2a**, K₂CO₃, Me₂SO₄, acetone, reflux, 13 h, 97%; (aii) **2b**, K₂CO₃, MeI, acetone, reflux, 8 h, 89%; (b) K₂CO₃, Br₂, CHCl₃, 70 °C, 3 h, 74% (for **2a**), 90% (for **2b**); (c) NaOH, EtOH, reflux, 3 h, 98% (**3a**), 90% (**3b**); (d) i) SOCl₂, pyridine, CH₂Cl₂, rt, 30 min; ii) **4a-g**, pyridine, toluene, reflux, 5 h, 51–77%; (e) NBS, CCl₄, hv, 2–3 h, 44–76%; (f) NaCl, [CH₃(CH₂)₃]₄N⁺ I⁻, CHCl₃, H₂O, reflux, 3–12 h, 68–88%; (g) acetone, reflux, 3–5 days, 12–50%, (**8b**, 2%).

Methylation of 7-hydroxy-4-methylcoumarin (**2a**) with $\text{Me}_2\text{SO}_4/\text{K}_2\text{CO}_3$ followed by bromination with $\text{Br}_2/\text{K}_2\text{CO}_3/\text{CHCl}_3$, then hydrolysis and subsequent rearrangement of the 3-bromocoumarin in ethanolic NaOH , produced acid **3a** in 85% overall yield. 5,6-Dimethoxy-4-methylcoumarin (**3b**) was also prepared, in similar fashion, from 6,7-dihydroxy-4-methylcoumarin (**2b**) in 72% overall yield.⁵⁵⁵ Treatment of acid **3a** with thionyl chloride followed by substituted pyridines and pyrimidines (**4a–g**) produced amides **5a–g** and acid **3b** reacted, under these conditions, with amine **4a** to give amide **5g**. It was found that when the reaction was carried out in the typical way *i.e.* addition of a solution of the amine (1.1 molar equiv.) in pyridine to the acid chloride, 2-amino-3-picoline (**4b**) reacted with **3a** to give imide **9** (96%). Under these conditions, 2-amino-5-picoline (**4d**) also reacted to produce imide **10** (26%) along with desired amide **5d** (56 %).



9. R= Me, R'= H

10. R= H, R'= Me

The experimental data confirmed the double acylation of **4b** and **4d** which was perhaps due to the effect of the electron donating methyl group in *ortho* and *para* positions respectively, to the reacting amino group. Synthesis of amide **5b** was achieved by slowly adding the acid chloride mixture to a solution of **4b** (3 molar equiv.) in pyridine then heating the mixture at reflux for 3 hours.

Attempts at allylic chlorination of the amides using *t*-butyl hypochlorite in methyl formate, dichloromethane or carbon tetrachloride to give chloromethyl amides **7a–h** were futile. Hence, amides **5a–h** were treated with NBS in CCl₄ and irradiated, in a darkened box, with a 150 W tungsten lamp for 2–2.5 hours to give the respective bromomethyl amides **6a–h** in modest yields. Formation of the allyl bromide was readily confirmed by both ¹H-NMR and ¹³C-NMR spectra. The methyl group attached to the benzofuran system of the respective amides appears at about δ 2.6 in the ¹H-NMR spectrum and at δ 9.5 in ¹³C-NMR spectrum, while the CH₂-Br of the same system resonates further downfield at about δ 5.2 in the ¹H-NMR spectrum and δ 21.20 in the ¹³C-NMR spectrum. It should be noted that irradiation of the amides with NBS for longer than 3 hours caused cyclization of the bromomethyl amides to their respective tetracyclic bromide salts. This was not surprising as Jackson and Williams had reported this in their reaction with **5a**.

Allylic bromination of **5b** and **5g** proved less straightforward than for the other analogues. When amide **5b** was treated with NBS in CCl₄ and light, 3-bromomethyl-6-methoxy-*N*-(3-methylpyridin-2-yl)benzofuran-2-carboxamide (**6b**) was obtained as a mixture with 6-methoxy-*N*-(3-bromomethylpyridin-2-yl)-3-methylbenzofuran-2-carboxamide, in a crude yield of 89%. Analysis of the crude mixture confirmed that ratio of the desired **6b** to the other product was 3:2 and this crude mixture was used in the next step *i.e.* halogen transfer. Treatment of amide **5g** with NBS in CCl₄ and light for 1-3 hours produced the desired bromomethyl amide **6g** as a mixture with the 1,3-diazepinium bromide **11** in a ratio of 1:2. When the reaction was extended beyond 3 hours, only the bromide salt **11** was obtained, indicating that bromomethyl amide **6g** is very susceptible to ring closure, and reacts to produce the salt **11** as soon as it is formed. Since intermediate **6g** consists of a pyrimidine ring with not one, but two ring nitrogen atoms in

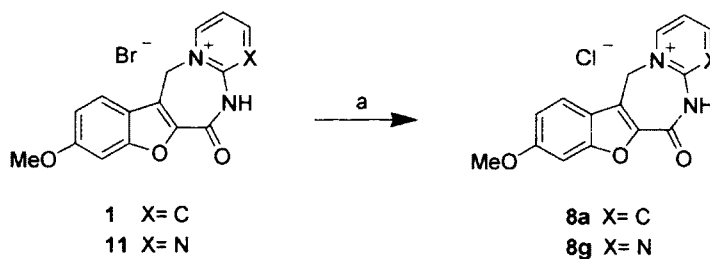
positions which are available for interaction with the $-\text{CH}_2\text{-Br}$ moiety of the molecule to effect cyclization, this process occurs readily.

Bromomethyl amides **6a–f** and **6h** were then converted to the respective chloromethyl amides **7a–f** and **7h** under phase transfer conditions,⁵¹² using a NaCl solution (25% aqueous) and tetra-*n*-butylammonium iodide as the phase transfer catalyst. The chloromethyl amides were easily distinguished from the corresponding bromomethyl compounds by their ^{13}C -NMR spectra, wherein the carbon atom of the $-\text{CH}_2\text{-Cl}$ group resonated at approximately δ 35.0, as compared to δ 21.2 for the analogous $-\text{CH}_2\text{-Br}$. Chloromethyl amides **7b** and **7d** were obtained in crude yields of 58 and 96% respectively. Analysis of NMR data confirmed the presence of the products and the crude products were used in the cyclization reaction.

Jackson and Williams accomplished cyclization of a 0.7% solution of bromomethyl amide **6a** in refluxing acetone in 70% yield⁵¹² however, when the corresponding chloro analogue **7a** was treated under similar conditions for 28 hours, 1,3-diazepinium chloride **8a** was obtained in only 6% yield. Heating 10–20% solutions of chloromethyl amides **7a–f** and **7h** at reflux in the more polar and higher boiling 1,4-dioxane for several days, however, furnished the corresponding 1,3-diazepinium chlorides in 12–50% yield, except in the case of **7b** where the tetracycle was obtained in only 2% yield. In the ^1H - and ^{13}C -NMR spectra, the methylene protons resonate at about δ 6.0 and δ 50.0 respectively.

Since the tetracyclic 1,3-diazepinium bromides were so readily formed, especially for compound **11**, we also considered converting these bromides to their respective chlorides. Yamazaki and later Cook reported the conversion of quaternary ammonium iodides to chlorides using AgCl in anhydrous MeOH. However, compounds **1** and **11**

were found to be insoluble in MeOH and even when the reaction was heated at reflux, only the starting bromides were obtained.



Scheme 2. Reagents and condition: (a) AgCl, MeOH, rt.

Experimental Data for the Tetracyclic 1,3-Diazepinium Chlorides

Chemistry

Unless otherwise stated, the following generalizations apply. Evaporation means evaporation under reduced pressure. Melting points were determined on a Thomas-Hoover apparatus and are uncorrected. ^1H -NMR and ^{13}C -NMR spectra were obtained in deuteriochloroform solution on ACE 200 Bruker spectrophotometers (200 MHz or 500 MHz) instruments. Chemical shifts are reported in ppm. The abbreviations are as follows: s, singlet; d, doublet; dd, double doublet; dt doublet of triplets; m, multiplet. Infrared spectra were obtained on a Bruker Vector FT-IR spectrophotometer and are for NaCl discs. Elemental analyses were carried out at MEDAC Ltd., Brunel Science Centre, United Kingdom. Column chromatography was performed using silica gel (40–63 μm). The solvent systems used were: A = ethyl acetate/hexane (1:1); B = ethyl acetate/hexane (1:2); C = ethyl acetate/dichloromethane (1:1) and D = ethyl acetate/dichloromethane (1:2).

General Preparation of 6-Methoxy-3-Methylbenzofuran-2-Carboxamides (5a-h)

To a 100 mL round bottom flask fitted with a reflux condenser and a calcium chloride guard tube was added a 10% mixture (wt./vol.) of acid **3** (1.00 g, 4.85 mmol) in

dichloromethane (10 mL). Thionyl chloride (2 molar equiv., 0.70 mL) and pyridine (2 mL) were then added to the mixture which was stirred at room temperature for 30 min. The amine (**4a–g**) (1.1 molar equiv.) in pyridine (4 mL) and toluene (3 mL) was then added and the mixture heated at reflux for 5 h. The mixture was concentrated then pyridine was removed by azeotroping with toluene and evaporating under vacuum. The crude was purified by flash-column chromatography on silica which had been treated with 5% triethylamine in eluting solvent, to give corresponding amides **5a–h**.

6-Methoxy-3-methyl-*N*-(pyridin-2-yl)benzofuran-2-carboxamide (5a)

Acid **3a** was reacted with 2-aminopyridine (**4a**) and column eluted with solvent system D to give amide **5a**, (0.92 g, 67%) as off-white crystals; mp 168–170 °C (MeOH), [lit. 167–169 °C]; IR ν_{\max} 1688, 3408 cm^{-1} ; $^1\text{H-NMR}$ δ = 2.57 (s, 3H, -CH₃), 3.81 (s, 3H, -OCH₃), 6.89 (m, 2H, H-5 and H-7), 7.00 (m, 1H, H-5'), 7.42 (m, 1H, H-4), 7.68 (m, 1H, H-4'), 8.28 (m, 2H, H-3', 6'), 9.00 ppm (1H, s, -NH); $^{13}\text{C-NMR}$ δ = 9.6, 56.2, 95.8, 113.5, 114.4, 120.2, 121.7, 123.5, 125.4, 138.8, 141.8, 148.4, 151.6, 155.1, 158.6, 161.1 ppm.

Di-(6-methoxy-3-methylbenzofuran-2-carbonyl)(3-methylpyridin-2-yl)amine (9)

Acid **3a** was reacted with 2-amino-3-picoline (**4b**) and column eluted with system B to give imide **9**, (1.13 g, 96%) as off-white crystals; mp > 300 °C (MeOH); IR ν_{\max} 1612, 1620 cm^{-1} ; $^1\text{H-NMR}$ δ = 2.43 (s, 3H, py-CH₃), 2.57 (s, 6H, furan-CH₃), 3.80 (s, 6H, -OCH₃), 6.73 (d, J = 2 Hz, 2H, H-7' and H-7''), 6.87 (dd, J = 2 and 9 Hz, 2H, H-5' and H-5''), 7.18 (dt, J = 5 and 8 Hz, 1H, H-5), 7.43 (d, J = 9 Hz, 2H, H-4' and H-4''), 7.67 (d, J

= 8 Hz, 1H, H-4), 8.92 ppm (d, J = 5 Hz, 1H, H-6); ^{13}C -NMR δ = 9.9, 18.2, 56.1, 95.6, 113.7, 121.8, 123.0, 123.5, 128.1, 131.2, 140.0, 145.4, 147.1, 151.9, 155.7, 161.3, 163.0 ppm. Anal. calcd for $\text{C}_{28}\text{H}_{24}\text{N}_2\text{O}_6$: C, 69.41; H, 4.99; N, 5.78. Found: C, 69.33; H, 4.84; N, 5.59.

6-Methoxy-3-methyl-*N*-(4-methylpyridin-2-yl)benzofuran-2-carboxamide (5c)

Acid **3a** was reacted with 2-amino-4-picoline (**4c**) and column eluted with system B to give amide **5c**, (0.73 g, 51%) as off-white crystals; mp 184.5–185.5 °C (MeOH); IR ν_{max} 1672, 3409 cm^{-1} ; ^1H -NMR δ = 2.40 (s, 3H, py- CH_3), 2.66 (s, 3H, furan- CH_3), 3.89 (s, 3H, - OCH_3), 6.94 (m, 3H, H-4, H-5 and H-7), 7.50 (dd, J = 3 and 5 Hz, 1H, H-5'), 8.20 (m, 2H, H-3' and H-6'), 8.92 ppm (s, 1H, -NH); ^{13}C -NMR δ = 9.6, 21.8, 56.2, 95.9, 113.5, 114.9, 121.4, 121.8, 123.5, 125.4, 141.8, 148.1, 150.3, 151.6, 155.1, 158.7, 161.1 ppm. Anal. calcd for $\text{C}_{17}\text{H}_{16}\text{N}_2\text{O}_3$: C, 68.91; H, 5.44; N, 9.45. Found: C, 68.60; H, 5.54; N, 9.00.

6-Methoxy-3-methyl-*N*-(5-methylpyridin-2-yl)benzofuran-2-carboxamide (5d)

Acid **3a** was reacted with 2-amino-5-picoline (**4d**) and column eluted with system B to give amide **5d**, (0.81 g, 56%) as cream needle-like crystals; mp 150–151 °C (MeOH); IR ν_{max} 1670, 3408 cm^{-1} ; ^1H -NMR δ = 2.35 (s, 3H, py- CH_3), 2.68 (s, 3H, furan- CH_3), 3.91 (s, 3H, - OCH_3), 6.96 (dd, J = 2 and 9 Hz, 1H, H-5), 6.98 (d, J = 2 Hz, 1H, H-7), 7.52 (d, J = 9 Hz, 1H, H-4), 7.58 (dd, J = 2 and 9 Hz, 1H, H-4'), 8.18 (d, J = 2 Hz, 1H, H-6'), 8.29 (d, J = 9 Hz, 1H, H-3'), 8.94 ppm (s, 1H, -NH); ^{13}C -NMR δ = 9.6, 18.2, 56.2, 96.0, 113.5, 113.9, 121.7, 123.6, 129.6, 139.3, 142.0, 148.4, 149.5, 155.1, 158.5, 161.1 ppm.

Anal. calcd for $C_{17}H_{16}N_2O_3$: C, 68.91; H, 5.44; N, 9.45. Found: C, 68.62; H, 5.31; N, 9.31.

Di-(6-methoxy-3-methylbenzofuran-2-carbonyl)(5-methylpyridin-2-yl)amine (10)

Acid **3a** was reacted with 2-amino-5-picoline (**4d**) and column eluted with system B to give imide **10**, (0.31 g, 26%) as off-white crystals; mp > 300 °C (MeOH); IR ν_{\max} 1634, 1628 cm^{-1} ; $^1\text{H-NMR}$ δ = 2.37 (s, 3H, py-CH₃), 2.59 (s, 6H, furan-CH₃), 3.82 (s, 6H, -OCH₃), 6.80 (d, J = 2 Hz, 2H, H-7' and H-7''), 6.91 (dd, J = 2 and 9 Hz, 2H, H-5' and H-5''), 7.31 (d, J = 8 Hz, 1H, H-4), 7.47 (d, J = 9 Hz, 2H, H-4' and H-4''), 7.60 (d, J = 8 Hz, 1H, H-3), 8.23 ppm (s, 1H, H-6); $^{13}\text{C-NMR}$ δ = 9.5, 18.0, 55.7, 95.4, 113.4, 120.8, 121.5, 122.6, 127.7, 131.6, 138.6, 143.2, 149.2, 150.6, 155.5, 161.0, 163.0 ppm. Anal. calcd for $C_{28}H_{24}N_2O_6$: C 69.41, H 4.99, N 5.78; found C 69.06, H 5.15, N 5.63.

6-Methoxy-3-methyl-N-(6-methylpyridin-2-yl)benzofuran-2-carboxamide (5e)

Acid **3a** was reacted with 2-amino-6-picoline (**4e**) and column eluted with system B to give amide **5e**, (1.09 g, 76%) as pale-yellow crystals; mp 130–132 °C (MeOH); IR ν_{\max} 1675, 3412 cm^{-1} ; $^1\text{H-NMR}$ δ = 2.51 (s, 3H, py-CH₃), 2.65 (s, 3H, furan-CH₃), 3.89 (s, 3H, -OCH₃), 6.94 (m, 3H, H-4, H-5 and H-7), 7.50 (d, J = 8 Hz, 1H, H-5'), 7.63 (t, J = 8 Hz, 1H, H-4'), 8.17 (d, J = 8 Hz, 1H, H-3'), 8.89 ppm (s, 1H, -NH); $^{13}\text{C-NMR}$ δ = 9.6, 24.5, 56.2, 95.9, 111.2, 113.5, 119.7, 121.7, 123.6, 125.2, 139.0, 141.9, 150.9, 155.1, 157.4, 158.6, 161.0 ppm. Anal. calcd for $C_{17}H_{16}N_2O_3$: C, 68.91; H, 5.44; N, 9.45. Found: C, 68.49; H, 5.45; N, 9.25.

***N*-(5-Chloropyridin-2-yl)-6-methoxy-3-methylbenzofuran-2-carboxamide (5f)**

Acid **3a** was reacted with 2-amino-5-chloropyridine (**4f**) and column eluted with system B to give amide **5f**, (1.19 g, 77%) as pale yellow crystals; mp 147–149 °C (MeOH); IR ν_{max} 1680, 3396 cm^{-1} ; $^1\text{H-NMR}$ δ = 2.63 (s, 3H, -CH₃), 3.88 (s, 3H, -OCH₃), 6.94 (m, 2H, H-5 and H-7), 7.48 (d, J = 9 Hz, 1H, H-4), 7.70 (dd, J = 3 and 9 Hz, 1H, H-4'), 8.29 (d, J = 3 Hz, 1H, H-6'), 8.36 (d, J = 9 Hz, 1H, H-3'), 9.01 ppm (s, 1H, -NH); $^{13}\text{C-NMR}$ δ = 9.2, 55.8, 95.4, 113.5, 113.3, 114.6, 121.4, 123.0, 125.5, 126.7, 138.0, 141.1, 146.7, 149.6, 154.7, 158.0, 160.8 ppm. Anal. calcd for C₁₆H₁₃N₂O₃Cl: C, 60.67; H, 4.14; N, 8.84. Found: C, 60.25; H, 4.10; N, 8.46.

6-Methoxy-3-methyl-*N*-(pyrimidin-2-yl)benzofuran-2-carboxamide (5g)

Acid **3a** was reacted with 2-aminopyrimidine (**4g**) and column eluted with system C to give amide **5g**, (0.98 g, 69%) as a cream crystals; mp 169–171 °C, [lit.⁵² 156–158 °C]; IR ν_{max} 1704, 3421 cm^{-1} ; $^1\text{H-NMR}$ δ = 2.58 (s, 3H, -CH₃), 3.80 (s, 3H, -OCH₃), 6.86 (m, 2H, H-5 and H-7), 7.00 (t, J = 5 Hz, 1H, H-5'), 7.42 (d, J = 8 Hz, 1H, H-4), 8.6 (d, J = 5 Hz, 2H, H-4' and H-6'), 9.04 ppm (s, 1H, -NH); $^{13}\text{C-NMR}$ δ = 9.6, 53.9, 56.2, 95.9, 113.7, 117.2, 122.0, 123.5, 126.7, 141.7, 155.1, 157.4, 157.9, 158.9, 161.3 ppm.

6-Methoxy-3-methyl-*N*-(3-methylpyridin-2-yl)benzofuran-2-carboxamide (5b)

To a 50 mL round bottom flask fitted with a calcium chloride guard tube was added a 10% mixture (wt./vol.) of acid **3a** (1.02 g, 4.97 mmol) in dichloromethane (10 mL). Pyridine (5 mL) and SOCl₂ (2 molar equiv.) were then added and the solution stirred at room temperature for 40 min. A 20% solution of amine **4b** (3 molar equiv.) in

pyridine/toluene (4:3) was made up in a 100 mL two-neck round bottom flask fitted with a constant pressure dropping funnel, reflux condenser and calcium chloride guard tube. The acid chloride mixture was transferred to the constant pressure dropping funnel and added dropwise over a period of 90 min then the whole heated at reflux for 3 h. The mixture was concentrated and pyridine removed by azeotroping with toluene and evaporating under vacuum. The crude was purified by flash-column chromatography on silica which had been treated with 5% triethylamine, and eluted with solvent system B, to give amide **5b** (1.03 g, 70%) as pale yellow crystals; mp 171–172 °C, IR ν_{\max} 1603, 3273 cm^{-1} ; $^1\text{H-NMR}$ δ = 2.41 (s, 3H, py-CH₃), 2.64 (s, 3H, furan-CH₃), 3.90 (s, 3H, -OCH₃), 6.97 (dd, J = 2 and 9 Hz, 1H, H-5), 6.99 (d, J = 2 Hz, 1H, H-7), 7.16 (dd, J = 5 Hz and 8 Hz, 1H, H-5'), 7.51 (d, J = 9 Hz, 1H, H-4), 7.64 (d, J = 8 Hz, 1H, H-4'), 8.35 (d, J = 5 Hz, 1H, H-6'), 8.64 ppm (s, 1H, -NH); $^{13}\text{C-NMR}$ δ = 9.1, 18.4, 55.8, 95.5, 113.0, 121.3, 121.7, 123.1, 124.7, 128.5, 139.8, 141.8, 145.9, 149.0, 154.7, 158.2, 160.5 ppm; Anal. calcd for C₁₇H₁₆N₂O₃: C, 68.91; H, 5.44; N, 9.45. Found: C, 68.86; H, 5.47; N, 9.29.

5,6-Dimethoxy-3-methyl-*N*-(pyridin-2-yl)benzofuran-2-carboxamide (5h)

5,6-Dimethoxy-3-methylbenzofuran-2-carboxylic acid (**3b**) (0.60 g, 2.53 mmol) was reacted with 2-aminopyridine (**4a**) (0.29 g, 3.03 mmol). Column was eluted with solvent system D to give amide **5h**, (0.49 g, 62%) as off-white crystals; mp 230–232 °C (EtOH); IR ν_{\max} 1695, 3417 cm^{-1} ; $^1\text{H-NMR}$ δ = 2.68 (s, 3H, -CH₃), 3.97 (s, 3H, -OCH₃), 3.98 (s, 3H, -OCH₃), 6.98 (s, 1H, H-7), 6.99 (s, 1H, H-4), 7.08 (m, 1H, H-4'), 7.76 (m, 1H, H-5'), 8.37 (m, 2H, H-3', 6'), 8.98 ppm (s, 1H, -NH); $^{13}\text{C-NMR}$ δ = 9.7, 56.7, 56.8, 95.3, 101.5, 114.4, 120.1, 122.0, 125.5, 138.7, 141.8, 147.7, 148.5, 149.0, 151.5, 151.7,

158.5 ppm. Anal. calcd for $C_{17}H_{16}N_2O_4$: C, 66.04; H, 5.85; N, 8.55. Found: C, 65.97; H, 5.81; N, 8.25.

General Preparation of Bromomethyl Amides (6a–h)

A solution of amide in carbon tetrachloride was made up in a round bottom flask fitted with reflux condenser and calcium chloride guard tube. *N*-bromosuccinimide (1.1 molar equiv.) was added with stirring and the mixture irradiated, in a darkened box, with a 150 W tungsten lamp for 2–3 h. The suspension was filtered and the filter cake washed with hot CCl_4 . The filtrate was then concentrated and recrystallized to give the respective bromomethyl amide. No elemental analysis was carried out on these allyl bromides.

3-(Bromomethyl)-6-methoxy-*N*-(pyridin-2-yl)benzofuran-2-carboxamide (6a)

Amide **5a** (0.40 g, 1.42 mmol) reacted in CCl_4 (24 mL) to give **6a** (0.39 g, 76%) as an off-white solid, mp 158–160 °C (MeOH); [lit. 123–124 °C]; IR ν_{\max} 1578, 1665, 3401 cm^{-1} ; 1H -NMR δ = 3.90 (s, 3H, $-OCH_3$), 5.14 (s, 2H, $-CH_2Br$), 7.00 (m, 3H, H-4, H-5 and H-7), 7.73 (m, 2H, H-4' and H-5'), 8.36 (m, 2H, H-3' and H-6'), 9.01 ppm (s, 1H, $-NH$); ^{13}C -NMR δ = 21.2, 56.2, 96.1, 114.3, 114.6, 120.6, 121.0, 122.1, 125.0, 138.8, 141.9, 148.5, 151.1, 155.3, 157.7, 161.4 ppm.

3-(Bromomethyl)-6-methoxy-*N*-(4-methylpyridin-2-yl)benzofuran-2-carboxamide (6c)

Amide **5c** (1.12 g, 3.78 mmol) reacted in CCl_4 (95 mL) to give **6c** (0.73 g, 51%) as a pale yellow solid, mp 191–193 °C (EtOH); IR ν_{\max} 1558, 1619, 3393 cm^{-1} ; IR ν_{\max}

1578, 1665, 3401 cm^{-1} ; $^1\text{H-NMR}$ δ = 2.41 (s, 3H, $-\text{CH}_3$) 3.90 (s, 3H, $-\text{OCH}_3$), 5.14 (s, 2H, $-\text{CH}_2\text{Br}$), 6.93 (dd, J = 1 and 5 Hz, 1H, H-5), 7.03 (m, 2H, H-4 and H-7), 7.67 (dd, J = 1 and 8 Hz, 1H, H-5'), 8.20 (m, 2H, H-3' and H-6'), 8.97 ppm (s, 1H, $-\text{NH}$); $^{13}\text{C-NMR}$ δ = 21.2, 21.8, 56.2, 96.1, 114.3, 115.2, 121.0, 121.8, 122.1, 125.0, 141.9, 147.9, 150.6, 151.1, 155.3, 157.7, 161.4 ppm.

3-(Bromomethyl)-6-methoxy-*N*-(5-methylpyridin-2-yl)benzofuran-2-carboxamide (6d)

Amide **5d** (0.80 g, 2.70 mmol) reacted in CCl_4 (80 mL) to give **6d** (0.45 g, 44%) as a pale yellow solid, mp 178–180 $^\circ\text{C}$ (EtOH); IR ν_{max} 1599, 1673, 3430 cm^{-1} ; $^1\text{H-NMR}$ δ = 2.36 (s, 3H, $-\text{CH}_3$), 3.91 (s, 3H, $-\text{OCH}_3$), 5.12 (s, 3H, $-\text{CH}_2\text{Br}$), 6.99 (dd, J = 2 and 9 Hz, 1H, H-5), 6.98 (d, J = 2 Hz, 1H, H-7), 7.52 (d, J = 9 Hz, 1H, H-4), 7.58 (dd, J = 2 and 9 Hz, 1H, H-4'), 8.18 (d, J = 2 Hz, 1H, H-6'), 8.29 (d, J = 9 Hz, 1H, H-3'), 8.98 ppm (s, 1H, $-\text{NH}$); $^{13}\text{C-NMR}$ δ = 18.3, 21.3, 56.3, 96.1, 114.2, 114.4, 121.1, 122.2, 125.4, 139.4, 139.7, 148.5, 149.0, 151.0, 155.3, 158.6, 161.4 ppm.

3-(Bromomethyl)-6-methoxy-*N*-(6-methylpyridin-2-yl)benzofuran-2-carboxamide (6e)

Amide **5e** (0.85 g, 2.87 mmol) reacted in CCl_4 (60 mL) to give **6e** (0.74 g, 69%) as a pale yellow solid, mp 150–152 $^\circ\text{C}$ (EtOH); IR ν_{max} 1597, 1670, 3414 cm^{-1} ; $^1\text{H-NMR}$ δ = 2.79 (s, 3H, $-\text{CH}_3$) 3.92 (s, 3H, $-\text{OCH}_3$), 5.07 (s, 2H, $-\text{CH}_2\text{Br}$), 7.02 (m, 3H, H-4, H-5 and H-7), 7.67 (m, 2H, H-4' and H-5'), 8.20 (d, J = 8 Hz, 1H, H-3'), 9.06 ppm (s, 1H, -

NH); ^{13}C -NMR δ = 21.2, 24.2, 56.2, 96.1, 112.0, 114.3, 120.1, 122.1, 123.9, 125.7, 139.9, 142.2, 151.0, 155.6, 157.8, 158.9, 161.6 ppm.

3-(Bromomethyl)-*N*-(5-chloropyridyl)-6-methoxybenzofuran-2-carboxamide (6f)

Amide **5f** (1.17 g, 3.70 mmol) reacted in CCl_4 (100 mL) to give **6f** (0.95 g, 65%) as a pale yellow solid, mp 218–220 °C (EtOH); IR ν_{max} 1577, 1678, 3394 cm^{-1} ; ^1H -NMR δ = 3.90 (s, 3H, $-\text{OCH}_3$), 5.12 (s, 2H, $-\text{CH}_2\text{Br}$) 7.01 (m, 2H, H-5 and H-7) 7.68 (d, J = 9 Hz, 1H, H-4), 7.73 (dd, J = 3 and 9 Hz, 1H, H-4'), 8.31 (d, J = 9 Hz, 1H, H-3'), 8.37 (d, J = 3 Hz, 1H, H-6'), 9.00 ppm (s, 1H, $-\text{NH}$); ^{13}C -NMR δ = 20.6, 55.8, 95.7, 114.0, 114.9, 120.6, 121.8, 125.1, 127.3, 138.1, 141.2, 146.7, 149.1, 155.0, 157.2, 161.2 ppm.

3-Methoxy-6-oxo-7,13-dihydro-6*H*-benzofuro[2,3-*e*]pyrimido[1,2-*a*][1,3]diazepin-12-ium bromide (11)

Amide **5g** (0.40 g, 1.41 mmol) reacted in CCl_4 (24 mL) to give **11** (0.11 g, 28%) as a light brown solid; mp. 283–285 °C (decomp.); IR ν_{max} (KBr) 1708, 3404 cm^{-1} ; ^1H -NMR ($\text{DMSO}-d_6$) δ = 3.86 (s, 3H, $-\text{OCH}_3$), 6.03 (s, 2H, $-\text{CH}_2\text{N}^+$), 7.18 (dd, J = 2 and 9 Hz, 1H, H-2), 7.41 (d, J = 2 Hz, 1H, H-4), 7.92 (m, 1H, H-10), 8.00 (d, J = 9, 1H, H-1), 9.30 (dd, J = 2 and 5 Hz, 1H, H-9), 9.38 ppm (dd, J = 2 and 5 Hz, 1H, H-11); ^{13}C -NMR ($\text{DMSO}-d_6$) δ = 51.8, 56.4, 96.4, 113.68, 115.1, 118.1, 119.0, 122.8, 123.3, 152.4, 152.7, 157.0, 157.2, 161.7, 166.2 ppm; Anal. calcd for $\text{C}_{15}\text{H}_{12}\text{N}_3\text{O}_3\text{Br}$: C, 49.74; H, 3.34; N, 11.60. Found: C, 49.46; H, 3.40; N, 11.67.

3-(Bromomethyl)-5,6-dimethoxy-*N*-(pyridin-2-yl)benzofuran-2-carboxamide (**6h**)

Amide **5h** (0.38 g, 1.20 mmol) reacted in CCl₄ (40 mL) to give **6h** (0.11 g, 23%) as an off-white solid, mp 216–218 °C (EtOH); IR ν_{max} 1574, 1643, 3379 cm⁻¹; ¹H-NMR δ = 4.01 (s, 3H, -OCH₃), 4.02 (s, 3H, -OCH₃), 5.18 (s, 2H, -CH₂Br), 7.05 (s, 1H, H-7), 7.14 (dd, J = 2 and 5 Hz, 1H, H-4'), 7.16 (s, 1H, H-4), 7.80 (dt, J = 2 and 8 Hz, 1H, H-5'), 8.38 (d, J = 5 Hz, 1H, H-3'), 8.41 (d, J = 8 Hz, 1H, H-6'), 9.05 ppm (s, 1H, -NH); ¹³C-NMR δ = 21.6, 56.8, 56.9, 95.4, 101.6, 114.7, 119.8, 120.6, 125.2, 139.0, 141.9, 148.2, 148.5, 149.3, 151.2, 151.9, 157.7 ppm.

Preparation of Chloromethyl Amides (**7a–f** and **7h**)

A solution of bromomethyl amide in chloroform was placed in a round bottom flask fitted with a reflux condenser. Tetra-*n*-butylammonium iodide (0.3 molar equiv.) was added to the solution with stirring, followed by an equal volume of 25% aqueous sodium chloride solution. The mixture was then heated at 90 °C for 3–12 h. The layers were separated and the organic layer washed with 2% HCl (2 × 20 mL), then 2% NaOH (2 × 20 mL) and finally water (2 × 20 mL). The resultant organic layer was dried with anhydrous sodium sulfate, filtered, concentrated and recrystallized to give the corresponding chloromethyl amide. No elemental analysis was carried out on these allyl chlorides.

3-(Chloromethyl)-6-methoxy-*N*-(pyridin-2-yl)benzofuran-2-carboxamide (7a)

Bromomethyl amide **6a** (0.43 g, 1.19 mmol) reacted in chloroform (20 mL) for 3 h to give **7a** (0.26 g, 68%) as light brown needle-like crystals, mp 163–165 °C (MeOH); IR ν_{\max} 1565, 1672, 3411 cm^{-1} ; $^1\text{H-NMR}$ δ = 3.90 (s, 3H, -OCH₃), 5.28 (s, 2H, -CH₂Cl), 7.07 (m, 3H, H-4, H-5 and H-7), 7.74 (m, 2H, H-4' and H-5'), 8.36 (m, 2H, H-3' and H-6'), 9.03 ppm (s, 1H, -NH); $^{13}\text{C NMR}$ δ = 35.0, 55.8, 95.7, 114.0, 114.3, 120.3, 120.7, 122.0, 124.3, 138.5, 141.8, 148.2, 150.8, 155.0, 157.3, 161.0 ppm.

3-(Chloromethyl)-6-methoxy-*N*-(4-methylpyridin-2-yl)benzofuran-2-carboxamide (7c)

Bromomethyl amide **6c** (0.29 g, 0.77 mmol) reacted in chloroform (25 mL) for 6 h to give **7c** (0.20 g, 81%) as beige crystals, mp 179–181 °C (EtOH); IR ν_{\max} 1524, 1602, 1675, 3427 cm^{-1} ; $^1\text{H-NMR}$ δ = 2.41 (s, 3H, -CH₃) 3.90 (s, 3H, -OCH₃), 5.28 (s, 2H, -CH₂Cl), 6.93 (dd, J = 2 and 5 Hz, 1H, H-5), 6.99 (d, J = 2 Hz, 1H, H-7) 7.03 (d, J = 5 Hz, 1H, H-4), 7.71 (dd, J = 2 and 7 Hz, 1H, H-5'), 8.19 (m, 2H, H-3' and H-6'), 8.97 ppm (s, 1H, -NH); $^{13}\text{C NMR}$ δ = 21.8, 35.3, 56.2, 96.0, 114.3, 115.1, 121.1, 121.8, 122.3, 124.5, 142.3, 148.1, 150.4, 151.1, 153.3, 155.3, 161.3 ppm.

3-(Chloromethyl)-6-methoxy-*N*-(6-methylpyridin-2-yl)benzofuran-2-carboxamide (7e)

Bromomethyl amide **6e** (0.55 g, 1.47 mmol) reacted in chloroform (40 mL) for 12 h to give **7e** (0.41 g, 88%) as beige crystals, mp 143–144 °C (EtOH); IR ν_{\max} 1544, 1664, 3413 cm^{-1} ; $^1\text{H-NMR}$ δ = 2.51 (s, 3H, -CH₃) 3.90 (s, 3H, -OCH₃), 5.28 (s, 2H, -CH₂Cl),

7.00 (m, 3H, H-4, H-5 and H-7), 7.69 (m, 2H, H-4' and H-5'), 8.17 (d, $J = 8$ Hz, 1H, H-3'), 8.94 ppm (s, 1H, -NH); ^{13}C NMR $\delta = 24.5, 35.4, 56.2, 96.0, 111.4, 114.3, 120.2, 122.4, 123.9, 125.5, 139.1, 142.1, 151.8, 155.3, 157.7, 158.7, 161.3$ ppm.

3-Chloromethyl-*N*-(5-chloropyridin-2-yl)-6-methoxybenzofuran-2-carboxamide (7f)

Bromomethyl amide **6f** (0.55 g, 1.47 mmol) reacted in chloroform (40 mL) for 4 h to give **7f** (0.41 g, 88%) as beige crystals, mp 207–208 °C (EtOH); IR ν_{max} 1549, 1666, 3398 cm^{-1} ; ^1H -NMR $\delta = 3.90$ (s, 3H, -OCH₃), 5.26 (s, 2H, -CH₂Cl), 7.01 (m, 2H, H-5 and H-7), 7.73 (m, 2H, H-4 and H-4'), 8.30 (d, $J = 6$ Hz, 1H, H-6'), 8.36 (d, $J = 9$ Hz, 1H, H-3'), 9.01 ppm (s, 1H, -NH); ^{13}C -NMR $\delta = 34.8, 55.8, 95.6, 114.0, 114.9, 120.6, 122.0, 125.1, 127.3, 138.1, 141.4, 146.7, 149.1, 155.8, 157.5, 161.4$ ppm.

3-(Chloromomethyl)-5,6-dimethoxy-*N*-(pyridin-2-yl)benzofuran-2-carboxamide (7h)

Bromomethyl amide **6h** (0.13 g, 0.33 mmol) reacted in chloroform (12 mL) to give **7h** (0.41 g, 68%) as beige crystals, mp 207–208 °C (EtOH); IR ν_{max} 1557, 1669, 3403 cm^{-1} ; ^1H -NMR $\delta = 4.00$ (s, 3H, -OCH₃), 4.01 (s, 3H, -OCH₃), 5.14 (s, 3H, -CH₂Cl), 6.99 (s, 1H, H-7), 7.00 (s, 1H, H-4), 7.13 (m, 1H, H-4'), 7.80 (m, 1H, H-5'), 8.40 (m, 2H, H-3' and H-6'), 8.98 ppm (s, 1H, -NH), ^{13}C -NMR $\delta = 35.6, 56.8, 56.9, 95.4, 101.9, 114.6, 119.9, 120.6, 125.2, 139.1, 142.0, 147.9, 148.0, 149.0, 151.5, 151.9, 157.8$ ppm.

Preparation of Tetracyclic Salts (8a–f, 8h)

In a round bottom flask fitted with a reflux condenser and calcium chloride guard tube, was placed a solution (10–20%) of chloromethyl amide in 1,4-dioxane. This was

heated at reflux for several days. The resultant precipitate was collected by filtration and was washed with hot acetone to give the respective tetracyclic chloride salt.

3-Methoxy-6-oxo-7,13-dihydro-6*H*-benzofuro[2,3-*e*]pyrido[1,2-*a*][1,3]diazepin-12-ium chloride (8a)

Chloromethyl amide **7a** (0.35 g, 1.11 mmol) in 1,4-dioxane (2 mL) for 3 days gave **8a** (0.15 g, 43%) as a pale gray solid, mp 285–287 °C; IR ν_{max} 1721, 3430 cm^{-1} , ^1H -NMR (DMSO- d_6) δ = 3.88 (s, 3H, -OCH₃), 6.10 (s, 2H, -CH₂N⁺), 7.17 (dd, J = 1 and 9 Hz, 1H, H-2), 7.43 (d, J = 1 Hz, 1H, H-4), 7.83 (dd, J = 2 and 8 Hz, 2H, H-8 and H-9), 8.07 (d, J = 9 Hz, 1H, H-1), 8.49 (dt, J = 2 and 6 Hz, 1H, H-10), 9.1 (d, J = 6 Hz, 1H, H-11), 12.21 ppm (s, 1H, -NH); ^{13}C -NMR (DMSO- d_6) δ = 50.2, 56.4, 96.5, 115.0, 118.1, 121.9, 122.9, 123.1, 123.6, 143.6, 143.7, 146.8, 148.4, 157.2, 157.8, 161.6 ppm; Anal. calcd for C₁₆H₁₃N₂O₃Cl: C, 60.67; H, 4.14; N, 8.84. Found: C, 60.49; H, 4.21; N, 8.82.

3-Methoxy-8-methyl-6-oxo-7,13-dihydro-6*H*-benzofuro[2,3-*e*]pyrido[1,2-*a*][1,3]diazepin-12-ium chloride (8b)

Crude chloromethyl amide **7b** (0.44 g) in 1,4-dioxane (4 mL) for 3 days gave **8b** (0.019 g, 2% from amide) as a brown solid, mp > 300 °C; IR ν_{max} 1708, 3467 cm^{-1} , ^1H -NMR (DMSO- d_6) δ = 2.42 (s, 3H, -CH₃), 3.90 (s, 3H, -OCH₃), 6.12 (s, 3H, -CH₂N⁺), 6.97 (dd, J = 2 and 9 Hz, 1H, H-2), 7.00 (d, J = 2 Hz, 1H, H-4), 7.23 (dd, J = 5 and 8 Hz, 1H, H-10), 7.58 (d, J = 9 Hz, 1H, H-1), 7.76 (d, J = 8 Hz, 1H, H-9), 8.64 (d, J = 5 Hz, 1H, H-11), 11.94 (s, 1H, -NH), ^{13}C -NMR (DMSO- d_6) δ = 18.6, 50.0, 55.9, 95.8, 113.0, 121.3, 121.7, 123.3, 124.8, 128.5, 139.8, 141.8, 146.2, 149.0, 155.2, 158.0, 160.9 ppm.

3-Methoxy-9-methyl-6-oxo-7,13-dihydro-6H-benzofuro[2,3-*e*]pyrido[1,2-*a*][1,3]diazepin-12-ium chloride (8c)

Chloromethyl amide **7c** (0.074 g, 0.23 mmol) in 1,4-dioxane (4 mL) for 3 days gave **8c** (0.036 g, 49%) as a cream solid, mp 283–285 °C; IR ν_{max} 1711, 3485 cm^{-1} , ^1H -NMR (DMSO- d_6) δ = 2.52 (s, 3H, -CH₃), 3.85 (s, 3H, -OCH₃), 5.90 (s, 2H, -CH₂N⁺), 7.13 (dd, J = 2 and 9 Hz, 1H, H-2), 7.38 (d, J = 2 Hz, 1H, H-4), 7.54 (s, 1H, H-8), 7.62 (d, J = 6, 1H, H-10), 8.01 (d, J = 9 Hz, 1H, H-1), 8.85 (d, J = 6 Hz, 1H, H-11), 12.13 ppm (s, 1H, -NH); ^{13}C -NMR (DMSO- d_6) δ = 22.2, 49.9, 56.9, 80.0, 97.0, 115.4, 118.6, 122.0, 123.4, 123.9, 143.0, 144.5, 148.5, 157.5, 158.6, 159.7, 161.9 ppm; Anal. calcd for C₁₇H₁₅N₂O₃Cl: C, 61.73; H, 4.57; N, 8.47. Found: C, 61.56; H, 4.50; N, 8.25.

3-Methoxy-10-methyl-6-oxo-7,13-dihydro-6H-benzofuro[2,3-*e*]pyrido[1,2-*a*][1,3]diazepin-12-ium chloride (8d)

Crude chloromethyl amide **7d** (0.20 g) in 1,4-dioxane (2 mL) for 3 days gave **8d** (0.05 g, 24%) as a pale gray solid, mp > 300 °C; IR ν_{max} 1716, 3465 cm^{-1} , ^1H -NMR (DMSO- d_6) δ = 2.41 (s, 3H, -CH₃), 3.88 (s, 3H, -OCH₃), 6.05 (s, 2H, -CH₂N⁺), 7.17 (dd, J = 2 and 9 Hz, 1H, H-2), 7.42 (d, J = 2 Hz, 1H, H-4), 7.76 (d, J = 9 Hz, 1H, H-1), 8.05 (d, J = 9 Hz, 1H, H-9), 8.37 (d, J = 9, 1H, H-8), 9.03 (s, 1H, H-11), 12.12 ppm (s, 1H, -NH); ^{13}C -NMR (DMSO- d_6) δ = 17.9, 50.6, 56.9, 97.0, 115.5, 118.6, 121.8, 123.6, 124.2, 133.8, 142.9, 144.1, 146.6, 148.2, 157.7, 158.4, 162.1; Anal. calcd for C₁₇H₁₅N₂O₃Cl: C, 61.73; H, 4.57; N, 8.47. Found: C, 61.56; H, 4.58; N, 8.41.

3-Methoxy-11-methyl-6-oxo-7,13-dihydro-6H-benzofuro[2,3-*e*]pyrido[1,2-*a*][1,3]diazepin-12-ium chloride (8e)

Chloromethyl amide **7e** (0.38 g, 1.20 mmol) in 1,4-dioxane (2 mL) for 5 days gave **8e** (45 mg, 12%) as a cream solid, mp 260–261 °C; IR ν_{max} 1707, 3458 cm^{-1} , $^1\text{H-NMR}$ (DMSO- d_6) δ = 2.82 (s, 3H, -CH₃), 3.76 (s, 3H, -OCH₃), 5.81 (s, 2H, -CH₂N⁺), 7.05 (dd, J = 2 and 9 Hz, 1H, H-2), 7.32 (d, J = 2 Hz, 1H, H-4), 7.63 (dd, J = 2 and 8 Hz, 2H, H-8 and H-10), 8.04 (d, J = 9 Hz, 1H, H-1), 8.56 (t, J = 8 Hz, 1H, H-9), 12.07 ppm (s, 1H, -NH); $^{13}\text{C-NMR}$ (DMSO- d_6) δ = 21.7, 45.0, 56.4, 96.6, 115.2, 117.9, 119.5, 122.9, 123.8, 124.6, 144.8, 145.8, 149.0, 152.9, 157.3, 158.0, 161.5 ppm; Anal. calcd for C₁₇H₁₅N₂O₃Cl: C, 61.73; H, 4.57; N, 8.47. Found: C, 61.37; H, 4.51; N, 7.91.

10-Chloro-3-methoxy-6-oxo-7,13-dihydro-6H-benzofuro[2,3-*e*]pyrido[1,2-*a*][1,3]diazepin-12-ium chloride (8f)

Chloromethyl amide **7f** (0.10 g) in 1,4-dioxane (0.5 mL) for 3 days gave **8f** (0.052 g, 50%) as a pale gray solid, mp 204–206 °C; IR ν_{max} 1720, 3431 cm^{-1} , $^1\text{H-NMR}$ (DMSO- d_6) δ = 3.88 (s, 3H, -OCH₃), 5.75 (s, 2H, -CH₂N⁺), 7.08 (dd, J = 2 and 9 Hz, 1H, H-2), 7.28 (d, J = 2 Hz, 1H, H-4), 7.80 (d, J = 9 Hz, 1H, H-1), 8.00 (dd, J = 2 and 9 Hz, 1H, H-9), 8.19 (d, J = 9 Hz, 1H, H-8), 8.48 (d, J = 2 Hz, 1H, H-11), 10.61 ppm (s, 1H, -NH); $^{13}\text{C-NMR}$ (DMSO- d_6) δ = 55.4, 56.3, 96.5, 114.4, 116.3, 120.4, 122.5, 124.0, 126.7, 138.5, 142.6, 147.1, 149.1, 150.1, 155.0, 157.9, 161.0 ppm; Anal. calcd for C₁₆H₁₂N₂O₃Cl₂: C, 54.72; H, 3.44; N, 7.98. Found: C, 54.40; H, 3.48; N, 8.01.

2,3-Dimethoxy-6-oxo-7,13-dihydro-6*H*-benzofuro[2,3-*e*]pyrido[1,2-*a*][1,3]diazepin-12-ium chloride (8h)

Chloromethyl amide **7h** (0.35 g, 1.11 mmol) in 1,4-dioxane (2 mL) for 3 days gave **8h** (0.15 g, 34%) as a pale gray solid, mp 256–258 °C; IR ν_{max} 1701, 3461 cm^{-1} , ^1H -NMR (DMSO- d_6) δ = 3.88 (s, 3H, -OCH₃), 3.90 (s, 3H, -OCH₃), 6.17 (s, 2H, -CH₂N⁺), 7.45 (s, 2H, H-1 and H-7), 7.84 (m, 2H, H-8 and H-10), 8.50 (t, J = 8 Hz, 1H, H-9), 9.11 (d, J = 6 Hz, 1H, H-11), 12.15 ppm (s, 1H, -NH); ^{13}C -NMR (DMSO- d_6) δ = 50.2, 56.8, 56.9, 95.5, 102.0, 114.5, 120.0, 120.8, 125.1, 139.1, 141.6, 147.9, 148.1, 149.0, 151.4, 152.3, 158.2 ppm; Anal. calcd for C₁₇H₁₅N₂O₄Cl: C, 58.88; H, 4.36; N, 8.07. Found: C, 58.74; H, 4.30; N, 7.96.

Appendix V. UWM Compound Table

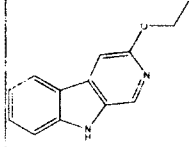
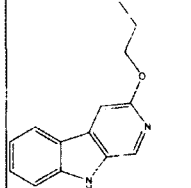
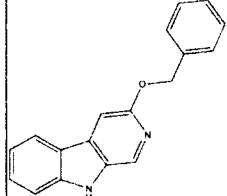
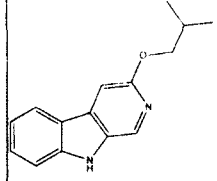
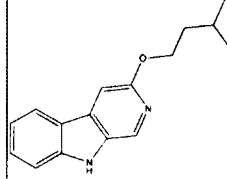
In the following pages is a reprint of the UWM compound table. The actual interactive database exists in a Microsoft excel spreadsheet with an add-in for ChemDraw Ultra 12.0. The add-in allows for additional spreadsheet functionality explained in the text. In the table, K_i values are reported in nM unless a percentage is listed.

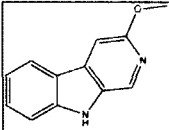
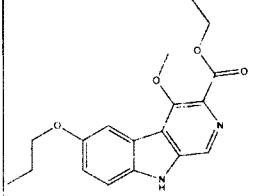
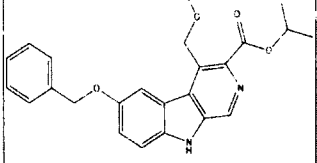
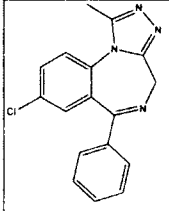
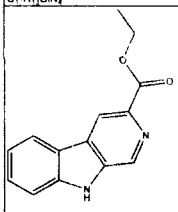
PDSP compound number assignment:

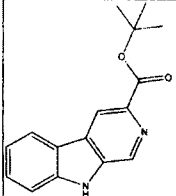
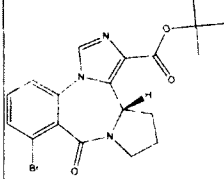
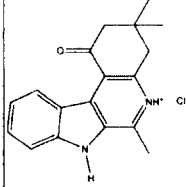
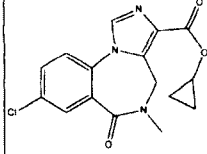
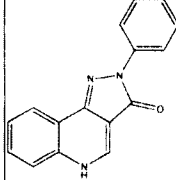
03-0934	DMH-D-070 (C ₃₉ H ₂₈ N ₆ O ₄ Br ₂)	802
03-0935	DMH-D-048 (C ₄₉ H ₄₆ N ₆ O ₄ Si ₂)	838
03-0936	DMH-D-053 (C ₄₃ H ₃₀ N ₆ O ₄)	694
03-0937	DM-II-26 (C ₄₁ H ₃₂ N ₆ O ₄ Br ₂)	830
03-0938	DM-II-41 (C ₅₁ H ₅₀ N ₆ O ₄ Si ₂)	866
03-0939	DM-III-97 (C ₄₅ H ₃₄ N ₆ O ₄)	722
03-0940	DM-III-93 (C ₄₀ H ₃₀ N ₆ O ₅ Br ₂)	832
03-0941	DM-III-94 (C ₅₀ H ₄₈ N ₆ O ₅ Si ₂)	868
03-0942	DM-III-96 (C ₄₄ H ₃₂ N ₆ O ₅)	724
03-0943	DM-II-20 (C ₂₂ H ₁₄ N ₃ O ₂ F ₃)	408
03-0944	DM-II-30 (C ₂₀ H ₁₃ N ₃ O ₂ BrF ₃)	463
03-0945	DM-II-33 (C ₂₀ H ₁₃ N ₃ O ₂ BrCl ₃)	511
03-0946	DM-II-35 (C ₂₅ H ₂₂ N ₃ O ₂ SiF ₃)	481
03-0947	DM-III-01 (C ₁₈ H ₁₂ N ₃ O ₂ Br)	381
03-0948	DM-II-72 (C ₁₅ H ₁₀ N ₂ OBrCl)	348
03-0949	DM-II-90 (C ₁₇ H ₁₂ N ₄ BrCl)	386
03-0950	XLi-JY-DMH-TMS C ₂₂ H ₂₁ N ₄ SiCl)	404
03-0951	XLi-JY-DMH (C ₁₉ H ₁₃ N ₄ Cl)	332
03-0952	Hz111 C ₂₀ H ₁₆ N ₃ ClO ₂	365.81
03-0953	Hz120 C ₂₀ H ₁₆ N ₃ IO ₂	457.26
03-0954	Hz141 C ₂₁ H ₂₃ N ₃ Si	345.51
03-0955	Hz146 C ₂₁ H ₂₃ N ₃ OSi	361.51
03-0956	Hz150 C ₁₆ H ₁₄ N ₃ OBr	344.21
03-0957	Hz147 C ₁₈ H ₁₅ N ₃ O	289.33
03-0958	Hz157 C ₁₉ H ₁₉ N ₃ OSi	333.46
03-0959	Hz158 C ₂₀ H ₂₁ N ₃ OSi	347.49
03-0960	Hz160 C ₁₇ H ₁₃ N ₃ O	275.3
03-0961	Hz165 C ₂₄ H ₂₄ N ₄ O ₂ Si	428.56
03-0962	Hz166 C ₂₁ H ₁₆ N ₄ O ₂	356.38
03-0963	Hz148 C ₁₈ H ₁₅ N ₃	273.33
03-0964	Hz135 C ₁₆ H ₁₄ N ₃ Br	328.21
03-0965	Hz164 C ₁₉ H ₁₅ N ₄ O ₂ Br	411.25
03-0966	WYS1 C ₄₅ H ₅₀ N ₄ O ₆	774.9
03-0967	WYS2 C ₃₅ H ₃₄ N ₄ O ₄	574.67
03-0968	WYS3 C ₃₅ H ₃₈ N ₄ O ₄	578.7
03-0969	WYS4 C ₄₈ H ₅₆ N ₄ O ₈	816.98
03-0970	WYS5 C ₃₇ H ₄₂ N ₄ O ₄	606.25
03-0971	WYS6 C ₃₇ H ₃₅ N ₄ O ₄	599.7
03-0972	WYS7 C ₂₁ H ₂₈ N ₄ O ₄ Si	364.51
03-0973	WYS8 C ₁₈ H ₁₆ N ₂ O ₂	292.33
03-0974	WYS9 C ₁₆ H ₁₅ N ₂ O ₂	394.21
03-0975	WYS10 C ₁₄ H ₉ F ₃ N ₂ O ₂	294.23
03-0976	WYS11 C ₁₅ H ₁₁ F ₃ N ₂ O ₃	324.25
03-0977	WYS12 C ₂₀ H ₁₈ N ₂ O ₂ S	350.44
03-0978	WYS13 C ₂₀ H ₁₈ N ₂ O ₃	334.37
03-0979	WYS14 C ₃₄ H ₂₉ F ₃ N ₄ O ₄	614.61
03-0980	WYS15 C ₂₂ H ₂₀ N ₂ O ₂	344.41
03-0981	WYS16 C ₁₈ H ₂₂ N ₂ O ₂	298.38
03-0982	WYS17 C ₁₇ H ₁₈ N ₂ O ₂	306.36
03-0983	WYS18 C ₂₁ H ₂₂ N ₂ O ₂	334.41
03-0984	WYS19 C ₂₆ H ₃₂ N ₂ O ₄ Si	464.63
03-0985	WYS20 C ₂₃ H ₂₄ N ₂ O ₄	392.45
03-0986	WYS21 C ₂₁ H ₂₃ I ₂ N ₂ O ₄	494.32
03-0987	WYSC1 C ₁₆ H ₁₆ N ₂ O ₂	268

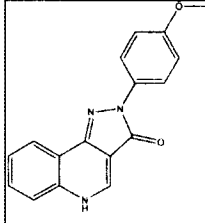
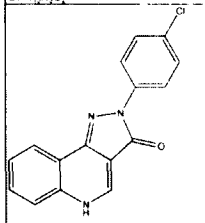
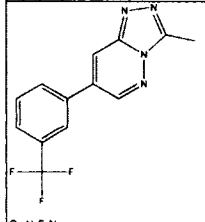
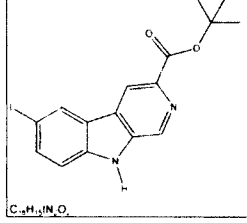
03-0988	WYSC2 C15H11F3N2O2	308
03-0989	JYI-01(C19H20N3O3Br)	418
03-0990	JYI-02 (C24H29N3O3Si)	437
03-0991	JYI-03 (C21H21N3O3)	363
03-0992	JYI-04 (C21H23N3O3)	365
03-0993	JYI-06 (C23H23N3O4)	405
03-0994	JYI-19 (C23H23N3O3S)	421
03-0995	JYI-20 (C25H25N3O3)	415
03-0996	JYI-10 (C17H13N3O3F3Br)	444
03-0997	JYI-11 (C22H22N3O3F3Si)	462
03-0998	JYI-15 (C19H14N3O3F3)	389
03-0999	JYI-12 (C19H16N3O3F3)	390
03-1001	JYI-13 (C21H16N3O4F3)	431
03-1002	JYI-14 (C17H14N3O3F3)	365
03-1003	JYI-21 (C23H17N3O3F3)	441
03-1004	JYI-32 (C20H15N3O2BrF)	428
03-1005	JYI-38 (C25H24N3O2FSi)	445
03-1006	JYI-56 (C24H18N3O4F)	373
03-1007	JYI-50 (C24H18N3O2SF)	469
03-1008	JYI-49 (C20H12N3O2F4Br)	482
03-1009	JYI-53 (C23H21N3O2F4Si)	475
03-1010	JYI-59 (C22H13N3O2F4)	427
03-1011	JYI-54 (C24H15N3O3F4)	469
03-1012	JYI-60 (C17H11N2OF)	278
03-1013	JYI-64 (C17H12N4FBr)	371
03-1014	JYI-70 (C19H13N4F)	316
03-1015	JYI-72 (C22H21N4SiF)	388
03-1016	PS-1-27 C21H16N5BrO	434.3
03-1017	PS-1-28 C26H25N5OSi	451.6
03-1018	PS-1-26 C23H17N5O	379.4
03-1019	PS-1-34B C20H17N	409.3
03-1020	PS-1-35 C23H22N:	464.4
03-1021	PS-1-36 C28H31N:	481.7
03-1022	PS-1-37 C25H23N:	409.5
03-1023	XLi268 C17H13BrN4	353
03-1024	XLi269 C22H22N4Si	370
03-1025	XLi270 C19H14N4	298.34
03-1026	XLi223 C22H20BrN3O2	438.32
03-1027	XLi224 C27H29N3O2Si	455.62
03-1028	XLi225 C24H21N3O2	383.44
03-1029	CM-D45 C19H21N3O4	355.39
03-1030	RY-024 C19H19N3O3	337.37
03-1031	XHeII-053 C22H17N3O2	355.39
03-1032	XLiXHeII-048 C25H25N3O2Si	427.57
03-1033	RY-023 C22H27N3O3Si	409.55
03-1034	RY-080 C17H15N3O3	309.32
03-1035	XLi337 C21H23N3O3	365.43
03-1036	XLi340 C26H25N3O2	411.5
03-1037	XLi339 C23H22N4	354.45
03-1038	XLi275 C20H19N3O3	349.38
03-1039	XLi356 C33H34N6O6	610.66
03-1040	XLi347 C34H28N6O7	632.62
03-1041	XLi351 C21H21CIN2OSi	380.94
03-1042	XLi343 C20H19CIN2OSi	366.92
03-1043	XLi350 C17H11CIN2O	294.73
03-1044	XLi352 C18H13CIN2O	308.76
03-1045	XLi338 C23H21CIN4	388.89

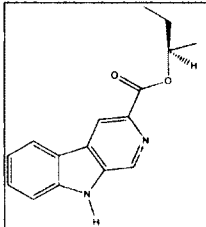
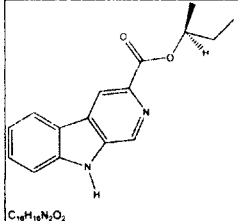
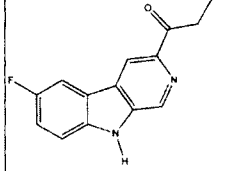
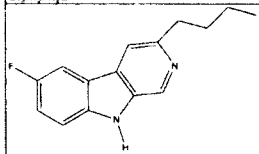
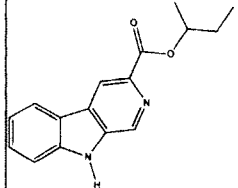
03-1046	Xli366	C22H21N3O2	359.42
03-1047	XLI368	C24H25N3O2	387.47
03-1048	JC184	C13H9BrN2OS	321
03-1049	JC207	C18H18N2OSSi	338
03-1050	JC208	C15H10N2OS	266
03-1051	JC209	C19H20N2OSSi	352
03-1052	JC222	C16H12N2OS	280
03-1053	JC217	C18H14BrN3O2S	416
03-1054	JC220	C23H23N3O2Ssi	433
03-1055	JC221	C20H15N3O2S	361

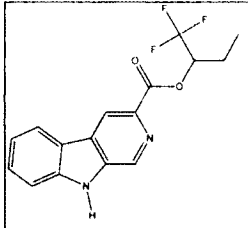
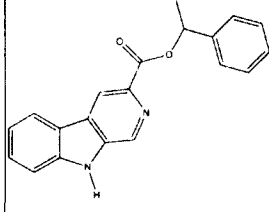
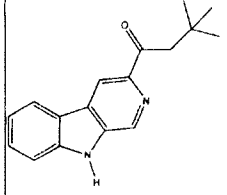
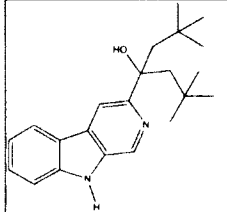
STRUCTURE	PDSP	COOK CODE	MOL FORMULA	MOL WEIGHT	a1	a2	a3	a4	a5	a6
										
C ₁₂ H ₁₂ N ₂ O		3 EBC	C13H12N2O	212.247	6.43	25.1	28.2		826	1000
										
C ₁₄ H ₁₄ N ₂ O		3 PBC	C14H14N2O	226.274	5.3	52.3	68.8		591	1000
										
C ₁₈ H ₁₄ N ₂ O		3-BENZOXY bC	C18H14N2O	274.317	830	3000	3000		10000	10000
										
C ₁₇ H ₁₈ N ₂ O		3-isobutoxy bC	C15H16N2O	240.3	24.9	123.6	139.2		1000	10000
										
C ₁₇ H ₁₈ N ₂ O		3-isopentoxy bC	C16H18N2O	254.327	350.2	3000	3000		3000	10000

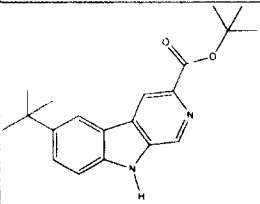
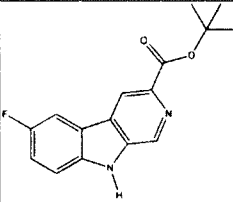
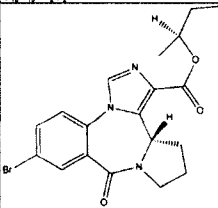
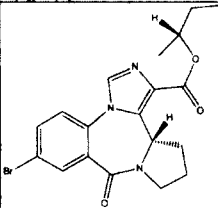
 $C_{17}H_{19}N_2O$		3MBC	C12H10N2O	198.221						
 $C_{18}H_{20}N_2O_4$		6-PBC	C18H20N2O4	328.362	0.49	1.21	2.2	2.39	1343	
 $C_{24}H_{24}N_2O_4$		ABECARNIL	C24H24N2O4	404.458	12.4	15.3	7.5	6	1000	
 $C_{17}H_{13}ClN_4$		alprazolam	C17H13ClN4	308.765	0.8	0.59	1.43	1.54	10000	
 $C_{14}H_{12}N_2O_2$		BCCE	C14H12N2O2	240.257	1.2	4.9	5.7	26.8	2700	

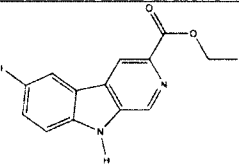
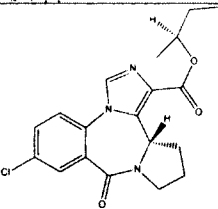
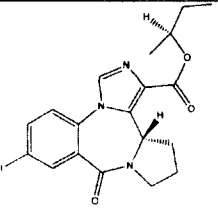
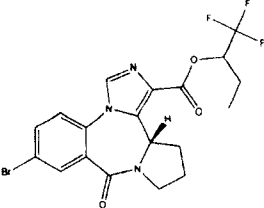
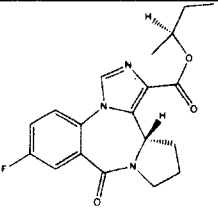
 $C_{16}H_{16}N_2O_2$		BCCl	$C_{16}H_{16}N_2O_2$	268.31	0.72	15	18.9		110.8	5000
 $C_{19}H_{20}BrN_3O_2$		BRETazenil	$C_{19}H_{20}BrN_3O_3$	418.284	0.35	0.64	0.2		0.5	12.7
 $C_{18}H_{19}ClN_4O$		C-383	$C_{18}H_{19}ClN_2O$	314.809	1000		1000	1000	1000	1000
 $C_{16}H_{14}ClN_3O_2$		CD-214	$C_{16}H_{14}ClN_3O_3$	331.754	16.4	48.2	42.5		9.8	168
 $C_{16}H_{11}N_3O$		CGS8216	$C_{16}H_{11}N_3O$	261.278	0.13					46

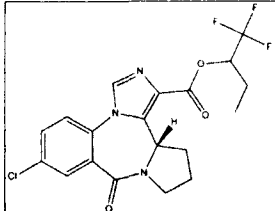
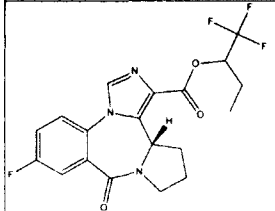
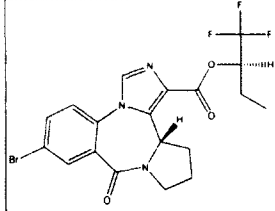
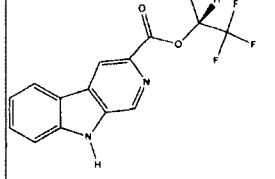
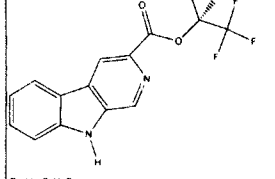
 $C_{17}H_{13}N_3O_2$		CGS9895	C17H13N3O2	291.304	0.21						9.3
 $C_{16}H_{10}ClN_3O$		CGS9896	C16H10ClN3O	295.723	0.28						181
 $C_{17}H_9F_3N_4$		CL 218,872	C13H9F3N4	278.233	57	1964	1161			561	10000
 $C_{21}H_{21}IN_2O_2$		CM-A100	C16H15IN2O2	394.207	14.49	44.91	123.8	1000		65.31	1000

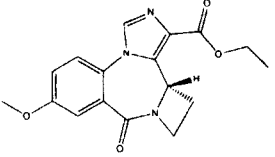
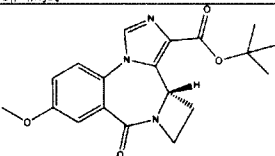
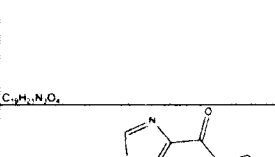
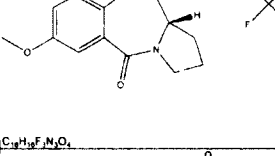
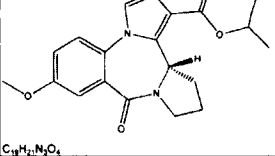
 $C_{16}H_{16}N_2O_2$		CM-A49(R)	C16H16N2O2	268.31	7.7	32.5	43	69	1000
 $C_{18}H_{18}N_2O_2$		CM-A50(S)	C16H16N2O2	268.31	17	59	88	144	1000
 $C_{15}H_{13}FN_2O$		CM-A57	C15H13FN2O	256.275	3.7	27	40	254	1000
 $C_{15}H_{13}FN_2$		CM-A58	C15H15FN2	242.291	16	120	184	1000	1012.2Nm
 $C_{16}H_{16}N_2O_2$		CM-A64	C16H16N2O2	268.31	18	60	116	216	1000

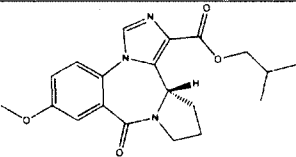
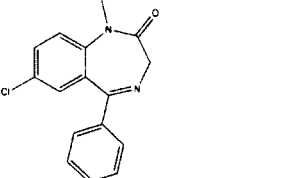
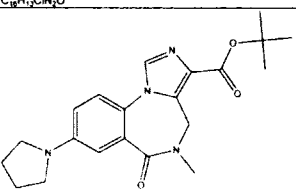
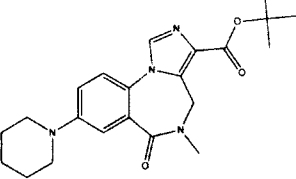
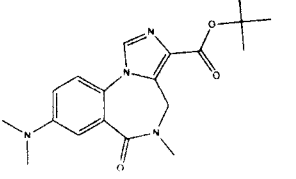
 $C_{16}H_{13}F_3N_2O_2$		CM-A69	C16H13F3N2O2	322.282	1000	1000	1000		1000	1000
 $C_{20}H_{19}N_2O_2$		CM-A71	C20H16N2O2	316.353	333.57	1000	1000	1000	1000	3000
 $C_{17}H_{19}N_2O$		CM-A77	C17H18N2O	266.338	11.51	51.9	105.16	1000	42.62	1000
 $C_{22}H_{30}N_2O$		CM-A77a	C22H30N2O	338.486	27.4	111.5	301.3	1000	61.61	1000

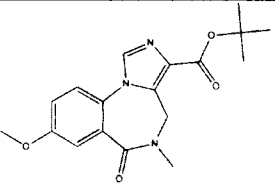
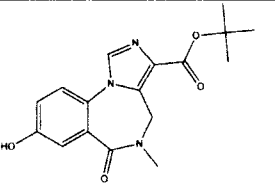
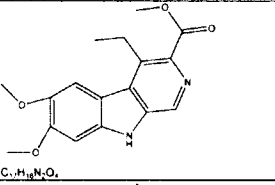
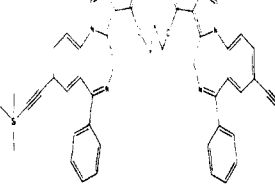
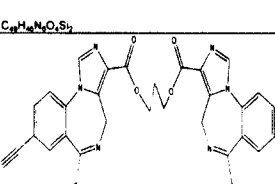
											
$C_{20}H_{24}N_2O_2$	CM-A82a	C20H24N2O2	324.417	2.78	8.93	24.51	1000	7.49	1000		
											
$C_{16}H_{15}FN_2O_2$	CM-A87	C16H15FN2O2	286.301	1.62	4.54	14.73	1000	4.61	1000		
											
$C_{19}H_{20}BrN_3O_3$	CM-A95(ss)	C19H20BrN3O3	418.284	141.5	225	59.45	30.36	146.3	107.1		
											
$C_{19}H_{20}BrN_3O_3$	CM-A97(sr)	C19H20BrN3O3	418.284	70.81	89.48	30.64	40.73	67.01	38.12		

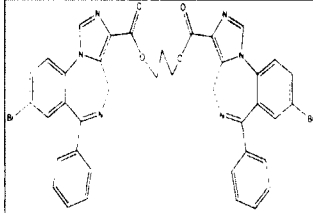
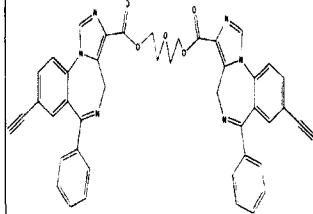
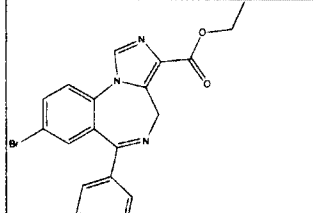
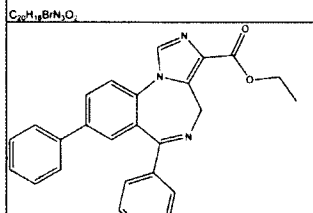
										
C ₁₄ H ₁₁ IN ₂ O ₂	CM-B01	C14H11IN2O2	366.154	4.8	31	34	1000	286	1000	
										
C ₁₉ H ₂₀ ClN ₃ O ₃	CM-B31c(ss)	C19H20ClN3O3	373.833	118	319	173	37	15	137	
										
C ₁₉ H ₁₉ FN ₃ O ₃	CM-B31i(ss)	C19H20IN3O3	465.285	90	184	78	18	4.9	121	
										
C ₁₉ H ₁₇ BrF ₃ N ₃ O ₃	CM-B34	C19H17BrF3N3O3	472.256	472	451	223	114	17	175	
										
C ₁₉ H ₁₆ FN ₃ O ₃	CM-B44(ss)	C19H20FN3O3	357.379	32	43	12	379	4.3	485	

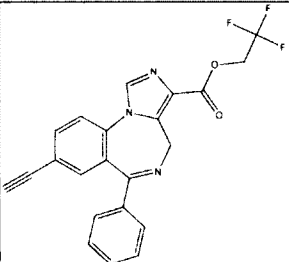
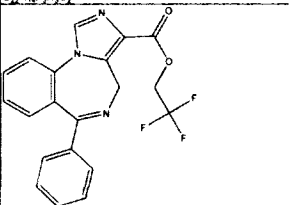
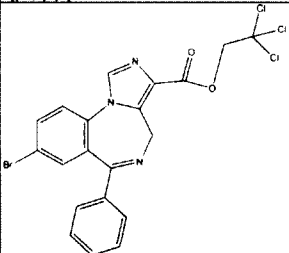
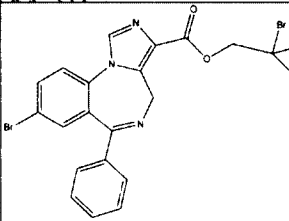
 $C_{19}H_{17}ClF_3N_3O_3$		CM-B45	C19H17ClF3N3O3	427.805	230	557	336	265	15	230
 $C_{19}H_{17}F_4N_3O_3$		CM-B47	C19H17F4N3O3	411.35	32	63	34	2007	4.4	717
 $C_{19}H_{17}BrF_3N_3O_3$		CM-C28(SR)	C19H17BrF3N3O3	472.256	176	752	244	290	14	141
 $C_{15}H_{11}F_3N_2O_2$		CM-D30(R)	C15H11F3N2O2	308.255	27	343.3	453	3000	1847	2000
 $C_{15}H_{11}F_3N_2O_2$		CM-D30(S)	C15H11F3N2O2	308.255	90	931	172	3000	1000	3000

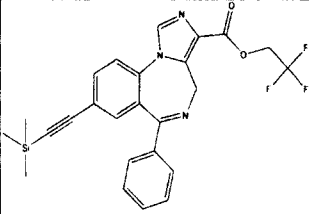

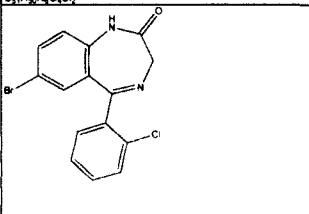
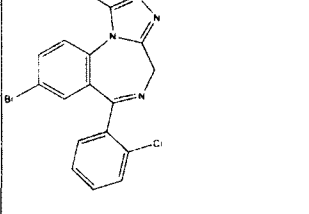
 $C_{17}H_{17}N_3O_4$		CM-D44	C17H17N3O4	327.335	34.3	56.3	20.7	0.33	0.57	0.92
 $C_{19}H_{21}N_3O_4$	03-1029	CM-D45	C19H21N3O4	355.388	90.5	65.5	30.3	0.15	1.65	0.23
 $C_{18}H_{15}F_3N_3O_4$		CM-E09a	C18H16F3N3O4	395.333	176	192	122	490	9.2	718
 $C_{19}H_{21}N_3O_4$		CM-E09b	C19H21N3O4	355.388	20	22	19	55	0.45	69
 $C_{23}H_{21}N_3O_4$		CM-E10	C23H21N3O4	403.431	23	26	14	215	0.51	96

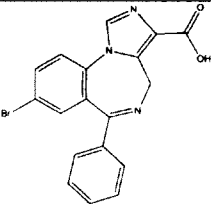
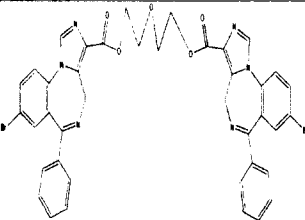
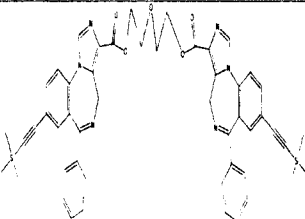
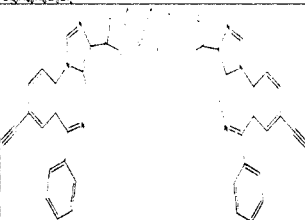
 $C_{20}H_{23}N_3O_4$		CM-E11	C20H23N3O4	369.414	333	308	161	394	14	750
 $C_{16}H_{12}ClN_2O$		diazepam	C16H13ClN2O	284.74	14	20	15		11	
 $C_{21}H_{26}N_4O_3$		DM-139	C21H26N4O3	382.456	5.8		169		9.25	325
 $C_{22}H_{28}N_4O_3$		DM-146	C22H28N4O3	396.483	6.44		148		4.23	247
 $C_{19}H_{24}N_4O_3$		DM-173	C19H24N4O3	356.419	13.1		38.1		0.78	118

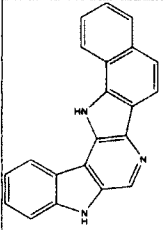
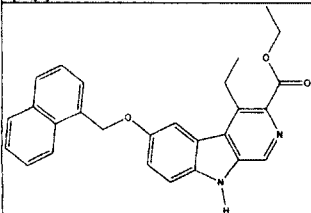
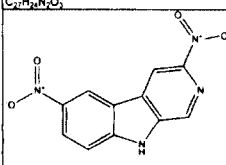
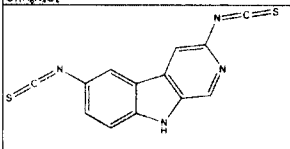
 $C_{18}H_{21}N_3O_4$		DM-215	C18H21N3O4	343.377	6.74		7.42	0.293	8.28
 $C_{17}H_{19}N_3O_4$		DM-239	C17H19N3O4	329.35	1.5		0.53	0.14	6.89
 $C_{17}H_{18}N_2O_4$		DMCM	C17H18N2O4	314.336	5.69	8.29	4	1.04	134
 $C_{49}H_{46}N_6O_4Si_2$	03-0935	DMH-D-048 (C49H46N6O4Si2)	C49H46N6O4Si2	839.098	5000	5000	5000	5000	5000
 $C_{43}H_{30}N_6O_4$	03-0936	DMH-D-053 (C43H30N6O4)	C43H30N6O4	694.736	236	7.4	272	5000	194.2 5000

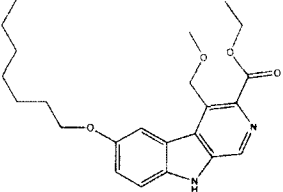
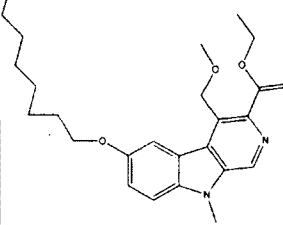
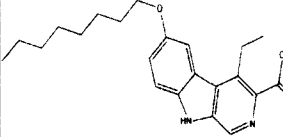
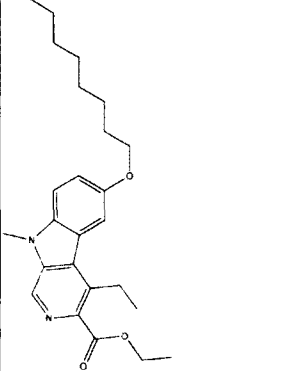
 $C_{39}H_{28}Br_2N_6O_4$	03-0934	DMH-D-070 (C ₃₉ H ₂₈ N ₆ O ₄ Br ₂)	C ₃₉ H ₂₈ Br ₂ N ₆ O ₄	804.485	5000	1901			5000	5000
 $C_{44}H_{28}N_6O_5$	03-0942	DMH-III-96 (C ₄₄ H ₃₂ N ₆ O ₅)	C ₄₄ H ₃₂ N ₆ O ₅	724.762	460	5000			5000	5000
 $C_{20}H_{16}BrN_3O_2$		DM-I-070	C ₂₀ H ₁₆ BrN ₃ O ₂	410.264						
 $C_{26}H_{21}N_3O_2$		DM-I-81	C ₂₆ H ₂₁ N ₃ O ₂	407.464	2000	2000	2000	2000	176	2000

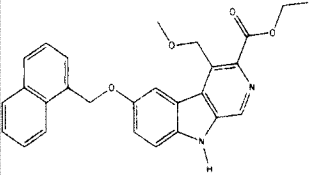
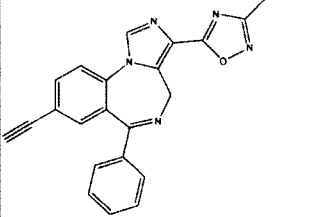
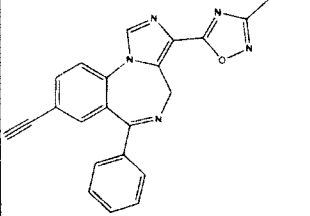
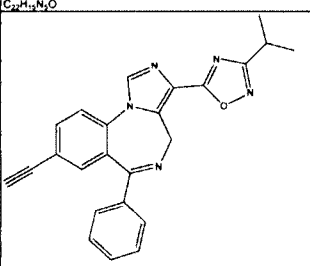
 $C_{22}H_{14}F_3N_3O_2$	03-0943	DM-II-20 (C ₂₂ H ₁₄ N ₃ O ₂ F ₃)	C ₂₂ H ₁₄ F ₃ N ₃ O ₂	409.361	54.3	27.14	35.68		15.35	5000
 $C_{22}H_{14}F_3N_3O_2$	03-0944	DM-II-30 C ₂₀ H ₁₃ N ₃ O ₂ BrF ₃)	C ₂₀ H ₁₄ F ₃ N ₃ O ₂	385.339	17.6	13.4	28.51		7.8	5000
 $C_{22}H_{13}BrCl_2N_3O_2$	03-0945	DM-II-33 (C ₂₀ H ₁₃ N ₃ O ₂ BrCl ₃)	C ₂₀ H ₁₃ BrCl ₃ N ₃ O ₂	513.599	88.6	85	11.6		26.2	5000
 $C_{20}H_{13}Br_2N_3O_2$	05-1734	DM-II-34	C ₂₀ H ₁₃ Br ₄ N ₃ O ₂	646.952						

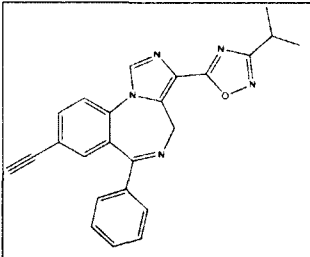
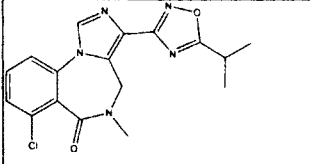
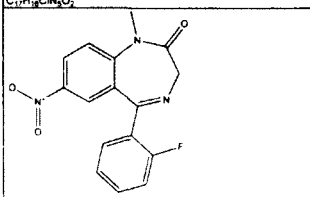
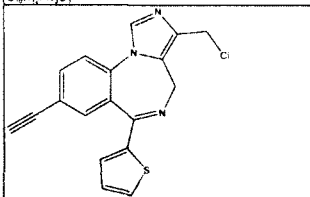
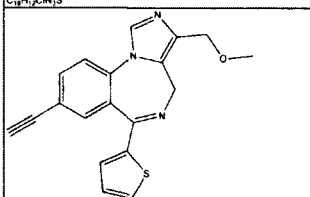
 $C_{25}H_{22}F_3N_3O_2Si$	03-0946	DM-II-35 (C25H22N3O2SiF3)	C25H22F3N3O2Si	481.542	11380	327			380	5000
 $C_{51}H_{50}N_6O_4Si_2$	03-0938	DM-II-41 (C51H50N6O4Si2)	C51H50N6O4Si2	867.152	missing					
 $C_{15}H_{10}BrClN_2O$	03-0948	DM-II-72 (C15H10N2OBrCl)	C15H10BrClN2O	349.61	5000	1.37			2.02	5000
 $C_{17}H_{12}BrClN_4$	03-0949	DM-II-90 (C17H12N4BrCl)	C17H12BrClN4	387.661	0.505	1	0.63		0.37	5000

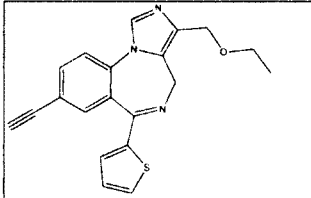
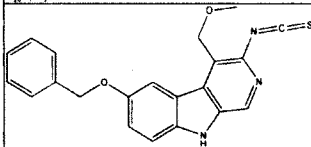
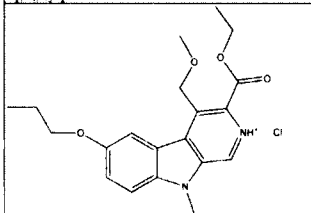
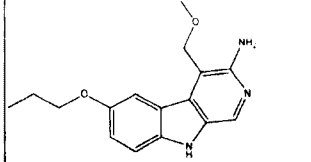
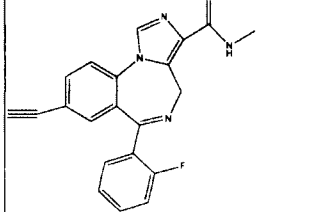
 $C_{18}H_{12}BrN_3O_2$	03-0947	DM-III-01 (C18H12N3O2Br)	C18H12BrN3O2	382.211	5000	12			4.73	5000
 $C_{40}H_{30}Br_2N_6O_5$	03-0940	DM-III-93 (C40H30N6O5Br2)	C40H30Br2N6O5	834.511	351	5000			179	5000
 $C_{50}H_{48}N_{10}O_5Si_2$	03-0941	DM-III-94 (C50H48N6O5Si2)	C50H48N6O5Si2	869.124	240	5000	5000		5000	5000
 $C_{45}H_{34}N_6O_4$	03-0939	DM-III-97 (C45H34N6O4)	C45H34N6O4	722.789	280	5000			5000	5000

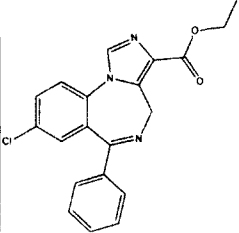
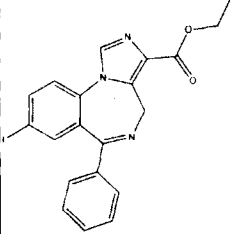
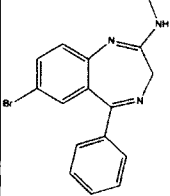
 $C_{21}H_{13}N_3$		EDC-I	C21H13N3	307.348	165		797		382.3	10000
 $C_{27}H_{24}N_2O_3$		EDC-I-042	C27H24N2O3	424.491	183	20.5	300		270	10000
 $C_{11}H_6N_4O_4$		EDC-I-071	C11H6N4O4	258.19	12.9	83.1			314	5000
 $C_{13}H_6N_4S_2$		EDC-I-093	C13H6N4S2	282.344	13.6	423			2912	5000

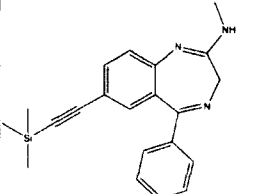
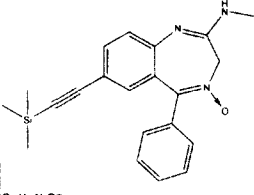
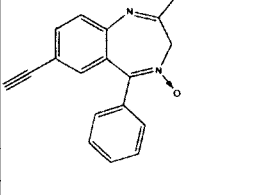
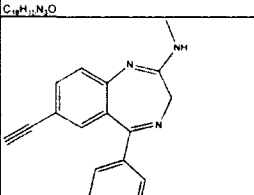
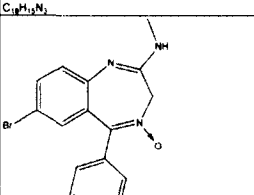
 $C_{24}H_{32}N_2O_4$		EDC-II-012	C24H32N2O4	412.522	1000	3000	3000		3000	3000
 $C_{25}H_{34}N_2O_4$		EDC-II-015	C25H34N2O4	426.548	3000	3000	3000		3000	3000
 $C_{24}H_{32}N_2O_4$		EDC-II-024	C24H32N2O3	396.522	3647	29749	35060		12683	30000
 $C_{25}H_{34}N_2O_4$		EDC-II-031	C25H34N2O3	410.549	1000	1000	1000		1000	1000

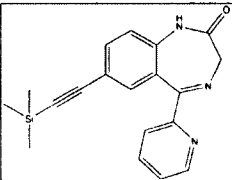
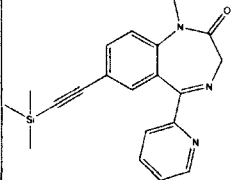
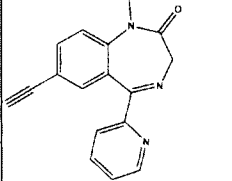
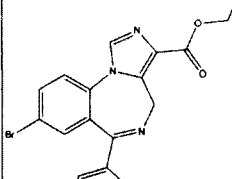
 $C_{27}H_{24}N_2O_4$		EDC-II-044	C27H24N2O4	440.49	15.4		293		323	1000
 $C_{22}H_{15}N_5O$	05-1713	EMJ-I-025	C22H15N5O	365.387	288	474	316		86	5000
 $C_{22}H_{15}N_5O$		EMJ-I-025	C22H15N5O	365.387						
 $C_{24}H_{19}N_5O$	05-1714	EMJ-I-026	C24H19N5O	393.441	5000	135	1027		152	5000

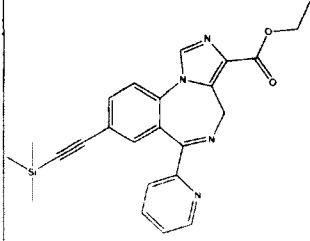
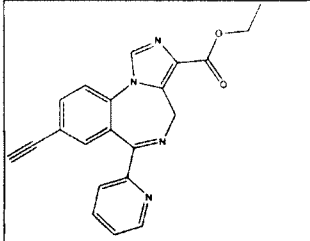
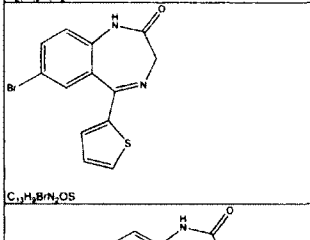
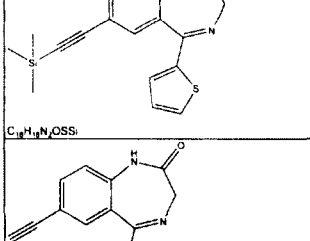
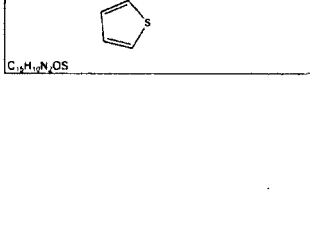
 C ₂₄ H ₁₉ N ₅ O		EMJ-I-026	C24H19N5O	393.441						
 C ₁₇ H ₁₃ ClN ₅ O ₂		FG8205	C17H16ClN5O2	357.794	0.4	2.08	1.16		1.54	227
 C ₁₆ H ₁₁ FN ₃ O ₃		FLUNITRAZEPAM	C16H12FN3O3	313.283	2.2	2.5	4.5		2.1	2000
 C ₁₈ H ₁₃ ClN ₃ S	05-1771	FMR-1	C18H12ClN3S	337.826						
 C ₁₉ H ₁₃ N ₃ OS	05-1772	FMR-2	C19H15N3OS	333.407						

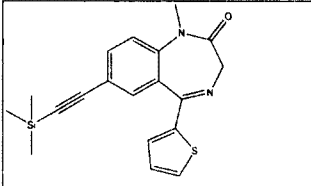
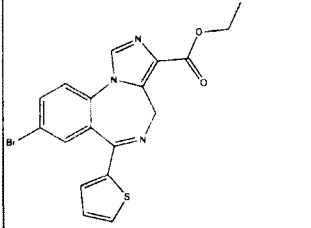
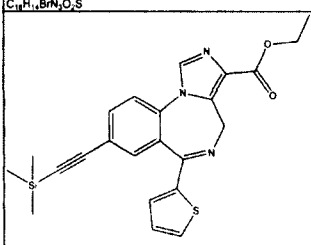
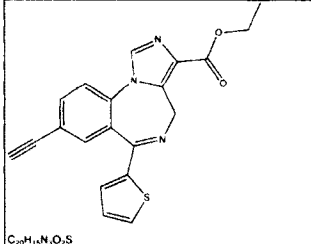
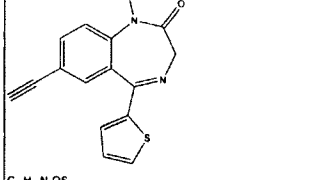
 $C_{20}H_{17}N_3OS$	05-1774	FMR-3	C20H17N3OS	347.433						
 $C_{21}H_{17}N_3O_2S$		HDA-343	C21H17N3O2S	375.444	25	82.6	58.8		159	10000
 $C_{22}H_{23}ClN_2O_4$		HDA-90-III	C20H25ClN2O4	392.877	25.6	105.4	163.6		160.6	10000
 $C_{16}H_{18}N_2O_2$		HDA-II-96	C16H19N3O2	285.341	236	3000	3000		3000	10000
 $C_{21}H_{15}FN_2O$	08-007	HJ-I-037	C21H15FN4O	358.368	15.07	8.127	28.29		0.818	

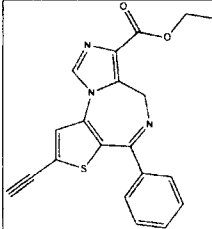
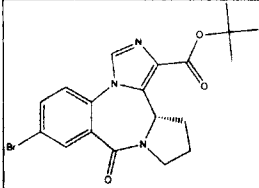
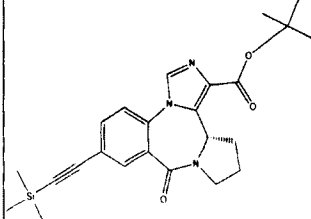
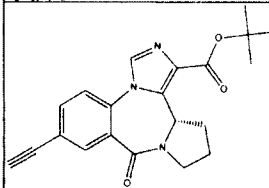
	08-010	HJ-I-040			1070	869.4	1123.6		1065	
 <chem>CCOC(=O)c1nc2c(ncn2C3=CC=CC=C3)c4ccc(Cl)cc4</chem> $C_{20}H_{16}ClN_3O_2$	03-0952	HZ111 C20H16N3ClO2	C20H16ClN3O2	365.813	46.65	34	77.6		24.6	842
 <chem>CCOC(=O)c1nc2c(ncn2C3=CC=CC=C3)c4ccc(F)cc4</chem> $C_{20}H_{14}FN_3O_2$	03-0953	HZ120 ANX2	C20H16IN3O2	457.264	5000	35	78.5		20.6	32.2
 <chem>Nc1nc2c(ncn2C3=CC=CC=C3)c4ccc(Br)cc4</chem> $C_{16}H_{14}BrN_3$	03-0964	HZ135 C16H14N3Br	C16H14BrN3	328.206	94.03	182			97	5000

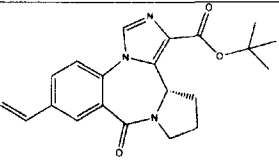
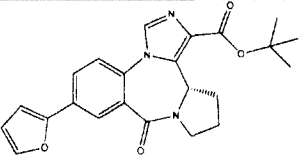
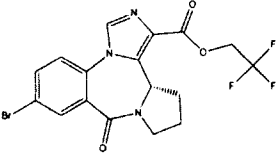
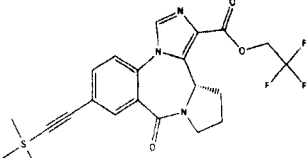
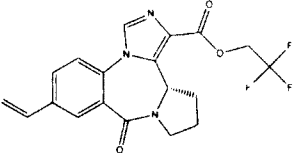
 $C_{21}H_{27}N_3Si$	03-0954	H _z 141 C ₂₁ H ₂₃ N ₃ Si	C ₂₁ H ₂₃ N ₃ Si	345.513	6480	5000	5000		737	5000
 $C_{21}H_{27}N_3OSi$	03-0955	H _z 146 C ₂₁ H ₂₃ N ₃ OSi	C ₂₁ H ₂₃ N ₃ OSi	361.512	5000	5000			5000	5000
 $C_{18}H_{15}N_3O$	03-0957	H _z 147 C ₁₈ H ₁₅ N ₃ O	C ₁₈ H ₁₅ N ₃ O	289.331	5000	5000			5000	5000
 $C_{18}H_{15}N_3$	03-0963	H _z 148 C ₁₈ H ₁₅ N ₃	C ₁₈ H ₁₅ N ₃	273.332	10.98	5000			256	5000
 $C_{16}H_{14}BrN_3O$	03-0956	H _z 150 C ₁₆ H ₁₄ N ₃ OBr	C ₁₆ H ₁₄ BrN ₃ O	344.206	485	469	5000		419	5000

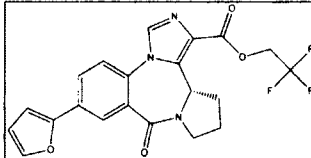
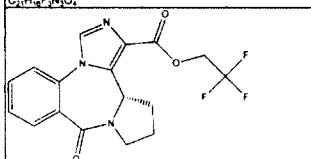
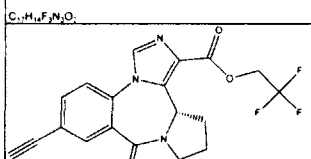
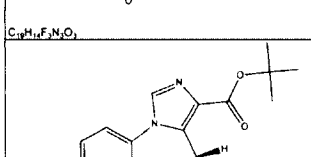
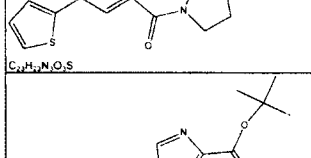
 $C_{19}H_{19}N_3OSi$	03-0958	Hz157 C19H19N3OSi	C19H19N3OSi	333.459	5000	5000	5000		5000	5000
 $C_{20}H_{21}N_3OSi$	03-0959	Hz158 C20H21N3OSi	C20H21N3OSi	347.486	5000	5000	5000		5000	5000
 $C_{17}H_{13}N_3O$	03-0960	Hz160 C17H13N3O	C17H13N3O	275.305	492	2633	334		87.3	5000
 $C_{19}H_{15}BrN_4O_2$	03-0965	Hz164 C19H15N4O2Br	C19H15BrN4O2	411.252	99.18	150	459		108.2	494

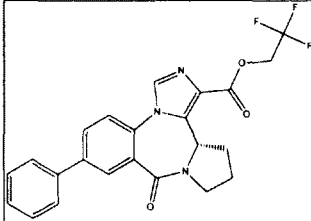
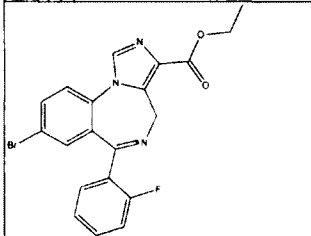
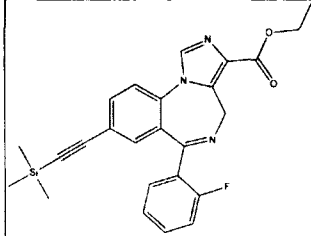
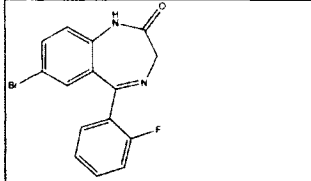
 $C_{24}H_{24}N_4O_2Si$	03-0961	HZ165 C24H24N4O2Si	C24H24N4O2Si	428.558	5000	5000			5000	5000
 $C_{21}H_{16}N_4O_2$	03-0962	HZ166 C21H16N4O2	C21H16N4O2	356.377	118	148	365	5000	76.88	5000
 $C_{17}H_9BrN_2OS$	03-1048	JC184 C13H9BrN2OSi	C13H9BrN2OS	321.192	9.606	10.5			6.709	
 $C_{18}H_{18}N_2OSSi$	03-1049	JC207 C18H18N2OSSi	C18H18N2OSSi	338.499	104.8	169.7			68.16	
 $C_{15}H_{12}N_2OS$	03-1050	JC208 C15H10N2OS	C15H10N2OS	266.318	22.42	18.89			5.039	

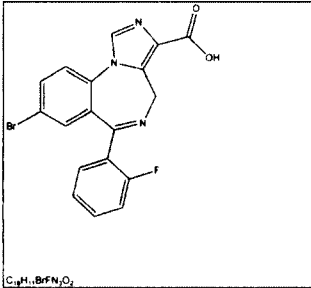
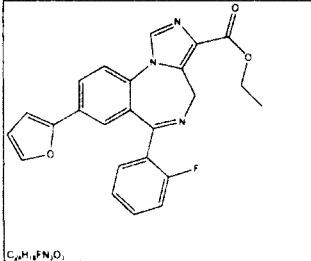
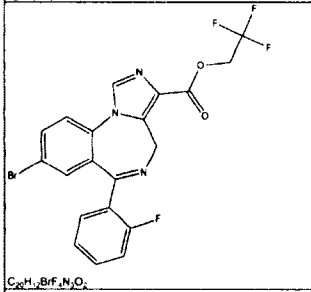
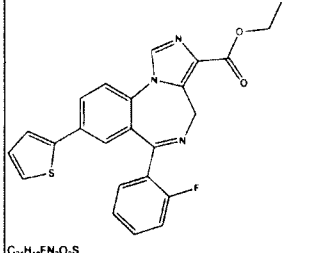
 <chem>C12H12N2O2Si</chem>	03-1051	JC209 C19H20N2O2Si	C19H20N2O2Si	352.525	294.6	334.7			249.5	
 <chem>C18H14BrN3O2S</chem>	03-1053	JC217 C18H14BrN3O2S	C18H14BrN3O2S	416.292						
 <chem>C23H23N3O2Si</chem>	03-1054	JC220 C23H23N3O2Si	C23H23N3O2Si	433.598						
 <chem>C20H15N3O2S</chem>	03-1055	JC221 ANX1	C20H15N3O2S	361.417	106.175	49.405	182		7.7495	362
 <chem>C16H12N2OS</chem>	03-1052	JC222 C16H12N2OS	C16H12N2OS	280.344	86.7	45.11			17.63	

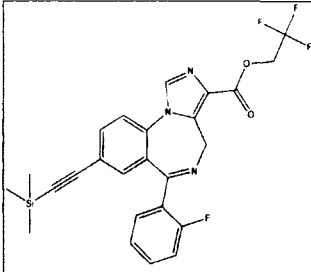
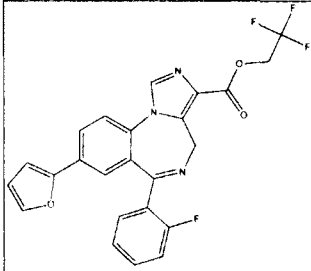
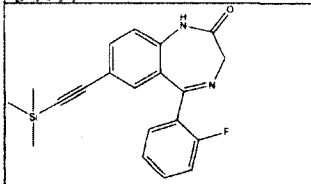
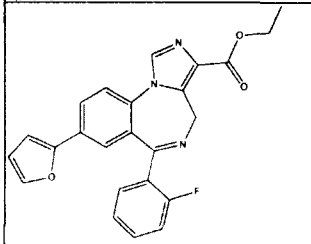
 $C_{20}H_{15}N_3O_2S$	08-26	JIE-I-12	C20H15N3O2S	361.417	3576	454.8	768.3		4416	
 $C_{19}H_{17}BrN_3O_3$	03-0989	JYI-01(C19H20N3O3Br)	C19H20BrN3O3	418.284	59.2	159	96		10.6	2.88
 $C_{24}H_{29}N_3O_3Si$	03-0990	JYI-02 (C24H29N3O3Si)	C24H29N3O3Si	435.591	missing					
 $C_{21}H_{21}N_3O_3$	03-0991	JYI-03 (C21H21N3O3)	C21H21N3O3	363.41	185.4	107			0.954	3.34

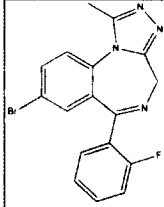
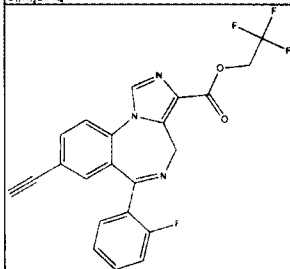
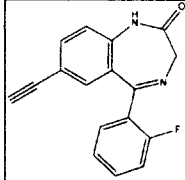
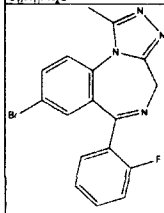
										
C ₂₁ H ₂₃ N ₃ O ₃	03-0992	JYI-04 (C ₂₁ H ₂₃ N ₃ O ₃)	C ₂₁ H ₂₃ N ₃ O ₃	365.426	28.3	16			0.51	1.57
										
C ₂₃ H ₂₃ N ₃ O ₄	03-0993	JYI-06 (C ₂₃ H ₂₃ N ₃ O ₄)	C ₂₃ H ₂₃ N ₃ O ₄	405.446	16.5	5.48	5000		12.6	5000
										
C ₁₇ H ₁₃ BrF ₃ N ₃ O ₃	03-0996	JYI-10 (C ₁₇ H ₁₃ N ₃ O ₃ F ₃ Br)	C ₁₇ H ₁₃ BrF ₃ N ₃ O ₃	444.203	5000	368			12.3	23
										
C ₂₂ H ₁₄ F ₃ N ₃ O ₃ Si	03-0997	JYI-11 (C ₂₂ H ₂₂ N ₃ O ₃ F ₃ Si)	C ₂₂ H ₂₂ F ₃ N ₃ O ₃ Si	461.509	5000	5000			648	3.97
										
C ₁₉ H ₁₆ F ₃ N ₃ O ₃	03-0999	JYI-12 (C ₁₉ H ₁₆ N ₃ O ₃ F ₃)	C ₁₉ H ₁₆ F ₃ N ₃ O ₃	391.344	91	39			4.5	6.8

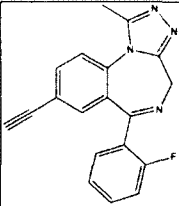
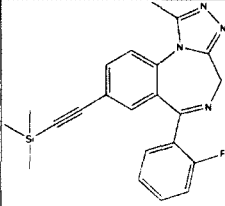
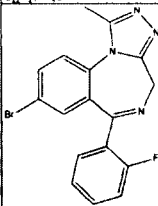
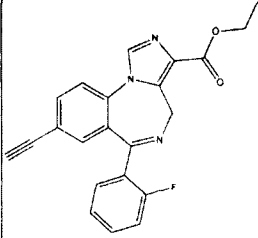
 $C_{21}H_{16}F_3N_3O_4$	03-1001	JYI-13 (C21H16N3O4F3)	C21H16F3N3O4	431.365	5000	63.7			16	8.38
 $C_{17}H_{14}F_3N_3O_4$	03-1002	JYI-14 (C17H14N3O3F3)	C17H14F3N3O3	365.307	32	25			13	565
 $C_{19}H_{14}F_3N_3O_4$	03-0998	JYI-15 (C19H14N3O3F3)	C19H14F3N3O3	389.328	205	812			4.8	22
 $C_{23}H_{23}N_3O_3S$	03-0994	JYI-19 (C23H23N3O3S)	C23H23N3O3S	421.512	2.176	205			34	12.7
 $C_{25}H_{25}N_3O_3$	03-0995	JYI-20 (C25H25N3O3)	C25H25N3O3	415.484	20.96	611			54	40.46

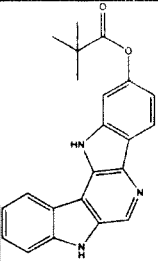
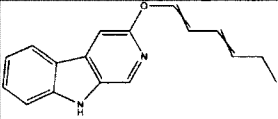
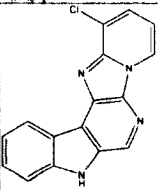
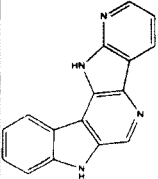
 $C_{23}H_{17}F_3N_3O_3$	03-1003	JYI-21 (C23H17N3O3F3)	C23H18F3N3O3	441.403	113.7	5000			209	60.96
 $C_{20}H_{12}BrFN_2O_2$	03-1004	JYI-32 (C20H15N3O2BrF)	C20H15BrFN3O2	428.254	3.07	4.96			2.92	52.24
 $C_{25}H_{24}FN_2O_2Si$	03-1005	JYI-38 (C25H24N3O2FSi)	C25H24FN3O2Si	445.561	5000	314			55.4	5000
 $C_{15}H_{10}BrFN_2O$	05-1737	JYI-42	C15H10BrFN2O	333.155	0.257	0.146	0.278		0.256	

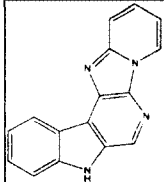
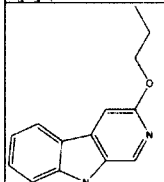
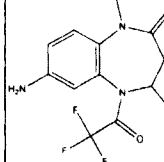
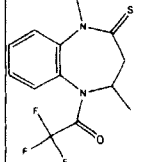
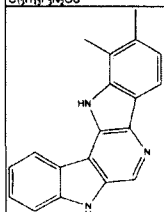
 $C_{18}H_{11}BrFN_3O_2$	05-1738	JYI-47	C18H11BrFN3O2	400.201	2.759	2.282	0.511	0.427	
 $C_{24}H_{18}FN_3O_3$	05-1735	JYI-48	C24H18FN3O3	415.416	75.59	90.68	12.78	31.28	
 $C_{20}H_{12}BrF_4N_3O_2$	03-1008	JYI-49 (C20H12N3O2F4Br)	C20H12BrF4N3O2	482.226	1.87	2.38		6.7	3390
 $C_{24}H_{18}FN_3O_2S$	03-1007	JYI-50 (C24H18N3O2SF)	C24H18FN3O2S	431.482	106.4	200		37.6	5040

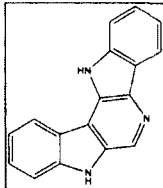
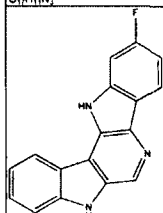
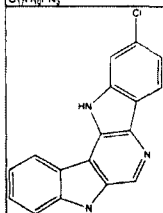
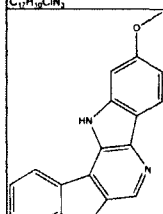
 $C_{25}H_{21}F_4N_3O_2Si$	03-1009	JYI-53 (C25H21N3O2F4Si)	C25H21F4N3O2Si	499.532	77.4	40.4	183		133	3650
 $C_{24}H_{15}F_4N_3O_2$	03-1011	JYI-54 (C24H15N3O3F4)	C24H15F4N3O3	469.388	2.89	172	6.7		57	1890
 $C_{20}H_{19}FN_2OSi$	05-1739	JYI-55	C20H19FN2OSi	350.462	41.39		0.504		24.75	
 $C_{24}H_{19}FN_3O_2$	03-1006	JYI-56 (C24H18N3O4F)	C24H18FN3O3	415.416	95.2	346	131		34.6	4140

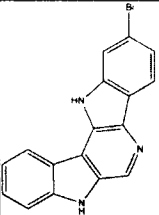
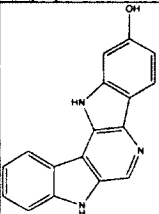
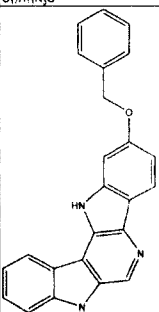
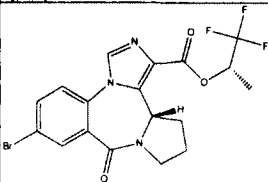
 $C_{17}H_{12}BrFN_4$	05-1736	JYI-57	C17H12BrFN4	371.206	0.076	0.076	0.131	0.036	
 $C_{22}H_{17}F_4N_3O_2$	03-1010	JYI-59 (C22H13N3O2F4)	C22H13F4N3O2	427.351	1.08	2.6	11.82	11.5	5000
 $C_{17}H_{11}FN_3O$	03-1012	JYI-60 (C17H11N2OF)	C17H11FN2O	278.28	3.73	1.635	4.3	1.7	5000
 $C_{17}H_{12}BrFN_4$	03-1013	JYI-64 (C17H12N4FBr)	C17H12BrFN4	371.206	0.305	1.111	0.62	0.87	5000

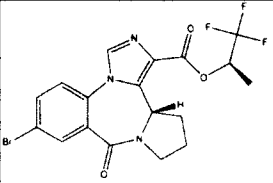
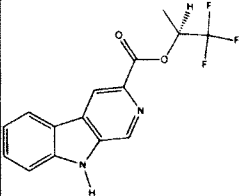
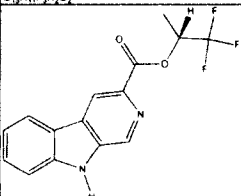
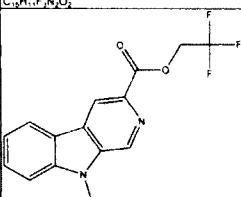
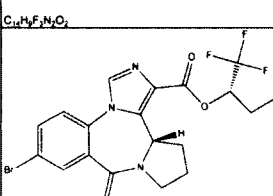
										
C ₁₉ H ₁₃ FN ₄	03-1014	JYI-70 (C ₁₉ H ₁₃ N ₄ F)	C ₁₉ H ₁₃ FN ₄	316.332	6.3	2.1			0.56	5000
										
C ₂₂ H ₁₇ FN ₄ Si	03-1015	JYI-72 (C ₂₂ H ₂₁ N ₄ SiF)	C ₂₂ H ₂₁ FN ₄ Si	388.513	48.5	18.5			11.5	5000
										
C ₁₇ H ₁₂ BrFN ₄		JYI-73	C ₁₇ H ₁₂ BrFN ₄	371.206						
										
C ₂₂ H ₁₆ FN ₄ O ₂		JY-XHE-053	C ₂₂ H ₁₆ FN ₄ O ₂	373.38						

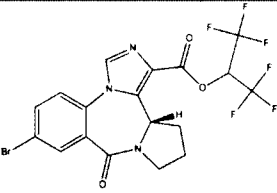
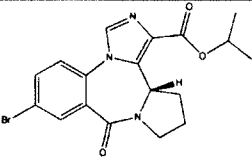
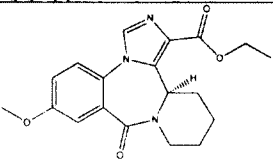
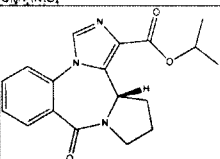
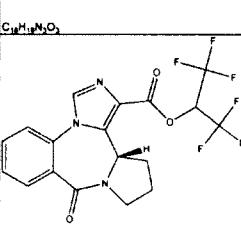
 $C_{27}H_{19}N_3O_2$		LD-9	C22H19N3O2	357.405	156				3000	10000
 $C_{17}H_{19}N_3O$		LJD-I-0036A	C17H16N2O	264.322	245	818	869		10000	10000
 $C_{17}H_9ClN_4$		LJD-II-87	C16H9ClN4	292.722	3000	3000	3000		10000	10000
 $C_{19}H_{12}N_4$		LJD-III-15E	C16H10N4	258.277	1.93	14	19		70.8	1000

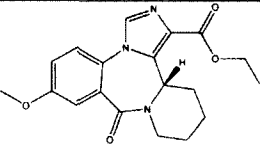
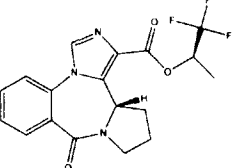
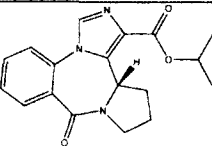
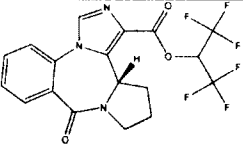
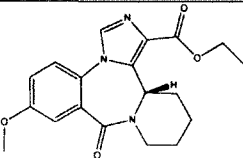
 C ₁₆ H ₁₀ N ₄		LJD-III-22A	C ₁₆ H ₁₀ N ₄	258.277	105	227.5	284		3000	10000
 C ₁₄ H ₁₄ N ₂ O		MA-3-PROPOXYL	C ₁₄ H ₁₄ N ₂ O	226.274	5.3	52.3	68.8		591	1000
 C ₁₇ H ₁₃ F ₃ N ₂ O ₂		MH-1 (Parkistan)	C ₁₃ H ₁₄ F ₃ N ₃ O ₂	301.264	3000	3000	3000	3000	3000	3000
 C ₁₇ H ₁₃ F ₃ N ₂ O ₂ S		MH-2 (Parkistan)	C ₁₃ H ₁₃ F ₃ N ₂ O ₂ S	302.315	3000	3000	3000	3000	3000	3000
 C ₁₉ H ₁₅ N ₃		MJP-II-34	C ₁₉ H ₁₅ N ₃	285.343	240		391		1360	10000

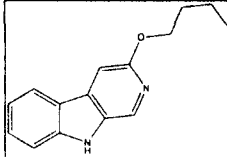
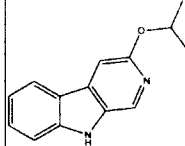
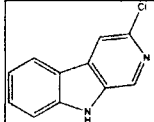
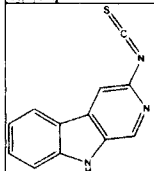
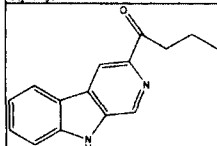
 <chem>C17H11N3</chem>		MLT-I-70	<chem>C17H11N3</chem>	257.289	1.1	1.2	1.1		40.3	1000
 <chem>C17H9FN3</chem>		MLT-II-16	<chem>C17H10FN3</chem>	275.28	5.05	10.41	18.4		260	10000
 <chem>C17H9ClN3</chem>		MLT-II-18	<chem>C17H10ClN3</chem>	291.734	3.9	12.2	24.4		210	10000
 <chem>C18H13NO</chem>		MLT-II-18	<chem>C18H13NO</chem>	287.315	3.4	11.7	11		225	10000

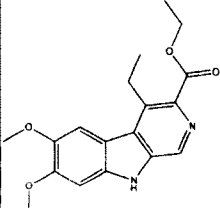
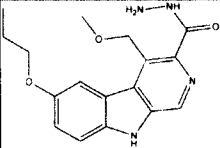
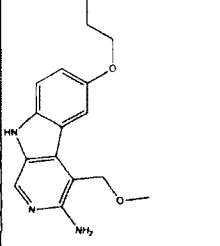
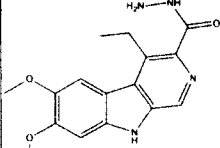
 $C_{17}H_{12}BrN_3$		MLT-II-29	C17H10BrN3	336.185							
 $C_{17}H_{11}N_3O$		MLT-II-34	C17H11N3O	273.289	7.04	15.95	22.3		158	1000	
 $C_{24}H_{17}N_3O$		MLT-II-87	C24H17N3O	363.411	432	3000	3000		10000	10000	
 $C_{18}H_{11}BrF_3N_3O_3$		MMB-II-37	C18H15BrF3N3O3	458.229	872	2602	1003	95	98	115	

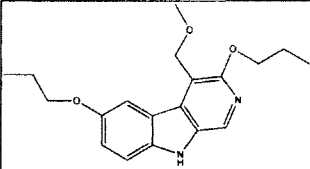
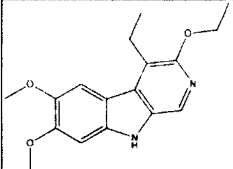
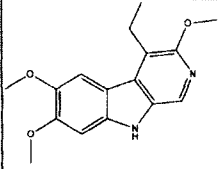
 $C_{18}H_{15}BrF_3N_3O_3$		MMB-II-43	C18H15BrF3N3O3	458.229	1353	5173	1535	98	132	78
 $C_{15}H_{11}F_3N_3O_2$		MMB-II-57	C15H11F3N2O2	308.255	90	931	172	3000	1000	3000
 $C_{15}H_{11}F_3N_3O_2$		MMB-II-68A	C15H11F3N2O2	308.255	27	343.3	453	3000	1847	3000
 $C_{14}H_9F_3N_3O_2$		MMB-II-74	C14H9F3N2O2	294.229	3	24.5	41.7	500	125.7	1000
 $C_{19}H_{17}BrF_3N_3O_3$		MMB-II-87	C19H17BrF3N3O3	472.256	200	333	107	109	5.4	333

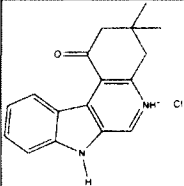
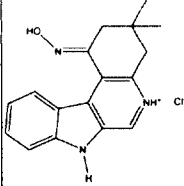
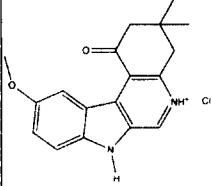
 $C_{18}H_{13}BrF_3N_3O_3$		MMB-II-89	C18H12BrF6N3O3	512.201	333	333	333	333	43	333
 $C_{18}H_{19}BrN_3O_3$		MMB-II-90	C18H18BrN3O3	404.258	20	24	5.7	9	0.25	36
 $C_{19}H_{21}N_3O_4$		MMB-II-99	C19H21N3O4	355.388	333	333	333	333	333	333
 $C_{18}H_{19}N_3O_3$		MMB-III-016	C18H19N3O3	325.362	3	1.97	2	1074	0.26	211
 $C_{18}H_{13}F_6N_3O_3$		MMB-III-018	C18H13F6N3O3	433.305	117	140	78	3500	14	976

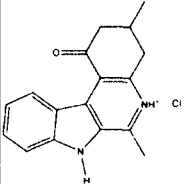
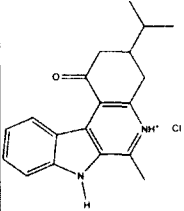
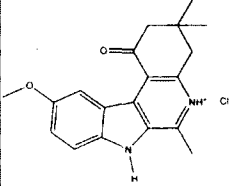
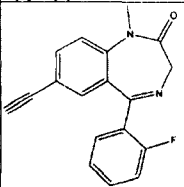
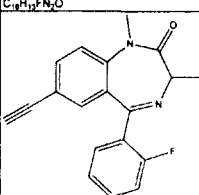
										
C ₁₉ H ₂₁ N ₃ O ₄	MMB-III-019	C19H21N3O4	355.388	3333	3333	3333	3500	889	3500	
										
C ₁₈ H ₁₅ F ₃ N ₃ O ₃	MMB-III-14	C18H16F3N3O3	379.333	13	13	6.9	333	1.1	333	
										
C ₁₈ H ₁₉ N ₃ O ₃	MMB-III-16	C18H19N3O3	325.362	3	1.97	2	1074	0.26	211	
										
C ₁₈ H ₁₃ F ₆ N ₃ O ₃	MMB-III-18	C18H13F6N3O3	433.305	117	140	78	3500	14	976	
										
C ₁₉ H ₂₁ N ₃ O ₄	MMB-III-19	C19H21N3O4	355.388	3333	3333	3300	3500	889	3500	

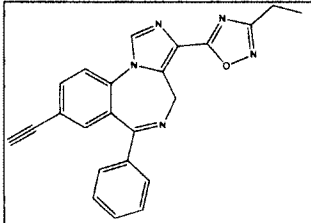
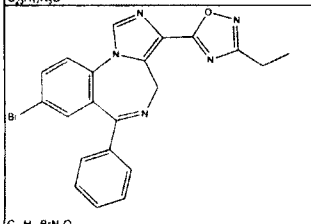
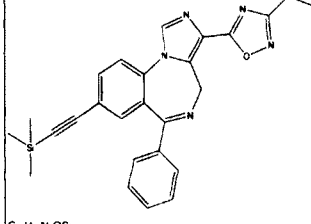
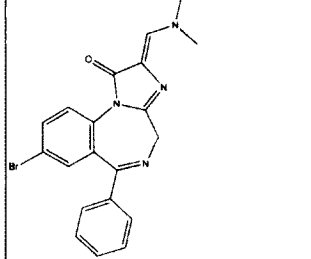
 $C_{15}H_{12}N_2O$		MSA-0-28	C15H16N2O	240.3	36.9	194	245		1000	1000
 $C_{14}H_{14}N_2O$		MSA-3-IPBC	C14H14N2O	226.274	283	3000	3000		10000	10000
 $C_{11}H_7ClN_2$		MSA-I-71	C11H7ClN2	202.64	60.4	125.3	126		1000	10000
 $C_{12}H_7N_3S$		MSA-II-35	C12H7N3S	225.269	67.2	120	141		3000	10000
 $C_{15}H_{14}N_2O$		MSA-IV-35	C15H14N2O	238.284	2.1	16	21		995	3000

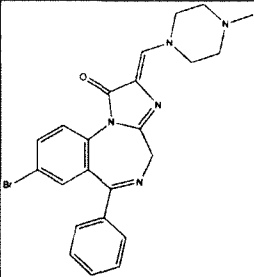
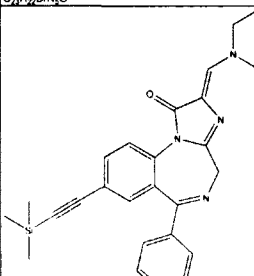
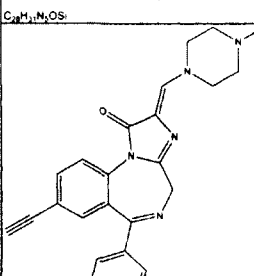
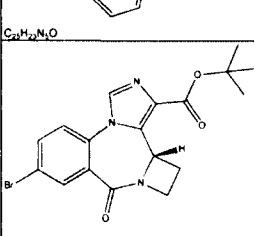
 $C_{18}H_{20}N_2O_4$		MSR-I-032	C18H20N2O4	328.362	6.2	18.7	4		3.3	74.9
 $C_{17}H_{20}N_2O_3$		MSR-I-036	C17H20N4O3	328.366	46	422	400		107.5	300
 $C_{16}H_{19}N_3O_2$		MSR-I-046	C16H19N3O2	285.341	45	540	700		380	3000
 $C_{16}H_{18}N_4O_3$		MSR-I-049	C16H18N4O3	314.339	896	1000	570		91.5	3000

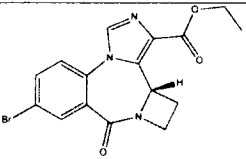
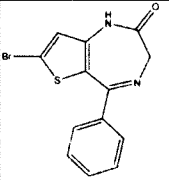
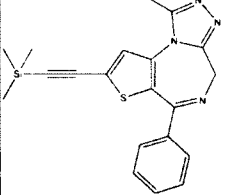
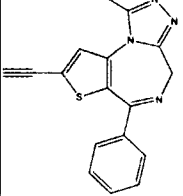
										
C ₂₃ H ₂₆ N ₂ O ₃		MSR-I-056	C ₁₉ H ₂₄ N ₂ O ₃	328.405	24.6	214.4	270.4		331.9	1000
										
C ₁₇ H ₂₀ N ₂ O ₃		MSR-I-057	C ₁₇ H ₂₀ N ₂ O ₃	300.352	300	300	300		300	300
										
C ₁₆ H ₁₈ N ₂ O ₃		MSR-I-100	C ₁₆ H ₁₈ N ₂ O ₃	286.326	300	300	300		300	300
	09-07	MVL-VI-13								

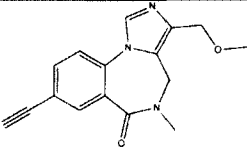
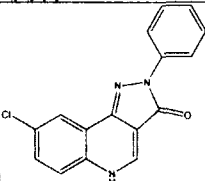
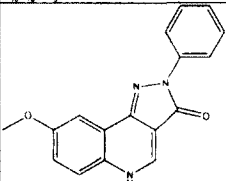
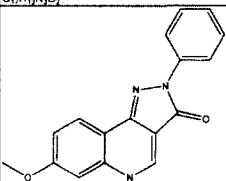
	09-08	MVL-VI-33									
	09-09	MVL-VI-34									
 <chem>C17H17ClN2O</chem>		N-111	C17H17ClN2O	300.783	691		4209	3000	3439	3000	
 <chem>C17H18ClN2O</chem>		N-112	C17H18ClN2O	315.797	296		5260	3000	3000	3000	
 <chem>C18H19ClN2O2</chem>		N-120	C18H19ClN2O2	330.809	422		1000	3000	932	3000	

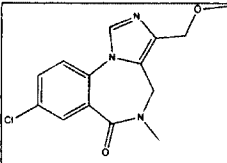
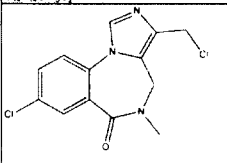
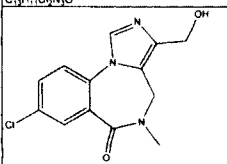
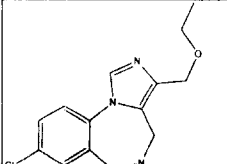
 $C_{17}H_{17}ClN_2O$		N-26	C17H17ClN2O	300.783	1000		3000	3000	3000	3000
 $C_{19}H_{21}ClN_2O$		N-30	C19H21ClN2O	328.836	1491		2000	2000	2000	2000
 $C_{19}H_{21}ClN_2O_2$		N-80	C19H21ClN2O2	344.835	1614.4		2000	2000	2000	2000
 $C_{18}H_{13}FN_2O$		OMB-18	C18H13FN2O	292.307	3.9	1.2	3.4	1733	0.8	5
 $C_{19}H_{15}FN_2O$		OMB-19	C19H15FN2O	306.334	22	4.6	20	3333	3.5	40

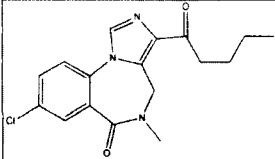
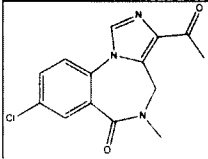
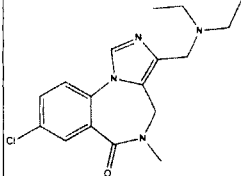
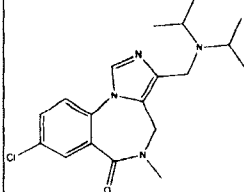
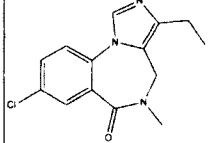
 $C_{22}H_{17}N_5O$	03-1018	PS-1-26 C23H17N5O	C23H17N5O	379.414	933.5	366	260		393.5	5000
 $C_{21}H_{16}BrN_5O$	03-1016	PS-1-27 C21H16N5BrO	C21H16BrN5O	434.289	182	294			86	5000
 $C_{26}H_{25}N_5OSi$	03-1017	PS-1-28 C26H25N5OSi	C26H25N5OSi	451.595	5000	5000			5000	5000
 $C_{20}H_{17}BrN_4O$	03-1019	PS-1-34B C20H17N4BrO	C20H17BrN4O	409.279		4.198	3.928			

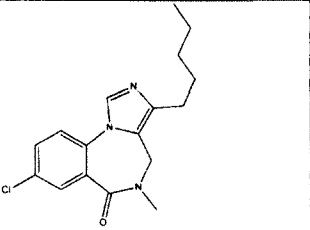
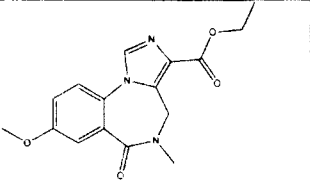
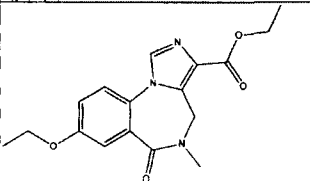
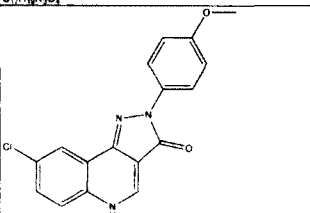
 $C_{23}H_{22}BrN_5O$	03-1020	S-1-35	C23H22N5C	C23H22BrN5O	464.358		16.03	24.41			
 $C_{28}H_{31}N_5OSi$	03-1021	S-1-36	C28H31N5C	C28H31N5OSi	481.664			939.1			
 $C_{25}H_{23}N_5O$	03-1022	S-1-37	C25H23N5C	C25H23N5O	409.483	193	35	435		22	5000
 $C_{18}H_{18}BrN_3O_3$		PS-2-58		C18H18BrN3O3	404.258						

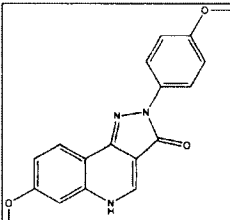
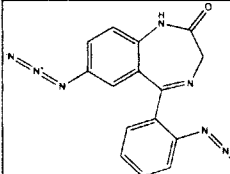
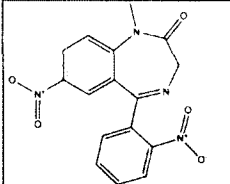
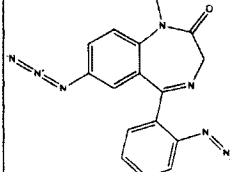
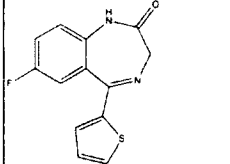
										
C ₁₈ H ₁₄ BrN ₃ O ₃		PS-2-58	C ₁₆ H ₁₄ BrN ₃ O ₃	376.205						
										
C ₁₇ H ₉ BrN ₂ OS	05-1742	PS-I-68	C ₁₃ H ₉ BrN ₂ OS	321.192	3134	481.3	679.5		101.3	
										
C ₂₀ H ₁₆ N ₄ SSi	05-1740	PS-I-71	C ₂₀ H ₂₀ N ₄ SSi	376.55	145.8	122.8	214.2		119.2	
										
C ₁₇ H ₁₂ N ₄ S	05-1741	PS-I-72	C ₁₇ H ₁₂ N ₄ S	304.369	123	31	386		34	5000

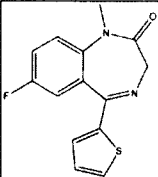
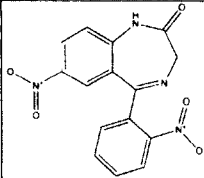
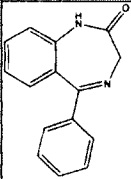
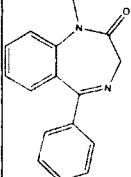
										
C ₁₆ H ₁₃ N ₃ O ₂		PWIII-012	C ₁₆ H ₁₅ N ₃ O ₂	281.309	1000	1000	1000		166	1000
										
C ₁₈ H ₁₃ ClN ₃ O		PWZ-0071	C ₁₆ H ₁₀ ClN ₃ O	295.723	0.23	0.17	0.12		0.44	17.31
										
C ₁₇ H ₁₃ N ₃ O ₂		PWZ-007A	C ₁₇ H ₁₃ N ₃ O ₂	291.304	0.11	0.1	0.09		0.2	10
										
C ₁₇ H ₁₃ N ₃ O ₂		PWZ-009A1	C ₁₇ H ₁₃ N ₃ O ₂	291.304	1.34	1.31	1.26		0.84	2.03

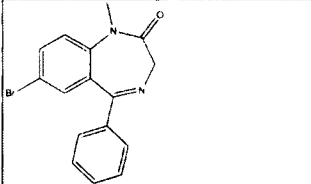
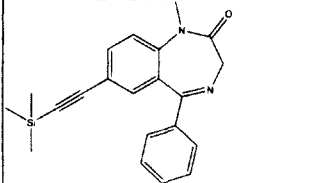
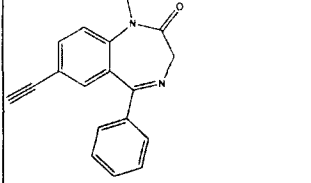
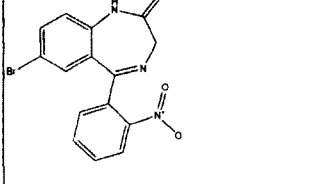
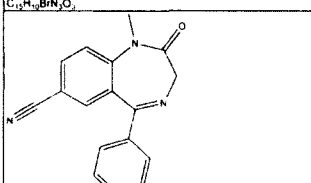
										
C ₁₄ H ₁₂ ClN ₃ O ₂		PWZ-029	C ₁₄ H ₁₄ ClN ₃ O ₂	291.733	300	300	300		38.8	300
										
C ₁₃ H ₁₁ Cl ₂ N ₃ O		PWZ-031A	C ₁₃ H ₁₁ Cl ₂ N ₃ O	296.152	300	300	300		28.5	300
										
C ₁₃ H ₁₂ ClN ₃ O ₂		PWZ-034A	C ₁₃ H ₁₂ ClN ₃ O ₂	277.706	300	300	300		300	300
										
C ₁₅ H ₁₄ ClN ₃ O ₂		PWZ-035A	C ₁₅ H ₁₆ ClN ₃ O ₂	305.759	300	300	300		82.7	300

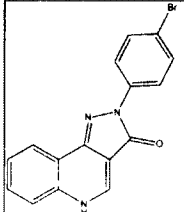
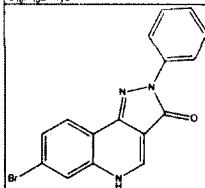
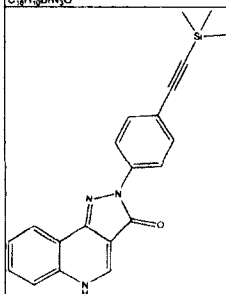
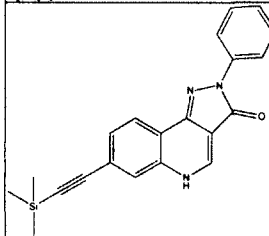
 $C_{17}H_{18}ClN_3O_2$		PWZ-049	C17H18ClN3O2	331.797	1581	2865	2739		166	2930
 $C_{14}H_{12}ClN_3O_2$		PWZ-051	C14H12ClN3O2	289.717	17535	33834	22125		2612	29500
 $C_{17}H_{21}ClN_4O$		PWZ-057	C17H21ClN4O	332.828	9483	30000	15409		2583	30160
 $C_{19}H_{25}ClN_4O$		PWZ-058	C19H25ClN4O	360.881	4201	12590	6266		1346	8600
 $C_{14}H_{14}ClN_3O$		PWZ-066	C14H14ClN3O	275.733	408	1527	1125		182	3648

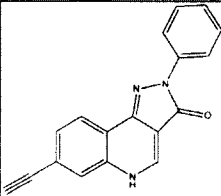
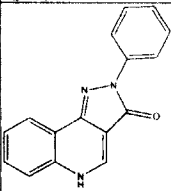
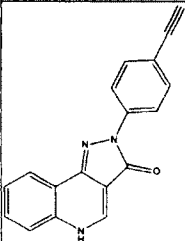
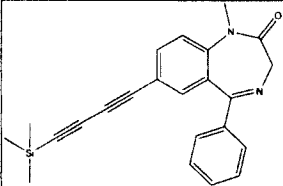
 $C_{17}H_{19}ClN_5O$		PWZ-068	C17H20ClN3O	317.813	2050	2900	2907		369	960
 $C_{19}H_{17}N_5O_4$		PWZ-085	C16H17N3O4	315.324	4.86	13	8.5		0.55	40
 $C_{21}H_{19}N_5O_4$		PWZ-096	C17H19N3O4	329.35	11.1	36	16.9		1.07	51.5
 $C_{17}H_{12}ClN_5O_2$		PZII-028	C17H12ClN3O2	325.749	0.2		0.2		0.32	1.9

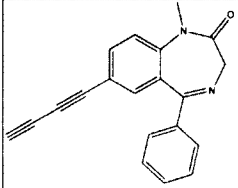
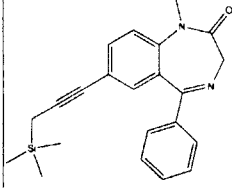
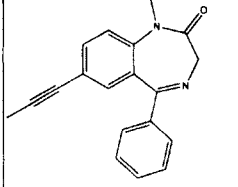
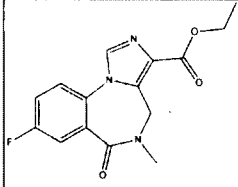
 <chem>COc1ccc(cc1)-n2c(=O)[nH]c3cc(OC)ccc3n2</chem> $C_{18}H_{15}N_2O_2$		PZII-029	C18H15N3O3	321.33	0.34	0.79	0.52	10	
 <chem>N=[N+]=[N-]c1ccc2c(c1)[nH]c(=O)nc2-c3ccccc3[N+]=[N-]</chem> $C_{15}H_{10}N_6O$		QH-133	C15H10N8O	318.293	2164	4620	1635	1000	
 <chem>O=[N+]([O-])c1ccc2c(c1)[nH]c(=O)nc2-c3ccccc3[N+](=O)[O-]</chem> $C_{16}H_{12}N_4O_5$		QH-146	C16H12N4O5	340.29	0.49	0.76	7.7	10000	
 <chem>N=[N+]=[N-]c1ccc2c(c1)[nH]c(=O)nc2-c3ccccc3[N+]=[N-]</chem> $C_{16}H_{12}N_6O$		QH-149	C16H12N8O	332.319					
 <chem>Fc1ccc2c(c1)[nH]c(=O)nc2-c3ccsc3</chem> $C_{13}H_9FN_2OS$		QH-27	C13H9FN2OS	260.287	175	335	405	150	300

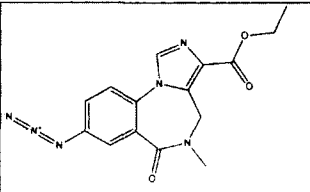
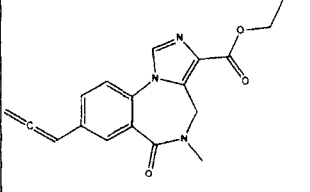
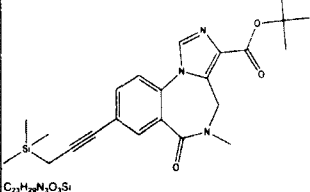
 $C_{14}H_{11}FN_2OS$		QH-28	C14H11FN2OS	274.313	141	215	205		65.5	300
 $C_{15}H_{10}N_4O_5$		QH-65	C15H10N4O5	326.264						
 $C_{15}H_{12}N_2O$		QH-II-058b	C15H12N2O	236.269	288	233	350		140	3000
 $C_{16}H_{14}N_2O$		QH-II-059	C16H14N2O	250.295	81	138	318		98	3000

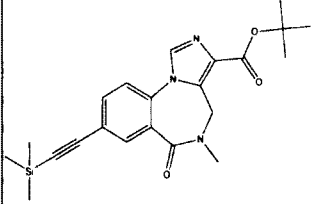
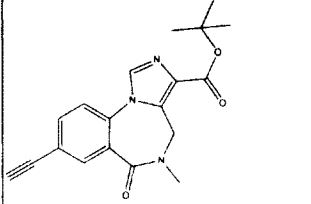
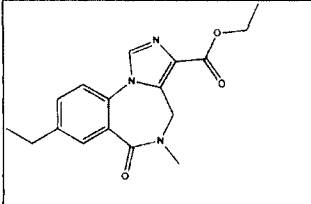
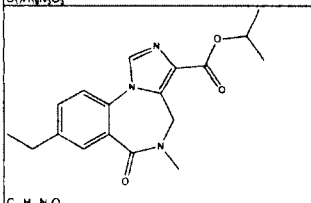
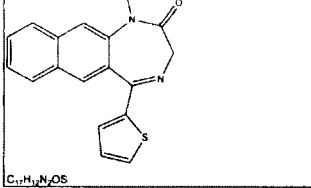
 $C_{16}H_{13}BrN_2O$		QH-II-063	$C_{16}H_{13}BrN_2O$	329.191	9.4	9.3	31		7.7	3000
 $C_{21}H_{22}N_2OSi$		QH-II-065	$C_{21}H_{22}N_2OSi$	346.498	94	73	203		63	3000
 $C_{18}H_{14}N_2O$		QH-II-066	$C_{18}H_{14}N_2O$	274.317	76.3	42.1	47.4	2000	6.8	3000
 $C_{15}H_{10}BrN_3O_2$		QH-II-067a	$C_{15}H_{10}BrN_3O_3$	360.162	16	31	52		199	3000
 $C_{17}H_{13}N_3O$		QH-II-072	$C_{17}H_{13}N_3O$	275.305	320	310	350		265	3000

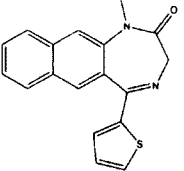
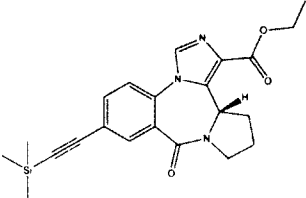
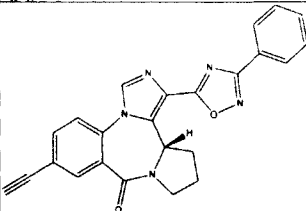
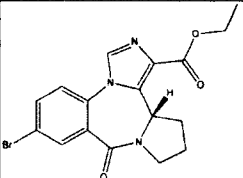
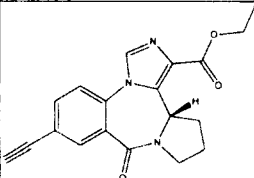
 <chem>C16H10BrN3O</chem>		QH-II-075	C16H10BrN3O	340.174	0.18	0.21	0.25		1.3	40
 <chem>C16H10BrN3O</chem>		QH-II-077	C16H10BrN3O	340.174	0.06	0.08	0.05		0.12	4
 <chem>C21H19N3OSi</chem>		QH-II-080b	C21H19N3OSi	357.481	3	3.7	4.7		24	1000
 <chem>C21H19N3OSi</chem>		QH-II-082	C21H19N3OSi	357.481	1.7	1.8	1.6		6.1	100

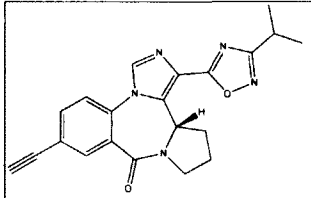
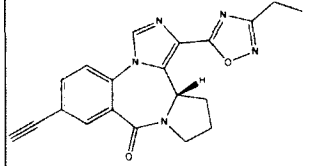
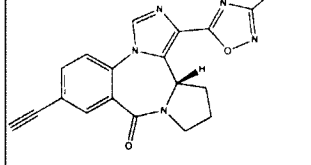
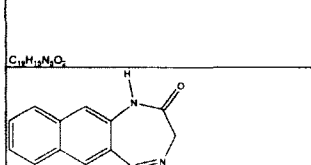
 $C_{18}H_{11}N_3O$		QH-II-085	C18H11N3O	285.299	0.08	0.06	0.02		0.08	
 $C_{16}H_{11}N_3O$		QH-II-090(CGS-8216)	C16H11N3O	261.278	0.05	0.08	0.12		0.25	17
 $C_{18}H_{11}N_3O$		QH-II-092	C18H11N3O	285.299	0.07	0.03	0.04		0.17	
 $C_{23}H_{22}N_2OSi$		QH-IV-014	C23H22N2OSi	370.519	3000	3000	3000		3000	3000

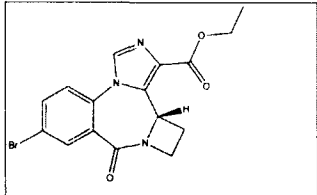
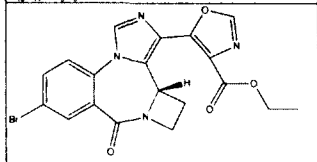
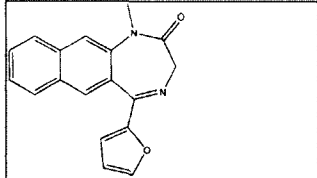
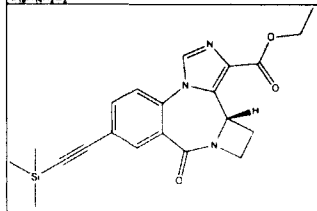
 $C_{20}H_{14}N_2O$		QH-IV-016	C20H14N2O	298.338	3000	3000	3000		3000	3000
 $C_{22}H_{24}N_2OSi$		QH-IV-019	C22H24N2OSi	360.524	3000	3000	3000		3000	3000
 $C_{19}H_{14}N_2O$		QH-IV-021	C19H16N2O	288.343	3000	3000	3000		3000	3000
 $C_{15}H_{14}FN_2O_3$		Ro15-1788	C15H14FN3O3	303.288	0.8	0.9	1.05		0.6	148

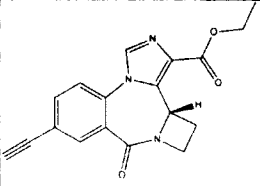
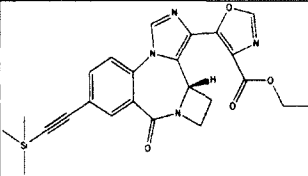
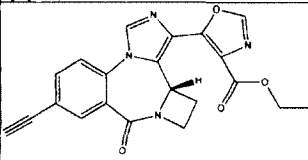
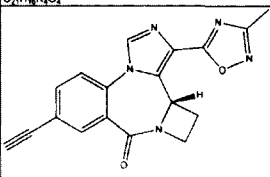
 $C_{15}H_{14}N_6O_3$		Ro15-4513	C15H14N6O3	326.31	3.3	2.6	2.5		0.26	3.8
	08-34	RSK-II-35			200.7	47.03	94.66		38.38	
 $C_{18}H_{17}N_5O_3$		RY-008	C18H17N3O3	323.346	3.75	7.2	4.14		1.11	44.3
 $C_{23}H_{29}N_5O_3Si$		RY-020	C23H29N3O3Si	423.58	275	387	337		23	301

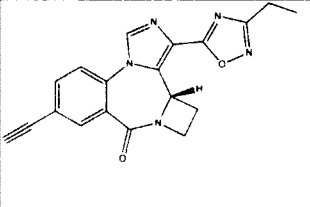
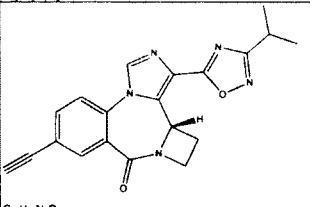
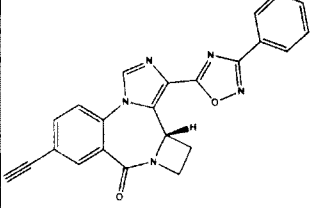
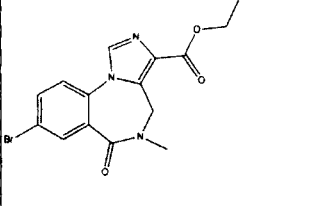
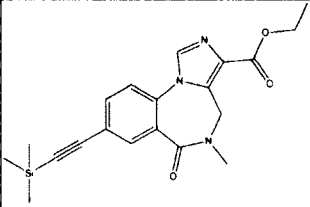
 $C_{22}H_{27}N_3O_3Si$	03-1033 merck?	RY-023	C22H27N3O3Si	C22H27N3O3Si	409.554	197	142.6	255	7.8	2.61	58.6
 $C_{19}H_{19}N_3O_3$	03-1030	RY-024	C19H19N3O3	C19H19N3O3	337.372	26.9	26.3	18.7		0.4	5.1
 $C_{17}H_{19}N_3O_3$		RY-031 (RY-10)		C17H19N3O3	313.351	20.4	27	26.1		1.5	176
 $C_{18}H_{21}N_3O_3$		RY-033		C18H21N3O3	327.378	14.8	56	25.3		1.72	22.9
 $C_{17}H_{12}N_2OS$		RY-035		C17H12N2OS	292.355	980	590	775		92.5	3000

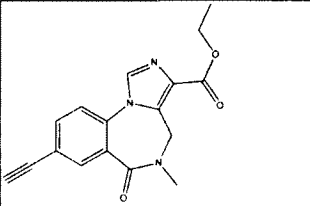
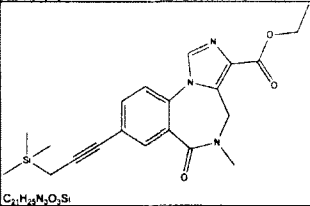
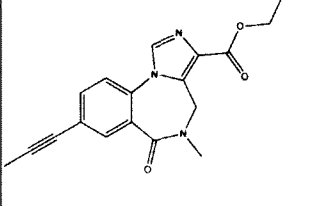
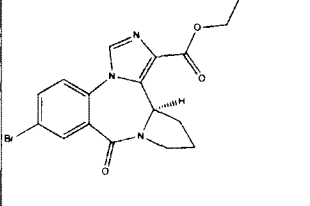
 $C_{18}H_{14}N_2OS$										
		RY-037	C18H14N2OS	306.382	300	300	300		300	300
 $C_{22}H_{22}N_2O_3Si$		RY-047	C22H25N3O3Si	407.538	200	124	79		4	340
 $C_{24}H_{17}N_5O_2$		RY-049	C24H17N5O2	407.424						
 $C_{17}H_{12}BrN_5O_2$		RY-053	C17H16BrN3O3	390.231	49	29	15		1	46
 $C_{19}H_{17}N_5O_2$		RY-054	C19H17N3O3	335.357	59	44	27		1.3	126

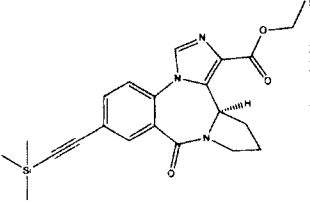
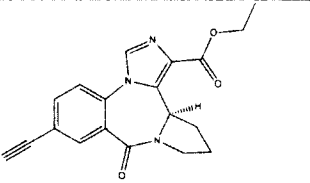
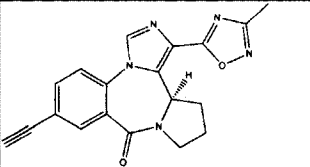
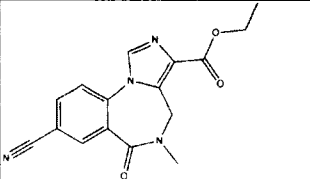
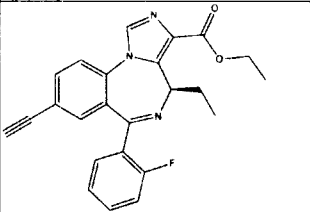
 $C_{21}H_{19}N_5O_2$		RY-057	C21H19N5O2	373.408	73	85	97		4.8	333
 $C_{20}H_{17}N_5O_2$		RY-058	C20H17N5O2	359.381	86	40	85		2.4	150
 $C_{19}H_{15}N_5O_2$		RY-059	C19H15N5O2	345.355	89	70	91		3.7	301
 $C_{17}H_{12}N_5O_2$		RY-060	C17H12N5O2	276.289	1000	1000	1000		1000	1000

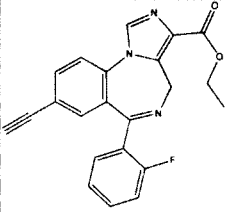
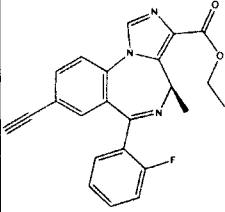
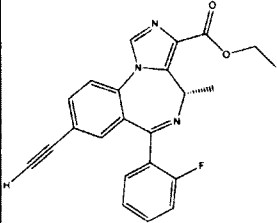
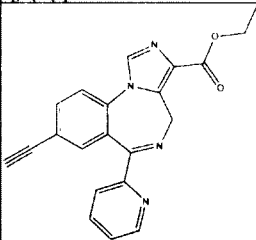
 $C_{16}H_{14}BrN_3O_3$										
		RY-061	C16H14BrN3O3	376.205	17	13	6.7		0.3	31
 $C_{19}H_{15}BrN_4O_4$										
		RY-062	C19H15BrN4O4	443.251	1000	1000	500		172	2000
 $C_{18}H_{14}N_2O_2$										
		RY-062	C18H14N2O2	290.316	300	300	300		300	300
 $C_{21}H_{23}N_3O_3Si$										
		RY-066	C21H23N3O3Si	393.511	83	60	48		2.6	180

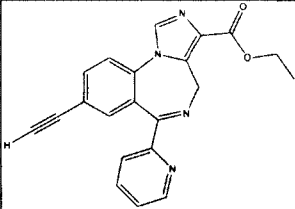
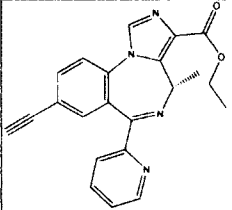
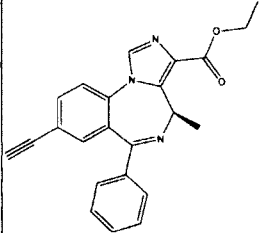
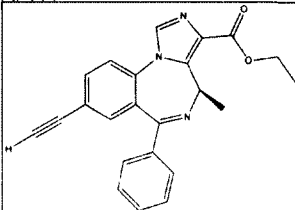
										
$C_{18}H_{15}N_3O_3$		RY-067	C18H15N3O3	321.33	21	12	10		0.37	42
										
$C_{24}H_{24}N_4O_4Si$		RY-068	C24H24N4O4Si	460.557	500	877	496		37	1000
										
$C_{21}H_{16}N_4O_4$		RY-069	C21H16N4O4	388.376	692	622	506		19	1000
										
$C_{18}H_{13}N_5O_2$		RY-071	C18H13N5O2	331.328	19	56	91		7.2	266

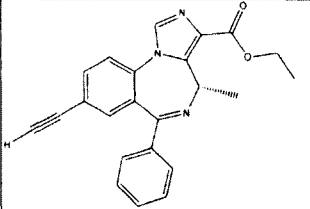
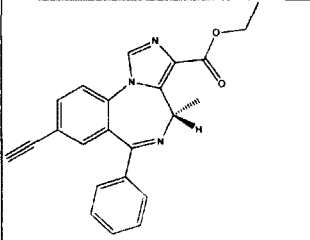
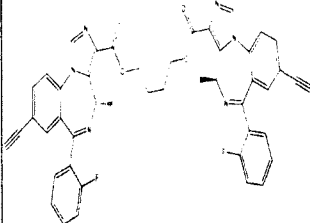
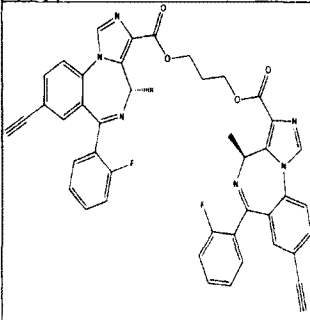
 $C_{19}H_{17}N_5O$		RY-072	C19H15N5O2	345.355	220	150	184		12.7	361
 $C_{20}H_{17}N_5O_2$		RY-073	C20H17N5O2	359.381	156	88	122		8.5	267
 $C_{23}H_{19}N_5O_2$		RY-075	C23H15N5O2	393.398						
 $C_{15}H_{14}BrN_3O_3$		RY-076	C15H14BrN3O3	364.194	26	27	13		0.7	22
 $C_{20}H_{27}N_3O_3Si$		RY-079	C20H23N3O3Si	381.5	121.1	141.9	198.4	159	5	113.7

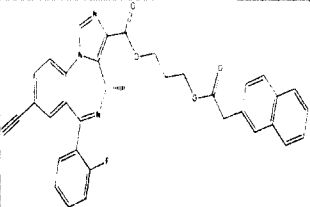
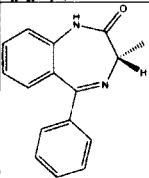
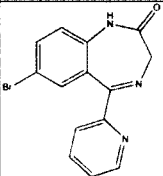
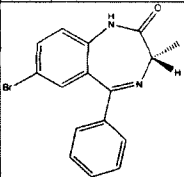
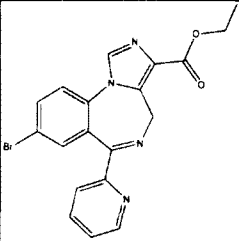
 $C_{17}H_{15}N_3O_3$	03-1034	RY-080	C17H15N3O3	C17H15N3O3	309.319	28.4	21.4	25.8	5.3	0.49	28.8
 $C_{21}H_{25}N_3O_3Si$		RY-097		C21H25N3O3Si	395.527	300	300	300		300	300
 $C_{18}H_{17}N_3O_3$		RY-098		C18H17N3O3	323.346	10.1	22.2	16.5		1.68	100
 $C_{17}H_{16}BrN_3O_3$		RY-I-26		C17H16BrN3O3	390.231	1000	1000	1000		1000	1000

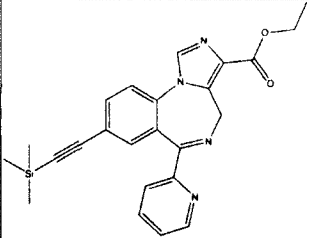
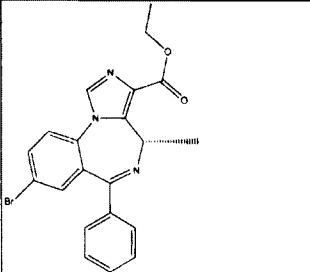
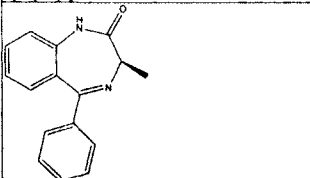
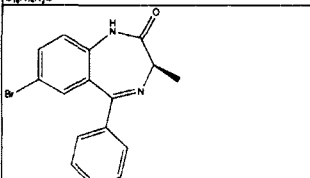
 $C_{22}H_{25}N_3O_3Si$		RY-I-27	C22H25N3O3Si	407.538	1000	1000	1000		1000	1000
 $C_{19}H_{17}N_3O_3$		RY-I-28	C19H17N3O3	335.357	283	318	102		7.2	61
 $C_{19}H_{15}N_3O_2$		RY-I-29	C19H15N3O2	345.355	1000	1000	1000		157	1000
 $C_{18}H_{14}N_4O_2$		RY-I-31	C16H14N4O3	310.307	10	45	19		6	1000
 $C_{24}H_{20}FN_3O_2$		SA-01-031	C24H20FN3O2	401.433	2013	1887			609.3	

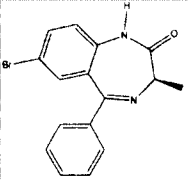
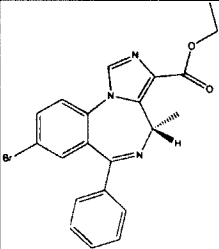
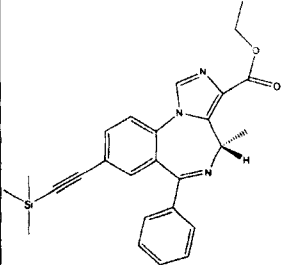
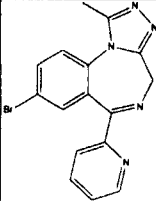
	09-95	SA-SH-053-2'N-R-CH3			406	73565	3392		16843	
 $C_{22}H_{16}FN_3O_2$	06-003	SH-053-2'F	C22H16FN3O2	373.38	21.99	12.34	34.9		0.671	
 $C_{22}H_{16}FN_3O_2$	06-009	SH-053-2'F-R-CH3	C23H18FN3O2	387.406	759.1	948.2	768.8		95.17	
 $C_{22}H_{16}FN_3O_2$	06-010	SH-053-2'F-S-CH3	C23H18FN3O2	387.406	468.2	33.27	291.5		19.2	
 $C_{21}H_{16}N_4O_2$	05-1768	SH-053-2'N	C21H16N4O2	356.377	300	160	527		82	5000

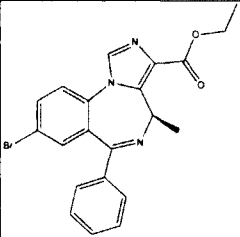
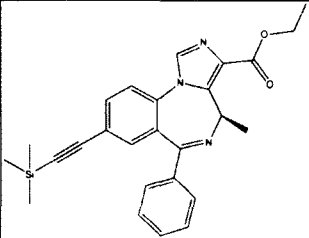
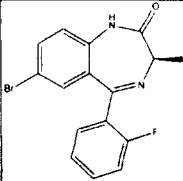
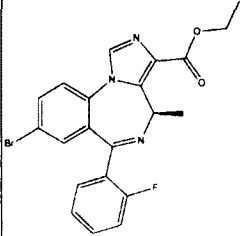
 $C_{21}H_{16}N_4O_2$		SH-053-2'N	C21H16N4O2	356.377						
 $C_{22}H_{18}N_4O_2$	06-002	SH-053-2'N-S-CH3	C22H18N4O2	370.404	6951	2331	2655		744.1	
 $C_{23}H_{19}N_4O_2$	06-001	SH-053-R-CH3	C23H19N3O2	369.416	2026	2377	1183		949.1	
 $C_{23}H_{19}N_4O_2$		SH-053-R-CH3	C23H19N3O2	369.416						

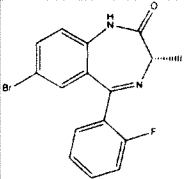
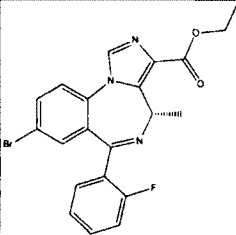
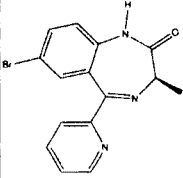
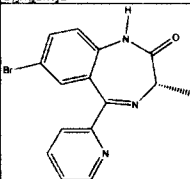
 $C_{23}H_{19}N_3O_2$	06-007	SH-053-S-CH3	C23H19N3O2	369.416	1666	1263	1249		206.4	
 $C_{23}H_{19}N_3O_2$	05-1750	SH-053-S-CH3	C23H19N3O2	369.416	5000	551	540.1		201	5000
 $C_{46}H_{34}F_2N_6O_4$	06-030	SH-222A	C46H34F2N6O4	772.797	2058	292.3			51.24	
 $C_{45}H_{32}F_2N_6O_4$	06-029	SH-223A	C45H32F2N6O4	758.77	1231	2008	3609		261.3	

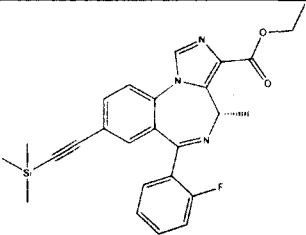
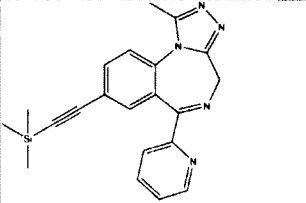
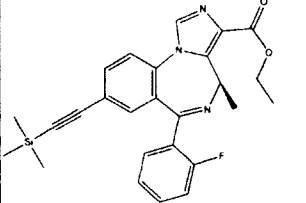
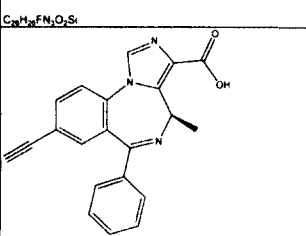
 $C_{36}H_{28}FN_3O_4$	06-028	SH-223B	C36H28FN3O4	585.624	4117	4785	10661	911	
 $C_{16}H_{14}N_2O$	06-020	SH-I-029B	C16H14N2O	250.295	489	576.5	706.1	208.8	
 $C_{14}H_{10}BrN_3O$	05-1762	SH-I-02B	C14H10BrN3O	316.153	29.82	1315	18	74.05	
 $C_{16}H_{13}BrN_3O$	06-005	SH-I-030	C16H13BrN3O	329.191	14.42	11.04	19.09	1.89	
 $C_{19}H_{15}BrN_4O_2$	05-1766	SH-I-031A	C19H15BrN4O2	411.252	84.05	141.3	150.5	151.2	

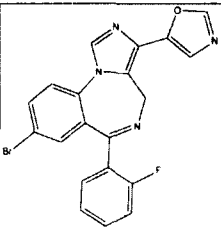
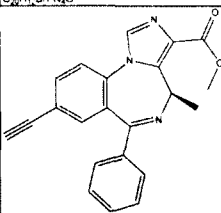
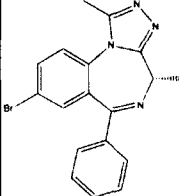
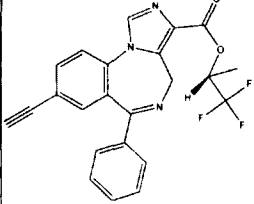
 $C_{24}H_{24}N_4O_2Si$	05-1767	SH-I-031B	$C_{24}H_{24}N_4O_2Si$	428.558	981.9	1004	2046	356.2	
 $C_{21}H_{18}BrN_3O_2$	06-017	SH-I-034(S)	$C_{21}H_{18}BrN_3O_2$	424.291	793.4	746.8	544.6	1564	
 $C_{16}H_{14}N_2O$	06-015	SH-I-035A	$C_{16}H_{14}N_2O$	250.295	7389	6049	16811	15793	
 $C_{16}H_{13}BrN_2O$	05-1752	SH-I-035B	$C_{16}H_{13}BrN_2O$	329.191	7439	11084	3021	4043	

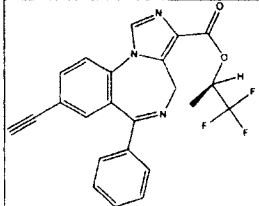
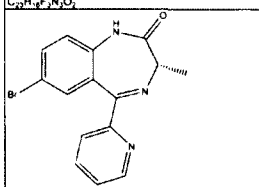
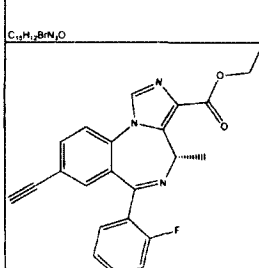
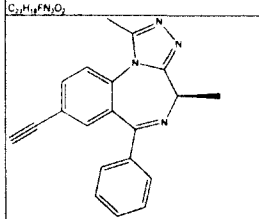
 $C_{16}H_{13}BrN_2O$	06-021	SH-I-035B	$C_{16}H_{13}BrN_2O$	329.191	11218	4571	3841		7035	
 $C_{21}H_{18}BrN_3O_2$	05-1748	SH-I-036	$C_{21}H_{18}BrN_3O_2$	424.291	587	587.9	280.2		150.8	
 $C_{26}H_{27}N_3O_2Si$	05-1749	SH-I-038	$C_{26}H_{27}N_3O_2Si$	441.597						
 $C_{16}H_{12}BrN_3$	05-1763	SH-I-04	$C_{16}H_{12}BrN_3$	354.204	7.3	6.136	5.1		7.664	

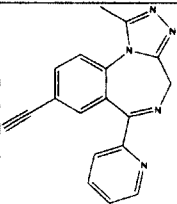
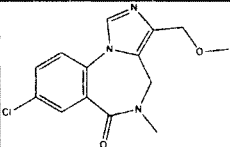
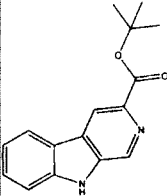
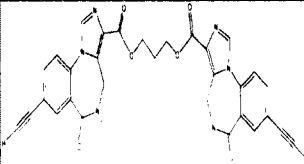
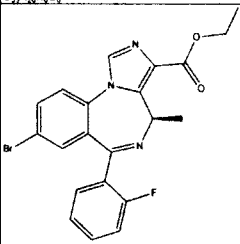
 $C_{21}H_{18}BrN_3O_2$	06-022	SH-I-040 R	C21H18BrN3O2	424.291	774.4	334.1	584	355.9	
 $C_{26}H_{27}N_3O_2Si$	05-1754	SH-I-041	C26H27N3O2Si	441.597					
 $C_{16}H_{12}BrFN_2O$	06-018	SH-I-044	C16H12BrFN2O	347.182	5633	2034	6658	3521	
 $C_{21}H_{17}BrFN_3O_2$	05-1761	SH-I-047	C21H17BrFN3O2	442.281	1710	17.52	1222	1519	

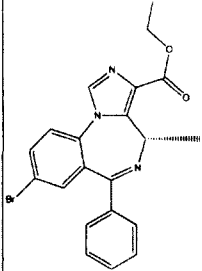
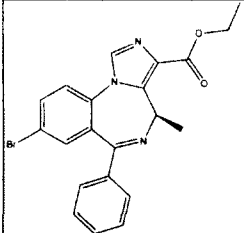
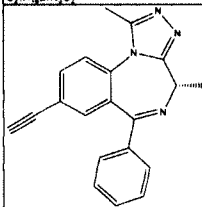
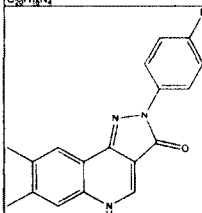
 <chem>C12=CC=C(C=C1C2=NC(=O)N1C=CC(=C1)Br)C3=CC=CC=C3F</chem> $C_{16}H_{12}BrFN_2O$	06-006	SH-I-048A	C16H12BrFN2O	347.182	0.774	0.1723	0.383	0.11	
 <chem>CCOC(=O)C1=NC2=C(N1C=CC(=C2)Br)C3=CC=CC=C3F</chem> $C_{21}H_{17}BrFN_2O_2$	05-1757	SH-I-048B	C21H17BrFN3O2	442.281					
 <chem>C[C@H]1C(=O)NC2=CC=C(C=C2C1=NC3=CC=CC=C3Br)C4=CC=CC=N4</chem> $C_{17}H_{12}BrN_3O$		SH-I-049R	C15H12BrN3O	330.179					
 <chem>C[C@H]1C(=O)NC2=CC=C(C=C2C1=NC3=CC=CC=C3Br)C4=CC=CC=N4</chem> $C_{17}H_{12}BrN_3O$	06-014	SH-I-049S	C15H12BrN3O	330.179	155.6	137.2	88.5	11094	

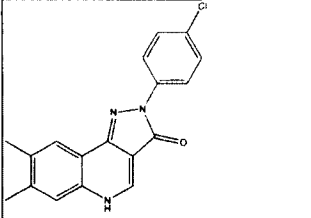
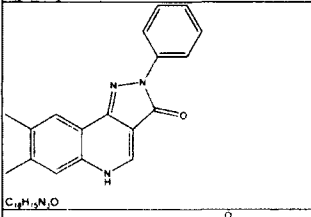
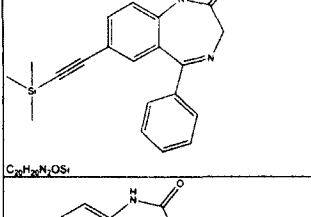
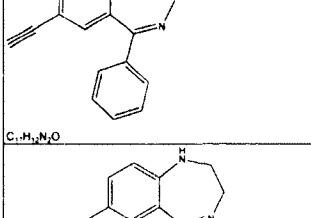
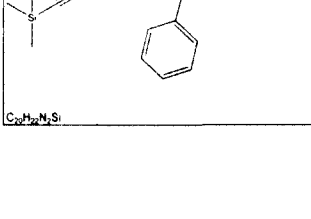
 $C_{26}H_{26}FN_3O_2Si$	06-013	SH-I-055	C26H26FN3O2Si	459.587	5109	1638	1394	223.4	
 $C_{21}H_{21}N_4Si$	05-1764	SH-I-06	C21H21N5Si	371.51					
 $C_{26}H_{26}FN_3O_2Si$	06-004	SH-I-064	C26H26FN3O2Si	459.587	4249	3970	3412	1215	
 $C_{21}H_{15}N_3O_2$		SH-I-067	C21H15N3O2	341.363					

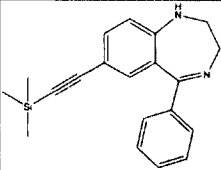
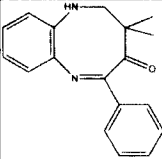
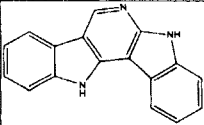
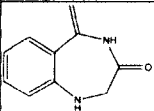
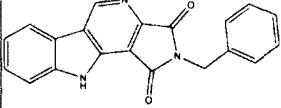
 $C_{20}H_{11}BrFN_4O$	06-011	SH-I-085	C20H12BrFN4O	423.238	11.08	4.866	13.75	0.24
 $C_{22}H_{17}N_3O_2$	06-023	SH-I-75	C22H17N3O2	355.389	1487	989.9	773	0.1825
 $C_{18}H_{13}BrN_4$	06-019	SH-I-89S	C18H15BrN4	367.242	12.78	8.562	8.145	3.23
 $C_{23}H_{16}F_3N_4O_2$	06-012	SH-I-R66	C23H16F3N3O2	423.387	219.5	169.1	87.01	47.97

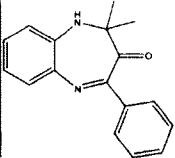
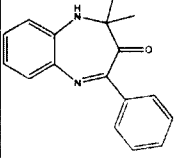
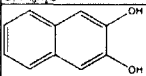
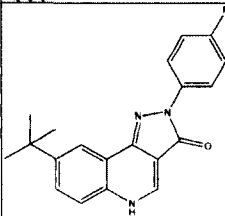
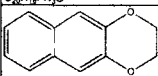
 $C_{27}H_{18}F_3N_3O_2$	06-008	SH-I-S66	C23H16F3N3O2	423.387	22.93	30.36	55.26	0.69	
 $C_{17}H_{12}BrN_3O$	05-1769	SH-O53-2'N-S-CH3	C15H12BrN3O	330.179					
 $C_{27}H_{18}FN_3O_2$	05-1759	SH-O53-S-CH3-2'F	C23H18FN3O2	387.406	350	141	1237	16	5000
 $C_{27}H_{18}N_4$	06-027	SH-TR-CH3	C20H16N4	312.368	7367	1534	8213	1948.5	
	06-027	SH-TR-CH3							

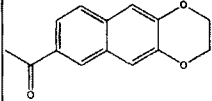
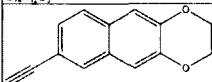
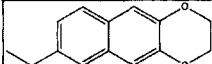
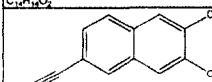
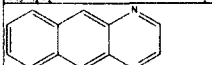
 $C_{24}H_{17}N_5$	05-1765	SH-TRI-108 ANX4	C18H13N5	299.329	143.9	81.29	103.9		45.64	
 $C_{14}H_{11}ClN_3O_2$	06-024	SH-TSC-1(PWZ-029)	C14H14ClN3O2	291.733	362.4	180.3	328.2		6.185	
 $C_{24}H_{18}N_2O_2$	06-025	SH-TSC-2(BCCT)	C16H16N2O2	268.31	0.03	0.0419	0.035		69.32	
 $C_{37}H_{28}N_4O_6$	06-026	SH-TSC-3(XLI-093)	C33H26N6O6	602.596	1295	744.9	1814		33.99	
 $C_{27}H_{17}BrFN_3O_2$		SH-TSC-5(SH-I-047)	C21H17BrFN3O2	442.281	356.7	169.4	285		75.31	

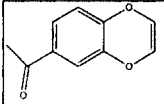
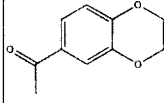
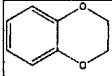
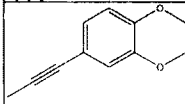
 <chem>CCOC(=O)c1nc2c(nc1c3ccccc3n2)c4ccccc4Br</chem> $C_{21}H_{18}BrN_3O_2$		SH-TSC-6(SH-I-034)	C21H18BrN3O2	424.291	913.2	283	300		436.8	
 <chem>CCOC(=O)c1nc2c(nc1c3ccccc3n2)c4ccccc4Br</chem> $C_{21}H_{18}BrN_3O_2$		SH-TSC-7(SH-I-040)	C21H18BrN3O2	424.291	709	1997	1256		727.4	
 <chem>CC1=CN2C(=N1)c3ccccc3N2C#Cc4ccccc4</chem> $C_{20}H_{16}N_4$	06-016	SH-TS-CH3	C20H16N4	312.368	107.2	50.09	20.95		8.068	
 <chem>CC1=CN2C(=N1)c3ccccc3N2C(=O)c4ccccc4Br</chem> $C_{18}H_{14}BrN_3O$		SHU-1-07	C18H14BrN3O	368.227	108	260	175	940	155	2535

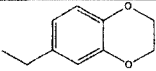
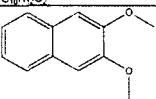
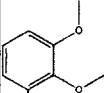
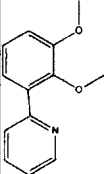
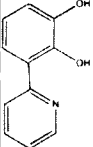
 $C_{18}H_{12}ClN_2O$		SHU-1-15	C18H14ClN3O	323.776	81	63	86	2175	174	2167
 $C_{18}H_{15}N_3O$		SHU-1-19	C18H15N3O	289.331	4	12	7	48	14	84
 $C_{20}H_{20}N_2OSi$		SHU-221 (XLI-250)	C20H20N2OSi	332.471	492	439	339	3000	118	3000
 $C_{17}H_{12}N_2O$		SHU-221-1	C17H12N2O	260.29	66	41	43	3000	9	3000
 $C_{20}H_{22}N_2Si$		SHU-223	C20H22N2Si	318.488	1000	1000	1000	1000	1000	1000

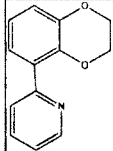
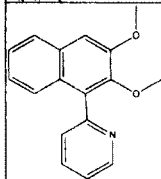
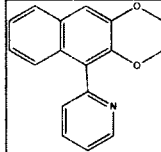
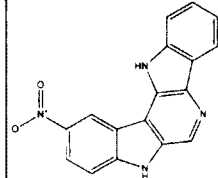
 $C_{20}H_{22}N_2Si$		SHU-224	C20H22N2Si	318.488	1000	1000	1000	1000	1000	1000
 $C_{18}H_{19}N_2O$		SHU-525	C18H18N2O	278.348	667	667	667	667	667	429
 $C_{17}H_{11}N_3$		SHU-528	C17H11N3	257.289	667	667	667	667	667	429
 $C_{10}H_{13}N_2O$		SHU-530	C10H10N2O	174.199	667	667	667	667	667	429
 $C_{20}H_{13}N_3O_2$		SHU-537	C20H13N3O2	327.336	333	333	333	333	667	429

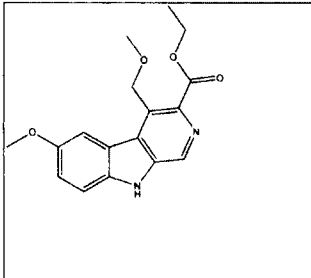
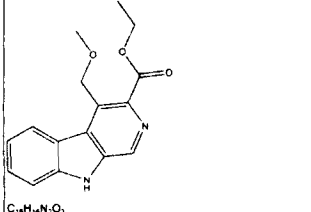
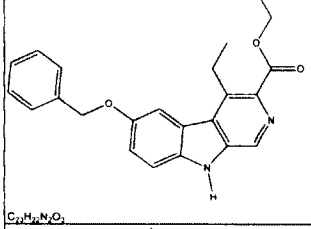
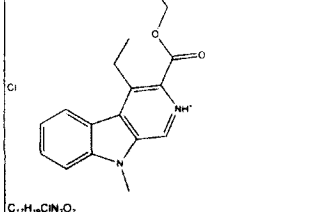
 $C_{17}H_{16}N_2O$		SHU-547	C17H16N2O	264.322	667	667	667	667	667	429
 $C_{17}H_{16}N_2O$		SHU-550	C17H16N2O	264.322	333	333	333	333	333	429
 $C_{10}H_{10}O_2$		SHU-III-032	C10H8O2	160.169	1000	1000	1000	1000	1000	1000
 $C_{20}H_{18}FN_2O$		SHU-III-24	C20H18FN3O	335.375	1000	1000	1000	1000	1000	1000
 $C_{21}H_{24}O_2$		SHU-III-32	C12H10O2	186.207	1000	1000	1000	1000	1000	1000

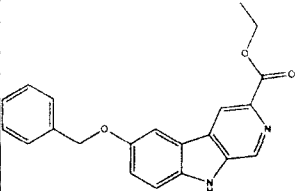
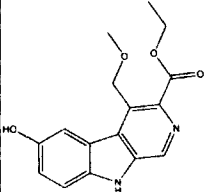
											
C ₁₉ H ₁₆ O ₂		SHU-III-33	C ₁₄ H ₁₂ O ₃	228.243	1000	1000	1000	1000	1000	1000	1000
											
C ₁₇ H ₁₂ O ₂		SHU-III-34	C ₁₄ H ₁₀ O ₂	210.228	1000	1000	1000	1000	1000	1000	1000
											
C ₁₇ H ₁₄ O ₂		SHU-III-36	C ₁₄ H ₁₄ O ₂	214.26	1000	1000	1000	1000	1000	1000	1000
											
C ₁₇ H ₁₂ O ₂		SHU-III-37	C ₁₅ H ₁₂ O ₂	224.255	1000	1000	1000	1000	1000	1000	1000
											
C ₁₂ H ₈ N ₂		SHU-III-40	C ₁₂ H ₈ N ₂	180.205	1000	1000	1000	1000	1000	1000	1000

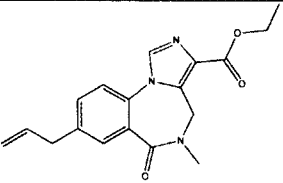
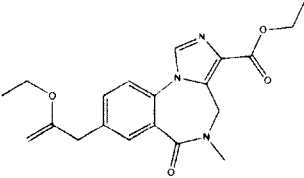
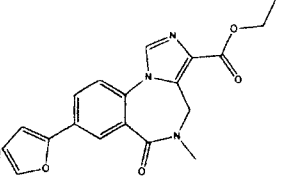
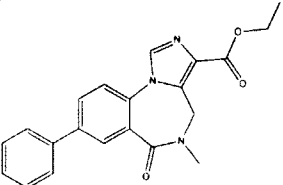
											
C ₁₀ H ₈ O ₃		SHU-III-42	C ₁₀ H ₈ O ₃	176.169	1000	1000	1000	1000	1000	1000	1000
											
C ₁₀ H ₁₀ O ₃		SHU-III-42A	C ₁₀ H ₁₀ O ₃	178.185	1000	1000	1000	1000	1000	1000	1000
											
C ₈ H ₈ O ₂		SHU-III-42B	C ₈ H ₈ O ₂	136.148	1000	1000	1000	1000	1000	1000	1000
											
C ₁₁ H ₁₀ O ₂		SHU-III-44	C ₁₁ H ₁₀ O ₂	174.196	1000	1000	1000	1000	1000	1000	1000

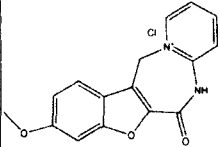
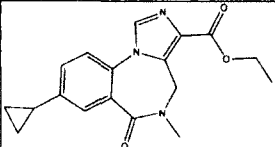
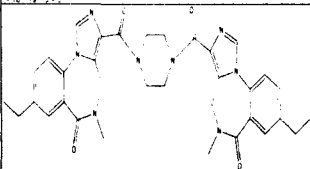
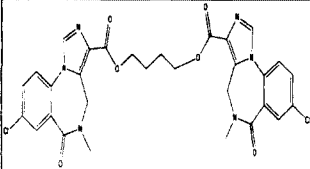
											
<chem>C18H18O2</chem> 		SHU-III-45	C10H12O2	164.201	1000	1000	1000	1000	1000	1000	1000
<chem>C12H12O2</chem> 		SHU-III-66	C12H12O2	188.222	1000	1000	1000	1000	1000	1000	1000
<chem>C13H11NO2</chem> 		SHU-III-87	C13H13NO2	215.248	1000	1000	1000	1000	1000	1000	1000
<chem>C11H9NO2</chem> 		SHU-III-88	C11H9NO2	187.195	1000	1000	1000	1000	1000	1000	1000

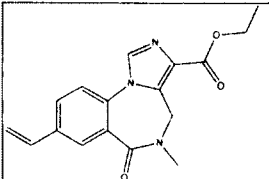
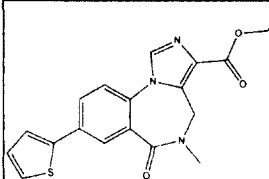
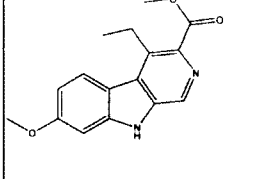
 $C_{13}H_{11}NO_2$		SHU-III-90	C13H11NO2	213.232	1000	1000	1000	1000	1000	1000
 $C_{17}H_{15}NO_2$		SHU-III-93	C17H15NO2	265.306	1000	1000	1000	1000	1000	1000
 $C_{17}H_{13}NO_2$		SHU-III-94	C17H13NO2	263.291	1000	1000	1000	1000	1000	1000
 $C_{17}H_{10}N_4O_7$		SLL-II-25	C17H10N4O2	302.287	244	500	532	1560	10000	

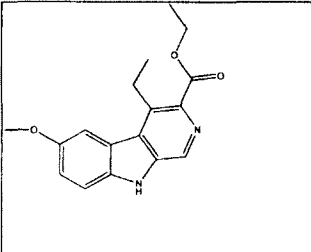
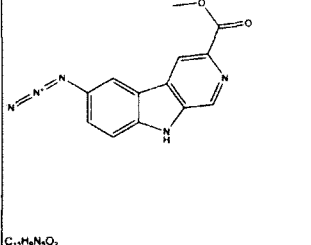
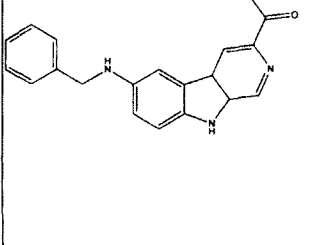
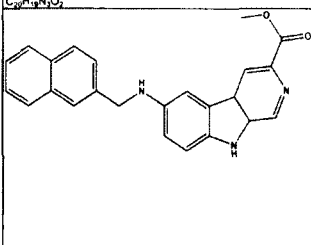
 <chem>CCOC(=O)C1=C2C(=C1)C(=CN2)C3=CC=C(C=C3)OC</chem> $C_{17}H_{18}N_2O_4$		SPH-121	C17H18N2O4	314.336	0.14	1.19	1.72		4	479
 <chem>CCOC(=O)C1=C2C(=C1)C(=CN2)C3=CC=CC=C3</chem> $C_{16}H_{16}N_2O_3$		SPH-165	C16H16N2O3	284.31	0.63	2.79	4.85		10.4	1150
 <chem>CCOC(=O)C1=C2C(=C1)C(=CN2)C3=CC=C(C=C3)OCC4=CC=CC=C4</chem> $C_{23}H_{22}N_2O_3$		SPH-166	C23H22N2O3	374.432	20.8	78.3	58.7		67.3	10000
 <chem>CCOC(=O)C1=C2C(=C1)C(=CN2)C3=CC=C(C=C3)Cl</chem> $C_{17}H_{19}ClN_2O_2$		SPH-178	C17H19ClN2O2	318.798	1000	1000	1000		1000	1000

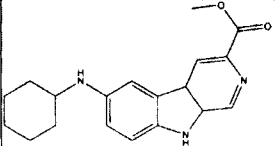
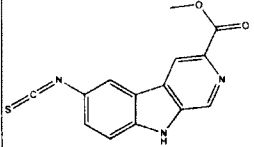
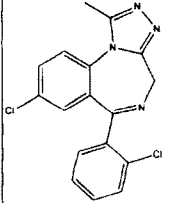
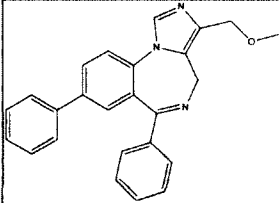
 $C_{21}H_{19}N_2O_3$		SPH-195	C ₂₁ H ₁₈ N ₂ O ₃	346.379	7.2	168.5	283.5		271	10000
 $C_{18}H_{15}N_2O_4$		SPH-38	C ₁₆ H ₁₆ N ₂ O ₄	300.309	2	5.4	10.8		18.5	3000
	09-01	SR-II-25			1593	2592	3919		1611	
	09-02	SR-II-30			724.1	470.6	790.2		770	
	09-03	SR-II-54			174.1	363.2	946.4		966.6	

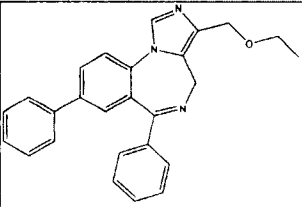
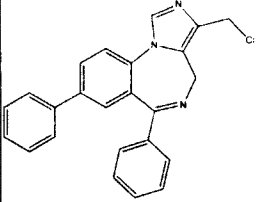
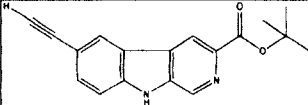
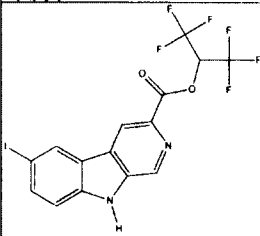
	09-04	SR-II-57				169.2	480.8	667.1		729.5
										
C ₁₈ H ₁₉ N ₃ O ₃		SVO-8-14	C18H19N3O3	325.362	8	25	8	6.9	0.9	14
										
C ₂₀ H ₂₃ N ₃ O ₄		SVO-8-20	C20H23N3O4	369.414	11	40	28	19	8.6	138
										
C ₁₉ H ₁₇ N ₃ O ₄		SVO-8-30	C19H17N3O4	351.356	1.1	5.3	5.3	2.8	0.6	15
										
C ₂₁ H ₁₉ N ₃ O ₃		SVO-8-67	C21H19N3O3	361.394	7	41	26	15	2.3	191

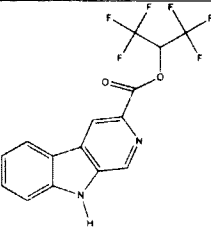
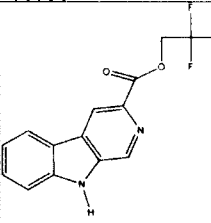
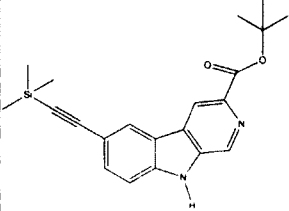
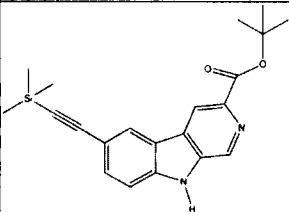
 <chem>COc1ccc2c(c1)oc3c2c(=O)[nH]c3c4ccccc4Cl</chem> $C_{16}H_{13}ClN_2O_3$	08-27	TC-T-JG-24	C16H13ClN2O3	316.739	746.5	8081	1543	2364	
 <chem>CCOC(=O)c1nc2cc3c(c1n2)C(=O)N(C)C3=CC=C4C5CC5C4</chem> $C_{17}H_{17}N_3O_3$	08-30	TC-YT-II-76	C18H19N3O3	325.362	101.1	1.897	5.816	11.99	
 $C_{34}H_{36}N_4O_4$	08-011	TC-YT-III-19	C34H36N8O4	620.701	2772	24918	4842.3	4925	
 $C_{30}H_{26}Cl_2N_6O_6$	08-25	TC-YT-TC-2	C30H26Cl2N6O6	637.47	2657	737.8	643	1973	

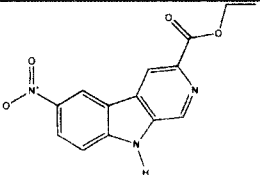
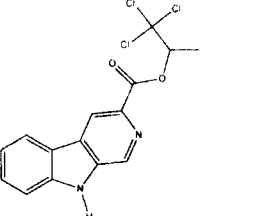
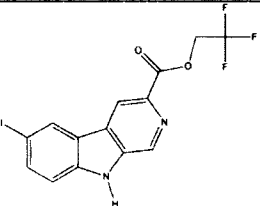
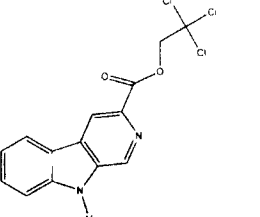
 $C_{17}H_{17}N_3O_3$		TG-4-29	C17H17N3O3	311.335	8.3	10.2	6.9		0.4	7.61
		TG-4-29			2.8	3.9	2.7	2.1	0.18	3.9
 $C_{19}H_{17}N_3O_3S$		TG-4-39	C19H17N3O3S	367.422	1.6	34	24	5.6	1.4	23
 $C_{16}H_{16}N_2O_3$		TG-I-97	C16H16N2O3	284.31						

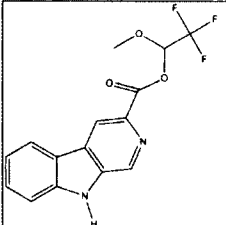
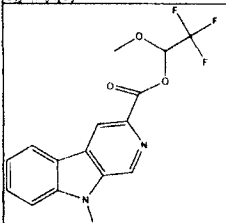
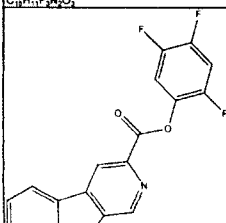
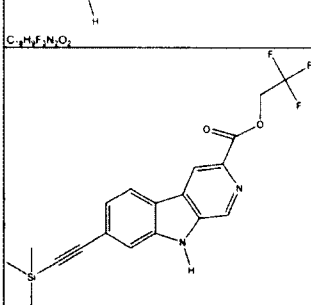
 <chem>CCOC(=O)c1c2c(c3cc(OC)ccc3n2)c4ccccc4n1</chem> $C_{17}H_{18}N_2O_3$		TG-II-82	C17H18N2O3	298.336	1.6	2.9	2.8		1	1000
 <chem>COC(=O)c1c2c(c3cc(N=[N+]=[N-])ccc3n2)c4ccccc4n1</chem> $C_{13}H_9N_5O_2$		TJH-6AZ	C13H9N5O2	267.243						
 <chem>COC(=O)c1c2c(c3cc(NCc4ccccc4)ccc3n2)c4ccccc4n1</chem> $C_{20}H_{19}N_2O_2$		TJH-IV-43	C20H19N3O2	333.384	5.42	30.19	48.9		475	10000
 <chem>COC(=O)c1c2c(c3cc(NCc4ccc5ccccc45)ccc3n2)c4ccccc4n1</chem> $C_{24}H_{21}N_2O_2$		TJH-IV-50	C24H21N3O2	383.442	30.7	205	271		814	10000

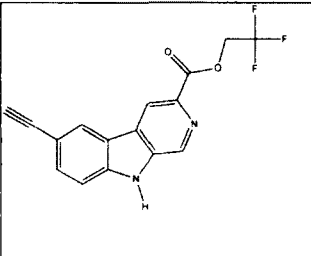
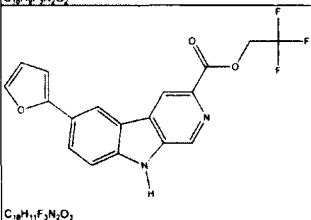
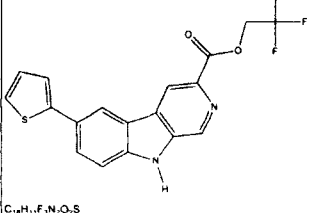
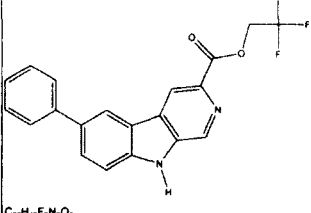
 $C_{19}H_{23}N_3O_2$		TJH-IV-51	C19H23N3O2	325.405	2.39	17.4	14.5		316	10000
 $C_{14}H_9N_3O_2S$		TJH-V-88	C14H9N3O2S	283.305	3.41		30		140.9	10000
 $C_{17}H_{12}Cl_2N_4$		triazolam	C17H12Cl2N4	343.21						
 $C_{25}H_{21}N_3O$	05-1745	TSC-I-93	C25H21N3O	379.454	5000	5000	5000		304	5000

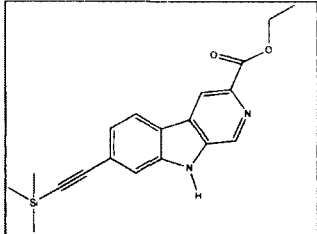
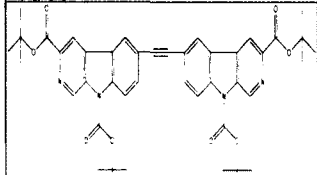
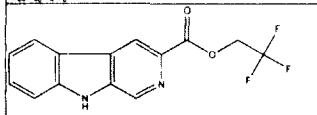
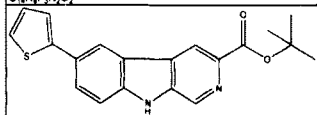
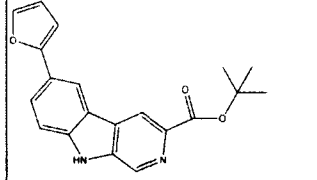
 $C_{26}H_{23}N_3O$	05-1744	TSC-I-94	C26H23N3O	393.48							
 $C_{24}H_{18}ClN_3$	05-1743	TSC-I-95	C24H18ClN3	383.873							
 $C_{17}H_{18}N_2O_2$	03-0973	WY-A-99-2(WYS8)	C18H16N2O2	292.332	0.972	111	102	2000	208	1980	
 $C_{15}H_7F_6N_2O_2$		WY-B-08	C15H7F6IN2O2	488.123	78	301	131	3000	681	3000	

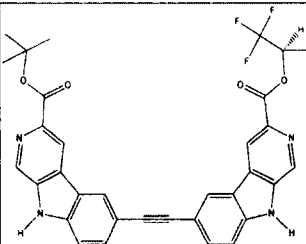
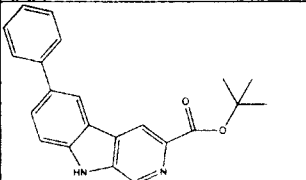
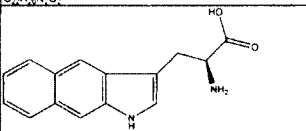
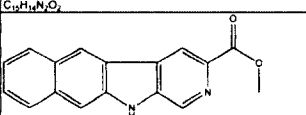
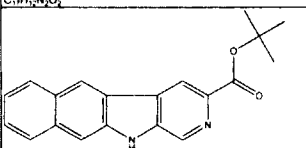
 $C_{15}H_8F_6N_2O_2$		WY-B-09-1	C15H8F6N2O2	362.227	3.99	8	32	1000	461	2000
 $C_{14}H_9F_3N_2O_2$		WY-B-09-2	C14H9F3N2O2	294.229	1000	2000	2000	3000	1000	3000
 $C_{21}H_{24}N_2O_2Si$	03-0972 merck	WY-B-14(WYS7)	C21H24N2O2Si	364.513	6.84	30	36	2000	108	1000
 $C_{21}H_{24}N_2O_2Si$	03-0972	WY-B-14(WYS7)	C21H24N2O2Si	364.513	8.5	165	245		1786	5000

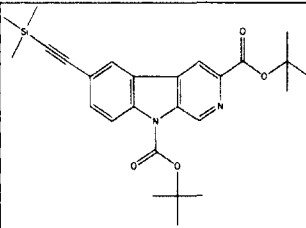
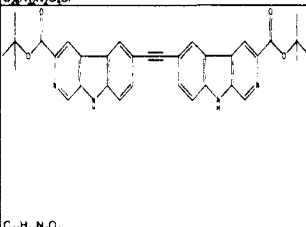
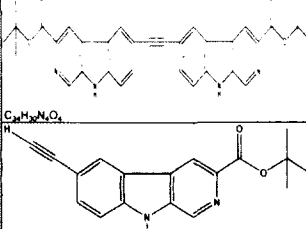
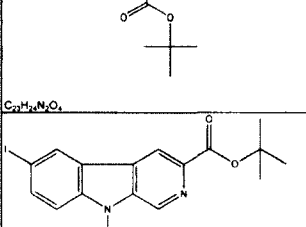
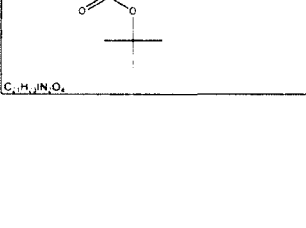
 $C_{14}H_{11}N_3O_4$		WY-B-15	C14H11N3O4	285.255	0.92	0.83	0.58	2080	4.42	646
 $C_{15}H_{11}Cl_2N_2O_2$		WY-B-17	C15H11Cl2N2O2	357.619	2000	2000	2000	3000	2000	5000
 $C_{14}H_8F_3IN_2O_2$		WY-B-20	C14H8F3IN2O2	420.125	12	39	47	2000	122	3000
 $C_{14}H_9Cl_2N_2O_2$		WY-B-23-1	C14H9Cl2N2O2	343.592	10	33	43	1000	189	2000

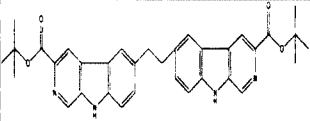
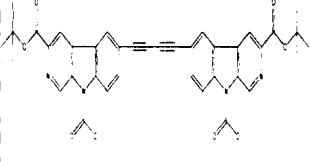
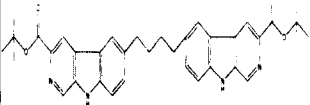
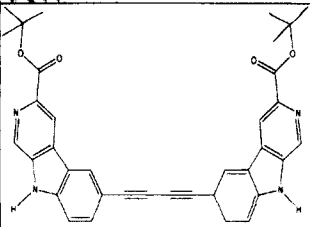
 $C_{15}H_{11}F_3N_2O_3$	03-0976 merck	WY-B-23-2(WYS11)	C15H11F3N2O3	324.255	4.2	37.7	39	2000	176	69.4
 $C_{15}H_{11}F_3N_2O_3$	03-0976	WY-B-23-2(WYS11)	C15H11F3N2O3	324.255	4.2	37.7	73		176	69.4
 $C_{18}H_9F_3N_2O_2$		WY-B-24	C18H9F3N2O2	342.271	22.02	177	44.78	3000	422	3000
 $C_{19}H_{17}F_3N_2O_2Si$		WY-B-25	C19H17F3N2O2Si	390.431	7.6	40	66	2000	263	2000

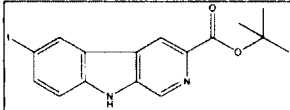
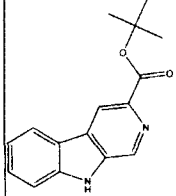
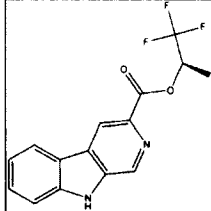
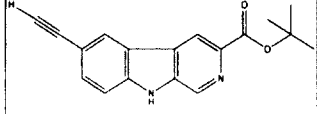
 $C_{16}H_9F_3N_2O_2$		WY-B-26-2	C16H9F3N2O2	318.25	4.45	44.57	42.66	2000	124	2000
 $C_{18}H_{11}F_3N_2O_3$		WY-B-27-1	C18H11F3N2O3	360.287	26	143	117	3000	127	2000
 $C_{18}H_{11}F_3N_2O_2S$		WY-B-27-2	C18H11F3N2O2S	376.352	9.19	111	72	2000	449	2000
 $C_{20}H_{13}F_3N_2O_2$		WY-B-29-2	C20H13F3N2O2	370.325	25	137	125	2000	299	2000

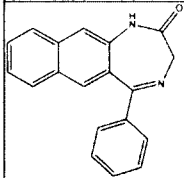
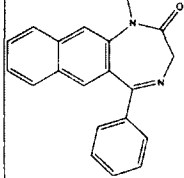
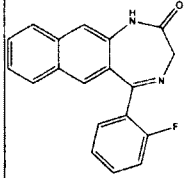
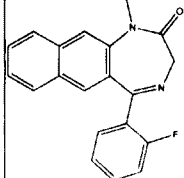
 $C_{19}H_{20}N_2O_2Si$		WY-B-99-1	C19H20N2O2Si	336.46	4.4	4.5	5.58	2000	47	2000
 $C_{44}H_{48}N_4O_6$	03-0966	WYS1 C45H50N4O6	C44H46N4O8	758.858	missing					
 $C_{14}H_9F_3N_2O_2$	03-0975	WYS10 C14H9F3N2O2	C14H9F3N2O2	294.229	0.88	36	25.6		548.7	15.3
 $C_{20}H_{18}N_2O_2S$	03-0977	WYS12 C20H18N2O2S	C20H18N2O2S	350.434	37	166	314		2861	5000
 $C_{20}H_{18}N_2O_3$	03-0978	WYS13 C20H18N2O3	C20H18N2O3	334.369	2.442	13	27.5		163	5000

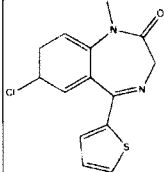
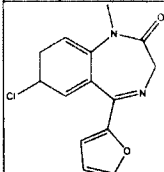
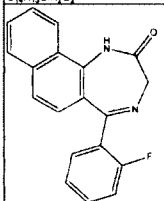
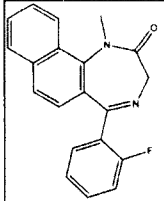
 <chem>CC(C)(C)OC(=O)c1ccc2c(c1)c(c[nH]2)C#Cc3ccc4c(c3)c(c[nH]4)C(=O)OC(C)(C)C</chem> $C_{33}H_{25}F_3N_4O_4$	03-0979	WYS14 C34H29F3N4O4	C33H25F3N4O4	598.571	798	5000			5000	5000
 <chem>CC(C)(C)OC(=O)c1ccc2c(c1)c(c[nH]2)c3ccccc3</chem> $C_{22}H_{19}N_2O_2$	03-0980	WYS15 C22H20N2O2	C22H20N2O2	344.406	3.63	2.02	44.3		76.5	5000
 <chem>N[C@@H](Cc1ccc2c(c1)c(c[nH]2)c3ccccc3)C(=O)O</chem> $C_{15}H_{14}N_2O_2$	03-0981	WYS16 C18H22N2O2	C15H14N2O2	254.284	5000	5000			5000	5000
 <chem>COC(=O)c1ccc2c(c1)c(c[nH]2)c3ccccc3</chem> $C_{17}H_{12}N_2O_2$	03-0982	WYS17 C17H18N2O2	C17H12N2O2	276.289	missing					
 <chem>CC(C)(C)OC(=O)c1ccc2c(c1)c(c[nH]2)c3ccccc3</chem> $C_{20}H_{14}N_2O_2$	03-0983	WYS18 C21H22N2O2	C20H18N2O2	318.369	missing					

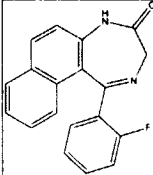
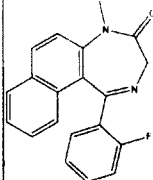
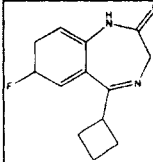
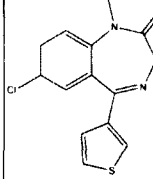
 $C_{26}H_{32}N_2O_4Si$	03-0984	WYS19 C26H32N2O4Si	C26H32N2O4Si	464.629			0.89			
 $C_{34}H_{32}N_4O_4$	03-0967	WYS2 C35H34N4O4	C34H30N4O4	558.626	5000	5000	5000		5000	5000
 $C_{34}H_{32}N_4O_4$	03-0967 (merck)	WYS2 C35H34N4O4	C34H30N4O4	558.626	30	124	100	300	300	4000
 $C_{27}H_{32}N_2O_4$	03-0985	WYS20 C23H24N2O4	C23H24N2O4	392.448	450	5000			5000	5000
 $C_{21}H_{23}N_2O_4$	03-0986	WYS21 C21H23N2O4	C21H23N2O4	494.323	missing					

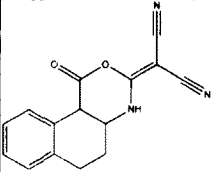
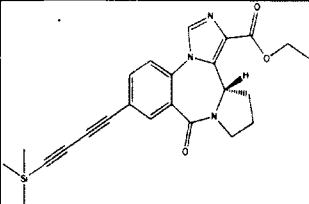
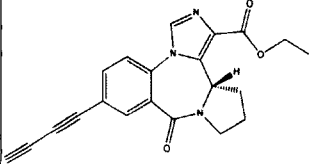
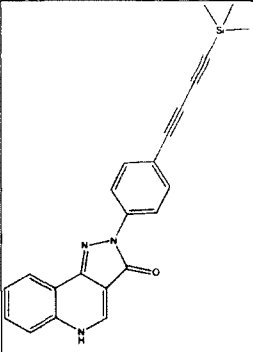
										
<chem>C_{34}H_{34}N_4O_4</chem>	03-0968	WYS3 C35H38N4O4	C34H34N4O4	562.658	241	5000	1841		5000	5000
										
<chem>C_{48}H_{56}N_4O_8</chem>	03-0969	WYS4 C48H56N4O8	C46H46N4O8	782.879	missing					
										
<chem>C_{37}H_{42}N_4O_4</chem>	03-0970	WYS5 C37H42N4O4	C37H42N4O4	606.754	5000	5000			5000	5000
										
<chem>C_{36}H_{32}N_4O_4</chem>	03-0971	WYS6 C37H35N4O4	C36H32N4O4	584.664	120	1059	3942		5000	5000

										
C ₁₆ H ₁₃ N ₂ O ₂	03-0974	WYSC9 C16H15IN2O2	C16H15IN2O2	394.207	2.72	22.2	23.1		562	122
										
C ₁₈ H ₁₃ N ₂ O ₂	03-0987	WYSC1 C16H16N2O2	C16H16N2O2	268.31	1.094	5.44	12.3		69.8	21.2
										
C ₁₉ H ₁₁ F ₃ N ₂ O ₂	03-0988	WYSC2 C15H11F3N2O2	C15H11F3N2O2	308.255	14.14	113	170		518	61.2
										
C ₁₈ H ₁₃ N ₂ O ₂		WY-TSC-4(WYS8)	C18H16N2O2	292.332	109.431	2374.5	1656.4		2663.5	

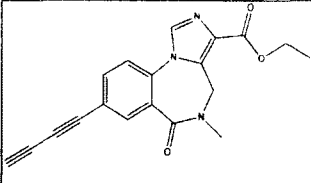
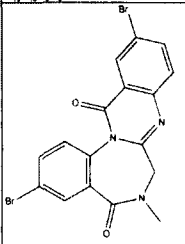
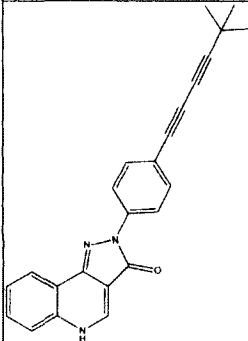
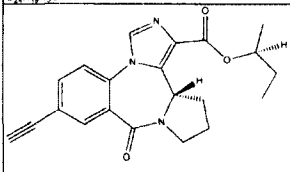
		WY-TSC-4(WYS8)			0.007	0.99	1.63		51.04	
 $C_{19}H_{14}N_2O$		WZ-030	C19H14N2O	286.327	279	210	200		45.15	1000
 $C_{20}H_{16}N_2O$		WZ-032	C20H16N2O	300.354	965	345	590		150	3000
 $C_{19}H_{13}FN_2O$		WZ-069	C19H13FN2O	304.318	40	30.5	38.5		12.6	1000
 $C_{20}H_{15}FN_2O$		WZ-070	C20H15FN2O	318.344	72.7	30.7	53.2		18.6	300

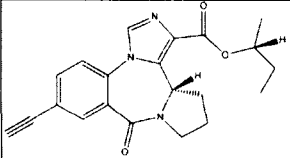
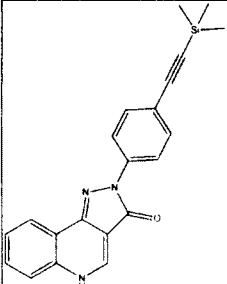
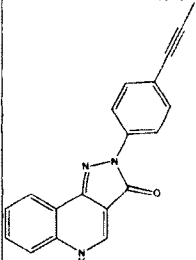
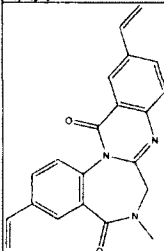
 $C_{14}H_{13}ClN_2OS$		WZ-113	C14H13ClN2OS	292.784	19.2	13.2	13.4		11.5	300
 $C_{14}H_{13}ClN_2O_2$		WZ-148	C14H13ClN2O2	276.718	300	300	300		300	300
 $C_{19}H_{13}FN_2O$		WZ-153	C19H13FN2O	304.318	199	151.3	191.6		73.5	1000
 $C_{20}H_{15}FN_2O$		WZ-154	C20H15FN2O	318.344	300	300	300		300	300

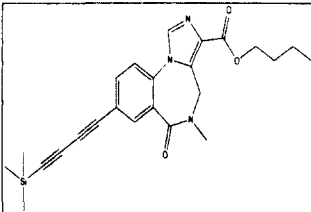
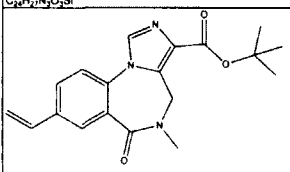
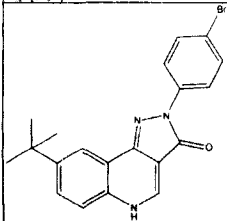
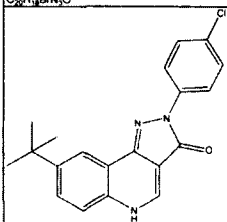
										
C ₁₉ H ₁₃ FN ₂ O	WZ-175	C ₁₉ H ₁₃ FN ₂ O	304.318	1000	1000	1000		1000	1000	
										
C ₂₀ H ₁₅ FN ₂ O	WZ-176	C ₂₀ H ₁₅ FN ₂ O	318.344	300	300	300		300	300	
										
C ₁₇ H ₁₅ FN ₂ O	WZ-185	C ₁₃ H ₁₅ FN ₂ O	234.269	300	300	300		300	300	
										
C ₁₄ H ₁₃ ClN ₂ OS	WZ-198	C ₁₄ H ₁₃ ClN ₂ OS	292.784	300	300	300		300	300	

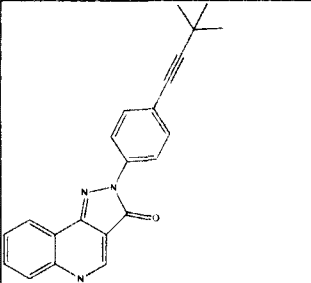
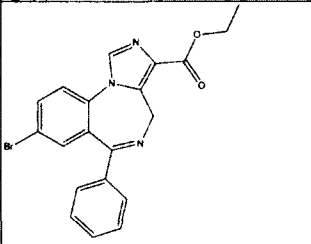
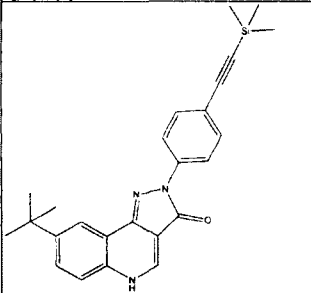
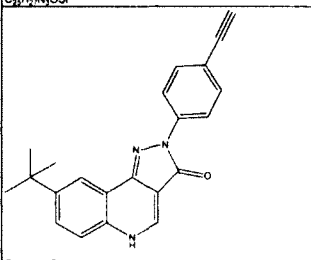
 $C_{15}H_{11}N_3O_2$		WZ-201	C15H11N3O2	265.267							
 $C_{24}H_{25}N_3O_3Si$		XHE-I-027	C24H25N3O3Si	431.559	1000	1000	1000		180		
 $C_{21}H_{17}N_3O_3$		XHE-I-030	C21H17N3O3	359.378	1000	1000	1000	1000	53	1000	
 $C_{23}H_{19}N_3OSi$		XHE-I-038	C23H19N3OSi	381.502	7.3	5	34		132	1000	

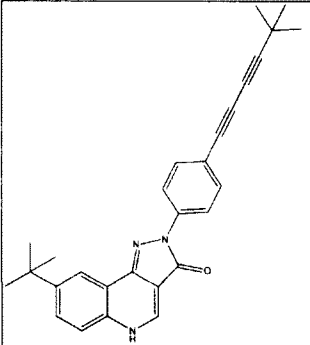
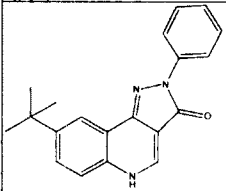
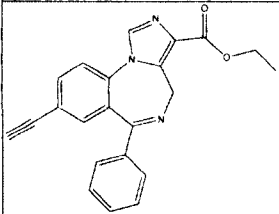
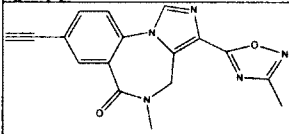
 $C_{20}H_{11}N_3O$		XHE-I-043	C20H11N3O	309.321	31	95	272		81	1000
 $C_{12}H_{10}BrN_2O_2$		XHE-I-046	C15H14BrN3O3	364.194	1000	1000	1000		1000	1000
 $C_{21}H_{19}N_3O_2$		XHE-I-048	C21H19N3O3	361.394	220	440	481		50	160
 $C_{22}H_{23}N_3O_2Si$		XHE-I-050	C22H23N3O3Si	405.522	254	300	300		195	3000

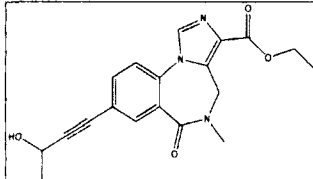
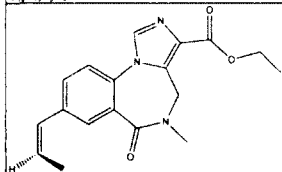
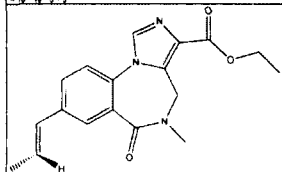
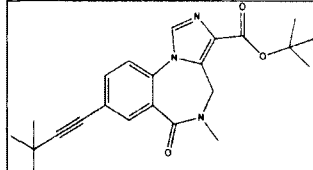
 $C_{19}H_{15}N_3O_3$		XHE-I-051	$C_{19}H_{15}N_3O_3$	333.341	35	39	42		5.3	979
 $C_{17}H_{11}Br_2N_3O_2$		XHE-I-055b	$C_{17}H_{11}Br_2N_3O_2$	449.096	615	1000	1000	2213	268	1524
 $C_{24}H_{19}N_3O$		XHE-I-065	$C_{24}H_{19}N_3O$	365.427	7.2	17	18	500	57	500
 $C_{21}H_{21}N_3O_3$		XHE-I-066A(SS)	$C_{21}H_{21}N_3O_3$	363.41	196.66	176.14	95.4	74.26	125.06	186.25

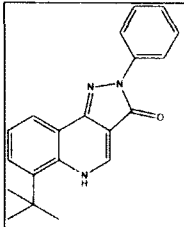
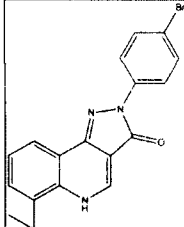
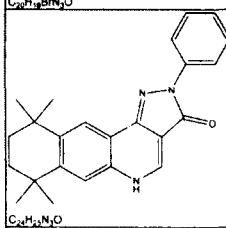
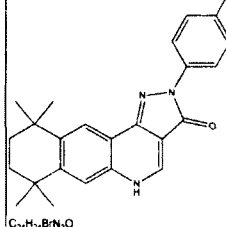
										
C ₂₁ H ₂₁ N ₃ O ₃	XHE-I-066B(SR)	C ₂₁ H ₂₁ N ₃ O ₃	363.41	76.04	73.56	45.05	22.72	53.42	51.32	
										
C ₂₁ H ₁₉ N ₃ O ₃ Si	XHE-I-073	C ₂₁ H ₁₉ N ₃ O ₃ Si	357.481	62	155	217	1000	393	1000	
										
C ₁₉ H ₁₃ N ₃ O	XHE-I-093	C ₁₉ H ₁₃ N ₃ O	299.326	2	7.1	8.9	1107	20	1162	
										
C ₂₁ H ₁₇ N ₃ O ₂	XHE-I-096	C ₂₁ H ₁₇ N ₃ O ₂	343.379	3079	1000	4636	1601	567	2712	

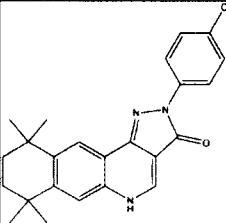
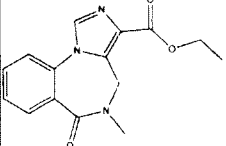
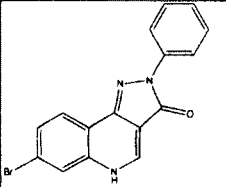
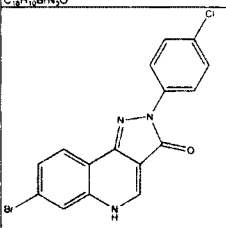
 $C_{24}H_{27}N_3O_3Si$		XHE-I-47	C ₂₄ H ₂₇ N ₃ O ₃ Si	433.575	705	2502	2460		480	10000
 $C_{19}H_{21}N_3O_3$		XHE-II-002	C ₁₉ H ₂₁ N ₃ O ₃	339.388	8.3	18	13	3.9	1.5	11
 $C_{20}H_{18}BrN_3O$		XHE-II-006a	C ₂₀ H ₁₈ BrN ₃ O	396.28	4.7	4.4	20	1876	89	3531
 $C_{20}H_{18}ClN_3O$		XHE-II-006b	C ₂₀ H ₁₈ ClN ₃ O	351.829	3.7	15	12	1897	144	1000

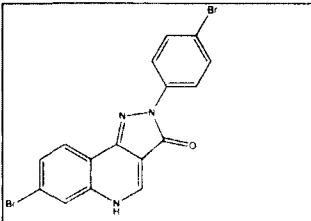
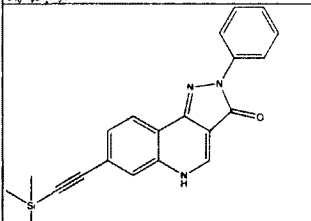
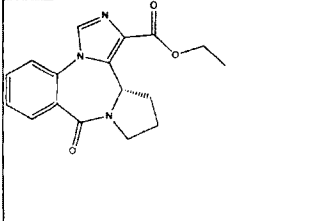
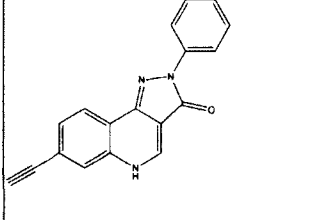
 <chem>CC(C)(C)C#Cc1ccc(cc1)n2c(=O)[nH]c3ccccc3n2</chem> $C_{22}H_{19}N_3O$		XHE-II-011	C22H19N3O	341.406	9	60	39	3233	90	1000
 <chem>CCOC(=O)c1nc2cc(Br)ccc2n1Cc3ccccc3</chem> $C_{20}H_{13}BrN_3O_2$		XHE-II-012	C20H16BrN3O2	410.264	49	24	31	1042	14	2038
 <chem>CC(C)(C)C#Cc1ccc(cc1)n2c(=O)[nH]c3ccccc3n2</chem> $C_{25}H_{27}N_3OSi$		XHE-II-014	C25H27N3OSi	413.587	329	1098	1156	1000	2462	1000
 <chem>CC(C)(C)C#Cc1ccc(cc1)n2c(=O)[nH]c3ccccc3n2</chem> $C_{22}H_{19}N_3O$		XHE-II-017	C22H19N3O	341.406	3.3	10	7	258	17	294

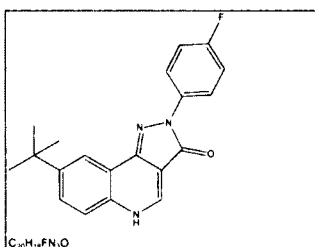
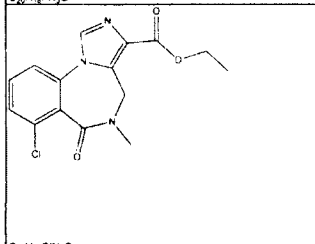
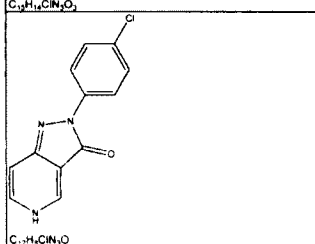
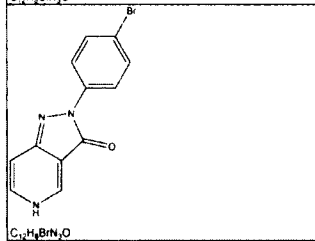
 $C_{28}H_{27}N_3O$		XHE-II-019	C28H27N3O	421.533	273	428	762	1000	1464	1000
 $C_{20}H_{19}N_3O$		XHE-II-024	C20H19N3O	317.384	0.09	0.18	0.32	14	0.24	11
 $C_{22}H_{17}N_3O_2$	03-1031	XHE-II-053	C22H17N3O2	355.389	287	45	96	1504	13.8	1000
 $C_{17}H_{13}N_5O_2$		XHE-II-065	C17H13N5O2	319.317	1000	409	216	37	6.4	175

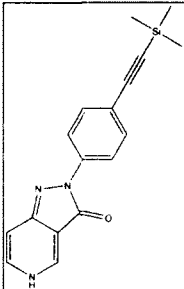
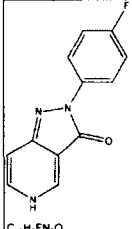
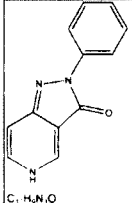
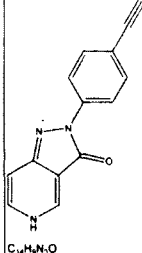
										
C ₂₃ H ₁₇ N ₃ O ₄	XHE-II-070	C ₁₉ H ₁₉ N ₃ O ₄	353.372	352	532	454	45%	55	1000	
										
C ₂₃ H ₁₉ N ₃ O ₃	XHE-II-073A (R ENRICHED)	C ₁₈ H ₁₉ N ₃ O ₃	325.362	5.9	11	10	15	1.18	140	
										
C ₂₃ H ₁₉ N ₃ O ₃	XHE-II-073B (S-ENRICHED)	C ₁₈ H ₁₉ N ₃ O ₃	325.362	11	17	12	33	2.1	269	
										
C ₂₃ H ₂₇ N ₃ O ₃	XHE-II-077	C ₂₃ H ₂₇ N ₃ O ₃	393.479	1363	1000	3403	3561	1000	1000	

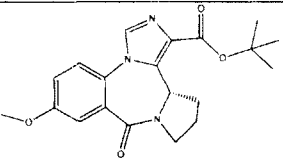
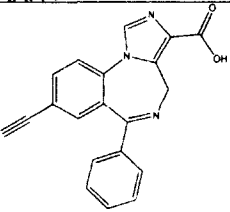
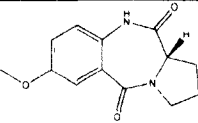
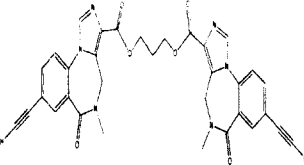
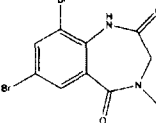
 $C_{20}H_{19}N_3O$		XHE-II-087a	C20H19N3O	317.384	1604	1000	1000	1000	1000	1000
 $C_{20}H_{18}BrN_3O$		XHE-II-087c	C20H18BrN3O	396.28	1000	1000	1000	1000	1000	1000
 $C_{24}H_{25}N_3O$		XHE-II-098a	C24H25N3O	371.475	1000	1000	1000	1000	1000	1000
 $C_{24}H_{24}BrN_3O$		XHE-II-098b	C24H24BrN3O	450.371	1000	1000	1000	1000	1000	1000

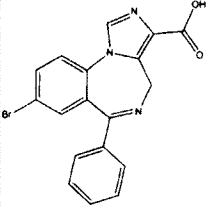
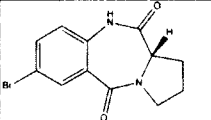
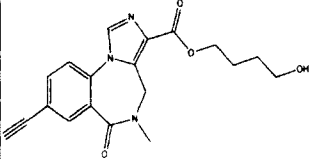
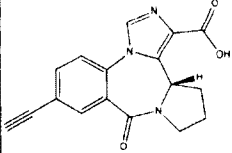
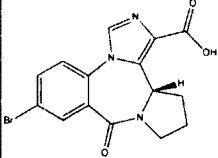
 <chem>C₂₄H₂₄ClN₃O</chem>		XHE-II-098c	C ₂₄ H ₂₄ ClN ₃ O	405.92	1000	1000	1000	1000	1000	1000
 <chem>C₁₅H₁₅N₃O₃</chem>		XHE-III-04	C ₁₅ H ₁₅ N ₃ O ₃	285.298	1.2	2	1.1	219	0.4	500
 <chem>C₁₆H₁₀BrN₃O</chem>		XHE-III-06a	C ₁₆ H ₁₀ BrN ₃ O	340.174	1	2	1	5	1.8	37
 <chem>C₁₆H₉BrClN₃O</chem>		XHE-III-06b	C ₁₆ H ₉ BrClN ₃ O	374.619	32	33	20	299	28.6	740

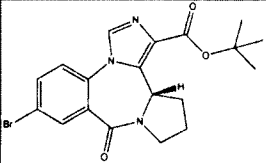
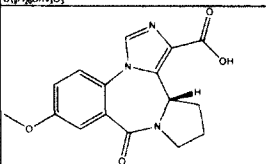
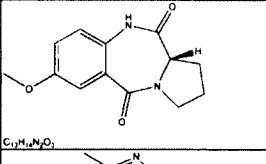
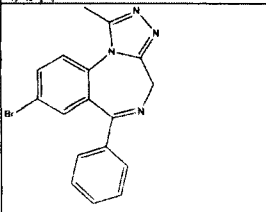
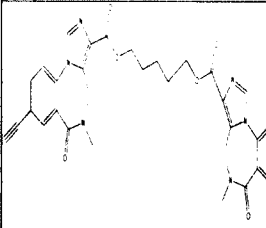
 $C_{16}H_9Br_2N_3O$		XHE-III-06c	C16H9Br2N3O	419.07	34	44	29	210	23	319
 $C_{21}H_{19}N_3OSi$		XHE-III-12	C21H19N3OSi	357.481	240		1000	1000	181	536
 $C_{27}H_{17}N_3O_3$		XHE-III-13	C17H17N3O3	311.335	7.3		7.1	880	1.6	311
 $C_{18}H_{11}N_3O$		XHE-III-14	C18H11N3O	285.299	2.6		10	13	2	7

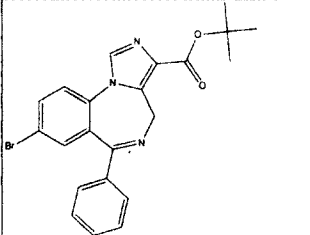
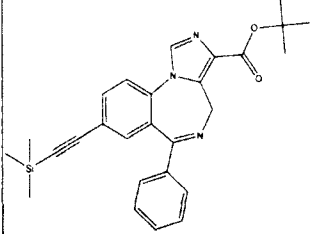
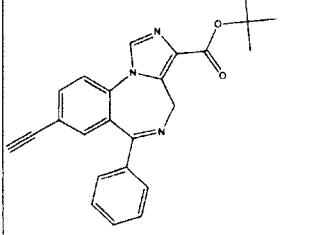
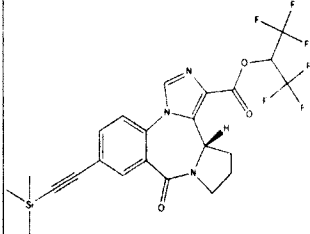
 $C_{20}H_{18}FN_3O$		XHE-III-24	C ₂₀ H ₁₈ FN ₃ O	335.375	0.25		8	222	10	328
 $C_{15}H_{14}ClN_2O_3$		XHE-III-49	C ₁₅ H ₁₄ ClN ₂ O ₃	319.743	1.3	5.5	4.2	38.7	11.3	85.1
 $C_{17}H_{12}ClN_3O$		XHE-III-54	C ₁₇ H ₁₂ ClN ₃ O	245.664	1071	1624	2048	1000	1158	1000
 $C_{17}H_{12}BrN_3O$		XHE-III-56b	C ₁₇ H ₁₂ BrN ₃ O	290.115	1005	1642	1928	1000	1300	1000

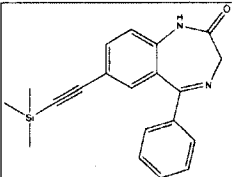
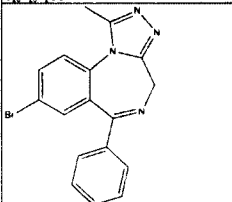
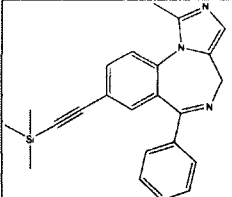
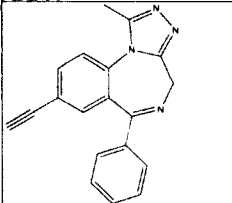
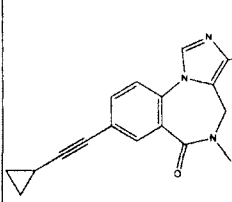
 $C_{17}H_{17}N_3OSi$		XHE-III-67	C17H17N3OSi	307.422	1000	1000	1000	1000	1000	1000
 $C_{12}H_8FN_3O$		XHE-III-69	C12H8FN3O	229.21	3433	1000	1000	1000	1000	1000
 $C_{12}H_9N_3O$		XHE-III-70	C12H9N3O	211.219	997.5	2356	2484	711	500	1000
 $C_{14}H_9N_3O$		XHE-III-73	C14H9N3O	235.241	1000	303	942	1000	492	1000

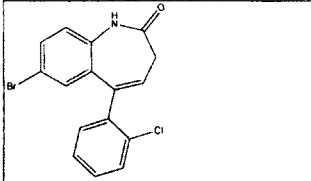
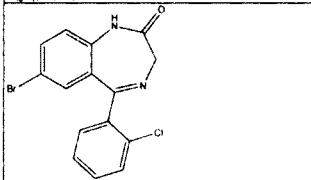
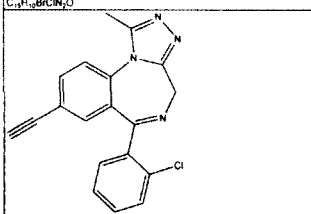
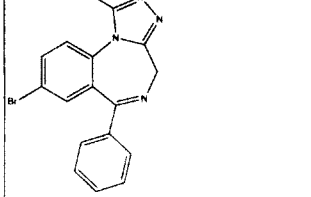
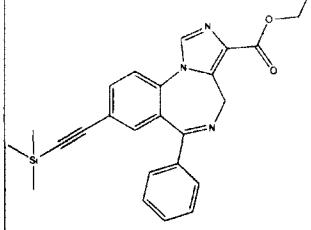
										
$C_{20}H_{23}N_3O_4$		XHE-III-74	C20H23N3O4	369.414	77	105	38	0.42	2.2	5.8
										
$C_{24}H_{17}N_3O_2$	05-1773	XHE-II-O53-ACID	C20H13N3O2	327.336	50.35	11.8	44		5.9	5000
										
$C_{13}H_{14}N_2O_3$		XLI-?	C13H14N2O3	246.262						
										
$C_{33}H_{26}N_6O_6$		XLI-093	C33H26N6O6	602.596	1000	1000	858	1550	15	2000
										
$C_{10}H_8Br_2N_2O_2$		XLI-1?	C10H8Br2N2O2	347.991						

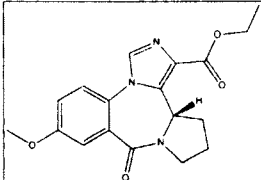
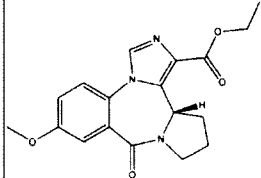
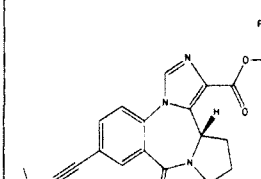
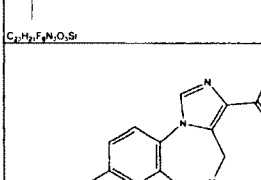
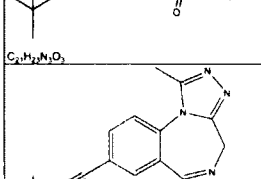
 $C_{18}H_{17}BrN_3O_2$	05-1724	XLI-12TC	$C_{18}H_{12}BrN_3O_2$	382.211						
 $C_{17}H_{11}BrN_3O_2$	05-1725	XLI-13TC	$C_{12}H_{11}BrN_2O_2$	295.132	2078	5289	618.7	8382		
 $C_{19}H_{19}N_3O_4$	05-1728	XLI-14TC	$C_{19}H_{19}N_3O_4$	353.372						
 $C_{17}H_{13}N_3O_3$	05-1729	XLI-15TC	$C_{17}H_{13}N_3O_3$	307.303						
 $C_{15}H_{12}BrN_3O_3$	05-1730	XLI-16TC	$C_{15}H_{12}BrN_3O_3$	362.178	7664	3515	787.4	1831		

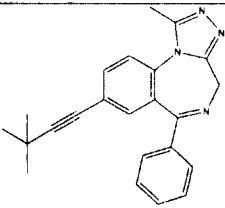
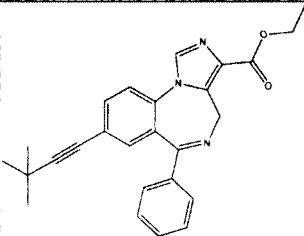
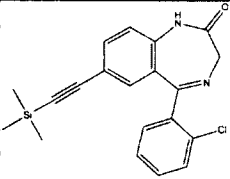
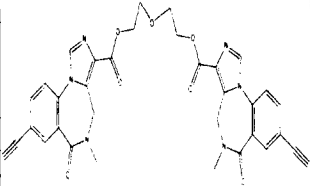
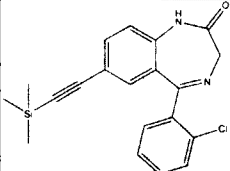
 $C_{19}H_{20}BrN_3O_3$	05-1731	XLI-17TC	$C_{19}H_{20}BrN_3O_3$	418.284	224.8	106.6	120.6		92.43	
 $C_{16}H_{15}N_3O_4$	05-1732	XLI-18TC	$C_{16}H_{15}N_3O_4$	313.308						
 $C_{13}H_{14}N_2O_3$	05-1733	XLI-19TC	$C_{13}H_{14}N_2O_3$	246.262						
 $C_{17}H_{13}BrN_4$		XLI-2?	$C_{17}H_{13}BrN_4$	353.216						
 $C_{35}H_{30}N_6O_6$	05-1727	XLI-210	$C_{35}H_{30}N_6O_6$	630.649	231	661	2666		5.4	54.22

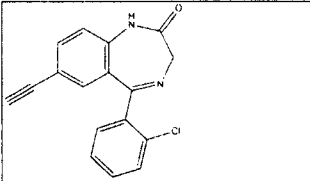
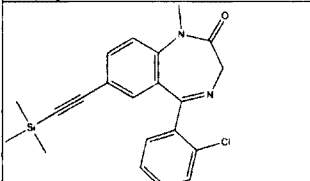
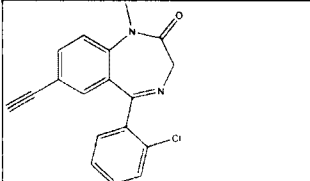
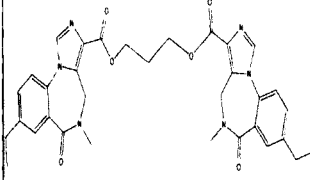
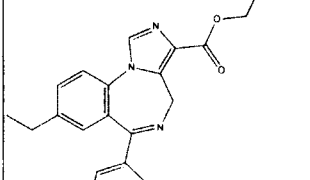
 $C_{22}H_{19}BrN_3O_2$	03-1026	XLI223	C22H20BrN3O2	C22H20BrN3O2	438.317	14	8.7	18	1000	10	2000
 $C_{27}H_{29}N_3O_2Si$	03-1027	XLI224	C27H29N3O2Si	C27H29N3O2Si	455.624	333	333	333	3000	333	2000
 $C_{24}H_{19}N_3O_2$	03-1028	XLI225	C24H21N3O2	C24H21N3O2	383.442	333	225	174	3000	110	2000
 $C_{23}H_{17}F_6N_3O_3Si$		XLI-232		C23H21F6N3O3Si	529.507						

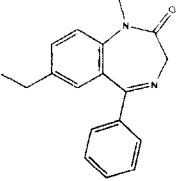
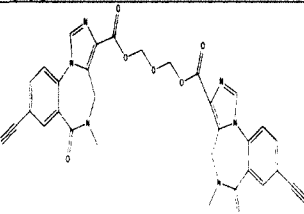
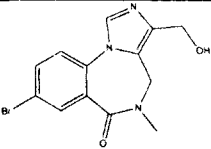
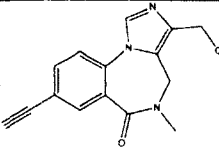
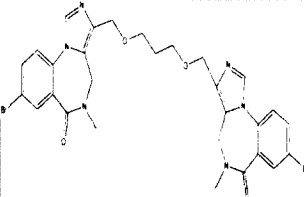
											
C ₂₀ H ₂₀ N ₂ OSi		XLI-250 (SHU-221)		C ₂₀ H ₂₀ N ₂ OSi	332.471	1000	1000	339	1000	118	1000
											
C ₁₇ H ₁₃ BrN ₄	03-1023	XLI268	C ₁₇ H ₁₃ BrN ₄	C ₁₇ H ₁₃ BrN ₄	353.216	2.8145	0.6862			0.6243	
											
C ₂₂ H ₂₂ N ₄ Si	03-1024	XLI269	C ₂₂ H ₂₂ N ₄ Si	C ₂₃ H ₂₃ N ₃ Si	369.534	221.8	154.2			15.51	
											
C ₁₉ H ₁₄ N ₄	03-1025	XLI270	C ₁₉ H ₁₄ N ₄	C ₁₉ H ₁₄ N ₄	298.341	36.39	25.81			5.291	
											
C ₂₀ H ₁₉ N ₃ O ₃	03-1038	XLI275	C ₂₀ H ₁₉ N ₃ O ₃	C ₂₀ H ₁₉ N ₃ O ₃	349.383	35.61					

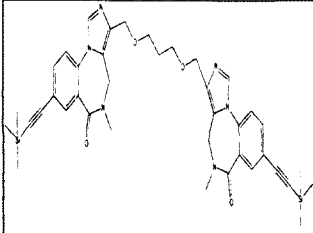
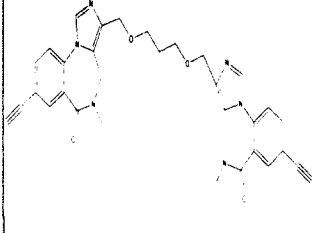
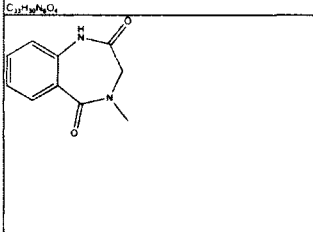
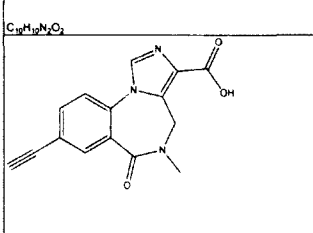
 $C_{16}H_{11}BrClNO$		XLI286	$C_{16}H_{11}BrClNO$	348.622						
 $C_{15}H_{10}BrClN_2O$	05-1715	XLI-286	$C_{15}H_{10}BrClN_2O$	349.61	0.051	0.064	0.118	0.684		
 $C_{19}H_{13}ClN_4$		xli296	$C_{19}H_{13}ClN_4$	332.786						
 $C_{17}H_{13}BrN_4$	05-1711	XLI-2TC	$C_{17}H_{13}BrN_4$	353.216	3.442	1.673	44.08	1.121		
 $C_{25}H_{25}N_3O_2Si$		XLI-3?	$C_{25}H_{25}N_3O_2Si$	427.57						

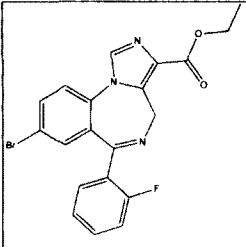
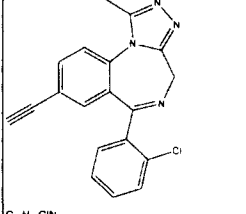
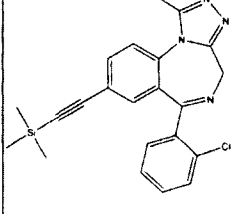
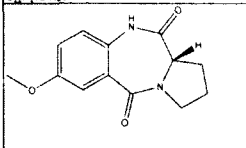
 $C_{18}H_{19}N_3O_4$	05-1712	XLI-317	C18H19N3O4	341.361	60.24	24.05	4.562	0.295	
 $C_{18}H_{19}N_3O_4$		XLI-317	C18H19N3O4	341.361					
 $C_{23}H_{27}F_6N_3O_3Si$	05-1710	XLI-332	C23H21F6N3O3Si	529.507	1390	1507	3405	132.1	
 $C_{21}H_{23}N_3O_3$	03-1035	XLI337 C21H23N3O3	C21H23N3O3	365.426					
 $C_{23}H_{21}ClN_4$	03-1045	XLI338 C23H21ClN4	C23H21ClN4	388.893	380	189	692	5000	5000

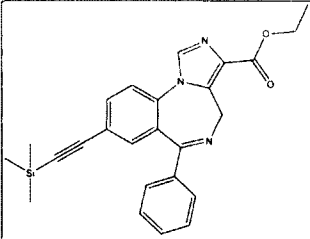
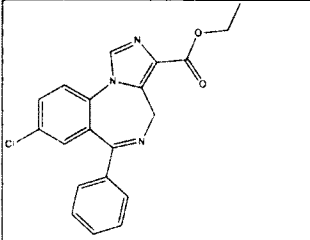
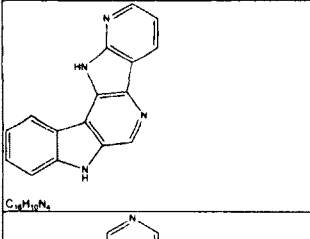
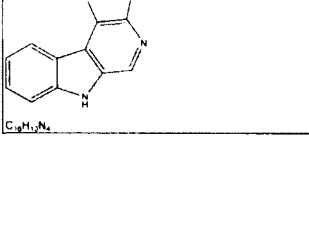
 $C_{22}H_{22}N_4$	03-1037	XLI339 C23H22N4	C23H22N4	354.448	5000	625	5000	5000	5000
 $C_{26}H_{24}N_4O_2$	03-1036	XLI340 C26H25N3O2	C26H25N3O2	411.496					
 $C_{28}H_{23}ClN_2OSi$	03-1042	XLI343 C20H19ClN2OSi	C20H19ClN2OSi	366.916	6.375	17.71		150.5	
 $C_{34}H_{28}N_6O_7$	03-1040	XII-347 C34H28N6O7	C34H28N6O7	632.622	828.05	690.2		13.87	
 $C_{28}H_{23}ClN_2OSi$	05-1723	XLI-348	C20H19ClN2OSi	366.916	13.56	11.17	1.578	82.05	

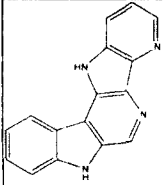
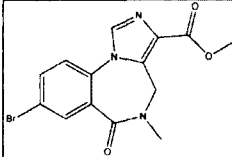
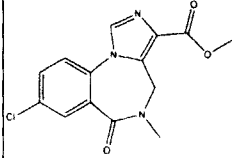
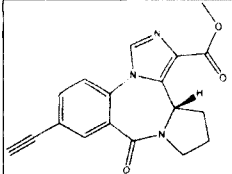
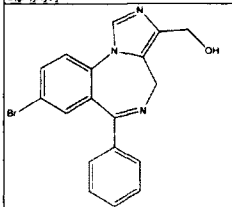
 $C_{17}H_{11}ClN_2O$	03-1043	XLI350 C17H11ClN2O	C17H11ClN2O	294.735	1.224	1.188			2.9	
 $C_{22}H_{21}ClN_2OSi$	03-1041	XLI351 C21H21ClN2OSi	C21H21ClN2OSi	380.943	1.507	0.967			1.985	
 $C_{18}H_{13}ClN_2O$	03-1044	XLI352 C18H13ClN2O	C18H13ClN2O	308.762	1.56	0.991			1.957	
 $C_{33}H_{34}N_6O_4$	03-1039	XLI356 C33H34N6O6	C33H34N6O6	610.66	1851.5	4702.5	8545		100.5	5000
 $C_{22}H_{21}N_3O_2$	03-1046	XLI366 C22H21N3O2	C22H21N3O2	359.421	1					

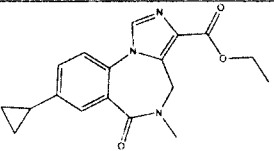
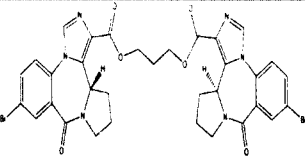
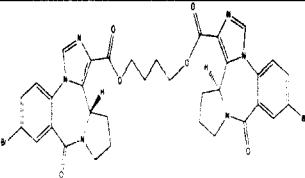
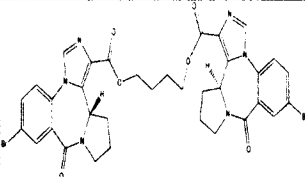
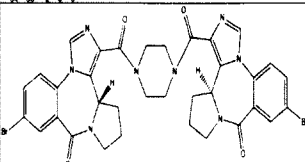
										
$C_{18}H_{18}N_2O$	03-1047	XLI368 C24H25N3O2	C18H18N2O	278.348						
										
$C_{32}H_{24}N_4O_7$	05-1721	XLI-374	C32H24N6O7	604.569	3795	2694	1864		76.14	
										
$C_{17}H_{12}BrN_3O_2$	05-1717	XLI-379	C13H12BrN3O2	322.157	1037	482.4	357.5		36.13	
										
$C_{15}H_{12}ClN_3O$	05-1720	XLI-381	C15H12ClN3O	285.728	619.9	285.6	3639		7.051	
										
$C_{29}H_{18}Br_2N_6O_4$	05-1718	XLI-382	C29H28Br2N6O4	684.378						

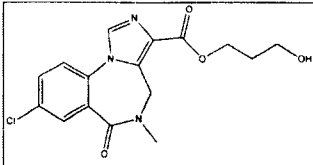
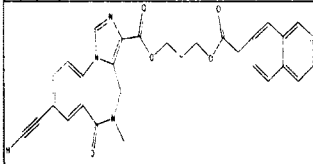
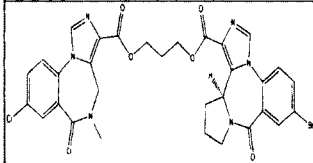
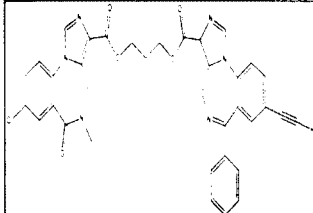
 $C_{39}H_{46}N_4O_4Si_2$	05-1722	XLI-385	C39H46N6O4Si2	718.991						
 $C_{33}H_{30}N_6O_4$	05-1726	XLI-387	C33H30N6O4	574.629	5454	5000	5000		5000	5000
 $C_{10}H_{10}N_2O_2$		XLI-4?	C10H10N2O2	190.199						
 $C_{15}H_{11}N_3O_3$	05-1716	XLI-6TC	C15H11N3O3	281.266	2371	1421	1840		1169	

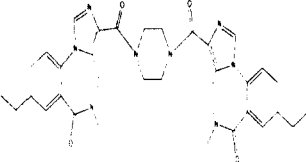
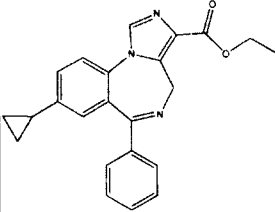
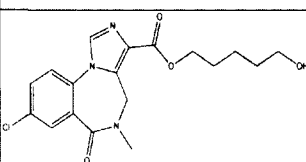
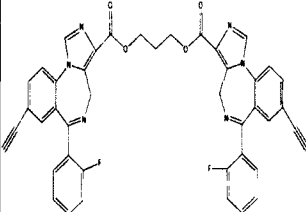
 <chem>CCOC(=O)c1nc2c(c1)cc(Br)cc2-c3ccccc3F</chem> $C_{20}H_{15}BrFN_2O_2$	05-1719	XLI-8TC	$C_{20}H_{15}BrFN_2O_2$	428.254	21.52	11.01	2.155		4.059	
 <chem>CC#Cc1cc2c(c1)nc3ccccc3n2-c4ccccc4Cl</chem> $C_{19}H_{13}ClN_4$	03-0951	XLI-JY-DMH ANX3	$C_{19}H_{13}ClN_4$	332.786	3.3	0.58	1.9		4.4	5000
 <chem>CC#C[Si](C)(C)Cc1cc2c(c1)nc3ccccc3n2-c4ccccc4Cl</chem> $C_{22}H_{21}ClN_4Si$	03-0950	XLI-JY-DMH-TMS C22H21N4SiCl)	$C_{22}H_{21}ClN_4Si$	404.967	35	63	99.13		69.7	5000
 <chem>COc1ccc2c(c1)nc3c2c(=O)[C@H]4CCCC4C3=O</chem> $C_{17}H_{14}N_2O_3$	05-1709	XLI-TC	$C_{13}H_{14}N_2O_3$	246.262	8155	7528	1036		508.9	

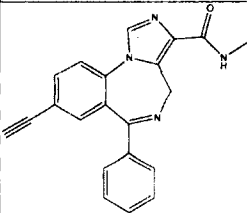
 $C_{25}H_{29}N_3O_2Si$	03-1032	XliXHe-II-048	C25H25N3O2Si	C25H25N3O2Si	427.57	5000	5000	5000	5000	
 $C_{20}H_{16}ClN_3O_2$			XZ112	C20H16ClN3O2	365.813					
 $C_{16}H_{10}N_4$			YCT-5	C16H10N4	258.277	2.2	11.46	16.3	200	10000
 $C_{16}H_{10}N_4$			YCT-7A	C16H10N4	258.277	3	23.8	30.5	240	10000

 $C_{19}H_{19}N_4$										
		YCT-7B	C16H10N4	258.277	28	118	156		1000	10000
 $C_{14}H_{11}BrN_3O_3$	08-001	YT-5	C14H12BrN3O3	350.167	0.421	0.6034	36.06		1.695	
 $C_{14}H_{11}ClN_3O_3$	08-004	YT-6	C14H12ClN3O3	305.716	15.31	87.8	60.49		1.039	
 $C_{19}H_{19}N_3O_3$	05-1770	YT-I-38	C18H15N3O3	321.33	945.9	326.8	245.9		4.07	
 $C_{18}H_{14}BrN_3O$	08-005	YT-II	C18H14BrN3O	368.227	6.932	0.8712	3.518		5.119	

 $C_{18}H_{19}N_3O_2$	08-009	YT-II-76	C18H19N3O3	325.362	95.34	2.797	0.056	0.04	
 $C_{33}H_{28}Br_2N_6O_6$	07-007	YT-II-791	C33H28Br2N6O6	764.42	1495	2681	527.4	144	
 $C_{34}H_{30}Br_2N_6O_6$	07-001	YT-II-792	C34H30Br2N6O6	778.447	789.6	599.5	1698	83.18	
 $C_{34}H_{30}Br_2N_6O_6$	07-002	YT-II-793	C34H30Br2N6O6	778.447	1383	2881	782.6	128.9	
 $C_{34}H_{30}Br_2N_6O_4$	07-011	YT-II-794	C34H30Br2N8O4	774.461	4536	126.2	4981	932.8	

 $C_{23}H_{29}ClN_2O_4$	08-002	YT-II-83	$C_{16}H_{16}ClN_3O_4$	349.769	32.74	13.22	24.1	3.548	
 $C_{30}H_{39}N_3O_5$		YT-III-1	$C_{30}H_{25}N_3O_5$	507.537					
 $C_{31}H_{39}BrClN_6O_9$	07-009	YT-III-10	$C_{31}H_{26}BrClN_6O_6$	693.932	1172	1915	1481	282.9	
 $C_{36}H_{47}ClN_4O_5$	07-008	YT-III-15	$C_{36}H_{27}ClN_6O_5$	659.09	73.19	90.45	141.4	114	

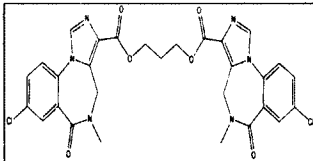
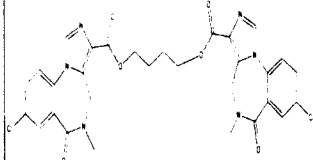
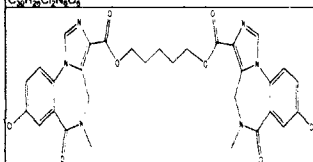
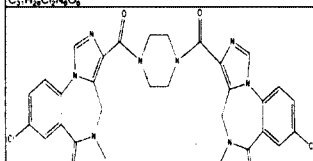
										
$C_{34}H_{36}N_4O_4$	07-010	YT-III-19	C34H36N8O4	620.701	5329	182.4	3817		3313	
										
$C_{27}H_{27}N_3O_2$	08-008	YT-III-23	C23H21N3O2	371.432	19.83	23.65	19.87		1.105	
	08-35	YT-III-231			51.09	61.46	26.34		9.124	
										
$C_{27}H_{26}ClN_3O_4$	08-003	YT-III-25	C18H20ClN3O4	377.822	2.531	5.786	5.691		0.095	
										
$C_{43}H_{28}F_2N_6O_4$	08-17	YT-III-271	C43H28F2N6O4	730.717	32.54	1.26	2.35		103	

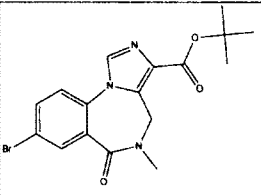
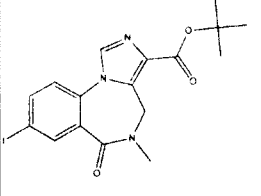
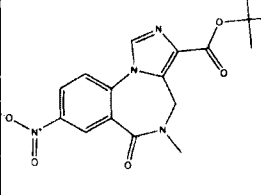
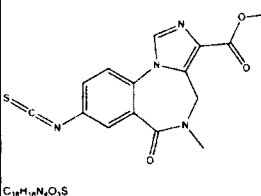
	08-28	YT-III-272			295.9	14.98	10.77		103.3	
	08-18	YT-III-273			245.1	366	389		879.4	
	08-14	YT-III-28			130.7	80.03	82.9		192	
 $C_{21}H_{16}N_4O$	08-006	YT-III-31	$C_{21}H_{16}N_4O$	340.378	36.39	67.85	129.7		7.59	
	08-15	YT-III-33			198.7	82.3	146		76.4	

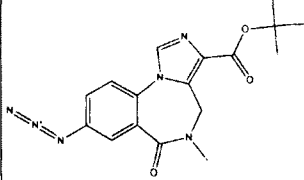
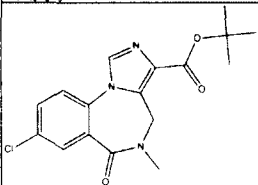
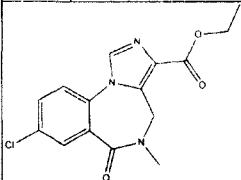
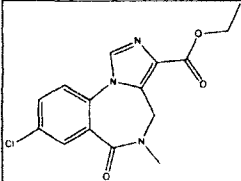
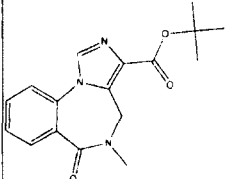
	08-19	YT-III-331			1199	665	759		1687	
	08-20	YT-III-332			526.4	168	148		1365	
	08-21	YT-III-333			459.7	298.3	447.6		718.2	
	08-22	YT-III-334			1930	1049	1102		3105	
	08-23	YT-III-341			370	196.5	203.7		673.3	

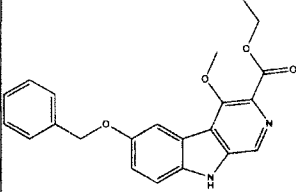
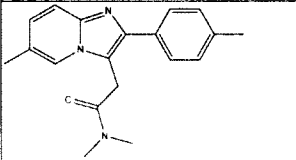
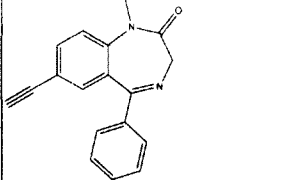
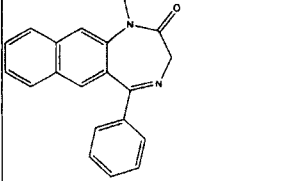
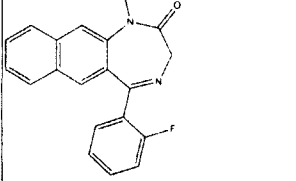
	08-24	YT-III-342			42.83	68.95	83.6		135.7	
	08-16	YT-III-36			74.96	195	90.9		262.5	
 $C_{23}H_{20}FN_3O_2$	08-33	YT-III-38	C23H20FN3O2	389.422	1461	18.21	14.63		3999	
	08-36	YT-III-39			161.5	336.3	412		224.4	

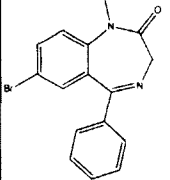
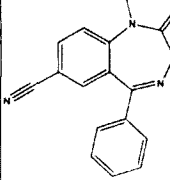
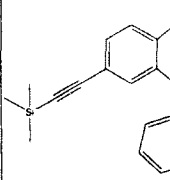
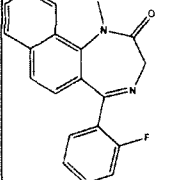
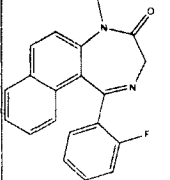
	08-37	YT-III-40			1454	2576	3543		112.6	
	08-29	YT-III-41			3052	745.7	510.8		416.8	
	08-31	YT-III-42			382.9	16.83	44.04		9.77	
	08-32	YT-III-44			37.83	9717	3739		24.04	

 $C_{29}H_{24}Cl_2N_6O_6$	07-003	YT-TC-1	C29H24Cl2N6O6	623.443	441.8	927.4	157.9	122.2	
 $C_{30}H_{26}Cl_2N_6O_6$	07-004	YT-TC-2	C30H26Cl2N6O6	637.47	839.1	1647	568.1	421.9	
 $C_{31}H_{28}Cl_2N_6O_6$	07-005	YT-TC-3	C31H28Cl2N6O6	651.497	141.4	11.43	118.1	29.22	
 $C_{30}H_{26}Cl_2N_6O_4$	07-006	YT-TC-4	C30H26Cl2N8O4	633.485	6291	3315	352.2	2881	

										
$C_{17}H_{18}BrN_3O_3$	ZG-168	C17H18BrN3O3	392.247	11.2	10.7	9.2		0.47	9.4	
										
$C_{17}H_{18}N_3O_3$	ZG-208	C17H18N3O3	439.248	9.7	11.2	10.9		0.38	4.6	
										
$C_{17}H_{16}N_4O_5$	ZG-213	C17H18N4O5	358.349	12.8	49.8	30.2		3.5	22.5	
										
$C_{18}H_{18}N_4O_3S$	ZG-224	C18H18N4O3S	370.426	17.1	33.7	50		2.5	30.7	

 $C_{17}H_{18}N_6O_3$		ZG-234	C17H18N6O3	354.363	7.25	22.14	9.84		0.3	5.25
 $C_{17}H_{16}ClN_6O_3$		ZG-63A	C17H16ClN6O3	347.796	17.3	21.6	29.1		0.65	4
 $C_{15}H_{14}ClN_6O_3$		ZG-69A	C15H14ClN6O3	319.743	6.8	16.3	9.2		0.85	54.6
 $C_{15}H_{14}ClN_6O_3$		ZG-69a(Ro15-1310)	C15H14ClN6O3	319.743	6.8	16.3	9.2		0.85	54.6
 $C_{17}H_{19}N_3O_3$	09-06	ZG-88 ZJW-II-040	C17H19N3O3	313.351						

 <chem>CCOC(=O)c1nc2cc(OC)c(OC)c2cc1OCc3ccccc3</chem> $C_{22}H_{20}N_2O_4$		ZK 93423	C22H20N2O4	376.405	4.1	4.2	6		4.5	1000
 <chem>CN(C)C(=O)Cc1c2ccccc2n1-c1ccc(C)cc1</chem> $C_{19}H_{19}N_2O$		ZOLPIDEM	C19H21N3O	307.39	26.7	156	383		10000	10000
	05-1751						462.2			
 <chem>O=C1Nc2cc(C#Cc3ccccc3)ccc2N1Cc4ccccc4</chem> $C_{18}H_{14}N_2O$			C18H14N2O	274.317	76.3	42.1	47.4		6.8	3000
 <chem>O=C1Nc2ccc3ccccc3c2N1Cc4ccccc4</chem> $C_{20}H_{16}N_2O$			C20H16N2O	300.354	965	345	590		150	1000
 <chem>O=C1Nc2ccc3ccccc3c2N1Cc4cc(F)cc4</chem> $C_{20}H_{15}FN_2O$			C20H15FN2O	318.344	73	31	53		19	1000

 <chem>C16H13BrN2O</chem>			<chem>C16H13BrN2O</chem>	329.191	9.4	9.3	31		7.7	3000
 <chem>C17H13N3O</chem>			<chem>C17H13N3O</chem>	275.305	320	310	350		265	3000
 <chem>C21H22N2OSi</chem>			<chem>C21H22N2OSi</chem>	346.498	94	73	203		63	3000
 <chem>C20H15FN2O</chem>			<chem>C20H15FN2O</chem>	318.344	1000	1000	1000		1000	1000
 <chem>C20H15FN2O</chem>			<chem>C20H15FN2O</chem>	318.344	1000	1000	1000		1000	1000

Appendix VI. PDSP Activity Data

The activity data at GABA and other receptors was carried out by Dr. Bryan Roth. The Roth Lab studies the structure and function of G-Protein coupled receptors (GPCRs). The Roth lab is the principal contractor for the NIMH Psychoactive Drug Screening Program which includes the PDSP K_i database. The lab operates within the Pharmacology Department at the University of North Carolina at Chapel Hill. The database can be accessed online at <https://kiddbdev.med.unc.edu/pdsp/>.

PDSP Compound List

Milwaukee Code # versus UNC Code Number for PDS

UNC Roth Compound #	Name	MW
401	BCCt C16H16N2O2	268.31
402	3 EBC C13H12N2O-HCl	248.5
403	3 PBC C14H14N2O-HCl	262.5
404	RY-080 C17H15N3O3	309.32
405	RY-024 C19H19N3O3	337.37
406	Xhe II-053 C22H17N3O2	335.39
407	RY-023 C22H27N3O3Si	409.55
408	RY-079 C20H23N3O3Si	381.5
409	QH II-066 C17H12N2O	260.29
410	CMD 30 C15H11F3N2O2	308.26
473	JY-HXE-053 C22H16FN3O2 (F.W. 373)	373
474	JY-032 C20H15BrFN3O2	428
475	JYI-70 C19H13FN4	316
477	XliHell-048 C25H25N3O2Si	427
479	Xli270 C19H14N	298
934	DMH-D-070 (C39H28N6O4Br2)	802
935	DMH-D-048 (C49H46N6O4Si2)	838
936	DMH-D-053 (C43H30N6O4)	694
937	DM-II-26 (C41H32N6O4Br2)	830
939	DM-III-97 (C45H34N6O4)	722
940	DM-III-93 (C40H30N6O5Br2)	832
941	DM-III-94 (C50H48N6O5Si2)	868
942	DM-III-96 (C44H32N6O5)	724
943	DM-II-20 (C22H14N3O2F3)	408
944	DM-II-30 C20H13N3O2BrF3)	463
945	DM-II-33 (C20H13N3O2BrCl3)	511
946	DM-II-35 (C25H22N3O2SiF3)	481
947	DM-III-01 (C18H12N3O2Br)	381
948	DM-II-72 (C15H10N2OBrCl)	348
949	DM-II-90 (C17H12N4BrCl)	386
950	XLi-JY-DMH-TMS C22H21N4SiCl)	404
951	XLi-JY-DMH (C19H13N4Cl)	332
952	H2111 C20H16N3ClO2	365.81
953	H2120 C20H16N3IO2	457.26
954	H2141 C21H23N3Si	345.51
955	H2146 C21H23N3OSi	361.51
956	H2150 C16H14N3OBr	344.21
957	H2147 C18H15N3O	289.33
958	H2157 C19H19N3OSi	333.46
959	H2158 C20H21N3OSi	347.49
960	H2160 C17H13N3O	275.3
961	H2165 C24H24N4O2Si	428.56

CMPD #	Name	MW
<u>963</u>	<u>Hz148 C18H15N3</u>	273.33
<u>964</u>	<u>Hz135 C16H14N3Br</u>	328.21
<u>965</u>	<u>Hz164 C19H15N4O2Br</u>	411.25
<u>966</u>	<u>WYS1 C45H50N4O6</u>	774.9
<u>967</u>	<u>WYS2 C35H34N4O4</u>	574.67
<u>968</u>	<u>WYS3 C35H38N4O4</u>	578.7
<u>969</u>	<u>WYS4 C48H56N4O8</u>	816.98
<u>970</u>	<u>WYS5 C37H42N4O4</u>	606.25
<u>972</u>	<u>WYS7 C21H28N4O4Si</u>	364.51
<u>973</u>	<u>WYS8 C18H16N2O2</u>	292.33
<u>974</u>	<u>WYS9 C16H15IN2O2</u>	394.21
<u>975</u>	<u>WYS10 C14H9F3N2O2</u>	294.23
<u>976</u>	<u>WYS11 C15H11F3N2O3</u>	324.25
<u>977</u>	<u>WYS12 C20H18N2O2S</u>	350.44
<u>978</u>	<u>WYS13 C20H18N2O3</u>	334.37
<u>979</u>	<u>WYS14 C34H29F3N4O4</u>	614.61
<u>980</u>	<u>WYS15 C22H20N2O2</u>	344.41
<u>981</u>	<u>WYS16 C18H22N2O2</u>	298.38
<u>986</u>	<u>WYS21 C21H23IN2O4</u>	494.32
<u>987</u>	<u>WYSC1 C16H16N2O2</u>	268
<u>988</u>	<u>WYSC2 C15H11F3N2O2</u>	308
<u>989</u>	<u>JYI-01(C19H20N3O3Br)</u>	418
<u>990</u>	<u>JYI-02 (C24H29N3O3Si)</u>	437
<u>991</u>	<u>JYI-03 (C21H21N3O3)</u>	363
<u>992</u>	<u>JYI-04 (C21H23N3O3)</u>	365
<u>993</u>	<u>JYI-06 (C23H23N3O4)</u>	405
<u>994</u>	<u>JYI-19 (C23H23N3O3S)</u>	421
<u>995</u>	<u>JYI-20 (C25H25N3O3)</u>	415
<u>996</u>	<u>JYI-10 (C17H13N3O3F3Br)</u>	444
<u>997</u>	<u>JYI-11 (C22H22N3O3F3Si)</u>	462
<u>998</u>	<u>JYI-15 (C19H14N3O3F3)</u>	389
<u>999</u>	<u>JYI-12 (C19H16N3O3F3)</u>	390
<u>1001</u>	<u>JYI-13 (C21H16N3O4F3)</u>	431
<u>1002</u>	<u>JYI-14 (C17H14N3O3F3)</u>	365
<u>1003</u>	<u>JYI-21 (C23H17N3O3F3)</u>	441
<u>1004</u>	<u>JYI-32 (C20H15N3O2BrF)</u>	428
<u>1005</u>	<u>JYI-38 (C25H24N3O2FSi)</u>	445
<u>1006</u>	<u>JYI-56 (C24H18N3O4F)</u>	373
<u>1007</u>	<u>JYI-50 (C24H18N3O2SF)</u>	469
<u>1008</u>	<u>JYI-49 (C20H12N3O2F4Br)</u>	482
<u>1009</u>	<u>JYI-53 (C23H21N3O2F4Si)</u>	475
<u>1010</u>	<u>JYI-59 (C22H13N3O2F4)</u>	427
<u>1011</u>	<u>JYI-54 (C24H15N3O3F4)</u>	469
<u>1012</u>	<u>JYI-60 (C17H11N2OF)</u>	278
<u>1013</u>	<u>JYI-64 (C17H12N4FBr)</u>	371
<u>1014</u>	<u>JYI-70 (C19H13N4F)</u>	316
CMPD #	Name	MW
<u>1016</u>	<u>PS-1-27 C21H16N5BrO</u>	434.3

<u>1017</u>	<u>PS-1-28 C26H25N5OSi</u>	451.6
<u>1018</u>	<u>PS-1-26 C23H17N5O</u>	379.4
<u>1019</u>	<u>PS-1-34B C20H17N4BrO</u>	409.3
<u>1020</u>	<u>PS-1-35 C23H22N5OBr</u>	464.4
<u>1021</u>	<u>PS-1-36 C28H31N5OSi</u>	481.7
<u>1022</u>	<u>PS-1-37 C25H23N5O</u>	409.5
<u>1023</u>	<u>XLi268 C17H13BrN4</u>	353
<u>1024</u>	<u>XLi269 C22H22N4Si</u>	370
<u>1025</u>	<u>XLi270 C19H14N4</u>	298.34
<u>1026</u>	<u>XLi223 C22H20BrN3O2</u>	438.32
<u>1027</u>	<u>XLi224 C27H29N3O2Si</u>	455.62
<u>1028</u>	<u>XLi225 C24H21N3O2</u>	383.44
<u>1029</u>	<u>CM-D45 C19H21N3O4</u>	355.39
<u>1030</u>	<u>RY-024 C19H19N3O3</u>	337.37
<u>1031</u>	<u>XHeII-053 C22H17N3O2</u>	355.39
<u>1032</u>	<u>XLiXHeII-048 C25H25N3O2Si</u>	427.57
<u>1033</u>	<u>RY-023 C22H27N3O3Si</u>	409.55
<u>1034</u>	<u>RY-080 C17H15N3O3</u>	309.32
<u>1035</u>	<u>XLi337 C21H23N3O3</u>	365.43
<u>1036</u>	<u>XLi340 C26H25N3O2</u>	411.5
<u>1037</u>	<u>XLi339 C23H22N4</u>	354.45
<u>1038</u>	<u>XLi275 C20H19N3O3</u>	349.38
<u>1039</u>	<u>XLi356 C33H34N6O6</u>	610.66
<u>1040</u>	<u>XLi347 C34H28N6O7</u>	632.62
<u>1041</u>	<u>XLi351 C21H21CIN2OSi</u>	380.94
<u>1042</u>	<u>XLi343 C20H19CIN2OSi</u>	366.92
<u>1043</u>	<u>XLi350 C17H11CIN2O</u>	294.73
<u>1044</u>	<u>XLi352 C18H13CIN2O</u>	308.76
<u>1045</u>	<u>XLi338 C23H21CIN4</u>	388.89
<u>1048</u>	<u>JC184 C13H9BrN2OS</u>	321
<u>1049</u>	<u>JC207 C18H18N2OSSi</u>	338
<u>1050</u>	<u>JC208 C15H10N2OS</u>	266
<u>1051</u>	<u>JC209 C19H20N2OSSi</u>	352
<u>1052</u>	<u>JC222 C16H12N2OS</u>	280
<u>1055</u>	<u>JC221 C20H15N3O2S</u>	361
<u>1684</u>	<u>RY069</u>	388.38
<u>1685</u>	<u>PS-I-26</u>	379.14
<u>1686</u>	<u>JC221</u>	361.42
<u>1687</u>	<u>H2166</u>	356.13
<u>1688</u>	<u>PS-I-28</u>	451.18
<u>1689</u>	<u>Xli-JY-DMH</u>	332.08
<u>1690</u>	<u>PS-I-37</u>	425.22
<u>1691</u>	<u>PWZ-031A</u>	296.15
<u>1692</u>	<u>XLI093</u>	602.19
<u>1693</u>	<u>XLI356</u>	610.66
	CMPD #	Name
<u>1695</u>	<u>CM-D45</u>	355.39
<u>1696</u>	<u>RY-059</u>	345.35
<u>1697</u>	<u>PWZ-035A</u>	305.76

<u>1698</u>	<u>RY068</u>	460.56
<u>1699</u>	<u>JY-I-70</u>	316.11
<u>1709</u>	<u>RY-I-29</u>	345.35
<u>3173</u>	<u>PWZ-029</u>	291.73
<u>7828</u>	<u>SH-TR-CH3</u>	312.37
<u>7829</u>	<u>SH-TS-CH3</u>	312.37
<u>7944</u>	<u>JIE-1-12</u>	361.43
<u>11461</u>	<u>TC-YJIG-24</u>	316.74
<u>14413</u>	<u>MVL-VI-33</u>	263.72
<u>14414</u>	<u>MVL-VI-34</u>	263.72
<u>14460</u>	<u>MVL-V1-52</u>	269.3
<u>14567</u>	<u>TC-YJIG-26</u>	250
<u>14575</u>	<u>TC-YJIG-24</u>	0
<u>16067</u>	<u>OJ-MPP-1</u>	269.1
<u>16068</u>	<u>YT-II-76</u>	325.36
<u>16069</u>	<u>HJ-I-040</u>	341.4
<u>16070</u>	<u>ZJW-II-040</u>	394.4
<u>16071</u>	<u>HZ-166 ACID</u>	328.3
<u>16072</u>	<u>SH-I-75</u>	355
<u>16073</u>	<u>YT-III-40</u>	411.43
<u>16074</u>	<u>YT-III-41</u>	409.48
<u>16075</u>	<u>XLI-210</u>	630.65
<u>16076</u>	<u>YT-II-794</u>	774.5
<u>16077</u>	<u>YT-II-792</u>	778.45
<u>16078</u>	<u>YT-II-793</u>	792.47
<u>16079</u>	<u>SR-II-97</u>	304.73
<u>16080</u>	<u>YT-III-331</u>	758.77
<u>16081</u>	<u>YT-III-332</u>	772.8
<u>16082</u>	<u>YT-III-333</u>	786.8
<u>16083</u>	<u>YT-III-15</u>	659.1
<u>16084</u>	<u>ZJW-II-065</u>	358.4
<u>16085</u>	<u>ZJW-II-067</u>	342.4
<u>16086</u>	<u>ZJW-II-061</u>	355.4
<u>16087</u>	<u>ON-I-29A</u>	305.71
<u>16088</u>	<u>XHE-II-53</u>	355.38
<u>16089</u>	<u>XLI-093</u>	603
<u>16090</u>	<u>PWZ-029</u>	291.73
<u>16091</u>	<u>BCCT</u>	268.3
<u>16092</u>	<u>3 PBC</u>	262.7
<u>16162</u>	<u>mlw-13</u>	301.68
<u>16163</u>	<u>mlw-21</u>	316.74
<u>16164</u>	<u>mlw-23</u>	335.58
<u>16165</u>	<u>mlw-29</u>	385.23
CMPD #	Name	MW
<u>16167</u>	<u>mlw-35</u>	380.03
<u>16168</u>	<u>mlw-36</u>	312.23
<u>16169</u>	<u>mlw-38</u>	346.13
<u>16170</u>	<u>mlw-58</u>	272.68
<u>16171</u>	<u>mlw-59</u>	286.71

<u>16172</u>	<u>mlw-62</u>	312.79
<u>16173</u>	<u>mlw-64</u>	272.68
<u>16174</u>	<u>mlw-65</u>	256.68
<u>16175</u>	<u>mlw-69</u>	316.74
<u>16176</u>	<u>mlw-70</u>	286.71
<u>16177</u>	<u>mlw-88</u>	299.75
<u>16178</u>	<u>mlw-89</u>	274.67
<u>16179</u>	<u>mlw-103</u>	324.68
<u>16180</u>	<u>mlw-104</u>	270.26
<u>16181</u>	<u>mlw-111</u>	257.26
<u>16182</u>	<u>mlw-112</u>	282.29
<u>16183</u>	<u>mlw-113</u>	282.29
<u>16184</u>	<u>mlw-116</u>	324.68
<u>16185</u>	<u>mlw-117</u>	281.69

CMPD	PI	Tier	5-HT1A	5-HT1B	5-HT1D	5-HT1e	5-HT2A
473	Cook	1		>10000			
474	Cook	1		>10000			
475	Cook	1					
476	Cook	1					
477	Cook	1			4,171.00		2,205.00
479	Cook	1					>10000
934	Cook	1					
935	Cook	1					
936	Cook	1					
937	Cook	1					
939	Cook	1					
940	Cook	1					
941	Cook	1					
942	Cook	1					
943	Cook	1					
944	Cook	1					

Unless otherwise indicated (see Note), data represent K_i (nM) values obtained from non-linear regression of radioligand competition binding isotherms. K_i values are calculated from best fit IC_{50} values using the Cheng-Prusoff equation.

Note: When the Hill coefficient (nH) is significantly different from -1 (assessed by F test), the IC_{50} and nH are reported instead of the K_i .

A * next to a value denotes IC_{50} .

To view the experiment error, source, species, concentration, etc, click on the result.

Legend:	Complete	2* Assay Scheduled					

CMPD	PI	Tier	5-HT1A	5-HT1B	5-HT1D	5-HT1e	5-HT2A
946	Cook	1					
947	Cook	1					
948	Cook	1					
949	Cook	1					
950	Cook	1					
951	Cook	1					
952	Cook	1					
953	Cook	1					
954	Cook	1					
955	Cook	1					
956	Cook	1					
957	Cook	1					
958	Cook	1					
959	Cook	1					
960	Cook	1					
961	Cook	1					
962	Cook	1					
963	Cook	1					
964	Cook	1					
965	Cook	1					
966	Cook	1					
967	Cook	1					
968	Cook	1					
969	Cook	1					
970	Cook	1					
972	Cook	1					
973	Cook	1					
974	Cook	1					
975	Cook	1					
976	Cook	1					
977	Cook	1					
CMPD	PI	Tier	5-HT1A	5-HT1B	5-HT1D	5-HT1e	5-HT2A
979	Cook	1					
980	Cook	1					
981	Cook	1					
986	Cook	1					
987	Cook	1					
988	Cook	1					
989	Cook	1					
990	Cook	1					
991	Cook	1					
992	Cook	1					
993	Cook	1					
994	Cook	1					
995	Cook	1					
996	Cook	1					
997	Cook	1					
998	Cook	1					
999	Cook	1					
1001	Cook	1					
1002	Cook	1					
1003	Cook	1					
1004	Cook	1					
1005	Cook	1					
1006	Cook	1					
1007	Cook	1					
1008	Cook	1					
1009	Cook	1					
1010	Cook	1					
1011	Cook	1					
1012	Cook	1					
1013	Cook	1					
1014	Cook	1					

CMPD	PI	Tier	5-HT1A	5-HT1B	5-HT1D	5-HT1e	5-HT2A
1016	Cook	1					
1017	Cook	1					
1018	Cook	1					
1019	Cook	1					
1020	Cook	1					
1021	Cook	1					
1022	Cook	1					
1023	Cook	1					
1024	Cook	1					
1025	Cook	1					
1026	Cook	1					
1027	Cook	1					
1028	Cook	1					
1029	Cook	1					
1030	Cook	1					
1031	Cook	1					
1032	Cook	1					
1033	Cook	1					
1034	Cook	1					
1035	Cook	1					
1036	Cook	1					
1037	Cook	1					
1038	Cook	1					
1039	Cook	1					
1040	Cook	1					
1041	Cook	1					
1042	Cook	1					
1043	Cook	1					
1044	Cook	1					
1045	Cook	1					
1048	Cook	1					
1050	Cook	1					
1051	Cook	1					
1052	Cook	1					
1055	Cook	1					
1684	Cook	1					
1685	Cook	1	1,715.00	>10,000	2,383.00	22.1	1,124.00
1686	Cook	1	4,573.00	>10,000		20.3	
1687	Cook	1					
1688	Cook	1		4,142.00		188.3	
1689	Cook	1					
1690	Cook	1					
1691	Cook	1					
1692	Cook	1		10,000.0(AVE)			
1693	Cook	1					
1694	Cook	1		>10,000		679.6	
1695	Cook	1		>10,000			
1696	Cook	1		2,078.00			
1697	Cook	1	>10,000				
1698	Cook	1					
1699	Cook	1	>10,000				
1709	Cook	1					
3173	Cook	1					
7828	Cook	1				>10000	
7829	Cook	1				>10000	
7944	Cook	1					
11461	Cook	1					
14413	Cook	1					
14414	Cook	1					
14460	Cook	1					
14567	Cook	1		261			
14575	Cook	1					

CMPD	PI	Tier	5-HT1A	5-HT1B	5-HT1D	5-HT1e	5-HT2A
16068	Cook	1					
16069	Cook	1					
16070	Cook	1					
16071	Cook	1					
16072	Cook	1					
16073	Cook	1					
16074	Cook	1					
16075	Cook	1					
16076	Cook	1					
16077	Cook	1					
16078	Cook	1					
16079	Cook	1					
16080	Cook	1					
16081	Cook	1					
16082	Cook	1					
16083	Cook	1					
16084	Cook	1					
16085	Cook	1					
16086	Cook	1					
16087	Cook	1					
16088	Cook	1					
16089	Cook	1					
16090	Cook	1					
16091	Cook	1					
16092	Cook	1					
16162	Cook	1					
16163	Cook	1					
16164	Cook	1					
16165	Cook	1					
16166	Cook	1					
16167	Cook	1					
16169	Cook	1					
16170	Cook	1					
16171	Cook	1					
16172	Cook	1					
16173	Cook	1					
16174	Cook	1					
16175	Cook	1					
16176	Cook	1					
16177	Cook	1					
16178	Cook	1					
16179	Cook	1					
16180	Cook	1					
16181	Cook	1					
16182	Cook	1					
16183	Cook	1					
16184	Cook	1					
16185	Cook	1					

CMPD	Alpha2C	AMPA*	82	Beta1	Beta2	Beta3	BZP Rat Brain Site	Calcium Channel
473	2,105.00							
474	1,597.00							1,590.00
475	1,809.00							
476								
477	2,004.00			3,918.00	>10,000			446.3
479	2,362.00							
934								
935								
936								
937								
939								
940								
941								
942								
943								
944								

--	--	--	--	--	--	--	--	--

CMPD	Alpha2C	AMPA*	B2	Beta1	Beta2	Beta3	BZP Rat Brain Site	Calcium Channel
946								
947								
948								
949								
950								
951								
952								
953								
954								
955								
956								
957								
958								
959								
960								
961								
962								
963								
964								
965								
966								
967								
968								
969								
970								
972								
973								
974								
975								
976								
977								
CMPD	Alpha2C	AMPA*	B2	Beta1	Beta2	Beta3	BZP Rat Brain Site	Calcium Channel
979								
980								
981								
986								
987								
988								
989								
990								
991								
992								
993								
994								
995								
996								
997								
998								
999								
1001								
1002								
1003								
1004								
1005								
1006								
1007								
1008								
1009								
1010								
1011								
1012								
1013								
1014								

CMPD	Alpha2C	AMPA*	B2	Beta1	Beta2	Beta3	BZP Rat Brain Site	Calcium Channel
1016								
1017								
1018								
1019								
1020								
1021								
1022								
1023								
1024								
1025								
1026								
1027								
1028								
1029								
1030								
1031								
1032								
1033								
1034								
1035								
1036								
1037								
1038								
1039								
1040								
1041								
1042								
1043								
1044								
1045								
1048								
1050								
1051								
1052								
1055								
1684								
1685	4,504.00							
1686								
1687								
1688								
1689								
1690								
1691								
1692								
1693								
1694								
1695								
1696								
1697								
1698								
1699								
1709								
3173								
7828				>10,000				
7829				>10,000				
7944								
11461								
14413							4	
14414							16.4	
14460				823			4.5	
14567	2,646.00							
14575	9,660.00							

CMPD	Alpha2C	AMPA*	B2	Beta1	Beta2	Beta3	BZP Rat Brain Site	Calcium Channel
16068								
16069								
16070								
16071								
16072								
16073								
16074								
16075								
16076								
16077								
16078								
16079								
16080								
16081								
16082								
16083								
16084								
16085								
16086								
16087								
16088								
16089								
16090								
16091								
16092								
16162								
16163								
16164								
16165								
16166								
16167								
16169								
16170								
16171								
16172								
16173								
16174								
16175								
16176								
16177								
16178								
16179								
16180								
16181								
16182								
16183								
16184								
16185								

CMPD	CB1	CB1 H	D1	D2	D3	D4	D5	DAT	DOR	EP1	EP2	EP3
1016												
1017												
1018												
1019												
1020												
1021												
1022												
1023												
1024												
1025												
1026												
1027												
1028												
1029												
1030												
1031												
1032												
1033												
1034												
1035												
1036												
1037												
1038												
1039												
1040												
1041												
1042												
1043												
1044												
1045												
1048												
1050												
1051												
1052												
1055												
1684												
1685												
1686												
1687												
1688								8,505.00	894.3			
1689												
1690												
1691				>10,000	7,148.00	>10,000						
1692												
1693												
1694			1,597.00	6,497.00			4,432.00		182.4			
1695			>10,000				>10,000					
1696								>10,000				
1697												
1698												
1699												
1709			>10,000				>10,000					
3173												
7828				>10,000			>10,000		>10,000			
7829				>10,000			>10,000		>10,000			
7944							3,600.00		>10,000			
11461								>10,000				
14413				>10,000		7,503.00		>10,000				
14414				>10,000	8,608.00	>10,000						
14460												
14567							3,792.00					
14575							>10,000					

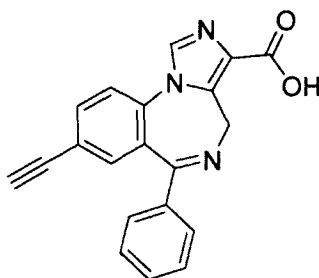
CMPD	EP4	GABA a1	GABAA	GABAa a2	GABAa a3	GABAa a6	GABAB	H1	H2
946		<u>1,127.00</u>							
947		<u>14.5</u>							
948		<u>3.9</u>							
949		<u>0.9</u>							
950		<u>137</u>							
951		<u>3.5</u>							
952		<u>32.5</u>							
953		<u>51.1</u>							
954									
955									
956		<u>491</u>							
957									
958									
959		<u>2,073.00</u>							
960		<u>481</u>							
961		<u>1,498.00</u>							
962									
963									
964		<u>271.6</u>							
965		<u>135.7</u>							
966		<u>2,432.00</u>							
967		<u>546.8</u>							
968		<u>264</u>							
969		<u>>10,000</u>							
970									
972		<u>83.4</u>							
973									
974		<u>30.5</u>							
975		<u>23.1</u>							
976		<u>47.2</u>							
977		<u>45.1</u>							
CMPD	EP4	GABA a1	GABAA	GABAa a2	GABAa a3	GABAa a6	GABAB	H1	H2
979		<u>1,179.00</u>							
980		<u>47</u>							
981									
986		<u>3,280.00</u>							
987									
988									
989									
990									
991		<u>221</u>							
992		<u>21.1</u>							
993		<u>6.1</u>							
994		<u>46.1</u>							
995		<u>288</u>							
996									
997		<u>288</u>							
998		<u>389</u>							
999		<u>99</u>							
1001		<u>1.6</u>							
1002		<u>111</u>							
1003		<u>115.8</u>							
1004		<u>21.9</u>							
1005									
1006		<u>121.1</u>							
1007		<u>123</u>							
1008		<u>0.3</u>							
1009		<u>120</u>							
1010		<u>1.4</u>							
1011		<u>117</u>							
1012		<u>17</u>							
1013		<u>0.3</u>							
1014		<u>8.4</u>							

CMPD	EP4	GABA a1	GABAA	GABAA a2	GABAA a3	GABAA a6	GABAB	H1	H2
1016		95							
1017		3,107.00							
1018		387							
1019		18.4							
1020		22.2							
1021		962							
1022		132.4							
1023		7.1							
1024		645.3							
1025		61.5							
1026		37							
1027									
1028									
1029									
1030		14							
1031									
1032		947							
1033		562							
1034		69.1							
1035									
1036									
1037		872							
1038		68							
1039		4.1							
1040		687							
1041		1.5							
1042		234							
1043		2.5							
1044		1.9							
1045		607							
1048		30							
1050		121.5							
1051		979							
1052		155							
1055		109.2							
1684									
1685									
1686									
1687									
1688									
1689									
1690									
1691									
1692									
1693									
1694									
1695									
1696									
1697									
1698									
1699									
1709									
3173									
7828								>10,000	
7829								>10,000	
7944									
11461									
14413									
14414									
14460									
14567		>10,000							
14575		7,460.00							

CMPD	EP4	GABA a1	GABAA	GABAa a2	GABAa a3	GABAa a6	GABAB	H1	H2
16068		5							
16069		178							
16070		161							
16071		283							
16072		1,424.00							
16073		157							
16074		387							
16075		234							
16076		1,640.00							
16077									
16078		453							
16079		79							
16080		1,682.00							
16081		409							
16082		895							
16083		146							
16084		1,456.00							
16085		1,437.00							
16086		2,942.00							
16087		330							
16088		714							
16089		711							
16090		1,338.00							
16091		202							
16092		1,626.00							
16162		1,631.00							
16163		3,188.00							
16164		150							
16165		764							
16166		348							
16167		326							
16169		1,864.00							
16170		4,445.00							
16171		1,368.00							
16172	3,281.00				9,417.00				
16173	904				612				
16174	1,223.00				1,944.00				
16175	4,970.00				1,684.00				
16176	8,816.00				1,460.00				
16177	1,590.00				1,141.00				
16178	1,171.00				1,853.00				
16179	3,781.00				383				
16180	3,615.00				8,578.00				
16181	2,232.00				9,732.00				
16182	1,111.00				>10,000				
16183	1,225.00				6,807.00				
16184	1,487.00				298				
16185	3,778.00				2,250.00				

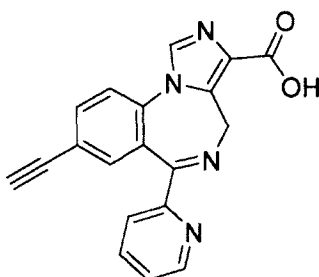
[illegible]

Appendix VII. In Vitro Metabolic Stability of Selected Compounds Using Human Liver Microsomes



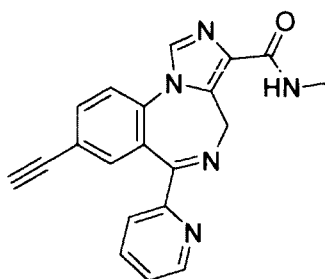
XHe-II-053 Acid

Not metabolized by human liver microsomes
at either of the concentrations tested (1 and 10 μ M)



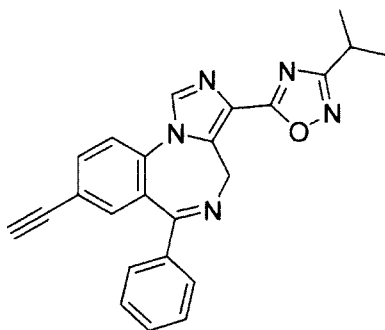
SR-II-54

Not metabolized by human liver microsomes
at either of the concentrations tested (1 and 10 μ M)



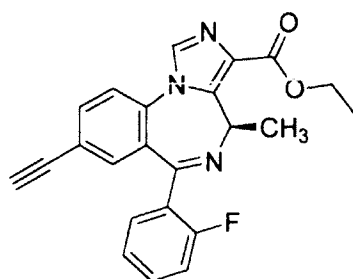
HJ-I-40

Not metabolized by human liver microsomes
at either of the concentrations tested (1 and 10 μM)



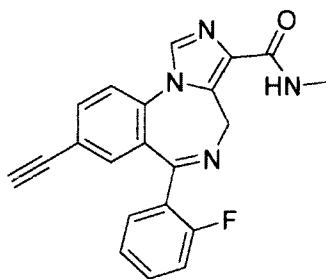
EMJ-I-026

Not metabolized by human liver microsomes
at either of the concentrations tested (1 and 10 μM)



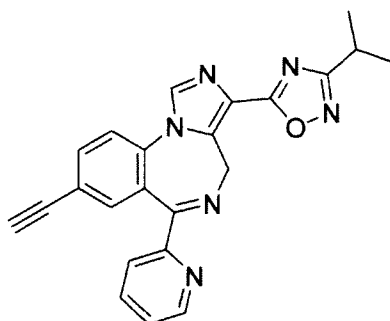
SH-053-2'F-RCH3

Not metabolized by human liver microsomes
at either of the concentrations tested (1 and 10 μ M)



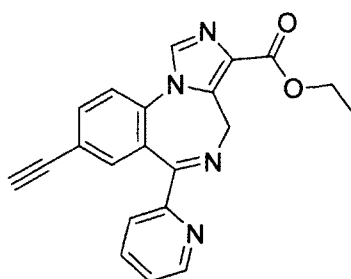
HJ-I-037

Not metabolized by human liver microsomes
at either of the concentrations tested (1 and 10 μ M)



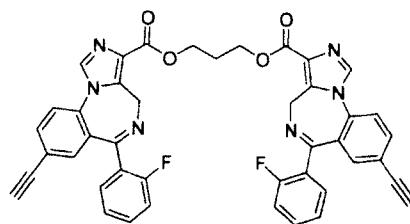
ZJW-II-040

Not metabolized by human liver microsomes
at either of the concentrations tested (1 and 10 μM)



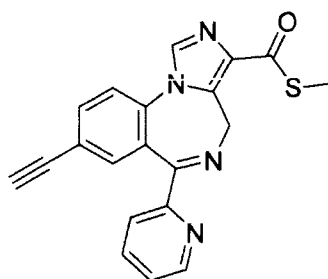
HZ-166

Showed only slight metabolism at 1 μM and 10 μM



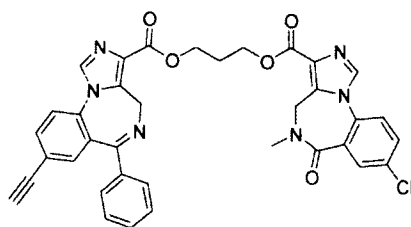
YT-III-271

Only slight metabolism at 1 μM and no metabolism at 10 μM



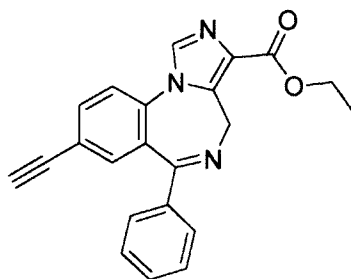
ZJW-II-065

Only slight metabolism at 1 μ M and no metabolism at 10 μ M



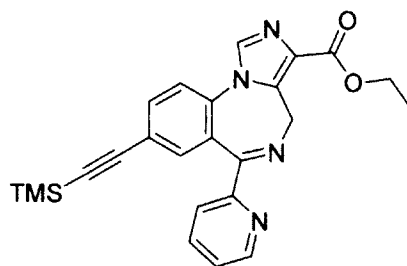
YT-III-15

Showed significant metabolism at 1 μ M but only slight metabolism at 10 μ M



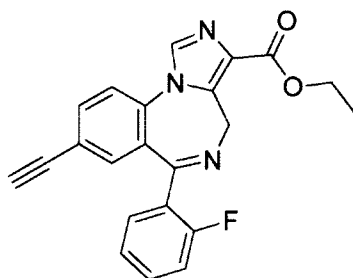
XHe-II-053

Showed significant metabolism at both 1 and 10 μ M
when incubated with human liver microsomes



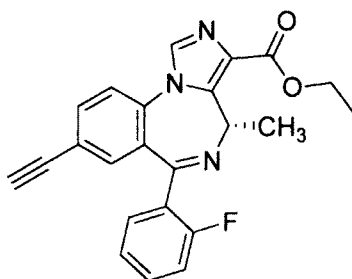
HZ-166-TMS

Shown significant metabolism at both 1 and 10 μ M
when incubated with human liver microsomes



JY-XHe-053

Shown significant metabolism at both 1 and 10 μ M
when incubated with human liver microsomes



SH-053-2'F-SCH3

Showned significant metabolism at both 1 and 10 μ M
when incubated with human liver microsomes

The metabolic stability of XHe-II-053(1), XHe-II-043 Acid(2), HZ-166(3), SR-II-54(4), HZ-166-TMS(5), HJ-I-40(6), EMJ-I-026(7), JY-XHe-053(8), SH-053-2'F-SCH3(9), SH-053-2'F-RCH3(10), YT-III-271(11), YT-III-15(12), HJ-I-037(13), ZJW-II-065(14), and ZJW-II-040(15) using human liver microsomes was studied. The test articles were incubated at two concentrations (1 and 10 μ M) and aliquots (100 μ l) were removed at various time points (0, 15, 30 and 60 minutes), and analyzed by LC-MS/MS.

The results for the metabolic stability of all 15 compounds using pooled human liver microsomes are summarized in Tables 1, 2 and 3. XHe-II-043 Acid(2), SR-II-54, HJ-I-40(6), EMJ-I-026(7), SH-053-2'F-RCH3(10), HJ-I-037(13), ZJW-II-040(15) were not metabolized by human liver microsomes at either of the concentrations tested (1 and 10 μ M). HZ-166(3) showed slight metabolism at 1 μ M and 10 μ M. YT-III-271(11) and ZJW-II-065(14) showed slight metabolism at 1 μ M and no metabolism at 10 μ M. YT-III-15(12) showed significant metabolism at 1 μ M but only slight metabolism at 10 μ M. XHe-II-053(1), HZ-166-TMS(5), JY-XHe-053(8), SH-053-2'F-SCH3(9) showed significant metabolism at both 1 and 10 μ M when incubated with human liver microsomes.

When incubated with heat-inactivated human liver microsomes, there was no significant change in the % remaining of any of the 15 compounds after 60 minutes. This

suggests that the compounds are stable in the incubation conditions used in these experiments.

The results for the metabolic stability of midazolam using active and heat-inactivated human liver microsomes are summarized in Table 4. Midazolam was consistently metabolized, indicating that the incubation conditions used were suitable for determining metabolic stability.

Table 47. In vitro metabolic stability of XHe-II-053(1), XHe-II-043 acid(2), HZ-166(3), SR-II-54(4), HZ-166-TMS(5) using human liver microsomes

Test Article	Time, min	Mean % Remaining vs T = 0 min ^a	
		Human Liver Microsomes	
		1 μ M ^b	10 μ M ^b
XHe-II-053(1)	15	41.4	47.6
	30	11.1	13.9
	60	1.46	1.74
XHe-II-053(1) with HI ^c Microsomes	60	107	102
XHe-II-043 Acid(2)	15	108	95.6
	30	106	95.0
	60	111	95.0
XHe-II-043 Acid(2) with HI ^c Microsomes	60	106	97.4
HZ-166(3)	15	106	104
	30	98.4	90.7
	60	80.4	76.3
HZ-166(3) with HI ^c Microsomes	60	94.1	95.4
SR-II-54(4)	15	102	91.4
	30	94.7	86.1
	60	110	86.9
SR-II-54(4) with HI ^c Microsomes	60	97.4	88.7
HZ-166-TMS(5)	15	78.0	77.1
	30	35.9	43.8
	60	7.8	13.8
HZ-166-TMS(5) with HI ^c Microsomes	60	108	84.7

^a % remaining at T=0 is 100%

^b Samples were assayed in duplicate.

^c HI = Heat Inactivated

Table 48. In vitro metabolic stability of HJ-I-40(6), EMJ-I-026(7), JY-XHE-053(8), SH-053-2'F-SCH3(9), SH-053-2'F-RCH3(10) using human microsomes

Test Article	Time, min	Mean % Remaining vs T = 0 min ^a	
		Human Liver Microsomes	
		1 μ M ^b	10 μ M ^b
HJ-I-40(6)	15	109	104
	30	126	106
	60	136	110
HJ-I-40(6) with HI ^c Microsomes	60	110	110
EMJ-I-026(7)	15	100	109
	30	107	108
	60	91.4	96.6
EMJ-I-026(7) with HI ^c Microsomes	60	137	119
JY-XHe-053(8)	15	13.5	20.0
	30	2.13	3.60
	60	0.27	0.56
JY-XHe-053(8) with HI ^c Microsomes	60	102	111
SH-053-2'F-SCH3(9)	15	6.18	11.7
	30	0.85	1.72
	60	3.85 ^d	0.20
SH-053-2'F-SCH3(9) with HI ^c Microsomes	60	110	114
SH-053-2'F-RCH3(10)	15	86.7	97.9
	30	86.7	105
	60	86.9	105
SH-053-2'F-RCH3(10) with HI ^c Microsomes	60	115	117

^a % remaining at T=0 is 100%

^b Samples were assayed in duplicate.

^c HI = Heat Inactivated

^d Suspected contamination, if deleted value = 0.20

Table . In vitro metabolic stability of YT-III-271(11), YT-III-15(12), HJ-I-037(13), ZJW-II-065(14), and ZJW-II-040(15) using human microsomes

Test Article	Time, min	Mean % Remaining vs T = 0 min ^a	
		Human Liver Microsomes	
		1 μ M ^b	10 μ M ^b
YT-III-271(11)	15	97.1	104
	30	83.5	102
	60	52.0	91.1
YT-III-271(11) with HI ^c Microsomes	60	117	97.0
YT-III-15(12)	15	87.3	107
	30	39.4	104
	60	5.2	82.8
YT-III-15(12) with HI ^c Microsomes	60	141	114
HJ-I-037(13)	15	97.7	96.8
	30	99.5	103
	60	92.7	103
HJ-I-037(13) with HI ^c Microsomes	60	117	108
ZJW-II-065(14)	15	98.4	111
	30	97.0	106
	60	82.5	95.6
ZJW-II-065(14) with HI ^c Microsomes	60	105	110
ZJW-II-040(15)	15	97.8	106
	30	98.7	99.3
	60	89.4	95.1
ZJW-II-040(15) with HI ^c Microsomes	60	113	92.0

^a % remaining at T=0 is 100%

^b Samples were assayed in duplicate.

^c HI = Heat Inactivated

Table 49. In vitro metabolic stability of Midazolam using human liver microsomes

Test Article	Time, min	Mean % Remaining vs T = 0 min ^a
		Human Liver Microsomes
		10 μ M ^b
Midazolam	15	36.9 \pm 13.5
	30	18.7 \pm 7.3
	60	4.2 \pm 2.2
Midazolam with HI ^c Microsomes	60	104 \pm 1.2

^a % remaining at T=0 is 100%

^b Data from three experiments (samples were assayed in duplicate in each experiment).

^c HI = Heat Inactivated

Curriculum Vitae

CURRICULUM VITAE

Full Name: Terrill S. Clayton

Email: terry_clayton@sbcglobal.net

Place and Date of Birth: Madison, Wisconsin, January 16, 1973

Education:

B.S., University of Wisconsin-Madison, May 1996
Major: Biology.

B.S., University of Wisconsin-Milwaukee, May 2001
Major: Chemistry.

Ph.D, University of Wisconsin-Milwaukee, December 2011
Major: Organic/Medicinal Chemistry.

Dissertation Title: I. Unified Pharmacophore Protein Models of the Benzodiazepine Receptor Subtypes. II. Subtype Selective Ligands for $\alpha 5$ GABA_A/Bz Receptors.

Affiliations/Memberships: American Chemical Society, Medicinal Chemistry

Publications:

Yin, W.; Majumder, S.; Clayton, T.; Petrouc, S.; VanLinn, M.L.; Namjoshia, O.A.; Ma, C.; Cromer, B.A.; Roth, B.L.; Platte, D.M. and Cook, J.M. Design, synthesis, and subtype selectivity of 3,6-disubstituted β -carboline at Bz/GABA(A)ergic receptors. SAR and studies directed toward agents for treatment of alcohol abuse. *Bioorg. and Med. Chem.* **2010**, 18, (21) pp 7548-7564.

Miroslav M Savic, Ph.D.; Samarpan Majumder; Shengming Huang; Rahul V Edwankar; Roman Furtmüller; Srđan Joksimović; Terry Clayton Sr.; Joachim Ramerstorfer; Marija M Milinković; Bryan L Roth; Werner Sieghart; James M Cook. Novel positive allosteric modulators of GABA_A receptors: Do subtle differences in activity at $\alpha 1$ plus $\alpha 5$ versus $\alpha 2$ plus $\alpha 3$ subunits account for dissimilarities in behavioral effects in rats? *Progress in Neuro-Psychopharmacology & Biological Psychiatry*. **2010**, 34, 2, 376-386.

Grant, J.A., Bonnick, T., Gossell-Williams, M., Clayton, T., Cook, J.M., Jackson, Y.A., Synthesis, pharmacological studies and molecular modeling of some tetracyclic 1,3-diazepinium chlorides. *Bioorg. Med. Chem.* **2010**, 18, 2, 909-921.

Takahashi, A.; Yap, J.J.; Bohager, D.Z.; Faccidomo, S.; Clayton, T.; Cook, J.M.; Miczek, K.A. Glutamatergic and GABAergic Modulations of Ultrasonic Vocalizations During Maternal Separation Distress in Mouse Pups. *Psychopharmacol.* **2009**, 204, 61-71.

Han, D., Forsterling, H.F., Li, X., Deschamps, J.R., Parrish, D., Cao, H., Rallapalli, S., Clayton, T., Teng, Y., Majumder, S., Sankar, S., Roth, B.L., Sieghart, W., Furtmuller, R., J.K., Weed, M.R., Cook, J.M. A Study of the Structure-activity Relationship of GABA_A-benzodiazepine Receptor Bivalent Ligands by Conformational Analysis with low Temperature NMR and X-ray Analysis, *Bioorg. and Med. Chem.*, **2008**, 16, 8853-8862.

Savic, M.M.; Milinkovic, M.M.; Clayton, T.; Rallapalli, R.; Joksimovic, Van linn, M.; Cook, J.M.; The differential role of $\alpha 1$ and $\alpha 5$ containing GABAA receptors in mediating diazepam effects on spontaneous locomotor activity and water maze learning and memory in rats. *International Journal of Neuropsychopharmacology*, **2009**, 12, 1179-1193.

Savic, M. M.; Clayton, T.; Furtmuller, R.; Gavrilovic, I.; Samardzic, J.; Savic, S.; Huck, S.; Sierhart, W.; Cook, J. M.; PWZ-029, A compound with moderate inverse agonist functional selectivity at GABAA receptors containing $\alpha 5$ subunits, improves passive, but not active, avoidance learning in rats. *Brain Research*, **2008**, 1208, 150-159.

Danni Harris, Terry Clayton, James Cook, Robert Halliwell, Peyman Sahbaie, Roman Furtmuller, Sigismund Huck, Werner Sieghart, Timothy M. DeLorey; Selective Influence on Contextual Memory: Physiochemical Properties Associated with Selectivity of Benzodiazepine Ligands at GABA_A Receptors Containing the $\alpha 5$ Subunit. *J. Med. Chem.*, **2008**, 51, 13, 3788-3803.

T. Clayton, J.L. Chen, M. Ernst, L. Richter, B.A. Cromer, C.J. Morton, H. Ng, C.C. Kaczorowski, F.J. Helmstetter, R. Furtmüller, G. Ecker, M.W. Parker, W. Sieghart and J.M. Cook.; Analysis of the Benzodiazepine Binding Site on γ -Aminobutyric acid_A Receptors: Correlation of Experimental Data with Pharmacophore and Comparative Models, *Current Medicinal Chemistry*, **2007**, 14, 26, 2755-2775.

Savic, M.M., Huang, S., Furtmüller, R., Clayton, T., Huck, S., Obradović, D.I., Ugrešić, N.D., Sieghart, W., Bokonjić, D.R., Cook, J.M.; Are GABA_A Receptors Containing $\alpha 5$ Subunits Contributing to the Sedative Properties of Benzodiazepine Site Agonists? *Neuropsychopharmacology*, **2008**, 33, 332-339.

Patents:

Roth, B.; Clayton, T. *Device, Method, and Composition For Reducing the Incidence of Tobacco Smoking*. U.S. Pat. 7,766,018; August 03, 2010.

Cook, J.M.; Clayton, T.; Johnson, Y.T.; Rallapalli, S.; Han, D.; *Gabaergic Agents to Treat Memory Deficits*. U.S. Pat. Appl. US 2010/0130479 A1. Pub. May 27, 2010.

Cook, J.M.; Han, D.; Clayton, T. *Imidazobenzodiazepines As Gabaergic Agents to Treat Memory Deficits and Their Preparation*. U.S. Pat. 7,595,395 B2; September 29, 2009.

Cook, J.M.; Clayton, T.; Jain, H.D.; Teng, Y.; Yang, J. *Selective Anticonvulsant Agents and Their Uses*. U.S. Pat. Appl. No. 61/038,184; Filed March 2008.

Barndt, J.A.; Barton, R.H.; Clayton, T.S.; Rose, M.J.; Volz, P.G. *Printing Using Color Changeable Material*. WO 2009/094063 A1. Pub. July 30, 2009.

Graushar, W.T; Barndt, J.A.; Barton, R.H.; Clayton, T.S.; *Ablative Printing*. US 2009/0128860 A1; Pub. May 21, 2009.

Presentations:

Clayton, Terry; *Computational Chemistry Methods: SAR, Pharmacophores & Protein Docking*. University of Wisconsin-Milwaukee, March 2nd, 2010.

Clayton, Terry; *Synthesis of Subtype Selective Ligands and Molecular Modeling for Alpha-5 Containing GABA_A/Bz Receptors to Treat Memory Deficits*. 235th ACS National Meeting, New Orleans, LA United States, April 6-10th, 2008.

J. A. Grant, Y. A. Jackson, M. Gossell-Williams, T. Bonnick, T. Clayton and J. M. Cook; *Synthesis, Pharmacological Studies and Molecular Modeling of Novel Tetracyclic 1,3-Diazepinium Chlorides*. The 22nd Mona Symposium on Natural Products and Medicinal Chemistry, Mona Jamaica, January 7-10 (2008).

James M. Cook, Harry June, Elise Weerts, Micheal L. Van Linn, Donna Platt, Tim DeLorey, Miroslav Savic, Terry Clayton. *Serendipity Rediscovered — An Oxymoron or Rational Drug Design: Studies on Subtype Selective BzR/GABAergic Ligands*. Division of Medicinal Chemistry-234th ACS National Meeting Boston, MA August 19-23, 2007.

Clayton, T.; *Synthesis of Subtype Selective Ligands for Alpha 5-Containing GABA_A/Bz Receptors to Treat Memory Deficits*. 233rd ACS National Meeting, Chicago, IL, United States, March 25-29th, 2007.

Huang, Shengming; Savic, Miroslav; Furtmuller, Roman; Duke, Angela; Clayton, Terry; Sieghart, Werner; Rowlett, James K.; Cook, James M. *Design and Synthesis of Stereoenantiomeric*

Benzodiazepine Receptor Ligands. Abstract of Papers, 233rd ACS National Meeting, Chicago, IL, United States, March 25-29th, 2007.

Platt, D.M.; Cook, J.M.; Van Linn, M.L.; Clayton, T.S.; *GABA_A/α5 Receptor Mechanisms in the Discriminative Stimulus Effects of GABA-A Modulators*. CPDD Meeting, Quebec, Canada. June 16-21, 2007.

M. Weed, T. Clayton, J.M. Cook, RY-023, *A Selective Inverse Agonist at the Benzodiazepine Binding Site on the GABA_A α5 Receptor, Improves Performance in a Delayed-Match-to-Sample Task in Rhesus Monkeys*. 46th American College of Neuropsychopharmacology, December 9-13, Boca Raton, FL, Abst. #158 (2007).

Faccidomo, S.; Maggin, J.G.; Melief, S.; Clayton, T.S.; Cook, J.M.; Miczek, K.A. *Modulation of Alcohol-Heightened Aggression in Mice by α5-Containing GABA_A Receptors*; Society for Neuroscience, Atlanta, GA October, 2006.

Grant, J.A.; Jackson, Y.A.; Gossel-Williams, M.; Clayton, T.; Cook, J.M.; *Synthesis, Pharmacological Studies, and Molecular Modeling of Novel 1,3-Diazepinium Chlorides*. In Latest Trends in Organic Synthesis, Brock University, St. Catharines, Ontario, 2006.

Clayton, T.; Sanker, S.; Delorey, T.; Sieghart, W.; Furtmueller, R.; Wenger, G.; Cook, J.M.; *Synthesis of Subtype Selective Ligands for α5-Containing GABA_A/Bz Receptors to Treat Memory Deficits*. ACS, Milwaukee, WI, May, 2006.

S. Huang, T. Clayton, M. Dai, W. Yin, J. Ma, R. Edwankar, C. Sawant, M. Van Linn, Y. Teng, M. Johnson, H. F. Forsterling, and J. M. Cook; *The SAR Study of Benzodiazepine Receptor Bivalent Ligands by Low Temperature NMR Spectroscopy and X-Ray Analysis*, Abstracts, 37th Great Lakes Regional Meeting of the American Chemical Society, Milwaukee, WI May 31 – June 2, 2006, GLRM-155.

S. Huang, T. Clayton, M. Dai, R. Edwankar, C. Sawant, J. M. Cook *Synthesis of Optically Active Subtype Selective BZR Ligands*, Abstracts of Papers, 232nd ACS National Meeting, San Francisco, CA, Sept. 10-14, 2006, MEDI-502.

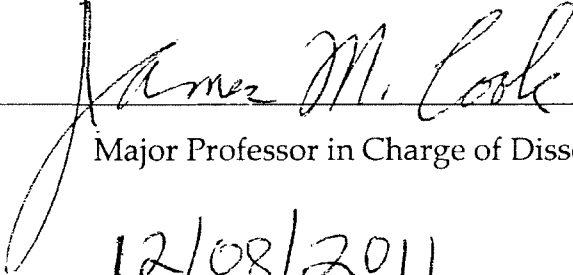
Clayton, T., *Prodrug Design and Synthesis*, Graduate Seminar, Milwaukee, WI 2004.

Clayton, T., *Stripping Potentiometry Studies of Inorganic Arsenic Oxyanions at Trace Levels*, Awards Day Finalist, Milwaukee, WI, 2003.

Clayton, T.; *Chemistry and Art*. National Chemistry Week. Discovery World, ACS - Milwaukee Section, Milwaukee, WI, 2001.

Minor: Analytical

Signed


Major Professor in Charge of Dissertation

Date

12/08/2011